THE MINOR PLANET BULLETIN

BULLETIN OF THE MINOR PLANETS SECTION OF THE ASSOCIATION OF LUNAR AND PLANETARY OBSERVERS

VOLUME 46, NUMBER 4, A.D. 2019 OCTOBER-DECEMBER 373.

H-G PARAMETERS FOR (37652) 1994 JS1

Lorenzo Franco
Balzaretto Observatory (A81), Rome, ITALY
lor_franco@libero.it

Alessandro Marchini
Astronomical Observatory, DSFTA - University of Siena (K54)
Via Roma 56, 53100 - Siena, ITALY

Riccardo Papini, Massimo Banfi, Fabio Salvaggio
Wild Boar Remote Observatory (K49)
San Casciano in Val di Pesa (FI), ITALY

Alfonso Noschese, Antonio Vecchione, Antonio Catapano
AstroCampania Associazione, Naples, ITALY

(Received: 2019 July 11)

For the asteroid (37652) 1994 JS1 the absolute (R band) magnitude and slope parameter was determined from the photometric data: H_R = 14.47 ± 0.02 mag, G = 0.25 ± 0.04. The slope parameter value is consistent with a medium albedo asteroid.

Photometric data, acquired independently from the authors, for the asteroid (37652) 1994 JS1 (Marchini et al., 2019; Noschese et al., 2019) was used for the H-G parameters determination using the H-G calculator function implemented in *MPO Canopus*.

For each measured lightcurve, we determined the half peak to peak R magnitude, using a 2nd order Fourier fit model (Buchheim, 2010). We found an absolute magnitude in R band, H_R = 14.47 ± 0.02 mag and a slope parameter G = 0.25 ± 0.04, that is compatible with a medium albedo asteroid (Lagerkvist et al. 1990; Shevchenko et al. 1998). The H value in V band was derived adding a color index V-R = 0.45 to H_R, obtaining H = 14.92 ± 0.05 mag, somewhat fainter compared to published values by Veres et al. (2015; 14.45 mag) and by Nugent et al. (2016; 14.59 mag).

References

Buchheim, R.K. (2010). "Methods and Lessons Learned Determining the H-G Parameters of Asteroid Phase Curves." *Society for Astronomical Sciences Annual Symposium*, **29**, 101-115

DSFTA (2019), Dipartimento di Scienze Fisiche, della Terra e dell'Ambiente – Astronomical Observatory. *https://www.dsfta.unisi.it/en/research/labs-eng/astronomical-observatory*

Lagerkvist, C.-I.; Magnusson, P. (1990). "Analysis of asteroid lightcurves. II - Phase curves in a generalized HG-system." Astronomy and Astrophysics Supplement Series, **86**, 119-165.

Marchini, A.; Papini, R.; Banfi, M.; Salvaggio, F.; Franco, L. (2019). "Rotation period determination for the asteroids 3329 Golay and (37652) 1994 JS1." *Minor Planet Bulletin* **46**, 338-339.

Noschese, A.; Vecchione, A.; Catapano, A. (2019). "Lightcurve analysis and rotation period for (37652) 1994 JS1." *Minor Planet Bulletin* **46**, 331-331.

Nugent, C. R.; Mainzer, A.; Baurer, J.; Cutri, R.M.; et al. (2016). "NEOWISE Reactivation Mission Year Two: Asteroid Diameters and Albedos." *Astron. J.* **152**, A63.

Shevchenko, V. G.; Lupishko D. F. (1998). "Optical properties of Asteroids from Photometric Data." *Solar System Research* **32**, 220-232.

Veres, P.; Jedicke, R.; Fitzsimmons, A.; Denneau, L.; et al. (2015). "Absolute magnitudes and slope parameters for 250,000 asteroids observed by Pan-STARRS PS1 - Preliminary results." *Icarus* **261**, 34-47.

Warner, B.D. (2016). MPO Software, MPO Canopus v10.7.7.0. Bdw Publishing. *http://minorplanetobserver.com*

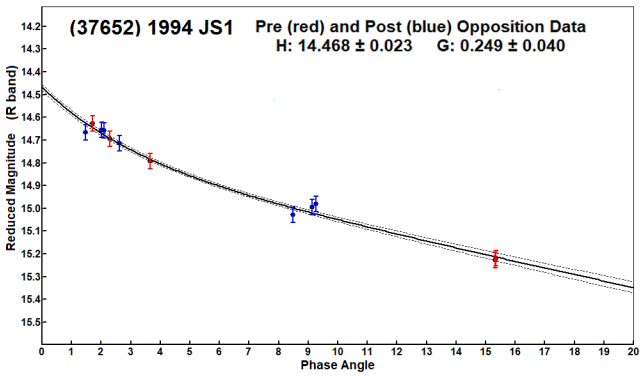

ROTATION PERIOD FOR 1711 SANDRINE

Stephen C. Percy
The Studios Observatory (Z52)
31 Ipswich Gardens, Grantham, NG31 8SE, U.K.
mail@opussoftware.co.uk

(Received: 2019 May 5)

CCD photometric observations of the outer main-belt asteroid 1711 Sandrine were performed over eight nights between 2019 February 23 and March 31. A synodic rotation period of 33.02 ± 0.02 h and lightcurve amplitude of 0.19 ± 0.05 mag were found.

The minor planet 1711 Sandrine (=1909 DJ = 1935 BB = 1938 SF1 = 1943 QE = 1949 WF = 1951 CX1 = 1952 HG1 = 1956 AH = 1956 AW = 1956 DC = 1959 TR = 1959 UH) is a member of the Eos family. It was discovered at Uccle on 1935 January 29 by E. Delporte and named in honor of a grand-niece of Uccle astronomer G. Roland. [Ref: Minor Planet Circ. 6832]. A search of the asteroid lightcurve database (LCDB, Warner *et al*, 2018) indicates no previous reported rotation period for this asteroid.

All observations were performed at the Studios Observatory, Grantham, U.K. (Z52) using a Meade 0.36-m LX200 ACF OTA operating at *f*/7 and a Takahashi FS-102 10-cm *f*/8 refractor as a guide scope. The OTAs are mounted on a Paramount MEII robotic mount. The 0.35-m OTA is equipped with Moonlite CSL 2.5-inch large format motorized focuser, Astro Physics AP CCDT67 focal reducer, and a QSI 683 cooled CCD camera (binned 2x2). An Astrodon Clear (UV blocking only) filter was used for all observations. All guiding was carried out using a ZWO ASI1600M-Cooled CMOS camera binned 2x2. The main imaging QSI 683 CCD is based on a Kodak KAF-8300 sensor with square 3326x2504x5.4 µm pixels. The image scale after 2x2 binning was 0.88 arcsecs/pixel.

TheSkyX Professional software (Software Bisque) was used for all telescope, focuser, camera control, and guiding. This software was also later used to calibrate all science images using bias, dark, dark-for-flat, and flat-field frames. All flat-field images were taken at the end of the observing sessions using a wall-mounted whiteboard illuminated by an A4-size electroluminescent (EL) panel. A recent library of bias, dark and dark-for-flat frames was used in the calibration process, no scaling of dark frames was necessary.

All data processing of the calibrated images and subsequent period analysis was performed using *MPO Canopus* (BDW Publishing 2018). Differential photometry measurements were performed using the Comp Star Selector (CSS) and Star-B-Gone procedures of *MPO Canopus*. The asteroid and up to five solar-like stars were used for all photometric comparisons. The KAF-8300 sensor has a peak spectral response in the green visual band so V band magnitudes and V-R colour indexes were used throughout the data processing. Even though the target declination remained below +20 deg, which favored the APASS catalog (Henden et al. 2009), the sparse star field surrounding the target required the MPOSC3 catalogue to be used for all plate solving (auto-match) and photometric reductions. The asteroid's magnitude ranged from V = 15.5-16.3 during the observing period. Period analysis used the Fourier analysis algorithm (FALC) developed by Alan Harris (Harris *et al.* 1989).

CCD photometric observations were performed over eight nights between 2019 February 23 and 2019 March 31. A total of 53 hours 48 minutes of observation resulted in 698 data points for analysis. All likely periods from 1 hour onwards were examined. The rotation period was found to be 33.02 ± 0.02 h with amplitude of 0.19 ± 0.05 mag.

The observing schedule is summarized in Table I. Table II provides an overview of the results. Individual raw lightcurves are shown for each observing run along with a period spectrum and final phased plot. All new data were deposited in the ALCDEF database.

2019 mm/dd	Dur	Pts	Exp	Phase	L_{PAB}	B_{PAB}
02/23	1:28	21	180	4.51	142.6	2.4
02/24	9:36	149	240	4.94	142.6	2.4
02/25	9:40	126	240	5.29	142.6	2.5
02/26	9:45	115	240	5.65	142.6	2.5
02/27	9:10	123	240	6.00	142.6	2.6
03/28	6:37	83	240	14.26	143.2	3.5
03/29	6:12	67	240	14.46	143.3	3.5
03/31	1:20	14	240	14.83	143.4	3.6

Table I. Observing schedule for 1711 Sandrine. Dur is duration of session (h:mm). Pts is the number of data points. Exp is the exposure in seconds. The phase angle and phase angle bisector (Harris et al., 1984) values are for mid-session.

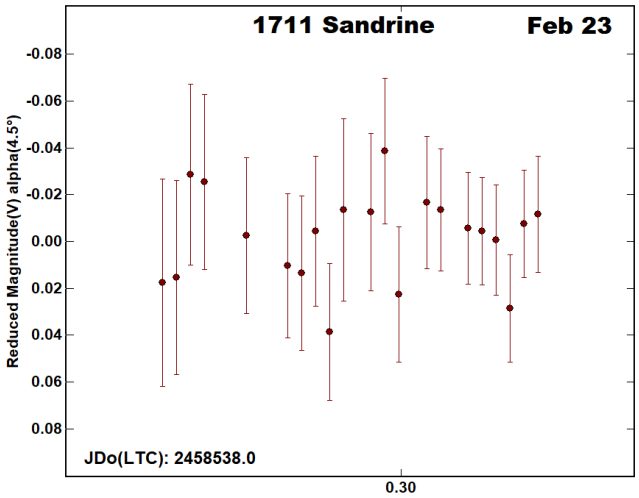

Number	Name	2019 mm/dd	Phase	L_{PAB}	B_{PAB}	Period(h)	P.E.	Amp	A.E.	Grp
1711	Sandrine	02/23-03/31	4.51,14.83	143	3	33.02	0.02	0.19	0.02	MB-O

Table II. Observing circumstances and results. Pts is the number of data points. The phase angle is given for the first and last date. L_{PAB} and B_{PAB} are the approximate phase angle bisector longitude and latitude at mid-date range (see Harris *et al.*, 1984). Grp is the asteroid family/group (Warner *et al.*, 2009). MB-O: Outer main-belt.

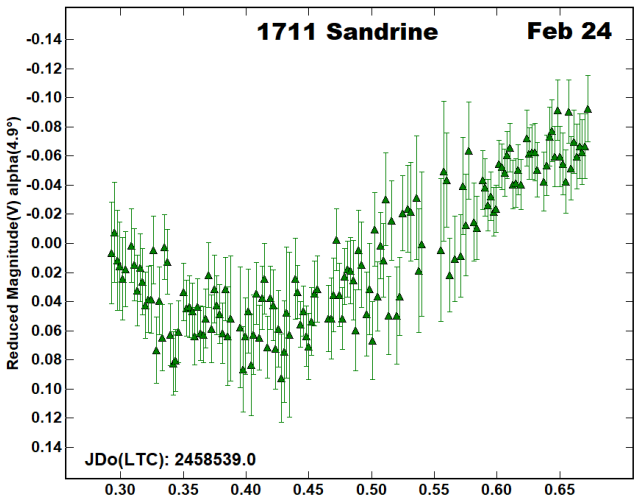
1711 Sandrine
Feb 24
Reduced Magnitude(V) alpha(4.9°)
JDo(LTC): 2458539.0

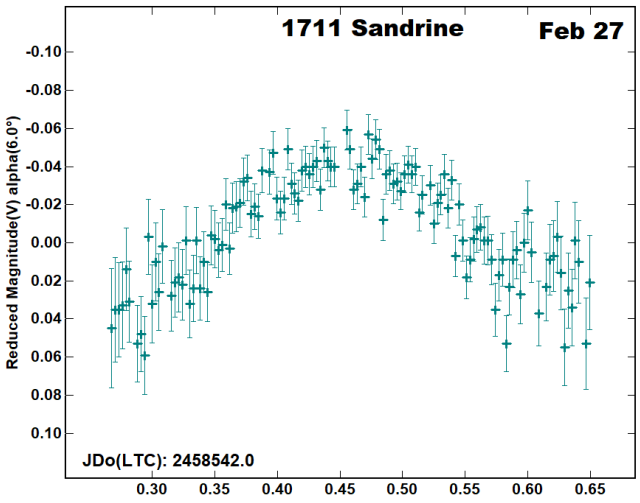
1711 Sandrine
Feb 27
Reduced Magnitude(V) alpha(6.0°)
JDo(LTC): 2458542.0

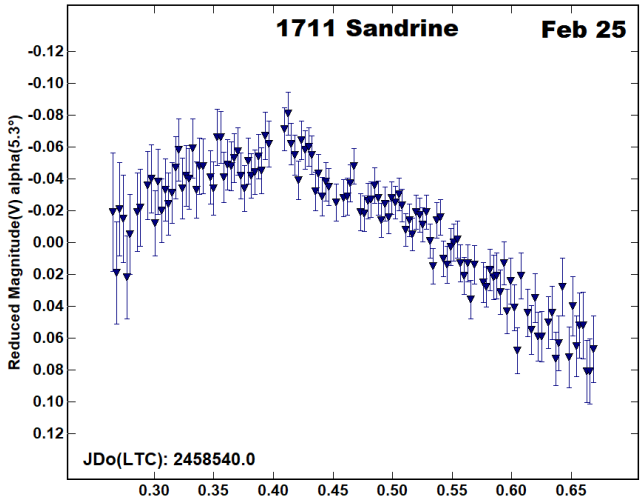
1711 Sandrine
Feb 25
Reduced Magnitude(V) alpha(5.3°)
JDo(LTC): 2458540.0

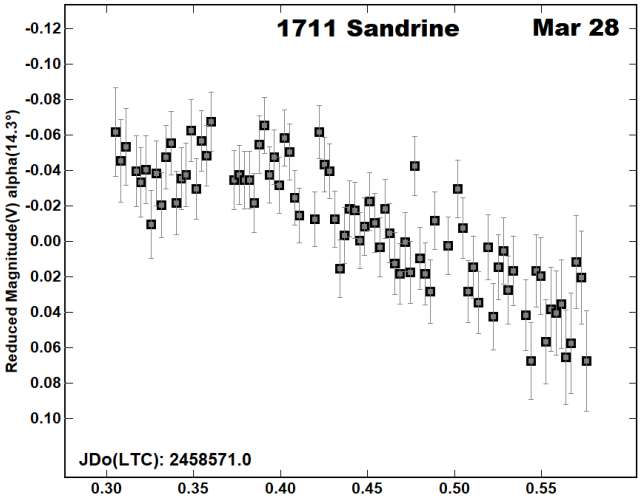
1711 Sandrine
Mar 28
Reduced Magnitude(V) alpha(14.3°)
JDo(LTC): 2458571.0

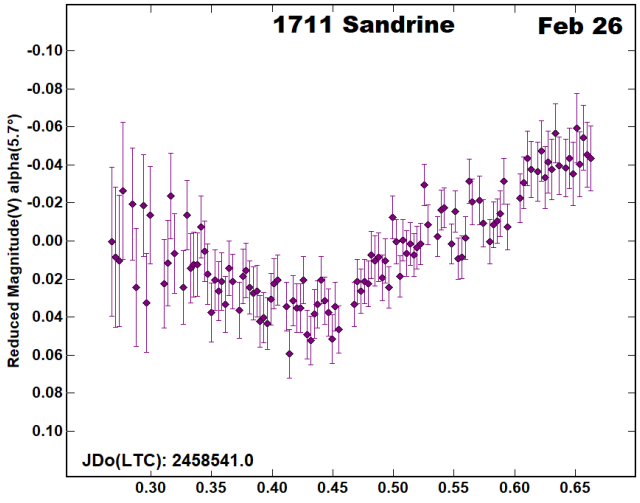
1711 Sandrine
Feb 26
Reduced Magnitude(V) alpha(5.7°)
JDo(LTC): 2458541.0

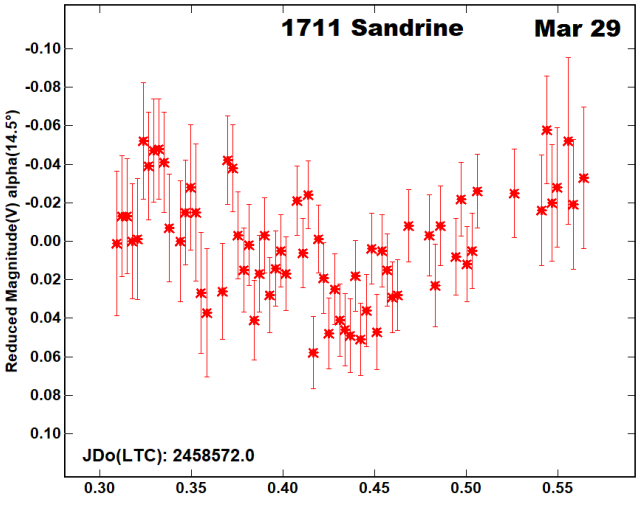
1711 Sandrine
Mar 29
Reduced Magnitude(V) alpha(14.5°)
JDo(LTC): 2458572.0

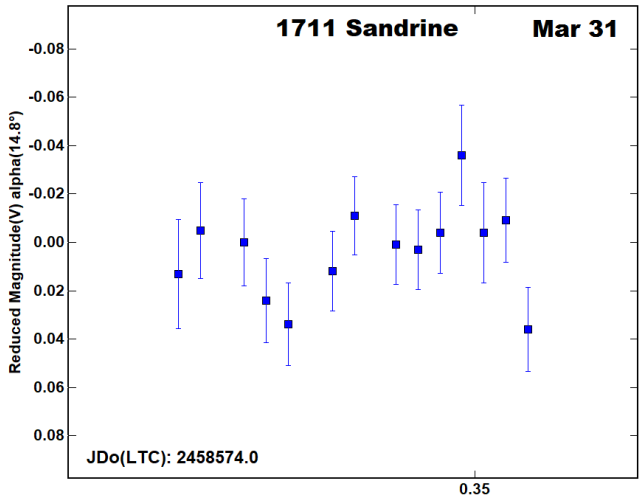

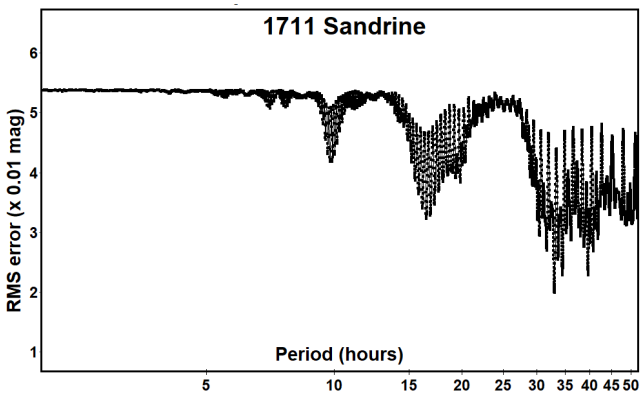

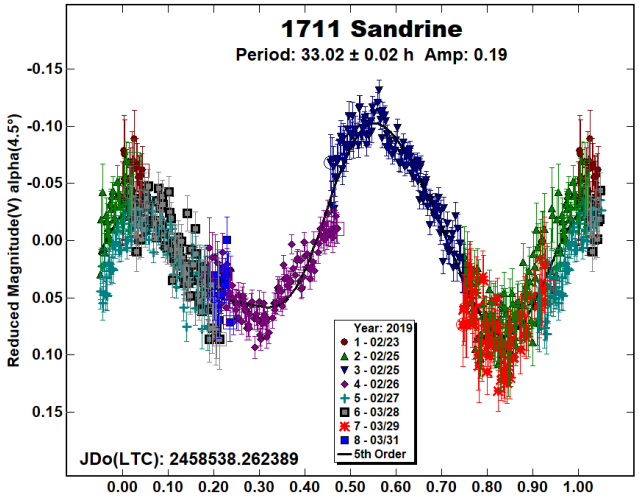

Acknowledgements

This research has made use of data and services provided by the International Astronomical Union's Minor Planet Center.

https://www.minorplanetcenter.net/iau/mpc.html

This research was made possible in part based on data from the MPCOSC3-2MASS catalog (a product of the Two Micron All Sky Survey), UCAC4 (the fourth U.S. Naval Observatory CCD Astrograph Catalog), and the AAVSO Photometric All-Sky Survey (APASS), funded by the Robert Martin Ayers Sciences Fund.

The author would like to express his gratitude to Brian D. Warner for his *MPO Canopus* software and support, along with the 2nd edition of his book *A Practical Guide to Lightcurve Photometry and Analysis*. Both have been invaluable in this research.

References

Minor Planet Circulars (MPCs) are published by the International Astronomical Union's Minor Planet Center. All Minor Planet Circulars are available from the Minor Planet Centre's MPC/MPO/MPS Archive. *https://www.minorplanetcenter.net/iau/ECS/MPCArchive/MPCArchive_TBL.html*

Henden, A.A.; Terrell, D.; Levine, S.E.; Templeton, M.; Smith,T.C.; Welch, D.L. (2009). "The AAVSO Photometric All-Sky Survey (APASS)." *http://www.aavso.org/apass*

Harris, A.W.; Young, J.W.; Scaltriti, F.; Zappala, V. (1984). "Lightcurves and phase relations of the asteroids 82 Alkmene and 444 Gyptis." *Icarus* **57**, 251-258.

Harris, A.W.; Young, J.W.; Bowel, E.; Martin, L.J.; Millis, R.L.; Poutanen, M.; Scaltriti, F.; Zappala, V.; Schober, H.J.; Debehogne, H.; Zeigler, K.W. (1989). "Photoelectric observations of asteroids 3, 24, 60, 261, and 863." *Icarus* **77**, 171-186.

Software Bisque (2019). *TheSkyX Professional* software. *http://www.bisque.com/sc/pages/TheSkyX-Professional-Edition.aspx*

Warner, B.D.; Harris, A.W.; Pravec, P. (2009). "The Asteroid Lightcurve Database." *Icarus* **202**, 134-146. Updated 2018 July. *http://www.minorplanet.info/lightcurvedatabase.html*

Warner, B.D. (2018). Asteroid Lightcurve Photometry Database (ALCDEF) website. *http://alcdef.org*

Warner, B.D. (2018). *MPO Canopus* v10.7.11.3. BDW Publishing. *http://www.minorplanetobserver.com/MPOSoftware/MPOCanopus.htm*

Warner, B.D. (2006). *A Practical Guide to Lightcurve Photometry and Analysis (2nd edition)*. Springer, New York.

THE ROTATION PERIOD OF 5351 DIDEROT

Luca Izzo, Sebastiano de Franciscis, Francisco Javier Rollin Sáenz de Rodrigáñez, Alvaro Castro Romero, Andrés Marín García, María Sánchez Martínez, Andrea García Roa, José Antonio Gallego Rodríguez, Paula Fabiola Freundlinger Lopez, Jaime Gómez Muñoz
IAA-CSIC, Granada, Spain
(izzo@iaa.es)

Alfonso Noschese, Maurizio Mollica, Antonio Vecchione
AstroCampania Associazione, Naples, Italy

(Received: 2019 May 9)

We present an analysis of the rotation period of 5351 Diderot. We found a period of P = 9.99 ± 0.01 h by using data collected on five nights of observations between April 19th and April 24th. Our result independently confirms the recent finding by Marchini et al. (2019) who found a period of P = 9.984 ± 0.003 h.

5351 Diderot is a main-belt asteroid with a diameter of about 3.7 km, a major semi-axis of a = 2.426 AU, an eccentricity of e = 0.14, and an inclination of i = 5.60 deg. Its rotation period was unknown until recent years: its only measurement was completed in the last months, when Marchini et al. (2019) found P = 9.984 ± 0.003.

We have observed Diderot from the Osservatorio Astronomico Salvatore di Giacomo (OASDG), Agerola (MPC code L07) on five consecutive nights from April 19th to April 24th 2018, see Table 1. Observations were conducted with a 0.50-m Ritchey–Chrétien telescope operating at f/8. The telescope is equipped with an FLI-PL4240 CCD camera with an array of 2048x2048 pixels of 13.5 micron size, and with a *Rc* filter. All the images have been astrometrically calibrated and corrected for the Dark frame and normalized by a Flat Field image. A total of 384 light curve data points have been collected on the five nights, with an exposure times of 180 s for each single data point.

This observational campaign was part of the PIIISA project (*http://www.piiisa.es*) sponsored by the Spanish MINECO, the Junta de Andalucia, the Universidad de Granada and the CSIC. The project consists in initiating young students to Astronomy through a direct contact with people working in an astronomical research and through a direct contact with the data analysis. Three student groups have been established and each analyzed independently the photometric data of 5351 Diderot, in search of its rotation period. The data analysis was coordinated by two astronomers (L. Izzo and S. de Franciscis, both at the IAA/CSIC) with the support of the staff of the OASDG. The software CANOPUS was used for the photometry (using up to five stars with near-solar colors and the 'comp-star selector' tool), and the search for the period using the FALC Fourier analysis algorithm. Finally, from each single power spectrum obtained by each group, we have derived a final average power spectrum and consequently the best measurement of the period through the minimization of the RMS value. All the three groups found the same rotation period of P = 9.99 ± 0.01 h, then it was trivial to conclude that the best-fit rotation period of 5351 Diderot is P = 9.99 ± 0.01 h, see Fig. 1. Our result confirms the recent finding of Marchini et al. (2019) for the rotation period of 5351 Diderot.

References

Marchini, A., Papini, R., Banfi, M., Salvaggio, F., (2019). "Rotation period determination for 5351 Diderot and 7230 Lutz" *MPB* 46, 90-91.

Warner, B., (2016) MPO Software, MPO Canopus version 10.7.7.0 Bdw Publishing. *http://minorplanetobserver.com*

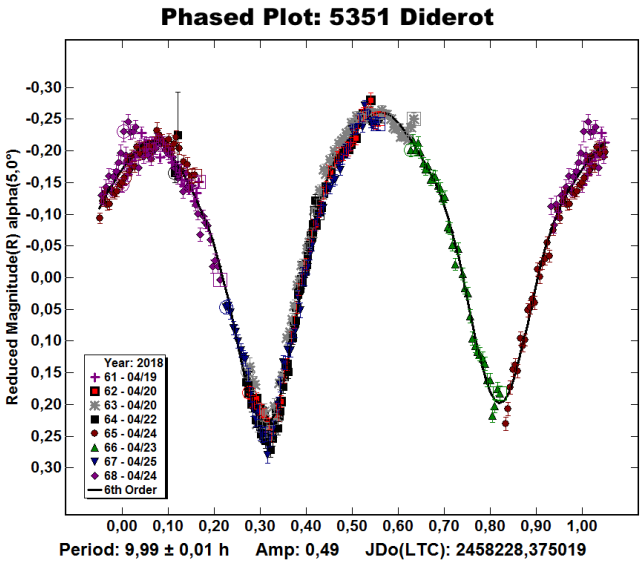

Fig.1 The best period of P = 9.99 ± 0.01 h found in one of the three independent analysis mentioned in this work

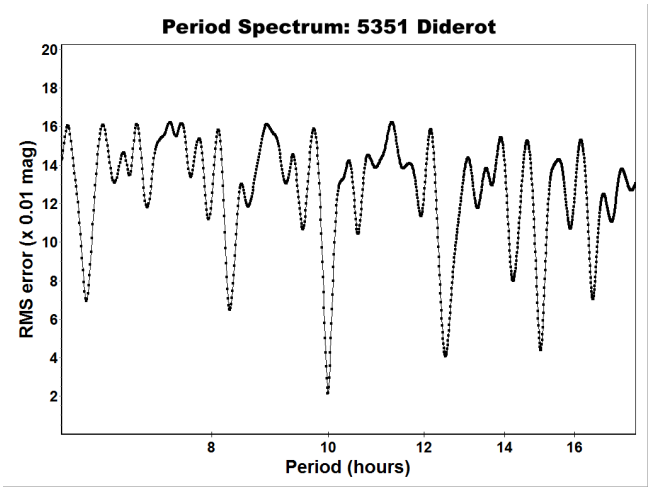

Fig.2 The distribution of the RMS value as function of the Diderot period (in hours) obtained in one of the three independent analysis.

Number	Name	2018 mm/dd	Pts	Phase	L_{PAB}	B_{PAB}	Period(h)	P.E.	Amp
5351	Diderot	04/19-04/24	384	5.00/4.47	213.6	6.9	9.99±0.01	0.01	0.49

Table I. Observing circumstances and results. Pts is the number of data points. The phase angle is given for the first and last date.

A MODEL OF MINOR PLANET NUMBER DISTRIBUTIONS: VISUAL OBSERVATIONS

Andrew Salthouse
560 Heritage Road
Millington NJ 07946 USA
asalthouse@hotmail.com

(Received: 2019 May 8)

In two earlier papers (Salthouse 2019a, 2019b) the author noted two specific patterns of minor planet number distributions within a large set of visual observations. These patterns revealed a strong relationship between the minor planet numbers and the total number of objects observed. The author introduces a probability model to explain this behavior.

The author visually observed over 2900 distinct minor planets, and found stable relationships among the minor planet numbers in the data. These relationships were reported earlier (Salthouse 2019a, 2019b). A probability model is introduced to explain these relationships; it is based entirely on the author's own data. As such, it is unique to his circumstances, but he is sharing it here since other visual observers may find similar patterns.

Let N be the total number of distinct objects observed, Q be the number of minor planets seen with assigned number $n \leq N$, and let p_{25}, p_{50}, and p_{75} be the 25th, 50th (median), and 75th percentile points of the distribution of observed values of n (whether less than or greater than N).

The specific findings were (for a fixed telescope aperture):

- The ratio of Q/N tended to an asymptote at large N
- The ratios p_{25}/N, p_{50}/N, and p_{75}/N also tended to asymptotes at large N

These imply that the distribution of observable minor planet numbers expands in direct proportion to N. As N increases, the values of p_{25}, p_{50}, and p_{75} increase proportionally, implying that the entire distribution scales, with the possible exception of the tails; that is, both the median and width increase proportionally.

The percentile distribution is an outcome of the probability distribution of observing these objects. The probability of observing a given minor planet depends to a large extent on its visual magnitude. The shape of the distribution of observable minor planet numbers for a given value of N has implications for the probability distribution, and therefore for the magnitude distribution.

Model Rationale

In an effort to explain the data, the author developed a probability model that replicates much of this effect. He used a deductive approach building up from the raw data to see if the observed patterns can be replicated, rather than an inductive approach working backward from the patterns. This probability function is unique to each observer's equipment and circumstances. Such a model is necessarily heuristic since there is no fundamental physical principle that ties observability to minor planet number.

In the two earlier papers (Salthouse 2019a, 2019b) the author showed the results of his observations in bins of 100 each for the variable N. However, in the approach used here, the author proceeds by using bins of 100 each for the variable n, not N. The distinction is important; whereas there are only 29 bins for N, there are a much larger number of bins for n, since n can reach very large numbers. Binning "n" rather than "N" simplifies the analysis. The bin size of 100 was selected as a compromise between smaller bins (with more noise in the parameter estimates) and larger bins (too few data points for good model fits).

There will be 100 distinct objects in each bin. We do not need to model the observability of each individual minor planet; we only need to model the average observability of the entire bin. We label the bins using k = 1, 2, 3, etc.

The values of k can run up to several thousand, but the author cut off the analysis at k = 100 (n = 10,000) since the data above that threshold was very sparse and represented only 6% of total observations. As one continues to observe and add more objects to the set of observed minor planets, each bin will gradually fill up. As each bin fills, there are fewer objects available to observe in that bin. Since the lower numbered objects tend to be brighter, the lowest numbered bins will fill the fastest, so that subsequent objects must come from higher bins. This drives the shape of the distribution higher as more objects are added to the total. Thus the median value of n necessarily increases as more objects are added to the total. The key is to understand why this increase is linear. In this paper, the goal is to derive the probability distribution of each bin and show that this leads to a linear relationship at the aggregate level, consistent with the two sets of findings described above.

Development of Bin Parameters

The data strongly suggested two primary effects. First, many of the bins contain minor planets that are beyond the reach of the author's equipment; each bin can be characterized by a bin size that is generally less than 100. The parameter $S(k) \leq 1$ represents the proportion of the k^{th} bin that is observable in principle, so that the effective bin size is 100S(k). Second, the probability of observing an object within a given bin is lower for higher numbered bins than for lower numbered bins, on average. The parameter P(k) represents the relative probability of observing an object in bin k, with bin k = 1 normalized to unity.

Using his raw data, the author estimated S(k) and P(k) for the first 30 bins. Next, using statistical modeling and experimenting with different forms, he developed nonlinear models that reproduced these estimates with minimal variance. The parameters in these models are unique to the author's telescope and observing site. Other observers would likely find different parameter values, but the overall shape of the models should be similar. The author found the following closed form models:

$$S(k) = 1/(1+\mu(k^{\beta}-1)) \quad (1)$$

where $\mu = 0.000077$ and $\beta = 3.045$

$$P(k) = k^{-\alpha} \quad (2)$$

where $\alpha = 1.380$

These are purely phenomenological forms. Figures 1 and 2 show the data and the fitted models for S(k) and P(k).

Recursive Relation and Numerical Integration

Once the observable bin size and relative probability of each bin has been estimated, the next step is to determine the rate at which

the bins will fill up. The author developed a recursive difference formula that expresses this idea. On any given observational attempt, three factors will come into play:

- The available size of each bin
- The relative probability of observing objects in each bin
- The proportion of the bin that is not yet filled by previous observations

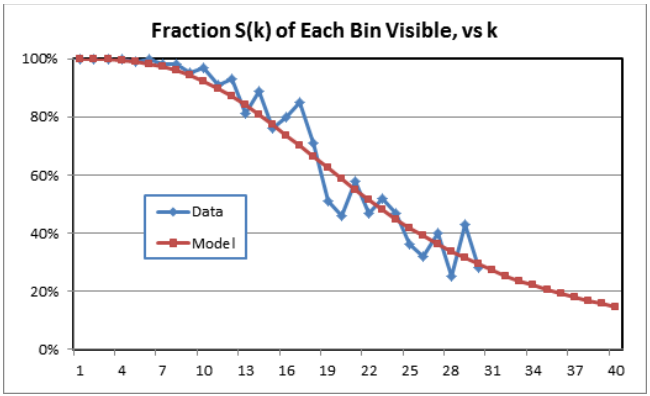

Figure 1. Fraction of each bin potentially visible in author's telescope vs k (x-axis)

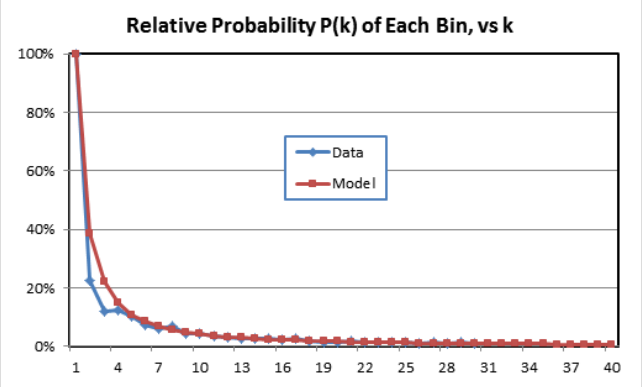

Figure 2. Relative probability of observing objects in each bin in author's telescope vs k (x-axis)

The first two factors are expressed by the Eqs. (1) and (2). The third factor will be a function of both k (the bin number) and N (the number of observations); we use the notation F(k,N) to represent the fraction of the bin k that has been filled after N observations. N represents total observations across all bins. Note that N represents successful observations, because unsuccessful attempts at observation have no impact on the functions defined below. Since P(k) is a relative probability, the probability distribution across all bins needs to be renormalized to 1. On the $(N+1)^{th}$ observational attempt, a fraction F(k,N) of bin k will be filled, leaving [1 – F(k,N)] available for observing. Thus the relative probability of observing an object in bin k will be the size of the bin S(k) multiplied by the relative probability of objects in that bin P(k), multiplied by the proportion of the bin not yet filled [1-F(k,N)]; this represents the incremental probability of finding a minor planet in bin k. We call this incremental factor I(k,N):

$$I(k,N) = S(k)P(k)[1-F(k,N)] \quad (3)$$

The normalization factor is

$$T(N) = \Sigma_k\, I(k,N) \quad (4)$$

Thus, the actual probability $\pi(k,N)$ of observing an incremental object in the k^{th} bin on the $(N+1)^{th}$ observation is

$$\pi(k,N) = I(k,N)/T(N) \quad (5)$$

This will sum to 1 across all bins. The rate $\Delta F(k,N)$ at which bin k will fill up is then given by

$$\Delta F(k,N) = \pi\,(k,N)\,/(100S(k)) \quad (6)$$

The denominator is the effective bin size. This leads to a recursive relationship that can be solved by iteration:

$$F(k,N+1) = F(k,N) + \Delta F(k,N) \quad (7)$$

The boundary condition is F(k,0) = 0 for each k. The author used numerical integration, starting at N = 0 and integrating up to N = 2500 in 500 steps of 5; the integration included the full range of k from 1 to 100. At each step of the process, he solved for I(k,N), T(N), $\pi(k,N)$, $\Delta F(k,N)$, F(k,N), Q(N), and the mean and median value of k. The mean and median value of n can be derived from that of k.

Because this is a probability model, it produces non-integer solutions to the number of objects observed in each bin. This is perfectly acceptable, as we are dealing with expected values.

Model Results

The results of the numerical integration were the mean(n), the 25^{th}, 50^{th}, and 75^{th} percentiles of the distribution of n, and Q. Each of these was plotted versus N. Figures 3 and 4 show the model output for mean(n) and median(n) versus N in steps of 5. The relationships were very nearly linear with $R^2 = 0.995$ for the mean and $R^2 = 0.999$ for the median over the range N = 0 to 2500.

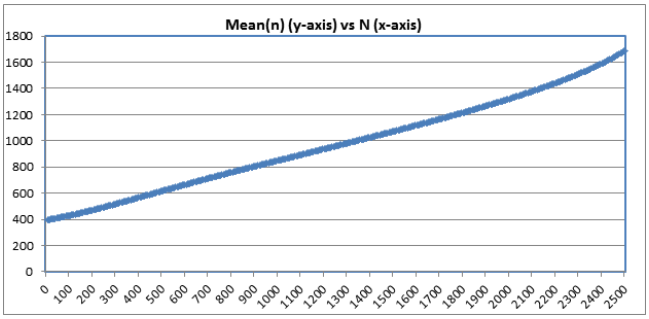

Figure 3. Model output of mean value of n versus N, in steps of 5 up to 2500 ($R^2 = 0.995$)

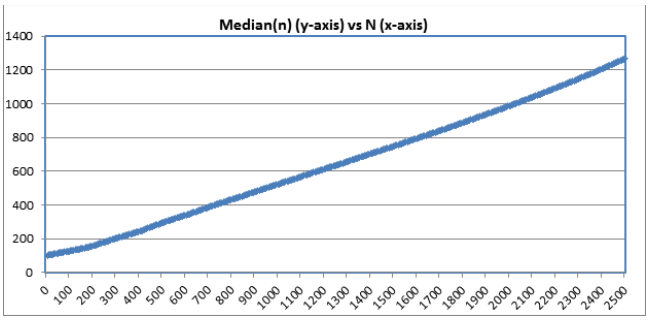

Figure 4. Model output of median value of n versus N, in steps of 5 up to 2500 ($R^2 = 0.999$)

The model also produced linear results for the 25th and 75th percentile of n. The 25th, 50th, and 75th percentiles of the distribution each had $R^2 = 1.000$ in the smaller range of N = 400 to 2000. This is also true for many other points on the percentile distribution.

However, the model has its limits. First, the functions S(k) and P(k) are extrapolated from the first 30 bins to 100 bins, so the formulae (1) and (2) might be an inadequate representation at larger values of k. Second, due to the large bin size of 100, it does a poor job of matching the observations for low N (below about 300-400). The author also encountered some computational issues at N beyond 2500, as the values of F(k,N) asymptotically approached 1 for many of the bins. Nevertheless it is quite remarkable that a model with highly nonlinear input assumptions leads to highly linear outputs as a result of the numerical integration.

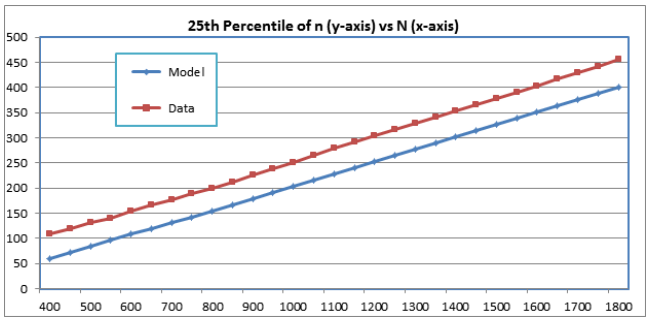

Figure 5. Result of the model output of 25th percentile of n versus observational data

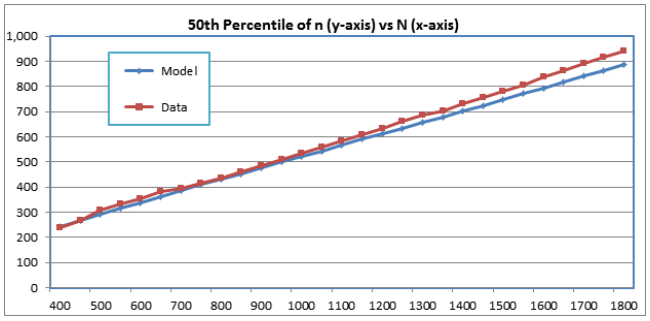

Figure 6. Result of the model output of 50th percentile of n versus observational data

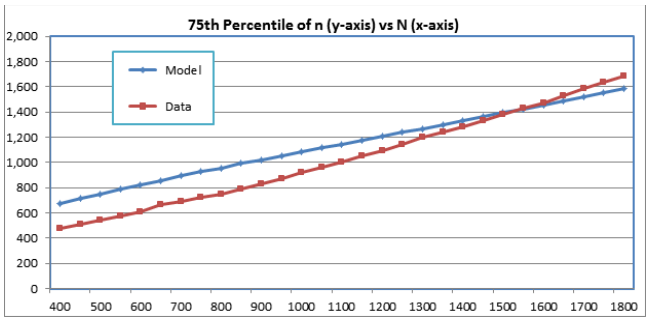

Figure 7. Result of the model output of 75th percentile of n versus observational data

Note that the mean curves upward slightly at higher N, as it is impacted more by higher numbered bins than is the case for the median. Figures 5 through 7 show the 25th, 50th, and 75th percentile points of the model distribution compared to the author's data from N = 400 to 1800 in steps of 50. From these graphs it is clear that the model accurately reproduces the 50th percentile of the observed distribution of n, but understates the 25th and mostly overstates the 75th percentile distribution of the observed values of n. Thus, although the model matches the center of the distribution, it tends to overstate the true width of the distribution.

Nevertheless, the author believes that this probability model captures the essential dynamics of the observational results rather well.

Finally, the author compared the model output of the variable Q to the observational data, as shown in Figure 8. Here the model slightly understates the data for Q.

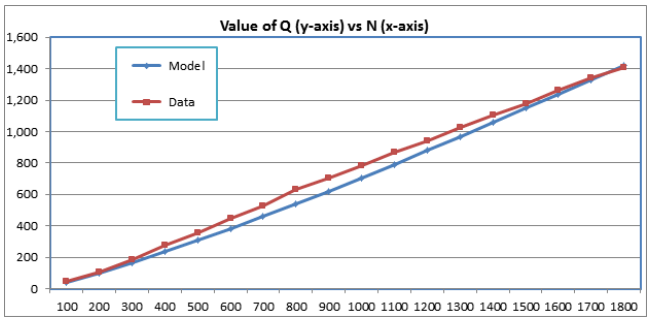

Figure 8. Result of the model output of Q versus observational data

The author performed a sensitivity analysis on some of the model parameters. He found that a slightly higher value of α in formula (2) improved the match between model and data in figures 7 and 8, but worsened the fit in figure 2, while having little effect on figures 5 and 6. The higher percentage points of the distribution were more sensitive to changes in α than were the lower points of the distribution. The author found that P(k) was the most difficult function to estimate from the raw data, so it is entirely possible that he has underestimated the value of α. However, the author prefers working forward from the data, rather than backward from the desired answer.

The model is based entirely on the author's visual observations collected over a period of many years. With somewhat different model parameters, it may also reproduce the key effects of other visual observers. The overall structure of this model, with suitable modifications, might even apply to the results from nonvisual observations.

Acknowledgements

The author thanks Mr. Brian Warner for providing the *Minor Planet Observer* (Warner, 2019) suite of products and services, without which this work would have been impossible.

References

Salthouse, A. (2019a). "Pattern of Minor Planet Numbers vs Cumulative Number Observed." *Minor Planet Bulletin* **46**, 118.

Salthouse, A. (2019b). "Distribution of Minor Planet Numbers vs Cumulative Number Observed.",*Minor Planet Bulletin* **46**, 235.

Warner, B. (2019). Minor Planet Info website. *http://www.MinorPlanet.info*

SIX ASTEROIDS FROM THE 2018 MEXICAN ASTEROID PHOTOMETRY CAMPAIGN

M.E. Contreras, L. Olguín, P. Loera-González, J.C. Saucedo
Departamento de Investigación en Física
Universidad de Sonora
Hermosillo, Sonora, México
contreras.maru@gmail.com

W.J. Schuster
Instituto de Astronomía-Ensenada
Universidad Nacional Autónoma de México
Ensenada, B.C., México

P. Valdés-Sada
Universidad de Monterrey
Av. I. Morones Prieto 4500 Pte.
San Pedro Garza García, N.L., 66238 México

Juan Segura-Sosa
Facultad de Ciencias Físico-Matemáticas
Universidad Autónoma de Coahuila
Saltillo, Coahuila, México

(Received: 2019 May 15)

We present photometric optical lightcurves and derived rotation periods for a sample of six asteroids: 767 Bondia (8.3402 ± 0.0007 h), 1229 Tilia (7.0353 ± 0.0005 h), 1475 Yalta (28.29 ± 0.01 h), 4807 Noboru (4.0415 ± 0.0005 h), 6582 Flagsymphony (70.288 ± 0.024 h), and 7305 Ossakajusto (15.3838 ± 0.0003 h). These observations were carried out at the Observatorio Astronómico Nacional at Sierra San Pedro Mártir (OAN-SPM), Baja California, México and at the Carl Sagan Observatory (OCS) of the Universidad de Sonora, México.

As part of the Mexican Asteroid Photometry Campaign (CMFA in Spanish), we obtained photometric data during the second half of 2018 for six main-belt asteroids: 767 Bondia, 1229 Tilia, 1475 Yalta, 4807 Noboru, 6582 Flagsymphony and 7305 Ossakajusto. Our observations were carried out at two observatories: the Observatorio Astronómico Nacional in San Pedro Mártir (OAN-SPM), Baja California, México, and the Carl Sagan Observatory (OCS) of the Universidad de Sonora, México.

Observations at the OAN-SPM were carried out with the 0.84-m *f*/15 Ritchey-Chretien telescope and a 2048×2048 pix E2V-4240 cryogenic CCD, operating at a temperature of −110 °C. Images were generally binned 2×2 with a final field of view of 9×9 arcmin. The equipment used at the OCS was a 3056×3056×12 µm Apogee Alta F9000 CCD camera mounted on a Meade LX-200GPS 0.41-m *f*/10 telescope. Images were trimmed to a subframe of 2000×2000 pixels and were generally 3×3 binned yielding a final plate scale of 1.8 arcsec/pix and an effective 20×20 arcmin FOV. Data reduction was made with *IRAF* or *MaximDL* following standard procedures to correct for bias, dark current and flat-field effects. Photometry and lightcurve analysis were made using *MPO Canopus (*V.9.5.0.14*,* Warner*,* 2017) software package, which allowed us to obtain the synodic period for each object.

767 Bondia is a main-belt asteroid. It was discovered in 1913 by J.H. Metcalf (Schmadel, 2003). It has a diameter of 45.3 km, an absolute magnitude H = 10, and an albedo of 0.09 reported by Ali-Lagoa et al. (2016). It has an estimated rotation period of > 60 h, with an approximate 30% error, reported by Szabó et al. (2016). We observed 767 Bondia during on three nights, 2018 October 20, 21, and 22 at the OAN-SPM. Based on these data, we obtained a quite nice lightcurve consisting of 1169 points and determined a period of 8.3402 ± 0.0007 h with an amplitude of 0.27 ± 0.02 mag.

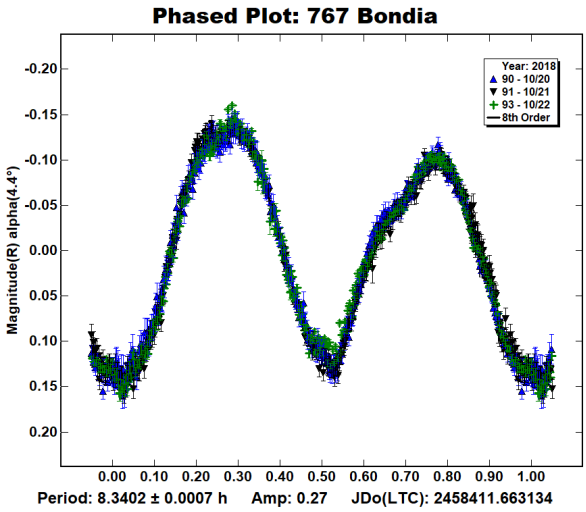

1229 Tilia is an outer main-belt asteroid discovered in 1931 by K. Reinmuth (Schmadel, 2003). It has a reported absolute magnitude of H = 11.3 (Usui et al., 2011; Mainzer et al., 2011; Alí-Lagoa et al., 2013, 2016; Veres et al., 2015; Mainzer et al., 2016) and diameter estimates of 27.57 km (Usui et al., 2011) to 29.1 km (Alí-Lagoa et al., 2016). Its reported albedo values are 0.086 (Usui et al., 2011) and 0.06-0.069 (Mainzer et al., 2011, 2016; Alí-Lagoa et al., 2013, 2016). Noschese et al. (2019a) and Kinglesmith and Lovato (2019a) reported rotation periods of 7.0355 ± 0.0007 h and 7.035 ± 0.001 h, respectively. We observed this object for five nights, 2018 August 18, 19, 20, 21 and 22, at the OAN-SPM. Our derived lightcurve allowed us to estimate a period of 7.0353 ±0.0005 h with a peak-to-peak amplitude of 0.29 ± 0.03 mag, which is in very good agreement with the values mentioned above.

Number	Name	2018 mm/dd	Phase	L_{PAB}	B_{PAB}	Period(h)	P.E.	Amp	A.E.	Grp
767	Bondia	10/20-10/22	4.5,3.7	36	-2	8.3402	0.0007	0.27	0.02	THM
1229	Tilia	08/18-08/22	8.8,7.3	345	1	7.0353	0.0005	0.29	0.03	THM
1475	Yalta	11/26-12/23	5.9,19.4	57	-4	28.29	0.01	0.20	0.04	FLOR
4807	Noboru	12/19-12/30	1.0,6.4	88	1	4.0415	0.0005	0.18	0.03	MB-I
6582	Flagsymphony	10/16-11/11	2.3,12.8	27	-1	70.288	0.024	0.21	0.03	MB-O
7305	Ossakajusto	06/23-09/14	22.0,17.0	318	3	15.3838	0.0003	0.23	0.03	MB-O

Table I. Observing circumstances and results. Pts is the number of data points. The phase angle is given for the first and last date. L_{PAB} and B_{PAB} are the approximate phase angle bisector longitude and latitude at mid-date range (see Harris *et al.*, 1984). Grp is the asteroid family/group (Warner *et al.*, 2009) FLOR:Flora; THM: Themis; MB-I/O: Main-belt inner/outer.

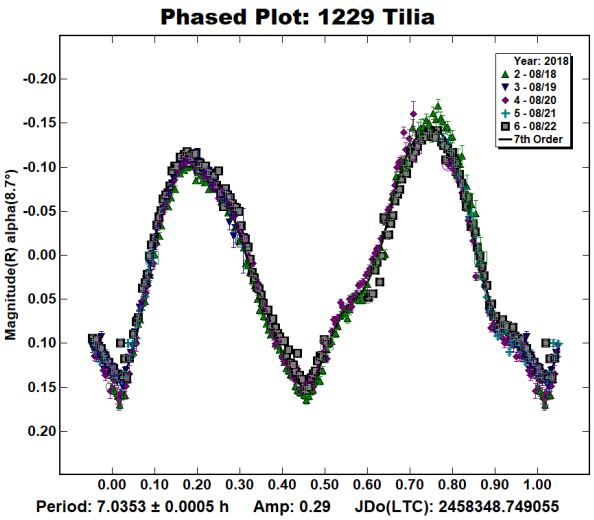

1475 Yalta. This main-belt asteroid was discovered by P.F. Shajn in 1935 (Schmadel, 2003). While a search in the literature did not find a reported diameter value for this object, its absolute magnitude H = 13.1 ± 0.2 is reported by Veres et al. (2015). There are two reported period values: 70.77 ± 0.05 h (Polakis and Skiff, 2019) and 36.62 ± 0.01 h (Noschese and Vecchione, 2019b). We carried out observations during nine nights at the OCS: 2018 November 26, 28, 29 and December 2, 10, 13, 14, 18, and 23, obtaining a total of 735 points. With these data, we derived a rotation period of 28.29 ± 0.01 h with an amplitude of 0.20 ± 0.04 mag. We can see that our period value is closer to the value reported by Noschese and Vecchione (2019b).

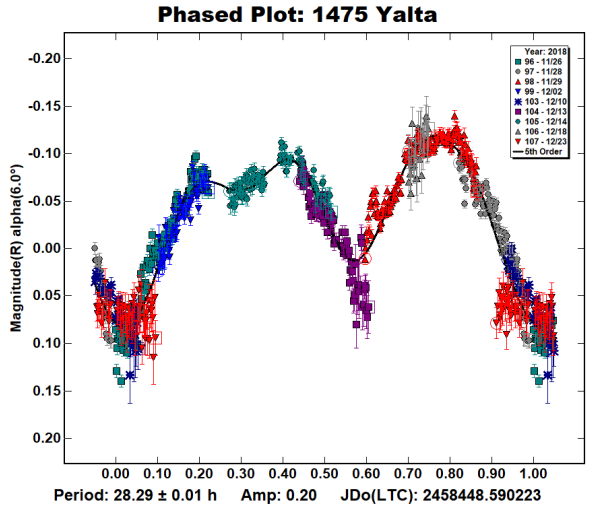

4807 Noboru is a main-belt asteroid. It was discovered in 1991 by T. Kobayashi at the Oizumi Observatory (Schmadel, 2003). It has an absolute magnitude of H = 13.5 (Mainzer et al., 2011) to H = 14.18 (Veres et al., 2015). An albedo of 0.321 ± 0.066 and a diameter of 4.682 ± 0.558 km are reported by Mainzer et al. (2011). Rotation period values are reported by Zeigler et al. (2019, 4.04 ± 0.02 h) and Kinglesmith and Lovato (2019b, 4.044 ± 0.002 h). We observed 4807 Noboru during three nights, 2018 December 19, 29 and 30. With these data we determined a rotation period of 4.0415 ± 0.0005 h with an amplitude of 0.18 ± 0.03 mag, which is consistent with previous values.

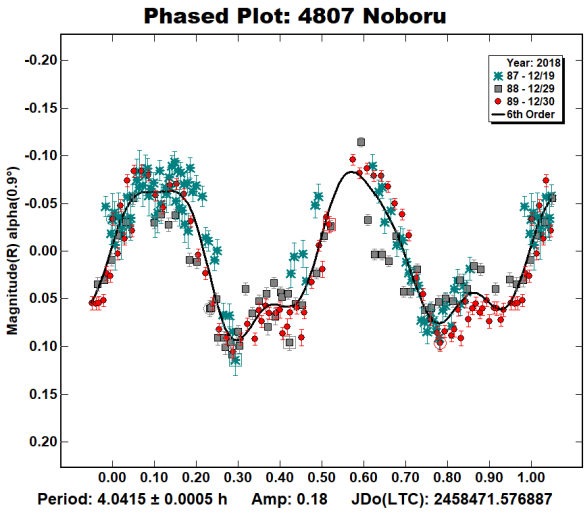

6582 Flagsymphony is a main-belt asteroid discovered by E. Bowell in 1981 (Schmadel, 2003). Its albedo of 0.03 ± 0.02, diameter of 18.42 ± 5.99 km, and absolute magnitude H = 13 were reported by Nugent et al. (2016). A rotation period value of 113.3 ± 0.2 h was reported by Polakis and Skiff (2019). Our data were collected during ten nights: three at the OAN-SPM, 2018 October 17, 18, 19, and seven at the OCS, 2018 October 16, 17, 18, November 6, 7, 8, and 11, giving a total of 1588 points. Based on these data, we estimated a period of 70.288 ± 0.024 h with an amplitude of 0.21 ± 0.03 mag. All our fits to the lightcurve yielded a long period of about 70 h with poor phase coverage. Although our period determination differs from that of Polakis and Skiff (2019), both values suggest that we are dealing with a slow rotator.

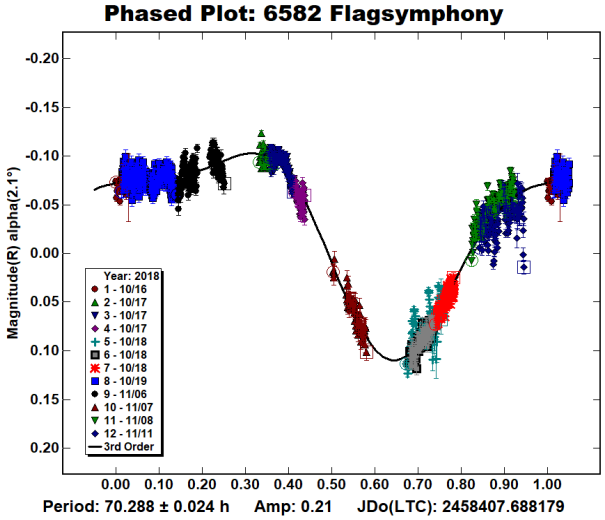

7305 Ossakajusto is a main-belt asteroid discovered in 1994 by K. Endate and K. Watanabe and named after Justo Ossaka (Minor Planet Circ. 33788). Its absolute magnitude is H = 12.1 (JPL Small-Body Database) with an albedo of 0.049 ± 0.004 and a diameter of 23.779 ± 0.999 reported by Masiero et al. (2012). A search of the asteroid lightcurve database (LCDB; Warner et al., 2009) as well the Astronomical Database (ADS), did not find any synodic period value reported. Our photometric data were obtained at the OAN-SPM during five nights, 2018 June 23, and 24, August 19, 21, and 22. Another set of observations were carried out at the OCS during the nights of 2018 September 10, 11

and 14. With a total of 511 points, we obtained a lightcurve and determined a rotation period of 15.3838 ± 0.0003 h with an amplitude of 0.23 ± 0.03 mag.

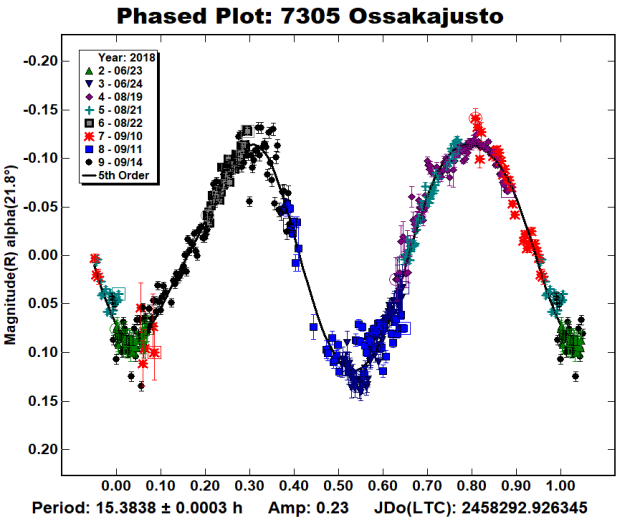

Acknowledgements

MEC acknowledges support from CONACyT Fellowship C-841/2018. LO, PLG and JCS acknowledge UNISON project USO315003483. This work was partially based upon observations acquired at the Observatorio Astronómico Nacional in the Sierra San Pedro Mártir, Baja California, México. We would like to thank the Departamento de Agricultura y Ganadería of the Universidad de Sonora for hosting OCS observatory and for their valuable support. This research has made use of data and/or services provided by the International Astronomical Union's Minor Planet Center, NASA JPL HORIZONS and Small-Body Databases, The Asteroid Light Curve Database (LCDB) and The Collaborative Asteroid Lightcurve Link (CALL). IRAF is distributed by the National Optical Astronomy Observatory, which is operated by the Association of Universities for Research in Astronomy (AURA) under a cooperative agreement with the National Science Foundation.

References

Alí-Lagoa, V.; de León, J.; Licandro, J.; Delbó, M.; Campins, H.; Pinilla-Alonso, N.; Kelley, M.S. (2013). "Physical properties of B-type asteroids from WISE data." *A&A* **574**, A71.

Alí-Lagoa, V.; Licandro, J.; Gil-Hutton, R.; Cañada-Assandri, M.; Delbó, M.; de León, J.; Campins, H.; Pinilla-Alosnso, N.; Kelley, M.S.P.; Hanuš, J. (2016). "Differences between the Pallas collisional family and similarly sized B-type asteroids." *A&A* **591**, A14.

Harris, A.W.; Young, J.W. (1984). "Lightcurves and Phased Relations of the Asteroids 82 Alkmene and 444 Gyptis." *Icarus* **57**, 251-258.

Kinglesmith III, D.A.; Lovato, E.A. (2019a). "Etscorn Asteroids: 2018 July-September." *Minor Planet Bull.* **46**, 81-82.

Kinglesmith III, D.A.; Lovato, E.A. (2019b). "Photometric Lightcurve for 4807 Noboru." *Minor Planet Bull.* **46**, 199.

Mainzer, A.; Grav, T.; Masiero, J.; Hand, E.; Bauer, J.; Tholen, D.; McMillan, R.S.; Spahr, T.; Cutri, R.M.; Wright, E.; Watkins, J.; Mo, W.; Maleszewski, C. (2011). "NEOWISE Study of Spectrophotometrically Classified Asteroids: Preliminary Results." *Ap. J.* **741**, 90.

Mainzer, A.K.; Bauer, J.M.; Cutri, R.M.; Grav, T.; Kramer, E.A.; Masiero, J.R.; Nugent, C.R.; Sonnett, S.M.; Stevenson, R.A.; Wright, E.L. (2016). NEOWISE Diameters and Albedos V1.0. EAR-A-COMPIL-5-NEOWISEDIAM-V1.0. NASA Planetary Data System.

Masiero, J.R.; Mainzer, A.K.; Grav, T.; Bauer, J.M.; Cutri, R.M.; Nugent, C.; Cabrera, M.S. (2012). "Preliminary Analysis of WISE/NEOWISE 3-Band Cryogenic and Post-cryogenic Observations of Main Belt Asteroids." *Ap J.* **759**, L8.

Noschese, A.; Vecchione, A. (2019a). "Rotation Period Determination for 1229 Tilia." *Minor Planet Bull.* **46**, 77.

Noschese, A.; Vecchione, A. (2019b). "Rotational Periods and Lightcurves of 1475 Yalta and 7230 Lutz." *Minor Planet Bull.* **46**, 194.

Nugent, C.R.; Mainzer, A.; Bauer, J.; Cutri, R.; Kramer, E.A.; Grav, T.; Masiero, J.; Sonnett, S.; Wright, E.L. (2016). "NEOWISE Reactivation Mission Year Two: Asteroid Diameters and Albedos." *AJ* **152**, A63.

Polakis, T.; Skiff, B. (2019). "Lightcurves of Eleven Main-belt Minor Planets." *Minor Planet Bull.* **46**, 132-137.

Schmadel, L.D. (2003). *Dictionary of Minor Planet Names*, pp. 73, 102, 118, 414, 543. Springer, New York.

Szabó, R.; Pál, A.; Sárneczky, K.; Szabó, Gy.M.; Molnár, L.; Kiss, L.L.; Hanyecz, O.; Plachy, E.; Kiss, Cs. (2016). "Uninterrupted optical light curves of main-belt asteroids from K2 Mission." *A&A* **596**, A40.

Usui, F.; Kuroda, D.; Müller, Th.G.; Hasegawa, S.; Ishiguro, M.; Ootsubo, T.; Ishihara, D.; Kataza, H.; Takita, S.; Oyabu, S.; Ueno, M.; Matsuhara, H.; Onaka, T. (2011). "Asteroid catalog Using AKARI: AKARI/IRC Mid-Infrared Asteroid Survey." *PASJ* **63**, 1117-1138.

Veres, P.; Jedicke, R.; Fitzsimmons, A.; Denneau, L.; Granvik, M.; Bolin, B.; Chastel, S.; Wainscoat, R.; Burgett, W.; Chambers, K.C.; Flewelling, H.; Kaiser, N.; Magnier, E.A.; Morgan, J.S.; Price, P.A.; and 2 colleagues. (2015). "Absolute magnitudes and slope parameters for 250,000 asteroids observed by Pan_STARRS PS1 – Preliminary results." *Icarus* **261**, 34-47.

Warner, B.D.; Harris, A.W.; Pravec, P. (2009). "The Asteroid Lightcurve Database." *Icarus* **202**, 134-146. Updated 2019 July. *http://www.minorplanet.info/lightcurvedatabase.html*

Warner, B.D. (2017). *MPO Canopus* software. *http://bdwpublishing.com*

Zeigler, K.; Barnhart,T.; Moser, A.; Rockafellow, T. (2019). "CCD Photometric Observations of Asteroids 2678 Aavasaksa, 3769 Arthurmiller, 4807 Noboru, (7520) 1990 BV, and (14510) 1996 ES2." *Minor Planet Bull.* **46**, 191-193.

2638 GADOLIN LIGHTCURVE ANALYSIS

Melissa N. Hayes-Gehrke, Eric Yates, Cameron Sewell,
Elliot Tapscott, Adam Margolis, Eric Goren, John Merlo-Coyne,
Samir Zahid, Alexander Reinhardt, Sean Malone, Casey Gardner,
Tim Seidell, Jordan Koehn, Soumya Pattanayak
Department of Astronomy, University of Maryland
College Park, MD, USA 20740
mhayesge@umd.edu

(Received: 2019 June 3)

Lightcurve analysis using *MPO Canopus* was completed by University of Maryland undergraduates and faculty. Data for 2638 Gadolin were collected over four nights in 2019 April. We found the rotation period to be 7.2174 ± 0.0149 h and the lightcurve amplitude to be 0.37 mag.

2638 Gadolin is situated within the asteroid main-belt and has a diameter of 12.1 km. It was first observed on 1939 Sept 19 by Y. Vaisala. It has an albedo of 0.284 and has an orbital period of 4.08 years. Its absolute magnitude is 11.8. (JPL, 2015)

Photometric observations of the asteroid were made on 2019 April 3, 6, 9, and 12 using the T-17 Planewave CDK 0.43-m iTelescope located at the Siding Spring Observatory in Siding Spring, Australia. Images were taken with an exposure time of 300 s, a binning of 1x1, and a luminance filter. The T-17 iTelescope uses an FLI ProLine PL4710 CCD with a 13x13 µm pixel size and a resolution of 0.92 arcsec per pixel. We took a total of 148 images; out of those, 102 were considered usable for photometry.

Aperture and differential photometry calculations were made from our data using the *MPO Canopus* software program. A Fourier analysis was performed on our data which allowed us to determine a rotation period with a reasonable uncertainty.

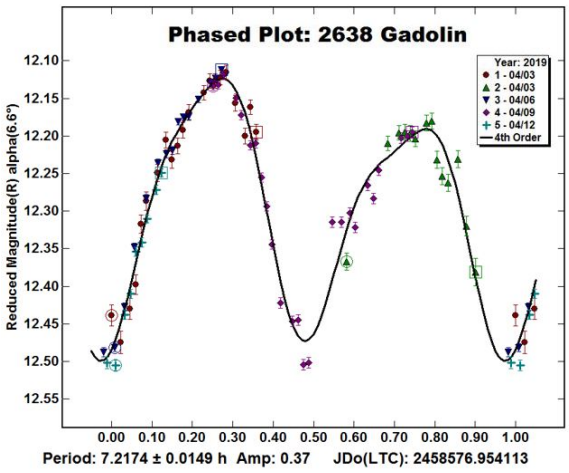

The phased plot for our observed nights shows a very distinct rotation period with minimal outlying data points. Because of the quality of our data, we were able to determine that 2638 Gadolin has a rotation period of 7.2174 ± 0.0149 h. Other rotation periods are possible; however, their fits produce higher RMS values when additional steps are calculated. Furthermore, the data points did not fit the curves of other potential rotation periods as well and left substantial gaps between data points. These alternative rotation periods yielded higher uncertainties, leading us to believe they were unlikely candidates.

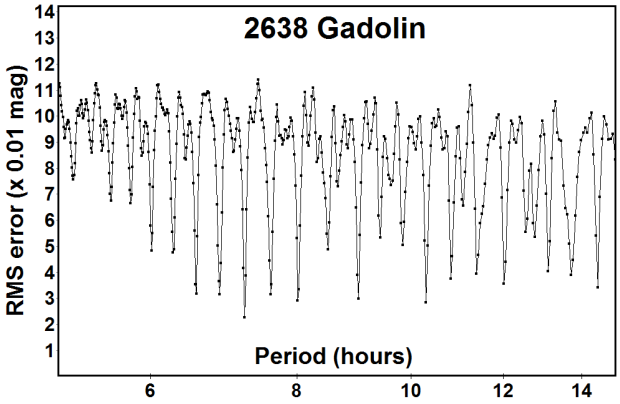

During one rotation, the magnitude of the asteroid varied by 0.37 mag peak-to-peak. The large change in the amplitude leads us to believe that 2638 Gadolin is oblong in shape. As of the most recent version of the lightcurve database (LCDB; Warner et al., 2009), no period for 2638 Gadolin has been published until now.

Acknowledgements

This research was funded by the Department of Astronomy at the University of Maryland, College Park. Observations were made via telescopes remotely controlled via the internet provided by iTelescope at the Siding Spring Observatory in Siding Spring, Australia. We want to send our thanks to Brian Warner for assisting us with our 2019 April 6 data in *MPO Canopus*.

References

Harris, A.W.; Young, J.W.; Scaltriti, F.; Zappala, V. (1984). "Lightcurves and phase relations of the asteroids 82 Alkmene and 444 Gyptis." *Icarus* **57**, 251-258.

iTelescope - T7 - Deep Field.
http://www. itelescope.net/telescope-t7/

JPL (2015). Small Body Database Browser.
http://ssd.jpl.nasa.gov/sbdb.cgi

Warner, B.D.; Harris, A.W.; Pravec, P. (2009). "The asteroid lightcurve database." *Icarus* **202**, 134-146. Updated 2019 Jan. *http://www.MinorPlanet.info/lightcurvedatabase.html*

Warner, B.D. (2013). MPO Software, *MPO Canopus* version 10.4.3.7, Bdw Publishing. *http:/Avww.minorplanetobserver.com/*

Number	Name	2019 mm/dd	Phase	L_{PAB}	B_{PAB}	Period(h)	P.E.	Amp	A.E.	Grp
2638	Gadolin	04/03-04/12	6.6,7.2	194	-14	7.2174	0.0149	0.37	0.00	EUN

Table I. Observing circumstances and results. Pts is the number of data points. The phase angle is given for the first and last date. LPAB and BPAB are the approximate phase angle bisector longitude and latitude at mid-date range (see Harris et al., 1984). Grp is the asteroid family/group (Warner et al., 2009). EUN: Eunomia.

LIGHTCURVE ANALYSIS OF FIVE MAIN-BELT ASTEROIDS: 3446 COMBES, (9410) 1995 BJ1, (17780) 1998 FY13, (24491) 2000 YT 123, AND 28341 BINGAMAN

Melissa N. Hayes-Gehrke, Ajay Singh, Andrew Malwitz, Caleb Wilson, Daniel Huang, Diego Nava, Iris Yu, Nick Chappell, Jonathan Lin, Lynn Du, Aishwarya Vijaykumar, Robert Dries, Yifan Lou
Department of Astronomy, University of Maryland
College Park, MD 20742
mhayesge@umd.edu

Stephen M. Brincat
Flarestar Observatory
San Gwann SGN 3160, MALTA

Charles Galdies
Znith Observatory
Naxxar NXR 2217, MALTA

Winston Grech
Antares Observatory
Fgura FGR 1555, MALTA

(Received: 2019 June 3)

An observing campaign was conducted among teams at the University of Maryland, College Park, and in Malta to determine the rotation period of 3446 Combes during 2019 March and April. Lightcurve analysis using *MPO Canopus* of the asteroid was conducted in order to determine its rotation period. Using the eight nights of data, 3446 Combes was found to have a rotation period of 5.6990 ± 0.0005 h and an amplitude of 0.18 mag. The University of Maryland team also observed four additional asteroids that serendipitously appeared in the images: (9410) 1995 BJ, (17780) 1998 FY13, (24491) 2000 YT123, and 28341 Bingaman. These were observed only one night each and only the raw data for them are presented.

One site of observations was in the United States, by the University of Maryland team. Five asteroids were observed using an online telescope-sharing website called itelescope.net. The telescope (T-21) is located in Mayhill, New Mexico at the New Mexico Skies Observatory (iTelescope.net). It was used on 2019 April 4, 7, 10, and 25. The primary diameter of the telescope is 0.43 m, with a focal length of 1.94 m. The CCD camera had a 3072x2048x9µm pixel array and a full well of 100,000 e^-. Each image had an exposure of 300 seconds, used clear filter, and 1x1 binning. All images were processed with standard bias, dark, and flat calibrations.

Other sites used to observe 3446 Combes were at the Flarestar Observatory, Antares Observatory, and the Znith Observatory by collaborators located in Malta. Images at the Flarestar Observatory in Malta were taken using a 0.25-m SCT telescope with a Moravian G2-1600/ KAF 1603ME CCD, and FOV of 25.5x17.0 arcmin. The pixel scale was 0.99 arcsec/pixel. Images taken at Antares Observatory in Fgura Malta, used a 0.28-m SCT telescope with a SBIG STL-11000/KAI-11000M CCD, and FOV of 45.9x30.6 arcmin. The scale was 1.37 arcsec/pixel. Images were taken from the Znith Observatory in Naxxar, Malta, using a 0.20-m SCT telescope with a Moravian G2-1600/ KAF 1603ME CCD, FOV of 30.0 x 20.0 arcmin and scale of 1.17 arcsec/pixel.

There were no previous rotation periods reported for any of the five asteroids based on a search through the lightcurve database (Warner et al., 2009).

3446 Combes was first discovered on 1942 March 12 by K. Reinmuth at the National Observatory for Homewaters - Königstuhl. Reinmuth named the asteroid after a French amateur astronomer Michel-Alain Combes (Schmadel, 2006). The asteroid has an orbital period of 3.66 yr, absolute magnitude H = 13.3, an albedo of 0.144, and a diameter of 8.411 km (NASA, 2007). Combes was observed across four days in New Mexico along with four days from international collaborators in Malta, collecting a total of 301 data points. The period was determined to be 5.6990 ± 0.0005 h and an amplitude of 0.18 mag.

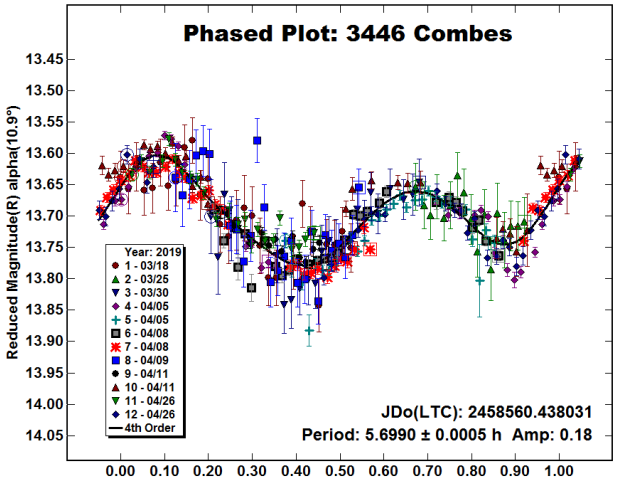

(9410) 1995 BJ1 was discovered on 1995 January 26 by astronomer Takeshi Urata at the Ohira station of the Nihondaira Observatory in Shimizu. The asteroid has an orbital period of 5.81 yr, absolute magnitude H = 12.6, and an albedo of 0.067 (NASA, 2007). 1995 BJ1 was observed on 2019 April 26 for a total of 21 images using the T-21 telescope. This is insufficient data to conclusively yield a rotation period, thus the raw data are provided for future analysis.

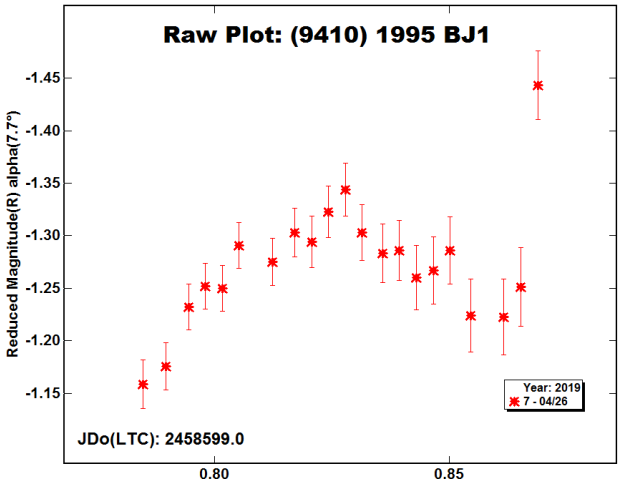

(17780) 1998 FY13 was first discovered on 1998 March 24 by Near Earth Asteroid Tracking (NEAT) from the station of Maui. It has an orbital period of 5.195 yr and absolute magnitude H = 12.9 (NASA, 2007). The asteroid was observed on 2019 April 10 for a total of 40 images using the T-21 telescope. This is insufficient

data to conclusively yield a rotation period, thus the raw data are provided for future analysis.

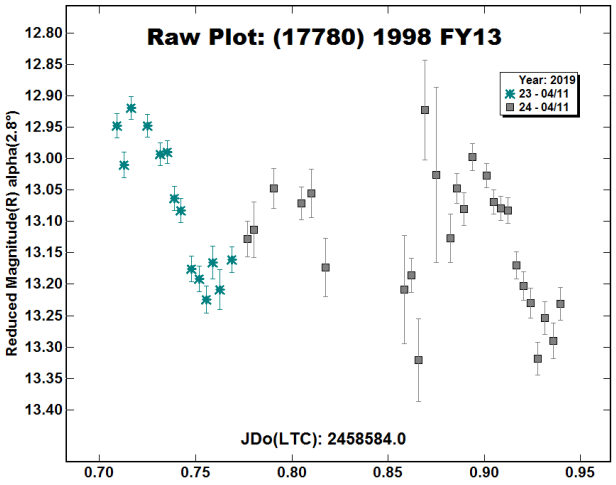

(24491) 2000 YT 123 was discovered on 2000 December 28 at the Magdalena Ridge Observatory in New Mexico through the Lincoln Near-Earth Asteroid Research Project (LINEAR). The asteroid has an orbital period of 5.91 yr and absolute magnitude H = 13.8 with an unknown albedo (NASA). The asteroid was observed on 2019 April 26 for a total of 21 images using the T-21 telescope. This is insufficient data to conclusively yield a rotation period, thus the raw data are provided for future analysis.

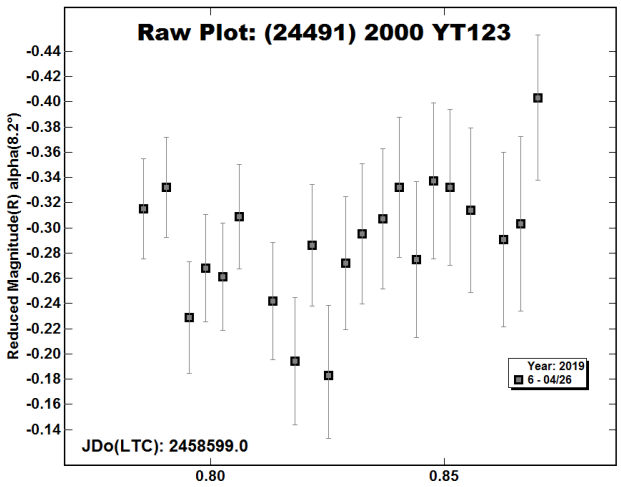

28341 Bingaman was first discovered on 1999 March 13 American astronomer Roy A. Tucker from Goodricke-Pigott Observatory in Tucson. It is named after a graphic artist Kory Bingaman. It has an orbital period of 4.94 yr and absolute magnitude of H = 13.6 (NASA, 2007). We observed it on 2019 April 10 for a total of 40 images using the T-21 telescope. This is insufficient data to conclusively yield a rotation period, thus the raw data are provided for future analysis.

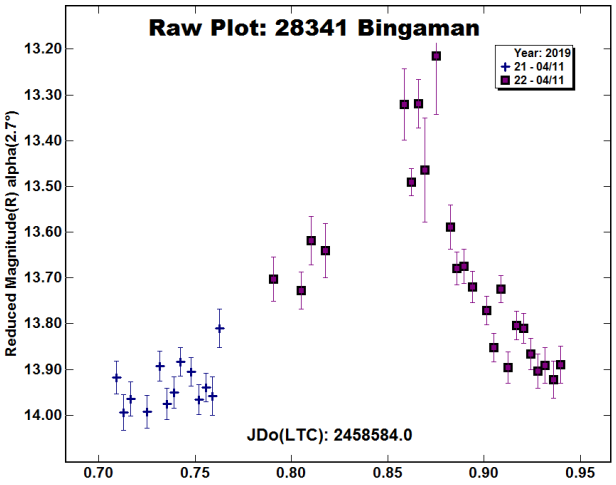

Acknowledgements

We thank the Department of Astronomy at the University of Maryland, College Park for funding and New Mexico Skies Observatory for allocating resources including the T-21 telescope.

References

Harris, A.W.; Young, J.W.; Scaltriti, F.; Zappala, V. (1984). "Lightcurves and phase relations of the asteroids 82 Alkmene and 444 Gyptis." *Icarus* **57**, 251-258.

iTelescope.net. "Remote Internet Telescope Network - Online Imaging & Telescope Hosting Service." Telescope T-21. iTelescope.net, n.d. Web. 2019 May 8. *http://www.itelescope.net/telescope-t21/*

NASA JPL. "JPL Small-Body Database Browser." Solar System Dynamics. NASA JPL, 23 Oct. 2007. *https://ssd.jpl.nasa.gov/sbdb.cgi*

Schmadel, L.D. (2006). *Dictionary of Minor Planet Names: Addendum For Fifth Edition, 2003-2005*. Springer.

Warner, B.D., Harris, A.W., Pravec, P. (2009). "The Asteroid Lightcurve Database." *Icarus* **202**, 134-146. Updated 2016 Sep. *http://www.minorplanet.info/lightcurvedatabase.html*

Warner, B.D. (2016). MPO Software, *MPO Canopus* version 10.7.7.0. *http://minorplanetobserver.com*

Number	Name	2019 mm/dd	Phase	L_{PAB}	B_{PAB}	Period(h)	P.E.	Amp	A.E.	Grp
3446	Combes	04/04-04/26	2.4,10.7	196	3	5.6990	0.0005	0.18	0.02	V
9410	1995 BJ1	04/26	7.6	195	3	-	-	-	-	THM
17780	1998 FY13	04/10	2.2	196	3	-	-	-	-	EOS
24491	2000 YT123	04/26	8.0	195	3	-	-	-	-	MB-O
28341	Bingaman	04/10	2.2	196	3	-	-	-	-	KOR

Table I. Observing circumstances and results. Pts is the number of data points. The phase angle is given for the first and last date. L_{PAB} and B_{PAB} are the approximate phase angle bisector longitude and latitude at mid-date range (see Harris *et al.*, 1984). Grp is the asteroid family/group (Warner *et al.*, 2009). KOR: Koronis; MB-O: Main-belt – outer; THM: Themis; V: Vestoid.

LIGHTCURVE FOR 3816 CHUGAINOV

Melissa Hayes-Gehrke, Akshay Anil, Pavlos Baffes, Brandon Ferrell, Satya Gandham, Michael Gregory, Rudra Menon, Conor Moore, Alex Pongchit, Anthony Proulx, Corey Sackalosky, Yavuz Sefik, Tyler Weddle, and Eric Yates
Department of Astronomy, University of Maryland
College Park, Maryland 20742 USA
mhayesge@umd.edu

(Received: 2019 June 3)

Lightcurve analysis using *MPO Canopus* of multiple nights of observations of 3816 Chugainov was unable to produce a rotation period due to a lack of fluctuations in the phased lightcurves.

We focused on finding a rotation period for 3816 Chugainov through remote observation. A total of 158 usable images were taken by the T17 telescope, a 0.43-m *f*/6.8 reflector, in Siding Spring, Australia (MPC Code - Q62) between 2019 April 4 and May 7. The CCD used was the FLI ProLine PL4710 which has a resolution of 0.92 arcsec/pixel, a FOV of 15.5 x 15.5 arcmin, and an array size of 1024x1024 pixels (iTelescope, 2018). Observation settings included a clear filter, binning 1x1, and exposure time of 300 seconds.

Prior to any analysis, we checked the Asteroid Lightcurve Database (LCDB; Warner et al., 2009) for any prior determinations of a rotation period and found none.

3816 Chugainov, a main-belt asteroid, was discovered by Nikolai Chernykh on 1975 November 8 at the Crimean Astrophysical Observatory near Nautschnyj, Crimea (Enacademic, 2010). It is 12.323 km in diameter and has an orbital period of 4.21 years (JPL, 2019).

MPO Canopus (Warner, 2018) was used to perform aperture and differential photometry. This was used to generate a series of phased lightcurves through Fourier analysis in an attempt to determine a period for 3816 Chugainov. Unfortunately, the analysis was inconclusive due to no significant fluctuations in the differential magnitudes and the time baseline of the data proved to be insufficient to determine a rotation period longer than typically expected. Perhaps a longer observation period might yield better results. The amplitude was approximately 0.06 magnitudes.

There are several possibilities to explain why we were unable to determine a rotation period for 3816 Chugainov. It may have a pole that is aligned or nearly aligned with our point of view, it may be spherical in shape, with little variation in the cross-sectional area over time, or it may simply just have a very long period. The asteroid may also exhibit some combination of these characteristics.

One should note that the lightcurve presented here does not represent the true period; it is simply the best way to present the data that we obtained.

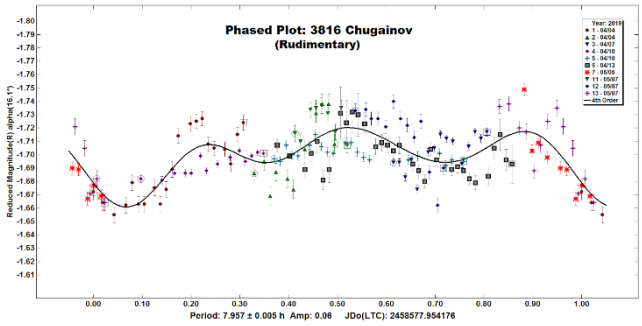

Acknowledgments

Thanks to the University of Maryland Astronomy Department for their funding and iTelescope.net for allowing us to use their telescope. Without their support, we would not have been able to study this asteroid.

References

Enacademic (2010). 3816 Chugainov. *https://enacademic.com/dic.nsf/enwiki/9331700/3816_Chugainov*

Harris, A.W.; Young, J.W.; Scaltriti, F.; Zappala, V. (1984). "Lightcurves and phase relations of the asteroids 82 Alkmene and 444 Gyptis." *Icarus* **57**, 251-258.

iTelescope (2018). iTelescope T17-Deep Field Research-Australia. *http://support.itelescope.net/support/solutions/articles/231915-telescope-17*

JPL (2019). Small-Body Database Browser. *http://ssd.jpl.nasa.gov/sbdb.cgi*

Warner, B.D.; Harris, A.W.; Pravec, P. (2009). "The Asteroid Lightcurve Database." Icarus **202**, 134-146. Updated 2016 Sep. *http://www.minorplanet.info/lightcurvedatabase.html*

Warner, B.D. (2018). *MPO Canopus* software V10.7.11.4. Bdw Publishing. *http://bdwpublishing.com/*

Number	Name	2019 mm/dd	Phase	L_{PAB}	B_{PAB}	Period(h)	P.E.	Amp	A.E.	Grp
3816	Chugainov	04/04-05/07	7.7,16.4	194	-15	-	-	-	-	EUN

Table I. Observing circumstances and results. Pts is the number of data points. The phase angle is given for the first and last date. L_{PAB} and B_{PAB} are the approximate phase angle bisector longitude and latitude at mid-date range (see Harris *et al.*, 1984). Grp is the asteroid family/group (Warner *et al.*, 2009). EUN: Eunomia.

LIGHTCURVE ANALYSIS AND ROTATION PERIOD OF 6372 WALKER

Melissa N. Hayes-Gehrke, Marley Berk, Abisola Fatodu, Bhargin Kanani, Quinn Kropschot, Julia Marks, Ella Misangyi, Matthew Nguyen, Julie Stone, Joshua Suniga,
Michael Thompson, Matthew Vorsteg, Timothy Wagman
Physical Sciences Complex (415), Room 1113
4296 Stadium Dr.
University of Maryland
College Park, MD 20742-2421
mhayesge@umd.edu

Alessandro Marchini
Astronomical Observatory, DSFTA - University of Siena (K54)
Via Roma 56, 53100 - Siena, ITALY

Massimo Banfi, Riccardo Papini, Fabio Salvaggio
Wild Boar Remote Observatory (K49)
San Casciano in Val di Pesa (FI), ITALY

Stephen M. Brincat
Flarestar Observatory
San Gwann SGN 3160, MALTA

Charles Galdies
Znith Observatory
Naxxar NXR 2217, MALTA

Winston Grech
Antares Observatory
Fgura FGR 1555, MALTA

(Received: 2019 June 3)

From 2019 March-May, images of minor planet 6372 Walker were captured to investigate its rotation period. Our analysis found a period of 44.25 ±0.01 h.

6372 Walker is a main-belt asteroid discovered in 1985 by C.S. Shoemaker at Palomar Observatory and was last observed in May of 2018 (JPL, 2019). It has a diameter of 42.13 km and orbital period of 5.68 yr.

Over the course of the observations, six telescopes were used for our observing campaign on 6372 Walker. Table I lists the basic equipment information for each observatory. All observations used a clear filter and images were processed with standard bias, dark, and flat calibrations. *MPO Canopus* (Warner, 2018) was used for standard aperture and differential photometry in order to generate the lightcurve. Images were taken on 2019 March 17, 29, 30, 31, April 4, 6, 7, 10, 11, 13, 25, 27, 29, and May 1, 4.

Our data analysis yielded a rotation period P = 44.25 ± 0.01 hours with an amplitude A = 0.19 ± 0.03 mag. There were no previously reported rotation periods in the asteroid lightcurve database (LCDB; Warner et al., 2009).

Obs	Scope	Cam	FOV arcmin	Scale "/pix
NMS	0.43-m CDK	FLI PL6303	33x49	0.96
DSFTA	0.32-m MC	SBIG STL-6303	59x39	2.30
WBRO	0.23-m SCT	SBIG ST-8XME	14x10	1.60
FO	0.25-m SCT	Moravian G2-1600	25x17	0.99
AO	0.28-m SCT	SBIG STL-11000	46x31	1.37
ZO	0.20-m SCT	Moravian G2-1600	30x20	1.17

Table I. Equipment used for observations. Obs column: NMS: New Mexico Skies. WBRO: Wild Boar. FO: Flarestar Obs. AO: Antares Obs. ZO: Znith Obs. Scope column: CDK corrected Dall-Kirkham; MC: Maksutov-Cassegrain; SCT: Schmidt-Cassegrain.

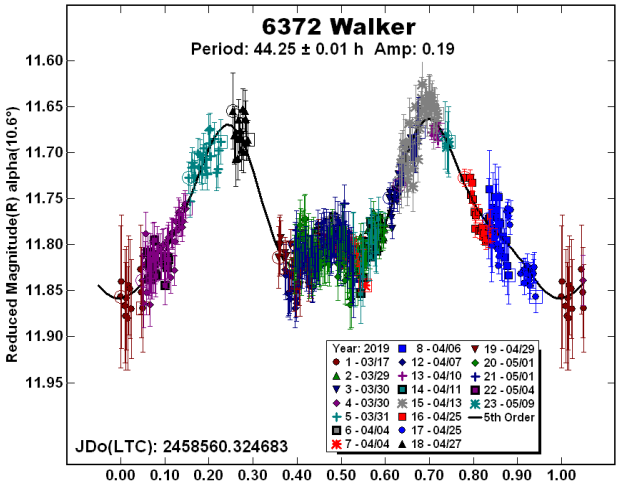

Acknowledgements

Funding for the observations at iTelescope (iTelescope, 2019) was provided by the University of Maryland Department of Astronomy.

References

Harris, A.W.; Young, J.W.; Scaltriti, F.; Zappala, V. (1984). "Lightcurves and phase relations of the asteroids 82 Alkmene and 444 Gyptis." *Icarus* **57**, 251-258.

iTelescope (2019). Remote Observatory. *https://www.itelescope.net/*

JPL (2019). Small Body Database Search Engine. *http://ssd.jpl.nasa.gov*

Warner, B.D. (2018). *MPO Canopus* software V10.2.1.0. Bdw Publishing. *http://bdwpublishing.com*

Warner, B.D.; Harris, A.W.; Pravec, P. (2009). "The Asteroid Lightcurve Database." *Icarus* **202**, 134-146. Updated 2019 Jan. *http://www.minorplanet.info/lightcurvedatabase.html*

Number	Name	2019 mm/dd	Phase	L_{PAB}	B_{PAB}	Period(h)	P.E.	Amp	A.E.	Grp
6372	Walker	03/17-05/09	10.7,12.1	199	14	44.25	0.01	0.19	0.03	MB-O

Table II. Observing circumstances and results. Pts is the number of data points. The phase angle is given for the first and last date. L_{PAB} and B_{PAB} are the approximate phase angle bisector longitude and latitude at mid-date range (see Harris *et al.*, 1984). Grp is the asteroid family/group (Warner *et al.*, 2009). MBO: outer main-belt.

LIGHTCURVE ANALYSIS OF L5 TROJAN ASTERIODS AT THE CENTER FOR SOLAR SYSTEM STUDIES: 2019 ARPIL TO JUNE

Robert D. Stephens
Center for Solar System Studies (CS3)/MoreData!
11355 Mount Johnson Ct., Rancho Cucamonga, CA 91737 USA
rstephens@foxandstephens.com

Brian D. Warner
Center for Solar System Studies (CS3)/MoreData!
Eaton, CO

(Received: 2019 July 7)

Lightcurves for five L_5 Jovian Trojan asteroids were obtained at the Center for Solar System Studies (CS3) from 2019 April to June.

CCD Photometric observations of five Trojan asteroids from the L_5 (Trojan) Lagrange point were obtained at the Center for Solar System Studies (CS3, MPC U81). For several years, CS3 has been conducting a study of Jovian Trojan asteroids. This is another in a series of papers reporting data analysis being accumulated for family pole and shape model studies. It is anticipated that for most Jovian Trojans, two to five dense lightcurves per target at oppositions well distributed in ecliptic longitudes will be needed and can be supplemented with reliable sparse data for the brighter Trojan asteroids. For most of these targets we were able to get preliminary pole positions and create shape models from sparse data and the dense lightcurves obtained to date. These preliminary models will be improved as more data are acquired at future oppositions and will be published at a later date.

Telescope	Camera
0.40-m f/10 Schmidt-Cass	FLI Proline 1001E
0.40-m f/10 Schmidt-Cass	Fli Microline 1001E
0.35-m f/10 Schmidt-Cass	Fli Microline 1001E

Table I. List of telescopes and CCD cameras used at CS3.

Table I lists the telescopes and CCD cameras that were used to make the observations. Images were unbinned with no filter and had master flats and darks applied. The exposures depended upon various factors including magnitude of the target, sky motion, and Moon illumination.

Image processing, measurement, and period analysis were done using *MPO Canopus* (Bdw Publishing), which incorporates the Fourier analysis algorithm (FALC) developed by Harris (Harris et al., 1989). The Comp Star Selector feature in *MPO Canopus* was used to limit the comparison stars to near solar color. Night-to-night calibration was done using field stars from the CMC-15 or the ATLAS catalog (Tonry et al., 2018), which has Sloan *griz* magnitudes that were derived from the GAIA and Pan-STARRS catalogs, among others. The authors state that systematic errors are generally no larger than 0.005 mag, although they can reach 0.02 mag in small areas near the Galactic plane. BVRI magnitudes were derived by Warner using formulae from Kostov and Bonev (2017). The overall errors for the BVRI magnitudes, when combining those in the ATLAS catalog and the conversion formulae, are on the order of 0.04-0.05 mag.

Even so, we found in most cases that nightly zero point adjustments for the ATLAS catalog to be on the order of only 0.02-0.03 mag were required during period analysis. There were occasional exceptions that required up to 0.10 mag. These may have been related in part to using unfiltered observations, poor centroiding of the reference stars, and not correcting for second-order extinction terms. Regardless, the systematic errors seem to be considerably less than other catalogs, which reduces the uncertainty in the results when analysis involves data from extended periods or the asteroid is tumbling.

In the lightcurve plots, the "Reduced Magnitude" is Johnson V corrected to a unity distance by applying $-5*\log(r\Delta)$ to the measured sky magnitudes with r and Δ being, respectively, the Sun-asteroid and the Earth-asteroid distances in AU. The magnitudes were normalized to the phase angle given in parentheses using $G = 0.15$. The X-axis rotational phase ranges from –0.05 to 1.05. The amplitude indicated in the plots (e.g. Amp. 0.23) is the amplitude of the Fourier model curve and not necessarily the adopted amplitude of the lightcurve. Targets were selected for this L_5 observing campaign based upon the availability of dense lightcurves acquired in previous years. We obtained two to four lightcurves for most of these Trojans at previous oppositions. For brevity, only some of the previously reported rotational periods may be referenced. A complete list is available at the lightcurve database (LCDB; Warner et al., 2009).

To evaluate the quality of the data obtained to determine how much more data might be needed, preliminary pole and shape models were created for all of these targets. Sparse data observations were obtained from the Catalina Sky Survey and USNO-Flagstaff survey using the AstDyS-3 site (*http://hamilton.dm.unipi.it/asdys2/*). These sparse data were combined with our dense data as well as any other dense data found in the ALCDEF asteroid photometry database (*http://www.alcdef.org/*) using *MPO LCInvert*, (Bdw Publishing). This Windows-based program incorporates the algorithms developed by Kassalainen et al (2001a, 2001b) and converted by Josef Durech from the original FORTRAN to C. A period search was made over a sufficiently wide range to assure finding a global minimum in χ^2 values.

2357 Phereclos. The synodic period found this year produced a low amplitude, lightcurve with three extrema consistent with rotational periods found in previous years (Mottola et al., 2011; Stephens et al., 2016b; 2017; 2018). These data were combined with our data from the last three years and available sparse data to create a preliminary shape model with a sidereal period of 14.36221 ± 0.00001 h.

Number	Name	2019 mm/dd	Phase	L_{PAB}	B_{PAB}	Period(h)	P.E.	Amp	A.E.
2357	Phereclos	03/31-04/15	*2.5,0.9	201	1	14.449	0.003	0.15	0.02
2363	Cebriones	05/29-06/04	6.9,7.8	214	4	20.099	0.003	0.34	0.02
3451	Mentor	12/31-12/31	*6.9,7.8	0	0	7.6922	0.0004	0.31	0.02
12929	1999 TZ1	05/26-06/02	7.3,8.3	208	11	13.73	0.02	0.08	0.02
17492	Hippasos	05/12-05/21	5.7,6.5	219	25	17.699	0.006	0.40	0.03

Table II. Observing circumstances and results. The phase angle is given for the first and last date. If preceded by an asterisk, the phase angle reached a minimum or maximum during the period. L_{PAB} and B_{PAB} are the approximate phase angle bisector longitude/latitude at mid-date range (see Harris et al., 1984).

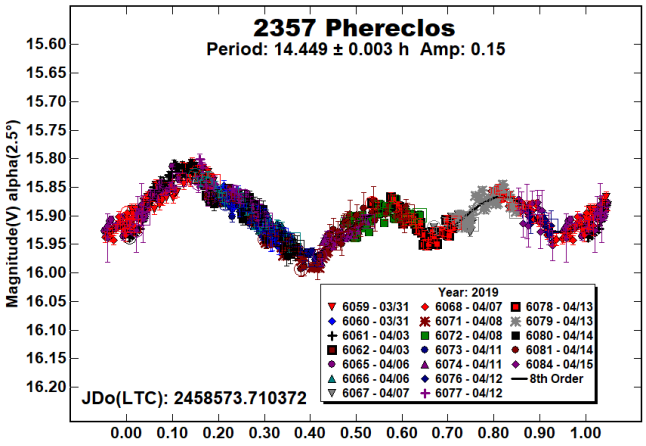

2363 Cebriones. Reliable rotational rates for this Trojan were obtained three times in the past (Galad et al., 2008; Mottola et al., 2011; Skiff et al., 2019), each time finding a period near 20.1 h. The 2019 results are in good agreement.

Using sparse data from the Asteroids – Dynamic Site and the Skiff data from the Asteroid Lightcurve Photometry Database, a preliminary shape model with a sidereal rotational period of 20.09748 ± 0.00001 h was created.

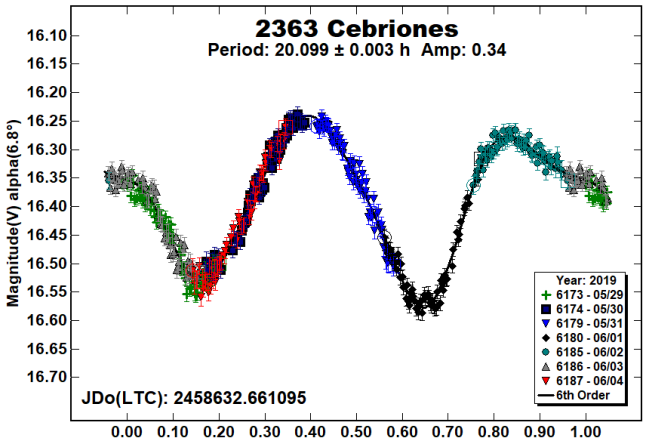

3451 Mentor. Judging by the number entries in the LCDB, this is one of the better-studied Trojans. All the results have been consistently near 7.7 h. Among those rated U ≥ 2+ are Melita et al. (2010; 7.68 h), French et al. (2011b; 7.730 h), Mottola et al. (2011; 7.675 h), and Stephens et al. (2014; 7.68 h). Our result of 7.6922 h is in good agreement.

This Trojan is obliging when it comes to trying to model its shape and spin axis. It has shown lightcurves amplitudes ranging from 0.13 mag (L_{PAB} = 59°) to 0.63 mag (L_{PAB} = 167°). From this, the spin axis should have an ecliptic longitude near 60° or 240°. This is confirmed by our preliminary model with ecliptic coordinates of λ,β = (255°, +60°) and sidereal period of 7.6966420 ± 0.000002 h.

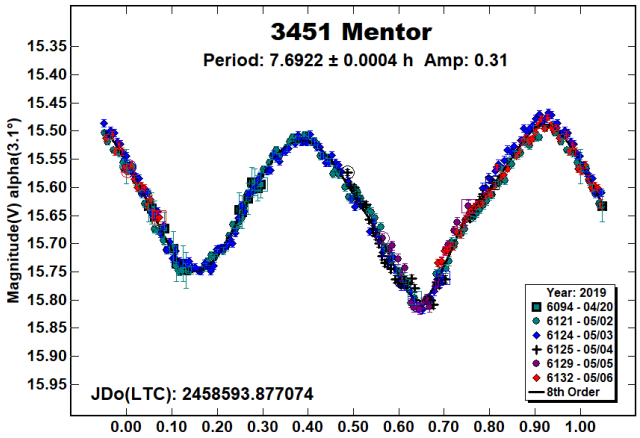

(12929) 1999 TZ1. This L_5 Jovian Trojan has been observed several times in the past. Moullet et al. (2008) observed it in 2007 reporting a rotational period of 10.4 h from sparse data over 12 nights. The resulting lightcurve was a poor fit. Over seven nights in 2009, Mottola et al. (2011) used sparse data and found a rotational period of 9.2749 h with a single extremum. Thirourin et al. (2010) used sparse data over six nights in 2007 to find two ambiguous periods, a bimodal 5.211 h period and a 10.422 h period with four extrema. Both lightcurves show scatter equal to the 0.07 mag. amplitude.

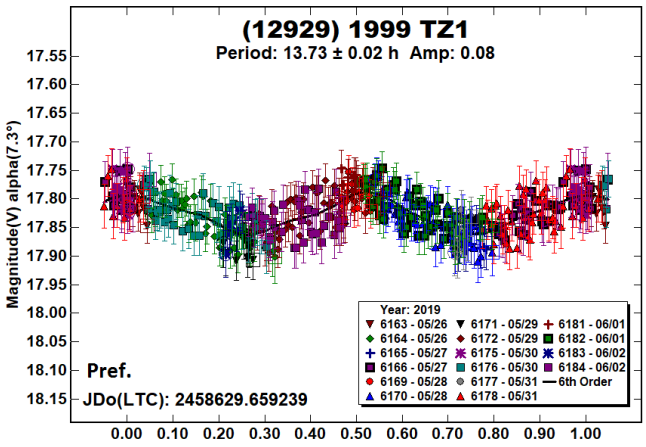

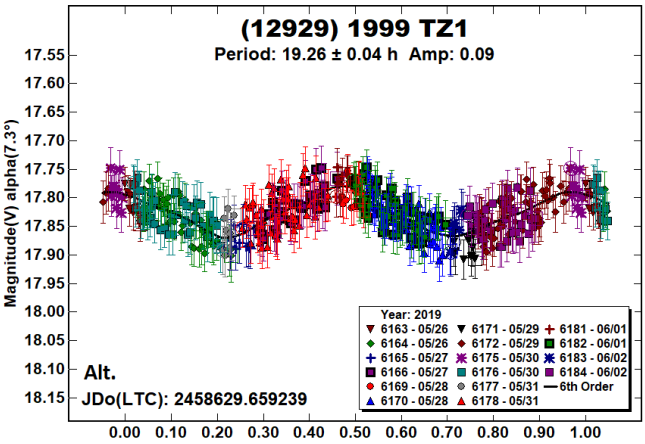

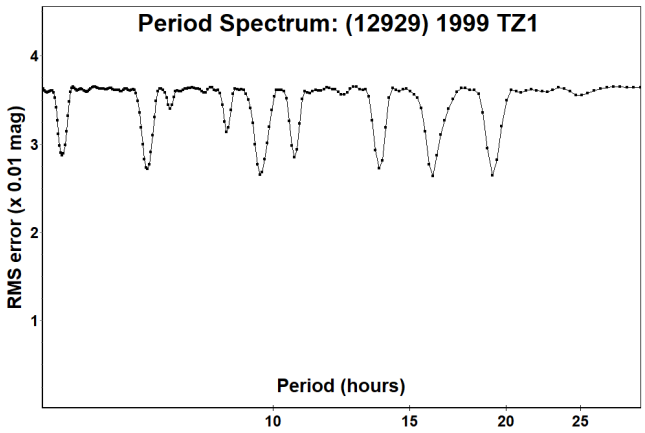

The results in 2019 are from a much denser dataset but still result in an ambiguous solution. Our preferred solution and the one adopted for this paper is 13.73 h which is a 3:4 alias of the previously reported 10.4 h period. A 19.26 h rotational period also produces a bimodal solution. Both solutions are low amplitude. 1999 TZ1 is yet another example of the problems involved in trying to use sparse observational data to determine low amplitude lightcurves.

17492 Hippasos. We observed this Trojan once before (Stephens and Warner, 2014) and found a synodic rotational period of 17.75 h. This 2019 result is in good agreement. Using sparse data from the Asteroids – Dynamic Site, we were able to create a preliminary shape model with a sidereal rotational period of 17.71126 ± 0.00001 h.

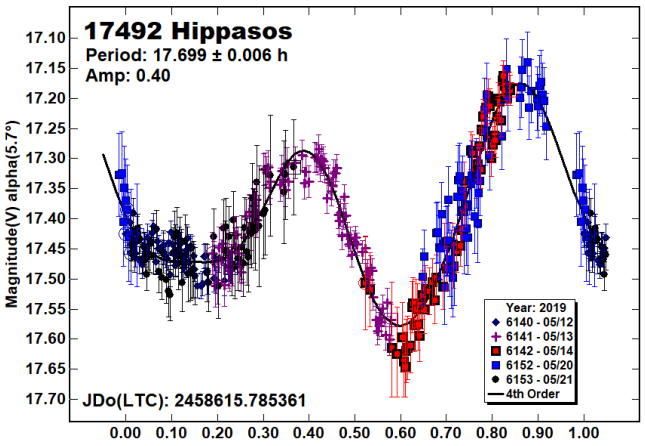

Acknowledgements

Observations at CS3 and continued support of the asteroid lightcurve database (LCDB; Warner et al., 2009) are supported by NASA grant 80NSSC18K0851. Work on the asteroid lightcurve database (LCDB) was also partially funded by National Science Foundation grant AST-1507535. This research was made possible in part based on data from CMC15 Data Access Service at CAB (INTA-CSIC) (*http://svo2.cab.inta-csic.es/vocats/cmc15/*). This work includes data from the Asteroid Terrestrial-impact Last Alert System (ATLAS) project. ATLAS is primarily funded to search for near earth asteroids through NASA grants NN12AR55G, 80NSSC18K0284, and 80NSSC18K1575; byproducts of the NEO search include images and catalogs from the survey area. The ATLAS science products have been made possible through the contributions of the University of Hawaii Institute for Astronomy, the Queen's University Belfast, the Space Telescope Science Institute, and the South African Astronomical Observatory. The purchase of a FLI-1001E CCD cameras was made possible by a 2013 Gene Shoemaker NEO Grants from the Planetary Society.

References

Asteroids – Dynamic Site. *https://newton.spacedys.com/astdys/*

Asteroid Lightcurve Photometry Database. *http://www.alcdef.org/*

French, L.M.; Stephens, R.D.; Lederer, S.M.; Coley, D.R.; Rohl, D.A. (2011). "Preliminary Results from a Study of Trojan Asteroids." *Minor Planet Bull*. **38**, 116-120.

Galad, A.; Kornos, L. (2008). "A Collection of Lightcurves from Modra: 2007 December- 2008 June." *Minor Planet Bull.* **35**, 114-146.

Harris, A.W.; Young, J.W.; Scaltriti, F.; Zappala, V. (1984). "Lightcurves and phase relations of the asteroids 82 Alkmene and 444 Gyptis." *Icarus* **57**, 251-258.

Harris, A.W.; Young, J.W.; Bowell, E.; Martin, L.J.; Millis, R.L.; Poutanen, M.; Scaltriti, F.; Zappala, V.; Schober, H.J.; Debehogne, H.; Zeigler, K.W. (1989). "Photoelectric Observations of Asteroids 3, 24, 60, 261, and 863." *Icarus* **77**, 171-186.

Kassalainen, M.; Torppa J. (2001a). "Optimization Methods for Asteroid Lightcurve Inversion. I. Shape Determination." *Icarus* **153**, 24-36.

Kassalainen, M.; Torppa J.; Muinonen, K. (2001b). "Optimization Methods for Asteroid Lightcurve Inversion. II. The Complete Inverse Problem." *Icarus* **153**, 37-51.

Kostov, A.; Bonev, T. (2017). "Transformation of Pan-STARRS1 gri to Stetson BVRI magnitudes. Photometry of small bodies observations." *Bulgarian Astron. J.* **28**, 3 (AriXiv:1706.06147v2).

Melita, M.D.; Duffard, R.; Williams, I.P.; Jones, D.C.; Licandro, J.; Ortiz, J.L. (2010). "Lightcurves of 6 Jupiter Trojan asteroids." *Planet. Space Sci.* **58**, 1035-1039.

Molnar, L.A.; Haegert, M.J.; Hoogenboom, K.M. (2008). "Lightcurve Analysis of an Unbiased Sample of Trojan Asteroids." *Minor Planet Bull*. **35**, 82-84.

Mottola, S.; Di Martino, M.; Erikson, A.; Gonano-Beurer, M.; Carbognani, A.; Carsenty, U.; Hahn, G.; Schober, H.; Lahulla, F.; Delbò, M.; Lagerkvist, C. (2011). "Rotational Properties of Jupiter Trojans. I. Light Curves of 80 Objects." *Astron. J.* **141**, A170.

Moullet, A.; Lellouch, E.; Doressoundiram, A.; Ortiz, J.L.; Duffard, R.; Morbidelli, A.; Vernazza, P.; Moreno, R. (2008). "Physical and dynamical properties of (12929) 1999 TZ{1} suggest that it is a Trojan." *Astro. and Astro.* ***483*** *L17-L20.*

Stephens, R.D.; French, L.; Davitt, C.; Coley, D. (2014). "At the Scaean Gates: Observations Jovian Trojan Asteroids, July-December 2013." *Minor Planet Bull.* **41**, 95-100.

Stephens, R.D.; Coley, D.R.; French, L.M. (2015). "Dispatches from the Trojan Camp – Jovian Trojan L5 Asteroids Observed from CS3: 2014 October – 2015 January." *Minor Planet Bull.* **42**, 216-224.

Stephens, R.D.; Warner, B.D. (2018). "Lightcurve Analysis of L5 Trojan Asteroids at the Center for Solar System Studies: 2018 January to March." *Minor Planet Bull.* **45**, 301-304.

Thirouin, A.; Ortiz, J. L.; Duffard, R.; Santos-Sanz, P.; Aceituno, F.J.; Morales, N. (2010). "Short-term variability of a sample of 29 trans-Neptunian objects and Centaurs." *Astro. and Astro.* ***522*** *A93.*

Tonry, J.L.; Denneau, L.; Flewelling, H.; Heinze, A.N.; Onken, C.A.; Smartt, S.J.; Stalder, B.; Weiland, H.J.; Wolf, C. (2018). "The ATLAS All-Sky Stellar Reference Catalog." *Astrophys. J.* **867**, A105.

Warner, B.D.; Harris, A.W.; Pravec, P. (2009). "The Asteroid Lightcurve Database." *Icarus* **202**, 134-146. Updated 2019 Feb. *http://www.minorplanet.info/lightcurvedatabase.html*

SPIN-SHAPE MODEL FOR 131 VALA

Lorenzo Franco
Balzaretto Observatory (A81), Rome, ITALY
lor_franco@libero.it

Frederick Pilcher
4438 Organ Mesa Loop
Organ Mesa Observatory (G50)
Las Cruces, NM 88011 USA

Alessandro Marchini
Astronomical Observatory, DSFTA - University of Siena (K54)
Via Roma 56, 53100 - Siena, ITALY

Giorgio Baj
M57 Observatory (K38), Saltrio, ITALY

Paolo Bacci, Martina Maestripieri
San Marcello Pistoiese (104), Pistoia, ITALY

Roberto Bacci
G. Pascoli Observatory (K63), Castelvecchio Pascoli, ITALY

(Received: 2019 June 22 Revised: 2019 August 2)

We present shape and spin axis model results for main-belt asteroid 131 Vala. The model was achieved with the lightcurve inversion process, using combined dense photometric data acquired from four apparitions, between 2007-2018 and sparse data from USNO Flagstaff. Analysis of the resulting data found a sidereal period P = 5.180810 ± 0.000023 h and two mirrored pole solutions at λ = 54°, β = 29° and λ = 243°, β = 30° with an uncertainty of ± 15 degrees.

We report that minor planet 131 Vala was recently observed in order to acquire data for lightcurve inversion work (Franco et al., 2019). A search in the asteroid lightcurve database (LCDB; Warner et al., 2009) shows many entries, covering a wide range of phase angle bisectors. Dense photometric data were downloaded from ALCDEF (ALCDEF, 2019) and sparse data instead were taken from the Asteroids Dynamic Site (AstDyS-2, 2018).

The observational details of the dense data used are reported in Table I with the mid date of the observing campaign, longitude and latitude of phase angle bisector (LPAB, BPAB).

Reference	Mid date	PABL°	PABB°
Pilcher (2008)	2007-10-22	48	-2
Pilcher (2009)	2009-02-18	167	7
Pilcher (2017)	2017-06-04	231	1
Franco et al. (2019)	2018-09-28	6	-6

Table I. Observational details for the data used in the lightcurve inversion process for 131 Vala.

Lightcurve inversion was performed using *MPO LCInvert* v.11.7.5.1 (BDW Publishing, 2016). For a description of the modeling process see *LCInvert Operating Instructions Manual* and Warner et al. (2017).

In order to find a better solution, we have also used sparse data from USNO Flagstaff Station (MPC Code 689) in addition to the dense data. Figure 1 shows the wide PAB longitude/latitude distribution for dense/sparse data used in the lightcurve inversion process. Figure 2 (top panel) shows the sparse photometric data

distribution (intensities vs JD) and (bottom panel) the corresponding phase curve (reduced magnitudes vs phase angle).

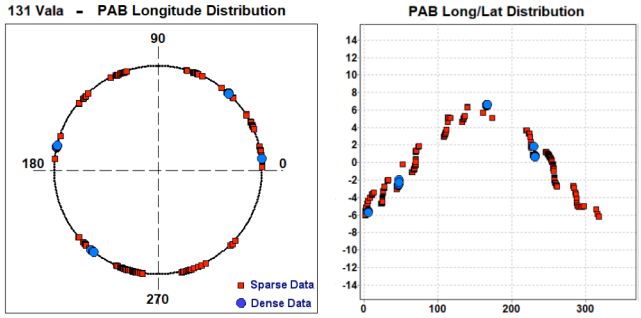

Figure 1: PAB longitude and latitude distribution of the data used for the lightcurve inversion model.

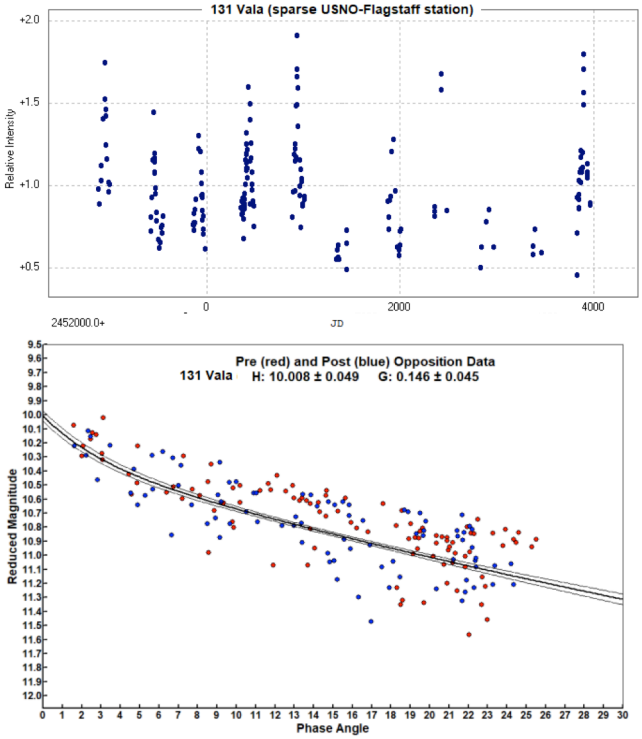

Figure 2: Top: sparse photometric data point distribution from (689) USNO Flagstaff station (relative intensity of the asteroid's brightness vs Julian Day). Bottom: phase curve obtained from sparse data (reduced magnitude vs phase angle).

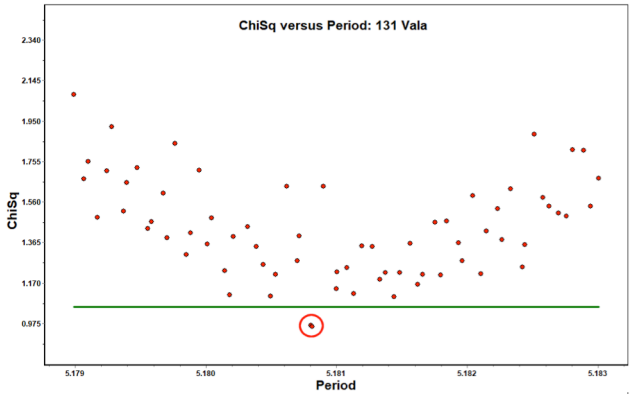

Figure 3: The period search for 131 Vala shows two overlapping sidereal periods with Chi-Sq values within 10% of the lowest value.

In the analysis the processing weighting factor was set to 1.0 for dense data and to 0.3 for sparse data. The "dark facet" weighting factor was set to 2.0 to keep the dark facet area below 1% of total area and the number of iterations was set to 50.

The sidereal period search was started around the average of the synodic periods found in the asteroid lightcurve database (LCDB; Warner et al., 2009). We found two very close sidereal periods within 0.000012 hours with a Chi-Sq value within 10% of the lowest Chi-Sq (Figure 3). Of these was chosen the one with the lowest Chi-Sq value.

The pole search was started using the "medium" option with the previously found sidereal period set to "float". From this step we found two roughly mirrored lower Chi-Sq solutions (Figure 4) separated by 180° in ecliptic longitude, (60°, 15°) and (240°, 30°).

The subsequent "fine" search that was centered on these rough positions, allowed us to refine the position of the pole (Figure 5). The analysis shows two clustered solutions of ecliptic longitude-latitude pairs within 15° of radius that had Chi-Sq values within 10% of the lowest value.

The two best solutions (lowest two Chi-Sq values) are reported in Table II. The sidereal period was obtained by averaging the two solutions found in the pole search process. Typical errors in the pole solution are ± 15° and the uncertainty in sidereal period has been evaluated as a rotational error of 30° over the total time span of the dense data set. Figure 6 shows the shape model (first solution) while Figure 7 shows the fit between the model (black line) and some observed lightcurves (red points).

λ °	β °	Sidereal Period (hours)	RMS
54	29	5.180810 ± 0.000023	0.0151
243	30		0.0153

Table II. The two spin axis solutions for 131 Vala (ecliptic coordinates). The sidereal period was the average of the two solutions found in the pole search process.

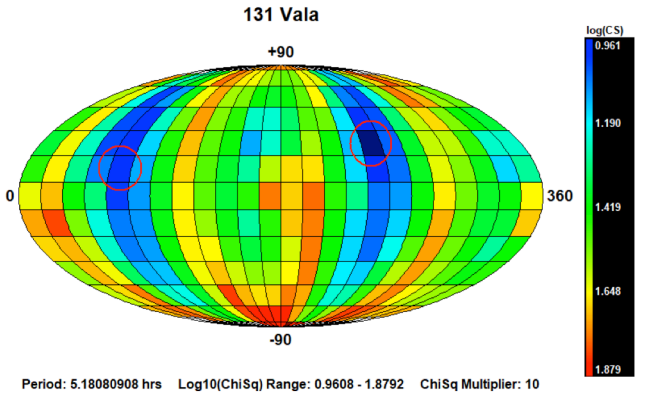

Figure 4: Pole search distribution. The dark blue indicates the better solutions (lower Chi-Sq), while maroon the worst ones.

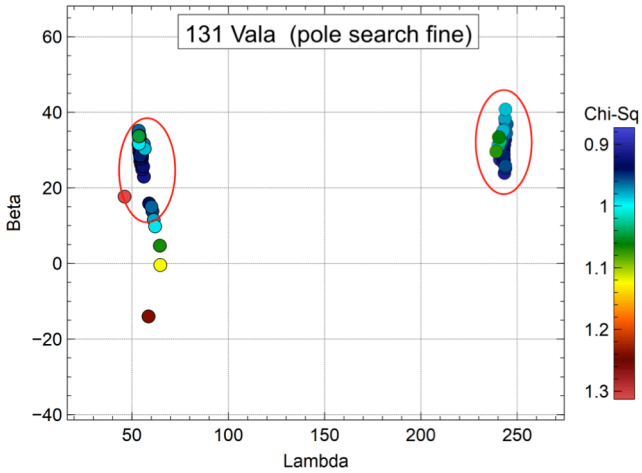

Figure 5: The "fine" pole search shows two clustered solutions centered at the ecliptic longitude/latitude (54°, 30°) and (243°, 31°) with radius approximately of 10° and Chi-Sq values within 10% of the lowest value.

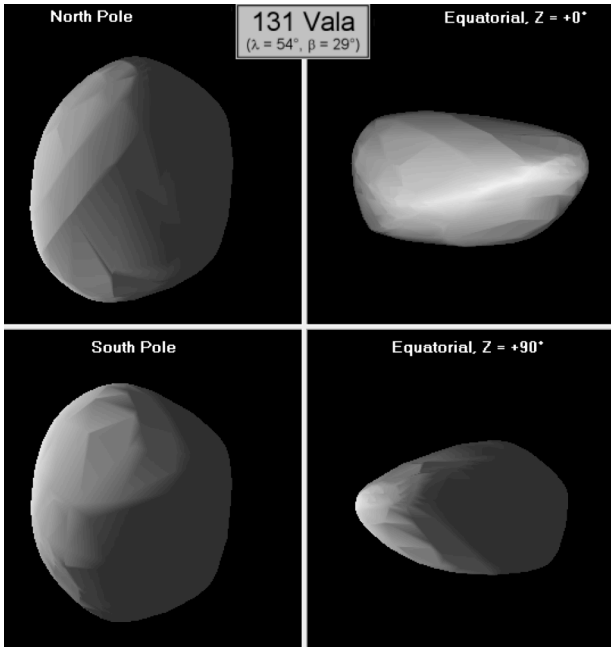

Figure 6: The shape model for 131 Vala (λ = 54°, β = 29°).

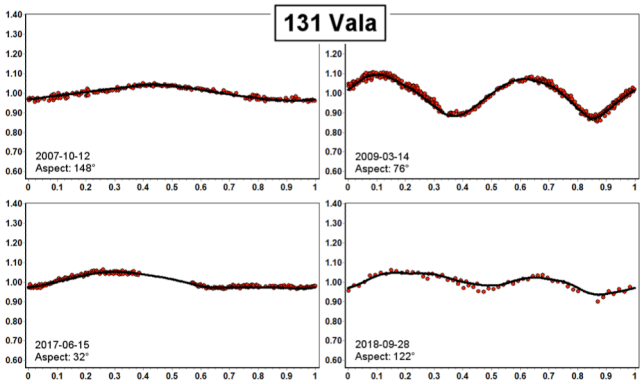

Figure 7: Model fit (black line) versus observed lightcurves (red points) for (λ = 54°, β = 29°) solution.

References

ALCDEF (2019). Asteroid Lightcurve Data Exchange Format web site. *http://www.alcdef.org/*

AstDyS-2 (2018), Asteroids - Dynamic Site. *http://hamilton.dm.unipi.it/astdys/*

BDW Publishing (2016). *http://www.minorplanetobserver.com/MPOSoftware/MPOLCInvert.htm*

DSFTA (2019). Dipartimento di Scienze Fisiche, della Terra e dell'Ambiente – Astronomical Observatory. *https://www.dsfta.unisi.it/en/research/labs-eng/astronomical-observatory*

Franco, L.; Marchini, A.; Baj, G.; Scarfi, G.; Bacci, P.; Maestripieri, M.; Bacci, R.; Papini, R.; Salvaggio, F.; Banfi, M. (2019). "Lightcurves for 131 Vala, 374 Burgundia, 734 Brenda, and 929 Algunde." *Minor Planet Bulletin* **46**, 86-86.

Pilcher, F. (2008). "Period Determination for 84 Klio, 98 Ianthe, 102 Miriam 112 Iphigenia, 131 Vala, and 650 Amalasuntha." *Minor Planet Bulletin* **35**, 71-72.

Pilcher, F. (2009). "Rotation Period Determinations for 120 Lachesis, 131 Vala 157 Dejanira, and 271 Penthesilea." *Minor Planet Bulletin* **36**, 100-102.

Pilcher, F. (2017). "Lightcurves of 131 Vala and 612 Veronika During Their 2017 Apparitions." *Minor Planet Bulletin* **44**, 317-318.

Warner, B.D.; Harris, A.W.; Pravec, P. (2009). "The asteroid lightcurve database." *Icarus* **202**, 134-146. Updated 2019 January. *http://www.minorplanet.info/lightcurvedatabase.html*

Warner, B.D.; Pravec, P.; Kusnirak, P.; Benishek, V.; Ferrero, A. (2017). "Preliminary Pole and Shape Models for Three Near-Earth Asteroids." *Minor Planet Bulletin* **44**, 206-212.

MAINBELT ASTEROIDS LIGHTCURVE ANALYSIS FROM *TAR* TELESCOPE NETWORK: 2018 OCTOBER - 2019 MAY

Amadeo Aznar Macías
APT Observatories Group, SPAIN
aptog@aptog.com

Javier Licandro
Instituto de Astrofísica de Canarias & Departamento de Astrofísica, Universidad de La Laguna
Tenerife, Spain

Miquel Serra-Ricart
Instituto de Astrofísica de Canarias Tenerife, Spain

(Received: 2019 June 20 Revised: 2019 August 9)

Lightcurves of twelve main-belt asteroids (MBA) obtained with the Telescopio Robótico Abierto network (TAR) and the Isaac Aznar Observatory from 2018 October to 2019 May are presented and analyzed to derive the rotation period, lightcurve amplitude, and axis size relationship.

CCD photometric observations of twelve main-belt asteroids (MBA) were obtained using the Telescopio Abierto Robótico (TAR) network between 2018 October and 2019 May. This work is included in the Mars-crossing survey we started with these telescopes in late 2018 (Licandro et al., in preparation). Due to the large field-of-view of the images obtained during the survey, we also obtained the lightcurve of every main-belt asteroid serendipitously identified in the images. Thus, it is necessary to remark that there is no previous asteroid selection process in this work, except for the three targets observed from the Isaac Aznar Observatory (IAO) in 2019 May.

Six of the observed asteroids do not have previously published lightcurves: 3830, 7673, 14105, 15925, 33729 and 62836. The others have been observed during previous apparitions and their rotation period is already determined. Even in those cases, the data presented in this paper are still useful to improve the rotation period determination and, combined with previous and future observations, to determine their spin orientation (pole position) and shape, e.g. using lightcurve inversion techniques (see e.g. Ďurech et al., 2010).

Our observations were made using the TAR network of robotic telescopes and the IAO 0.35m telescope. TAR telescope network consists of three telescopes located at Teide Observatory (Tenerife, Canary Islands, Spain, at 2390 meters above sea level). Two (TAR1 and TAR2) are 0.46-meter *f*/2.8 telescopes; TAR 3 is a 0.40-meter *f*/10 telescope. TAR1 and TAR2 use an SBIG ST11000 CCD camera with 4008x2672 pixels. The plate scale is 1.5 arcsec/pix. TAR 3 is equipped with an FLI MicroLine fitted with an E2V CCD47-10, 1024x1024 pixels. Combined with a focal reducer, the system has a plate scale of 1.5 arcsec/pixels.

Isaac Aznar Observatory (IAO) is located in Alcublas, Valencia, Spain, at an altitude of 870 meters and under dark skies (21.7 mag/arcsec^2 on average). It has a 0.35-meter telescope with an SBIG STL 1001+AO camera. The CCD is 1024x1024 pixels with a plate scale of 1.45 arsec/pixel.

A series of images, typically of 60s exposure time, were obtained in 1x1 binning mode and without any filter on different nights. Images were bias, dark, and flat field corrected using bias, dark, and twilight sky flat-fields obtained during the same night using the corrections routines included in *MaximDL*.

Aperture photometry was done using *MPO Canopus*. The Comp Star Selector utility in *MPO Canopus* found up to five comparison stars of near solar-color allowing to obtain accurate differential and calibrated photometry. The comp star magnitudes were taken from the APASS (Henden et al., 2009) and MPOSC3 catalogs, depending on the availability of comparison stars. The nightly zero points for both catalogs have been found to be generally consistent to about ± 0.05 mag or better, but on occasion reach 0.1 mag and more.

The StarBGone star subtraction algorithm in *MPO Canopus* was used when needed in order to remove the effect of stars located in the asteroid's path. This is most effective when the star's SNR is equal to or lower than asteroid's SNR (Aznar, 2013). The rotation period analysis was doing using the FALC period analysis algorithm developed by Harris (Harris et al., 1989) also included in *MPO Canopus*.

In Table I, we list the date of the observations, the derived rotation period, amplitude of the lightcurve, the axis ratio for an assumed triaxial ellipsoid *a/b*, and the telescope used. The ellipsoid is assumed to be $a > b$ and the rotation is about the *c*-axis (Harris and Lupishko, 1989). These were derived after reducing the lightcurve amplitude to zero phase angle (Zappala et al., 1980).

We note that for the axis size relationship, we have assumed an equator-on viewing geometry. In this case, the *a/b* ratio is a lower limit since it depends in the observing geometry. More observations made in future are necessary to determine the proper shape of the asteroid.

261 Prymno. This asteroid was discovered in 1886. During the last years of the 20th century, this target was analyzed several times using photometric techniques. All recent measurements match with a rotation period of 9.44 h. We found a similar period (9.44 ± 0.01 h) based on 187 data points over one unique session. The main difference with respect to previous lightcurves is the amplitude. In our case the maximum amplitude reaches 0.23 mag, thus *a/b* = 1.20.

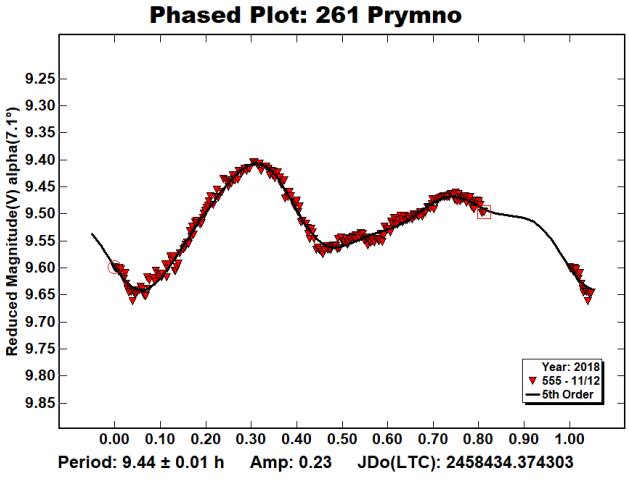

338 Budrosa. All previous analysis indicates a rotation period of about 4.608 h, e.g., Behrend (2016) and Hamanowa and Hamanowa (2011). We report a period of 4.6079 ± 0.0005 h based on a lightcurve with 420 data points. Previous results found a maximum amplitude of 0.46 mag; we found a maximum amplitude of 0.07 mag. L_{PAB} = 171°. The *a/b* axis relationship is 1.06.

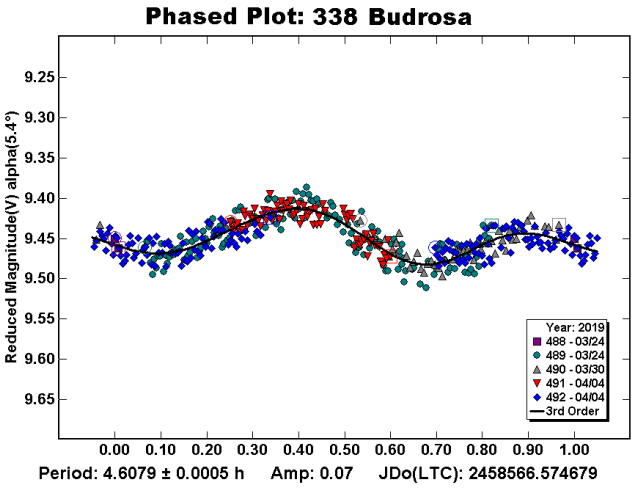

714 Ulula. The rotation period of 6.9938 ± 0.0412 h reported here matches the period reported in Lightcurve Database (LCDB; Warner et al., 2009). This period was based on data from one night. Since 1990 this asteroid has been analyzed ten times with different maximum lightcurve amplitudes, from 0.02 in 2008 to 0.65 mag in 2005 (Marciniak, 2011).

Ulula has a pole and shape determination based on lightcurve inversion techniques in the DAMIT database (*http://astro.troja.mff.cuni.cz/projects/damit* by Ďurech et al., 2010). Our lightcurve has a shape and amplitude, 0.17 mag, that is similar to that expected using the DAMIT shape model and pole (Fig. 1). L_{PAB} = 83°, *a/b* = 1.14.

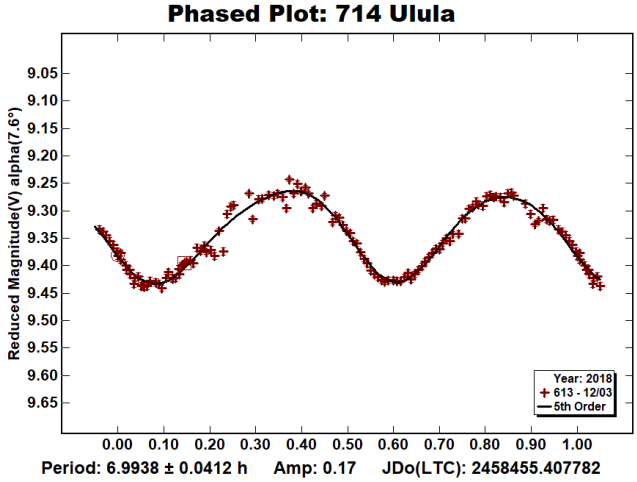

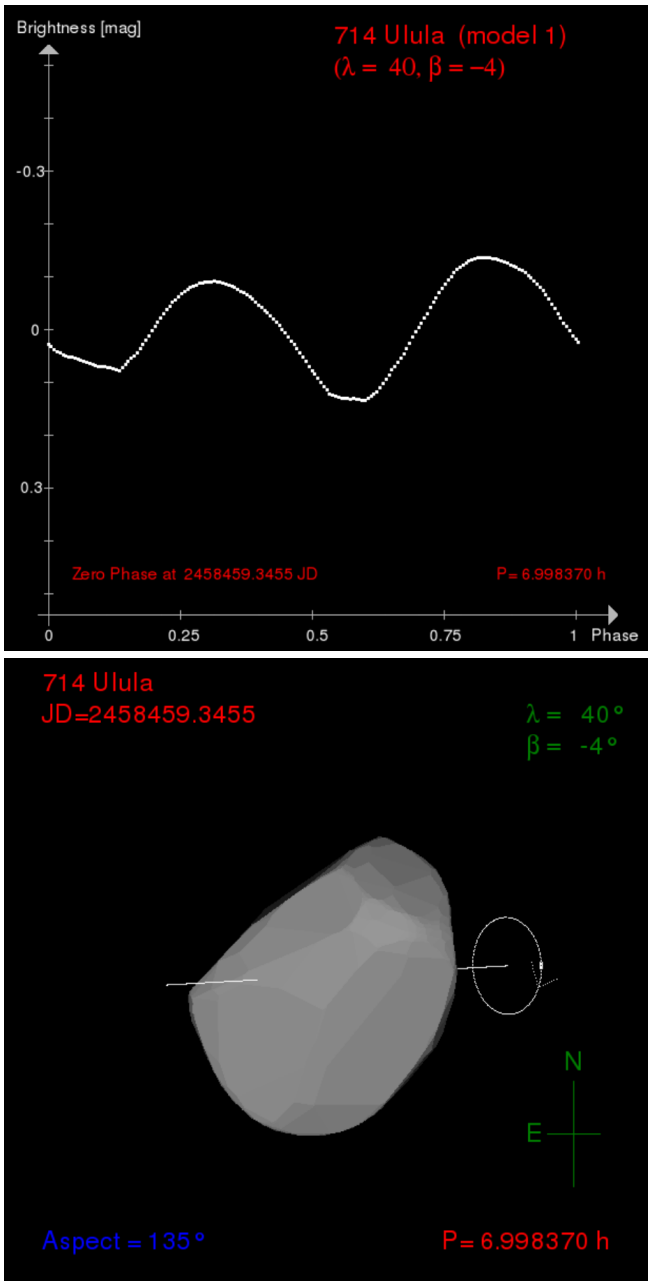

Figure 1. Expected lightcurve of 714 Ulula for the date of our observations (upper figure) produced with the shape model in the DAMIT database (lower figure). The images are produced using the Interactive Service for Asteroid Models (*http://isam.astro.amu.edu.pl/*).

2956 Yeomans. There are three entries in LCDB regarding this main-belt asteroid. It was first analyzed in 2015 (Aznar, 2015) with a rotation period of 3.40 h. A few years later, it was analyzed again (Waszczak et al., 2015; Oey, 2018), both authors suggested different rotation period values.

Our photometric work during 2019 derived a rotation period of 3.57 ± 0.01 h and a maximum lightcurve amplitude of 0.27 mag. L_{PAB} = 241°. The *a/b* axis relationship is 1.10.

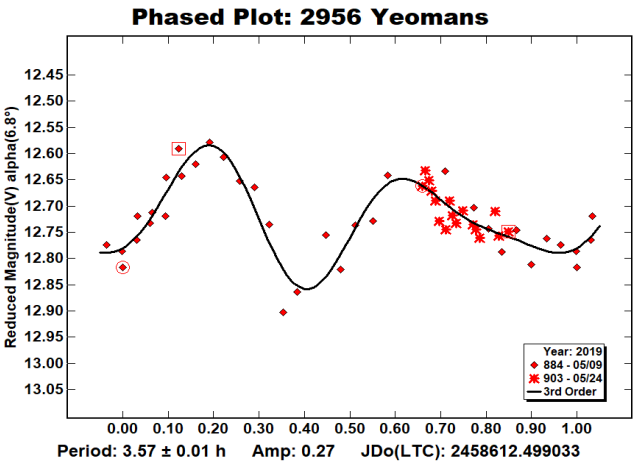

3147 Samantha. There is no entry in the most recent release of the lightcurve database (LCDB; Warner et al., 2009) for this main-belt asteroid. We report a rotation period of 5.2724 ± 0.0136 h from one observing session. The lightcurve shows a maximum amplitude of 0.62 mag, which suggests a very elongated shape (*a*/*b* = 1.68) for this asteroid.

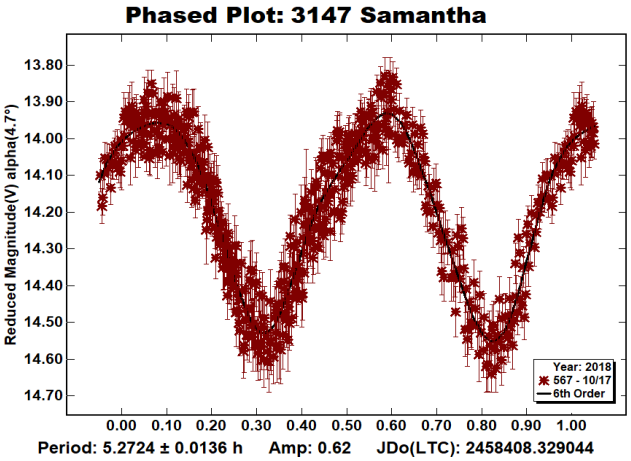

6329 Hikonejyo. The LCDB reports two different rotation periods for this object: 6.064 h (Behrend, 2012) and 8.066 h (Klinglesmith, 2012). Analysis of data obtained from 2019 May 11-25 provides a rotation period of 6.064 ± 0.003 h. The lightcurve shows a maximum amplitude of 0.15 mag. L_{PAB} = 225°. The *a*/*b* axis relationship is 1.13.

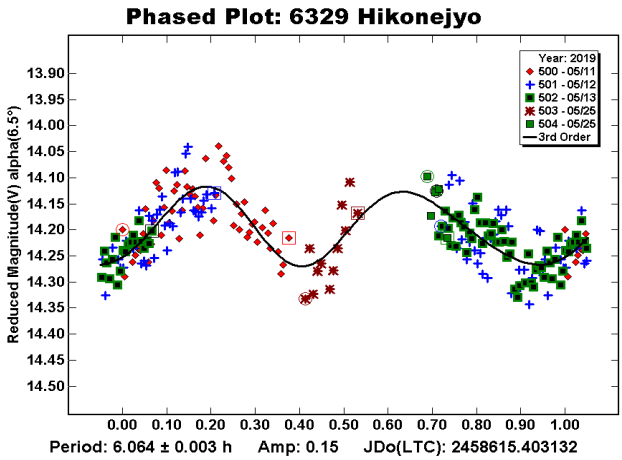

7673 Inohara. This the rotation period for this main-belt asteroid did not appear to be known prior to our work. We obtained a rotation period of 3.4 ± 0.01 h. This period should be considered as provisional. More data are necessary during future apparitions in order to confirm it. The lightcurve shows a maximum amplitude of 0.23 mag. L_{PAB} = 91°. The *a*/*b* axis relationship is 1.22.

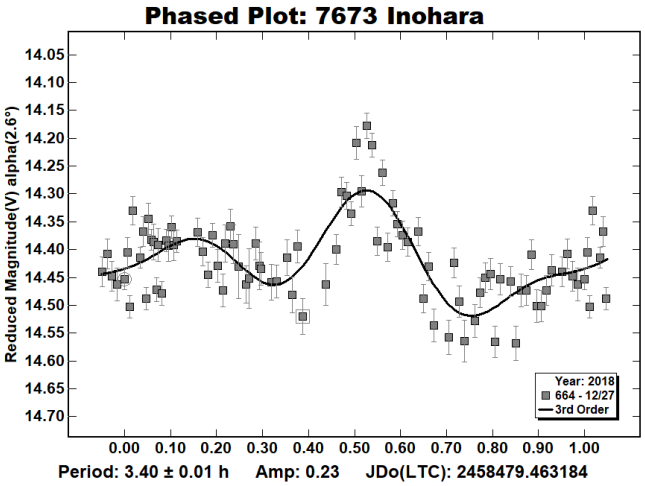

10997 Gahm. There are three entries in the LCDB for this asteroid. All of them match with a rotation period of about 3.2 h. We have calculated a rotation period of 3.209 ± 0.006 h and amplitude of 0.57 mag. The lightcurve shows a typical bimodal shape and its amplitude maximum suggests a very elongated shape for this asteroid. The *a*/*b* axis relationship is 1.58.

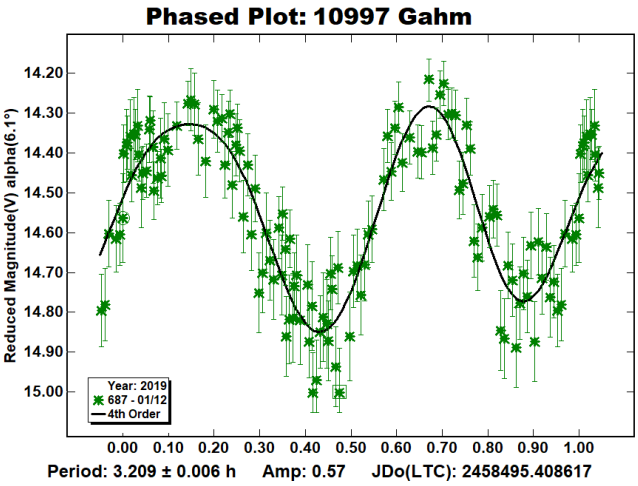

14105 Nakadai. There is no entry in the LCDB for this asteroid. We report a lightcurve composed of 211 points that has a period of 6.674 ± 0.049 h. The amplitude of 0.70 mag suggests a very elongated shape for this asteroid. L_{PAB} = 67°. The *a/b* axis relationship is 1.80

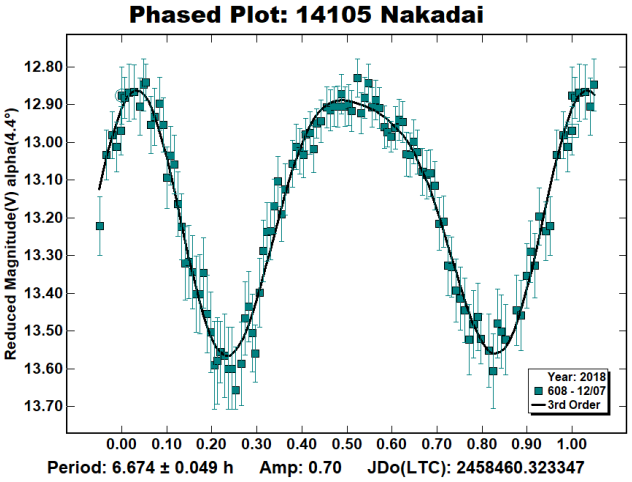

15925 Rokycany. This is a 6.4-km asteroid discovered in 1997 by L. Šarounová at Ondřejov observatory. No previous lightcurves of Rockycany are published, so this is the first photometric analysis of this asteroid.

We found a period of 3.01 ± 0.001 h based on 325 data points over one unique session. Its maximum amplitude suggests a moderate ellipsoidal shape when assuming an equatorial view of the asteroid. The *a/b* axis relationship is 1.14.

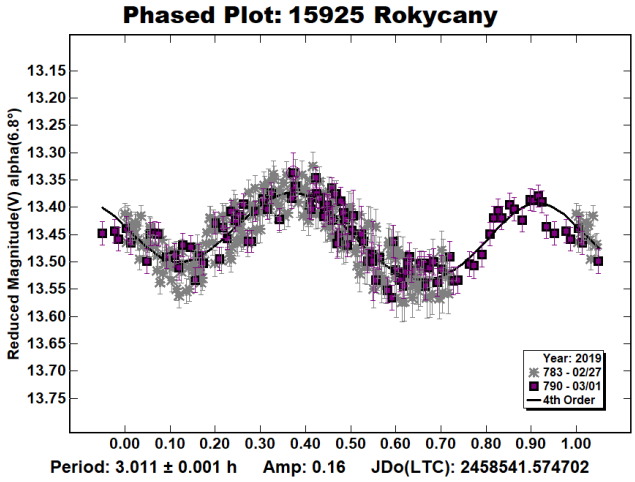

(33729) 1999 NJ21. This is a 12-km asteroid discovered in 1999 by LINEAR survey. There is no entry in the latest release of the LCDB.

We observed this target during one night only, 2018 Nov 3. The derived rotation period is 4.56 ± 0.27 h based on 178 points. The curve shows a typical bimodal shape with a maximum amplitude of 0.12 magnitudes at L_{PAB} = 27°. This suggests a very moderate ellipsoid asteroid shape. We recommend new observations in future apparitions for the purpose of supplementing this analysis. The *a/b* axis relationship is 1.01.

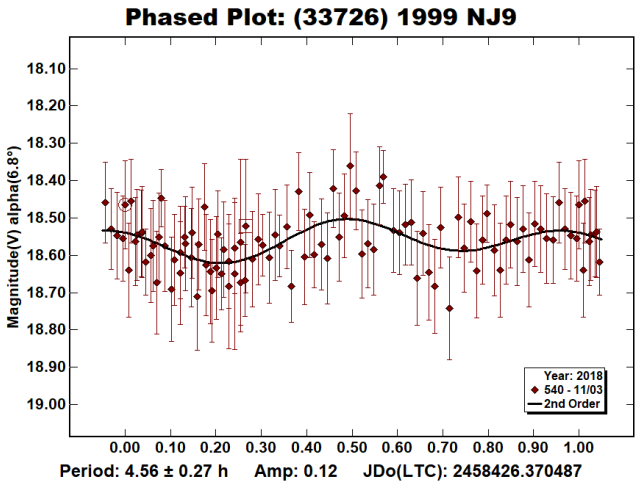

(62836) 2000 UC59. This is a main-belt asteroid with an estimated diameter of 3.4 km; it was discovered in 2000 by the LINEAR survey. There is no published photometric study of this asteroid. After six nights of observing, we concluded that the rotation period is around 10.73 ± 0.01 h. More data are needed in order to improve this determination.

The lightcurve obtained shows a maximum amplitude of 0.88 mag at L_{PAB} = 190°. This amplitude suggests a very elongated shape. The *a/b* axis relationship is 2.12.

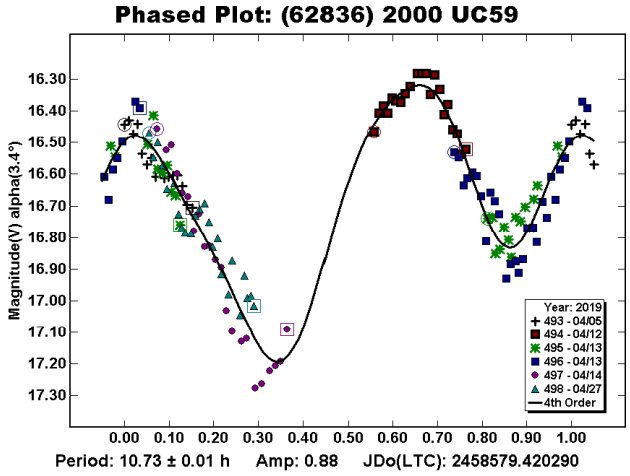

Acknowledgements

I would like to express my gratitude to Brian Warner for supporting LCDB as the main database for study of asteroids. Thanks to Solar System Group of Instituto de Astrofísica de Canarias for the effort supporting this work. Thanks to J. Licandro and M. Serra-Ricart acknowledge support from the AYA2015-67772-R project (MINECO, Spain).

References

Aznar. A. (2013). "Lightcurve of 3422 Reid Using Star Subtraction Techniques." *Minor Planet Bull*. **40**, 214-215.

Aznar. A. (2015). "Asteroid Lightcurve Analysis at Isaac Aznar Observatory." *Minor Planet Bull*. **42,** 4–6.

Behrend, R. (2012, 2016) Observatoire de Geneve web site. *http://obswww.unige.ch/~behrend/page_cou.html*

Ďurech J.; Sidorin, V.; Kaasalainen, M. (2010). "DAMIT: a database of asteroid models." *Astron. Astrophys.* **513**, A46.

Harris, A.W.; Lupishko, D.F. (1989). "Photometric lightcurve observations and reduction techniques." in *Asteroids II* (R.P. Binzel, T. Gehrels, M.S. Matthews eds.) pp. 39-53. University of Arizona Press. Tucson, AZ.

Hamanowa, H.; Hamanowa, H. (2011). *http://www2.ocn.ne.jp/~hamaten/astlcdata.htm*

Harris, A.W.; Young, J.W.; Scaltriti, F.; Zappala, V. (1984). "Lightcurves and phase relations of the asteroids 82 Alkmene and 444 Gyptis." *Icarus* **57**, 251-258.

Harris, A.W.; Young, J.W.; Bowell, E.; Martin, L.J.; Millis, R.L.; Poutanen, M.: Scaltriti, F.; Zappala, V.; Schober, H.J.; Debehogne, H.; Zeigler, K.W. (1989). "Photoelectric Observations of Asteroids 3, 24, 60, 261, and 863." *Icarus* **77**, 171-186.

Henden, A.A.; Terrell, D.; Levine, S.E.; Templeton, M.; Smith, T.C.; Welch, D.L. (2009). *http://www.aavso.org/apass*

Marciniak, A.; Michałowski, T.; Polińska, M.; Bartczak, P.; Hirsch, R.; Sobkowiak, K.; Kamiński, K.; Fagas, M.; Behrend, R.; Bernasconi, L.; Bosch, J. -G.; Brunetto, L.; Choisay, F.; Coloma, J.; Conjat, M.; Farroni, G.; Manzini, F.; Pallares, H.; Roy, R.; Kwiatkowski, T. Kryszczyńska, A.; Rudawska, R.; Starczewski, S.; Michałowski, J.; Ludick, P. (2011). "Photometry and models of selected main belt asteroids. VIII. Low-pole asteroids." *Astron. Astrophys.* **529**, A107.

Oey, J.; Groom, R. (2018). "Lightcurve Analysis of Main-belt Asteroids from BMO and DRO in 2016: I." *Minor Planet Bull*. **45**, 363-366.

Warner, B.D.; Harris, A.W.; Pravec, P. (2009). "The asteroid lightcurve database." *Icarus* **202**, 134-146. Updated 2019 Jan. *http://www.MinorPlanet.info/lightcurvedatabase.html*

Waszczak, A.; Chang, C.-K.; Ofek, E.O.; Laher, R.; Masci, F.; Levitan, D.; Surace, J.; Cheng, Y.-C.; Ip, W.-H.; Kinoshita, D.; Helou, G.; Prince, T.A.; Kulkarni, S. (2015). "Asteroid Light Curves from the Palomar Transient Factory Survey: Rotation Periods and Phase Functions from Sparse Photometry." *Astron. J.* **150**, A75.

Zappala, V.; Cellini, A.; Barucci, A.M.; Fulchignoni, M.; Lupishko, D.E. (1990). "An analysis of the amplitude-phase relationship among asteroids." *Astron. Astrophys*. **231**, 548-560.

Number	Name	20xx mm/dd	Phase	L_{PAB}	B_{PAB}	Period (h)	P.E.	Amp	A.E.	a/b	Scope
261	Prymno	18/11/12-11/12	7.2	63	38	9.44	0.01	0.23	0.01	1.20	TAR 2
338	Budrosa	19/03/24-04/04	5.3,9.0	171	-7	4.6079	0.0005	0.07	0.01	1.06	OIA
714	Ulula	18/12/03-12/03	7.6	83	8	6.9938	0.0041	0.17	0.01	1.14	TAR 2
2956	Yeomans	19/05/09-05/24	6.8,1.5	241	3	3.57	0.01	0.27	0.03	1.10	TAR 2
3147	Samantha	18/10/17-10/17	4.6	14	2	5.2724	0.0136	0.62	0.02	1.68	TAR 2
6329	Hikonejyo	19/05/11-05/25	6.5,11.6	225	9	6.064	0.003	0.15	0.03	1.13	OIA
7673	Inohara	18/12/27-12/27	2.6	91	-9	3.40	0.01	0.23	0.03	1.22	TAR 3
10997	Gahm	19/01/12-01/12	6.1	125	2	3.209	0.006	0.57	0.09	1.58	TAR 3
14105	Nakadai	18/12/07-12/07	4.1	67	-7	6.674	0.049	0.70	0.05	1.80	TAR 3
15925	Rokycany	19/02/27-03/04	6.8	160	-13	3.011	0.001	0.16	0.03	1.14	TAR 1
33729	1999 NJ21	18/11/09-11/09	6.5	27	8	4.56	0.27	0.12	0.08	1.01	TAR 1
62836	2000 UC59	19/04/05-04/27	2.8,14.8	190	-2	10.73	0.01	0.88	0.06	2.12	OIA

Table I. Observing circumstances and results. Pts is the number of data points used in the analysis. The phase angle values are for the first. L_{PAB} and B_{PAB} are the average phase angle bisector longitude and latitude. Period is in hours. Amp is peak-to-peak amplitude in magnitudes. The last column gives the a/b ratio for an assumed triaxial ellipsoid viewed equatorially based on the amplitude.

PHOTOMETRIC OBSERVATIONS OF SEVENTEEN MINOR PLANETS

Tom Polakis
Command Module Observatory
121 W. Alameda Dr.
Tempe, AZ 85282 USA
tpolakis@cox.net

(Received: 2019 June 20)

Lightcurves and synodic rotation periods are presented for 15 main-belt asteroids. Results are: 722 Frieda, 131.1 ± 0.2 h; 856 Backlunda, 11.965 ± 0.007 h; 1178 Irmela, 11.985 ± 0.004 h; 1199 Geldonia, 57.82 ± 0.21 h; 1397 Umtata, 240.6 ± 0.8 h; 1483 Hakoila, 239.1 ± 0.9 h; 1516 Henry, 17.599 ± 0.014 h; 1517 Beograd, 6.945 ± 0.014 h; 1558 Jarnefelt, 6.252 ± 0.003 h; 1914 Hartbeespoortdam, 6.330 ± 0.009 h; 2396 Kochi, 26.17 ± 0.11 h; 2433 Sootiyo, 7.234 ± 0.004 h; 2784 Domeyko, 6.025 ± 0.009 h; 3570 Wuyeesun, 15.432 ± 0.006 h; 5262 Brucegoldberg, 16.428 ± 0.008 h. No period solutions were found for 805 Hormuthia or 904 Rockefellia. All data were submitted to the ALCDEF database.

CCD photometric observations of seventeen main-belt asteroids were performed at Command Module Observatory (MPC V02) in Tempe, AZ. Images were taken using a 0.32-m *f*/6.7 modified Dall-Kirkham telescope, SBIG STXL-6303 CCD camera, and a 'clear' glass filter. Exposure time for all images was 2 min. The image scale was 1.76 arcsec/pixel (2x2 binning). Table I shows the observing circumstances and results. All of images for these seventeen asteroids were obtained between 2019 April and June.

Images were calibrated using a dozen bias, dark, and flat frames. Flat-field images were made using an electroluminescent panel. Image calibration and alignment was performed using *MaxIm DL* software.

The data reduction and period analysis were done using *MPO Canopus* (Warner, 2019). The 45x30 arcmin field of the CCD typically enables using the same field center for three consecutive nights. In these fields, the asteroid and three to five comparison stars were measured. Comparison stars were selected with colors within the range of 0.5 < B-V < 0.95 to correspond with color ranges of asteroids. In order to reduce the internal scatter in the data, the brightest stars of appropriate color that had peak ADU counts below the range where chip response becomes nonlinear were selected. The *MPO Canopus* internal star catalogue was useful in selecting comp stars of suitable color and brightness.

Since the sensitivity of the KAF-6303 chip peaks in the red, the clear-filtered images were reduced to Sloan r′ to minimize color term errors. Comp star magnitudes were derived from a combination of CMC15 (Muiñoz et al., 2014), APASS DR9 (Munari et al., 2015), and GAIA2 G (Sloan r′ = G for stars of asteroidal color) catalogues to set the zero-points each night. In most regions, the Sloan r′ data sources for brighter stars yielded very similar magnitudes (within about 0.05 mag total range), so mean values rounded to 0.01 mag precision were used.

This careful adjustment of the comp star magnitudes and color-indices allowed the separate nightly runs to be linked often with no zero-point offset required, or shifts of only a few hundredths of a magnitude in a series.

A 9-pixel (16 arcsec) diameter measuring aperture was used for asteroids and comp stars. It was typically necessary to employ star subtraction to remove contamination by field stars. For the asteroids described here, the RMS scatter on the phased lightcurves gives an indication of the overall data quality including errors from the calibration of the frames, measurement of the comp stars, the asteroid itself, and the period-fit. Period determination was done using the *MPO Canopus* Fourier-type FALC fitting method (Harris et al., 1989). Phased lightcurves show the maximum at phase zero. Magnitudes in these plots are apparent and scaled by *MPO Canopus* to the first night.

Asteroids were selected from the CALL website (Warner, 2011) using the criteria of magnitude greater than 15.0 and quality of results U < 2+. In this set of observations, 2 of the 17 asteroids had no previous period analysis, and two had U = 1.

The Asteroid Lightcurve Database (LCDB; Warner et al., 2009) was consulted to locate previously published results. All the new data for these 17 asteroids can be found in the ALCDEF database.

Number	Name	2019 /mm/dd	Phase	L_{PAB}	B_{PAB}	Period (h)	P.E.	Amp	A.E.	Grp
722	Frieda	04/23-05/04	*3.9,8.6	209	2	131.1	0.2	0.45	0.05	FLOR
805	Hormuthia	06/07-06/12	13.5,14.8	256	18	-	-	-	-	MB-O
856	Backlunda	05/26-05/31	10.5,9.6	234	16	11.965	0.007	0.09	0.02	MB-I
904	Rockefellia	04/01-04/22	*2.9,5.3	198	0	-	-	-	-	MB-O
1178	Irmela	04/03-04/11	7.7,4.3	206	5	11.985	0.004	0.25	0.04	MB-M
1199	Geldonia	05/26-06/03	4.3,1.8	255	3	57.82	0.21	0.20	0.04	EOS
1397	Umtata	04/01-04/25	*5.2,7.4	200	4	240.6	0.8	0.35	0.03	MB-M
1483	Hakoila	05/01-05/11	*2.7,3.0	225	3	239.1	0.9	0.62	0.05	MB-O
1516	Henry	04/07-04/11	11.7,10.3	213	12	17.599	0.014	0.35	0.03	MB-M
1517	Beograd	05/03-05/08	*1.4,1.7	224	2	6.945	0.014	0.09	0.04	MB-O
1558	Jarnefelt	06/04-06/09	*2.8,2.9	255	8	6.252	0.003	0.28	0.06	MB-O
1914	Hartbeespoortdam	05/05-05/08	8.7,7.4	236	8	6.330	0.009	0.11	0.02	V
2396	Kochi	*06/04-06/12	10.0,12.1	239	16	26.17	0.11	0.26	0.07	MB-O
2433	Sootiyo	04/23-04/25	8.5,7.7	224	8	7.234	0.004	0.38	0.02	MB-M
2784	Domeyko	06/01-06/03	7.8,6.8	260	5	6.025	0.009	0.22	0.05	FLOR
3570	Wuyeesun	05/26-06/23	*3.6,8.2	252	3	15.432	0.006	0.45	0.01	EOS
5262	Brucegoldberg	04/26-05/02	8.4,7.3	225	15	16.428	0.008	0.43	0.05	MB-O

Table I. Observing circumstances and results. *Observations in 2018. The phase angle (α) is given at the start and end of each date range, and marked with an asterisk if it reached a minimum between the two values. LPAB and BPAB are each the average phase angle bisector longitude and latitude (see Harris et al., 1984). Grp is the asteroid family/group (Warner et al., 2009). FLOR: Flora; MB-I/M/O: main-belt inner/middle/outer. V: Vestoid.

722 Frieda is a Flora-family asteroid that was discovered by Johann Palisa at Vienna in 1911. No rotation periods for it have been published. During 14 observing nights, 892 images were gathered, supporting a synodic period of 131.1 ± 0.2 h. The amplitude is 0.45 ± 0.05 mag; the RMS scatter on the fit shown in the phased plot is 0.051 mag.

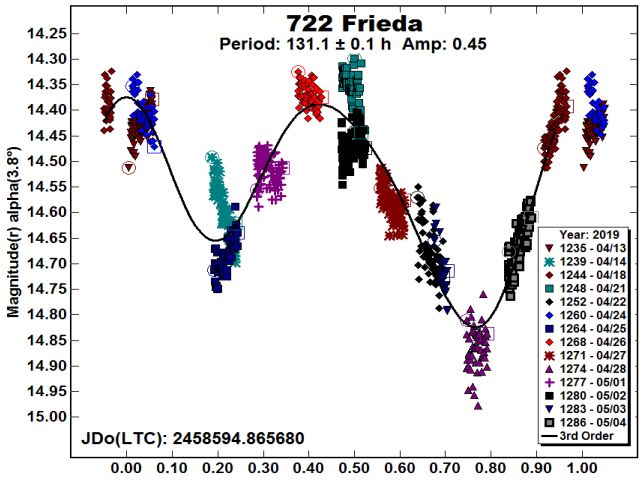

805 Hormuthia. Max Wolf made this discovery at Heidelberg in 1915. Behrend (2008) found a period of 8 h, while Pilcher and Benishek (2009) used a denser observation set to find 9.510 ± 0.001 h.

A total of 268 images taken during six nights showed that an unambiguous period solution would not be found. The period spectrum has no significant minima out to 20 h and the raw lightcurve does not show a gradual change in brightness that one would associate with a slow rotator. Follow-up study with a larger telescope, or at a higher phase angle is encouraged.

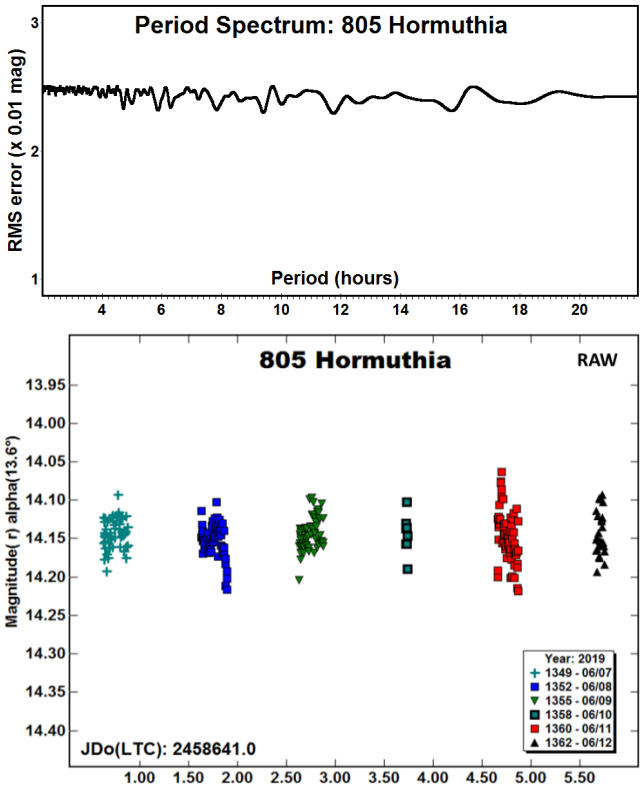

856 Backlunda. Sergey Belyavsky discovered this minor planet from Simeis in 1916. Three similar period solutions appear in the LCDB. They are: Binzel (1987) 12.08 h, Behrend (2007) 12.02 ± 0.05 h, and Hanus (2016) 12.02894 ± 0.00005 h.

During five nights, 234 data points were collected. A period of 11.965 ± 0.007 h was obtained, in agreement with published values. Since this rotation period is so close to half an Earth day, only half of the phase coverage could be obtained. The full amplitude in this region is 0.09 ± 0.02 mag, and the RMS scatter of the fit is 0.020 mag.

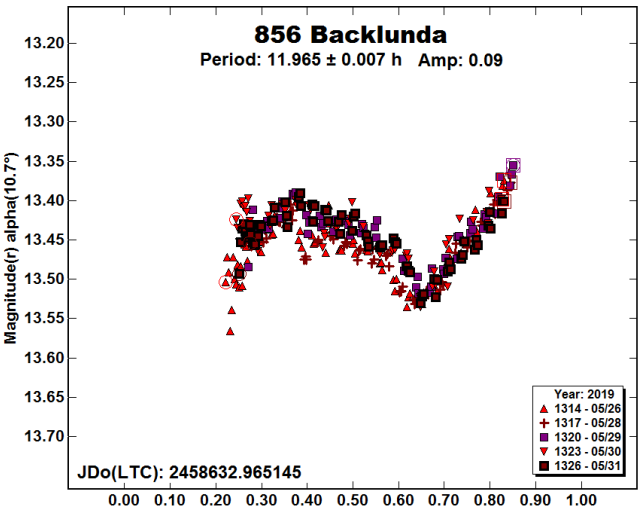

904 Rockefellia was discovered by Max Wolf at Heidelberg in 1918. Three dissimilar period solutions have been published. Fauvaud and Fauvaud (2013) published 5.82 ± 0.01 h, Behrend (2014) shows 12.72 ± 0.05 h, and Polakis (2018) obtained 6.826 ± 0.004 h.

The minor planet was monitored during 13 nights, and 514 images were recorded. While the period spectrum did show some minima, none of these correspond with a phased lightcurve with acceptable RMS error. A raw lightcurve for a typical night of observations is shown, in which all the data points lie in a band of roughly 0.1 mag. Again, follow-up observations may resolve this object's ambiguous period.

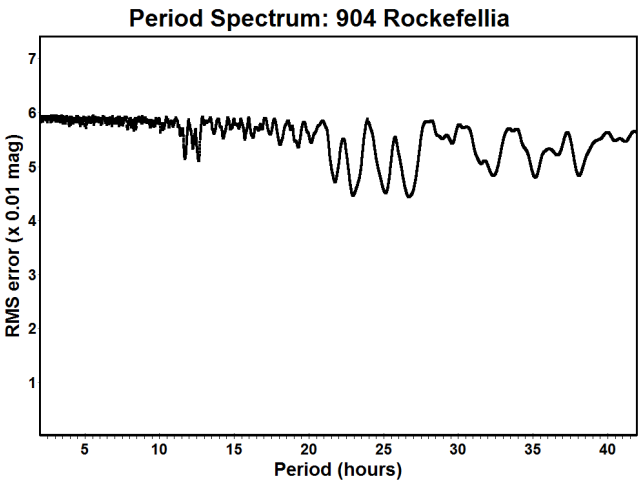

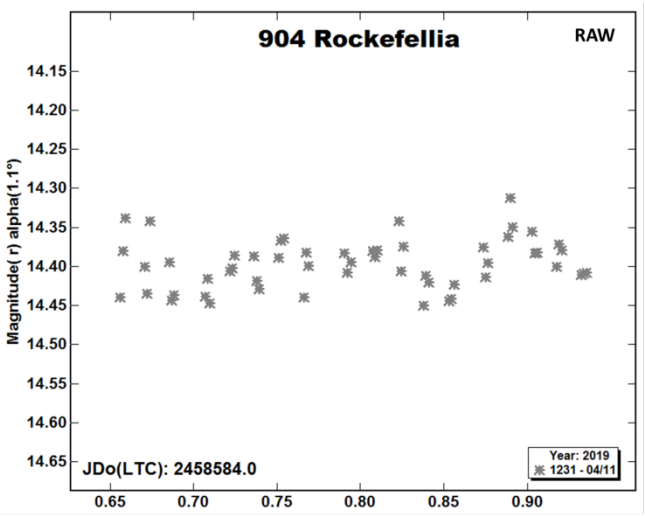

1178 Irmela is another of Max Wolf's discoveries. *Binzel (1987) published a period of 19.17 h*. Much more recently, Stephens (2012) computed 11.989 ± 0.001 h and was able to show half of the phase coverage.

During four nights, 198 images were sufficient to produce a satisfactory period solution of 11.985 ± 0.004 h, agreeing with Stephens' result. Again, it was possible to obtain only half of the phase coverage. The RMS scatter on the fit is 0.037 mag. The amplitude is 0.25 ± 0.04 mag.

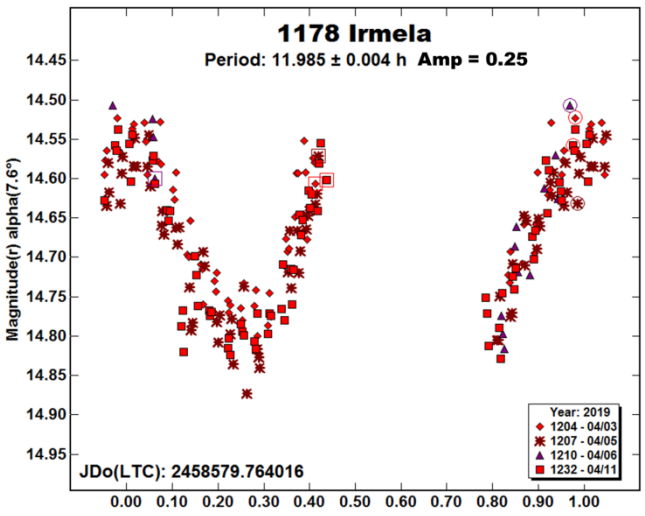

1199 Geldonia. This minor planet was discovered in 1931 by Eugène Joseph Delporte while working at Uccle. Behrend (2010) shows a synodic period of 28.3 ± 0.2 h; Durech (2018) published a value of 57.969 ± 0.002 h.

A total of 426 images were taken during eight nights. The period analysis produced a result of 57.82 ± 0.21 h, which is in good agreement with Durech. The amplitude of the lightcurve is 0.20 ± 0.04 mag and the RMS error on the fit is 0.041 mag.

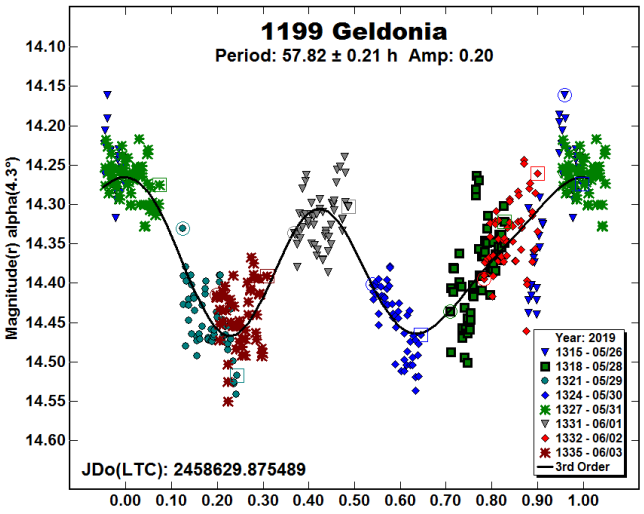

1397 Umtata was discovered at Johannesburg by Cyril Jackson in 1936. The only rotation period in the LCDB is that of Binzel (1987), who published a value of 30 h.

The minor planet revolves in an eccentric orbit and was observed around a favorable opposition on 17 nights in 2019 April. During this period, 543 data points were collected. The slow rotator has a period of 240.6 ± 0.8 h, which disagrees with Binzel's value. The lightcurve shows an amplitude of 0.35 ± 0.03 mag with an RMS error on the fit of 0.028 mag.

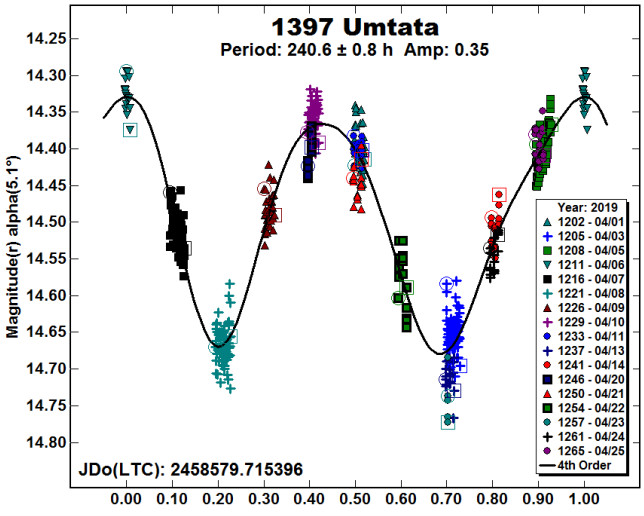

1483 Hakoila is an outer-belt asteroid discovered at Turku in 1938 by Yrjö Väisälä and named for his assistant. Only one analysis has been published, that of Behrend (2010) who shows >12 h.

This is another slow rotator, requiring 11 nights and 491 images to arrive at the unique solution of 239.1 ± 0.9 h. The Fourier fit shows an RMS error of 0.051 mag on a lightcurve with an amplitude of 0.62 ± 0.05 mag.

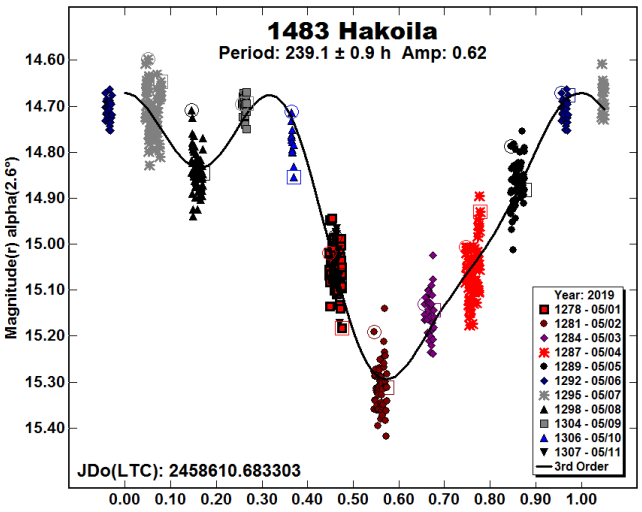

1516 Henry was discovered in 1938 at Nice by André Petry. Behrend (2002) obtained a period of 17.370 ± 0.006 h.

A total of 213 images were acquired during five nights, resulting in a good solution of 17.599 ± 0.014 h, agreeing with Behrend. The lightcurve's amplitude is 0.35 ± 0.03 mag and the RMS error of the curve fit is 0.032 mag.

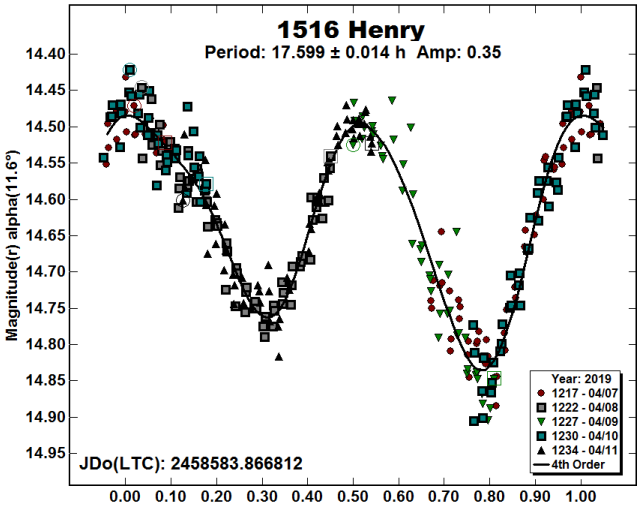

1517 Beograd. The discovery of this outer-belt asteroid was made at Belgrade in 1938 by Milorad Protić. Behrend (2005) and Benishek and Pilcher (2014) both studied the asteroid and found similar periods of 6.943 ± 0.004 and 6.9490 ± 0.0006 h, respectively.

During six nights, 224 data points were acquired, revealing a low amplitude. The period solution produced a value of 6.945 ± 0.014 h using binning of sets of three points shown in the figure. The RMS error of 0.035 mag is significant relative to the amplitude of 0.09 ± 0.04 mag, but the period solution closely matches previous assessments.

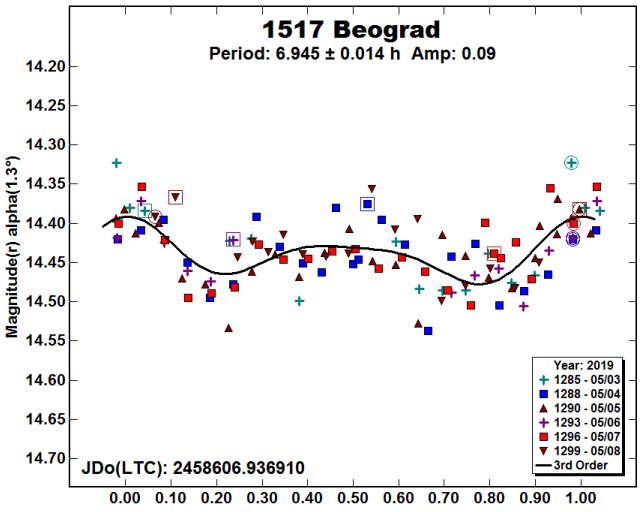

1558 Jarnefelt. This outer-belt asteroid was discovered in 1942 by Liisi Oterma at Turku. Only one period, by Hawkins and Ditteon (2008), is in the LCDB: 18.22 ± 0.06 h.

The asteroid was monitored on six nights, during which 255 images were obtained. A 4th-order fit produced a period of 6.252 ± 0.003 h, disagreeing with Oterma's result. The RMS error is 0.060 mag and the amplitude is 0.28 ± 0.06 mag.

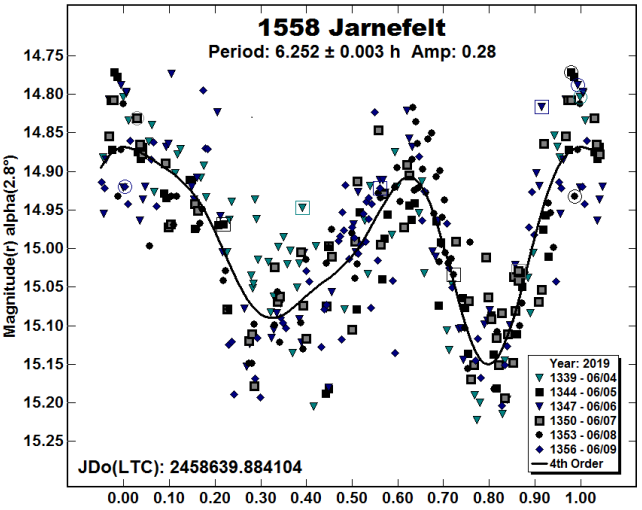

1914 Hartbeespoortdam is a Vestoid that was discovered at Johannesburg in 1938 by Hendrik Van Gent. Pravec (2015) published a synodic period of 6.331 ± 0.003 h.

Four nights and 173 images were sufficient to assess its short period of 6.330 ± 0.009 h, in good agreement with Pravec. The amplitude of the fit is 0.11 ± 0.02 mag and the RMS scatter of the curve fit is 0.020 mag. The lightcurve shows binned sets of three data points.

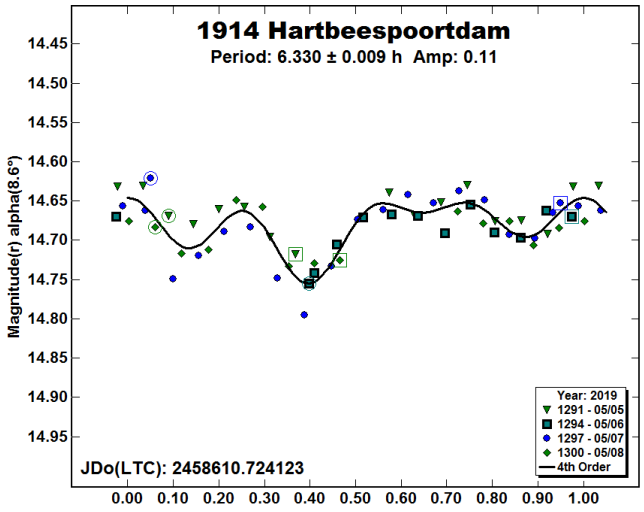

2396 Kochi. The discovery of this outer-belt minor planet was made by Tsutomu Seki in 1981 at Geisei. There are no published periods.

Observations were made on nine nights, and 439 images were obtained. The period spectrum shows a minimum point corresponding with a bimodal solution at 26.17 ± 0.11 h. The amplitude is 0.26 ± 0.07 mag, and the RMS scatter of the curve fit is 0.068 mag.

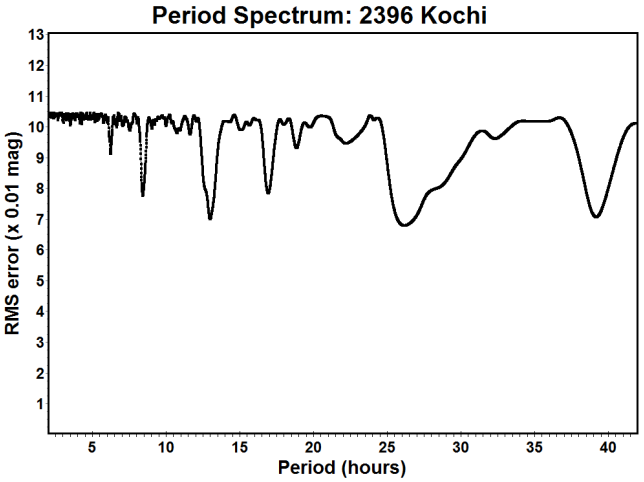

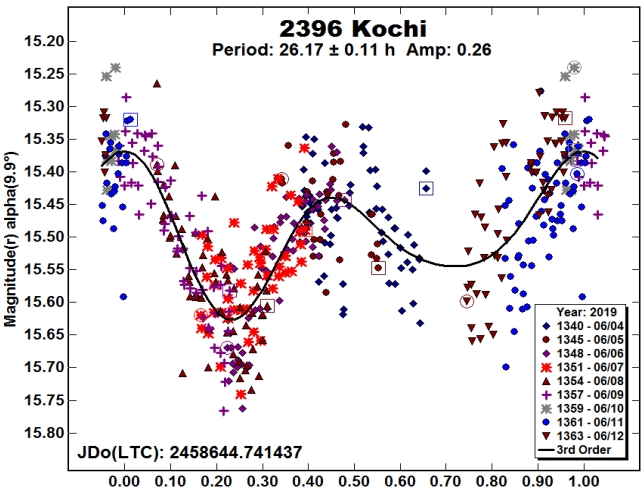

2433 Sootiyo was discovered at Lowell in 1981 by Ted Bowell. Its name is Hopi for "star boy." Both Angeli (2001) and Behrend (2007) show a period of 7 h. Proyecto ECLA (2011) gives the more precise value of 7.2298 ± 0.0002 h.

A total of 239 images were taken on three nights to obtain a period solution of 7.234 ± 0.004 h, in accordance with previous results. The lightcurve has a tight RMS scatter of 0.018 mag. The amplitude of the fit is 0.38 ± 0.02 mag. Due to its eccentric orbit, 2433 Sootiyo will be 70 percent farther away from earth at its next opposition.

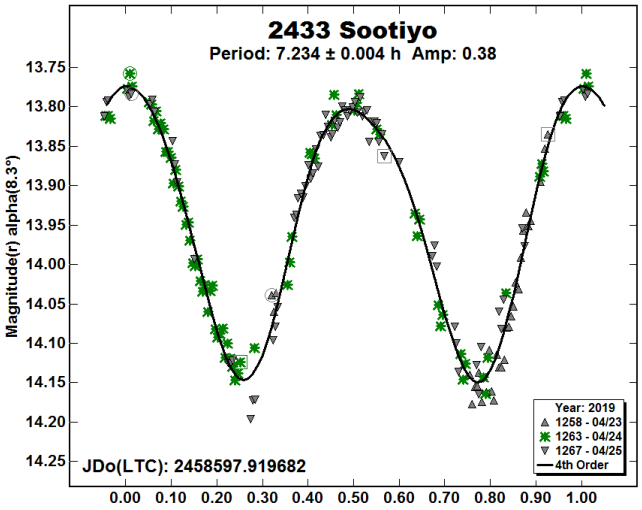

2784 Domeyko. This Flora-family asteroid was discovered by Carlos Torres at Cerro El Roble in 1974. Almeida (2004) shows a period of 5.98 h.

During three nights, 145 data points were captured. The period is 6.025 ± 0.009 h, similar to Almeida's result. The lightcurve amplitude is 0.22 ± 0.05 mag and the RMS scatter of the curve fit is 0.045 mag. Since 2784 Domeyko is also in an eccentric orbit, it will be 1.5 magnitudes fainter during the December 2020 opposition.

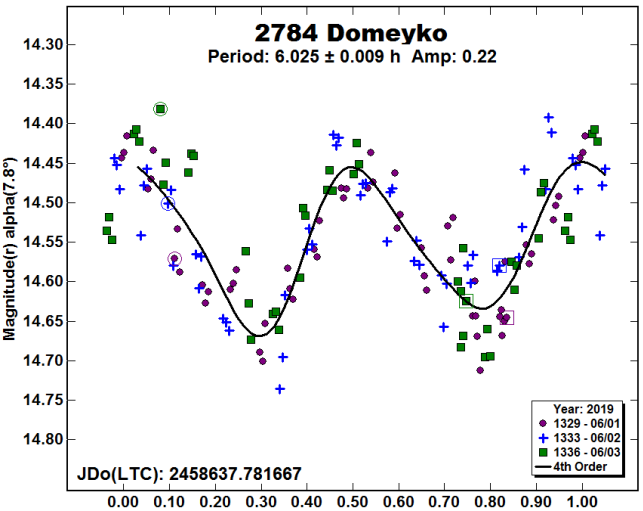

3570 Wuyeesun was discovered at Purple Mountain in 1979. The period shown by Waszczak et al. (2015) is 15.459 ± 0.0442 h.

The asteroid was followed for eight nights, and 252 images were captured. The period solution produced a value of 15.432 ± 0.006 h, in accordance with Waszczak's period. The 5th-order Fourier fit has an RMS error of 0.05 mag, and an amplitude of 0.45 ± 0.01 mag.

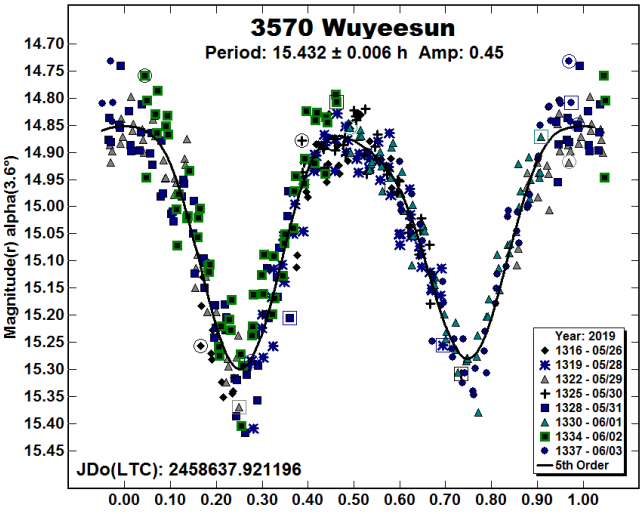

5262 Brucegoldberg. This outer-belt asteroid was discovered by Elanor Helin at Palomar in 1990. Three similar period solutions appear in the LCDB. They are: Gross (2003) 16.430 ± 0.001 h, Behrend (2008) 16.410 ± 0.001 h, and Behrend (2011) 16.422 ± 0.003 h.

A set of 225 images were taken during five nights. The period of 16.428 ± 0.008 h is in good agreement with published values. The amplitude of the lightcurve is 0.43 ± 0.05 h and the RMS error of the fit is 0.046 mag.

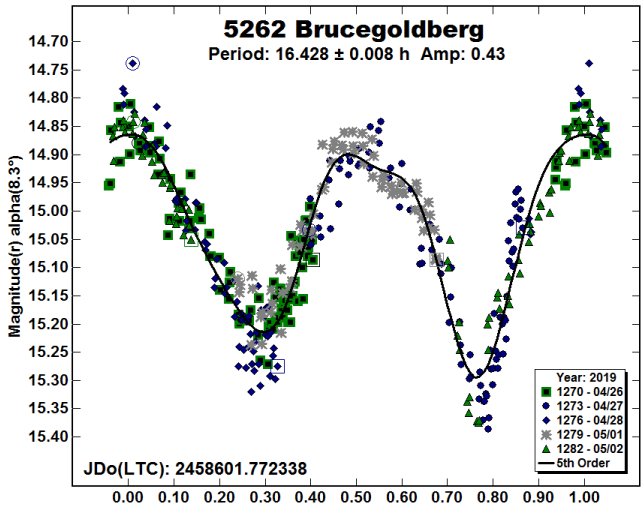

Acknowledgments

The author would like to express his gratitude to Brian Skiff for his indispensable mentoring in data acquisition and reduction. Thanks also go out to Brian Warner for support of his *MPO Canopus* software package.

References

Almeida, R.; Angeli, C.A.; Duffard, R.; Lazzaro, D. (2004). "Rotation periods for small main-belt asteroids." *Astron. Astrophys.* **415**, 403-406.

Angeli, C.A.; Guimaraes, T.A.; Lazzaro, D.; Duffard, R.; Fernandez, S.; Florczak, M.; Mothe-Diniz, T.; Varvano, J.M. (2001). "Rotation Periods for Small Main-Belt Asteroids From CCD Photometry." *Astron. J.* **121**, 2245-2252.

Behrend, R.(2002, 2005, 2007, 2008, 2010, 2014). Observatoire de Geneve web site.
http://obswww.unige.ch/~behrend/page_cou.html

Benishek, V.; Pilcher, F. (2014). "Rotation Period Determination for the Main-belt Asteroid 1517 Beograd." *Minor Planet Bull.* **41**, 263-264.

Binzel, R. (1987). "A photoelectric survey of 130 asteroids." *Icarus* **72**, 135.

Durech, J.; Hanus, J.; Ali-Lagoa, V. (2018). "Asteroid models reconstructed from the Lowell Photometric Database and WISE data." *Astron. Astrophys.* **617**, A57.

Fauvaud, S.; Fauvaud, M. (2013). "Photometry of Minor Planets. I. Rotation Periods from Lightcurve Analysis for Seven Main-belt Asteroids." *Minor Planet Bull.* **40**, 224-229.

Gross, J. (2003). "Sonoran Skies Observatory lightcurve results for asteroids 1054, 1390, 1813 1838, 2988, 3167, 4448, and 5262." *Minor Planet Bull.* **30**, 44-46.

Hanus, J.; Durech, J.; Oszkiewicz, D.A.; Behrend, R.; Carry, B.; Delbo, M.; Adam, O.; Afonina, V.; Anquetin, R.; Antonini, P.; and 159 coauthors. (2016). "New and updated convex shape models of asteroids based on optical data from a large collaboration network." *Astron. Astrophys.* **586**, A108.

Harris, A.W.; Young, J.W.; Scaltriti, F.; Zappala, V. (1984). "Lightcurves and phase relations of the asteroids 82 Alkmene and 444 Gyptis." *Icarus* **57**, 251-258.

Harris, A.W.; Young, J.W.; Bowell, E.; Martin, L.J.; Millis, R.L.; Poutanen, M.; Scaltriti, F.; Zappala, V.; Schober, H.J.; Debehogne, H.; Zeigler, K.W. (1989). "Photoelectric Observations of Asteroids 3, 24, 60, 261, and 863." *Icarus* **77**, 171-186.

Hawkins, S.; Ditteon, R. (2008). "Asteroid Lightcurve Analysis at the Oakley Observatory - May 2007." *Minor Planet Bull.* **35**, 1-4.

Muiñoz, J.L.; Evans, D.W. (2014). "The CMC15, the last issue of the series Carlsberg Meridian Catalogue, La Palma." *Astron. Nach.* **335**, 367.

Munari, U.; Henden, A.; Frigo, A.; Zwitter, T.; Bienayme, O.; Bland-Hawthorn, J.; Boeche, C.; Freeman, K.C.; Gibson, B.K.; Gilmore, G.; Grebel, E.K.; Helmi, A.; Kordopatis, G.; Levina, S.E.; and 13 coauthors. (2015). "APASS Landolt-Sloan BVgri photometry of RAVE stars. I. Data, effective temperatures, and reddenings." *Astron. J.*; **148**, 81.

Pilcher, F.; Benishek, V. (2009). "Period Determinations for 634 Ute and 805 Hormuthia." *Minor Planet Bull.* **36,** 29-30.

Polakis, T. (2018). "Lightcurve Analysis for Eleven Main-belt Asteroids." *Minor Planet Bull.* **45**, 199-203.

Pravec, P.; Wolf, M.; Sarounova, L. (2015). Ondrejov Asteroid Photometry Project web site. *http://www.asu.cas.cz/~ppravec/neo.htm*

Proyecto ECLA (Silvia Alonso Perez) (2011). *http://www.geocities.ws/proyectoecla/*

Stephens, R.D. (2012). "Asteroids Observed from GMARS and Santana Observatories: 2011 October- December." *Minor Planet Bull.* **39**, 80-82.

Warner, B.D.; Harris, A.W.; Pravec, P. (2009). "The Asteroid Lightcurve Database." *Icarus* **202**, 134-146. Updated 2019 Jan. *http://www.minorplanet.info/lightcurvedatabase.html*

Warner, B.D. (2011). Collaborative Asteroid Lightcurve Link website. *http://www.minorplanet.info/call.html*

Warner. B.D. (2019). *MPO Canopus* software. *http://bdwpublishing.com*

Waszczak, A.; Chang, C.-K.; Ofek, E.O.; Laher, R.; Masci, F.; Levitan, D.; Surace, J.; Cheng, Y.-C.; Ip, W.-H.; Kinoshita, D.; Helou, G.; Prince, T.A.; Kulkarni, S. (2015). "Asteroid Light Curves from the Palomar Transient Factory Survey: Rotation Periods and Phase Functions from Sparse Photometry." *Astron. J.* **150**, A75.

LIGHTCURVE ANALYSIS OF HILDA ASTEROIDS AT THE CENTER FOR SOLAR SYSTEM STUDIES: 2019 APRIL-JUNE

Brian D. Warner
Center for Solar System Studies / MoreData!
446 Sycamore Ave.
Eaton, CO 80615 USA
brian@MinorPlanetObserver.com

Robert D. Stephens
Center for Solar System Studies / MoreData!
Rancho Cucamonga, CA

(Received: 2019 July 10 Revised: 2019 July 17)

CCD photometric observations of seven Hilda asteroids were made at the Center for Solar System Studies (CS3) from 2019 April and June. Analysis of data for 1269 Rollandia and 3843 OISCA based on 2019 data led to review of our earlier results. For both objects, this resulted not in solving but deepening the mystery of the their true rotation periods.

CCD photometric observations of three Hilda asteroids were made at the Center for Solar System Studies (CS3) from 2019 April-June. This is another installment of an on-going series of papers on this group of asteroids, which is located between the outer main-belt and Jupiter Trojans in a 3:2 orbital resonance with Jupiter. The goal is to determine the spin rate statistics of the group and find pole and shape models when possible. We also look to examine the degree of influence that the YORP (Yarkovsky–O'Keefe–Radzievskii–Paddack) effect (Rubincam, 2000) has on distant objects and to compare the spin rate distribution against the Jupiter Trojans, which can provide evidence that the Hildas are more "comet-like" than main-belt asteroids.

Telescopes	Cameras
0.30-m *f*/6.3 Schmidt-Cass	FLI Microline 1001E
0.35-m *f*/9.1 Schmidt-Cass	FLI Proline 1001E
0.35-m *f*/11 Schmidt-Cass	SBIG STL-1001E
0.40-m f/10 Schmidt-Cass	
0.50-m *f*/8.1 Ritchey-Chrétien	

Table I. List of available telescopes and CCD cameras at CS3. The exact combination for each telescope/camera pair can vary due to maintenance or specific needs.

Table I lists the telescopes and CCD cameras that are combined to make observations. Up to nine telescopes can be used for the campaign, although seven is more common. All the cameras use CCD chips from the KAF blue-enhanced family and so have essentially the same response. The pixel scales ranged from 1.24-1.60 arcsec/pixel. All lightcurve observations were unfiltered since a clear filter can result in a 0.1-0.3 magnitude loss. The exposures varied depending on the asteroid's brightness and sky motion.

Measurements were made using *MPO Canopus*. The Comp Star Selector utility in *MPO Canopus* found up to five comparison stars of near solar-color for differential photometry. Comp star magnitudes were taken from ATLAS catalog (Tonry et al., 2018), which has Sloan *griz* magnitudes that were derived from the GAIA and Pan-STARR catalogs, among others. The authors state that systematic errors are generally no larger than 0.005 mag, although they can reach 0.02 mag in small areas near the Galactic plane. BVRI magnitudes were derived by Warner using formulae

from Kostov and Bonev (2017). The overall errors for the BVRI magnitudes, when combining those in the ATLAS catalog and the conversion formulae, are on the order of 0.04-0.05.

Even so, we found in most cases that nightly zero point adjustments on the order of only 0.02-0.03 mag were required during period analysis. There were occasional exceptions that required up to 0.10 mag. These may have been related in part to using unfiltered observations, poor centroiding of the reference stars, and not correcting for second-order extinction terms. Regardless, the systematic errors seem to be considerably less than other catalogs, which reduces the uncertainty in the results when analysis involves data from extended periods or the asteroid is tumbling.

Period analysis was done with *MPO Canopus*, which implements the FALC algorithm by Harris (Harris *et al.,* 1989). The same algorithm is used in an iterative fashion when it appears there is more than one period. This works well for binary but not for tumbling asteroids.

In the plots below, the "Reduced Magnitude" is Johnson V. These have been converted from sky magnitudes to unity distance by applying –5*log (rΔ) with r and Δ being, respectively, the Sun-asteroid and Earth-asteroid distances in AU. The magnitudes were normalized to the phase angle in parentheses using G = 0.15. The X-axis is the rotational phase ranging from –0.05 to 1.05. If the plot includes an amplitude, it is for the Fourier model curve and *not necessarily the adopted amplitude for the lightcurve*.

Our initial search for previous results started with the asteroid lightcurve database (LCDB; Warner *et al.,* 2009) found on-line at *http://www.minorplanet.info/lightcurvedatabase.html*. Readers are strongly encouraged to obtain, when possible, the original references listed in the LCDB.

1269 Rollandia. Finding a definitive period for this 105-km Hilda has been difficult over the years. Franco (2012) reported a period of 15.4 h. This was based on data obtained on three nights in 2012 March. The data set was noisy and the lightcurve was mostly flat except for a 0.08 mag "bump" from 0.3-0.8 rotation phase. Slyusarev et al. (2012) reported a period of 31 h and amplitude of 0.02 mag. No lightcurve was published in their ACM poster. Fauvaud and Fauvaud (2013), who observed almost the same time as Franco, determined P = 15.32 h, A = 0.13 mag. Their lightcurve was monomodal but had a gap between 0.1-0.3 rotation phase.

We observed Rollandia in 2016 August and found P = 19.98, A = 0.06 mag. Our hope was that new data in 2019 would resolve the ambiguities or at least reduce them. This would not be the case. The period spectrum was not helpful, showing several possible solutions and favoring an entirely new period.

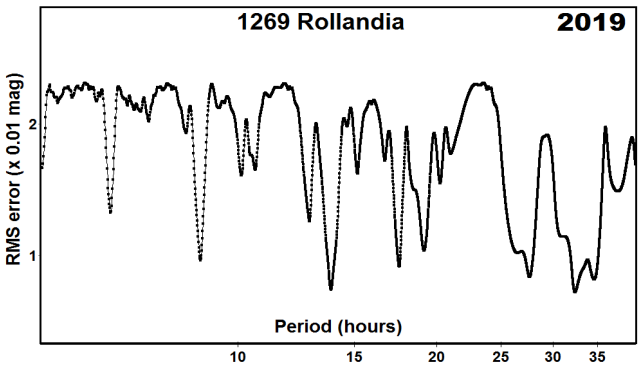

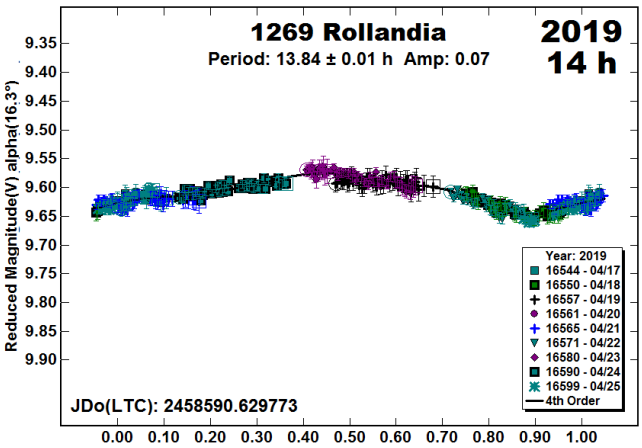

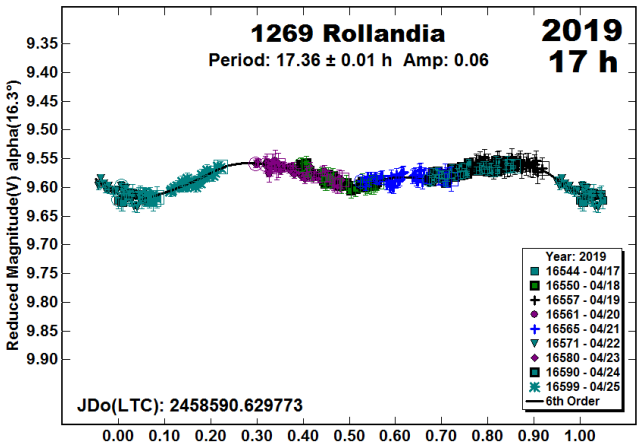

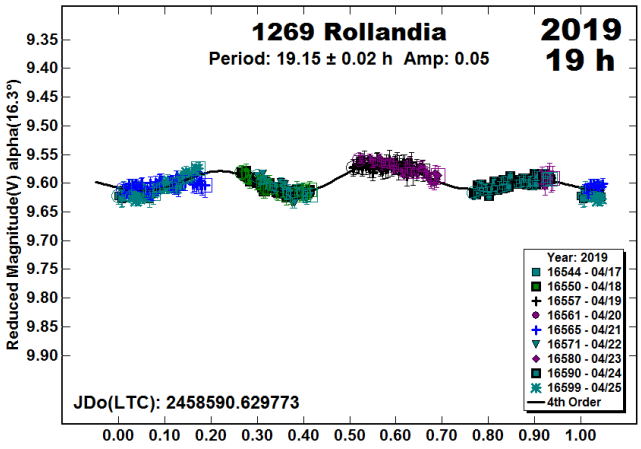

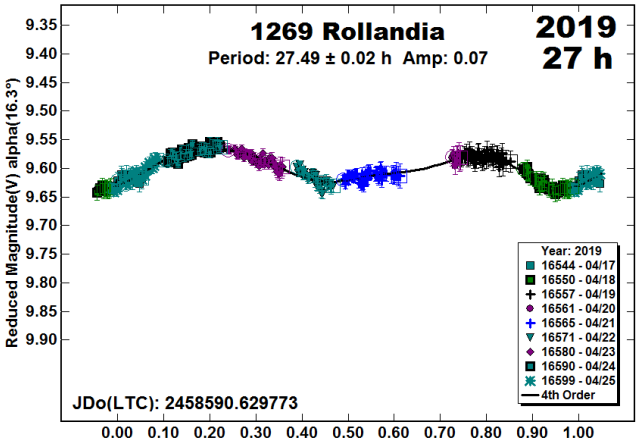

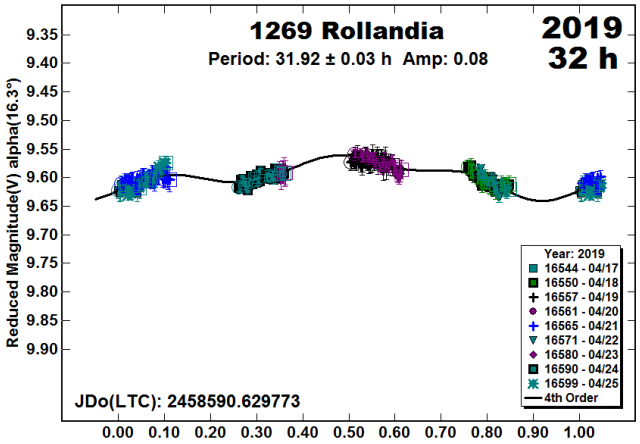

Looking at the plots from 2019 individually, the solution at 13.84 h is *almost* monomodal, but the disjoint in the slopes between 0.2 to 0.5 rotation phase was concerning. A solution near 19 hours produced a trimodal curve, which is not improbable given the low amplitude (Harris et al., 2014). The apparently bimodal lightcurve at P = 27.49 h was rejected because of the slight asymmetry, i.e., the maximums or minimums were not 0.5 rotation apart. This does not automatically preclude the solution, but it close to the double period of 13.84 h, which we eventually put aside. The fit to near 32 hours has an unusual shape. In addition, the slopes of some of the individual nights don't quite fit the model curve.

This left us with a solution of P = 17.36 h, which we have adopted for this paper because the curve is bimodal and more symmetrical than at 27 h and fits the model curve the best. This leaves a half-period solution of 8.68 h as another possibility. We returned to the data from 2016 to see if they could be fit to the new result or one of the other possibilities.

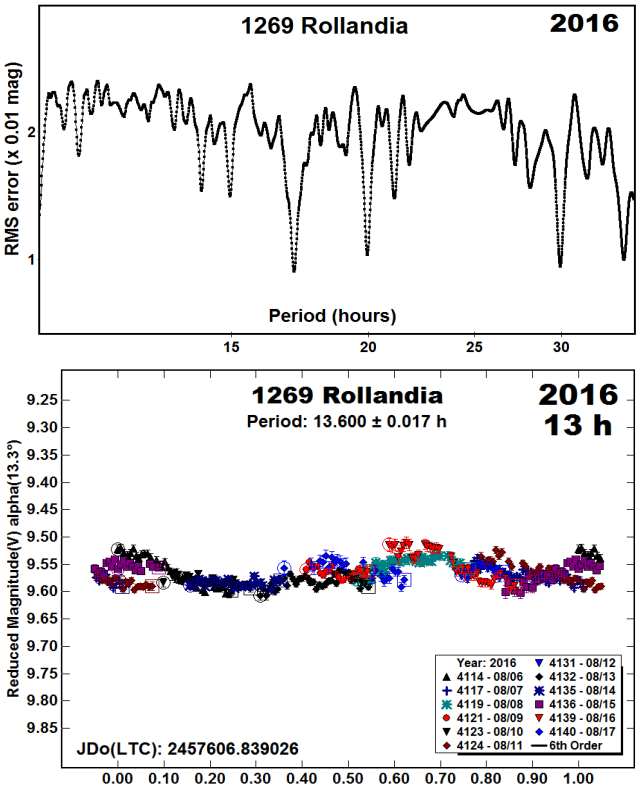

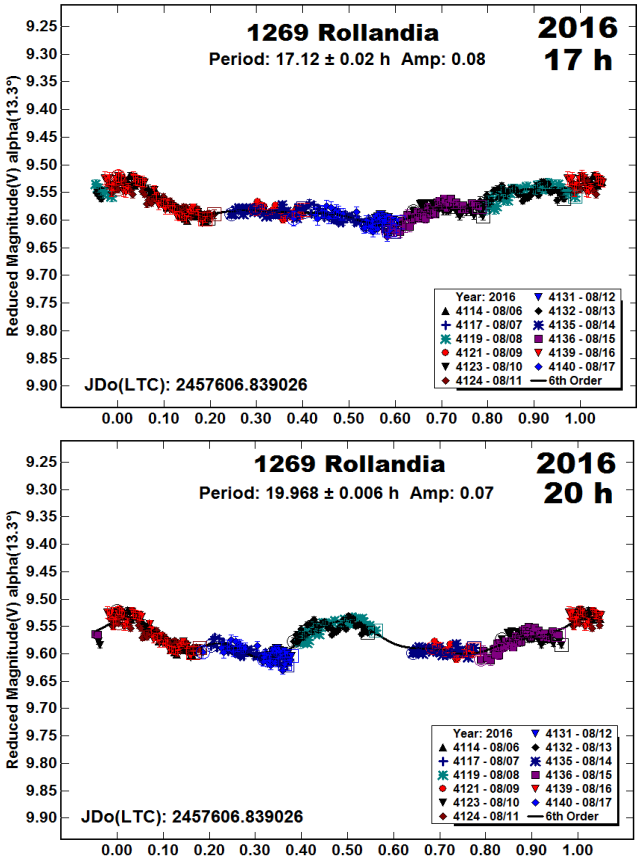

If nothing else, a period near 14 hours was eliminated. The best fit was again for a period of about 17 hours, but it is significantly different from the 2019 result. A definitive solution for 1269 Roliandia still proves elusive.

1902 Shaposhnikov. There are numerous results in the LCDB for the 97-km Shaposnikov. Early results include Dahlgren et al (1998; 21.2 h). We observed it twice in recent years: Warner and Stephens (2017b, 20.987 h; 2018b, 20.988 h). The latest results are in good agreement with our previous periods.

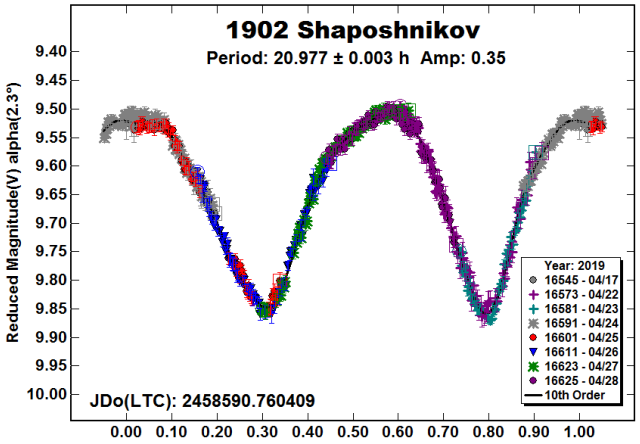

3577 Putilin. Previous results include Dahlgren et al. (1998, 29.0 h) and Warner and Stephens (2017b, 14.30 h). Brinsfield (2011) found yet another period: 18.270 h. Analysis of our data from the observations in 2019 April found P = 18.239 h. The solution is not fully secure but the period spectrum showed few alternate solutions of note. We turned to

half-period plots. The only one that worked was near 9 hours, confirming the final result of 18.239 h. Our reanalysis of the 2016 data was able to find a similar period, 18.324 h.

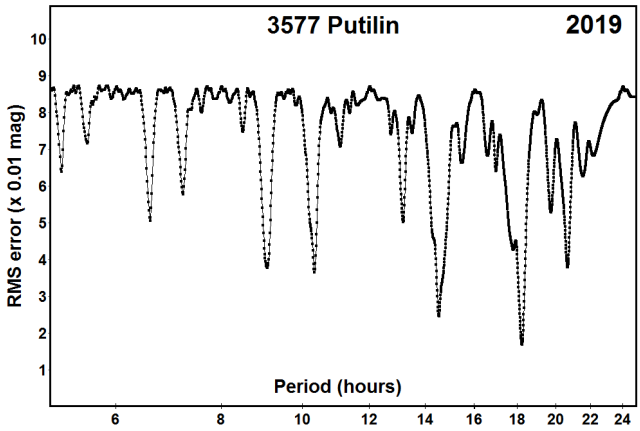

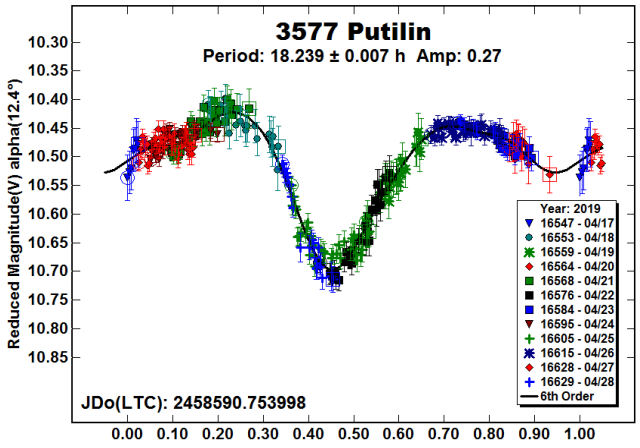

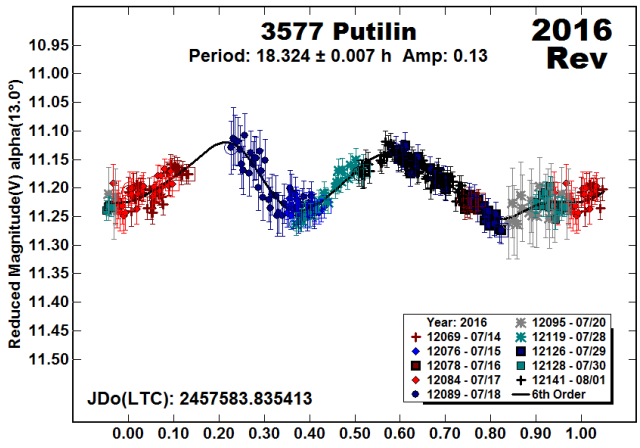

3843 OISCA. This is a 40-km member of the Hilda group. De Sanctis et al. (1994) found only lower limits of $P > 16$ h and $A > 0.2$ mag. Dalhgren et al. (1998) followed up with $P = 19.078$ and $A = 0.28$ mag. Our results from 2016 data (Warner and Stephens, 2018a) were $P = 19.089$ h and $A = 0.32$ mag, in good agreement with Dahlgren et al. Our analysis of data from 2019 turned an effort to refine the period and obtain more data for modeling into an effort just to find any period to which our 2016 and 2019 data sets would have a reasonable fit. It was not entirely successful. An unusual number of lightcurves are presented here to show the conundrum that was encountered more clearly.

Initial analysis of the full 2019 data set using as small of zero point adjustments as possible found a period of 29.41 h, or some 10 hours longer than previously reported ("2019 29h Full Data Set"). The "2019 29h" period spectrum was generated using the original zero points.

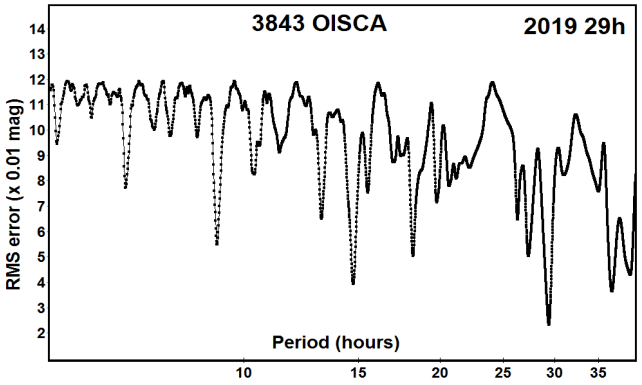

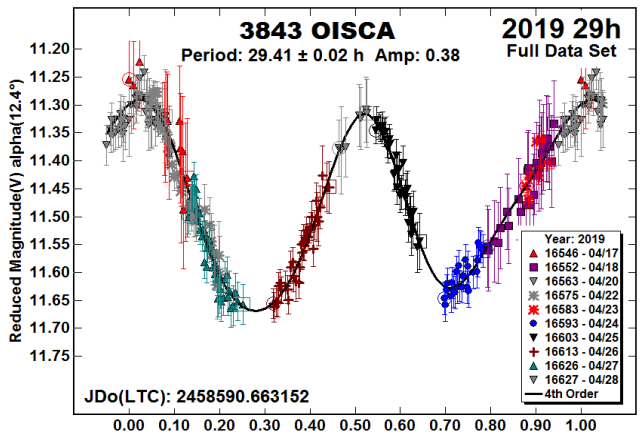

We then forced a period of 19.09 hours and adjusted zero points until we were able to get a match. The only way that this was possible was to use a subset of the 2019 data, eliminating the nights of 2019 April 22 and 23, which could not be fit no matter how severe the zero point adjustments. The period spectrum "2019 19h" shows the results of search after finding a fit using the subset. It is noticeably different from the previous one.

The period search range was narrowed and allowed to float instead of remain a fixed value. This produced a lightcurve with a period of 19.137 h that has a reasonable bimodal shape, albeit with significant gaps in coverage ("2019 19h Partial Data Set").

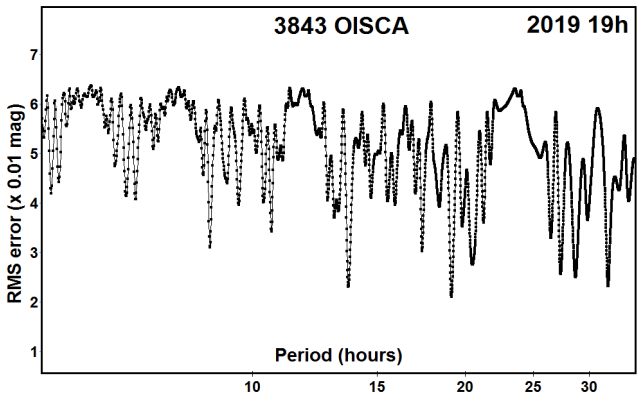

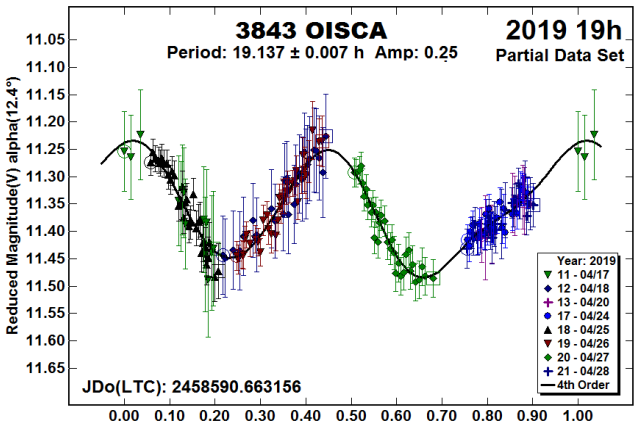

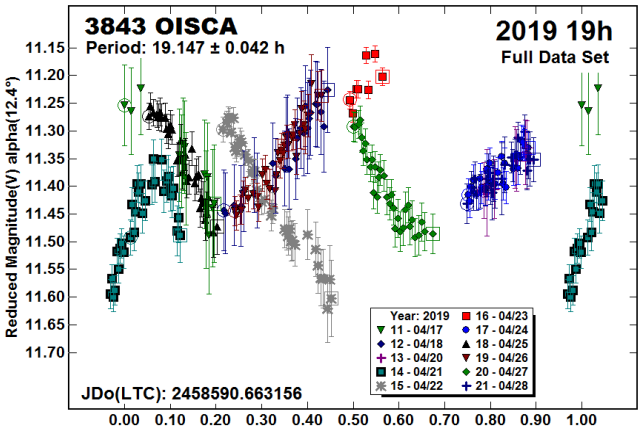

The next step was to try to force the full set to the 19-hour solution. This was futile ("2019 19h Full Data Set"). No amount of zero point adjustments could get the data to fit a trimodal lightcurve, let alone bimodal, which would be more likely given the low phase angle and amplitude (Harris et al., 2014).

We revisited our 2016 data to force the data to see if they would fit with the new, longer period. The period spectrum using the original zero points, with very minor adjustments, showed a strong preference for a period of 19.075 h ("2016 19h"). This is slightly shorter than previously found with the same data. The two are statistically the same and so there was no concern about the very minor difference. The "2016 28h" plot shows the results of trying to force the data to near 29 h. Here again, no amount of zero point shifts would allow a fit to a bimodal or trimodal lightcurve.

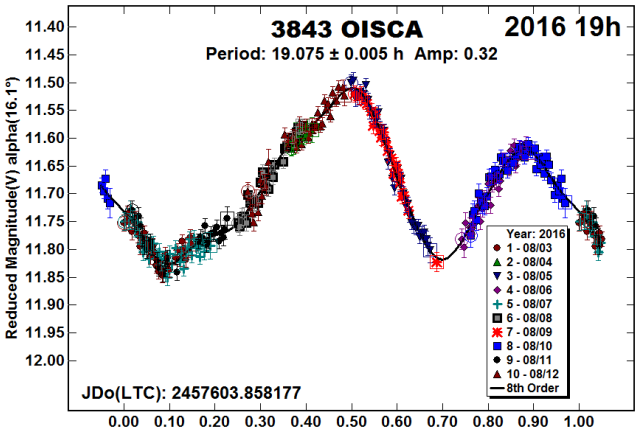

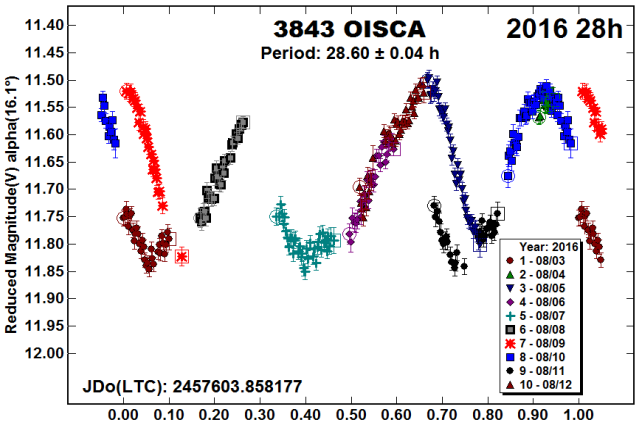

We considered the possibility that the asteroid might be tumbling but the diameter and periods make tumbling highly unlikely (Pravec et al., 2014; 2005), but not impossible.

Because there is no reasonable fit to be found near 29 h using the 2016 data and because we can find a 19-h period using a subset of the 2019 data, we are adopting the revised 2016 period of P = 19.075 h for this paper. We have no explanation at this time for why two consecutive nights, 2019 Aug 22-23, deviated so much from the fit to a period near previous results.

(36274) 2000 AV107, (39266) 2001 AT2. This appears to be the first reported rotation period for either asteroid. 2000 AV107 has a diameter of 18.38 km (Mainzer et al., 2016). The estimated diameter for 2001 AT2 is 17-km. The noisy data set makes the solution less than fully secure for the latter asteroid.

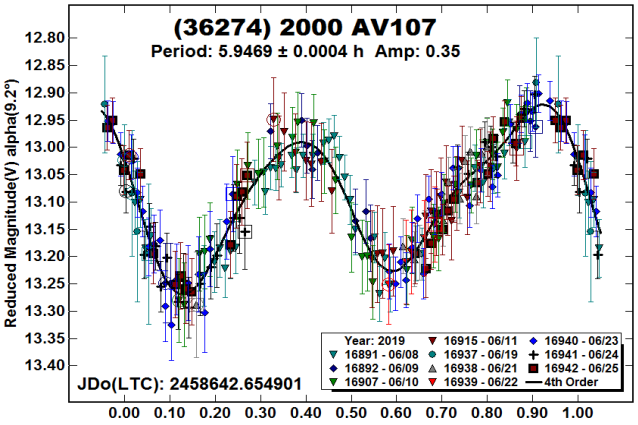

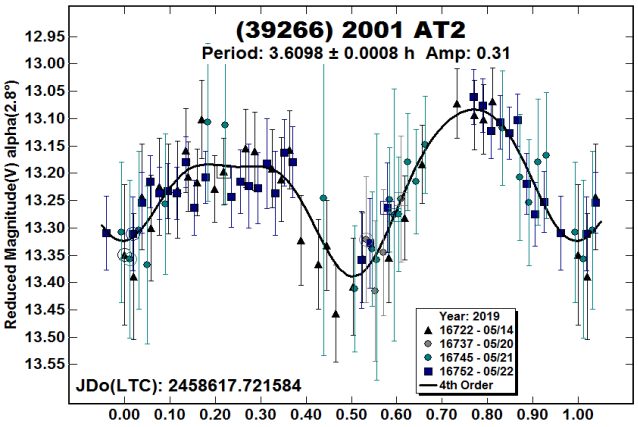

Number	Name	20xx/mm/dd	Phase	L_{PAB}	B_{PAB}	Period(h)	P.E.	Amp	A.E.
1269	**Rollandia**	**19/04/17-04/25**	**16.3,16.6**	**136**	**0**	**17.36**	**0.01**	**0.06**	**0.01**
1269	Rollandia	16/08/06-08/17	1.5,2.2	137	4	17.12	0.02	0.08	0.01
1902	Shaposhnikov	19/04/17-04/28	2.3,4.1	204	8	20.977	0.003	0.35	0.02
3577	**Putilin**	**19/04/17-04/28**	**16.8,17.3**	**141**	**-3**	**18.239**	**0.007**	**0.27**	**0.02**
3577	Putilin	16/07/14-08/01	13.0,10.7	351	4	18.324	0.007	0.13	0.01
3843	OISCA	19/04/17-04/28	12.4,13.5	153	3	19.137	0.007	0.25	0.02
	Alternate					29.41	0.02	0.38	0.03
3843	**OISCA**	**16/08/03-08/12**	**16.1,15.3**	**19**	**-1**	**19.075**	**0.005**	**0.32**	**0.02**
36274	2000 AV107	19/06/08-06/25	9.2,12.6	231	14	5.9469	0.0004	0.35	0.03
39266	2001 AT2	19/05/14-05/21	2.8,4.5	229	7	3.6098	0.0008	0.31	0.03

Table II. Observing circumstances. The phase angle (α) is given at the start and end of each date range. L_{PAB} and B_{PAB} are the average phase angle bisector longitude and latitude (see Harris *et al*., 1984). When there is more than one line for an asteroid, the one in bold text gives the period adopted for this work.

Acknowledgements

Funding for observations at CS3 and work on the asteroid lightcurve database (Warner et al., 2009) and ALCDEF database (*alcdef.org*) are supported by NASA grant 80NSSC18K0851.

This work includes data from the Asteroid Terrestrial-impact Last Alert System (ATLAS) project. ATLAS is primarily funded to search for near earth asteroids through NASA grants NN12AR55G, 80NSSC18K0284, and 80NSSC18K1575; byproducts of the NEO search include images and catalogs from the survey area. The ATLAS science products have been made possible through the contributions of the University of Hawaii Institute for Astronomy, the Queen's University Belfast, the Space Telescope Science Institute, and the South African Astronomical Observatory.

The authors gratefully acknowledge Shoemaker NEO Grants from the Planetary Society (2007, 2013). These were used to purchase some of the telescopes and CCD cameras used in this research.

References

Brinsfield, J.W. (2011). "Asteroid Lightcurve Analysis at the Via Capote Observatory: 1st Quarter 2011." *Minor Planet Bull*. **38**, 154-155.

Dahlgren, M.; Lahulla, J.F.; Lagerkvist, C.-I.; Lagerros, J.; Mottola, S.; Erikson, A.; Gonano-Beurer, M.; Di Martino, M. (1998). "A Study of Hilda Asteroids. V. Lightcurves of 47 Hilda Asteroids." *Icarus* **133**, 247-285.

De Sanctis, M.C.; Barucci, M.A.; Angeli, C.A.; Fulchignoni, M.; Burchi, R.; Angelini, P. (1994). "Photoelectric and CCD observations of 10 asteroids." *Planet. Space Sci.* **42**, 859-864.

Fauvaud, S.; Fauvaud, M. (2013). "Photometry of Minor Planets. I. Rotation Periods from Lightcurve Analysis for Seven Main-belt Asteroids." *Minor Planet Bull*. **40**, 224-229.

Franco, L. (2012). Balzaretto Observatory web site. *https://digilander.libero.it/A81_Observatory/4435/index.html*

Harris, A.W.; Young, J.W.; Scaltriti, F.; Zappala, V. (1984). "Lightcurves and phase relations of the asteroids 82 Alkmene and 444 Gyptis." *Icarus* **57**, 251-258.

Harris, A.W.; Young, J.W.; Bowell, E.; Martin, L.J.; Millis, R.L.; Poutanen, M.; Scaltriti, F.; Zappala, V.; Schober, H.J.; Debehogne, H.; Zeigler, K.W. (1989). "Photoelectric Observations of Asteroids 3, 24, 60, 261, and 863." *Icarus* **77**, 171-186.

Harris, A.W.; Pravec, P.; Galad, A.; Skiff, B.A.; Warner, B.D.; Vilagi, J.; Gajdos, S.; Carbognani, A.; Hornoch, K.; Kusnirak, P.; Cooney, W.R.; Gross, J.; Terrell, D.; Higgins, D.; Bowell, E.; Koehn, B.W. (2014). "On the maximum amplitude of harmonics on an asteroid lightcurve." *Icarus* **235**, 55-59.

Kostov, A.; Bonev, T. (2017). "Transformation of Pan-STARRS1 gri to Stetson BVRI magnitudes. Photometry of small bodies observations." *Bulgarian Astron. J.* **28**, 3 (AriXiv:1706.06147v2).

Mainzer, A.K.; Bauer, J.M.; Cutri, R.M.; Grav, T.; Kramer, E.A.; Masiero, J.R.; Nugent, C.R.; Sonnett, S.M.; Stevenson, R.A.; Wright, E.L. (2016). "NEOWISE Diameters and Albedos V1.0." NASA PDS. EAR-A-COMPIL-5-NEOWISEDIAM-V1.0.

Pravec, P.; Harris, A.W.; Scheirich, P.; Kušnirák, P.; Šarounová, L.; Hergenrother, C.W.; Mottola, S.; Hicks, M.D.; Masi, G.; Krugly, Yu.N.; Shevchenko, V.G.; Nolan, M.C.; Howell, E.S.; Kaasalainen, M.; Galád, A.; Brown, P.; Degraff, D.R.; Lambert, J. V.; Cooney, W.R.; Foglia, S. (2005). "Tumbling asteroids." *Icarus* **173**, 108-131.

Pravec, P.; Scheirich, P.; Durech, J.; Pollock, J.; Kusnirak, P.; Hornoch, K.; Galad, A.; Vokrouhlicky, D.; Harris, A.W.; Jehin, E.; Manfroid, J.; Opitom, C.; Gillon, M.; Colas, F.; Oey, J.; Vrastil, J.; Reichart, D.; Ivarsen, K.; Haislip, J.; LaCluyze, A. (2014). "The tumbling state of (99942) Apophis." *Icarus* **233**, 48-60.

Rubincam, D.P. (2000). "Relative Spin-up and Spin-down of Small Asteroids." *Icarus* **148**, 2-11.

Slyusarev, I.G.; Shevchenko, V.G.; Belskaya, I.N.; Krugly, Yu.N.; Chiorny, V.G. (2012). **ACM 2012**, #6398.

Tonry, J.L.; Denneau, L.; Flewelling, H.; Heinze, A.N.; Onken, C.A.; Smartt, S.J.; Stalder, B.; Weiland, H.J.; Wolf, C. (2018). "The ATLAS All-Sky Stellar Reference Catalog." *Astrophys. J.* **867**, A105.

Warner, B.D.; Harris, A.W.; Pravec, P. (2009). "The Asteroid Lightcurve Database." *Icarus* **202**, 134-146. Updated 2018 June. *http://www.minorplanet.info/lightcurvedatabase.html*

Warner, B.D.; Stephens, R.D. (2017a). "Lightcurve Analysis of Hilda Asteroids at the Center for Solar System Studies: 2016 June-September." *Minor Planet Bull*. **44**, 36-41.

Warner, B.D.; Stephens, R.D (2017b). "Lightcurve Analysis of Hilda Asteroids at the Center for Solar System Studies: 2016 December thru 2017 April." *Minor Planet Bull.* **44**, 220-222.

Warner, B.D.; Stephens, R.D.; Coley, D.R. (2017). "Lightcurve Analysis of Hilda Asteroids at the Center for Solar System Studies: 2016 September-December." *Minor Planet Bull*. **44**, 130-137.

Warner, B.D.; Stephens, R.D. (2018a). "Lightcurve Analysis of Hilda Asteroids at the Center for Solar System Studies: 2017 July Through September." *Minor Planet Bull*. **45**, 35-39.

Warner, B.D.; Stephens, R.D. (2018b). "Lightcurve Analysis of Hilda Asteroids at the Center for Solar System Studies: 2018 January-April." *Minor Planet Bull*. **45**, 262-265.

POTENTIAL BINARY AND TUMBLING ASTEROIDS FROM THE CENTER FOR SOLAR SYSTEM STUDIES

Brian D. Warner
Center for Solar System Studies / MoreData!
446 Sycamore Ave.
Eaton, CO 80615 USA
brian@MinorPlanetObserver.com

Robert D. Stephens
Center for Solar System Studies / MoreData!
Rancho Cucamonga, CA

(Received: 2019 July 10)

CCD photometric observations of four main-belt and one near-Earth asteroid were made in 2019. Of these, the Vestoid 2602 Moore and Hungaria (27568) 2000 PT6 were confirmed to be binary asteroids. The Hungaria 3880 Kaiserman is a suspected binary. Near-Earth asteroid (142040) 2002 QE15 was found to have a long period (46.4 h). Re-evaluation of data for the asteroid from two previous apparitions found a secondary period that is consistent with the system being a candidate for the rare class of very wide binary asteroids. New analysis of the data from 2016 for Phocaea member 2937 Gibbs found two periods (the second being ambiguous). It could not be determined if the asteroid is binary or in a tumbling state.

CCD photometric observations of five asteroids were conducted in 2019 April-July as part of ongoing work at the Center for Solar System Studies (CS3) to find the rotation periods of asteroids. The primary targets are near-Earth asteroids but, when there are no such objects within reach of our instruments or they are poorly placed, we observe main-belts objects, concentrating on Jupiter Trojans, Hildas, and Hungarias.

Telescopes	Cameras
0.30-m *f*/6.3 Schmidt-Cass	FLI Microline 1001E
0.35-m *f*/9.1 Schmidt-Cass	FLI Proline 1001E
0.35-m *f*/11 Schmidt-Cass	SBIG STL-1001E
0.40-m f/10 Schmidt-Cass	
0.50-m *f*/8.1 Ritchey-Chrétien	

Table I. List of available telescopes and CCD cameras at CS3. The exact combination for each telescope/camera pair can vary due to maintenance or specific needs.

Table I lists the telescopes and CCD cameras that are combined to make observations. Up to nine telescopes can be used for the campaign, although seven is more common. All the cameras use CCD chips from the KAF blue-enhanced family and so have essentially the same response. The pixel scales ranged from 1.24-1.60 arcsec/pixel. All lightcurve observations were unfiltered since a clear filter can result in a 0.1-0.3 magnitude loss. The exposures varied depending on the asteroid's brightness and sky motion.

Measurements were made using *MPO Canopus*. The Comp Star Selector utility in *MPO Canopus* found up to five comparison stars of near solar-color for differential photometry. Comp star magnitudes were taken from ATLAS catalog (Tonry et al., 2018), which has Sloan *griz* magnitudes that were derived from the GAIA and Pan-STARR catalogs, among others. The authors state that systematic errors are generally no larger than 0.005 mag, although they can reach 0.02 mag in small areas near the Galactic plane. BVRI magnitudes were derived by Warner using formulae

Number	Name	20xx/mm/dd	Phase	L_{PAB}	B_{PAB}	Period(h)	P.E.	Amp	A.E.	Grp
2602	Moore	19/04/17-05/15	22.1,27.1	164	2	3.46723	0.00003	0.43	0.01	V
	Satellite					27.455	0.003	0.15	0.01	
2937	Gibbs	16/12/17-12/19	8.8,7.9	103	-7	2.984	0.001	0.25	0.02	MC
	P2 Alt1					5.62	0.01	0.14	0.02	
	P2 Alt2					7.49	0.01	0.14	0.02	
3880	Kaiserman	19/07/01-07/07	11.9,23.4	280	10	5.2694	0.0007	0.14	0.01	H
	Satellite?					16.09	0.02	0.05	0.01	
27568	2000 PT6	19/06/26-07/07	21.9,43.4	268	31	3.5006	0.0003	0.25	0.02	H
	Satellite					16.099	0.008	0.18	0.02	
142040	2002 QE15	19/05/24-06/02	9.6,11.7	245	15	46.4	0.2	0.19	0.03	NEA
142040	2002 QE15	15/07/14-07/21	51.7,53.4	349	43	47.1	0.1	0.11	0.01	
	Satellite?					3.891	0.001	0.15	0.02	
142040	2002 QE15	17/08/21-08/29	46.6,48.7	288	44	48.1	0.2	0.20	0.03	
	Satellite?					3.856	0.003	0.11	0.02	

Table II. Observing circumstances. The phase angle (α) is given at the start and end of each date range. L_{PAB} and B_{PAB} are the average phase angle bisector longitude and latitude (see Harris *et al*., 1984). The additional lines after the first, complete line give the periods associated with a satellite or alternate solutions for a second period. The Grp column gives the family/group (Warner et al., 2009). H: Hungaria; MC: Mars-crosser; NEA: Near-Earth asteroid; V: Vestoid.

from Kostov and Bonev (2017). The overall errors for the BVRI magnitudes, when combining those in the ATLAS catalog and the conversion formulae, are on the order of 0.04-0.05.

Even so, we found in most cases that nightly zero point adjustments on the order of only 0.02-0.03 mag were required during period analysis. There were occasional exceptions that required up to 0.10 mag. These may have been related in part to using unfiltered observations, poor centroiding of the reference stars, and not correcting for second-order extinction terms. Regardless, the systematic errors seem to be considerably less than other catalogs, which reduces the uncertainty in the results when analysis involves data from extended periods or the asteroid is tumbling.

Period analysis was done with *MPO Canopus*, which implements the FALC algorithm by Harris (Harris *et al.,* 1989). The same algorithm is used in an iterative fashion when it appears there is more than one period. This works well for binary but not for tumbling asteroids.

In the plots below, the "Reduced Magnitude" is Johnson V. These have been converted from sky magnitudes to unity distance by applying –5*log (rΔ) with r and Δ being, respectively, the Sun-asteroid and Earth-asteroid distances in AU. The magnitudes were normalized to the phase angle in parentheses using G = 0.15. The X-axis is the rotational phase ranging from –0.05 to 1.05. If the plot includes an amplitude, it is for the Fourier model curve and *not necessarily the adopted amplitude for the lightcurve*.

Our initial search for previous results started with the asteroid lightcurve database (LCDB; Warner *et al.,* 2009) found on-line at *http://www.minorplanet.info/lightcurvedatabase.html*. Readers are strongly encouraged to obtain, when possible, the original references listed in the LCDB.

2602 Moore. Stephens observed this asteroid in 2019 April and May. Soon after the observations began, there were indications of attenuations that might be attributed to a satellite. An extensive campaign covered almost a month and confirmed the attenuations as being occultation and/or eclipses (*mutual events*) due to a satellite.

The three plots show the data without subtracting a second period followed by the results of the dual-period search. The depth of the attenuations ranged from 0.08-0.14 mag. Using the smaller value, we estimate an effective diameter ratio of satellite-to-primary $Ds/Dp \geq 0.28 \pm 0.02$. There were no previous lightcurve results posted in the LCDB.

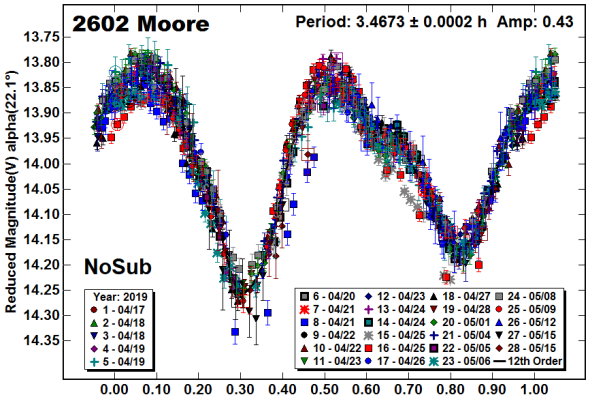

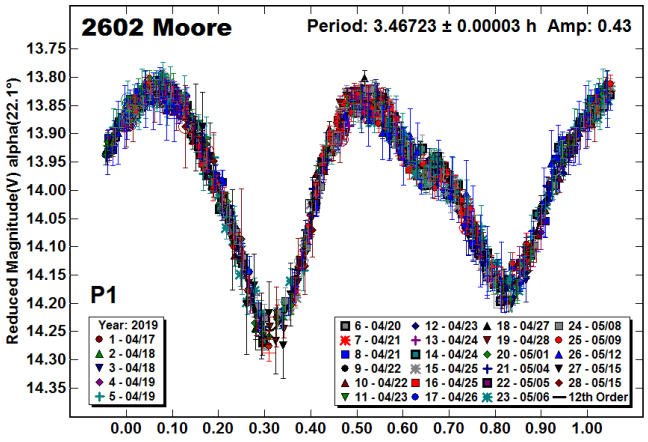

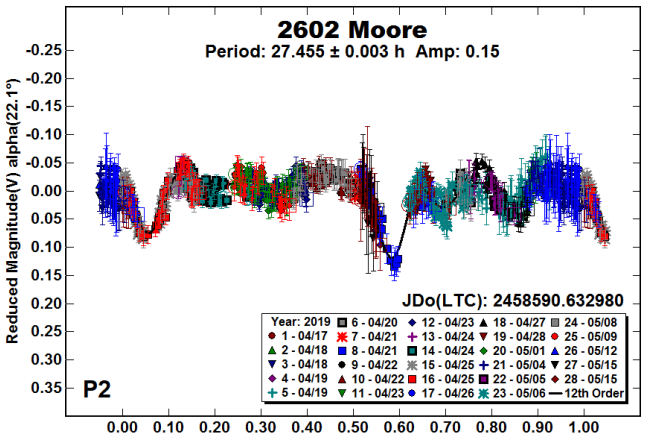

2937 Gibbs. There were several results posted in the LCDB for this 6-km Phocaea asteroid. Behrend (2005) reported 3.06153 h based on observations in 2005 August. His group observed again four months later and found a similar but less precise P = 3.06 h. Co-author Stephens (2017) found P = 3.189 h using data from 2016 December. This is similar to the Behrend results but differs by several sigma.

New observations made in 2019 June led to a significantly shorter period of 2.982 h. The new data could not be fit to the previous results. Given the large amplitude and relatively low solar phase angle, we adopted 2.982 h to be the true period and took another look at the data from 2016, forcing it to be near 2.98 h.

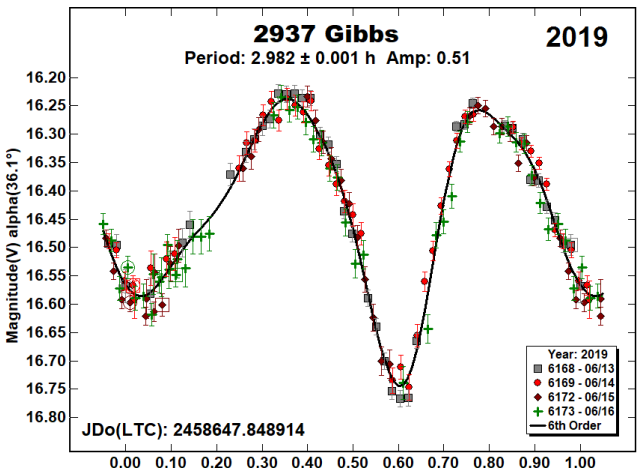

The "NoSub" plot shows what appear to be deviations in the lightcurve but the nosier data and smaller amplitude made those uncertain, at least to start. Our dual-period search found a very good fit to P_1 = 2.984 h after subtracting each of several possible secondary periods, P_2. Regardless of which secondary period was used, the result for P_1 remained the same.

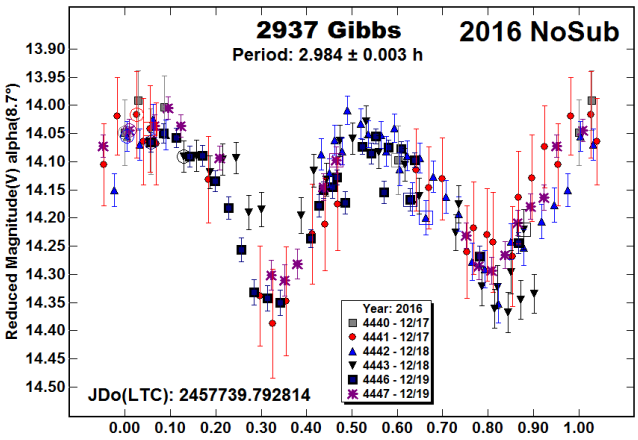

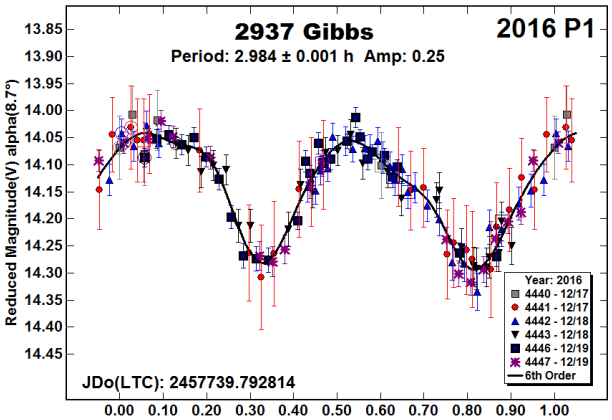

The period spectrum for the secondary period ("2016 P2") showed four possibilities with the one near 11 hours being the half-period of the longest solution of about 22 hours.

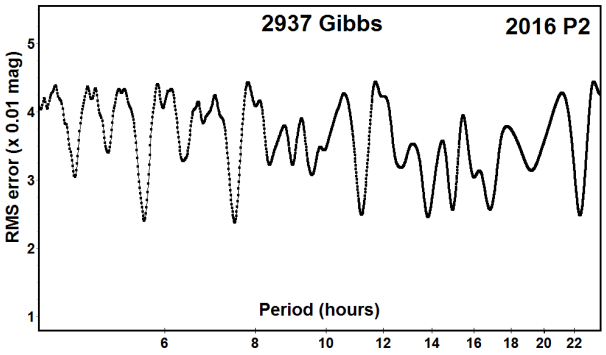

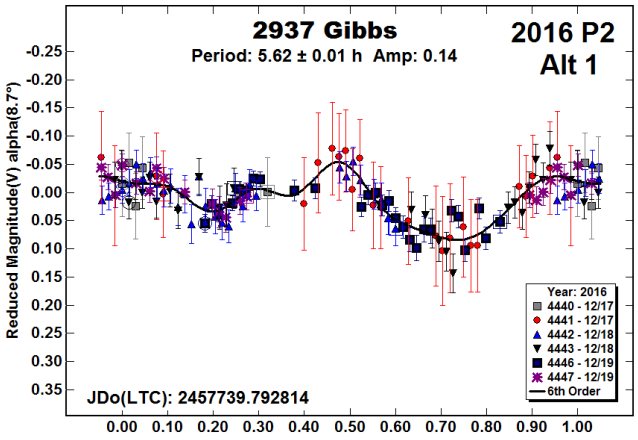

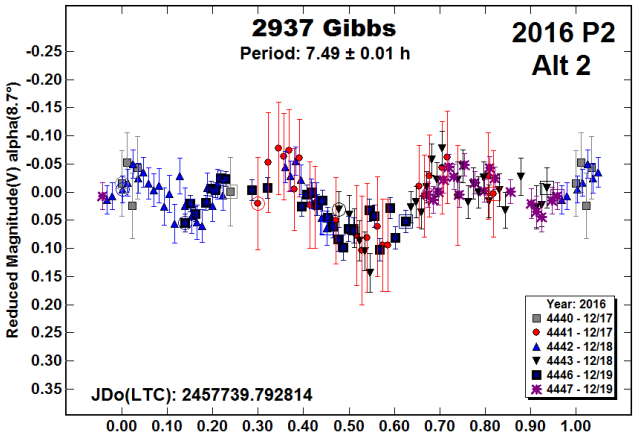

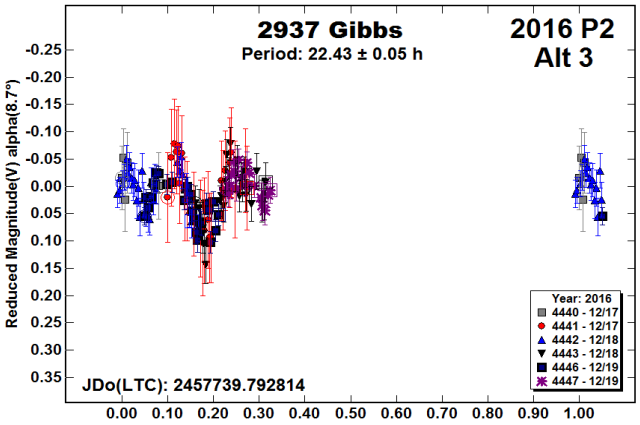

We examined the solutions at 5.6 h, 7.49 h, and 22.43 h to see which would produce the most plausible result. At P_2 = 5.62 h, the fit is acceptable given the scatter in the data set. It's important to note that this P_2 is not harmonically related to P_1, i.e., they do not have an integer ratio.

On the other hand, the remaining two solutions have *nearly* integral ratios with P_1. The lightcurve at P_2 = 7.49 h is almost trimodal, which is possible because of the low amplitude (Harris et al., 2014). The lightcurve at P_2 = 22.43 h is clearly wrong and simply a *fit by exclusion*, which is where the Fourier algorithm finds a local RMS minimum by minimizing the number of overlapping data points.

The harmonic relation between P_1 and P_2 = 7.49 h raises the possibility that the asteroid is in a low-level tumbling state where P_1 = 2.984 h dominates the solution and a linear combination of rotation and precession frequencies produces a "beat frequency" that is n/7.49, with n being an integer value. This is not uncommon (see Harris et al., 2014; Pravec et al., 2014; 2005).

3880 Kaiserman. We observed this Hungaria member twice before the latest observations. Warner (2012b) found a period of 5.270 h. In 2014 Warner (2015b) found a period of 5.227 h as well as indications of a secondary period of 22.16 h that was attributed to a possible satellite.

Our 2019 data also gave indications of a secondary period. The dual-period analysis found P_1 = 5.271 h, in agreement with Warner (2012b), and P_2 = 16.09 h. The lightcurve for P_2 is low amplitude (0.05 mag) but appears to be bimodal and has a shape typically seen for elongated satellites that are tidally-locked to the orbital period.

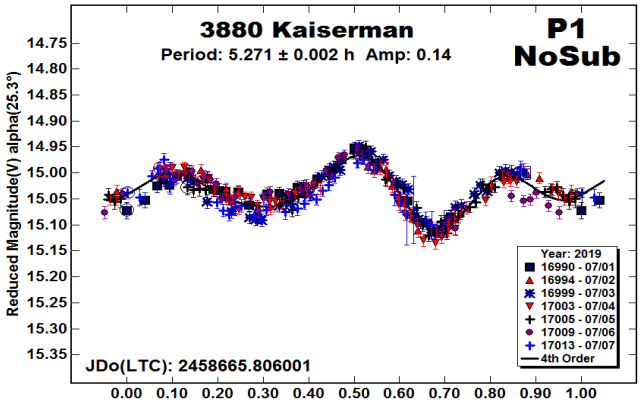

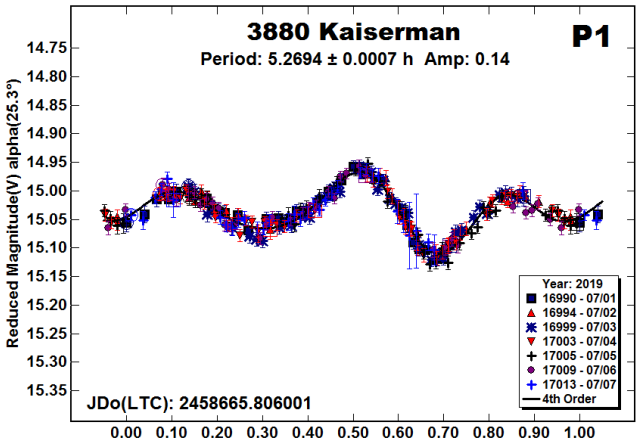

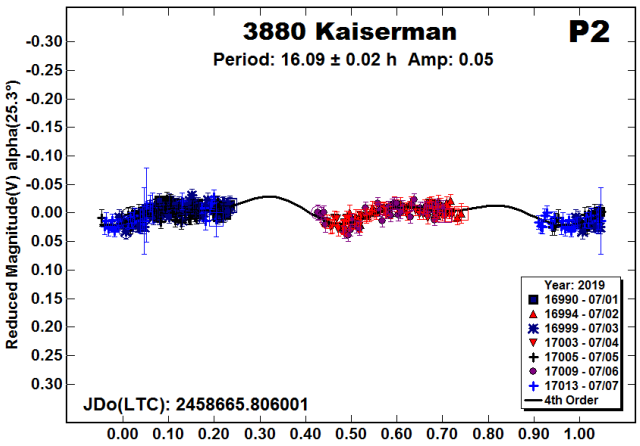

(27568) 2000 PT6. This was the fourth time we observed this Hungaria. Warner (2012a) reported a period of 3.624 h, but this was revised to 3.493 h after the data from observations in 2013 (Warner and Stephens, 2013) led to a period of 3.4885 h. They also reported the possibility of the asteroid being binary, with an orbital period of 16.353 h and estimated *Ds/Dp* of 0.22. Follow-up observations in 2014 (Warner, 2015a) found indications of a satellite but the orbital period was 11.73 h and there was no estimate of the effective diameters ratio.

The 2019 data leave little doubt that the asteroid is binary with an the satellite tidally-locked to an orbital period of 16.099 h. The satellite's lightcurve shape indicates an elongated body. We estimate $Ds/Dp \geq 0.23 \pm 0.04$

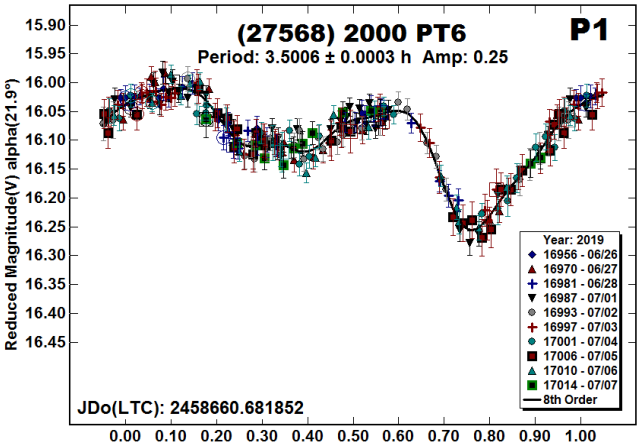

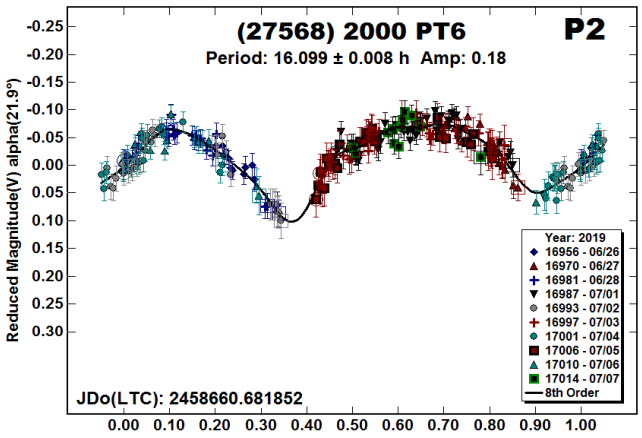

(142040) 2002 QE15. Pravec et al. (2002) observed this NEA in 2002 September-October and reported a period of 2.5811 h. When we observed it in 2015 (Warner, 2016) and 2017 (Warner, 2018), we did not think that our 3.88 h lightcurves were superimposed on a long period lightcurve. Then again, as we found we did in the past, the adjustments of the nightly zero points maybe have removed the traces of a long period.

We observed the asteroid again in 2019 May and June. With the ATLAS catalog (Tonry et al., 2018) and the higher confidence in nightly zero points, we found a $P = 46.4$ h. This made it a possible *very wide binary asteroid* (see, e.g., Warner and Stephens, 2019; and references therein). This rare class has about 30 candidates, some with very convincing evidence, that features a primary long primary period (> 24 h to 500+ h) with an underlying short period (usually 2-5 h) with a lightcurve that looks like a typical primary of an "ordinary" binary asteroid.

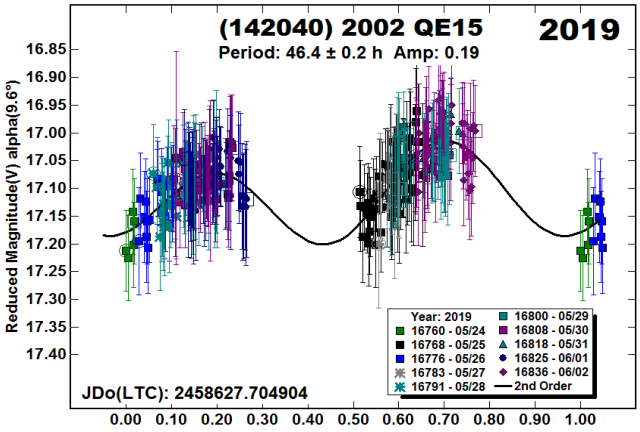

The data set in 2019 was too sparse and noisy to find a secondary period, especially if it had a particularly low amplitude. However, we returned to our previous data sets to see if we might have overlooked something. Part of this was to reset zero points and not change them significantly.

The new analysis of the 2015 data set found a low-amplitude (0.11 mag) lightcurve with a period of 47.1 h, which was in reasonable agreement with the 2019 result. Once that long period was subtracted in a dual-period search, we found a convincing solution of 3.891 h, which is close to what we found in the previous single period result. The 2017 data set provided a convincing case as well with the long-period lightcurve period of 48.1 h and a short period of 3.856 h, in reasonable agreement with the short period from the 2015 reanalysis and single period results.

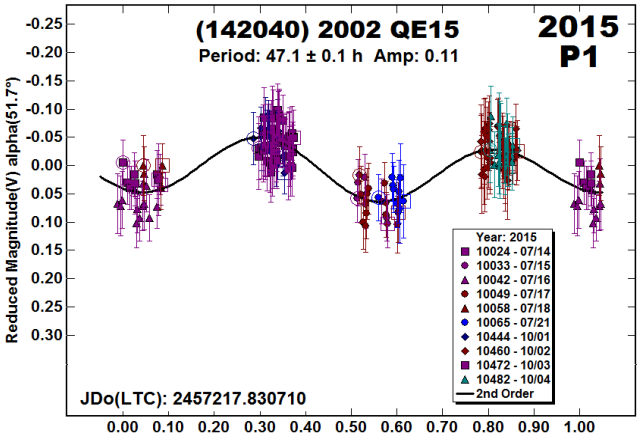

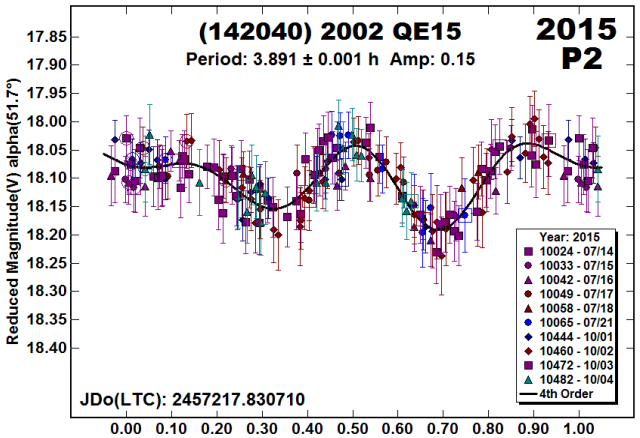

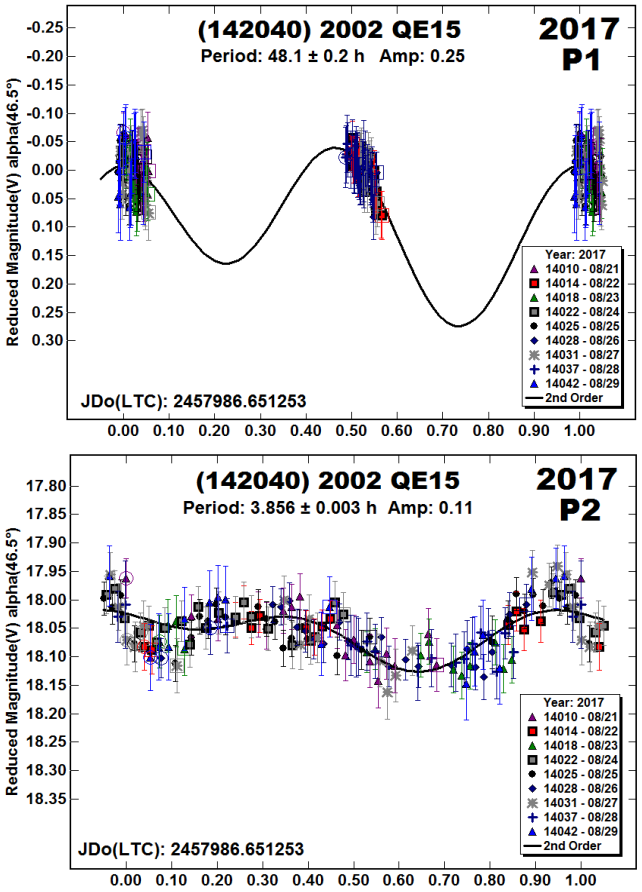

Acknowledgements

Funding for observations at CS3 and work on the asteroid lightcurve database (Warner et al., 2009) and ALCDEF database (*alcdef.org*) are supported by NASA grant 80NSSC18K0851.

This work includes data from the Asteroid Terrestrial-impact Last Alert System (ATLAS) project. ATLAS is primarily funded to search for near earth asteroids through NASA grants NN12AR55G, 80NSSC18K0284, and 80NSSC18K1575; byproducts of the NEO search include images and catalogs from the survey area. The ATLAS science products have been made possible through the contributions of the University of Hawaii Institute for Astronomy, the Queen's University Belfast, the Space Telescope Science Institute, and the South African Astronomical Observatory.

The authors gratefully acknowledge Shoemaker NEO Grants from the Planetary Society (2007, 2013). These were used to purchase some of the telescopes and CCD cameras used in this research.

References

Behrend, R. (2005). Observatoire de Geneve web site. *http://obswww.unige.ch/~behrend/page_cou.html*

Harris, A.W.; Young, J.W.; Scaltriti, F.; Zappala, V. (1984). "Lightcurves and phase relations of the asteroids 82 Alkmene and 444 Gyptis." *Icarus* **57**, 251-258.

Harris, A.W.; Young, J.W.; Bowell, E.; Martin, L.J.; Millis, R.L.; Poutanen, M.; Scaltriti, F.; Zappala, V.; Schober, H.J.; Debehogne, H.; Zeigler, K.W. (1989). "Photoelectric Observations of Asteroids 3, 24, 60, 261, and 863." *Icarus* **77**, 171-186.

Harris, A.W.; Pravec, P.; Galad, A.; Skiff, B.A.; Warner, B.D.; Vilagi, J.; Gajdos, S.; Carbognani, A.; Hornoch, K.; Kusnirak, P.; Cooney, W.R.; Gross, J.; Terrell, D.; Higgins, D.; Bowell, E.; Koehn, B.W. (2014). "On the maximum amplitude of harmonics on an asteroid lightcurve." *Icarus* **235**, 55-59.

Kostov, A.; Bonev, T. (2017). "Transformation of Pan-STARRS1 gri to Stetson BVRI magnitudes. Photometry of small bodies observations." *Bulgarian Astron. J.* **28**, 3 (AriXiv:1706.06147v2).

Pravec, P.; Harris, A.W.; Scheirich, P.; Kušnirák, P.; Šarounová, L.; Hergenrother, C.W.; Mottola, S.; Hicks, M.D.; Masi, G.; Krugly, Yu.N.; Shevchenko, V.G.; Nolan, M.C.; Howell, E.S.; Kaasalainen, M.; Galád, A.; Brown, P.; Degraff, D.R.; Lambert, J. V.; Cooney, W.R.; Foglia, S. (2005). "Tumbling asteroids." *Icarus* **173**, 108-131.

Pravec, P.; Wolf, M.; Sarounova, L. (2002). *http://www.asu.cas.cz/~ppravec/neo.htm*

Pravec, P.; Scheirich, P.; Durech, J.; Pollock, J.; Kusnirak, P.; Hornoch, K.; Galad, A.; Vokrouhlicky, D.; Harris, A.W.; Jehin, E.; Manfroid, J.; Opitom, C.; Gillon, M.; Colas, F.; Oey, J.; Vrastil, J.; Reichart, D.; Ivarsen, K.; Haislip, J.; LaCluyze, A. (2014). "The tumbling state of (99942) Apophis." *Icarus* **233**, 48-60.

Stephens, R.D. (2017). "Asteroids Observed from CS3: 2016 October - December." *Minor Planet Bull.* **44**, 120-122.

Tonry, J.L.; Denneau, L.; Flewelling, H.; Heinze, A.N.; Onken, C.A.; Smartt, S.J.; Stalder, B.; Weiland, H.J.; Wolf, C. (2018). "The ATLAS All-Sky Stellar Reference Catalog." *Astrophys. J.* **867**, A105.

Warner, B.D.; Harris, A.W.; Pravec, P. (2009). "The Asteroid Lightcurve Database." *Icarus* **202**, 134-146. Updated 2019 Jul. *http://www.minorplanet.info/lightcurvedatabase.html*

Warner, B.D (2012a). "Asteroid Lightcurve Analysis at the Palmer Divide Observatory: 2011 June – September." *Minor Planet Bull.* **39**, 16-21.

Warner, B.D (2012b). "Asteroid Lightcurve Analysis at the Palmer Divide Observatory: 2011 September - December." *Minor Planet Bull.* **39**, 69-80.

Warner, B.D.; Stephens, R.D. (2013). "Asteroid Lightcurve Analysis at the Palmer Divide Observatory: 2011 September - December." *Minor Planet Bull.* **40**, 175-176.

Warner, B.D. (2015a). "A Sextet of Main-belt Binary Asteroid Candidates." *Minor Planet Bull.* **42**, 60-66.

Warner, B.D. (2015b). "Two New Binaries and Continuing Observations of Hungaria Group Asteroids." *Minor Planet Bull.* **42**, 132-136.

Warner, B.D. (2016). "Near-Earth Asteroid Lightcurve Analysis at CS3-Palmer Divide Station: 2015 June-September." *Minor Planet Bull.* **43**, 66-79.

Warner, B.D. (2018). "Near-Earth Asteroid Lightcurve Analysis at CS3-Palmer Divide Station: 2017 July Through October." *Minor Planet Bull*. **45**, 19-34.

Warner, B.D.; Stephens, R.D. (2019). "Near-Earth Asteroid Lightcurve Analysis at the Center for Solar System Studies: 2019 January-April." *Minor Planet Bull.* **43**, 304-314.

PHOTOMETRIC OBSERVATIONS FOR 7 MAIN-BELT ASTEROIDS: 2019 FEBRUARY – MAY

Michael Fauerbach
Florida Gulf Coast University
and SARA Observatories
10501 FGCU Blvd.
Ft. Myers, FL33965-6565
mfauerba@fgcu.edu

(Received: 2019 July 13)

Photometric observations of seven main-belt asteroids were obtained on four nights between 2019 February 13 and May 26. The following rotational periods were determined: 1551 Argelander, 4.066 ± 064 h; 1677 Tycho Brahe, 3.86 ± 0.01 h; 1774 Kulikov, 3.823 ± 0.001 h; 2564 Kayala, 3.01 ± 0.01 h; 26355 Grueber, 4.495 ± 0.028 h; and (47369) 1999 XA88, 2.56 ± 0.09 h. No well-defined period could be derived for 11155 Kinpu.

Photometric observations of asteroids obtained with two of the Southeastern Association for Research in Astronomy (SARA) consortium telescopes are reported. For the nights of 2019 February 13 and March 10, the 1-m Jacobus Kapteyn Telescope at the Observatorio del Roque de los Muchachos on the Spanish island of La Palma was used. The telescope is coupled with an Andor iKon-L series CCD. For the nights of 2019 March 24 and May 26, we used the 0.9-m telescope at Kitt Peak National Observatory. The telescope is coupled with an ARC CCD. A detailed description of the instrumentation and setup can be found in the paper by Keel et al. (2017). The data were calibrated using *MaximDL* and photometric analysis was performed using *MPO Canopus* (Warner, 2017).

1551 Argelander. Our group observed this asteroid previously in 2017 (Fauerbach and Brown, 2018). It was observed again in order to confirm the earlier result and lay the basis for shape modeling of it. Observations were made on a single night for approximately 5 hours.

A rotational period of 4.066 ± 064 h with lightcurve amplitude of 0.50 mag was derived. This is in excellent agreement with two previous measurements based on sparse data (Waszczak et al., 2015; Ďurech at al., 2016), as well as the data from our group from 2017. Baxter et al. (2019) reported a period of 2.313 ± 0.011 h based on data obtained in 2016. Neither our data from 2017 nor the current data can reproduce the result by Baxter et al. (2019).

Number	Name	yyyy mm/dd	Phase	L_{PAB}	B_{PAB}	Period(h)	P.E.	Amp	A.E.	Grp
1551	Argelander	2019 02/13-02/13	16.3	106	1	4.066	0.064	0.50	0.04	MB-I
1677	Tycho Brahe	2019 03/10-03/10	11.7	141	4	3.86	0.01	0.42	0.03	EUN
1774	Kulikov	2019 02/14-03/25	11.5,3.4	176	0	3.823	0.001	0.40	0.02	KOR
2564	Kayala	2019 03/10-03/25	6.4,14.0	158	0	3.01	0.01	0.39	0.02	FLOR
11155	Kinpu	2019 02/14-03/25	12.4,12.1	155	-8			0.16	0.02	EUN
26355	Grueber	2019 02/13-02/13	15.4	109	6	4.495	0.028	0.74	0.06	MB-I
47369	1999 XA88	2019 05/26-05/26	26.2	184.4	8	2.56	0.09	0.28	0.06	V

Table I. Observing circumstances and results. The phase angle is given for the first and last date. If preceded by an asterisk, the phase angle reached an extrema during the period. L_{PAB} and B_{PAB} are the approximate phase angle bisector longitude/latitude at mid-date range (see Harris et al., 1984). Grp is the asteroid family/group (Warner et al., 2009).

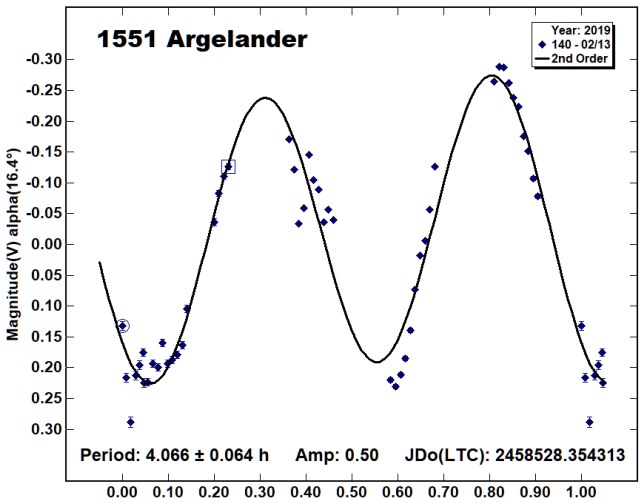

1677 Tycho Brahe is a member of the Eunomia family of asteroids. The asteroid was observed over a single night for a period of about 6.5 hours. The derived period of 3.86 ± 0.01 h with lightcurve amplitude of 0.42 mag are in excellent agreement with prior measurements (Violante and Leake, 2012; Benishek, 2018). Ďurech et al. (2018) were able to determine a pole position for this asteroid by combining sparse data from the Lowell Photometric database with date from WISE (Mainzer et al., 2016). Combining the denser photometric observations from 2012, 2017 and 2019 can provide an independent test of the pole orientation and the shape model.

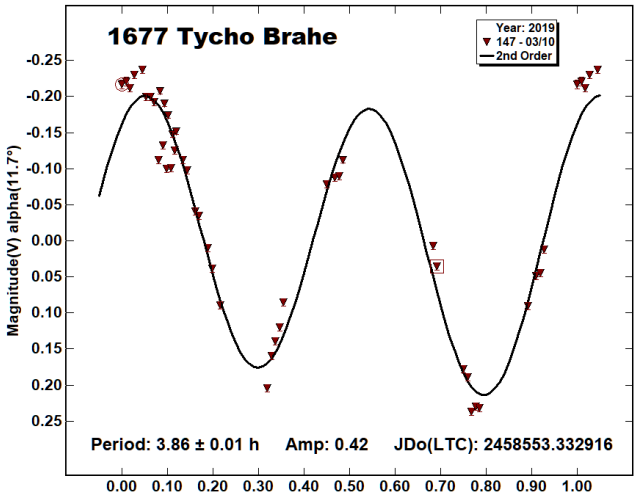

1774 Kulikov is a member of the Koronis family. The asteroid was observed on two nights, roughly 6 weeks apart. The derived rotational period of 3.823 ± 0.001 h with an amplitude of 0.40 mag is in good agreement with the result previously obtained by our group (Fauerbach and Nelson, 2019) and the result reported by Ďurech et al. (2016). We will combine our data from 2018 and 2019 to produce a shape model and then compare it to the one provided by Ďurech et al. (2016) based on sparse data.

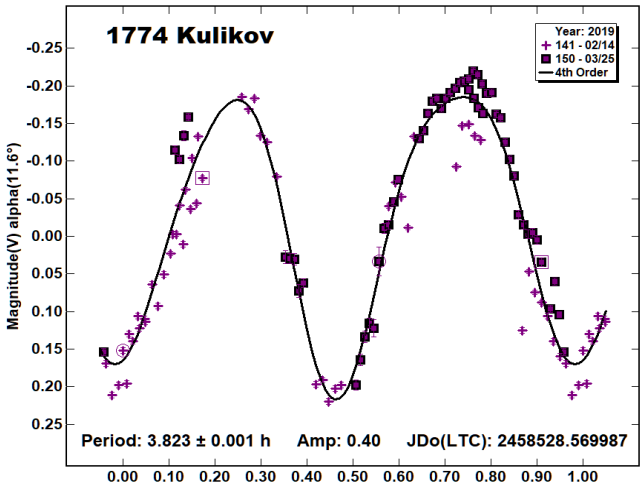

2564 Kayala is a member of the Florina family of asteroids. Only one prior period measurement, by Chang et al. (2016), has been reported. They derived a period of 2.95 ± 0.01 h with an amplitude of 0.36 mag. The best bimodal fit to the current data provides a period of 3.01 ± 0.01 h with an amplitude of 0.39 mag. This is in good agreement with the previous measurement.

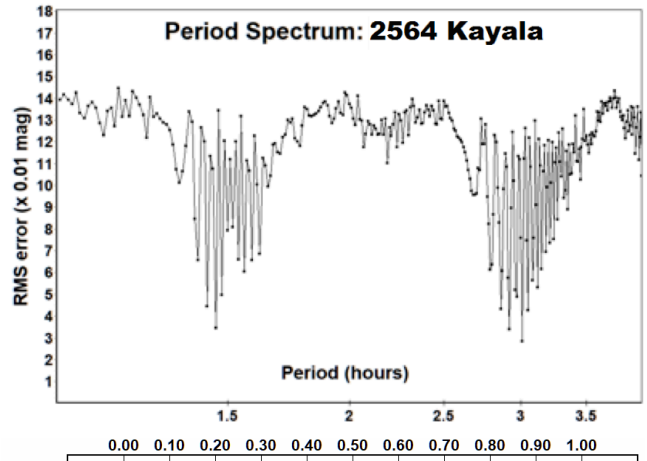

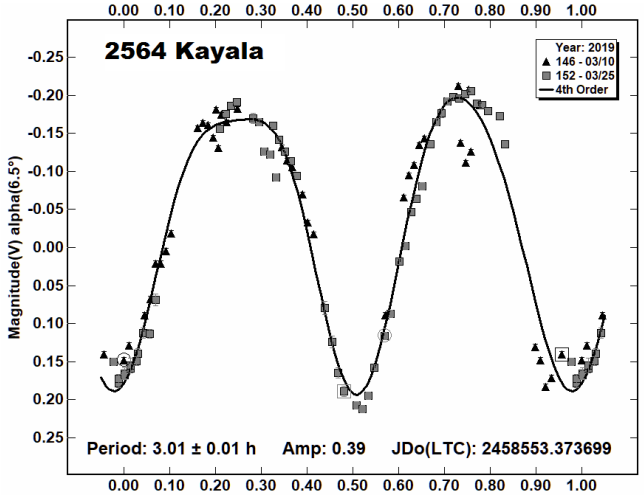

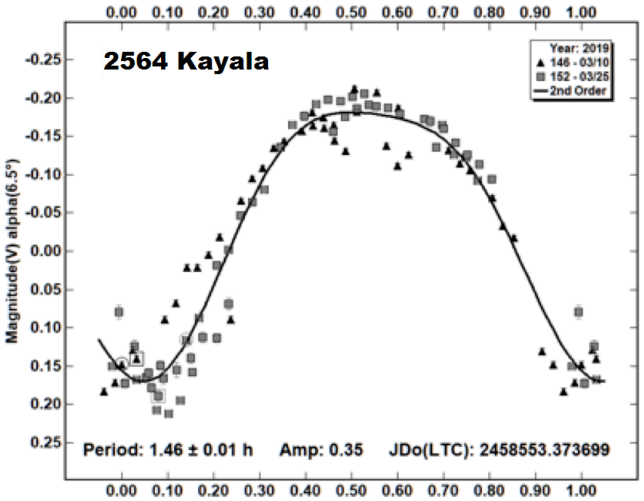

A closer look at the period spectrum reveals that a monomodal curve with a half-period of about 1.49 ± 0.01 h yields a similarly good fit and therefore cannot be excluded. For this paper it is assumed that the bimodal solution with a period of 3.01 ± 0.01 h is the preferred solution.

11155 Kinpu is a member of the Eunomia family of asteroids. The only previously reported rotational period is by Waszczak et al. (2015) based on a fit to sparse data. They reported a period of 2.208 ± 0.002 h with an amplitude of 0.06 mag.

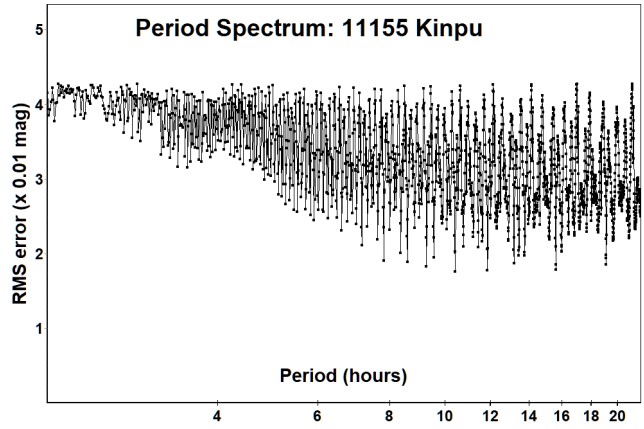

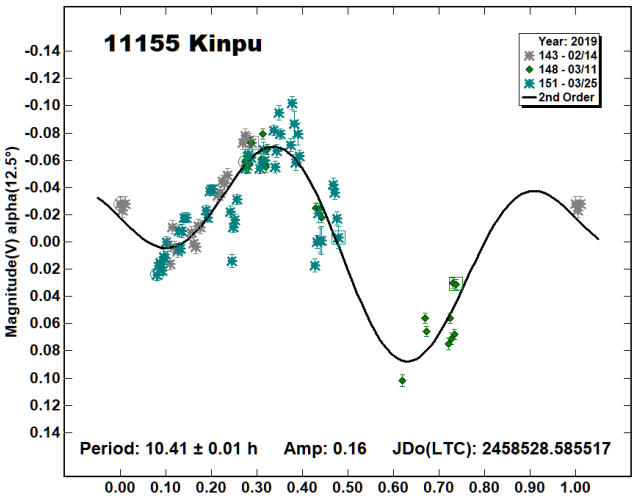

We observed 11155 Kinpu on three nights over a six-week period. On two of the nights, we studied the asteroid for more than four hours, thereby covering almost two complete rotations, if the period of 2.208 h is correct. Unfortunately, we were not able to confirm this period.

The best fit to our data is a rotational period of 10.41 ± 0.01 h with an amplitude of 0.16 mag. However, additional data are needed to confirm this result, since a look at the period spectrum shows that there are many solutions with a similar good fit to the data. Therefore, we will limit ourselves to stating the amplitude and the fact that the period seems to be substantially longer than the previously reported period of 2.208 h.

26355 Grueber. This asteroid was observed by our group in 2018 December (Fauerbach and Fauerbach, 2019). Our reported result did not agree with the only prior measurement by Waszczak et al. (2015), which was based on a fit to sparse data. Therefore, we jumped at the chance to verify our results two months later at a very different phase angle. The asteroid was observed for roughly 5.5 hours, which would mean covering more than one complete rotational period. The measured period of 4.495 ± 0.028 h with an amplitude of 0.74 mag fits well with our previous result of 4.539 ± 0.001 h. Combining the datasets from our 2018 and 2019 observations, we derive a period of 4.540 ± 0.001 h with an amplitude of 0.88 mag.

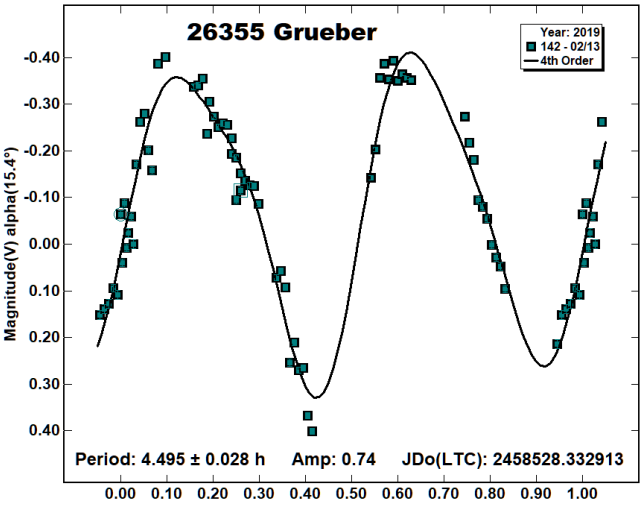

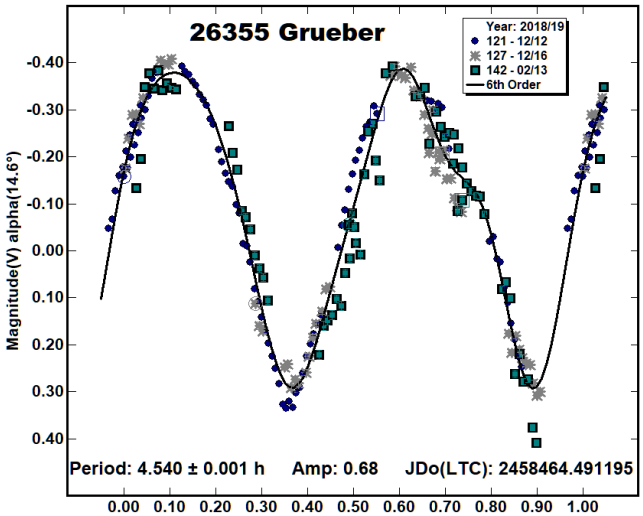

(47369) 1999 XA88 is a member of the Vesta family of asteroids. Only one prior period measurement, by Chang et al. (2016), has been reported. They derived a period of 2.55 ± 0.06 h with an amplitude of 0.19 mag. The best bimodal fit to the current data provides a period of 2.56 ± 0.09 h with an amplitude of 0.28 mag. This is in excellent agreement with the previous measurement.

A closer look at the period spectrum reveals that a monomodal curve with approximately half the period, 1.32 ± 0.04 h, yields a similarly good fit and therefore cannot be excluded. For this paper it is assumed that the bimodal solution with a period of 2.56 ± 0.09 h is the preferred solution.

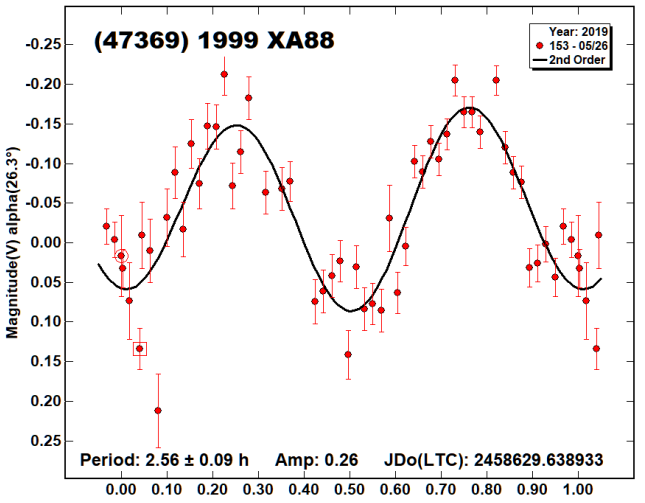

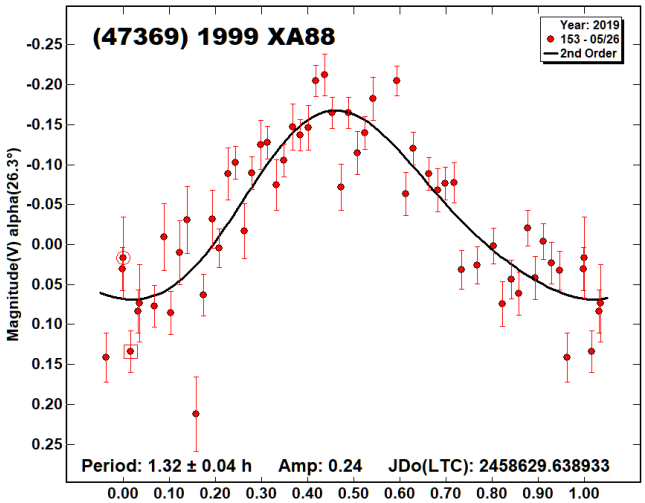

References

Baxter, N.; Vent, A.; Montgomery, K.; Davis, C.; Cantu, S.; Lyons, V. (2019). "Lightcurves and Rotational Periods of Five Main-belt Asteroids." *Minor Planet Bulletin* **46**, 111-114.

Benishek, V. (2018). "Lightcurve and Rotation Period Determinations for 8 Asteroids." *Minor Planet Bulletin* **45**, 187-189.

Chang, C.-K.; Lin, H.-W.; Ip, W.-H.; Prince, T.A.; Kulkarni, S. R.; Levitan, D.; Laher, R.; Surace, J. (2016). "Large Super-fast Rotator Hunting Using the Intermediate Palomar Transient Factory." *Astrophysical Journal Supplement Series* **227**, A20.

Ďurech, J.; Hanuš, J.; Oszkiewicz, D.; Vančo, R. (2016). "Asteroid models from the Lowell photometric database." *Astronomy & Astrophysics*, **587**, A48.

Ďurech, J.; Hanuš, J.; Alí-Lagoa, V. (2018). "Asteroid models reconstructed from the Lowell Photometric Database and WISE data." *Astronomy & Astrophysics* **617**, A57.

Fauerbach, M.; Brown, A. (2018). "Lightcurve Analysis of Minor Planets 1132 Hollandia, 1184 Gaea 1322 Coppernicius, 1551 Argelander, and 3230 Vampilov." *Minor Planet Bulletin* **45**, 240-241.

Fauerbach, M.; Fauerbach, M. (2019). "Lightcurve Analysis of Asteroids 131 Vala, 1184 Gaea, 7145 Linzexu, and 26355 Grueber." *Minor Planet Bulletin* **46**, 236-237.

Fauerbach, M.; Nelson, K.M. (2019). "Photometric Observations of 1007 Pawlowia, 1774 Kulikov, 2764 Moeller, 5110 Belgirate, (8505) 1990 YK, and (34459) 2000 SC91." *Minor Planet Bulletin* **46**, 21-23.

Harris, A.W.; Young, J.W.; Scaltriti, F.; Zappala, V. (1984). "Lightcurves and phase relations of the asteroids 82 Alkmene and 444 Gyptis." *Icarus* **57**, 251-258.

Keel, W.C.; Oswalt, T.; Mack, P.; Henson, G.; Hillwig, T.; Batcheldor, D.; Berrington, R.; De Pree, C.; Hartmann, D.; Leake, M.; Licandro, J.; Murphy, B.; Webb, J.; Wood, M.A. (2017). "The Remote Observatories of the Southeastern Association for Research in Astronomy (SARA)," *PSAP* **129**:015002 (12pp). *http://iopscience.iop.org/article/10.1088/1538-3873/129/971/015002/pdf*

Mainzer, A.K., Bauer, J.M., Cutri, R.M., Grav, T., Kramer, E.A., Masiero, J.R., Nugent, C.R., Sonnett, S.M., Stevenson, R.A., Wright, E.L. (2016). "NEOWISE Diameters and Albedos V1.0." NASA Planetary Data System. EAR-A-COMPIL-5-NEOWISEDIAM-V1.0.

Violante, R.; Leake, M.A. (2012). "Photometry and Lightcurve Analysis of 7 Main-Belt Asteroids." *Journal of the Southeastern Association for Research in Astronomy* **7**, 41-44.

Warner, B.D. (2017). *MPO Canopus* software version 10.7.10.0. *http://www.bdwpublishing.com*

Warner, B.D., Harris, A.W., Pravec, P. (2009). "The Asteroid Lightcurve Database." *Icarus* **202**, 134-146. *http://www.minorplanet.info/lightcurvedatabase.html*

Waszczak, A.; Chang; C.-K.; Ofek, E. O.; Laher, R.; Masci, F.; Levitan, D.; Surace, J.; Cheng, Y.-C.; Ip, W.-H.; Kinoshita, D.; Helou, G.; Prince, T.A.; Kulkarni, S. (2015). "Asteroid Light Curves from the Palomar Transient Factory Survey: Rotation Periods and Phase Functions from Sparse Photometry." *Astronomical Journal* **150**, A75.

ROTATION PERIOD OF ASTEROID 349 DEMBOWSKA

Alberto Colognese
P.O.C. – Piccolo Osservatorio Corsionese
Corsione (AT), Italy
alberto@colognese.it

(Received: 2019 June 28)

Here we present the result of an observing campaign for asteroid 349 Dembowska. In addition to period determination, we show how to use the result to determine absolute magnitude using the H-G system and how to derive the diameter for an equivalent spherical shape.

Asteroid 349 Dembowska was discovered on 1892 Dec. 9 by A. Charlois at Nice and named in honor of astronomer Ercole Dembowski (1812-1881), Dembowski is also honored by a lunar crater. According to JPL Small-Body Database, it is a relatively uncommon inner belt R-type asteroid (Tholen spectral type) located just prior the 7:3 resonance with Jupiter, showing a high albedo value (p = 0.384). According to MPC Database it has an estimated spherical diameter of ~140 km with an absolute magnitude of 5.93, a phase slope of 0.37 and a semi-major axis of 2.92 AU, with an eccentricity of 0.092 (MPC).

From February 27, 2019 to March 23, 2019, we carried out 4 CCD observations at P.O.C. observatory, making the photometric analysis of asteroid 349 Dembowska. Images were taken using a V photometric filter with an Atik 314L+ b/w and a RC 8". Exposures ranged from 15 to 20 seconds. The image scale after 2x2 binning was 1.66 arcsec/pixel. All images have been corrected with dark frame, bias and flat field images.

At the end of the work, after deleted spurious data, we used Canopus to analyze 683 fits for about 11.4 hours of observation, as presented in the table below, finding a synodic period of 4.6957 ± 0.0007 h that agrees rather well with that of 4.70117 h (Zappalà) and 4.7029 ± 0.0054 h (MPB No.35-2 2008) reported in literature even if our phase plot was derived with an incomplete dataset.

The lightcurve has an amplitude A=0.08 mag. Using this value we can estimate the approximate ratio between the major and minor axis of the asteroid shape:

$$a/b = 10^{\left(\frac{A}{2.5}\right)}$$

For (349) Dembowska, we get

$$10^{\left(+0.08/2.5\right)} = 1.0765$$

The H-G plot obtained with Canopus and the data gathered yields to an H value of 5.96 ± 0.18 assuming a fixed G value of 0.37. This H value can be used to estimate the asteroid spherical diameter with the formula (from JPL/NASA CNEOS):

$$D = 10^{[3.1236 - 0.5 \cdot log_{10}(p) - 0.2H]} = \frac{1329.23}{\sqrt{p}} \cdot 10^{-0.2H}$$

that, for 349 Dembowska, leads to

$$D = \frac{1329.23}{\sqrt{0.384}} \cdot 10^{-0.2 \cdot 5.955} = 138.64 \mp 11.28\ km$$

References

Alton, Kevin B. "CCD Photometry Lightcurve of Three Main Belt Asteroids". *Minor Planet Bulletin*. Vol. 42, No. 2 (2015)

JPL/NASA CNEOS, Center for Near Earth Objects Studies, *https://cneos.jpl.nasa.gov/tools/ast_size_est.html* (accessed June 21, 2019*)*

JPL Small-Body Database
https://ssd.jpl.nasa.gov/sbdb.cgi?sstr=2000349#phys_par(accessed July 30, 2019)

LiangLiang Yu; Bin Yang; Jianghui Ji; Wing-Huen Ip, (2017). "Thermophysical characteristics of the large main-belt asteroid (349) Dembowska." MNRAS, 472, 2388-2397

Majaess, D.J.; Tanner, J.; Savoy, J.; Sampson, B. (2008). "349 Dembowska: A Minor Study of its Shape and Parameters". *Minor Planet Bulletin*. Vol. 35, No. 2

MPC Database Search
https://www.minorplanetcenter.net/db_search/show_object?utf8=%E2%9C%93&object_id=dembowska (accessed June 21, 2019)

Schmadel, "Dictionary of Minor planets Names." Springer, 5th Ed.

UnderOak Observatory
http://www.underoakobservatory.com/Minor%20Planet%20LCs/349_Dembowska_17Apr-25Apr2014_v1.png (accessed June 21, 2019)

2019 mm/dd	Pts	Phase	LPAB	BPAB
02/27	195	-3.09	158.47	8.21
02/28	278	-3.12	158.45	8.20
03/22	119	+8.90	158.20	7.64
07/23	91	+9.19	158.21	7.61

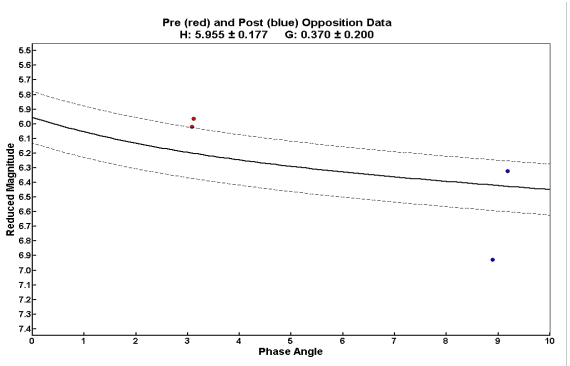

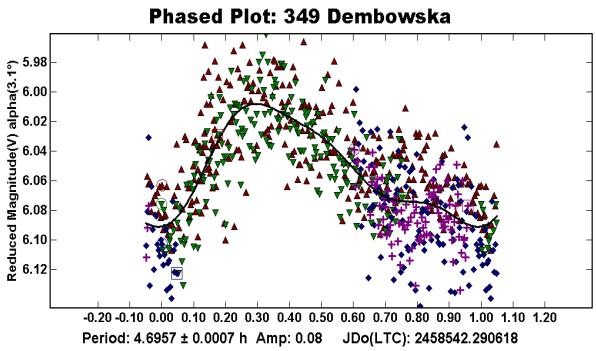

NEAR-EARTH ASTEROID LIGHTCURVE ANALYSIS AT THE CENTER FOR SOLAR SYSTEM STUDIES: 2019 MARCH-JULY

Brian D. Warner
Center for Solar System Studies / MoreData!
446 Sycamore Ave.
Eaton, CO 80615 USA
brian@MinorPlanetObserver.com

Robert D. Stephens
Center for Solar System Studies / MoreData!
Rancho Cucamonga, CA 91730

(Received: 2019 July 15)

Lightcurves for 38 near-Earth asteroids (NEAs) obtained at the Center for Solar System Studies (CS3) from 2019 March-July were analyzed for rotation period, peak-to-peak amplitude, and signs of satellites or tumbling.

CCD photometric observations of 38 near-Earth asteroids (NEAs) were made at the Center for Solar System Studies (CS3) from 2019 March-July. Table I lists the telescopes and CCD cameras that are combined to make observations.

Up to nine telescopes can be used for the campaign, although seven is more common. All the cameras use CCD chips from the KAF blue-enhanced family and so have essentially the same response. The pixel scales ranged from 1.24-1.60 arcsec/pixel.

Telescopes	Cameras
0.30-m *f*/6.3 Schmidt-Cass	FLI Microline 1001E
0.35-m *f*/9.1 Schmidt-Cass	FLI Proline 1001E
0.40-m *f*/10 Schmidt-Cass	SBIG STL-1001E
0.40-m *f*/10 Schmidt-Cass	
0.50-m *f*/8.1 Ritchey-Chrétien	

Table I. List of available telescopes and CCD cameras at CS3. The exact combination for each telescope/camera pair can vary due to maintenance or specific needs.

All lightcurve observations were unfiltered since a clear filter can cause a 0.1-0.3 mag loss. The exposure duration varied depending on the asteroid's brightness and sky motion. Guiding on a field star sometimes resulted in a trailed image for the asteroid.

Measurements were made using *MPO Canopus*. The Comp Star Selector utility in *MPO Canopus* found up to five comparison stars of near solar-color for differential photometry. Comp star magnitudes were taken from ATLAS catalog (Tonry et al., 2018), which has Sloan *griz* magnitudes that were derived from the GAIA and Pan-STARR catalogs, among others. The authors state that systematic errors are generally no larger than 0.005 mag, although they can reach 0.02 mag in small areas near the Galactic plane. BVRI magnitudes were derived by Warner using formulae from Kostov and Bonev (2017). The overall errors for the BVRI magnitudes, when combining those in the ATLAS catalog and the conversion formulae, are on the order of 0.04-0.05.

Even so, we found in most cases that nightly zero point adjustments on the order of only 0.02-0.03 mag were required during period analysis. There were occasional exceptions that required up to 0.10 mag. These may have been related in part to using unfiltered observations, poor centroiding of the reference stars, and not correcting for second-order extinction terms. Regardless, the systematic errors seem to be considerably less than other catalogs, which reduces the uncertainty in the results when analysis involves data from extended periods or the asteroid is tumbling.

In the plots below, the "Reduced Magnitude" is Johnson V as indicated in the Y-axis title. These are values that have been converted from sky magnitudes to unity distances by applying –5*log (rΔ) to the measured sky magnitudes with r and Δ being, respectively, the Sun-asteroid and Earth-asteroid distances in AU. Unless otherwise stated, the magnitudes were normalized to the phase angle in parentheses using G = 0.15. The X-axis is the rotational phase, ranging from –0.05 to +1.05.

If the plot includes an amplitude, e.g., "Amp: 0.65", this is the amplitude of the Fourier model curve and *not necessarily the adopted amplitude for the lightcurve*.

Our initial search for previous results started with the asteroid lightcurve database (LCDB; Warner *et al.,* 2009) found on-line at *http://www.minorplanet.info/lightcurvedatabase.html*. Readers are strongly encouraged to obtain, when possible, the original references listed in the LCDB.

1036 Ganymed. There are several references in the LCDB giving rotational values for this 32-km NEA. The most extensive report was by Pilcher et al. (2012), who followed the asteroid for several months and were able to make a detailed account of lightcurve synodic period and amplitude. They gave P = 10.309 h when using the entire data set. Using subsets, they found periods 10.280-10.345, making our result of 10.318 h in good agreement.

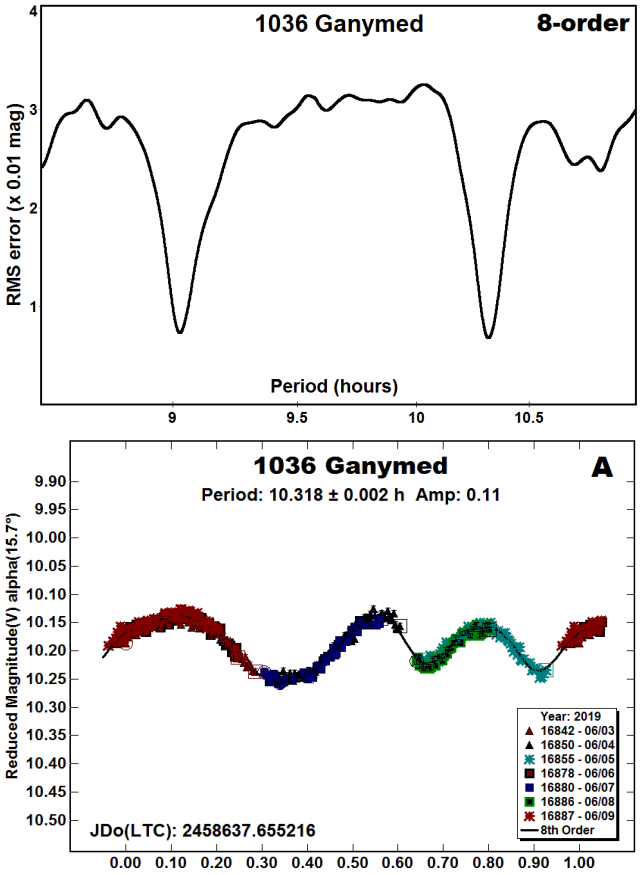

The trimodal shape is unusual but entirely possible because of the low phase angle and amplitude (Harris et al., 2014).

3103 Eger. This 2-km NEA has been well-studied over the years. Durech et al. (2012) used sparse and dense lightcurve data to determine that the YORP (Yarkovsky–O'Keefe–Radzievskii–Paddack; Rubincam, 2000) effect was causing the asteroid's rotation period to decrease. The uncertainty was significant; additional lightcurves extending the total range of observations will be useful for refining their result.

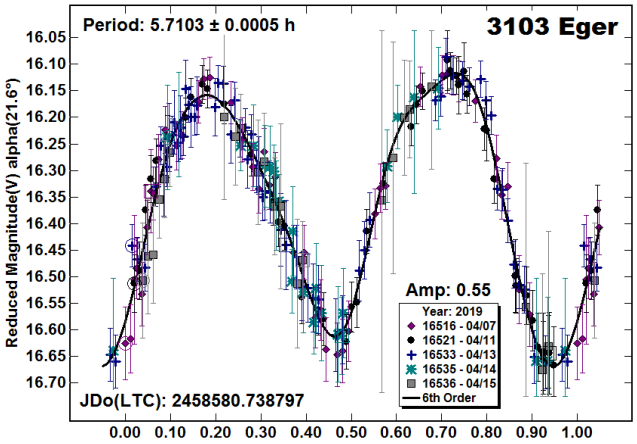

4581 Asclepius. The period spectrum showed several nearly equal solutions from our 2019 data. The only previous results in the LCDB were from Pravec et al. (2019), who found a secure solution at 8.008 h. Our data fit to 8.006 h, but there is a significant gap in coverage. A review of solutions between 3-7 hours for a good half-period (4.805 h, "Alt 1") made an argument for a solution near 9.6 h ("Alt 2"). We have adopted P = 8.006 h for this paper but consider it ambiguous and note that the other solutions cannot be formally excluded.

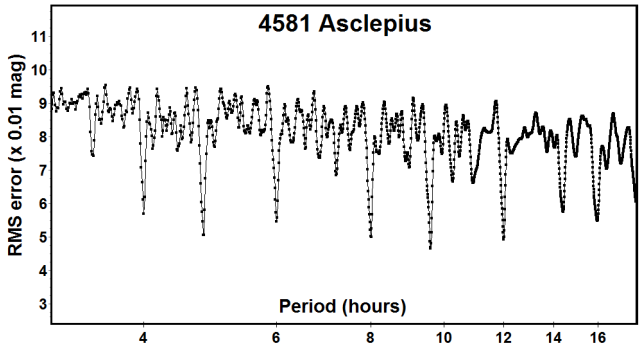

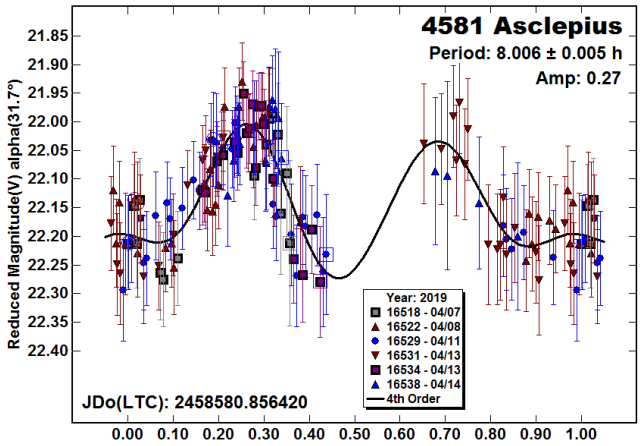

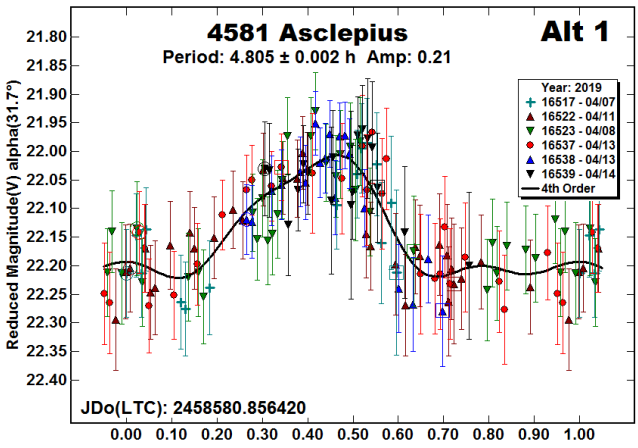

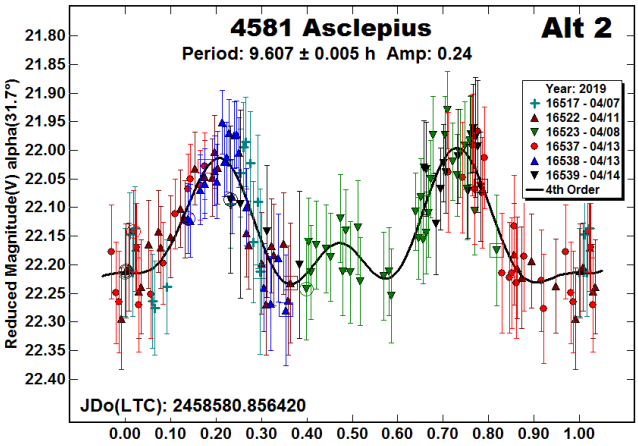

5332 Davidaguilar. The earliest result for this 3-km NEA is from Binzel (1990; 5.82 h), who observed it when it had only the designation 1990 DA. The rotation period was subsequently refined to 5.803 h (Wisniewski et al., 1997). Other than a sidereal period derived through shape modeling (Hanus et al., 2016), those are the only previously reported periods. Our result of 5.821 h is a little longer in comparison, but that may be due in part to sidereal-synodic period differences. It's also possible that another night or two, e.g., to get better coverage from 0.8-1.0 rotation phase, would have made our period match the others.

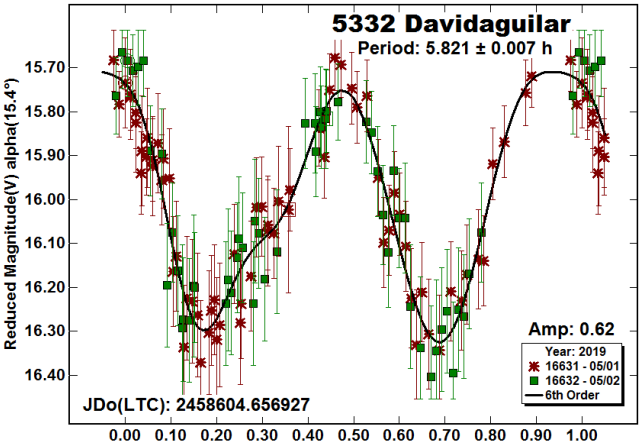

(5693) 1993 EA. We observed 1993 EA in 2017 January (Warner, 2017b). At the time, a period of 2.496 h was found along with a second period of 16.55 h, which was suspected to have been due to a satellite. We observed the asteroid again in 2018 April when

the phase angle bisector longitude (L_{PAB}) was about 80° from the 2017 apparition. We found P = 2.4956 h but no traces of a second period. This is not surprising since our data were noisy and the lightcurve amplitude only 0.06 mag.

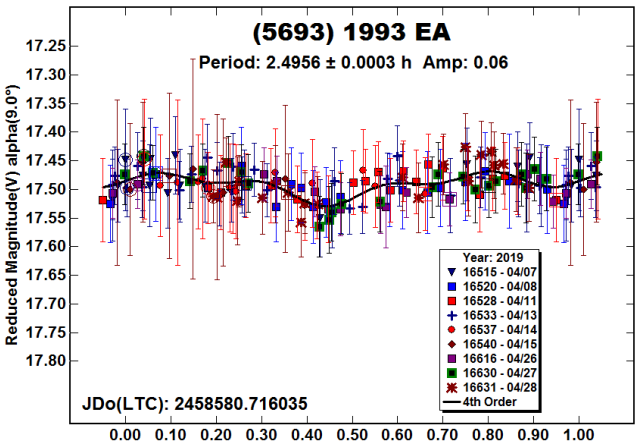

(12538) 1998 OH. The diameter of 1998 OH is about 2 km. We worked it several times in the past. First was Warner (2015a), when an ambiguous solution of 5.833 h or 2.914 h was reported. Using data from 2016 (Warner, 2017a), a new solution of 5.154 h was found and the previous result was revised to 5.191 h. Most recently (Warner, 2019), we used data from 2018 to find a period of 2.592. Revisits to the previous data sets revised those results as well, but all new results were considered ambiguous, with a double-period still possible.

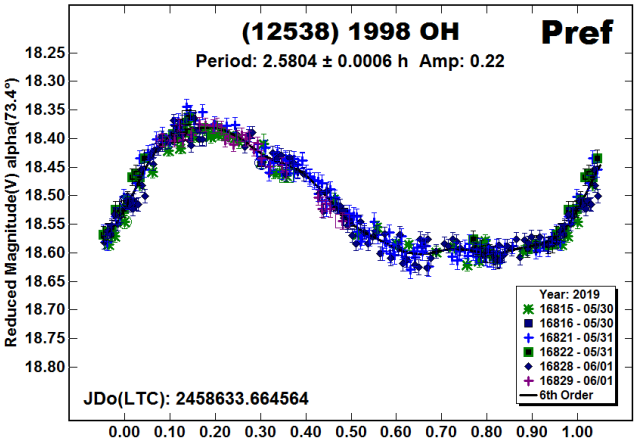

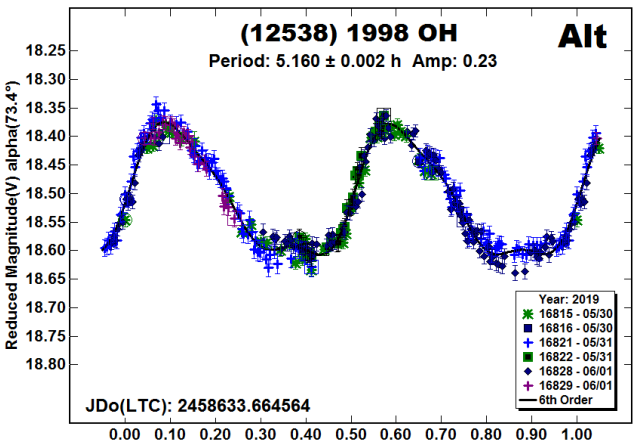

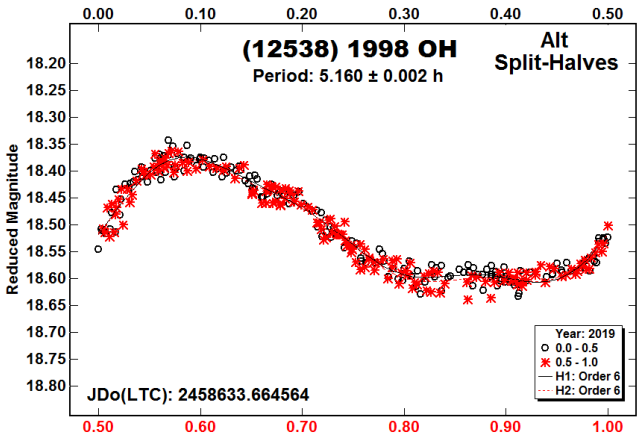

The period spectrum using the 2019 data shows the shorter period, 2.5804 h, is favored while a check of the double period using a split-halves plot shows mirrored halves, which is highly unlikely. This, along with results from Skiff et al. (2019b), leads to the conclusion that the true period is about 2.58 h and that the double solution, even though it cannot be formally excluded, can be safely rejected.

(68216) 2001 CV26. Stephens et al. (2015) reported this to be a suspected binary asteroid, finding P_1 = 2.429 h and P_2 = 21.89 h. They also reported that previous radar observations did not show traces of a satellite and so the claim of being binary was considered tenuous at best.

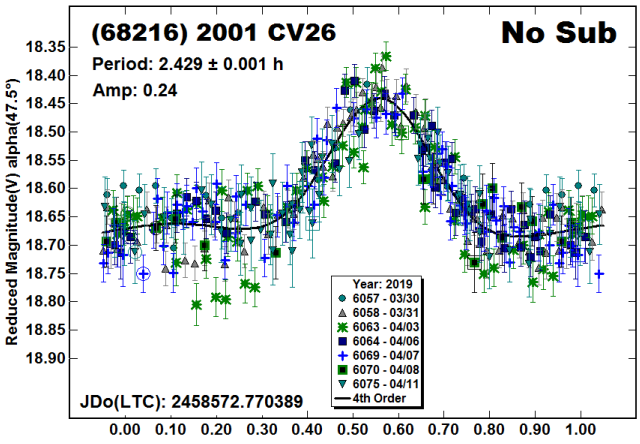

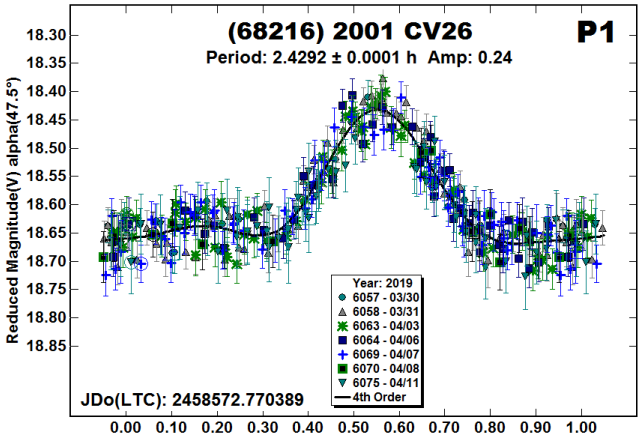

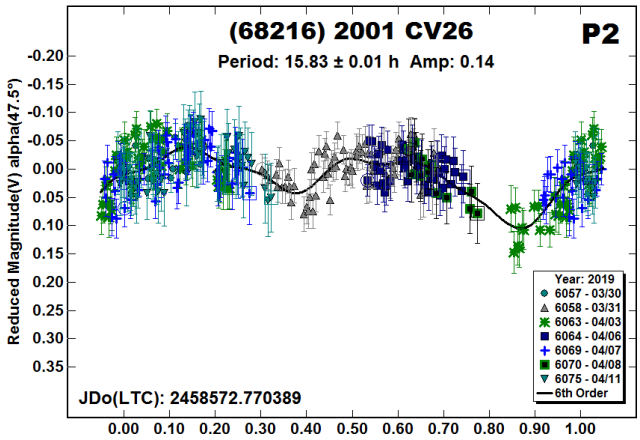

Our data from 2019 led to P_1 = 2.4292 h. The difference between the "NoSub" and "P1" plots again raised the possibility of a binary asteroid. We eventually found P_2 = 15.83 h and a bimodal lightcurve that resembles a typical case of a tidally-locked, elongated satellite. The new period is not an integral multiple with the one from Stephens et al. Here again, the evidence is weak and so the true nature of the asteroid remains a mystery.

(68950) 2002 QF15. Shepard et al. (2008) reported results from radar observations in 2003 and radar and photometric observations in 2006. The radar data indicated a size of about 2 km and a preferred rotation period of about 47 h, which was the period found from the photometric data, although the half-period (23.5 h) could not be excluded at the time.

We observed the asteroid in 2019 June. The data analysis found a period of 45.24 h, in close agreement with the preferred radar period. Despite the lack of coverage, the asymmetric shape made the half-period solution implausible, and so the longer solution is confirmed.

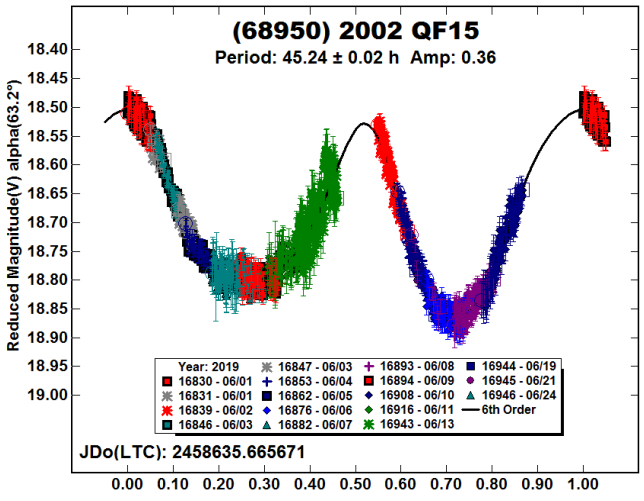

(85236) 1993 KH. The LCDB did not list any rotation periods for 1993 KH, which has an estimated diameter of 540 meters. While the data were noisy, we're confident that the result of P = 5.057 h is secure since the somewhat low phase angle and amplitude strongly favor a bimodal solution (Harris et al., 2014). Other factors favoring the solution are the asymmetry of the lightcurve (which ruled out the half-period solution) and that fact that some sessions covered almost a complete rotation of the presumed period.

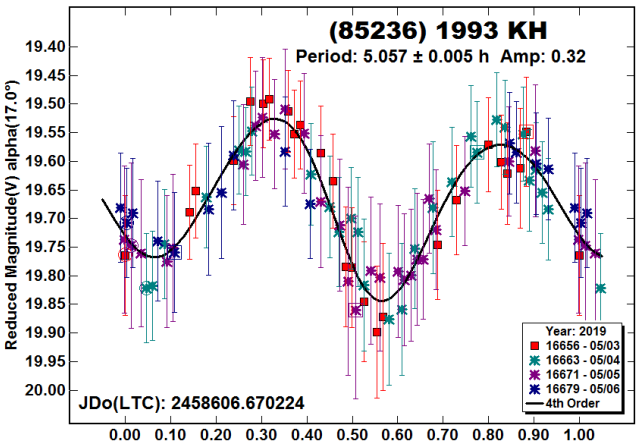

(85989) 1999 JD6. There are numerous results in the LCDB for this 1.1 km asteroid, e.g., Polishook and Brosch (2008, 7.6638 h), Warner (2015b, 7.673 h), and Aznar et al. (2018, 7.685 h). Our latest result is consistent with those.

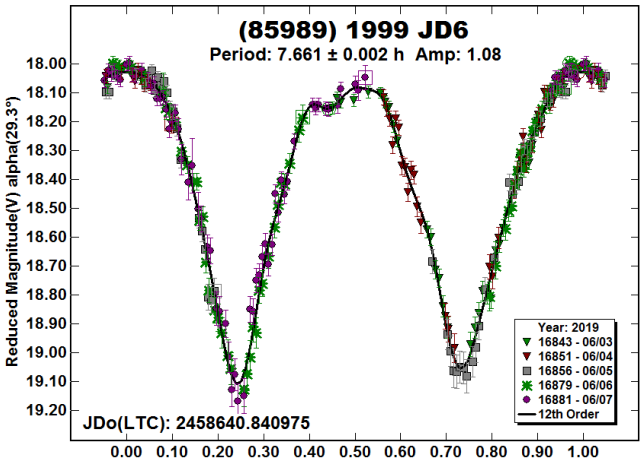

(112221) 2002 KH4. In the absence of other information, the lightcurve closely resembles one of an elongated satellite that is tidally-locked to its orbital period and shows mutual events. The estimated diameter is 2.4 km and so the size and putative orbital period are consistent with known binary asteroids. Subtracting the period from data in a dual-period search finds a nearly flat, noisy "curve" with a period of 2.479 h. This is also consistent with being a binary. This asteroid warrants detailed observations at future apparitions.

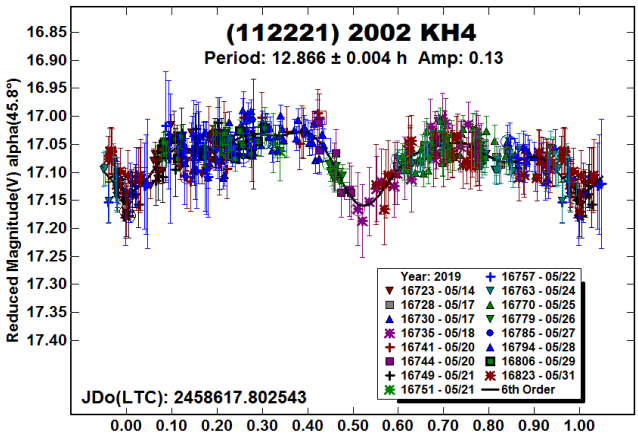

(141525) 2002 FV5. The estimated diameter is 750 meters. There were no listings in the LCDB prior to this.

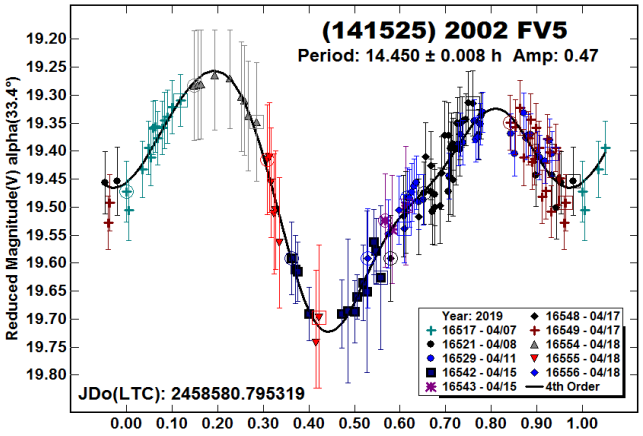

(144898) 2004 VD17. De Luise et al. (2007) found a period of 1.99 h. The period is slightly below the "spin barrier" of $P < 2.0$-2.2 h, which might imply a strength-bound structure or strong cohesive forces in a "rubble pile." Our result of 3.369 h puts the asteroid back into the league of ordinary asteroids.

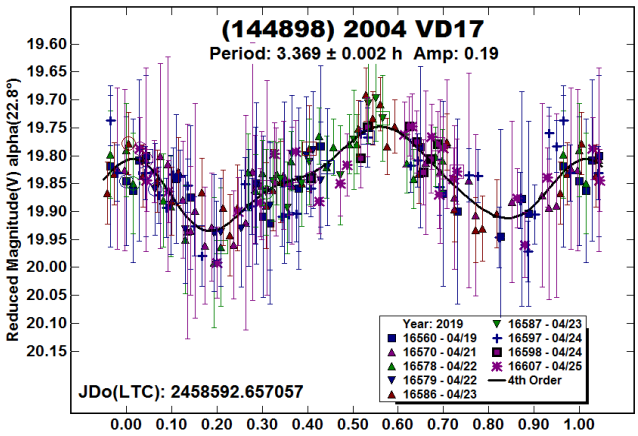

(162181) 1999 LF6. Pravec et al. (1999) found a period of 16.007 h. Warner (2014) reported 14.77 h.

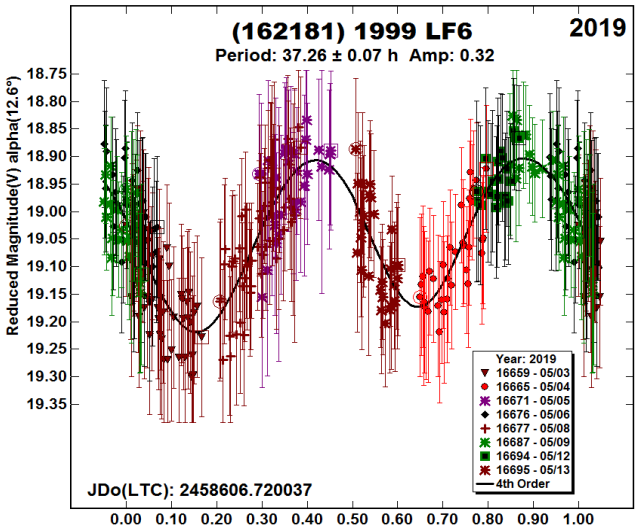

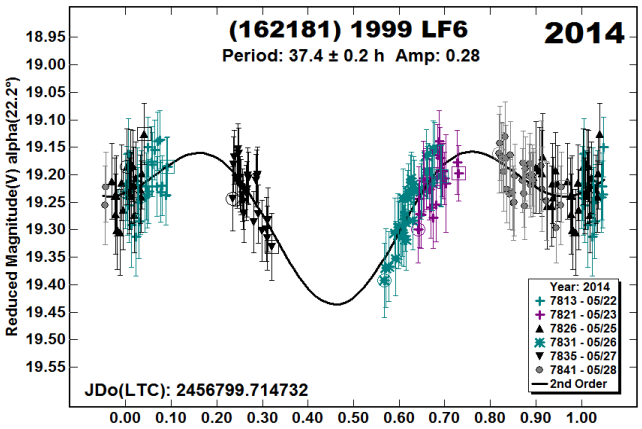

The data from our 2019 observations led to a period of 37.26 h. The noisy data do make the solution somewhat suspect but the slopes of the individual sessions are a good match to the Fourier curve. To be sure, we reviewed the 2014 data and found that a solution of 14.69 h was still slightly favored over one of 37.4 h but both showed an asymmetry of the maximums being 0.6 rotation phase apart and the longer period lightcurve with radically different minimum depths. We have adopted the 2019 result for this paper.

(163696) 2003 EB50. Pravec et al. (2019) found a period of 62.31 h based on data obtained in 2015. Our result is in good agreement.

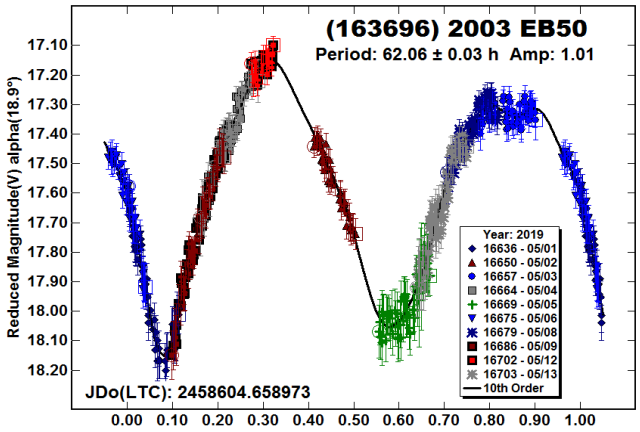

(244670) 2003 KN18. The period spectrum showed numerous solutions with nearly equal RMS minimum values. After single- and dual-period analysis, we suspect that the asteroid is in a low-level state of tumbling (see Pravec et al., 2014; 2005).

MPO Canopus does not implement an algorithm suitable for analyzing tumbling asteroids, which is to solve for two periods simultaneously instead of iteratively. In some cases, however, when the two periods are similar or have a readily identified "beat period" (when the two periods repeat in an almost perfect integral ratio), *MPO Canopus* can be used to get a first-order solution for the two periods.

This seemed to be the case here and so we did a dual-period search that found two distinct periods of P_1 = 20.887 and P_2 = 37.06 h. These have a beat period of P_{Beat} = 146.2 h, or a 7:4 ratio. When we forced a period of P_{Beat}, two pairs of sessions were found in which the two sessions in each pair overlapped about every 6 days (144 h).

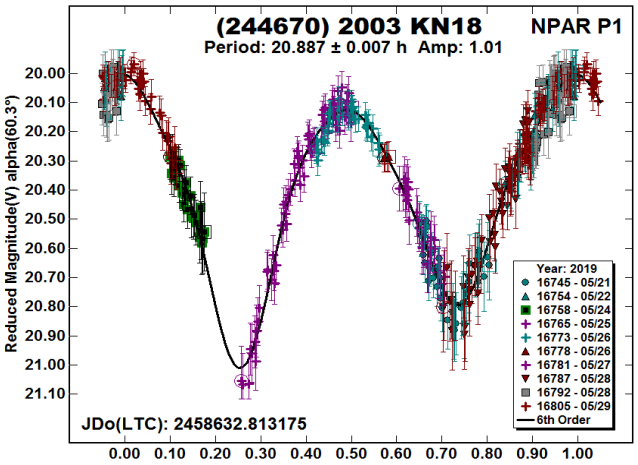

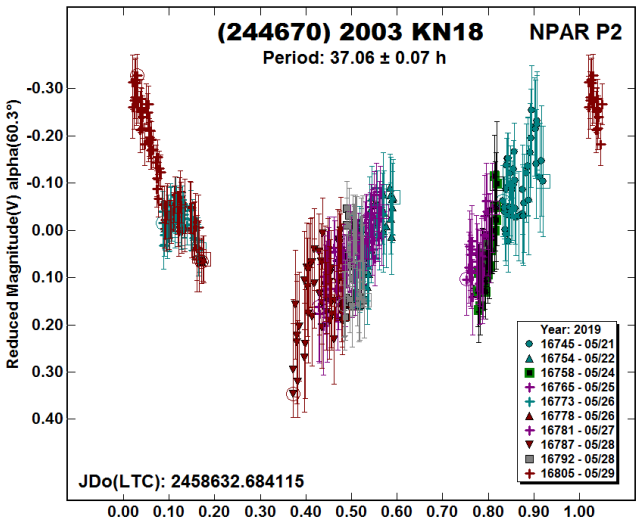

(257744) 2000 AD205. Skiff et al. (2012; 2019a) reported on one night of observations in 2008 June to say that no period could be found.

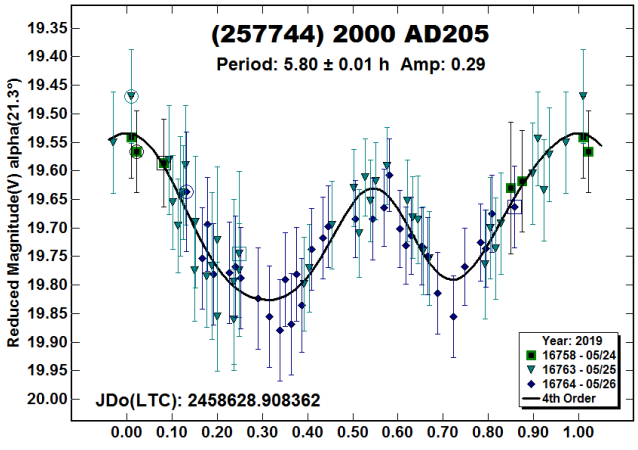

(326777) 2003 SV222. There were no previous lightcurve results in the LCDB. The period spectrum showed some alternate solutions but the RMS for a period of 28.01 h was clearly favored.

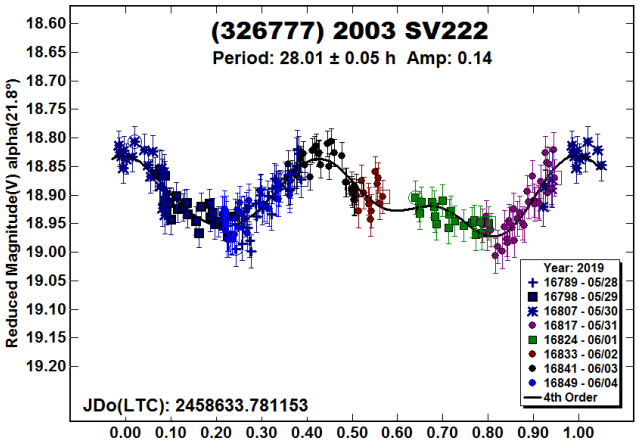

(355256) 2007 KN4. Waszczak et al. (2015) found a period of 7.141 h and amplitude of 0.40 mag using a "dense sparse" data set. Our result is very similar.

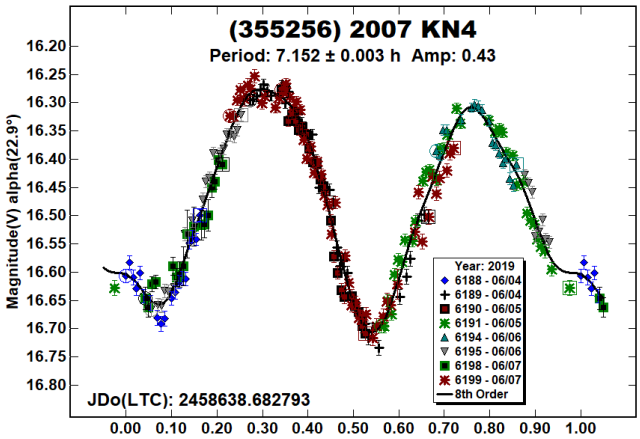

(453778) 2011 JK. Skiff et al. (2019b) found a period of 2.4567 h using a very high-quality data set obtained about two weeks after ours. Our result is in good agreement.

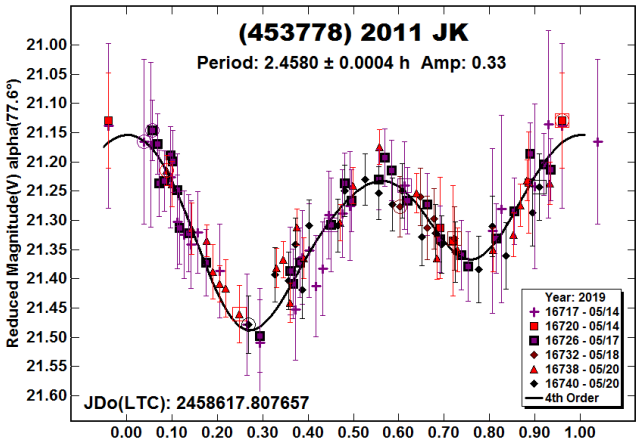

(455736) 2005 HC3, (494999) 2010 JU39. There were no previous entries of any kind for either of these NEAs. 2005 HC3 has an estimated diameter of 820 meters; the diameter of 2010 JU39 is about 360 m. The solution for 2010 JU39 is based on fitting a presumed half-period of 15.11 h. Neither the half- or full-period lightcurve is complete. Given the amplitude, it's likely that P = 30.2 h is the correct solution.

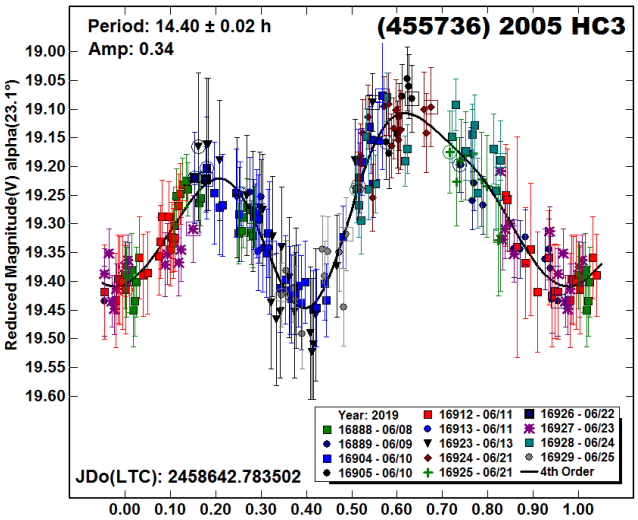

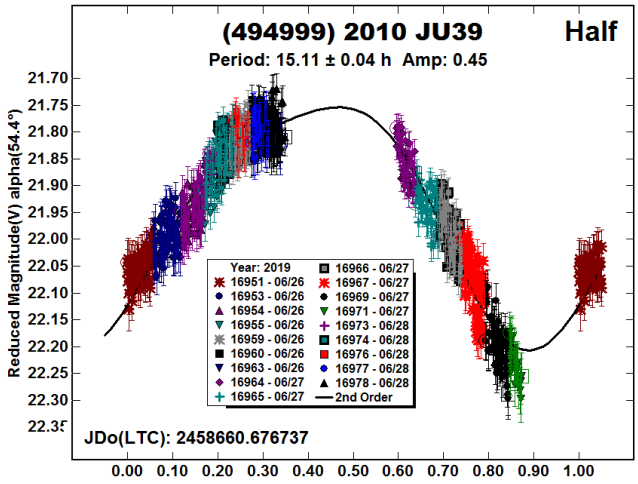

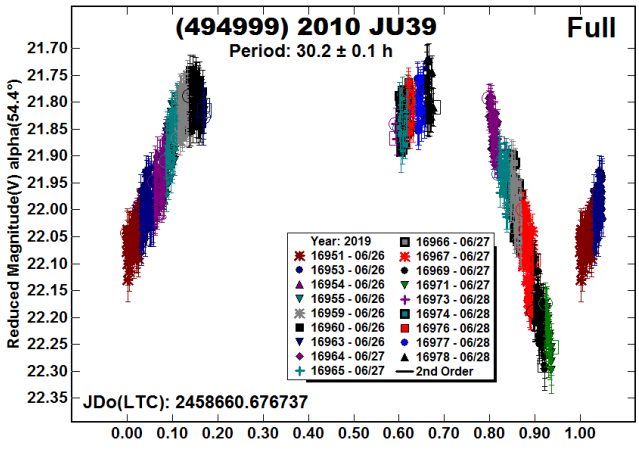

2002 JW15. Pravec et al. (2019) found a period of 11.489 h. Our period of 11.44 h is in good agreement with theirs when considering the generally lesser quality of our data.

In most cases, we assume G = 0.15 to normalize the data to the earliest session. In this case, that led to some larger than expected, or wanted, zero point shifts. We then tried G = 0.05 and G = 0.3-0.5 and found that the zero point shifts were essentially removed when using G = 0.5. When using G = 0.5, we found an absolute magnitude H = 20.92 ± 0.44. Pravec et al. used G = 0.24 to determine H = 20.60.

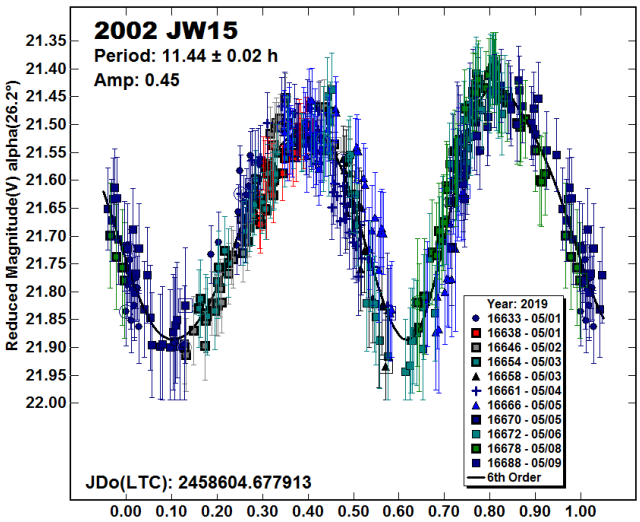

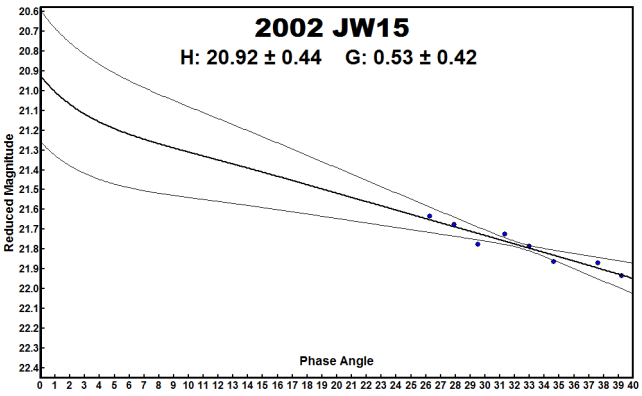

2006 KE. This appears to be the first reported rotation period for this 370-meter NEA. Fortunately, the amplitude was sufficient to overcome the low SNR. Even so, the solution is not considered secure but is still very likely correct.

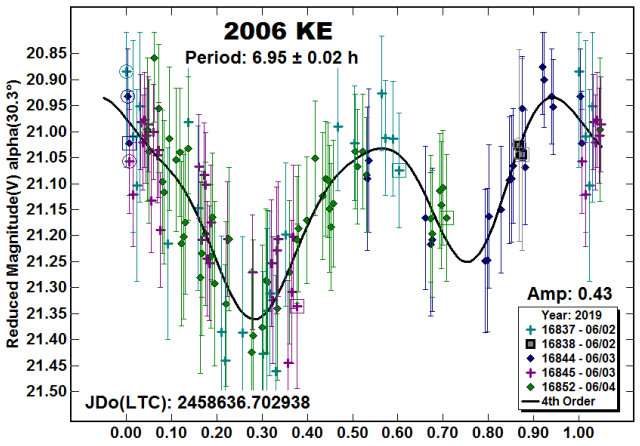

2008 HS3. Using data centered on 2019 May 1, Pravec et al. (2019) reported P = 10.75 h and amplitude A = 0.17 mag. We followed the asteroid from 2019 May 12-20 to track how its lightcurve shape, period, and amplitude changed as the phase angle increased from 21° to 44° over that time.

A solution using the entire data set ("May 12-20") is a bit confusing since the amplitude increased significantly at the end. We found a period such that the extrema lined-up to the same

rotation phase as much as possible. The period we adopt for this paper is 10.67 ± 0.01 h but we note that the synodic period varied considerably when using subsets of the data and, in some cases, was ambiguous to where we report more than one period for a given subset. The most interesting solution was the trimodal lightcurve that gave the best fit for the subset May 17-20.

Needless to say, many of the solutions are far from the adopted period because of significant gaps in lightcurve coverage. Still, this made for an interesting exercise and demonstration of lightcurve evolution.

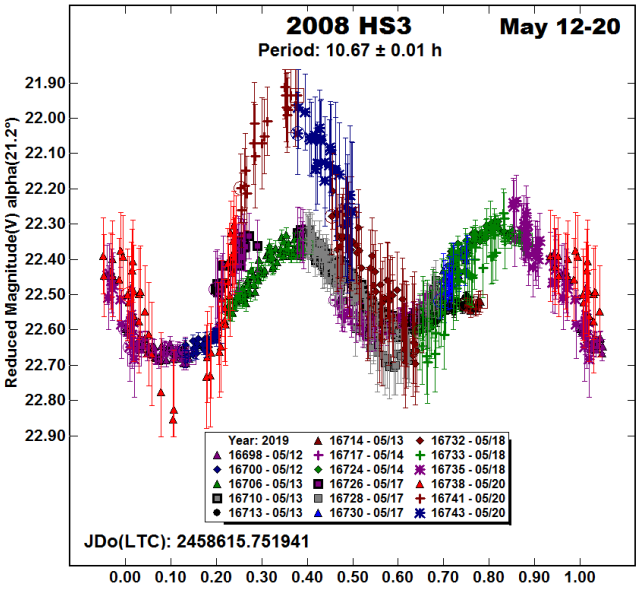

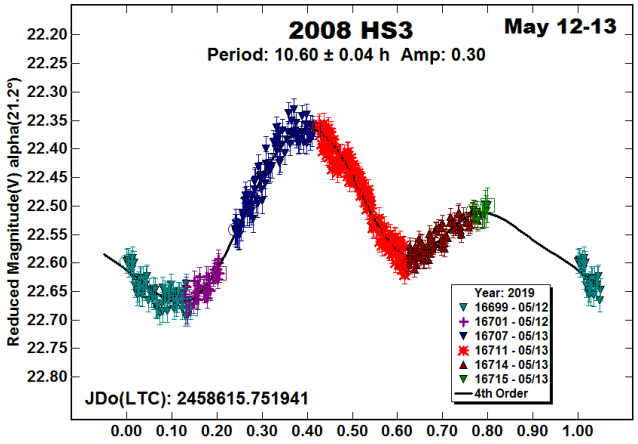

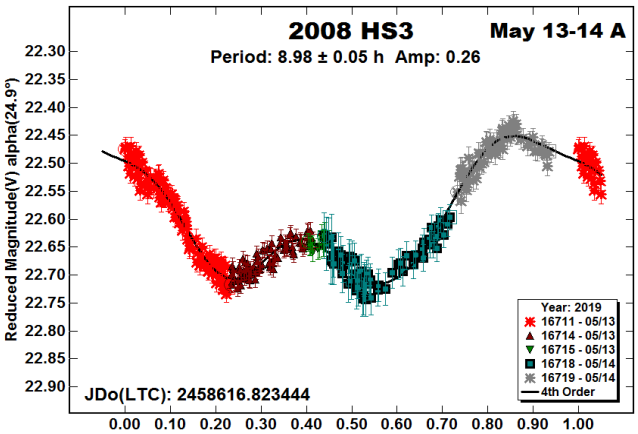

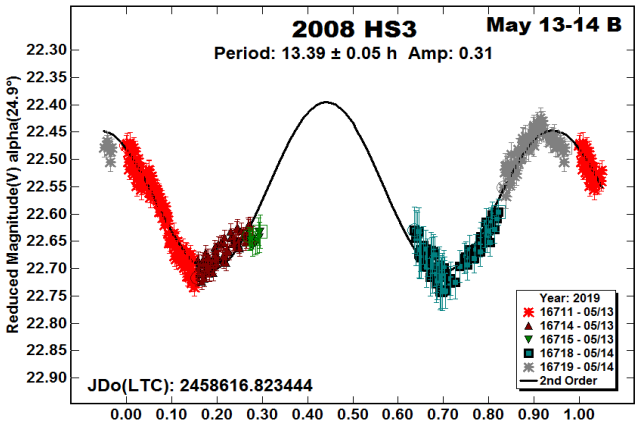

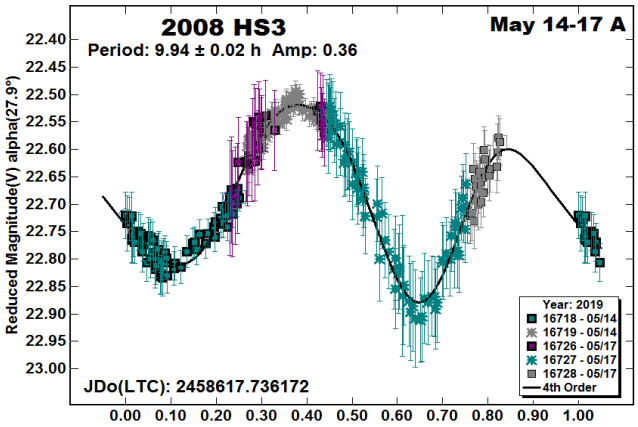

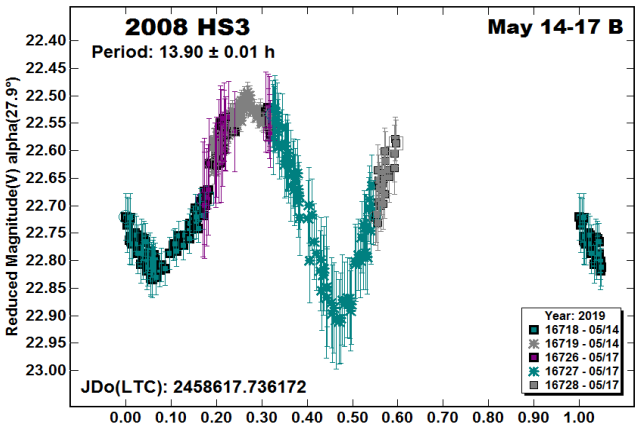

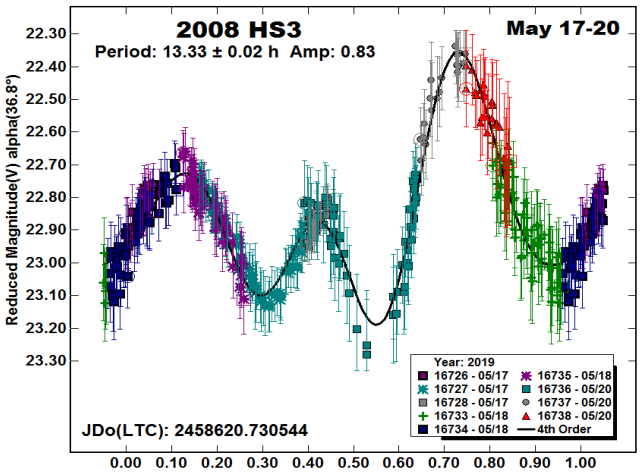

2008 WX32, 2009 DL1. Both of these NEAs are first-time entries in the LCDB. The solution for 2008 WX32 is considered secure. Its estimated diameter is 410 meters. The solution for 2009 DL1 is less secure. Given the unusual shape and somewhat sparse coverage, we included the period spectrum to show that P = 31.83 h is the only valid result – until a denser and/or higher-quality data set comes along.

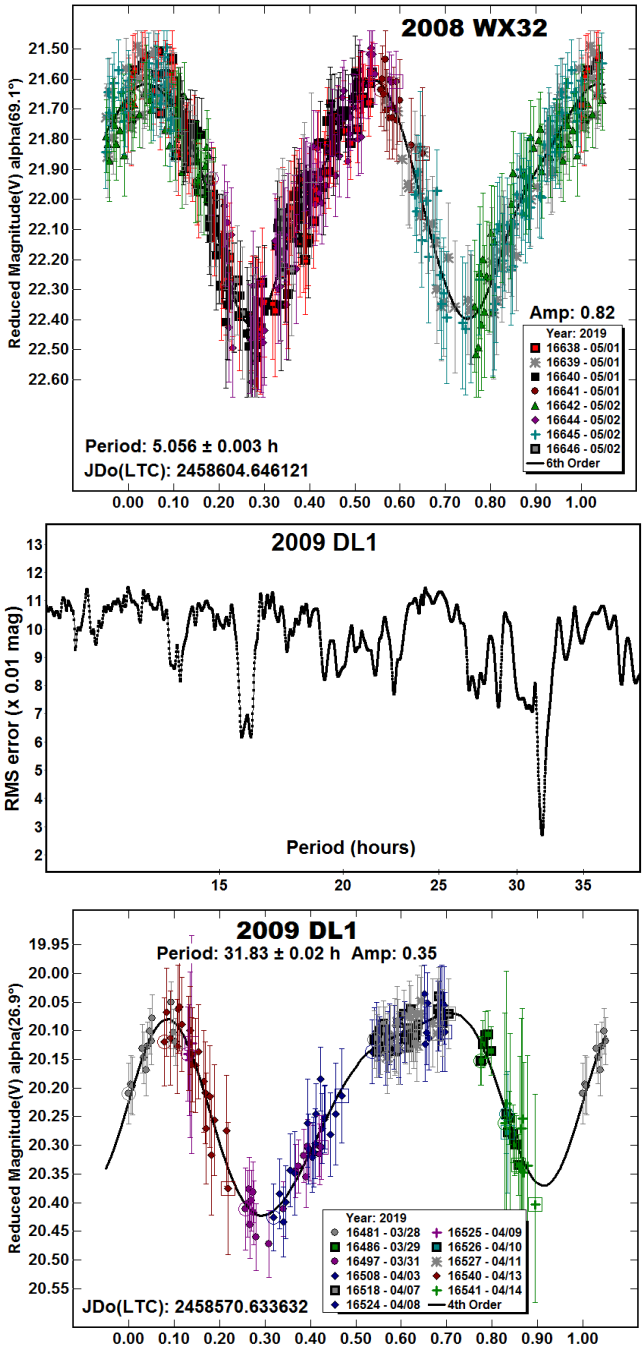

2011 HP. Pravec et al. (2019) found a period of 3.939 h using data from 2019 April. About the same time, Skiff (2011) reported a period of 3.942 h. As we did for 2008 HS3, we followed the NEA over a wide range of phase angles (15°-51°) to demonstrate lightcurve synodic period and amplitude changes. Using the entire data set ("All"), we have adopted a period of 3.9398 ± 0.0003 h and amplitude 0.40 mag.

Most nights allowed capturing all or most of a complete rotation assuming the adopted period and so the individual lightcurves give a good sense of the changing lightcurve properties.

Data over the large range of phase angles allowed us to try finding the H and G parameters. The plot shows a very good fit to the solution of H = 21.76 ± 0.04, G = –0.121 ± 0.012. Pravec et al. found H = 21.90 ± 0.04 using an assumed G = 0.12 ± 0.08.

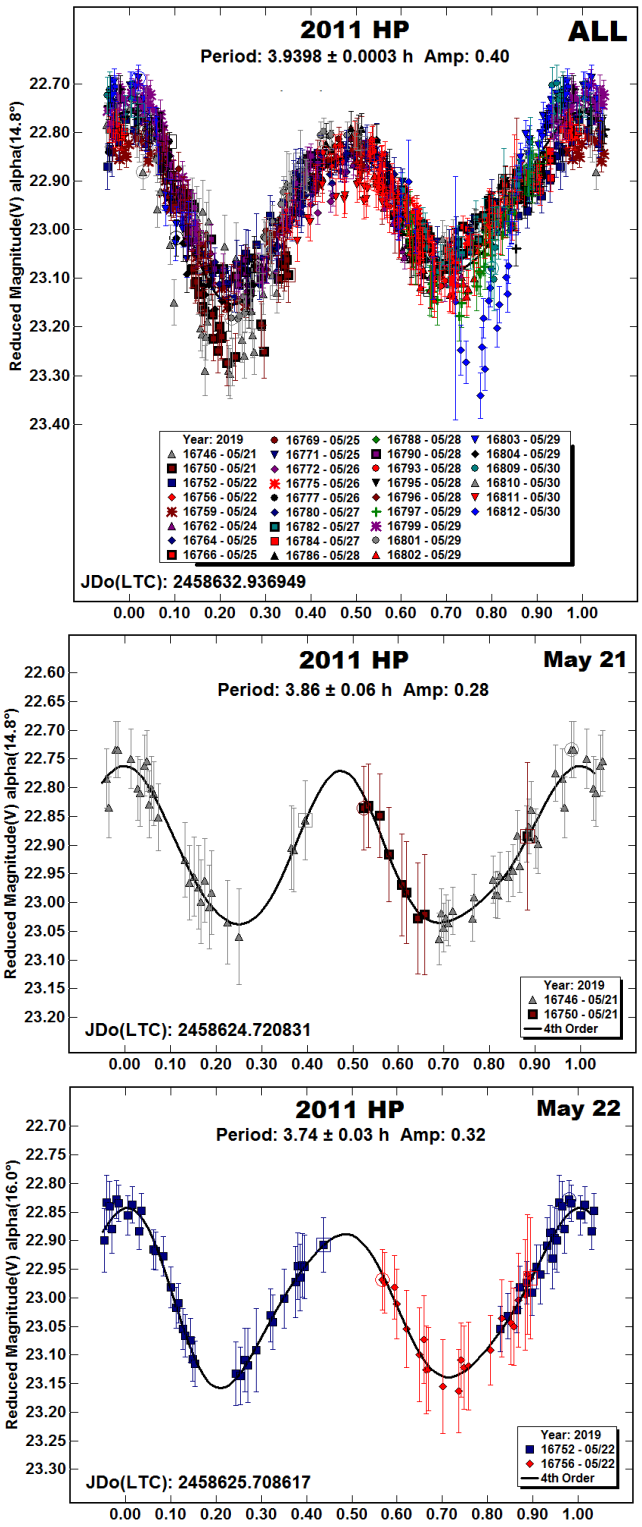

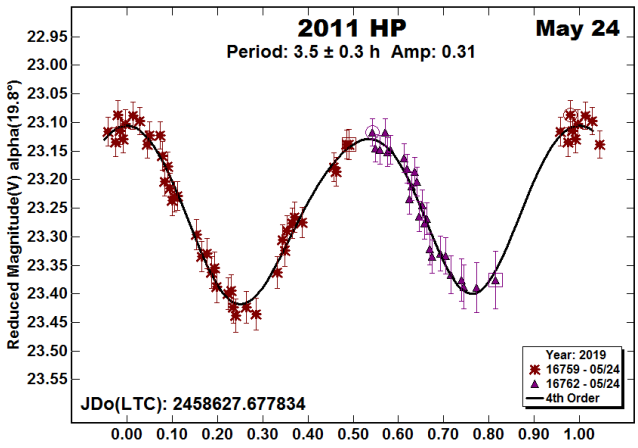
2011 HP
May 24
Period: 3.5 ± 0.3 h Amp: 0.31
Reduced Magnitude(V) alpha(19.8°)
JDo(LTC): 2458627.677834
Year: 2019
16759 - 05/24
16762 - 05/24
4th Order

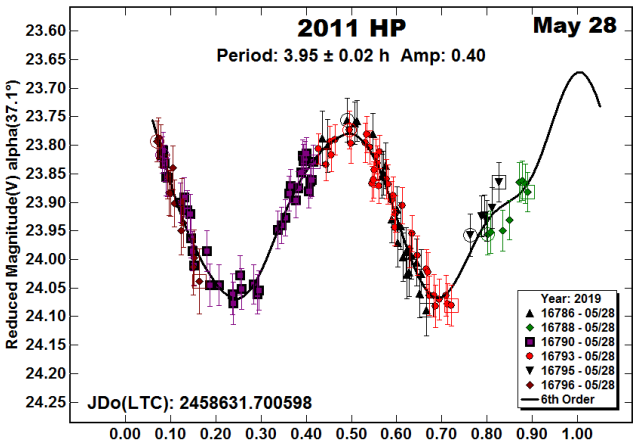
2011 HP
May 28
Period: 3.95 ± 0.02 h Amp: 0.40
Reduced Magnitude(V) alpha(37.1°)
JDo(LTC): 2458631.700598
Year: 2019
16786 - 05/28
16788 - 05/28
16790 - 05/28
16793 - 05/28
16795 - 05/28
16796 - 05/28
6th Order

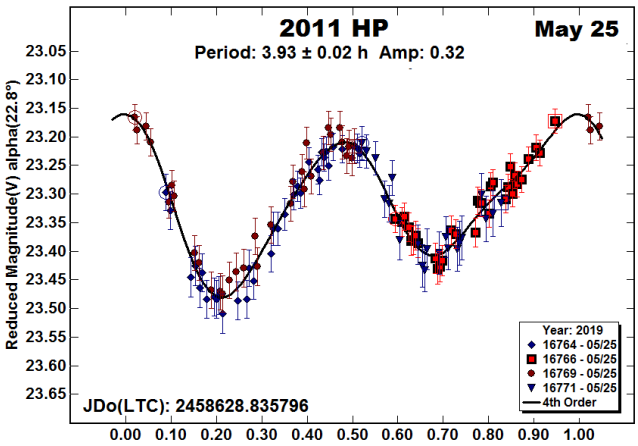
2011 HP
May 25
Period: 3.93 ± 0.02 h Amp: 0.32
Reduced Magnitude(V) alpha(22.8°)
JDo(LTC): 2458628.835796
Year: 2019
16764 - 05/25
16766 - 05/25
16769 - 05/25
16771 - 05/25
4th Order

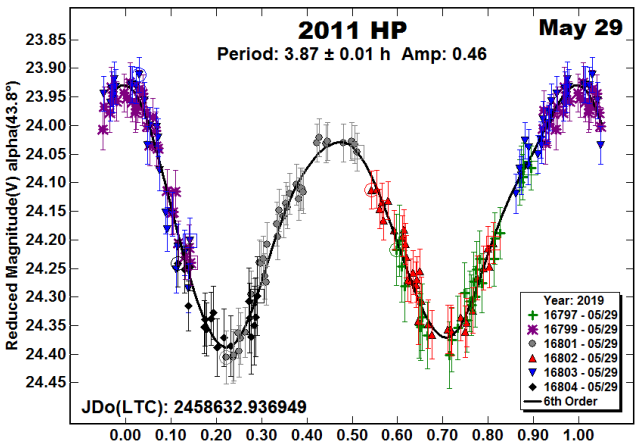
2011 HP
May 29
Period: 3.87 ± 0.01 h Amp: 0.46
Reduced Magnitude(V) alpha(43.8°)
JDo(LTC): 2458632.936949
Year: 2019
16797 - 05/29
16799 - 05/29
16801 - 05/29
16802 - 05/29
16803 - 05/29
16804 - 05/29
6th Order

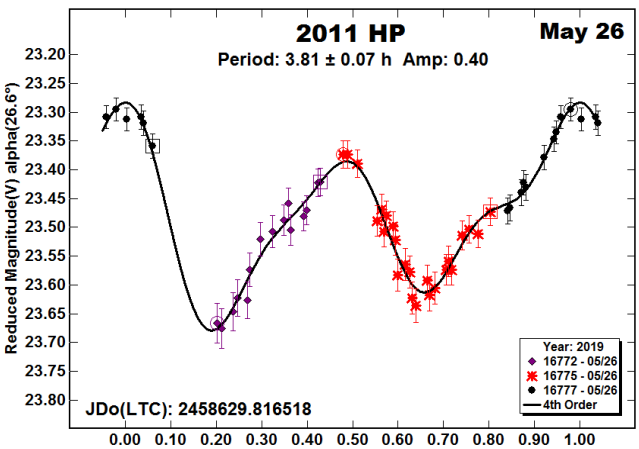
2011 HP
May 26
Period: 3.81 ± 0.07 h Amp: 0.40
Reduced Magnitude(V) alpha(26.6°)
JDo(LTC): 2458629.816518
Year: 2019
16772 - 05/26
16775 - 05/26
16777 - 05/26
4th Order

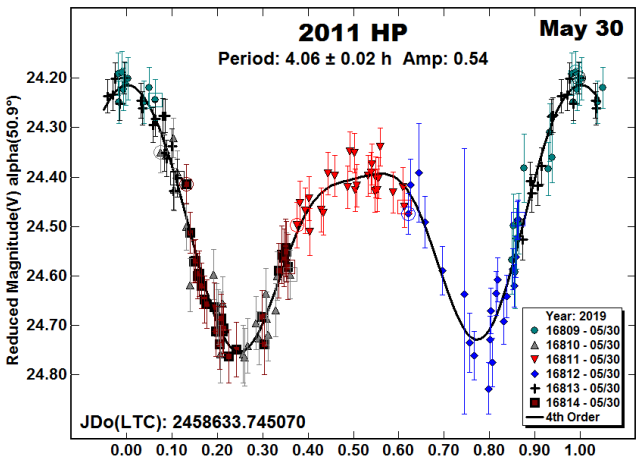
2011 HP
May 30
Period: 4.06 ± 0.02 h Amp: 0.54
Reduced Magnitude(V) alpha(50.9°)
JDo(LTC): 2458633.745070
Year: 2019
16809 - 05/30
16810 - 05/30
16811 - 05/30
16812 - 05/30
16813 - 05/30
16814 - 05/30
4th Order

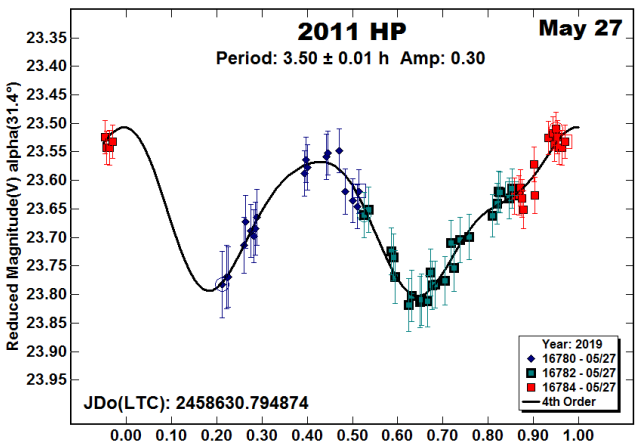
2011 HP
May 27
Period: 3.50 ± 0.01 h Amp: 0.30
Reduced Magnitude(V) alpha(31.4°)
JDo(LTC): 2458630.794874
Year: 2019
16780 - 05/27
16782 - 05/27
16784 - 05/27
4th Order

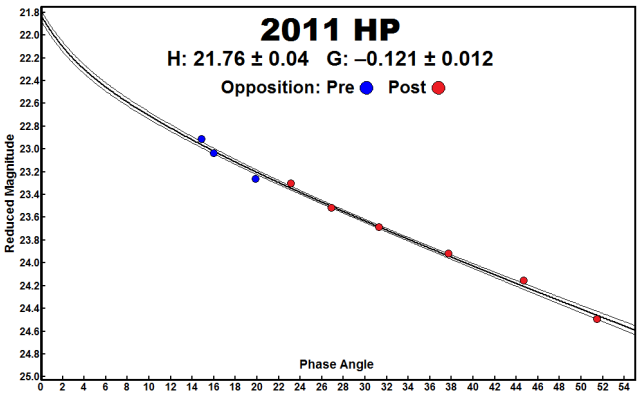
2011 HP
H: 21.76 ± 0.04 G: –0.121 ± 0.012
Opposition: Pre Post
Reduced Magnitude
Phase Angle

2014 LJ21, 2014 SZ303. This appears to be the first reported rotation period for both asteroids. 2014 LJ21 has an estimated diameter of 1.8 km. The estimated diameter for 2014 SZ303 is 700 meters.

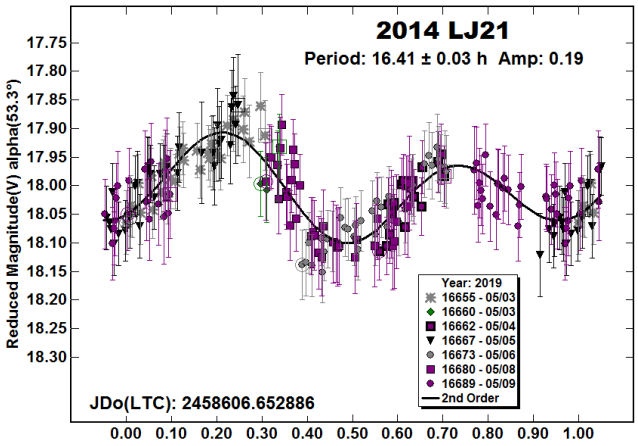

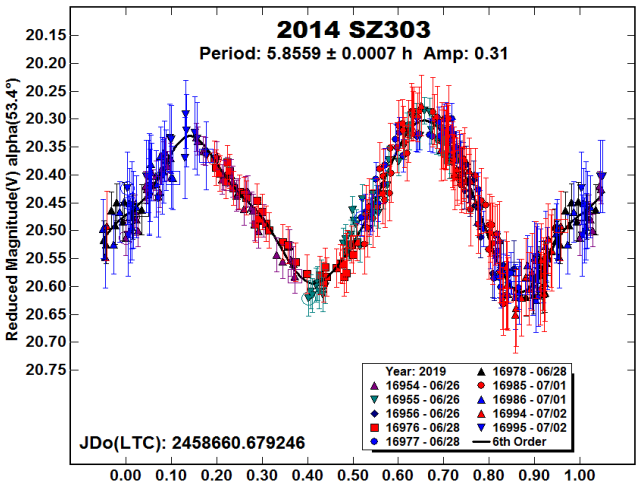

2018 EB. Here was a case where combined radar and photometric observations helped find the most likely correct period. Radar observations clearly showed that the asteroid was binary with the satellite being a few tens of meters in size (Brozovic et al., 2019). Unfortunately the radar data could not uniquely identify the rotation period of the asteroid or the orbital period of the satellite. Photometric observations from other locations showed no significant trend in the data, i.e., a "flat" lightcurve.

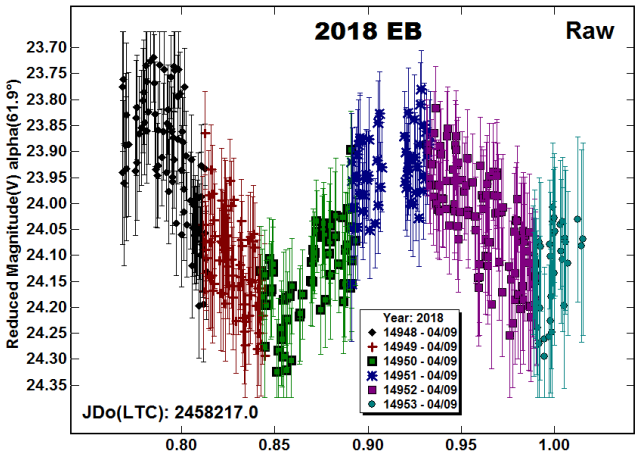

Our raw lightcurve data showed what appeared to be a bimodal lightcurve that fit to a period of 6.32 h. However, this was incompatible with the radar data. Looking at the period spectrum, a solution near 3.1 h shows a distinct RMS minimum while solutions $P > 5$ h "faded away" in what we call *harmonic ringing*. Such behavior is often seen as the Fourier analysis finds progressively longer periods that differ by a half- or full- rotation over the span of the observations.

We have adopted $P = 3.16$ h for this paper even though it has a monomodal shape. The amplitude is under the "limit" where a bimodal solution is almost required (Harris et al., 2014) but, more important, this period helps make sense of the radar observations.

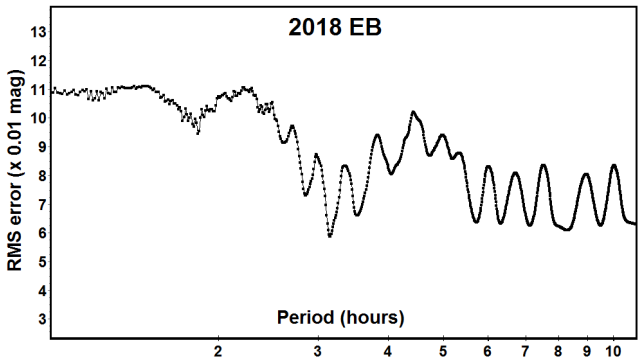

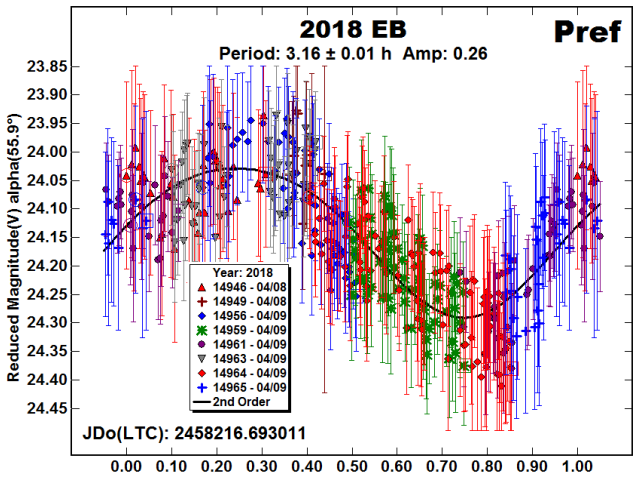

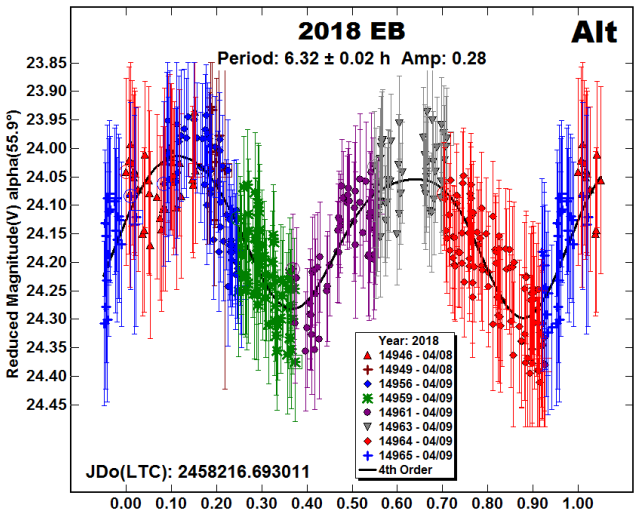

2018 XG5, 2019 HC. Both of these NEAs are newcomers to the LCDB listings. The estimated diameter of 2018 XG5 is 280 meters. The short period for 2019 HC, P = 1.2612 h, is somewhat unusual for an object its size, which puts it noticeably above the so-called "spin barrier." However, it has plenty of neighbors in the frequency-diameter plot from the LCDB data.

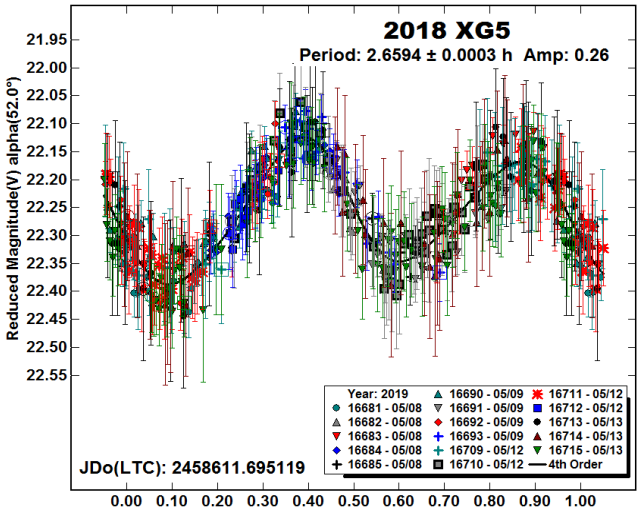

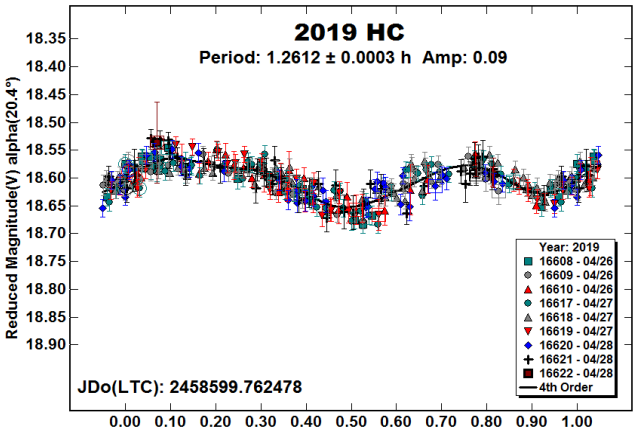

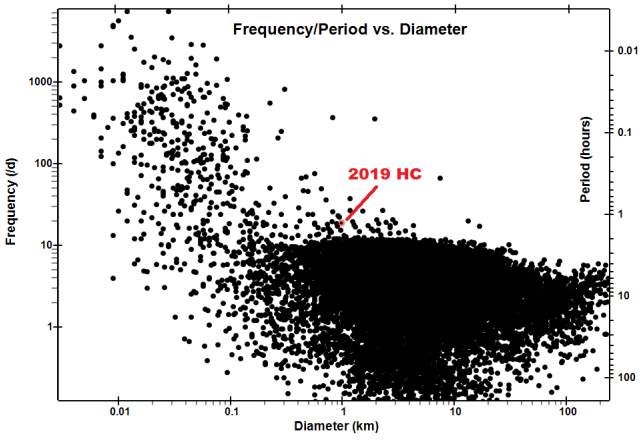

2019 JB1, 2019 FP2. Neither of these NEAs was in the LCDB prior to our observations. The solution for 2019 JB1 is ambiguous. We have adopted the period P = 8.30 h as being very likely. For 2019 FP, there is a Fourier curve in the lightcurve that is clearly the result of a failed attempt to fit to the noise. We offer no period or amplitude. The asteroid is included to note that data are available.

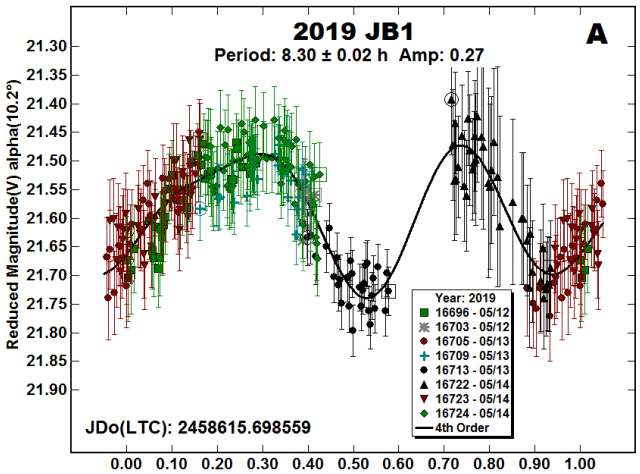

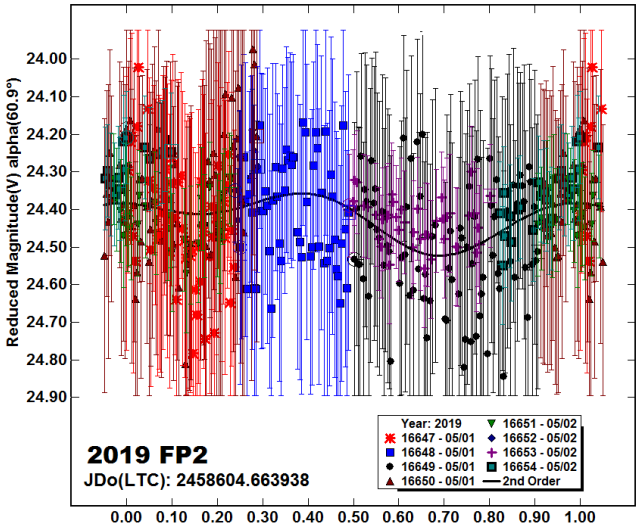

2019 KZ3. We suspect that this 40-meter asteroid might be binary, or is in a state of non-principle axis rotation (NPAR, *tumbling*). At the scale presented here, it is difficult to see that a second period might be in the lightcurve plot without subtraction of a second period.

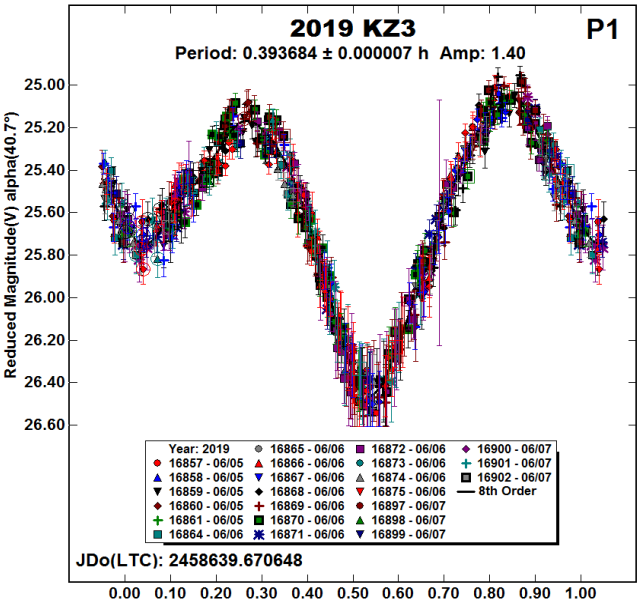

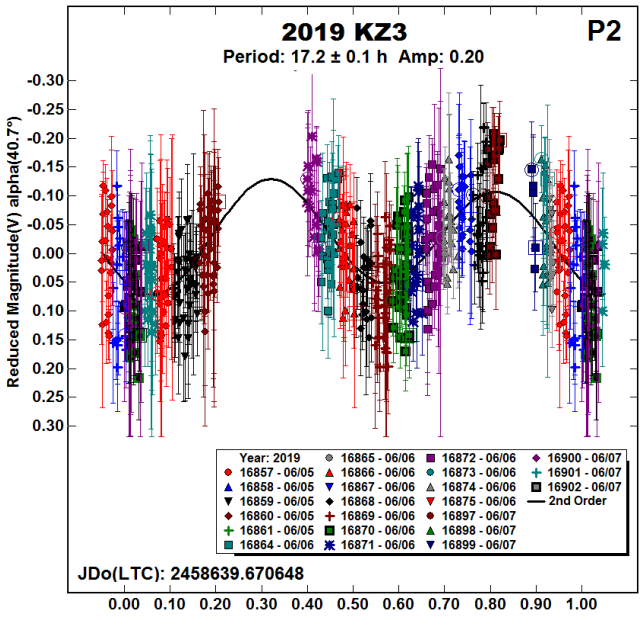

However, after close examination, we tried a dual-period search and found a clear secondary period, the low SNR data notwithstanding. As of 2019 July, the binary with the smallest primary is 2015 TD144 (D = 0.09 km; Radar Team, 2015).

2019 MB4, 2019 JX7. These are both new entries to the LCDB. The estimated size of 2019 MB4 is only 20 meters, so its super-fast rotation period of 0.134411 h (8.06 min; 483.6 s) is not surprising. We were fortunate that the asteroid was sufficiently bright so the required short exposures due to sky motion still allowed reasonably high SNR values.

The estimated diameter of 2019 JX7 is 150 meters. At this size, it is not uncommon for an asteroid to have a rotation period $P < 2$ h. Our period of 14.09 h is not extraordinary for being long. In fact, it is somewhat short among the 57 objects in the LCDB (2019 July 14) with a reliable period, $D < 0.2$ km, and $P > 10$ h. The longest belongs to 2013 US3 at 450 h.

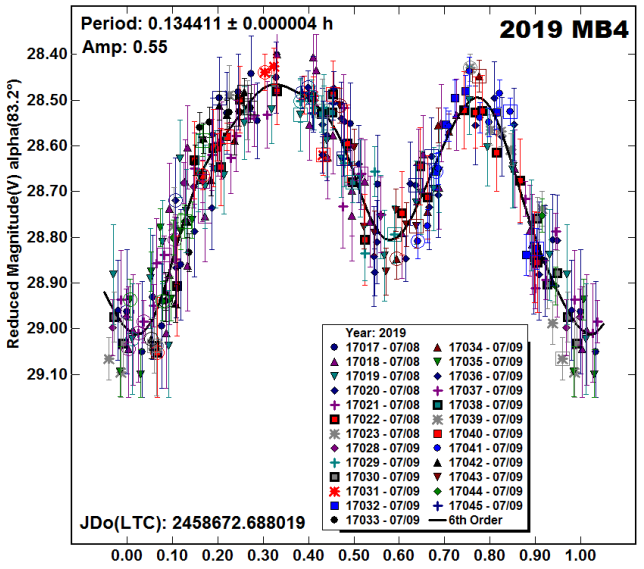

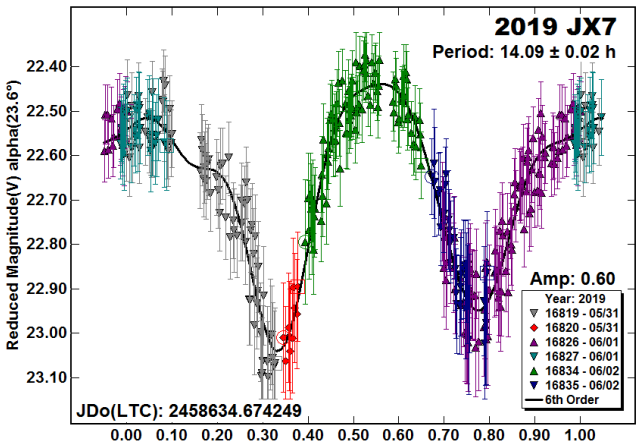

Acknowledgements

Funding for observations at CS3 and work on the asteroid lightcurve database (Warner et al., 2009) and ALCDEF database (*alcdef.org*) are supported by NASA grant 80NSSC18K0851.

The authors gratefully acknowledge Shoemaker NEO Grants from the Planetary Society (2007, 2013). These were used to purchase some of the telescopes and CCD cameras used in this research.

This work includes data from the Asteroid Terrestrial-impact Last Alert System (ATLAS) project. ATLAS is primarily funded to search for near earth asteroids through NASA grants NN12AR55G, 80NSSC18K0284, and 80NSSC18K1575; byproducts of the NEO search include images and catalogs from the survey area. The ATLAS science products have been made possible through the contributions of the University of Hawaii Institute for Astronomy, the Queen's University Belfast, the Space Telescope Science Institute, and the South African Astronomical Observatory.

References

References from web sites should be considered transitory, unless from an agency with a long lifetime expectancy. Sites run by private individuals, even if on an institutional web site, do not necessarily fall into this category.

Aznar Macias, A.; Predatu, M.; Vaduvescu, O.; Oey, J. (2018). "EURONEAR - First Light Curves and Physical Properties of Near Earth Asteroids." *arXiv*:1801.09420.

Binzel, R.P. (1990). "1990 DA." *IAUC* **4969**.

Brozovic, M.; Benner, L.A.M.; Naidu, S.P.; Hughes, R.S.; Giorgini, J.D.; Warner, B.D.; Virkki, A.K.; Marshall, S.E.; Tayloer, P.A.; Rivera-Valentin, E.G.; Lister, T.A.; Chatelain, J.P.; Pollock, J.T.; Busch, M.W. (2019). "Radar and Lightcurve Observations of Binary Near-Earth Asteroid 2019 EB." Binary Asteroids 5 Workshop, Fort Collins, CO. 2019 Sep 3-5.

De Luise, F.; Perna, D.; Dotto, E.; Fornasier, S.; Belskaya, I.N.; Boattini, A.; Valsecchi, G.B.; Milani, A.; Rossi, A.; Lazzarin, M.; Paolicchi, P.; Gulchignoni, M." (2007). "Physical investigation of the potentially hazardous Asteroid (144898) 2004 VD17." *Icarus* **191**, 628-635.

Durech, J.; Vokrouhlicky, D.; Baransky, A.R.; Breiter, S.; Burkhonov, O. A.; Cooney, W.; Fuller, V.; Gaftonyuk, N. M.; Gross, J.; Inasaridze, R.Ya.; and 21 others (2012). "Analysis of the rotation period of asteroids (1865) Cerberus, (2100) Ra-Shalom, and (3103) Eger - search for the YORP effect." *Astron. Astrophys*. **547**, A10.

Hanus, J.; Durech, J.; Oszkiewicz, D.A.; Behrend, R.; Carry, B.; Delbo, M.; Adam, O.; Afonina, V.; Anquetin, R.; Antonini, P.; and 159 coauthors. (2016). "New and updated convex shape models of asteroids based on optical data from a large collaboration network." *Astron. Astrophys.* **586**, A108.

Harris, A.W.; Young, J.W.; Scaltriti, F.; Zappala, V. (1984). "Lightcurves and phase relations of the asteroids 82 Alkmene and 444 Gyptis." *Icarus* **57**, 251-258.

Harris, A.W.; Young, J.W.; Bowell, E.; Martin, L.J.; Millis, R.L.; Poutanen, M.; Scaltriti, F.; Zappala, V.; Schober, H.J.; Debehogne, H.; Zeigler, K.W. (1989). "Photoelectric Observations of Asteroids 3, 24, 60, 261, and 863." *Icarus* **77**, 171-186.

Harris, A.W.; Pravec, P.; Galad, A.; Skiff, B.A.; Warner, B.D.; Vilagi, J.; Gajdos, S.; Carbognani, A.; Hornoch, K.; Kusnirak, P.; Cooney, W.R.; Gross, J.; Terrell, D.; Higgins, D.; Bowell, E.; Koehn, B.W. (2014). "On the maximum amplitude of harmonics on an asteroid lightcurve." *Icarus* **235**, 55-59.

Kostov, A.; Bonev, T. (2017). "Transformation of Pan-STARRS1 gri to Stetson BVRI magnitudes. Photometry of small bodies observations." *Bulgarian Astron. J.* **28**, 3 (AriXiv:1706.06147v2).

Pilcher, F.; Benishek, V.; Briggs, J.W.; Ferrero, A.; Klinglesmith, D.A.; III; Warren, C.A. (2012). "Eight Months of Lightcurves of 1036 Ganymed." *Minor Planet Bull*. **39**, 141-144.

Polishook, D.; Brosch, N. (2008). "Photometry of Aten asteroids—More than a handful of binaries." *Icarus* **194**, 111-124.

Pravec, P.; Wolf, M.; Sarounova, L. (1999, 2019)
http://www.asu.cas.cz/~ppravec/neo.htm

Pravec, P.; Harris, A.W.; Scheirich, P.; Kušnirák, P.; Šarounová, L.; Hergenrother, C.W.; Mottola, S.; Hicks, M.D.; Masi, G.; Krugly, Yu.N.; Shevchenko, V.G.; Nolan, M.C.; Howell, E.S.; Kaasalainen, M.; Galád, A.; Brown, P.; Degraff, D.R.; Lambert, J. V.; Cooney, W.R.; Foglia, S. (2005). "Tumbling asteroids." *Icarus* **173**, 108-131.

Pravec, P.; Scheirich, P.; Durech, J.; Pollock, J.; Kusnirak, P.; Hornoch, K.; Galad, A.; Vokrouhlicky, D.; Harris, A.W.; Jehin, E.; Manfroid, J.; Opitom, C.; Gillon, M.; Colas, F.; Oey, J.; Vrastil, J.; Reichart, D.; Ivarsen, K.; Haislip, J.; LaCluyze, A. (2014). "The tumbling state of (99942) Apophis." *Icarus* **233**, 48-60.

Radar Team (2015). Observers at Arecibo and/or Goldstone.
http://www.naic.edu/~pradar/
http://www.jpl.nasa.gov/asteroidwatch

Rubincam, D.P. (2000). "Relative Spin-up and Spin-down of Small Asteroids." *Icarus* **148**, 2-11.

Shepard, M.K.; Benner, L.A.M.; Ostro, S.J.; Nolan, M.C.; Giorgini, J.D.; Magri, C.; Warner, B.D. (2008). "Radar Observations of Potentially Hazardous Asteroid 68950 (2002 QF15)." *Asteroids, Comets, Meteors 2008*, Baltimore, MD.; id.8029.

Skiff, B.A. (2011). Posting on CALL web site.
http://www.minorplanet.info/call.html

Skiff, B.A.; Bowell, E.; Koehn, B.W.; Sanborn, J.J.; McLelland, K.P.; Warner, B.D. (2012). "Lowell Observatory Near-Earth Asteroid Photometric Survey (NEAPS) - 2008 May through 2008 December." *Minor Planet Bull*. **39**, 111-130.

Skiff, B.A.; McLelland, K.P.; Sanborn, J.J.; Pravec, P.; Koehn, B.W. (2019a). "Lowell Observatory Near-Earth Asteroid Photometric Survey (NEAPS): Paper 3." *Minor Plantet Bull.* **46**, 238-265.

Skiff, B.A.; McLelland, K.P.; Sanborn, J.; Pravec, P.; Koehn, B.W. (2019b). "Lowell Observatory Near-Earth Asteroid Photometric Survey (NEAPS): Paper 3." *Minor Planet Bull*. **46**, THIS ISSUE.

Stephens, R.D.; French, L.M.; Warner, B.D.; Connour, K. (2015). "Lightcurve Analysis of Two Near-Earth Asteroids." *Minor Planet Bull.* **42**, 276-277.

Tonry, J.L.; Denneau, L.; Flewelling, H.; Heinze, A.N.; Onken, C.A.; Smartt, S.J.; Stalder, B.; Weiland, H.J.; Wolf, C. (2018). "The ATLAS All-Sky Stellar Reference Catalog." *Astrophys. J.* **867**, A105.

Warner, B.D.; Harris, A.W.; Pravec, P. (2009). "The Asteroid Lightcurve Database." *Icarus* **202**, 134-146. Updated 2019 July. *http://www.minorplanet.info/lightcurvedatabase.html*

Warner, Brian D. (2014). "Near-Earth Asteroid Lightcurve Analysis at CS3-Palmer Divide Station: 2014 March-June." *Minor Planet Bull*. **41**, 213-224.

Warner, B.D. (2015a). "Near-Earth Asteroid Lightcurve Analysis at CS3-Palmer Divide Station: 2014 October-December." *Minor Planet Bull*. **42**, 115-127.

Warner, B.D. (2015b). "Near-Earth Asteroid Lightcurve Analysis at CS3-Palmer Divide Station: 2015 March-June." *Minor Planet Bull*. **42**, 256-266.

Warner, B.D. (2017a). "Near-Earth Asteroid Lightcurve Analysis at CS3-Palmer Divide Station: 2016 October-December." *Minor Planet Bull*. **44**, 98-107.

Warner, B.D. (2017b). "Near-Earth Asteroid Lightcurve Analysis at CS3-Palmer Divide Station: 2016 December thru 2017 April." *Minor Planet Bull*. **44**, 223-237.

Warner, B.D. (2019). "(12538) 1998 OH: A Continuing Non-resolution." *Minor Planet Bull*. **46**, 157-160.

Wisniewski, W.Z.; Michalowski, T.M.; Harris, A.W.; McMillan, R.S. (1997). "Photometric Observations of 125 Asteroids ." *Icarus* 1**26**, 395-449.

Number	Name	20xx mm/dd[#]	Phase	L_{PAB}	B_{PAB}	Period(h)	P.E.	Amp	A.E.
1036	Ganymed	06/03-06/09	15.7,17.0	205	-1	10.318	0.002	0.11	0.01
3103	Eger	04/07-04/15	21.6,20.7	212	30	5.7103	0.0005	0.55	0.03
4581	**Asclepius**	**04/07-04/14**	**31.8,19.0**	**215**	**8**	**8.006**	**0.005**	**0.27**	**0.03**
	Alternate 1					4.805	0.002	0.21	0.03
	Alternate 2					9.607	0.005	0.24	0.03
5332	Davidaguilar	05/01-05/02	15.4,15.4	218	32	5.821	0.007	0.62	0.05
5693	1993 EA	04/07-04/28	*9.0,15.1	204	8	2.4956	0.0003	0.06	0.02
12538	**1998 OH**	**05/30-06/01**	**73.3,71.2**	**207**	**28**	**2.5804**	**0.0006**	**0.22**	**0.02**
	Alternate					5.160	0.002	0.23	0.02
68216	2001 CV26	03/30-04/11	47.5,45.5	151	15	2.4292	0.0001	0.24	0.02
	P2 (satellite?)					15.83	0.02	0.13	0.02
68950	2002 QF15	06/01-06/24	63.1,53.0	224	21	45.24	0.02	0.36	0.03
85236	1993 KH	05/03-05/06	17.1,19.7	209	8	5.057	0.005	0.32	0.03
85989	1999 JD6	06/03-06/07	29.3,28.0	262	27	7.661	0.002	1.08	0.03
112221	2002 KH4	05/14-05/31	45.8,46.8	254	48	12.866	0.004	0.13	0.02
141525	2002 FV5	04/07-04/18	*33.4,34.0	212	24	14.450	0.008	0.47	0.03
144898	2004 VD17	04/19-04/25	23.0,34.2	190	-4	3.369	0.002	0.19	0.03
162181	**1999 LF6**	**05/03-05/13**	***12.6,15.0**	**229**	**13**	**37.26**	**0.07**	**0.32**	**0.04**
	Revised	14/05/22-05/28	22.0,26.1	236	21	37.4	0.2	0.33	0.03
163696	2003 EB50	05/01-05/13	18.9,22.0	217	22	62.06	0.03	1.01	0.03
244670	2003 KN18	05/21-05/29	60.2,53.0	212	30	20.887	0.007	1.01	0.05
	P2 (NPAR?)					37.06	0.07	0.5	0.1
257744	2000 AD205	05/24-05/26	21.4,23.0	238	18	5.80	0.01	0.29	0.03
326777	2003 SV222	05/28-06/04	*21.8,31.2	228	6	28.01	0.05	0.14	0.01
355256	2007 KN4	06/04-06/07	23.0,25.6	235	7	7.152	0.003	0.43	0.02
453778	2011 JK	05/14-05/20	77.5,73.4	194	16	2.4580	0.0004	0.33	0.03
455736	2005 HC3	06/08-06/25	*23.1,13.2	263	14	14.40	0.02	0.34	0.04
494999	2010 JU39	06/26-06/28	55.2,69.1	247	19	30.2	0.1	0.48	0.05
	2002 JW15	05/01-05/08	26.3,37.8	203	0	11.44	0.02	0.45	0.04
	2006 KE	06/02-06/04	30.4,32.5	260	22	6.95	0.02	0.43	0.05
	2008 HS3	**05/12-05/20**	**21.3,43.6**	**245**	**14**	**10.67**	**0.01**	**0.26-0.83**	
	2008 HS3	05/12-05/13	21.3,24.7	240	9	10.60	0.04	0.30	0.02
	2008 HS3	05/13-05/14	24.7,28.0	242	11	8.98	0.05	0.26	0.02
	Alternate					13.39	0.05	0.31	0.03
	2008 HS3	05/14-05/17	28.0,36.9	245	14	9.94	0.02	0.36	0.03
	Alternate					13.90	0.01	0.36	0.03
	2008 HS3	05/17-05/20	36.9,43.6	248	19	13.33	0.02	0.83	0.05
	2008 WX32	05/01-05/02	68.9,66.8	199	39	5.056	0.003	0.82	0.05
	2009 DL1	03/28-04/14	27.0,39.1	169	-2	31.83	0.02	0.35	0.03
	2011 HP	**05/21-05/30**	**14.9,51.5**	**246**	**15**	**3.9398**	**0.0003**	**0.40**	**0.05**
		05/21-05/21	14.9	234	6	3.86	0.06	0.28	0.02
		05/22-05/22	16.2	236	8	3.74	0.03	0.32	0.02
		05/24-05/24	20.1	240	11	3.5	0.3	0.31	0.02
		05/25-05/25	23.2	243	12	3.93	0.02	0.32	0.02
		05/26-05/26	27.1	245	15	3.81	0.07	0.40	0.02
		05/27-05/27	32.0	249	17	3.50	0.01	0.30	0.02
		05/28-05/28	37.8	252	19	3.95	0.02	0.40	0.03
		05/29-05/29	44.4	257	22	3.87	0.01	0.46	0.03
		05/30-05/30	51.5	262	24	4.06	0.02	0.54	0.03

Table II. Observing circumstances. # All dates are in 2019 unless the first date includes a two-digit year. The phase angle (α) is given at the start and end of each date range. If there is an asterisk before the first phase value, the phase angle reached a maximum or minimum during the period. L_{PAB} and B_{PAB} are, respectively the average phase angle bisector longitude and latitude (see Harris et al.,1984). Some asteroids have more than one line. If the additional lines have "Alternate", the result is ambiguous. The line in bold text is the period adopted for this work and the additional lines give the alternate solutions. If "P2" is the second line, it is a secondary period that is due to a confirmed or suspected satellite. "NPAR" indicates that the line has the second period of a tumbling asteroid. "Revised" indicates a new period using a previous data set that is based on the period adopted in this work. See the text for additional details.

Number	Name	20xx mm/dd[#]	Phase	L_{PAB}	B_{PAB}	Period(h)	P.E.	Amp	A.E.
	2014 LJ21	05/03-05/08	53.2,48.8	171	36	16.41	0.03	0.19	0.03
	2014 SZ303	06/26-07/02	53.1,40.8	251	19	5.8559	0.0007	0.31	0.02
	2018 EB	18/04/08-04/09	55.9,62.9	197	31	3.16	0.01	0.26	0.05
	Alternate					6.32	0.02	0.28	0.05
	2018 XG5	05/08-05/13	51.6,41.1	209	17	2.6594	0.0003	0.26	0.02
	2019 HC	04/26-04/27	20.4,21.3	227	9	1.2624	0.0003	0.09	0.01
	2019 JB1	05/12-05/14	10.1,11.8	229	5	8.30	0.02	0.27	0.03
	2019 FP2	05/01-05/02	60.8,60.4	199	26	-	-	-	-
	2019 KZ3	06/05-06/08	*39.8,36.0	261	13	0.393684	0.000007	1.40	0.05
	P2 (satellite?)					17.2	0.1	0.20	0.04
	2019 MB4	07/08-07/09	82.7,72.4	271	30	0.134411	0.000004	0.55	0.05
	2019 JX7	05/31-06/02	23.7,26.8	237	8	14.09	0.02	0.60	0.03

Table II (*contd*). Observing circumstances. # All dates are in 2019 unless the first date includes a two-digit year. The phase angle (α) is given at the start and end of each date range. If there is an asterisk before the first phase value, the phase angle reached a maximum or minimum during the period. L_{PAB} and B_{PAB} are, respectively the average phase angle bisector longitude and latitude (see Harris et al.,1984). See the text when there is more than one line for the same asteroid.

LIGHTCURVE ANALYSIS, ROTATION PERIOD AND H-G PARAMETERS DETERMINATION FOR 2727 PATON

A. Noschese
AstroCampania Associazione Naples (Italy)
and
Osservatorio Elianto (K68)
via V. Emanuele III, 95, 84098
Pontecagnano (SA) Italy

M. Mollica
AstroCampania Associazione
via Servio Tullio 101, 80126 Naples (Italy)
m.mollica@astrocampania.it

A. Catapano
AstroCampania Associazione Naples (Italy)

A. Vecchione
AstroCampania Associazione Naples (Italy)

(Received: 2019 July 10)

Data for asteroid 2727 Paton were collected from February 5th to March 4th 2019. The lightcurve analysis obtained has led to a bimodal curve with a period of 5.325 ± 0.001 h, amplitude 0.26 mag, with a full coverage. We have also obtained data in V and Rc filters, alternately, for color index V-R found to be 0.50 ±0.06 mag. Maximum reduced magnitudes have been extrapolated from each session in order to determine H and G parameters, found to be, respectively, 12.46±0.05 mag and 0.25 ±0.09 mag. Values found are consistent with an S-type taxonomy.

2727 is a main-belt asteroid (middle belt), discovered by N. Chernykh, in 1979. It has a semi-major axis of 2.609 AU, orbital period of 4.21 years, eccentricity of 0.102 and inclination of 3.509 deg (JPL Small-Body Database Browser). This nine-kilometer-sized asteroid has an absolute magnitude of 12.2 and a geometric albedo of 0.311 (from NEOWISE Diameters and Albedos V2.0, Mid-IR Photometry). No rotation period and lightcurve were reported for this object at the best of our knowledge. Observations were conducted by a 0,30 m Newtonian telescope at f/4, with a KAF 1603 ME 1536x1024 x 9.0-micron, unfiltered (Elianto Observatory, K68) and a 0.50-m Ritchey-Chretien telescope operating at f/8, using a FLI-PL4240 CCD camera with 2048x2048 array of 13.5 micron pixels and equipped with a Rc and V photometric filters (OASDG, Agerola, Naples. L07).

A total of 504 lightcurve data points were collected in eight observing sessions from 2019 February 5th, to 2019 March 4th, with exposing times ranging from 240 s through 360 s, seven of which were divided in two parts (before and after meridian flip). For this reason, sessions shown are a total of fifteen.

Table I lists the telescope/CCD camera combination used to collect the data. Master dark and flat were obtained using CCD Stack (CCD Ware). MPO Canopus (Warner, 2016) was used to measure the magnitudes with CMC15 catalogue. This catalogue has a very high internal consistency in r' (sdss) and J, K (2MASS) bands. r' magnitudes has been converted to standard Cousin R band, by using R = r' - 0.22 (R. Dymock and R. Miles, 2009).

This Rc derived magnitude has been reduced for unity Sun-asteroid and Earth-asteroid distances in AU and normalized to the given phase angle of 11.2°, using G= 0.15. Night-to-night zero-point calibration was accomplished by selecting up to five comparison stars with near-solar colors, using the "comp star selector" feature. The "starBgone" routine within MPO Canopus was used, as well, in order to subtract stars that occasionally merged with the asteroid during the observations. MPO Canopus was also used for rotation period analysis, adopting FALC method by Harris (Harris, 1989).

We found a period of 5.325 ± 0.001 hours. The data indicate a lightcurve amplitude change of 0.26 magnitudes with two maximum (figure 1). Table II gives the observing circumstances and results. The period spectrum provided, shows that the best solution (thus with lowest RMS) is the one adopted here (figure 2).

With two nights spent gathering data in V and Rc bands (alternately), using 0.50 m R.C. telescope, we obtained V-R plots separated by V-R = 0.50 mag. We used two nights to be more confident with the result (figure 3). Apass9 catalogue was used for reducing data. This catalogue provides native Johnson V band with a very high internal consistency, usually within 0.03 magnitudes. Using VizieR web site, Sloan r' band was converted in standard Cousin R by R = r' - 0.065 × (g' – i') - 0.174 (North Equator, U. Munari, 2012). The same comparison solar color star were used for both sets of images. Finally, the average value from two nights has been found. Using polynomial fit, maximum reduced magnitudes was extrapolated from any raw session in order to obtain H-G plot in R-band. The curve fit was performed using MPO Canopus utility, "H/G Calculator".

The absolute magnitude H obtained, has been converted in V band by adding the V-R color index previously found, resulting with Hv = 12.463 mag. The slope parameter found is G = 0.25±0.09 (figure 4). Both the color index (V-R) and the slope parameter determined here, are consistent with an S-type taxonomy (Shevchenko-Lupishko, 1998).

Site	Ap (m)	Type	f/	Camera	Array	Filter
Pontecagnano,(SA),Italy	0.30-m	N	4.0	KAF1603ME	1536x1024x9.0µ	C
Agerola (NA),Italy	0.50-m	RC	8.0	FLI-PL4240	2048x2048x13.5µ	Rc

Table I. List of telescope/camera combinations. RC=Ritchey-Chrétien, N=Newton,

Number	Name	2019 mm/dd	Pts	Phase	L_{PAB}	B_{PAB}	Period(h)	P.E.	Amp	A.E.	U	Exp
2727	Paton	02/05-03/04	504	11.2,2.7	159.2	-3.3	5.325	0.001	0.26	0.01	2	180/360

Table II. Observing circumstances and results. The phase angle is given for the first and last date. L_{PAB} and B_{PAB} are the approximate phase angle bisector longitude and latitude at mid-date range (see Harris *et al.*, 1984). The U rating is our estimate and not necessarily the one assigned in the asteroid lightcurve database (Warner *et al.*, 2009). Exp is average exposure, seconds.

Finally, using the obtained data and the value of the geometric albedo from NEOWISE, we calculated the asteroid diameter, using the following relation (Harris and Harris, 1997):

$$D = 1329/(p_V)^{0.5} * 10^{0.2H_v}$$

to be 7.7 Km.

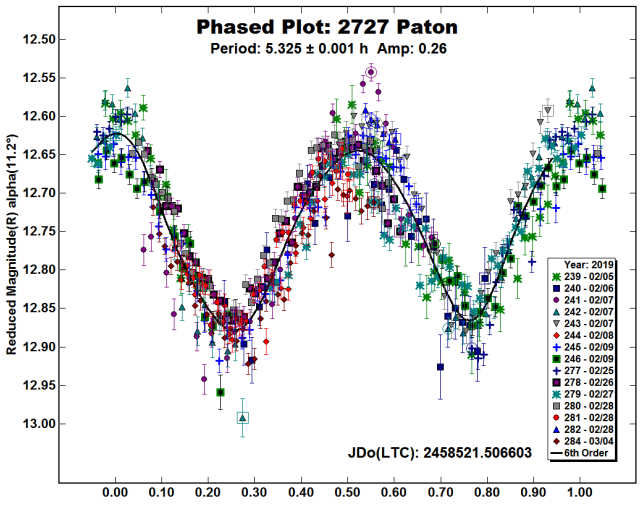

Figure 1: Lightcurve of (2727) Paton phased to a period of 5.325 h, Amp. 0.26 mag.

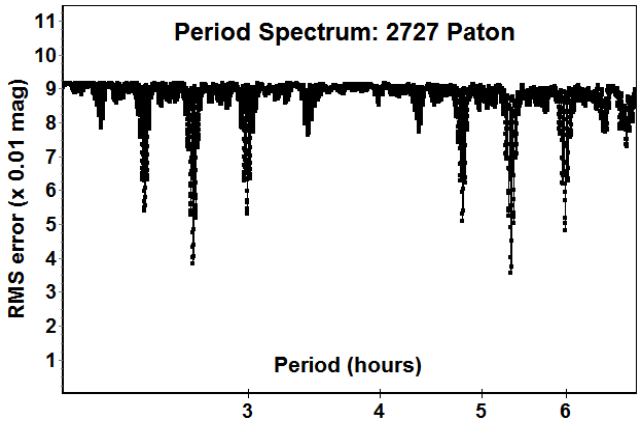

Figure 2: Minimum RMS found for our solution 3.65.

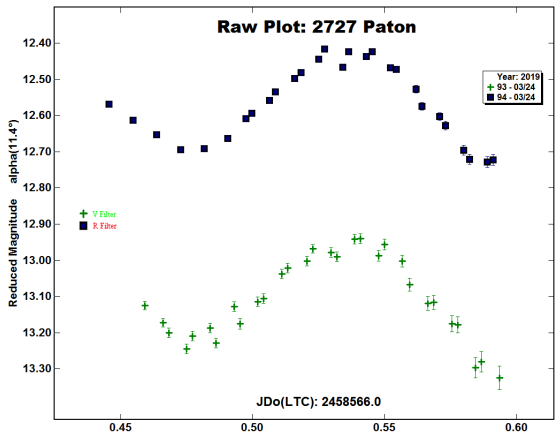

Figure 3: Observations of 2727 Paton, 2019 March 24 in R and V magnitudes.

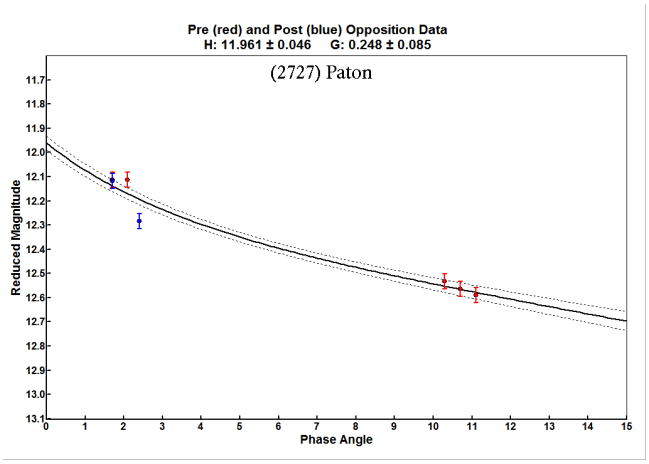

Figure 4: H-G plot for 2727 Paton for maximum light data points, in R band.

References

Dymock R.; Miles R. (2009). "A method for determining the V magnitude of asteroids from CCD images." *(JBAA, 119,3).*

Harris, A.W.; Young, J.W.; Scaltriti, F.; Zappala, V. (1984). "Lightcurves and phase relations of the asteroids 82 Alkmene and 444 Gyptis." *Icarus* **57**, 251-258.

Harris, A.W.; Harris A.W. (1997). "On the Revision of Radiometric Albedos and Diameters of Asteroids". *Icarus,* Vol. 126, Issue *2, pp. 450-454.*

Harris, A.W.; Young, J.W.; Bowell, E.; Martin, L.J.; Millis, R.L.; Poutanen, M.; Scaltriti, F.; Zappala, V.; Schober, H.J.; Debehogne, H.; Zeigler, K.W. (1989). "Photoelectric Observations of Asteroids" 3, 24, 60, 261, and 863." *Icarus* **77**, 171-186.

JPL (2018). Small-Body Database Browser. *http://ssd.jpl.nasa.gov/sbdb.cgi#top*

Munari, U. (2012) "Classical and Recurrent Novae". *JAAVSO,* Vol. 40*, 2012.*

Shevchenko, V.G.; Lupishko, D. (1998). "Optical Properties of Asteroids from Photometric Data." *Solar System Research,* Vol. 32, No. 3, 220-232.

Warner, B.D. (2016). MPO Software, MPO Canopus version 10.7.7.0 Bdw Publishing. *http://minorplanetobserver.com*

Warner, B.D.; Harris, A.W.; Pravec, P. (2009). "The Asteroid Lightcurve Database." Icarus **202**, 134-146. *http://www.minorplanet.info/lightcurvedatabase.html*

VizieR (2016). *https://vizier.u-strasbg.fr/viz-bin/VizieR*

COLLABORATIVE ASTEROID PHOTOMETRY FROM UAI: 2019 MAY-JUNE

Lorenzo Franco
Balzaretto Observatory (A81), Rome, ITALY
lor_franco@libero.it

Alessandro Marchini
Astronomical Observatory, DSFTA - University of Siena (K54)
Via Roma 56, 53100 - Siena, ITALY

Giorgio Baj
M57 Observatory (K38), Saltrio, ITALY

Riccardo Papini, Massimo Banfi, Fabio Salvaggio
Wild Boar Remote Observatory (K49)
San Casciano in Val di Pesa (FI), ITALY

Paolo Bacci, Martina Maestripieri
San Marcello Pistoiese (104), Pistoia, ITALY

Gianni Galli
GiaGa Observatory (203), Pogliano Milanese, ITALY

Giovanni Battista Casalnuovo, Benedetto Chinaglia
Filzi School Observatory, Laives, ITALY

Mauro Bachini, Giacomo Succi
Santa Maria a Monte (A29), ITALY

(Received: 2019 July 10)

Photometric observations of four main-belt and one near-Earth asteroids were made in order to acquire lightcurves for shape/spin axis models. The synodic period and lightcurve amplitude were found for: 234 Barbara: 26.482 ± 0.006 h, 0.21 mag; 1166 Sakuntala: 6.2918 ± 0.0006 h, 0.24 mag.; 1914 Hartbeespoortdam: 6.3398 ± 0.0006 h, 0.10 mag; 2433 Sootiyo: 7.235 ± 0.005 h, 0.35 mag; (66391) 1999 KW4: 2.7644 ± 0.0002 h, 0.15 mag. We also confirmed the binary nature of the asteroid (66391) 1999 KW4.

Collaborative asteroid photometry was made inside the UAI (Italian Amateur Astronomers Union) group. The targets were selected in order to acquire lightcurves for shape/spin axis models. The CCD observations were made in 2019 May-June using the instrumentation described in Table I. Lightcurve analysis was performed at the Balzaretto Observatory with *MPO Canopus* (BDW Publishing, 2016). All the images were calibrated with dark and flat frames and converted to R magnitudes using solar colored field stars from CMC15 catalogue, distributed with *MPO Canopus*. Table II shows the observing circumstances and results.

234 Barbara is an Ld-type (Bus & Binzel, 2002) inner main-belt asteroid discovered on 1883 August 12 by Peters, C. H. F. at Clinton. Collaborative observations were made over ten nights. We found a synodic period of P = 26.482 ± 0.006 h with an amplitude A = 0.21 ± 0.02 mag. The period is close to the previously published results in the asteroid lightcurve database (LCDB; Warner et al., 2009).

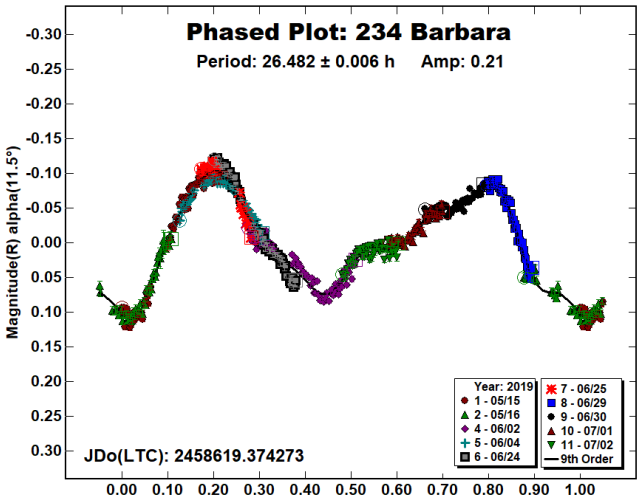

1166 Sakuntala is an inner main-belt asteroid, discovered on 1930 June 27 by Parchomenko, P. at Simeis. Collaborative observations were made over six nights. We found a synodic period of P = 6.2918 ± 0.0006 h with an amplitude A = 0.24 ± 0.02 mag. The period is close to the previously published results in the asteroid lightcurve database (LCDB; Warner et al., 2009).

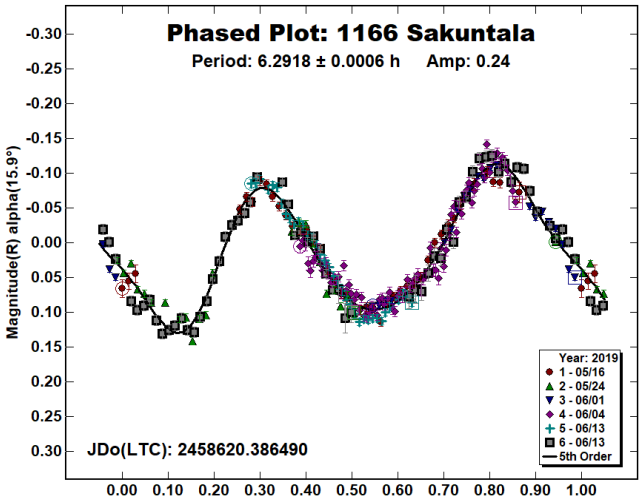

Observatory (MPC code)	Telescope	CCD	Filter	Observed Asteroids
DSFTA Observatory (K54)	0.30-m MCT f/5.6	SBIG STL-6303e (bin 2x2)	Rc,C	234,1166,2433,66391
M57 (K38)	0.30-m RCT f/5.5	SBIG STT-1603	C	1914,66391
WBRO (K49)	0.235-m SCT f/10	SBIG ST8-XME	Rc,C	234,1166,2433
GAMP(104)	0.60-m NRT f/4	Apogee Alta	C	1914,66391
GiaGa Observatory (203)	0.36-m SCT f/5.8	Moravian G2-3200	C	66391
Filzi School Observatory	0.35-m RCT f/8	QHY9 (KAF8300)	Rc	1166,1914
Santa Maria a Monte (A29)	0.40-m NRT f/5	DTA Discovery plus Kaf 260	C	66391

Table I. Observing Instrumentations. MCT: Maksutov-Cassegrain, RCT: Ritchey-Chretien, SCT: Schmidt-Cassegrain, NRT: Newtonian Reflector, SCT: Schmidt-Cassegrain.

1914 Hartbeespoortdam is an inner main-belt asteroid, member of the Vestoid *group*, discovered on 1930 September 28 by Van Gent, H. at Johannesburg. Collaborative observations were made over six nights. We found a quadrimodal lightcurve with a synodic period of P = 6.3398 ± 0.0006 h and an amplitude A = 0.10 ± 0.02 mag. The period is close to the solution published by Pravec et al. (2015; 6.331 ± 0.003 h).

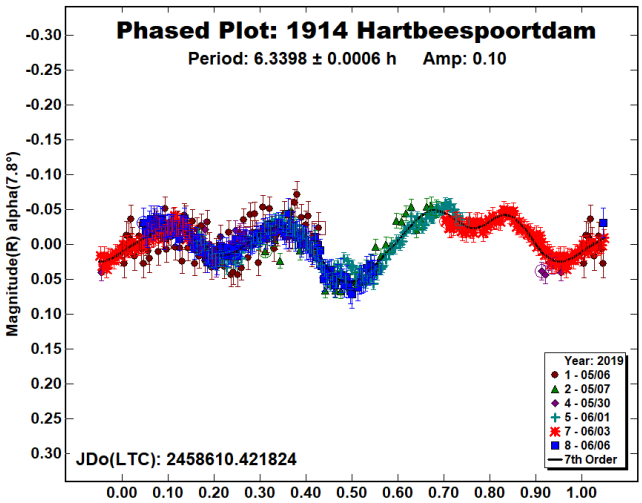

2433 Sootiyo is a middle main-belt asteroid discovered on 1981 April 05 by Bowell, E. at Flagstaff. Collaborative observations were made over three nights. We found a synodic period of P = 7.235 ± 0.005 h with an amplitude A = 0.35 ± 0.03 mag. The period is close to the solution published by Behrend (2007; 7.2298 ± 0.0002 h).

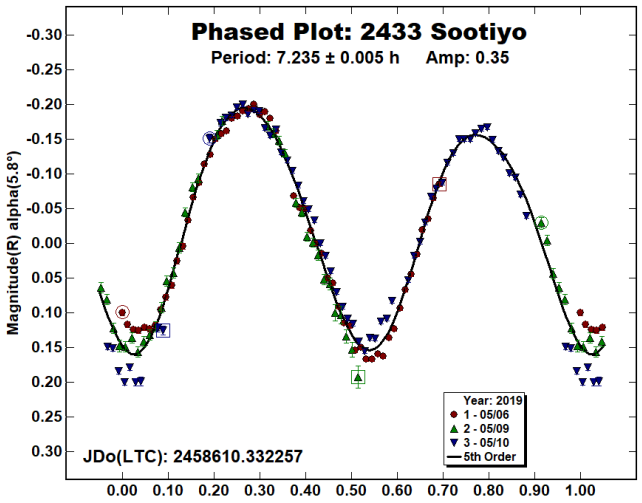

(66391) 1999 KW4 is an S-type Aten near-Earth asteroid, discovered on 1999 May 20 by LINEAR at Socorro. This asteroid is a binary system as reported by Benner et al. (2001) and Pravec et al. (2001). Collaborative observations were made over ten nights. The analysis was done using the dual period search function implemented in *MPO Canopus*. We found a primary synodic rotational period of P_1 = 2.7644 ± 0.0002 h with an amplitude A_1 = 0.15 ± 0.04 mag; orbital period P_2 = 17.468 ± 0.008 h with a maximum attenuation for the deeper event of 0.27 ± 0.03 mag, observed on May 30, 2019. Those periods are consistent with the previously published results in the asteroid lightcurve database (LCDB; Warner et al., 2009).

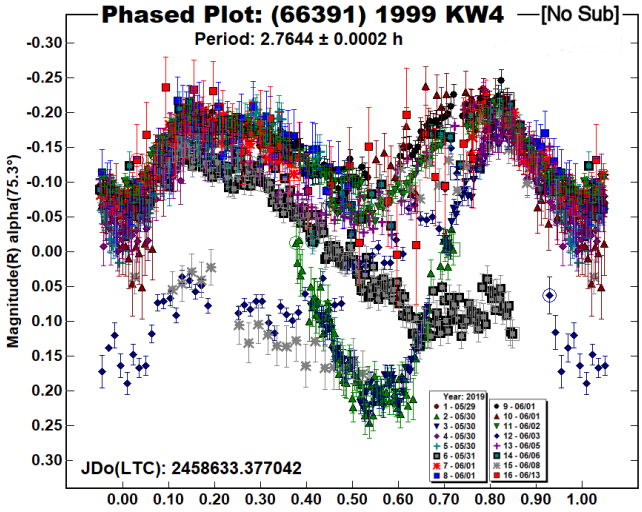

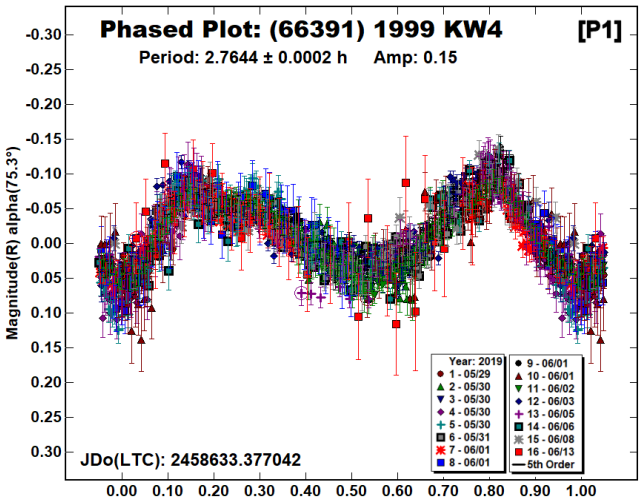

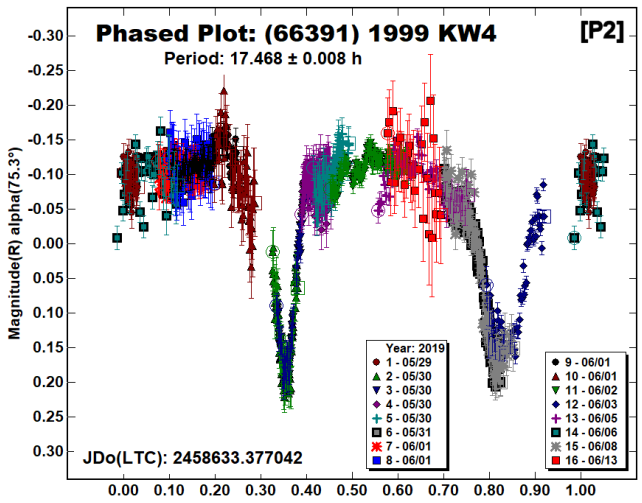

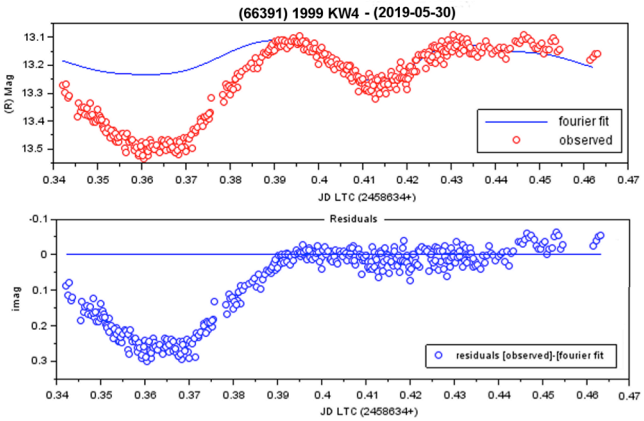

Top: data points observed on May 30, 2019 superimposed to the 2nd order Fourier model curve. Bottom: residuals after the Fourier model curve has been subtracted to the observed data.

References

Behrend, R. (2007). Observatoire de Geneve web site. *http://obswww.unige.ch/~behrend/page_cou.html*

Benner, L.A.M.; Ostro, S.J.; Giorgini, J.D.; Jurgens, R.F.; Margot, J.L.; Nolan, M.C. (2001). "1999 KW4" IAU Circ. **7632**, 1.

Bus S.J.; Binzel R.P. (2002). "Phase II of the Small Main-Belt Asteroid Spectroscopic Survey - A Feature-Based Taxonomy." *Icarus* **158**, 146-177.

DSFTA (2019), Dipartimento di Scienze Fisiche, della Terra e dell'Ambiente – Astronomical Observatory. *https://www.dsfta.unisi.it/en/research/labs-eng/astronomical-observatory*

Harris, A.W.; Young, J.W.; Scaltriti, F.; Zappala, V. (1984). "Lightcurves and phase relations of the asteroids 82 Alkmene and 444 Gyptis." *Icarus* **57**, 251-258.

Pravec, P.; Sarounova, L. (2001), "1999 KW4" *IAU Circ.* **7634**, 2.

Pravec, P.; Wolf, M.; Sarounova, L. (2015). web site. *http://www.asu.cas.cz/~ppravec/neo.htm*

UAI (2019). "Unione Astrofili Italiani" web site. *https://www.uai.it*

Warner, B.D.; Harris, A.W.; Pravec, P. (2009). "The asteroid lightcurve database." *Icarus* **202**, 134-146. Updated 2019 January 31. *http://www.minorplanet.info/lightcurvedatabase.html*

Warner, B.D. (2016). MPO Software, MPO Canopus v10.7.7.0. Bdw Publishing. *http://minorplanetobserver.com*

Number	Name	2019 mm/dd	Phase	L_{PAB}	B_{PAB}	Period(h)	P.E.	Amp	A.E.	Grp
234	Barbara	05/15-07/02	11.5,21.4	240	21	26.482	0.006	0.21	0.02	MB-I
1166	Sakuntala	05/16-06/13	16.2,8.1	259	14	6.2918	0.0006	0.24	0.02	MB-I
1914	Hartbeespoortdam	05/06-06/06	8.2,11.1	237	7	6.3398	0.0006	0.10	0.02	V
2433	Sootiyo	05/06-05/10	5.7,6.4	225	9	7.235	0.005	0.35	0.03	MB-M
66391	1999 KW4	05/29-06/13	77.7,69.2	213	11	2.7644	0.0002	0.15	0.04	NEA
						17.468	0.008	0.27	0.03	

Table II. Observing circumstances and results. The first line gives the results for the primary of a binary system. The second line gives the orbital period of the satellite and the maximum attenuation. The phase angle is given for the first and last date. If preceded by an asterisk, the phase angle reached an extrema during the period. L_{PAB} and B_{PAB} are the approximate phase angle bisector longitude/latitude at mid-date range (see Harris et al., 1984). Grp is the asteroid family/group (Warner et al., 2009).

THE COLOR INDICES OF THE NEA (66391) 1999 KW4

Albino Carbognani
Astronomical Observatory of the
Aosta Valley Autonomous Region (OAVdA),
Lignan 39, 11020 Nus (Aosta), ITALY
albino.carbognani@gmail.com

(Received: 2019 June 29)

This paper presents the results of photometric observations with standard broad-band Bessel filters B, V, R and I, on near-Earth asteroid (66391) 1999 KW4. The analysis shows that the mean color indices are the following: *B-V* = 0.85 ± 0.01 mag, *V-R* = 0.44 ± 0.02 mag, *B-R* = 1.29 ± 0.01 mag and *V-I* = 0.65 ± 0.03 mag.

The binary asteroid (66391) 1999 KW4 was discovered by LINEAR at Socorro on 1999 May 20. Based on the orbital parameters 1999 KW4 belongs to the Aten class of near-Earth asteroids (NEAs). This asteroid passed close to the Earth on 2019 May 25 at about 0.0346 AU and was observed from OAVdA after the Earth flyby to find the *B-V*, *V-R*, *B-R* and *V-I* standard colors using all-sky photometry with Landolt's stars calibration.

Instruments, Observations and Reduction Procedure

The images were collected with a modified 0.81-m *f*/4.75 Ritchey-Chrétien telescope and FLI 1001E CCD camera with an array of 1024×1024 pixels and equipped with BVRI filters. The field-of-view of the camera is 22×22 arcmin, while the plate scale is 2.57 arcsec/pixel in 2×2 binning mode. The target was observed from OAVdA on 2019 May 31 and June 01, from about 21:20 UT to 22:40 UT for both nights (see Table I). On these dates 1999 KW4 was about 0.075 AU away from the Earth but still bright, V ≈ +13.6 mag. The sky was very clear and there were no passing clouds, so the transparency conditions were reasonably stable in both nights.

During photometric observations images of different Landolt's fields were taken with the same BVRI filters used for the target (see Table II).

Target Set	Date (yyyy/mm/dd)	UT	Airmass
BVRI Set 1	2019/05/31	21:28	1.629
BVRI Set 2	2019/05/31	22:06	1.844
BVRI Set 3	2019/06/01	21:06	1.435
BVRI Set 4	2019/06/01	21:11	1.460

Table I. Date, mean UT and mean airmass for the four BVRI asteroid images set. The exposure time is 60 s for all the images.

Chart	RA (h m)	Dec (° ′)	yyyy/mm/dd	UT	Airmass
095	13:26	-08:50	2019/05/31	21:49	1.897
104	15:39	-00:14	2019/05/31	22:18	1.448
109	16:35	+09:47	2019/05/31	22:26	1.283
090	12:42	-00:40	2019/06/01	21:20	1.614
095	13:26	-08:50	2019/06/01	21:32	1.845

Table II. Landolt's charts, RA, Dec (J2000.0), date, mean UT and mean airmass.

Landolt fields are very useful for reducing observations to a standard photometric system as the Johnson/Cousins (Landolt, 1992). In our case we used the Landolt's fields to calibrate a simple instrumental-atmospheric model (Harris et al., 1981):

$$V - v = Zv - k_v \cdot X + C_v(B - V) \qquad (1)$$

In equation (1) B and V are the true apparent magnitude of the Landolt's stars; Zv is the zero point magnitude; v is the instrumental magnitude in V band, k_v is the first-order atmospheric extinction coefficient, $X = 1/\cos(z)$ is the air mass and C_v is the instrument color-correction coefficient. We can write analogous equations for B, R and I filters:

$$B - b = Zb - k_b \cdot X + C_b(B - V) \qquad (2)$$

$$R - r = Zr - k_r \cdot X + C_r(V - R) \qquad (3)$$

$$I - i = Zi - k_i \cdot X + C_i(V - I) \qquad (4)$$

Measuring the instrumental magnitude of the reference stars in the Landolt's fields and solving, in the least squares sense, the corresponding linear system for each filter in the unknown parameters *Z*, *k* and *C*, we found the best coefficients values listed in Table III and IV. In the June 1 session the airmass differences between the Landolt fields are not very high so we assumed the atmospheric absorption coefficients determined in the previous night, i.e. $k_b = 0.26$, $k_v = 0.15$, $k_r = 0.13$ and $k_i = 0.09$ (Table III).

Zero Point Mag.	Atmospheric Ext.	Color-Correction
Z_b=22.38 ± 0.05	k_b=0.26 ± 0.03	C_b=+0.14 ± 0.02
Z_v=22.39 ± 0.04	k_v=0.15 ± 0.02	C_v=-0.04 ± 0.01
Z_r=22.69 ± 0.04	k_r=0.13 ± 0.03	C_r=-0.12 ± 0.02
Z_i=21.89 ± 0.05	k_i=0.09 ± 0.03	C_i=+0.01 ± 0.02

Table III. Coefficients values of the instrumental-atmospheric model for 2019 May 31.

Zero Point Mag.	Color-Correction
Z_b = 22.21 ± 0.02	C_b = +0.13 ± 0.04
Z_v = 22.27 ± 0.02	C_v = -0.06 ± 0.03
Z_r = 22.62 ± 0.02	C_r = -0.17 ± 0.05
Z_i = 21.87 ± 0.05	C_i = +0.03 ± 0.07

Table IV. Coefficients values of the instrumental-atmospheric model for 2019 June 01.

The Visible Wavelength Colors of 1999 KW4

Using the previous coefficients determined from Landolt's fields, the equations that allows us to move from target instrumental colors to true ones are the difference between equations (1)-(4). For example, the *B-V* color is given by:

$$(B - V) = \frac{(b - v) - X \cdot (k_v - k_b) + Zb - Zv}{1 - (C_b - C_v)} \qquad (5)$$

and similar for *V-R*, *B-R* and *V-I*. By measuring 1999 KW4 instrumental colors using the four different sets of Table I and taking into account the different airmass values to which they were taken, we found four distinct values for each color. The mean colors are the following: *B-V* = 0.85 ± 0.01 mag, *V-R* = 0.44 ± 0.02 mag, *B-R* = 1.29 ± 0.01 mag and *V-I* = 0.65 ± 0.03 mag.

References

Harris, W.E.; Fitzgerald, M.P.; Reed, B.C. (1981). "Photoelectric Photometry: an Approach to Data Reduction." *Publications of the Astronomical Society of the Pacific*, **93**, 507-517.

Landolt, A.U. (1992). "UBVRI photometric standard stars in the magnitude range 11.5-16.0 around the celestial equator." *A.J.* **104**, 340-371. *http://web.pd.astro.it/blanc/landolt/landolt.html*

NEW LIGHTCURVES OF 50 VIRGINIA, 57 MNEMOSYNE, 59 ELPIS, 194 PROKNE, 444 GYPTIS, AND 997 PRISKA

Frederick Pilcher
Organ Mesa Observatory (G50)
4438 Organ Mesa Loop
Las Cruces, NM 88011 USA
fpilcher35@gmail.com

(Received: 2019 July 9 Revised: 2019 August 3)

Synodic rotation periods and amplitudes are found for 50 Virginia 14.313 ± 0.001 h, 0.13 ± 0.01 mag; 57 Mnemosyne 25.324 ± 0.002 h, 0.09 ± 0.01 mag; 59 Elpis 13.676 ± 0.001 h, 0.12 ± 0.01 mag; 194 Prokne 15.683 ± 0.002 h, 0.15 ± 0.01 mag; 444 Gyptis 6.215 ± 0.001 h, 0.13 ± 0.01 mag; 997 Priska 16.241 ± 0.001 h, 1.05 ± 0.05 mag.

Observations to obtain the data used in this paper were made at the Organ Mesa Observatory with a 0.35-meter Meade LX200 GPS Schmidt-Cassegrain (SCT) and SBIG STL-1001E CCD. Exposures were 60 seconds, unguided, with a clear filter except for the faint object 997 Priska where exposure time of 120 seconds was required. Photometric measurement and lightcurve construction are with MPO Canopus software. To reduce the number of points on the lightcurves and make them easier to read, data points have been binned in sets of 3 with a maximum time difference of 5 minutes.

50 Virginia. The lightcurve data base (LCDB; Warner et al., 2009) lists a period of 14.315 h based on several secure U = 3 published periods within 0.005 h of this value. New observations on six nights 2019 Apr. 11-May 6 provide a good fit to a lightcurve with period 14.313 ± 0.001 h, amplitude 0.13 ± 0.01 mag. This value is consistent with previous determinations.

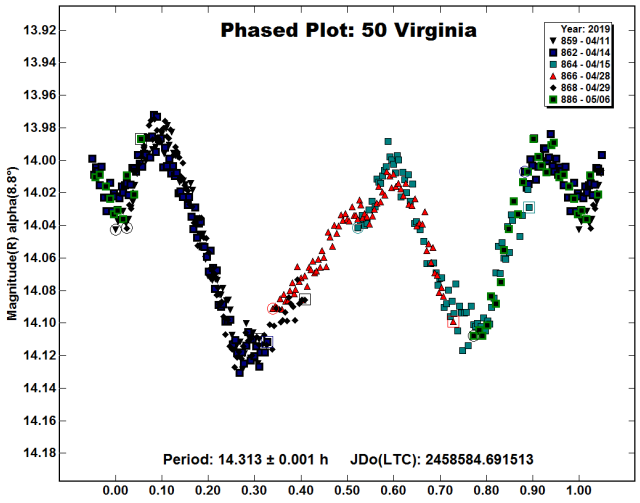

57 Mnemosyne. Among the 100 lowest numbered asteroids, 57 Mnemosyne is one of the least frequently observed. Previously published rotation periods are by Harris and Young (1992, 12.463 h, Ditteon and Hawkins (2007, 12.66 h), and Behrend (2016, 12.92 h). This project is an example of "too little, too late." As with minor planets 50, 59, 194, and 444 also described in this paper, the goal was to obtain data for an object whose rotation period was considered secure at a new celestial longitude to contribute to future lightcurve inversion modeling. The project was much delayed by bad weather and the need to complete other projects. It was nearly two months after opposition before it became apparent that a good fit could not be made to a period near 12.5 h. It was not feasible to continue observations after June 9 since early evening sessions were becoming increasingly shorter.

After the first few sessions, a fit to the new observations was found near 25.32 h, approximately twice the previously accepted period. The instrumental magnitude of each additional session was adjusted by a few 0.01 mag to a good fit near this period. After the observing campaign was concluded with new observations on 10 nights 2019 April 8 – June 9, a good fit could be made to a monomodal lightcurve with period 25.324 ± 0.002 h, amplitude 0.09 ± 0.01 mag.

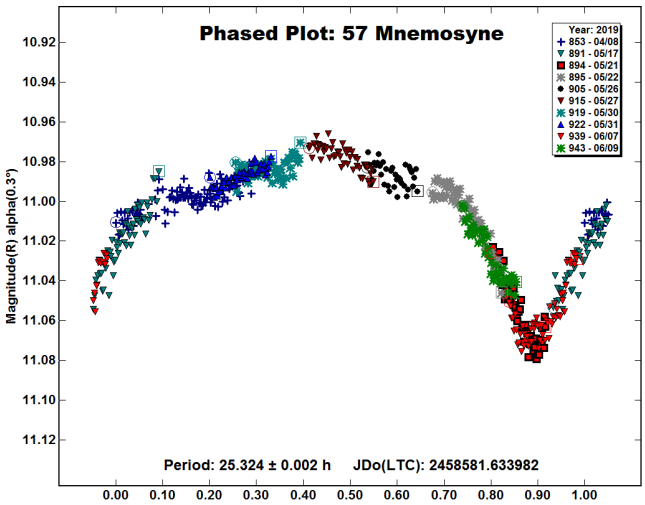

This lightcurve contains one maximum and minimum per cycle, a circumstance fairly often found when the viewing aspect (completely unknown for 57 Mnemosyne) is fairly close to polar. A period spectrum covering 10-60 h shows the deepest minimum at 25.32 h.

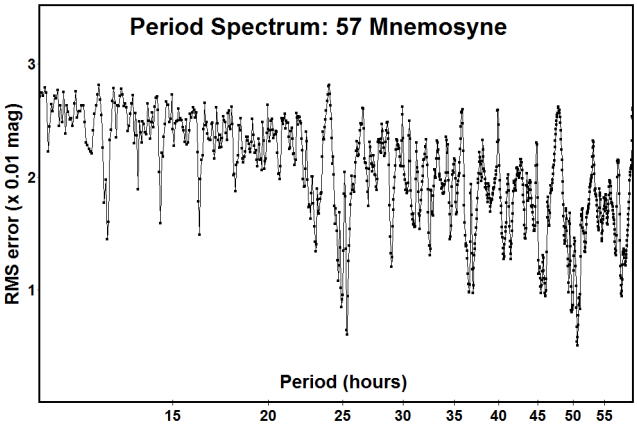

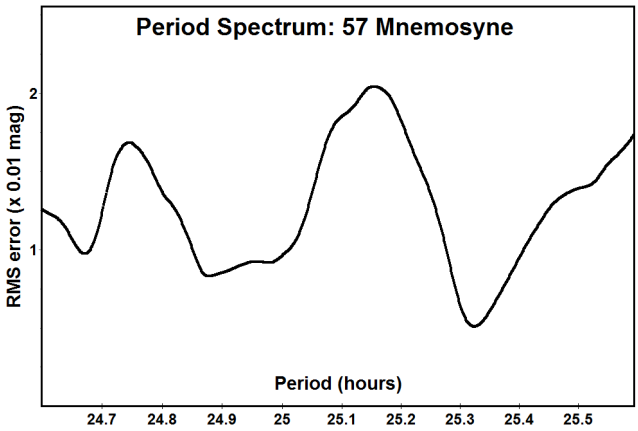

A period spectrum between 24.6-25.6 h shows a second minimum near 24.88 h nearly as deep as the minimum at 25.32 h. A lightcurve phased to this secondary minimum with a period 24.878 h shows two closely spaced narrow minima.

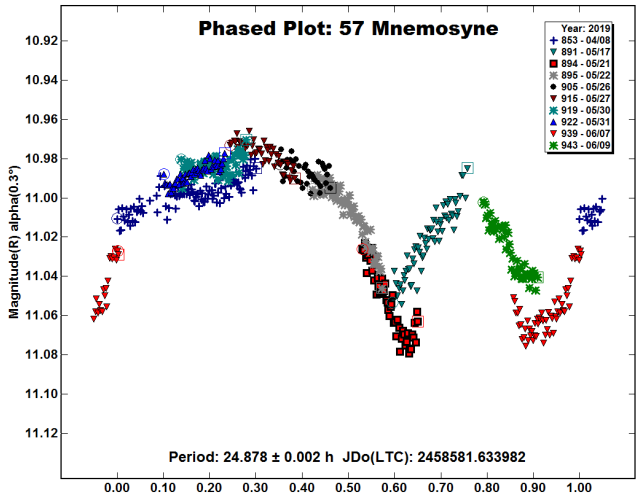

The fit of the individual sessions is as good as for 25.324 h except that sessions 891 (May 17) and 943 (June 9) are about 0.025 mag too high. The instrumental magnitudes of these two sessions are adjusted downward to best fit at 24.877 h.

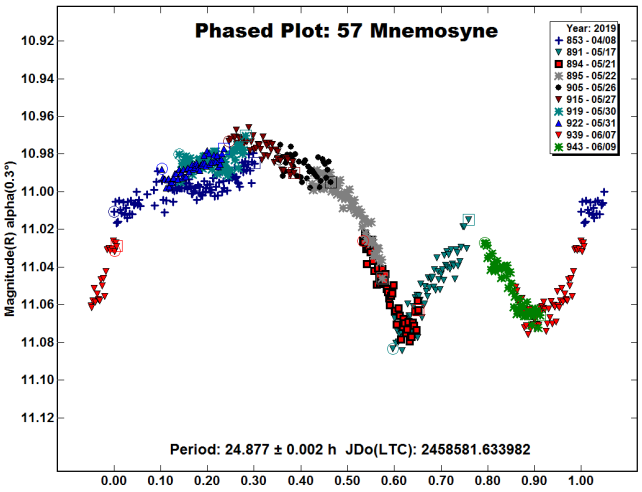

A period spectrum between 24.6-25.6 h after this adjustment now shows the lowest minimum at 24.88 h.

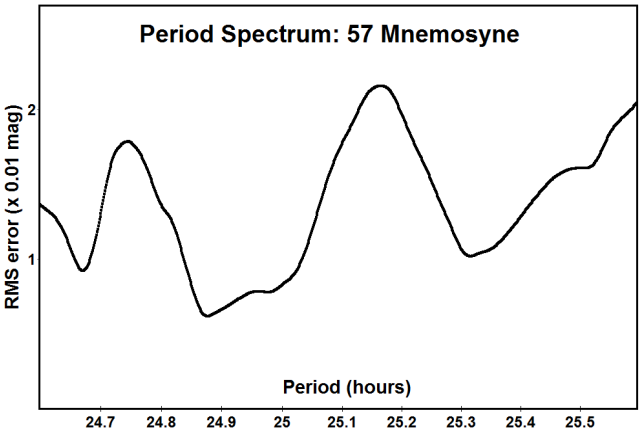

At least one, and perhaps both, of the respective 25.324 h and 24.877 h periods must be aliases. A caution is made to all observers. Merely adopting the period corresponding to the deepest minimum in a period spectrum does not assure that one has not selected an alias. Lightcurves phased to all likely minima in the period spectra should be plotted and examined for reasonable shape and also for slope discordances as are discussed below.

An effort was also made to find a lightcurve with period between 12.0-13.0 h, as had been accepted prior to this study. The best fit was to 12.329 h and the period spectrum between 12.0-13.0 h is also shown.

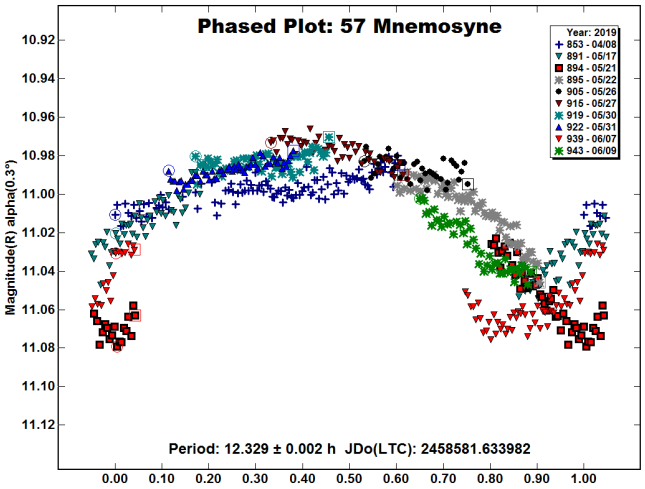

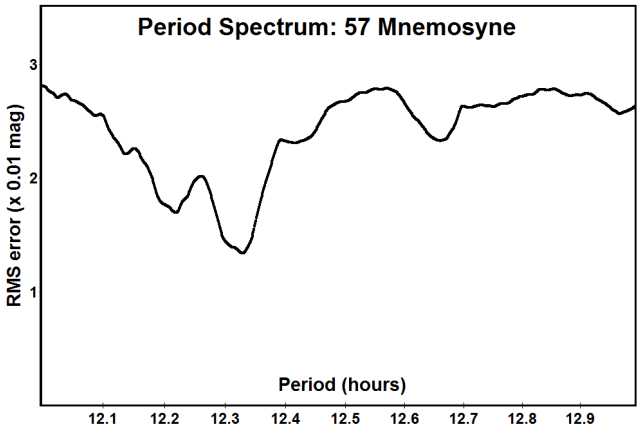

In the phased lightcurve, separate sessions show discordances in slope that remain even with adjustments of instrumental magnitudes. Their presence is strong evidence against the 12.329 h period. A lightcurve phased to the 12.20 h minimum in the period spectrum, not shown here, also shows slope discordances. The slope discordances of a lightcurve plotted to any period near 12.329 h appear to rule out all previously published periods.

In this study, the period of 25.324 h is adopted. Lightcurves with one maximum and minimum per rotational cycle are encountered fairly often, and are especially prevalent when the viewing aspect is fairly close to polar. Near polar viewing aspect at the phase angle bisector of 57 Mnemosyne in the current study should not, however, be assumed. An asteroid lightcurve with two closely spaced narrow minima is hardly ever encountered, and it is hard to imagine an asteroid shape that would produce such a lightcurve. Therefore, the 24.877 h period can be safely rejected.

There have been several other instances where low-numbered minor planets with few observations and periods considered secure had rotation periods twice as great as had been long believed. Examples are 49 Pales (Pilcher et al., 2016), 74 Galatea (Pilcher, 2008), 128 Nemesis (Pilcher, 2015), and 200 Dynamene (Pilcher, 2012). One wonders how many more brighter asteroids not recently observed have rotation periods greatly different from those now listed as secure U = 3.

59 Elpis. The lightcurve data base (LCDB; Warner et al., 2009) lists a period of 13.671 h based on several secure U = 3 published periods within 0.03 h of this value. New observations on five nights 2019 Apr. 6–May 5 provide a good fit to a lightcurve with period 13.676 ± 0.001 h, amplitude 0.12 ± 0.01 mag. This value is consistent with previous determinations.

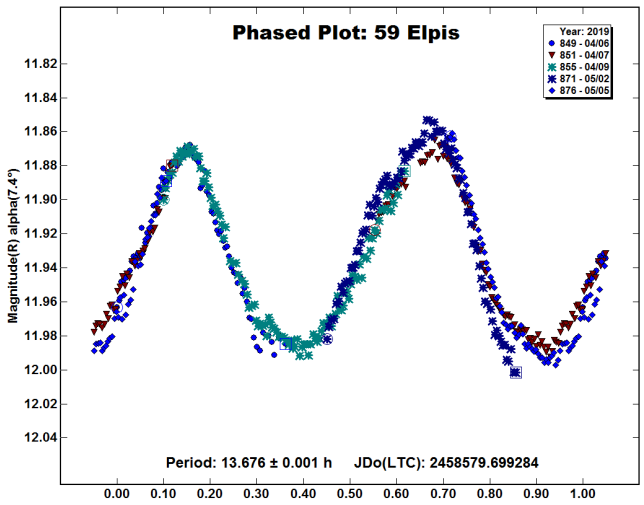

194 Prokne. The lightcurve data base (Warner et al., 2009) lists a period of 15.679 h based on several published periods within 0.01 h of this value. New observations on four nights from 2019 May 15-28 provide a good fit to an irregular lightcurve with period 15.683 ± 0.002 h, amplitude 0.15 ± 0.01 mag. This value is consistent with previous determinations.

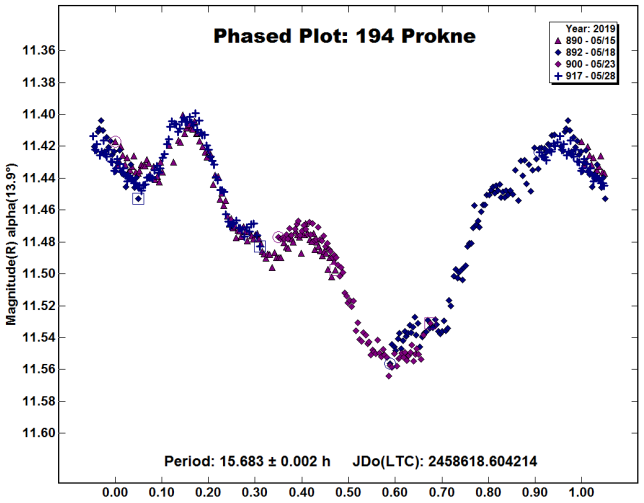

444 Gyptis. The lightcurve data base (Warner et al., 2009) lists a period of 6.214 h based on several secure U = 3 published periods within 0.005 h of this value. New observations on four nights from 2019 Mar. 28-Apr. 10 provide a good fit to a lightcurve with period 6.215 ± 0.001 h, amplitude 0.13 ± 0.01 mag. This value is consistent with previous determinations.

Number	Name	2019/mm/dd	Phase	L_{PAB}	B_{PAB}	Period(h)	P.E.	Amp	A.E.
50	Virginia	04/11-05/06	8.7,14.6	174	0	14.313	0.001	0.13	0.01
57	Mnemosyne	04/08-06/09	0.3,15.7	197	1	25.324	0.002	0.09	0.01
59	Elpis	04/06-05/05	7.4,15.7	177	2	13.676	0.001	0.12	0.01
194	Prokne	05/15-05/28	13.9,17.4	208	19	15.683	0.002	0.15	0.01
444	Gyptis	03/28-04/10	5.4,10.8	202	1	6.215	0.001	0.13	0.01
997	Priska	05/30-07/09	23.4,11.0	299	10	16.241	0.001	1.05	0.05

Table I. Observing circumstances and results. Pts is the number of data points. The phase angle is given for the first and last date, unless a minimum (second value) was reached. L_{PAB} and B_{PAB} are the approximate phase angle bisector longitude and latitude at mid-date range (see Harris *et al.*, 1984).

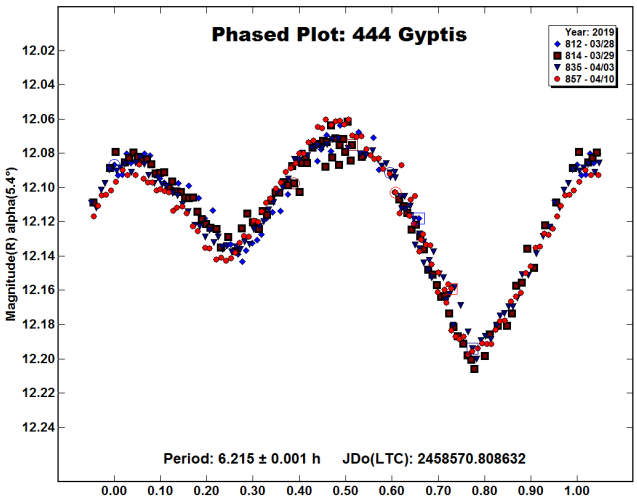

997 Priska. The only previously published rotation period is by Behrend (2006) who found 16.22 h, amplitude 0.61 mag. New observations on 11 nights from 2019 May 30–July 9 provide a good fit to a lightcurve with period 16.241 ± 0.001 h, amplitude 1.05 ± 0.05 mag. This period is consistent with Behrend (2006).

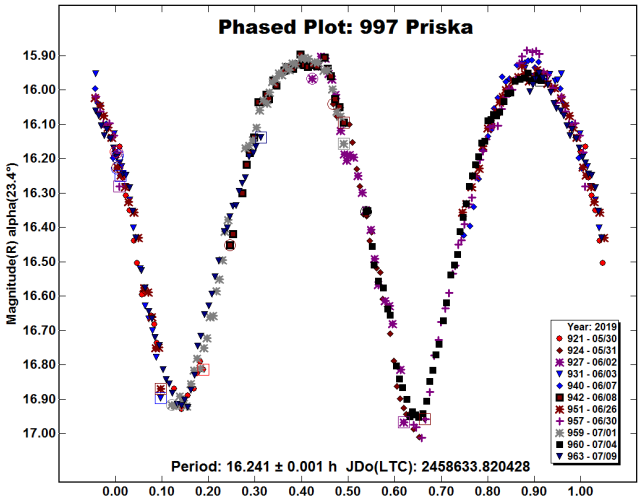

References

Behrend, R. (2006, 2016). Observatoire de Geneve web site. *http://obswww.unige.ch/~behrend/page_cou.html*.

Ditteon, R.; Hawkins, S. (2007). "Asteroid lightcurve analysis at the Oakley Observatory – November 2006." *Minor Planet Bull.* **34**, 59-64.

Harris, A.W.; Young, J W.; Scaltriti, F.; Zappala, V. (1984). "Lightcurves and phase relations of the asteroids 82 Alkmene and 444 Gyptis." *Icarus* **57**, 251-258.

Harris, A. W.; Young, J. W. (1992). "Asteroid rotation III. 1978 observations." *Icarus* **43**, 20-32.

Pilcher, F. (2008). "Period determinations for 26 Proserpina, 34 Circe, 74 Galatea, 143 Adria, 272 Antonia, 419 Aurelia, and 557 Violetta." *Minor Planet Bull.* **35**, 135-138.

Pilcher, F. (2012). "Rotation period determinations for 31 Euphrosyne, 65 Cybele, 154 Bertha, 177 Irma, 200 Dynamene, 724 Hapag, 880 Herba, and 1470 Carla." *Minor Planet Bull.* **39**, 57-60.

Pilcher, F. (2015). "New photometric observations of 128 Nemesis, 249 Ilse, and 279 Thule." *Minor Planet Bull.* **42**, 190-192.

Pilcher, F.; Benishek, V.; Klinglesmith III, D. A. (2016). "Rotation period, color indices, and H-G parameters for 49 Pales." *Minor Planet Bull.* **43**, 182-183.

Warner, B. D.; Harris, A. W.; Pravec, P. (2009). "The Asteroid Lightcurve Database." *Icarus* **202**, 134-146. Updated 2019 January. *http://www.minorplanet.info/lightcurvedatabase.html*

MAIN-BELT ASTEROIDS OBSERVED FROM CS3: 2019 APRIL TO JUNE

Robert D. Stephens
Center for Solar System Studies (CS3)/MoreData!
11355 Mount Johnson Ct., Rancho Cucamonga, CA 91737 USA
rstephens@foxandstephens.com

Brian D. Warner
Center for Solar System Studies (CS3)/MoreData!
Eaton, CO

(Received: 2019 July 9)

CCD photometric observations of 19 main-belt asteroids were obtained at the Center for Solar System Studies (CS3) from 2019 April to June.

The Center for Solar System Studies (CS3) has seven telescopes which are normally used for specific topic studies. The usual focus is on near-Earth asteroids, but when suitable targets are not available, Jovian Trojans and Hildas are observed. When a nearly full moon is too close to the primary targets being studied, targets of opportunity amongst the main-belt regions were selected.

Table I lists the telescopes and CCD cameras that were used to make the observations. Images were unbinned with no filter and had master flats and darks applied. The exposures depended upon various factors including magnitude of the target, sky motion, and Moon illumination.

Telescope	Camera
0.30-m f/6.3 Schmidt-Cass	FLI Microline 1001E
0.35-m f/9.1 Schmidt-Cass	FLI Microline 1001E
0.35-m f/9.1 Schmidt-Cass	FLI Microline 1001E
0.35-m f/9.1 Schmidt-Cass	FLI Microline 1001E
0.35-m f/11 Schmidt-Cass	FLI Microline 1001E
0.40-m f/10 Schmidt-Cass	FLI Proline 1001E
0.50-m F8.1 R-C	FLI Proline 1001E

Table I: List of CS3 telescope/CCD camera combinations.

Image processing, measurement, and period analysis were done using *MPO Canopus* (Bdw Publishing), which incorporates the Fourier analysis algorithm (FALC) developed by Harris (Harris et al., 1989). The Comp Star Selector feature in *MPO Canopus* was used to limit the comparison stars to near solar color. Night-to-night calibration was done using field stars from the CMC-15 or the ATLAS catalog (Tonry et al., 2018), which has Sloan *griz* magnitudes that were derived from the GAIA and Pan-STARR catalogs, among others. The authors state that systematic errors are generally no larger than 0.005 mag, although they can reach 0.02 mag in small areas near the Galactic plane. BVRI magnitudes were derived by Warner using formulae from Kostov and Bonev (2017). The overall errors for the BVRI magnitudes, when combining those in the ATLAS catalog and the conversion formulae, are on the order of 0.04-0.05 mag.

Even so, we found in most cases that nightly zero point adjustments for the ATLAS catalog to be on the order of only 0.02-0.03 mag were required during period analysis. There were occasional exceptions that required up to 0.10 mag. These may have been related in part to using unfiltered observations, poor centroiding of the reference stars, and not correcting for second-order extinction terms. Regardless, the systematic errors seem to be considerably less than other catalogs, which reduces the uncertainty in the results when analysis involves data from extended periods or the asteroid is tumbling.

In the lightcurve plots, the "Reduced Magnitude" is Johnson V corrected to a unity distance by applying $-5*\log(r\Delta)$ to the measured sky magnitudes with r and Δ being, respectively, the Sun-asteroid and the Earth-asteroid distances in AU. The magnitudes were normalized to the phase angle given in parentheses using $G = 0.15$. The X-axis rotational phase ranges from –0.05 to 1.05.

The amplitude indicated in the plots (e.g. Amp. 0.23) is the amplitude of the Fourier model curve and not necessarily the adopted amplitude of the lightcurve.

For brevity, only some of the previously reported rotational periods may be referenced. A complete list is available at the lightcurve database (LCDB; Warner et al., 2009).

Number	Name	2019 mm/dd	Phase	L_{PAB}	B_{PAB}	Period(h)	P.E.	Amp	A.E.	Grp
2025	Nortia	04/18-04/22	17.0,17.1	136	1	5.522	0.002	0.33	0.03	MB-O
2378	Pannekoek	04/22-04/27	4.0,5.5	205	8	11.874	0.003	0.19	0.01	MB-O
2510	Shandong	06/08-06/18	20.1,23.6	223	5	5.949	0.001	0.29	0.04	FLOR
2778	Tangshan	06/09-06/11	17.2,17.8	220	4	3.468	0.003	0.26	0.02	FLOR
4160	Sabrina-John	04/21-04/25	25.2,25.5	145	-3	5.735	0.002	0.41	0.03	V
4892	Chrispollas	04/21-05/18	*25.4,28.4	167	-7	1584	16	0.71	0.05	MB-I
5627	1991 MA	04/15-04/18	*21.7,20.8	266	16	5.365	0.002	0.48	0.03	H
6310	Jankonke	06/08-06/10	22.7,23.3	224	15	3.071	0.002	0.18	0.01	H
6859	Datemasamune	06/11-06/28	31.4,27.4	312	20	5.944	0.001	0.12	0.01	H
9564	Jeffwynn	05/24-05/25	26.2,26.1	263	32	3.03	0.003	0.11	0.02	MC
10480	Jennyblue	04/24-04/26	24.3,24.6	159	3	5.356	0.003	0.92	0.03	FLOR
20936	Nemrut Dagi	05/18-05/21	23.0,24.1	198	-1	3.328	0.002	0.26	0.02	H
32772	1986 JL	05/14-05/24	9.4,12.0	228	12	6.046	0.001	0.25	0.03	H
33324	1998 QE56	06/01-06/06	24.8,24.7	261	35	6.188	0.001	0.64	0.02	H
53440	1999 XQ33	06/09-06/25	21.3,23.3	248	26	5.3276	0.0005	0.34	0.04	H
55854	Stoppani	06/11-06/25	26.3,28.7	214	2	3.06	0.001	0.45	0.03	H
66346	1999 JU71	05/14-05/22	4.7,8.4	229	7	5.233	0.004	0.14	0.03	FLOR
162820	2001 BK36	03/16-03/17	3.4,3.2	178	-5	3.95	0.01	0.33	0.03	EUN
302111	2001 MM3	06/06-06/08	25.5,25.6	274	31	3.217	0.001	0.38	0.03	MC

Table II. Observing circumstances and results. The phase angle is given for the first and last date. If preceded by an asterisk, the phase angle reached an extrema during the period. L_{PAB} and B_{PAB} are the approximate phase angle bisector longitude/latitude at mid-date range (see Harris et al., 1984). Grp is the asteroid family/group (Warner et al., 2009).

2025 Nortia. The LCDB listed no previous rotation periods for this outer main-belt asteroid. Assuming an albedo of 0.057, the estimated diameter is 40 km. The lightcurve shows three maximums. This is unusual but possible with low amplitudes and phase angles (Harris et al., 2014).

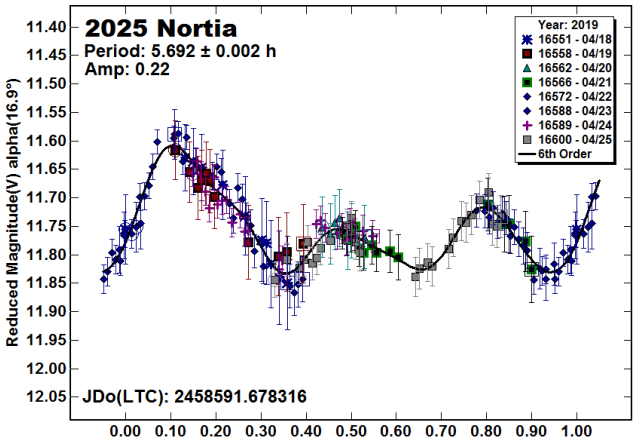

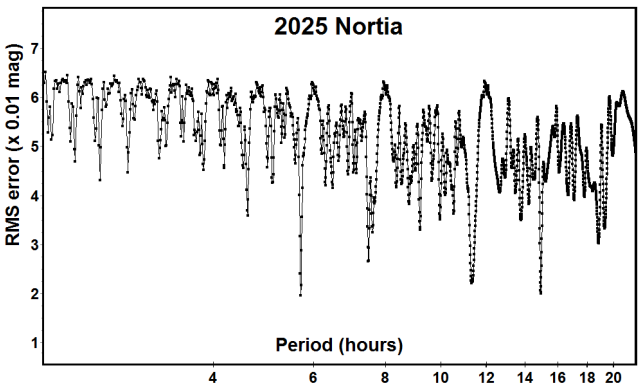

2378 Pannekoek. Previous results gave 5.943 h (Higgins, 2008) and 11.8806 h (Oey 2011 web), for this outer main-belt asteroid. Our results from 2019 show several aliases with our preference for P = 11.874 h even though the lightcurve is missing about 30% of a full rotation. This is based on the half-period plot showing the asymmetry of the full period solution. The spacing of extrema doesn't seem right for the near 7.9 h solution, but because of the amplitude, an unusual shape cannot be formally excluded (Harris et al., 2014), especially when the period spectrum shows sharp RMS minimums near 6 and 8 hours.

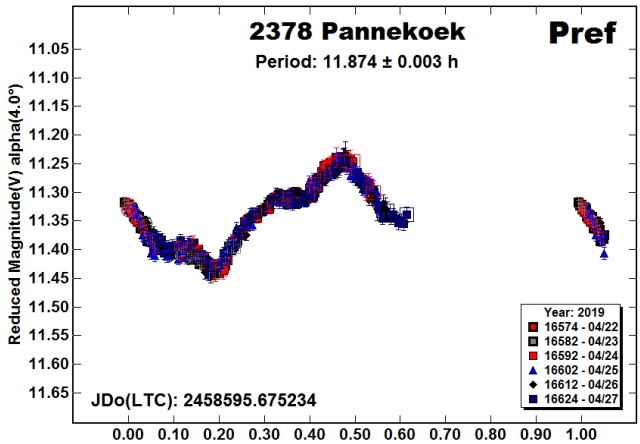

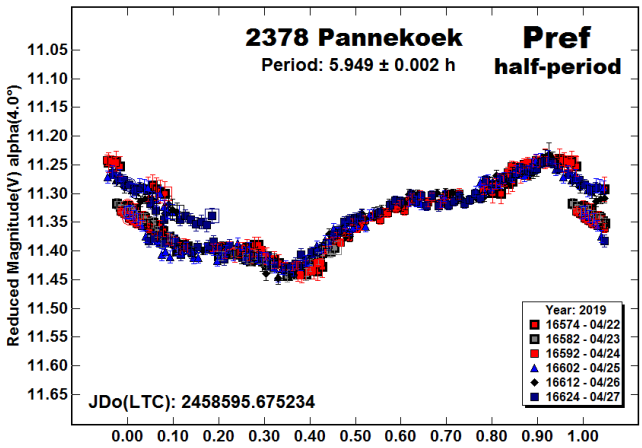

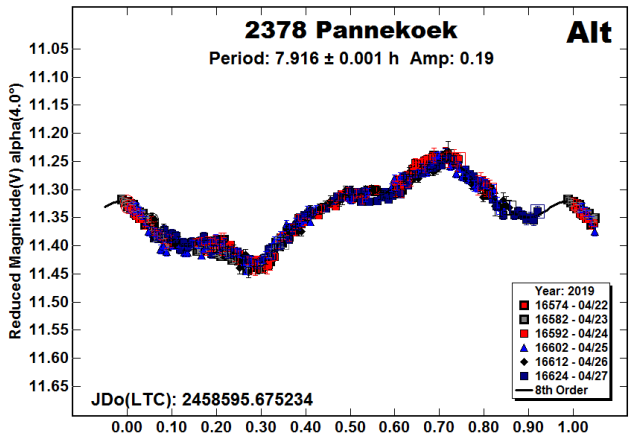

2510 Shandong. This inner main-belt asteroid has a diameter of about 9 km. Higgins and Goncalves (2007) found a period of 5.9463 h. Using a combination of dense and sparse lightcurve data, Hanus et al. (2013) found $P_{sidereal}$ = 5.94639 h and a preferred spin axis with ecliptic coordinates λ,β = (256°, 27°)

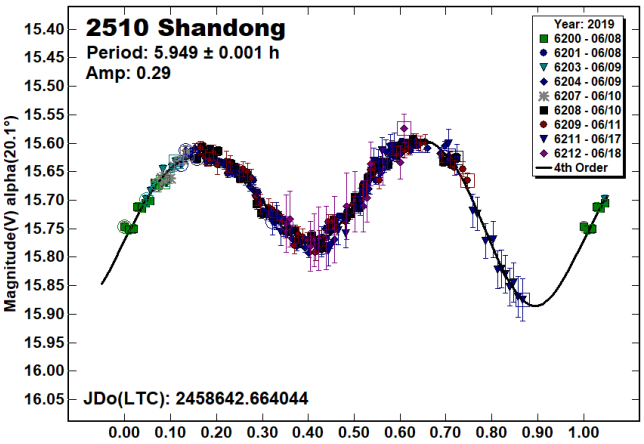

2778 Tangshan. Rotational periods for this member of the Flora group near 3.46 h have been reported twice before (Behrend et al., 2018, Warner, 2004). The result found this year is in good agreement.

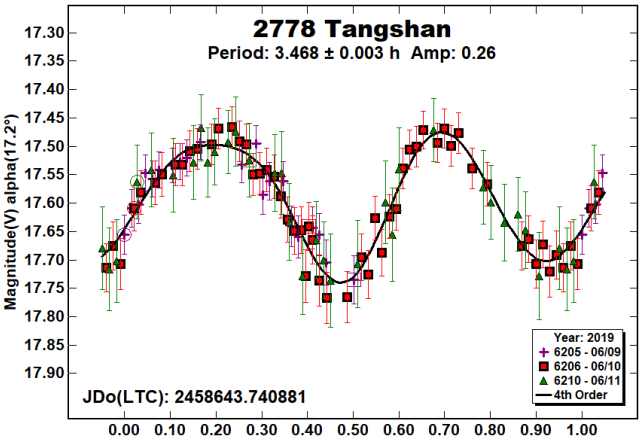

4160 Sabrina-John. This appears to be the first rotation period for Sabrina-John, which is classified as a Vestoid (i.e., possibly a fragment off Vesta) with a diameter of about 7 km.

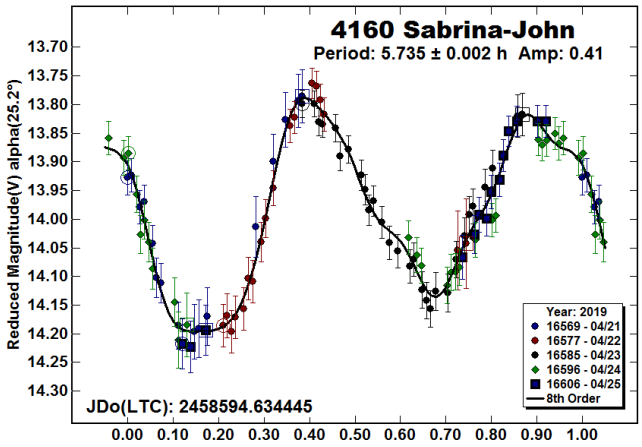

4892 Chrispollas. This 8-km inner main-belt asteroid had no previously reported period in the LCDB. There may be good reason for that: the extremely long period that we report here. In our data, night-to-night runs showed almost no ascending or descending trend. Given limited telescope time for many, this might have led most observers to give up in lieu of working other targets that had better opportunities for success.

Our program is dedicated to working potentially long-period objects until it is certain that the data are "flat" (low amplitude) or at least an approximate estimate of the period can be found. Even so, it was not possible to follow this asteroid long enough to obtain a full lightcurve and so our result is based on the presumed monomodal lightcurve at the half-period (Harris et al., 2014). Even this lightcurve is incomplete and so the true error in the resulting full-period is probably larger than the formal value given here. Because of the long period and estimated diameter, this is a good candidate for tumbling (Pravec et al., 2014; 2005). There are some indications of this with at least two sessions falling below the Fourier curve.

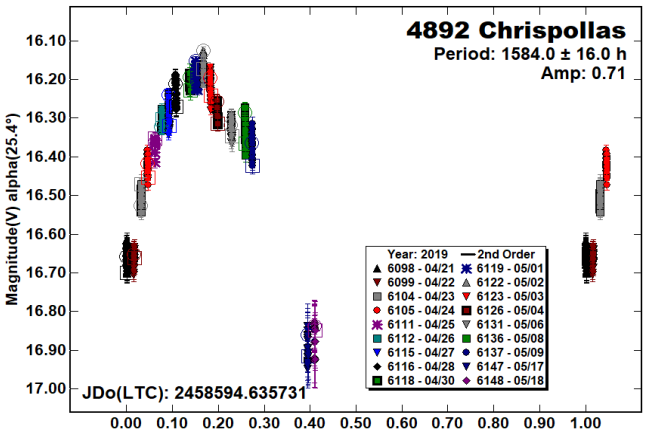

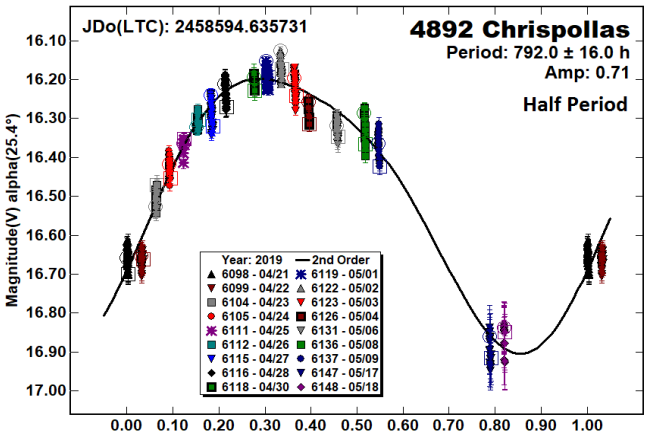

(5267) 1991 MA. Our result is about 0.15 h longer than previous results: Waszczak et al. (2015) and Zeigler et al. (2017). The former is a survey with a "dense sparse" data set. Zeigler et al. had two non-consecutive nights that produced a lightcurve that did not have full double coverage. For these reasons, we have high confidence in our result.

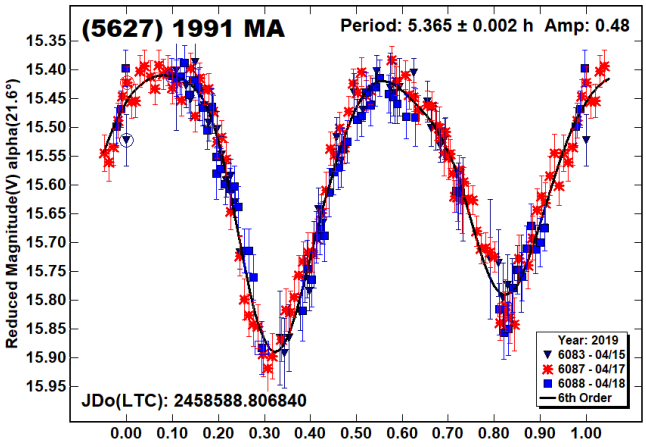

6310 Jankonke is a Hungaria asteroid that has been observed at several previous apparitions, in particular by Warner (see LCDB references) as part of an on-going project to find spin axes for members of the group. The period given here is consistent with previous results; the data should improve a preliminary spin axis.

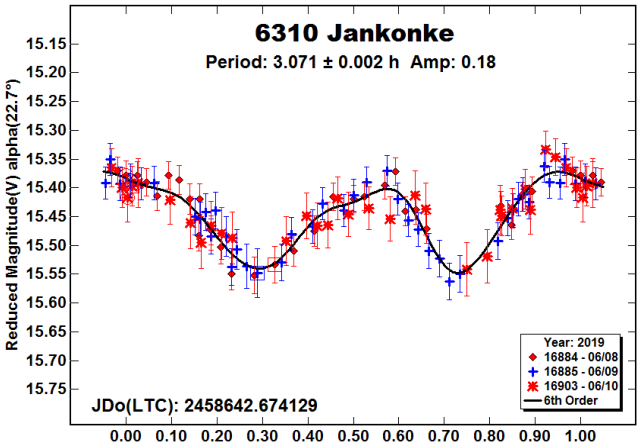

6859 Datemasamune is another Hungaria member that is part of the spin axis project. Finding the period has been difficult because of amplitudes < 0.2 mag. Previous results by Warner are 2006, 12.95 h; 2010, 22.1 h; 2011, 86.1 h.; and 2016b, 5.2879 h. The 2019 data excluded the very long periods and favored one close to the 2016 result. We have adopted the 2019 period of 5.944 h, but other solutions cannot be formally excluded.

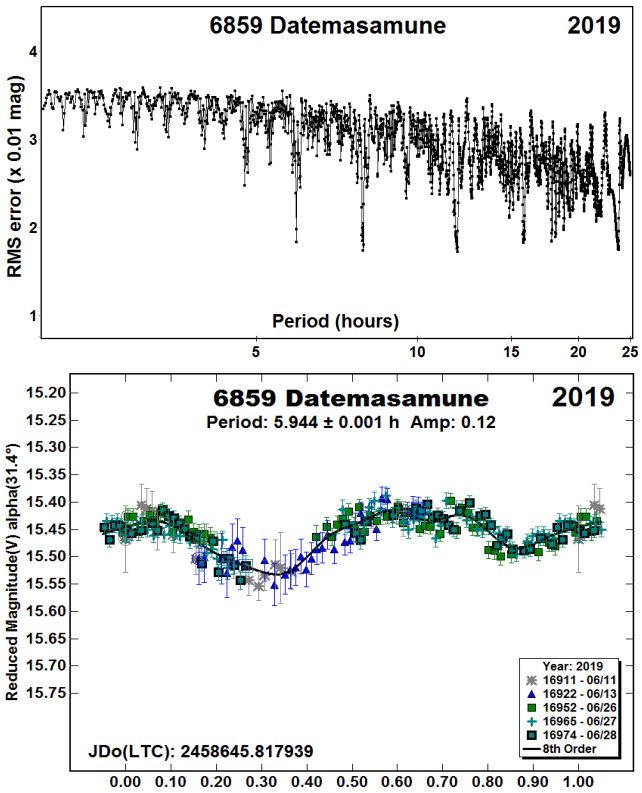

The data sets from 2006-2016 were reanalyzed to see if they would support the adopted period given here. The fits in 2006, 2011, and 2016 are very plausible. The 2009 data set was somewhat noisy and so the fit to the new period is not as convincing.

We note that having the ATLAS star catalog with highly-reliable magnitudes played an important role in our 2019 analysis because there was high confidence in zero point matching from night-to-night. In previous years, as can be seen with the wide range of periods, zero point adjustments were much more arbitrary.

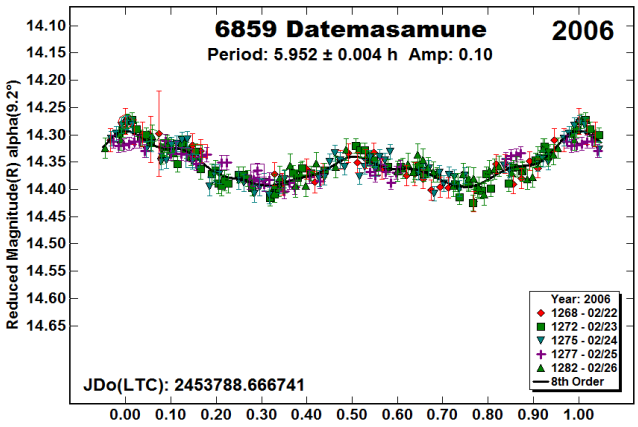

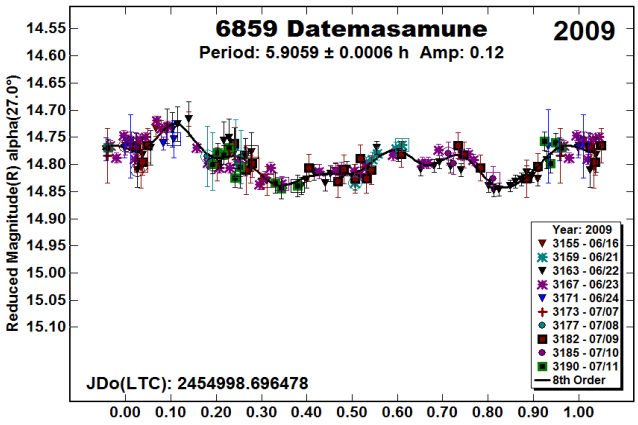

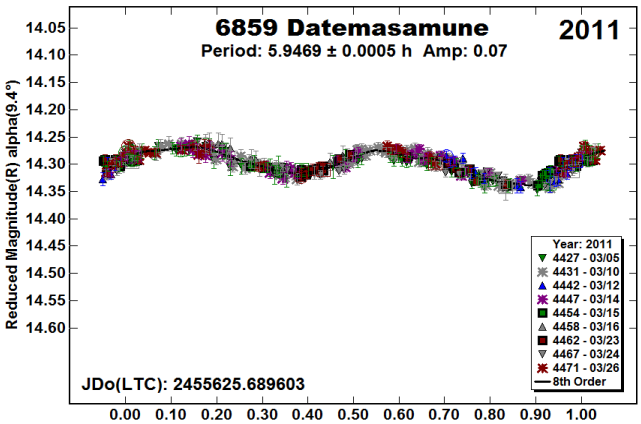

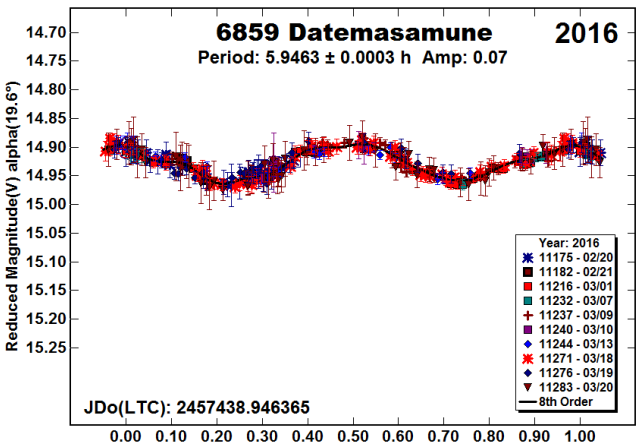

9564 Jeffwynn. The only previously reported period (3.035 h) was by Warner (2013a). Our most recent result is in good agreement.

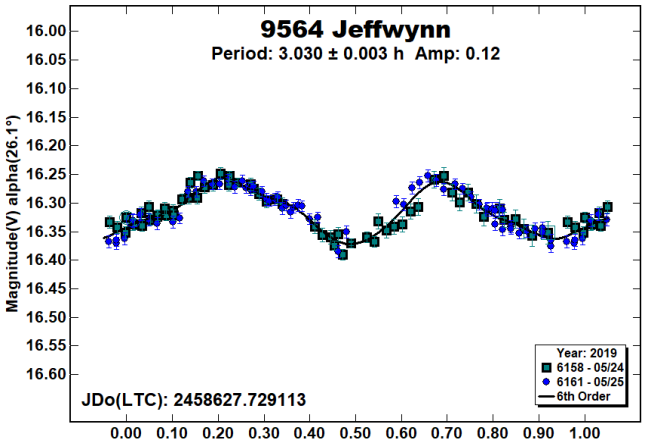

10480 Jennyblue. This was a target of opportunity in the field of a Hilda asteroid. Waszczak et al. (2015) found a period of 6.019 h. Forcing the 2019 data to something near that has the maximums only 0.4 rotation phase apart. There's a good chance of a *rotational alias* being involved since the two periods differ by almost exactly 0.5 rotations over 24 hours. Given the sparser data set used by Waszczak et al., it's reasonably safe to adopt our period of 5.356 h as the more likely.

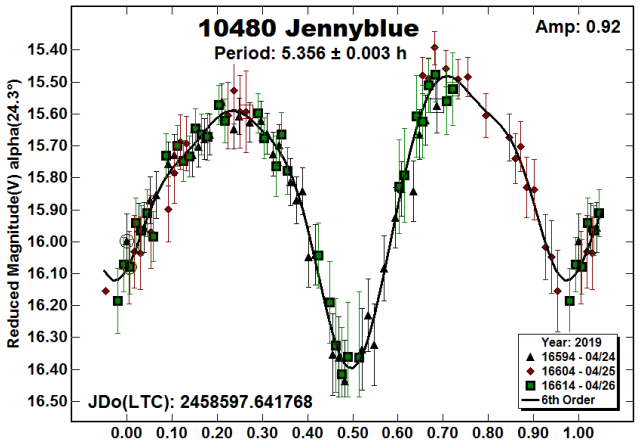

20936 Nemrut Dagi. There are several previous results in the LCDB for this 5-km Hungaria, e.g. Skiff (2011, 3.293 h) and Warner (2016a, 3.2754 h). Our data set was relatively sparse compared to others, enough that we had to force the period search to a small range covering a range a little larger than the full range of reported periods.

While the 2019 data can be fit to 3.328 h, the solution is hardly conclusive. Regardless, the data will be used to try to improve a preliminary spin axis.

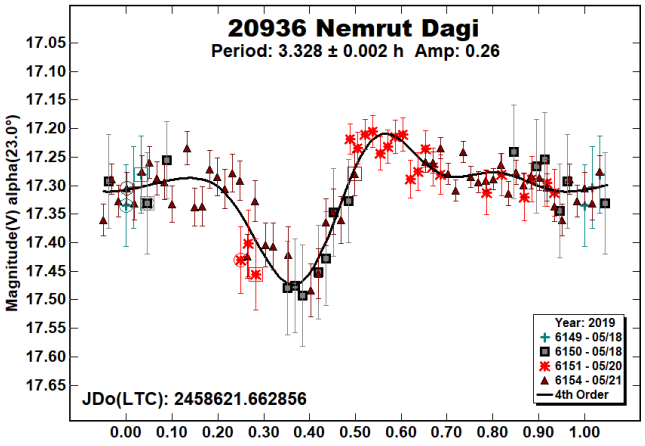

(32772) 1986 JL. We observed this twice before: Warner (2013c) and Stephens (2016). Those two and our result are in excellent agreement. The seemingly monomodal solution in 2019 is unusual given the amplitude, but not impossible (Harris et al., 2014).

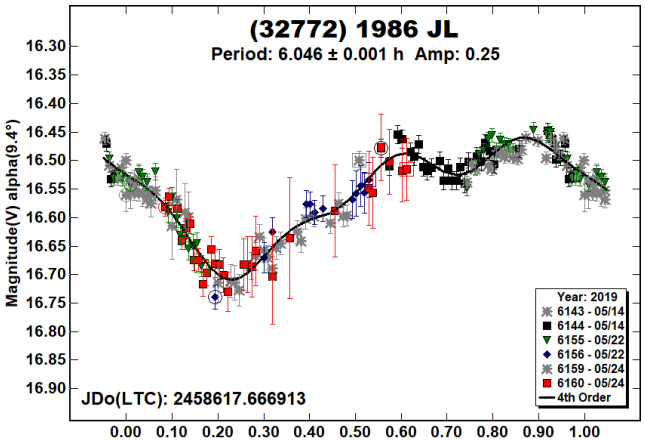

(33324) 1998 QE56. The latest data set extends our dense lightcurve observations from 2011 to 2019 (see LCDB references). As a result, we hope that, combined with sparse data, a good spin axis model can be developed.

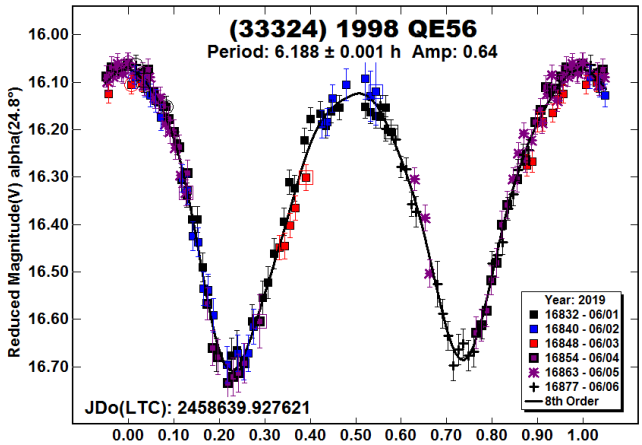

(53440) 1999 XQ33. This appears to be the first reported rotation period for 1999 XQ33. It is another member of the Hungaria group. It would be required to determine its taxonomic class before calling it a family member.

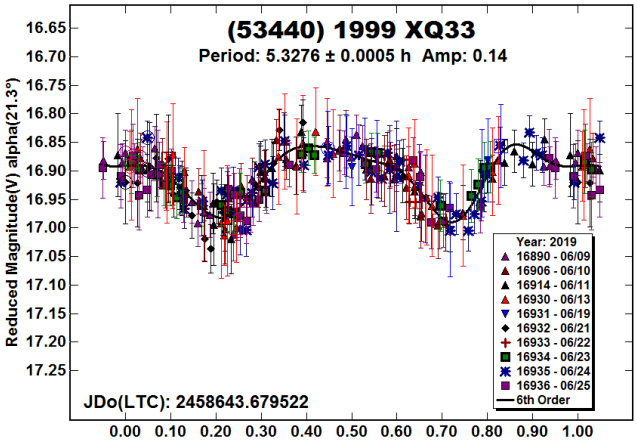

55854 Stoppani. Previous results from Skiff (2011) and Warner (2011, 2013b) are all in close agreement with our 2019 analysis. Were it not for the large amplitude overcoming the noisy data on some nights, it may not have been possible to find a period.

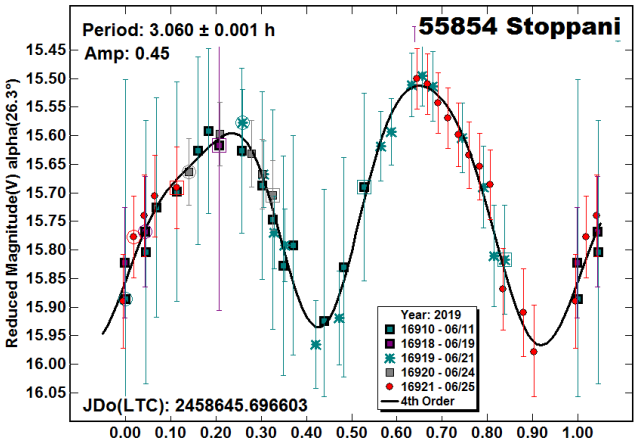

(66346) 1999 JU71. This is a member of the Flora group but it could actually belong to one of the subgroups in the region. The estimated diameter, assuming p_V = 0.24, is 2.3 km. There were no previously reported periods in the LCDB to serve as a starting point for analysis. Unfortunately, the data set was too noisy and too sparse to allow finding a definitive solution.

We show two plots phased to two of the possible solutions. Both have gaps in coverage, which might imply a *fit by exclusion*, which is when the Fourier algorithm finds a local RMS minimum that minimizes the number of overlapping data points. The two periods do not seem to be harmonically related.

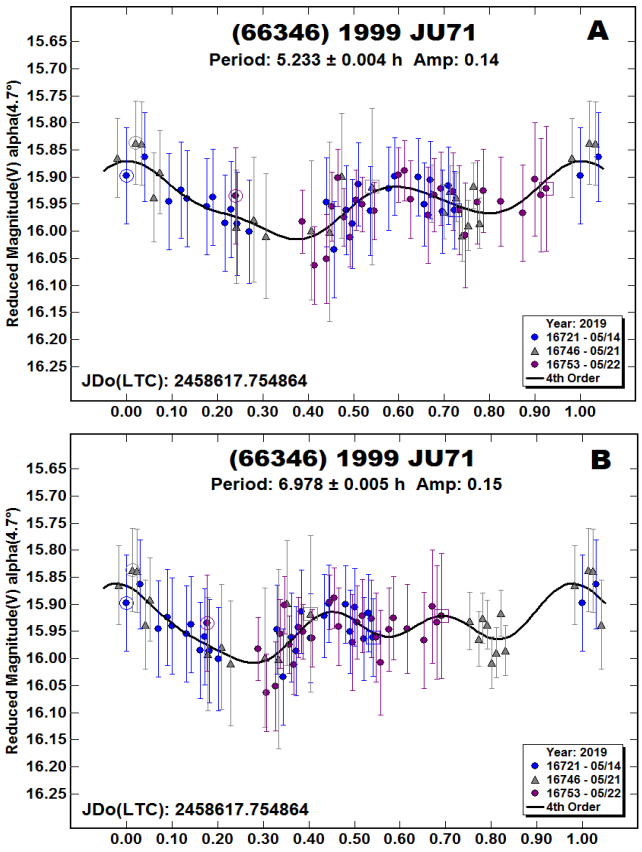

(162820) 2001 BK36. Assuming a default albedo of 0.21 for Eunomia group (or at least region) members gives an estimated diameter of 2.5 km. However, Mainzer et al. (2016) found the asteroid to have an albedo of 0.062. Using H = 15.10, this gave a diameter of 4.8 km.

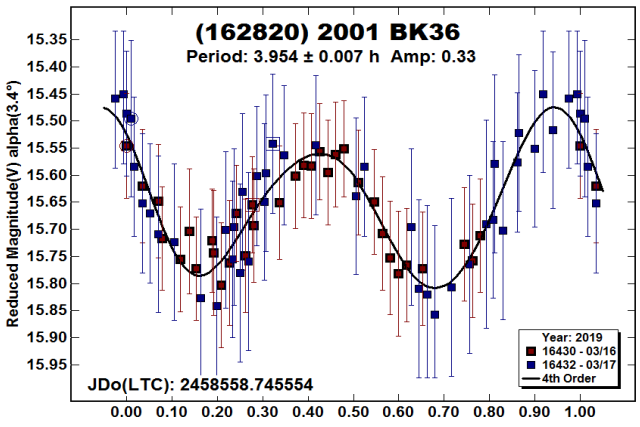

(302111) 2001 MM3. We observed this Mars-crosser for three nights in 2019 June. The resulting data was of high quality and almost covered the adopted period of 3.217 h completely each night. That and the large amplitude make the period solution secure. There were no previous period results in the LCDB.

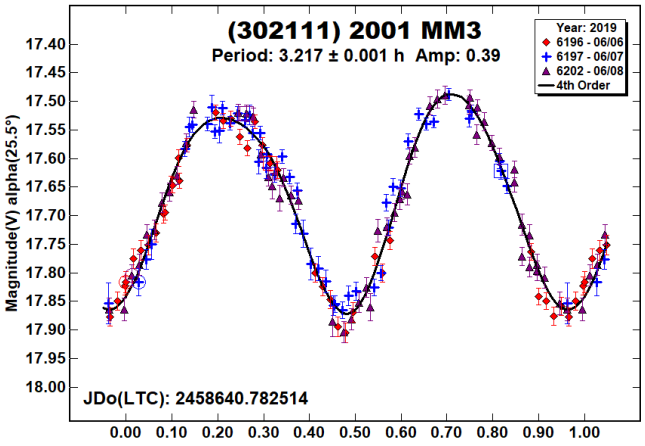

Acknowledgements

Observations at CS3 and continued support of the asteroid lightcurve database (LCDB; Warner et al., 2009) are supported by NASA grant 80NSSC18K0851. Work on the asteroid lightcurve database (LCDB) was also partially funded by National Science Foundation grant AST-1507535. This research was made possible in part based on data from CMC15 Data Access Service at CAB (INTA-CSIC) (http://svo2.cab.inta-csic.es/vocats/cmc15/). This work includes data from the Asteroid Terrestrial-impact Last Alert System (ATLAS) project. ATLAS is primarily funded to search for near earth asteroids through NASA grants NN12AR55G, 80NSSC18K0284, and 80NSSC18K1575; byproducts of the NEO search include images and catalogs from the survey area. The ATLAS science products have been made possible through the contributions of the University of Hawaii Institute for Astronomy, the Queen's University Belfast, the Space Telescope Science Institute, and the South African Astronomical Observatory. The purchase of a FLI-1001E CCD cameras was made possible by a 2013 Gene Shoemaker NEO Grants from the Planetary Society.

References

Behrend, R., (2005, 2018, 2019). Observatoire de Geneve web site, *http://obswww.unige.ch/~behrend/page_cou.html*

Hanuš, J.; Ďurech, J.; Brož, M.; Marciniak, A.; Warner, B.D.; Pilcher, F.; Stephens, R.; Behrend, R.; Carry, B.; and 111 coauthors (2013). "Asteroids' physical models from combined dense and sparse photometry and scaling of the YORP effect by the observed obliquity distribution." *Astron. Astrophys.* **551**, A67.

Harris, A.W.; Young, J.W.; Scaltriti, F.; Zappala, V. (1984). "Lightcurves and phase relations of the asteroids 82 Alkmene and 444 Gyptis." *Icarus* **57**, 251-258.

Harris, A.W.; Young, J.W.; Bowell, E.; Martin, L.J.; Millis, R.L.; Poutanen, M.; Scaltriti, F.; Zappala, V.; Schober, H.J.; Debehogne, H.; Zeigler, K.W. (1989). "Photoelectric Observations of Asteroids 3, 24, 60, 261, and 863." *Icarus* **77**, 171-186.

Harris, A.W., Pravec, P., Galad, A., Skiff, B.A., Warner, B.D., Vilagi, J., Gajdos, S., Carbognani, A., Hornoch, K., Kusnirak, P., Cooney, W.R., Gross, J., Terrell, D., Higgins, D., Bowell, E., Koehn, B.W. (2014). "On the maximum amplitude of harmonics on an asteroid lightcurve." *Icarus* **235**, 55-59.

Higgins, D.; Pravec, P.; Kusnirak, Pe.; Hornoch, K.; Brinsfield, J.; Allen, B.; Warner, B.D. (2004). "Asteroid Lightcurve Analysis at Hunters Hill Observatory and Collaborating Stations: November 2007 - March 2008." *Minor Planet Bull*. **35**, 123-126.

Higgins, D.; Goncalves, R.M.D. (2007). "Asteroid Lightcurve Analysis at Hunters Hill Observatory and Collaborating Stations - June-September 2006." *Minor Planet Bull*. **34**, 16-18.

Kostov, A.; Bonev, T. (2017). "Transformation of Pan-STARRS1 gri to Stetson BVRI magnitudes. Photometry of small bodies observations." *Bulgarian Astron. J.* **28**, 3 (AriXiv:1706.06147v2).

Mainzer, A.K., Bauer, J.M., Cutri, R.M., Grav, T., Kramer, E.A., Masiero, J.R., Nugent, C.R., Sonnett, S.M., Stevenson, R.A., Wright, E.L. (2016). "NEOWISE Diameters and Albedos V1.0." NASA Planetary Data System.
EAR-A-COMPIL-5-NEOWISEDIAM-V1.0.

Pravec, P.; Harris, A.W.; Scheirich, P.; Kušnirák, P.; Šarounová, L.; Hergenrother, C.W.; Mottola, S.; Hicks, M.D.; Masi, G.; Krugly, Yu.N.; Shevchenko, V.G.; Nolan, M.C.; Howell, E.S.; Kaasalainen, M.; Galád, A.; Brown, P.; Degraff, D.R.; Lambert, J. V.; Cooney, W.R.; Foglia, S. (2005). "Tumbling asteroids." *Icarus* **173**, 108-131.

Pravec, P.; Scheirich, P.; Durech, J.; Pollock, J.; Kusnirak, P.; Hornoch, K.; Galad, A.; Vokrouhlicky, D.; Harris, A.W.; Jehin, E.; Manfroid, J.; Opitom, C.; Gillon, M.; Colas, F.; Oey, J.; Vrastil, J.; Reichart, D.; Ivarsen, K.; Haislip, J.; LaCluyze, A. (2014). "The tumbling state of (99942) Apophis." *Icarus* **233**, 48-60.

Skiff, B.A. (2011). Posting on CALL web site.
http://www.minorplanet.info/call.html

Stephens, R.D. (2016). "Asteroids Observed from CS3: 2016 January-March." *Minor Planet Bull*. **43**, 252-255.

Stephens, R.D. (2017). "Asteroids Observed from CS3: 2016 October – December." *Minor Planet Bull*. **44**, 120-122.

Tonry, J.L.; Denneau, L.; Flewelling, H.; Heinze, A.N.; Onken, C.A.; Smartt, S.J.; Stalder, B.; Weiland, H.J.; Wolf, C. (2018). "The ATLAS All-Sky Stellar Reference Catalog." *Astrophys. J.* **867**, A105.

Warner, B.D. (2004). "Lightcurve analysis for numbered asteroids 1351, 1589, 2778, 5076, 5892, and 6386." *Minor Planet Bull*. **31**, 36-39.

Warner, B.D. (2006). "Asteroid lightcurve analysis at the Palmer Divide Observatory - February - March 2006." *Minor Planet Bull.* **33**, 82-84.

Warner, B.D. (2010). Asteroid Lightcurve Analysis at the Palmer Divide Observatory: 2009 June-September." *Minor Planet Bull*. **37**, 24-27.

Warner, B.D. (2011). "Asteroid Lightcurve Analysis at the Palmer Divide Observatory: 2011 March - July." *Minor Planet Bull*. **38**, 190-195.

Warner, B.D. (2013a). "Asteroid Lightcurve Analysis at the Palmer Divide Observatory: 2012 June – September." *Minor Planet Bull*. **40**, 26-29.

Warner, B.D. (2013b). "Asteroid Lightcurve Analysis at the Palmer Divide Observatory: 2012 September - 2013 January." *Minor Planet Bull*. **40**, 71-80.

Warner, B.D. (2013c). "Asteroid Lightcurve Analysis at the Palmer Divide Observatory: 2013 January – March." *Minor Planet Bull*. **40**, 137-145.

Warner, B.D. (2016a). "Asteroid Lightcurve Analysis at CS3-Palmer Divide Station: 2015 October-December." *Minor Planet Bull*. **43**, 137-140.

Warner, B.D. (2016b). "Asteroid Lightcurve Analysis at CS3-Palmer Divide Station: 2015 December - 2016 April." *Minor Planet Bull*. **43**, 227-233.

Warner, B.D.; Harris, A.W.; Pravec, P. (2009). "The Asteroid Lightcurve Database." *Icarus* **202**, 134-146. Updated 2019 Feb. *http://www.minorplanet.info/lightcurvedatabase.html*

Waszczak, A.; Chang, C.-K.; Ofek, E.O.; Laher, R.; Masci, F.; Levitan, D.; Surace, J.; Cheng, Y.-C.; Ip, W.-H.; Kinoshita, D.; Helou, G.; Prince, T.A.; Kulkarni, S. (2015). "Asteroid Light Curves from the Palomar Transient Factory Survey: Rotation Periods and Phase Functions from Sparse Photometry." *Astron. J.* **150**, A75.

Zeigler, K.; Banshaw, B.; Gass, J. (2017). "Photometric Observations of Asteroid 4742 Caliumi, 5267 Zegmott (18429) 1994 AO1, (26421) 1999 XP113, and (27675) 1981 CH." *Minor Planet Bull*. **44**, 259-260.

1744 HARRIET: ANOTHER VERY SLOWLY ROTATING ASTEROID

Frederick Pilcher
Organ Mesa Observatory
4438 Organ Mesa Loop
Las Cruces, NM 88011 USA
fpilcher35@gmail.com

Daniel Klinglesmith III
Etscorn Campus Observatory
New Mexico Tech
101 East Road
Socorro, NM 87801 USA

Julian Oey
Blue Mountains Observatory
94 Rawson Pde., Leura, NSW, AUSTRALIA

(Received: 2019 July 10)

Minor planet 1744 Harriet has a synodic rotation period near 724 hours, amplitude increasing from 0.95 ± 0.05 magnitudes to 1.10 ± 0.05 magnitudes.

The Asteroid Lightcurve Data Base (Warner et al., 2009) lists no previous observations of 1744 Harriet. First author Pilcher found very slow magnitude change in his first three nights of observation 2019 Apr. 11-14 and recognized that 1744 Harriet has a very long rotational period. He invited Daniel Klinglesmith and Julian Oey to collaborate in obtaining a long series of observations. Both graciously accepted the invitation and contributed many useful sessions.

Pilcher at Organ Mesa Observatory used a Meade 0.35 meter f/10 Meade LX200 GPS SCT and SBIG STL-1001E CCD to obtain sessions 860, 861, 863, 865, 867, 869, 874, 875, 885, 887, 888, 893, 896, 898, 902, 903, 904, 916, 920, 923, 925, 926, 930. 936, 937, 941, 944, 950. Klinglesmith at Etscorn Campus Observatory used a 0.35 cm Celestron SCT and SBIG STL-11000M CCD to obtain sessions 870, 872, 873, 889, 897, 899, 901, 918, 928, 929, 932, 938, 945, 946, 947, 948, 949. Oey at Blue Mountains Observatory used a 14 inch Schmidt Cassegrain telescope and SBIG ST8XME CCD to obtain sessions 877, 878, 879, 881, 882, 883, 884, 906, 907, 908, 909, 910, 911, 912, 913, 933, 934, 935, 952, 953, 954, 955, 956. The three observers obtained 69 sessions, many of them only one to two hours, 2019 Apr. 11 – June 26.

Petr Pravec (private communication) has kindly analyzed the data and finds no evidence of tumbling (Par = +2, Pravec, 2005) or any short term variation with amplitude > 0.038 magnitude. For all sessions 2019 Apr. 11 – June 2 for which the phase angle is less than 16 degrees, he finds a period 724 ± 5 hours. At larger phase angles the amplitude is appreciably greater and this period does not strictly apply.

The authors have performed a separate period search with *MPO Canopus* software. For 50 sessions with phase angle <16 degrees, 2019 Apr. 11 – June 2, they find a period 723.8 ± 0.4 hours,

Number	Name	yyyy/mm/dd	Pts	Phase	LPAB	BPAB	Period(h)	P.E	Amp	A.E.
1744	Harriet	2019/04/11-2019/06/26	2401	13.6, 1.2, 24.1	224	-2	719.5	0.4	1.0	0.1

Table I. Observing circumstances and results. Pts is the number of data points. The phase angle is given for the first and last date, unless a minimum (second value) was reached. LPAB and BPAB are the approximate phase angle bisector longitude and latitude at mid-date range (see Harris *et al.*, 1984).

amplitude 1.0 ± 0.1 magnitudes. For all 69 sessions April 11 – June 26, best fit is found for a period 719.5 ± 0.4 hours. In both cases the real error should be larger than the formal error. We provide lightcurves for both of these intervals. We also provide a raw lightcurve for the entire interval of observation to show that the amplitude has increased from 0.95 ± 0.05 magnitudes in April and May to 1.10 ± 0.05 magnitudes in June. The expected minimum near April 20 was missed because no observations were obtained in the in the interval April 14 – 27. The commonly encountered behavior of increased amplitude at larger phase angles holds also for 1744 Harriet.

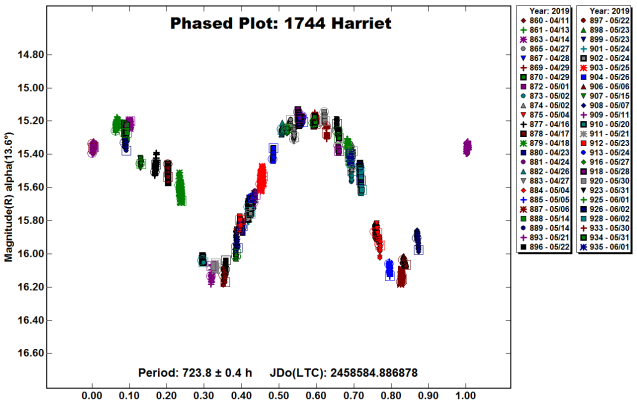

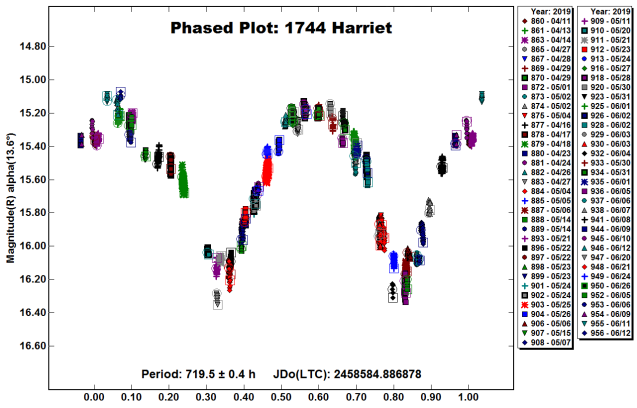

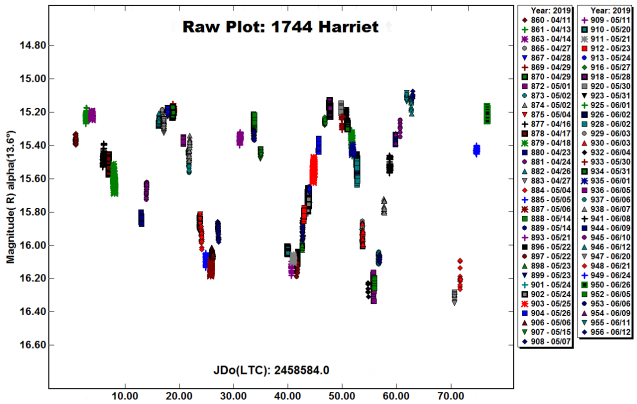

References

Harris, A.W., Young, J.W., Scaltriti, F., Zappala, V. (1984). "Lightcurves and phase relations of the asteroids 82 Alkmene and 444 Gyptis." *Icarus* **57**, 251-258.

Pravec, P.; Harris, A.W.; Scheirich, P.; Kusnirak, P.; Sarounova, L.; Hergenrother, C.W.; Mottola, S.; Hicks, M.D.; Masi, G.; Krugly, Yu.N.; Shevchenko, V.G.; Nolan, M.C.; Howell, E.S.; Kaasalainen, M.; Galad, A.; Brown, P.; DeGraff, D.R.; Lambert, J.V.; Cooney, W.R. Jr.; Foglia, S. (2005). "Tumbling Asteroids." *Icarus* **173**, 108-131.

Warner, B.D.; Harris, A.W.; Pravec, P. (2009). "The Asteroid Lightcurve Database." *Icarus* **202**, 134-146. Updated 2019 January. *http://www.minorplanet.info/lightcurvedatabase.html*

Acknowledgments

The authors thank P. Pravec for an independent analysis of the data. The Etscorn Campus Observatory operations are supported by the Research and Economic Development Office of New Mexico Institute of Mining and Engineering.

STAFF POSITION OPENING - ASSOCIATE PRODUCER, *MINOR PLANET BULLETIN*

The *Minor Planet Bulletin* announces the opening of a new staff position of Associate Producer, with the probability of taking over the *MPB* Producer's position in late 2020 following a period of mentoring and collaboration. The current Producer, Bob Werner, wishes to retire then after a 35-year run. The responsibilities will be to assist Werner with the layout construction of each quarterly issue of the *Minor Planet Bulletin*.

Producing an MPB issue requires the following:

- Reformatting approximately 30–40 manuscript documents from the editors.
- Responsive communication with the editorial and distribution staff.
- Able to commit to and adhere to deadlines throughout the calendar year.
- Corresponding with authors via email with article proofs.
- Handling formatting inquiries from new and seasoned authors who contribute manuscripts to the *MPB*.
- Laying out an issue's articles in a single master document, resulting in the ready-to-print and ready-to-release electronic version of each *MPB* issue.
- Constructing a full index of each annual volume.
- Maintaining a long-term electronic archive of all issues.

The skills required include:

- Proficiency with Microsoft Word 2013/2010, Portable Document Format (pdf) computer documents, and email. Production status is tracked using Excel.
- Knowledgeable expertise with asteroid astronomy sufficient for some error checking and recommending editorial corrections.
- Strong skills with written English.

The time commitment required varies from issue to issue, but typically occupies 25 or 30 hours each quarter, mostly in the month preceding an issue's release, February, May, August, and November. All *MPB* staff positions, including this announced opening for Associate Producer, are volunteer positions without pay or other compensation. Materials and postage costs, as necessary, are reimbursed.

Anyone interested in the Associate Producer position should send a cover letter with a statement on the level of available commitment and a summary of qualifications to the Editor: rpb@mit.edu The position will remain open until filled.

LOWELL OBSERVATORY NEAR-EARTH ASTEROID PHOTOMETRIC SURVEY (NEAPS): PAPER 4.

Brian A. Skiff
Lowell Observatory
1400 West Mars Hill Road
Flagstaff AZ 86001 USA
bas@lowell.edu

Kyle P. McLelland
Northern Arizona University
(now at Linn-Benton College, Oregon)

Jason J. Sanborn
Lowell Observatory
Discovery Channel Telescope

Petr Pravec
Academy of Sciences of Czech Republic
Astronomical Institute Ondřejov, Czech Republic

Bruce W. Koehn
Edward Bowell
Lowell Observatory (retired)

(Received: 2019 July 14)

Revised photometry and lightcurves are reported for 144 asteroids from the NEAPS project and later work at Lowell Observatory. This completes revision of objects from Paper 1 and 2 and adds previously unpublished data acquired between 2008 and 2019. In several cases we provide lightcurves over several lunations within an apparition and also at multiple apparitions with different phase-angle bisectors.

In a recent report Skiff et al. (2019, Paper 3) began revising the photometry and lightcurve analysis of mostly near-Earth asteroids obtained at Lowell Observatory starting in 2008. Much of the data were originally published in two earlier papers in this journal (Skiff et al. 2012, Paper 1; Koehn et al. 2014, Paper 2). The present publication completes work on the 86 asteroids appearing in Papers 1 and 2. This places the data more consistently on the Sloan r′ system in hopes of fulfilling the "photometric" element of the project acronym. In many cases revision of the comparison star photometry allowed us to rescue previously abandoned datasets, improve the precision of rotation periods, and to find rotation periods where we were not able to extract them previously. Hitherto unpublished results are added from observations taken between 2008 and 2019.

The telescopes involved in the present work are the same as before. These include the 0.55-m *f*/1.9 LONEOS Schmidt, the 0.7-m robotic, Hall 1.1-m, and Perkins 1.8-m reflectors; these are described in detail in Paper 1 and Paper 3. All are located at Lowell Observatory's Anderson Mesa Station (latitude +35.1°) outside Flagstaff, Arizona, at 2200 m elevation, and assigned MPC observatory codes 699 (LONEOS) and 688 (other telescopes). The LONEOS Schmidt was operated unfiltered with a CCD having strong far-red sensitivity. Images with the other telescopes were taken mostly with an R_c or a 'VR' filter that is similar to Sloan r′. All the photometry has been reduced to the extent possible to the standard Sloan r′ system.

We mention that for data taken using the 0.7-m and 1.1-m telescopes, it was usual to start observations in the evening with Sun altitude only –10° if exposures were less than about 90 seconds, and to continue them similarly late into morning twilight. We observed continuously through the Full Moon period apart from avoiding pointing near the Moon itself. Thanks to the high altitude, we also conducted observations to airmass sec z ~3.0 toward the eastern and western horizons, or higher for far-southern targets (within ~1 hour of the meridian as far south as –40° Dec). These procedures extend the observing windows significantly. Several targets presented in this paper show that data quality in such cases is not seriously compromised.

Further to the discussion in Paper 3 with regards photometry catalogues, we note that median per-star external errors in the Pan-STARRS catalogue are 0.014 mag for Sloan r′ (Magnier et al. 2019, specifically text section 6.4 and Figure 2). The SkyMapper DR1 southern survey (Wolf et al. 2018) inherits zonal errors from APASS DR9 (cf. Tonry et al. 2018), but these should be removed in later versions. SkyMapper external errors per star are roughly 0.02–0.03 mag. These figures thus set lower limits on the external zero-point errors in our data, even if internal errors are better. We also make much implicit use of the GAIA2 'G' magnitudes in this report. These are different than in GAIA1, specifically about 0.03 mag *fainter* than Pan-STARRS Sloan r′ for stars of intermediate 'asteroidal' color. The GAIA2 internal photometric precision is very high, at the few-millimag level. Their main use has been to control the lower-quality CMC15 and APASS Sloan r′ magnitudes when comparison stars are brighter than the Pan-STARRS saturation limit.

Careful use of even the new catalogues remains necessary due to resolved, unresolved, or poorly resolved binaries (compared to our relatively low resolution images), regions with few observations, cloudy night data included in the mix, and various other issues. Even GAIA2 has weird (wrong) stuff in it. The datasets are not perfectly clean!

985 Rosina. Two nights of photometry on this Mars-crosser were obtained in 2019 May using the 0.7-m telescope. The phase-angle bisector (PAB) longitudes were offset about 90° from previous observations (Behrend 2002web; Bernasconi data). The lightcurve morphology, however, is not dramatically different. The RMS scatter on the fit is 0.014 mag.

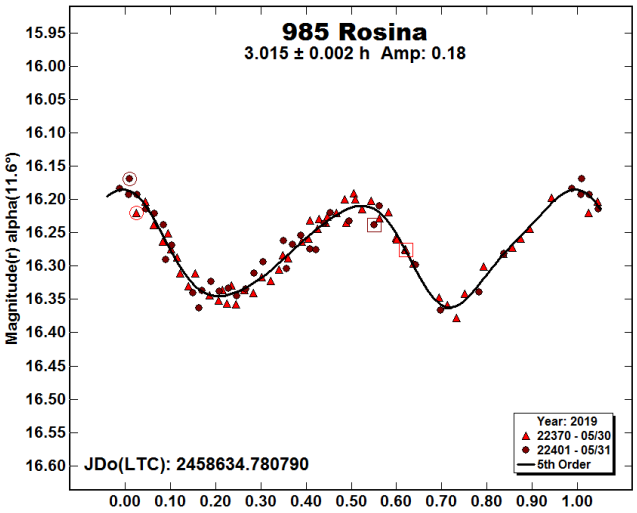

1090 Sumida. Wisniewski (1991) obtained the first photometry of this Phocaea; his single-night run shows a double-mode lightcurve of the approximately correct period. We obtained two nights of data near Full Moon in 2019 Jun using the 1.1-m telescope and 'VR' filter. The PAB longitude was similar to the circumstances of 2012 data by Warner and Megna (2012). Our triple-mode lightcurve shows the morphology much more clearly thanks to RMS scatter of 0.010 mag, compared to ~0.05 mag for theirs. The high-precision observations requested there are herewith fulfilled.

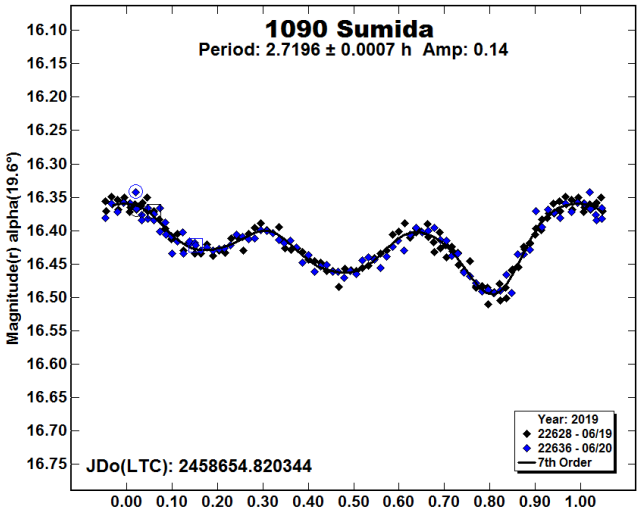

1293 Sonja. This Mars-crosser has been well-observed since Higgins et al. (2007) first determined the rotation period. We obtained three nights in 2019 Apr using the 0.7-m telescope when the object was in the southern sky at previously unobserved PABs. The resulting lightcurve has morphology somewhat different from the earlier ones and should help with shape-modeling. The RMS scatter on the fitted lightcurve is 0.021 mag.

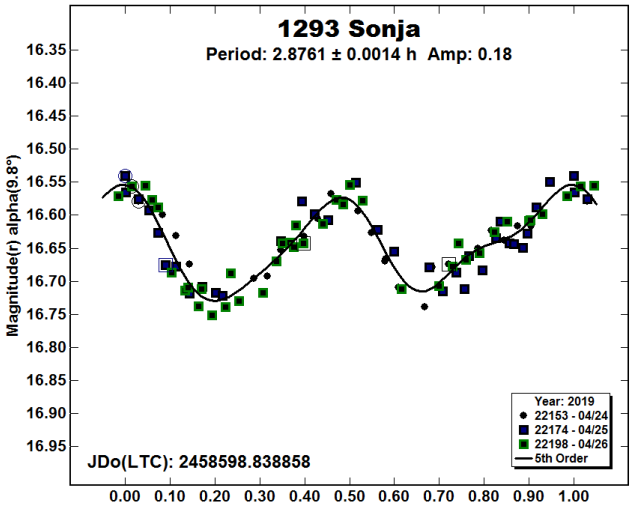

1387 Kama. The relatively long period of this main-belt asteroid prevented us from getting complete rotational phase coverage within the three nights devoted to the object in 2010 Dec. We show a force-fit of 0.7-m telescope data to the period of Pravec (2013web). The RMS scatter on the fit is 0.021 mag.

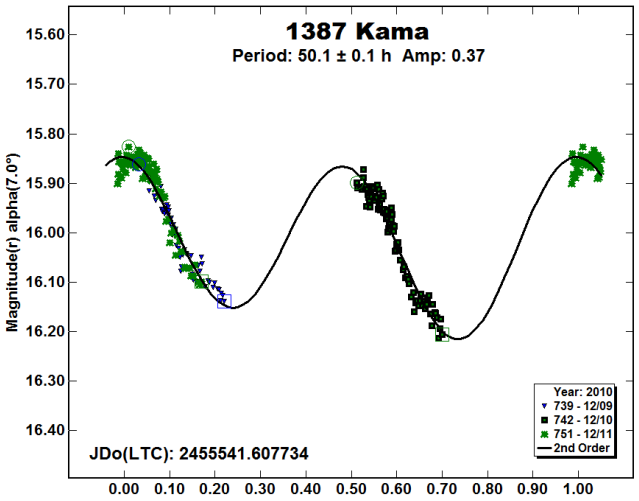

1468 Zomba. As with 1293 Sonja, we took the opportunity to follow this Mars-crosser in 2019 Apr at previously unobserved PABs when the asteroid was at southern Declinations. The rotation period agrees with several previous determinations. The two nights of 3-minute exposures using the 0.7-m telescope gave RMS scatter of 0.019 mag.

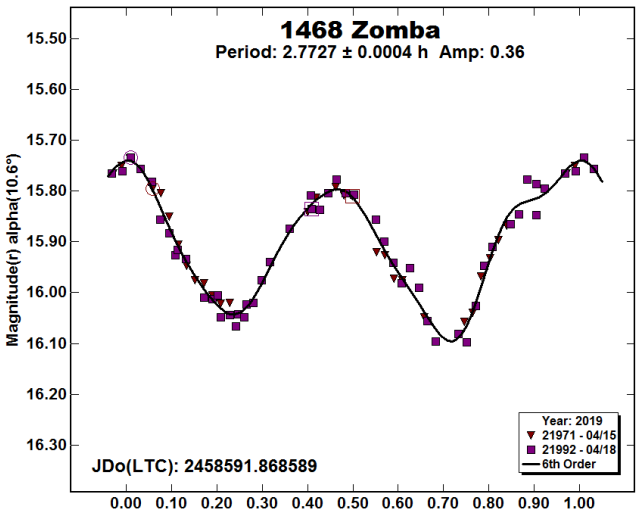

1865 Cerberus. Our sixteen nights on this Apollo can be divided into three groups, though in Paper 1 we showed only a composite lightcurve. The period has been known since the 1980 lightcurve of Harris and Young (1989), which also revealed the extreme amplitude. Our data were obtained in 2008 Oct-Nov using the LONEOS Schmidt with 3-minute exposures. The sharp minima were down near mag 18, so the RMS scatter on the three fits is 0.05, 0.07, and 0.07 mag, respectively, which is poor by our standards, though not obvious here due to the very large amplitudes.

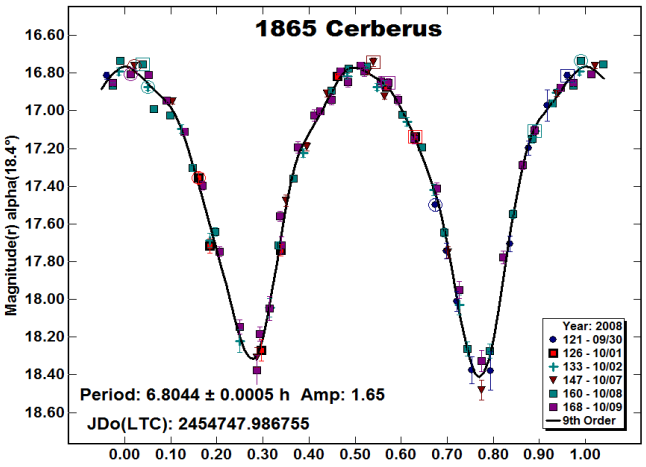

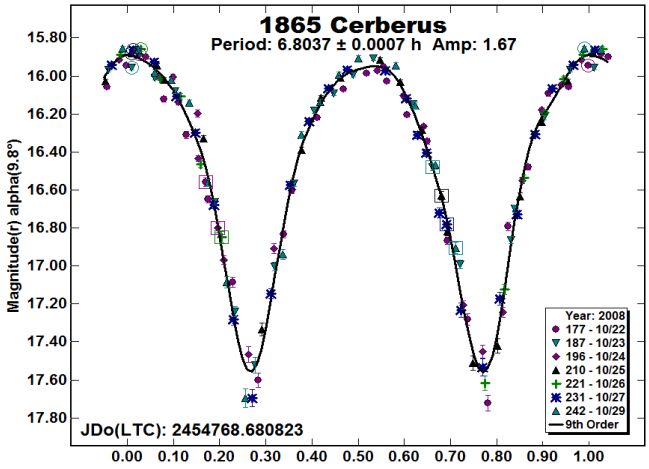

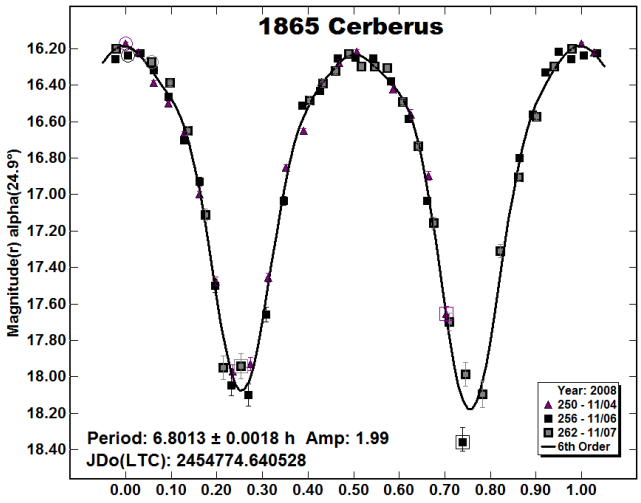

1943 Anteros. We presented uncertain results for this Amor in Paper 2. Fixing the comparison stars improves things marginally. We show a phased lightcurve from four of five nights of Schmidt data; the final night, 2009 Aug 10, is isolated in time and of poor quality. Using 54 images of mostly 90 seconds exposure, we find a minimum in the period spectrum at the 2.87-hour period first defined by Pravec et al. (1998a), which we round here to 0.01-h precision. The RMS scatter is 0.034 mag, about 25% of the full amplitude. The lightcurve morphology is very similar to those presented by Pravec et al., and more recently by Warner et al. (2017) and Warner and Stephens (2019b), where two different binary solutions are offered.

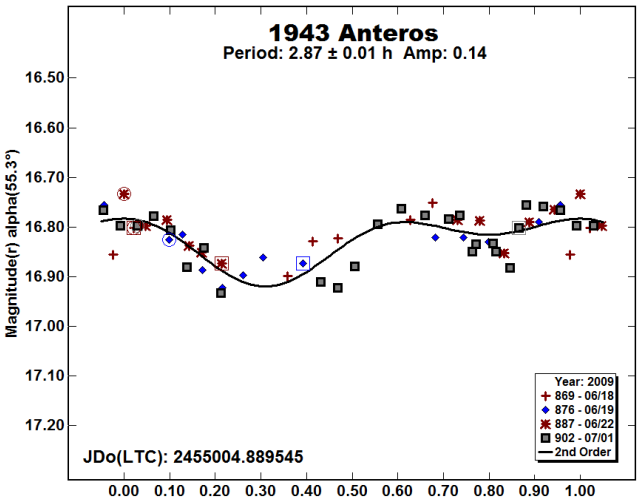

2212 Hephaistos. Despite getting continuous 6- to 7-hour runs over four consecutive 'photometric' (cloud-free) nights using the Schmidt in 2010 Sep, we found no indication of a reliable rotation period for this high-eccentricity Apollo. A total of 1650 30-second exposures were obtained. There seem to be small bumps and wiggles during each night, but these do not repeat in a cyclic manner. We show a raw plot from the first night, which is representative in exhibiting small oscillations, possibly superposed on a longer second period of several tens of hours.

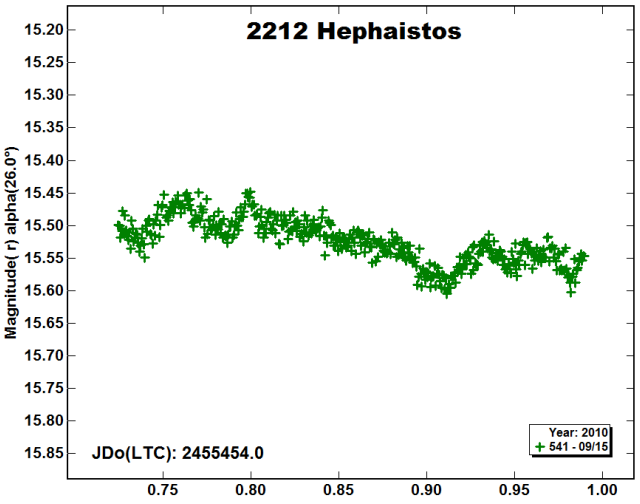

2281 Biela. Two nights of data on this main-belt asteroid using the 0.7-m telescope in 2010 Dec showed only that the 4.9-hour period reported from sparse PTF survey data (Waszczak et al., 2015) is far too short. The correct period is likely to be some tens of hours and with small amplitude. Our notional fit is indicative only (N.B. the very large uncertainty).

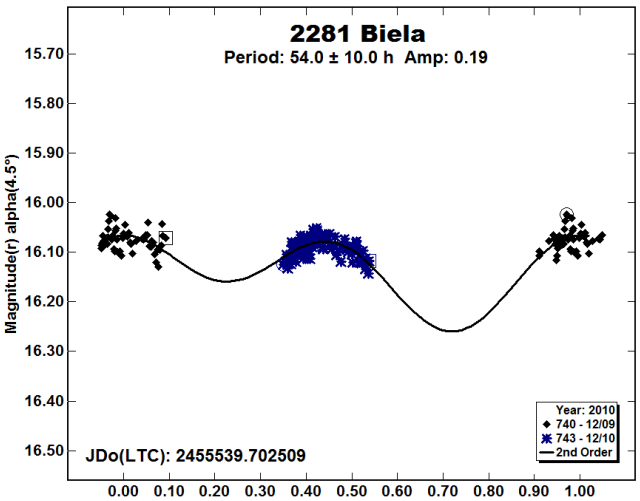

2525 O'Steen. This outer main-belt Themis-family asteroid was found on Lowell 'Pluto Camera' 33-cm astrograph plates in 1981. It was the first asteroid discovered by Skiff to be numbered. Three previous period determinations gave discrepant results. We obtained two nights of photometry early in the 2019 apparition using the 0.7-m telescope. The triple-mode lightcurve confirms the period found by Apolstolovska et al. (2004) and by Aznar Macías (2014web), and suggests the rough data (~0.1 mag scatter) reported by Clark (2006) is a 3:2 alias of the true period. Our data were taken at fresh PAB values, so they should also contribute to shape-modelling. The RMS scatter is 0.012 mag.

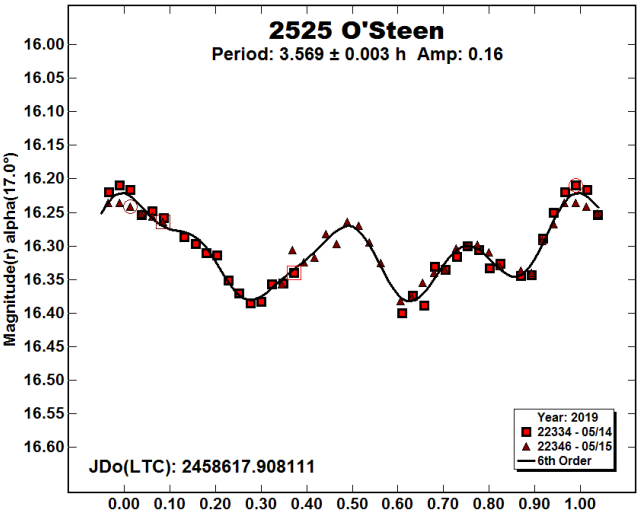

2585 Irpedina. All we can say about this main-belt object from two nights of data is that the period is long and possibly of substantial amplitude. These data were taken in 2010 Dec using the 0.7-m telescope. A raw plot covering about 30 hours is suggestive of the much longer trend.

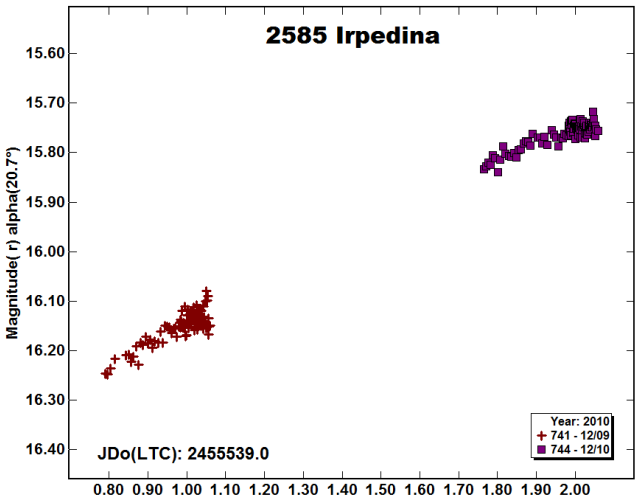

2629 Rudra. Three successive nights on this Mars-crosser using the 0.7-m telescope in 2010 Oct covered less than half the likely long rotation period near 123 hours reported by Waszczak et al. (2015). We offer here simply a raw plot of the data, which shows roughly two maxima and an intervening minimum over the 50-hour observation interval. The asteroid was too faint for the 60-second R_c filter exposures that were adopted, so the per-point scatter is large.

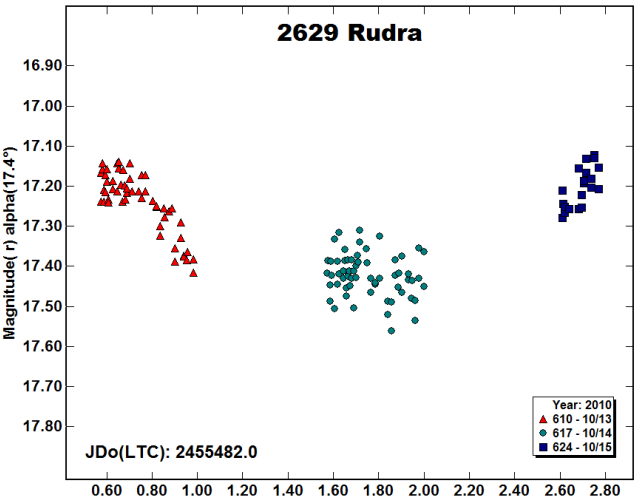

2744 Birgitta. Using photographic plates on the 1-m Kvistaberg Schmidt, Claes-Ingvar Lagerkvist (1976) both discovered and did immediate lightcurve follow-up on this Mars-crossing asteroid in 1975 Sep. We obtained long runs on two consecutive nights using the 0.7-m telescope in 2010 Oct. Each night produced a clean lightcurve with nearly complete rotational phase coverage, so the period is secure. The RMS scatter on the fit is 0.017 mag.

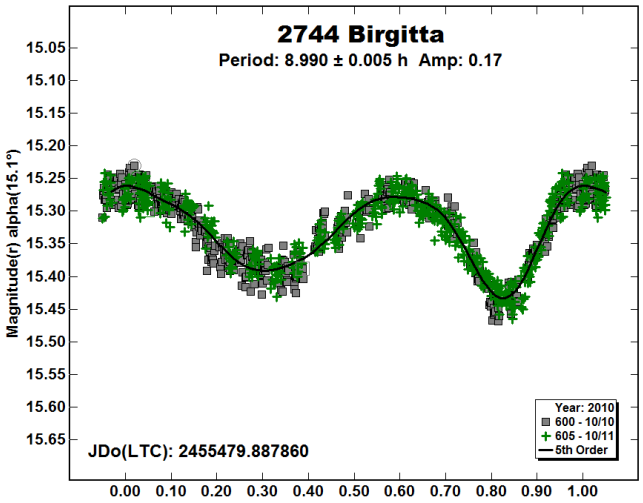

3040 Kozai. This Mars-crosser was observed by Pravec and Pray (Pravec 2019web), by Stephens and Warner (2019), and by Polakis (2019) in the same apparition as our observations. We got four nights subsequent to all these in 2019 Mar using both the 0.7-m and 1.1-m telescopes. The various rotation periods determined are identical within errors. The shapes and depths of the lightcurve minima shift noticeably in a matter of days among the three datasets having internal good precision. The RMS scatter on our fitted curve is 0.014 mag.

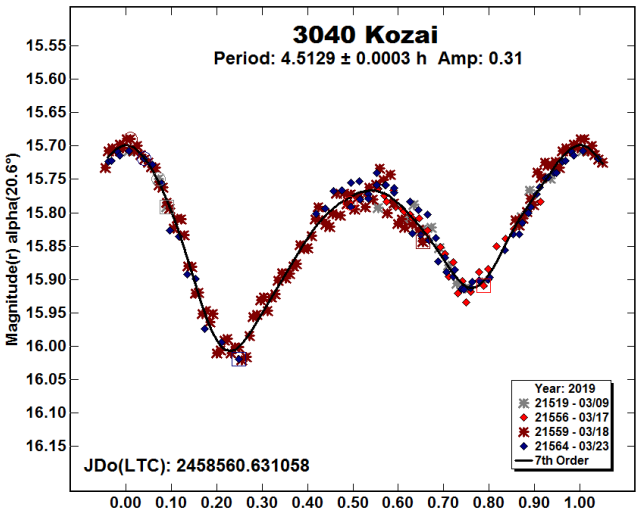

3073 Kursk. Smooth lightcurve traces with small internal errors on four consecutive 'photometric' nights 2008 Apr 12-15 using the 1.1-m telescope are each somewhat different. This confirms the binary nature of this main-belt Flora-family asteroid first reported by Kušnirák et al. (2007). The data are insufficient in themselves to resolve the two periods, however, so we show only a mean fit to the shorter period, which highlights the non-repeating nature of the nightly variations.

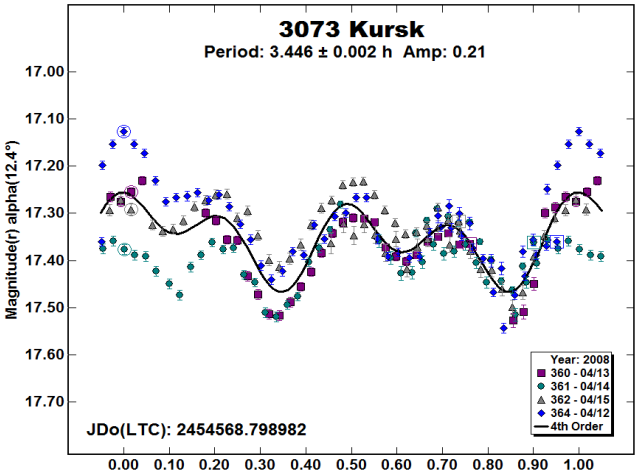

3086 Kalbaugh. This Hungaria was found on photographic plates taken in the 1980s with the Lowell 'Pluto Camera' astrograph. The lightcurve has been well observed starting with Warner (2005). An opportunity arose in 2019 Mar to get another series while it was as far south as –30° Dec and at previously unobserved PAB values. Thus the purpose was not to improve the period determination, but to provide data with fresh viewing geometry to aid in shape modelling. Two nights of 0.7-m data were obtained; the resulting lightcurve exhibits the largest amplitude yet observed for this object. The RMS scatter on the order-13 fit is 0.017 mag.

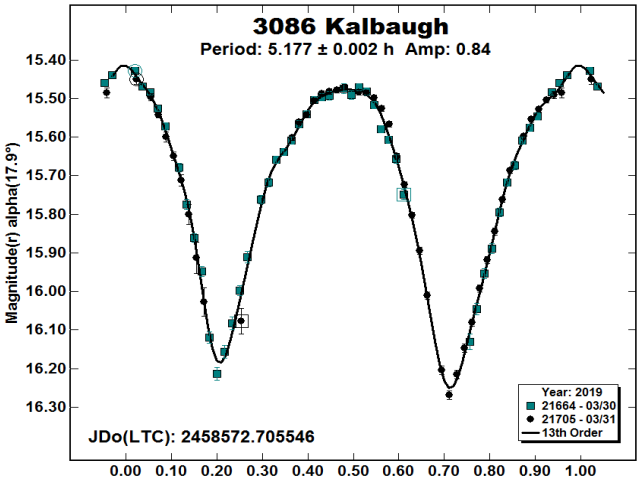

3552 Don Quixote. This Amor has an unusual, comet-like orbit, and is known to be active near perihelion. Detection of gas (likely CO or CO^+) was made in the thermal-IR using Spitzer Space Telescope in 2009 Aug, and a dust tail was visible in 2018 Mar (Mommert et al., 2014; 2018). We obtained data as early as 2009 Nov using the LONEOS Schmidt, and again in 2018 Aug-Sep with the 0.7-m telescope. We did not see activity directly, but it was likely to be present since the object was not far from perihelion in both instances.

In order to fit the photometry without large systematic zero-point offsets trending with date, the phase-function coefficient *G* was changed to –0.1 for the 2009 data and –0.3 for the 2018 data. The first value is not atypical for a dark D-type asteroid like this, but the effect of scattered light from some amount of translucent dusty coma is unknown. The *G* parameter itself is probably an inappropriate physical description in this circumstance, so the adjustment is an arbitrary 'fudge factor'.

The lightcurves are shown at the same vertical scale to highlight the difference in amplitude. The RMS scatter on the 2009 lightcurve fit is 0.040 mag; for the 2018 data it is 0.033 mag. The morphology of the two lightcurves is distinct and different again from those presented by Warner and Stephens (2019a) and by Benishek (2019a), who both observed the asteroid only a few weeks prior to our 2018 series. There was much additional data obtained by the planetary-science community during the 2018 apparition, so a shape-model and other results will be forthcoming.

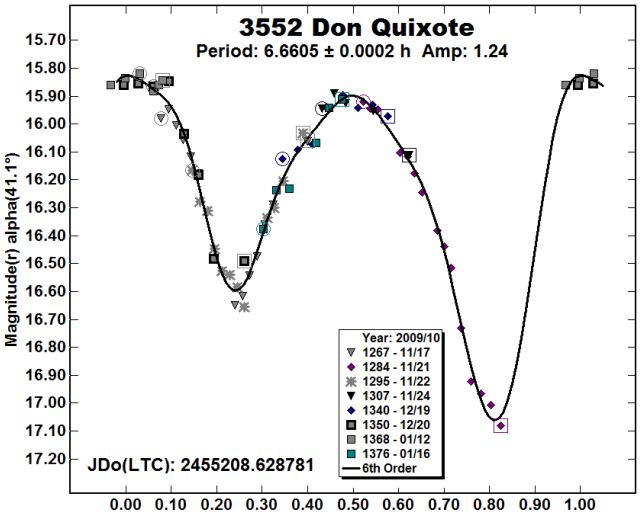

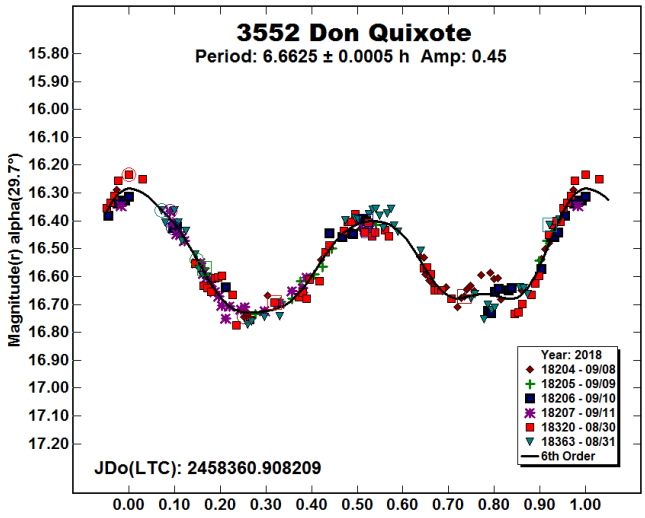

3554 Amun. Wisniewski et al. (1997) obtained the first lightcurve of this Aten-type asteroid in 1987, determining the correct period from three nights of data. In Paper 2 we showed a composite lightcurve spanning two calendar *years*, which fit together surprisingly well. The two apparitions are parsed out below. The 2009 data were taken with the LONEOS Schmidt using exposures between 2 and 3 minutes. The RMS scatter on the fitted curve is 0.020 mag. The dense series in 2011 was done using the Schmidt on the first night (30-second exposures) followed by two more nights with the 0.7-m telescope (90-second exposures). The second phased plot has these data averaged by pairs (392 points). The RMS scatter here is 0.015 mag. A single short night of observation was taken on an intervening date. We include these few data in the ALCDEF dataset for the sake of completeness, but make no further use of them.

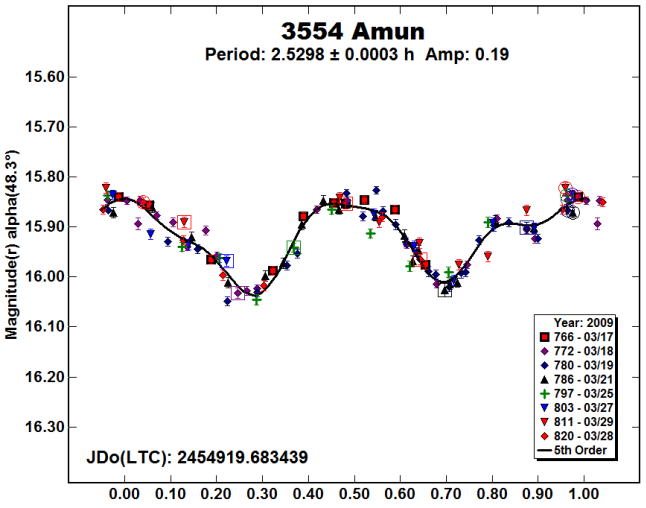

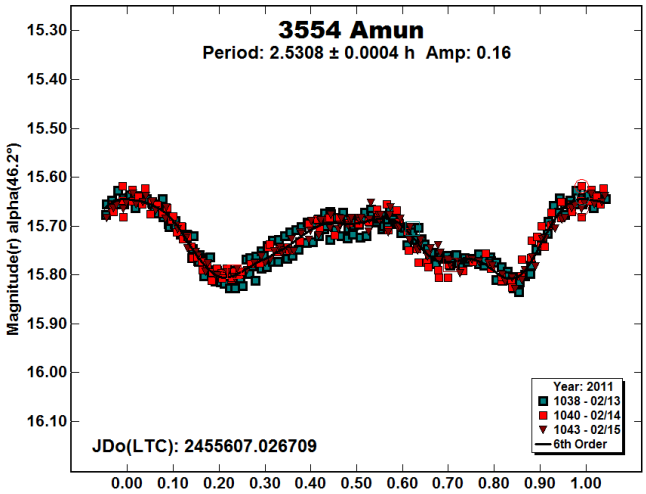

3671 Dionysus. We obtained two nights on this binary Apollo using 3-minute exposures with the LONEOS Schmidt in 2010 Apr. The asteroid was fairly faint, and so the results are poor. We show the data force-fit to the period of Pravec et al. (2006); the RMS scatter is 0.034 mag.

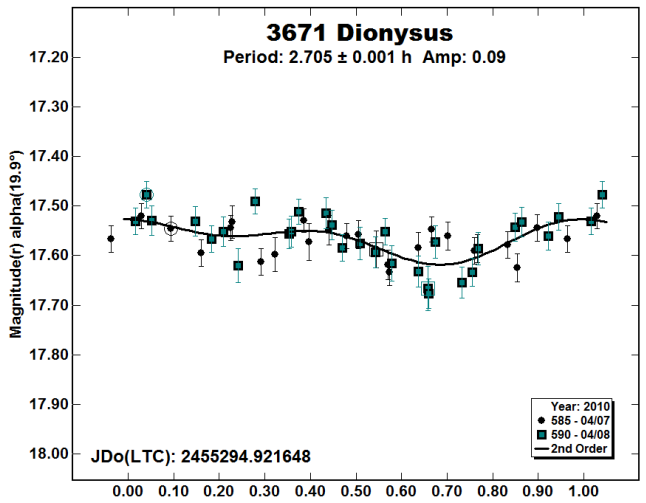

3672 Stevedberg. Ken Menzies (2011web) obtained the first lightcurve of this main-belt Flora, which is another Lowell 'Pluto Camera' discovery. Four nights of sparse data taken with the 0.7-m telescope in 2014 Aug-Sep confirms his rotation period at distinct phase-angle bisectors. The RMS scatter on the fitted curve is 0.023 mag.

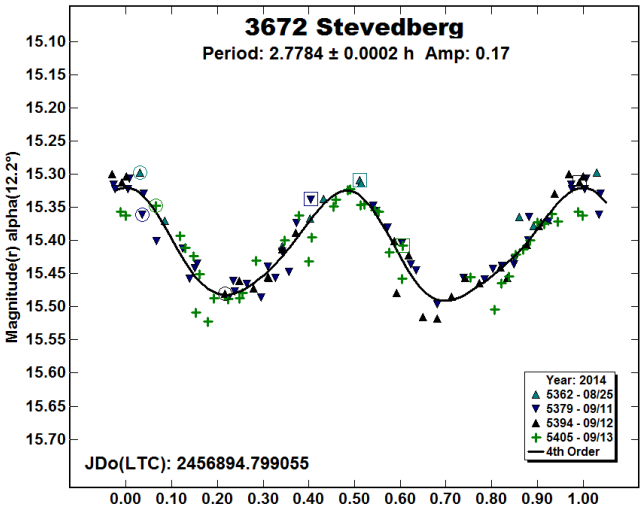

3838 Epona. There are no formally published lightcurves for this Apollo, but both we and Pravec (1999web) have made results available on the Web. We observed it for only about 4½ hours on one night in 2010 Nov using the Schmidt. This was sufficient to show the small-amplitude, short rotation period. Within the large uncertainty of the short run, the period matches the better determinations by Pravec. The phased plot shows the 298 original 30-second exposures averaged by pairs. The RMS scatter on the fit is 0.013 mag.

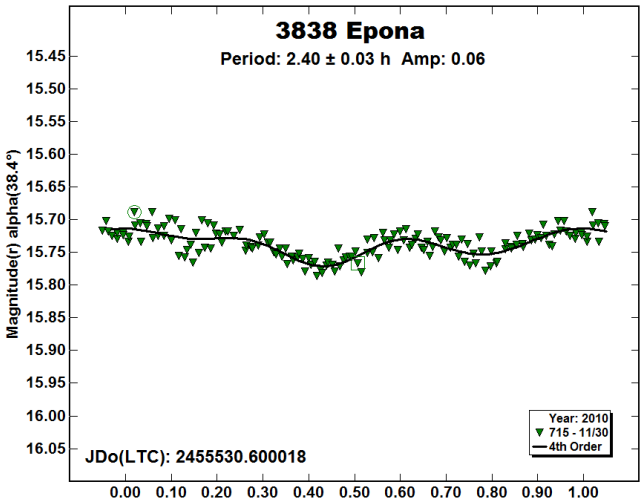

3875 Staehle. A previously unobserved main-belt Flora asteroid, this object was observed on eight nights using the 0.7-m telescope in 2011 Apr-May. The large-amplitude lightcurve has a moderately-long period, so rotational phase coverage is incomplete. Since only one extremum was properly witnessed, there remains some uncertainty on the period, which could differ by several tenths of an hour from what's shown. The RMS scatter on the fit is 0.041 mag.

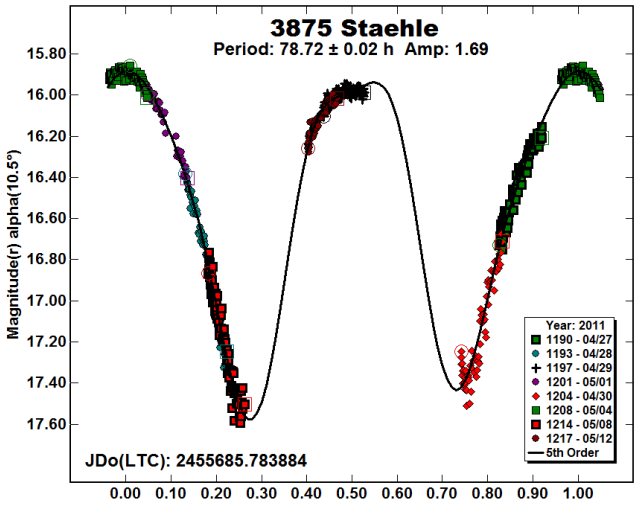

4179 Toutatis. As outlined in Paper 1, we obtained nearly 700 useful measurements over 29 nights with the Schmidt for this tumbling Apollo in late 2008 and early 2009. To give a summary of our coverage by date, a raw plot is shown without H,G correction of the magnitudes, now all fairly close to Sloan r′. The data are insufficient for an independent determination of the two tumbling periods, but might have other uses. Spencer et al. (1996) presented analysis of early results for this asteroid.

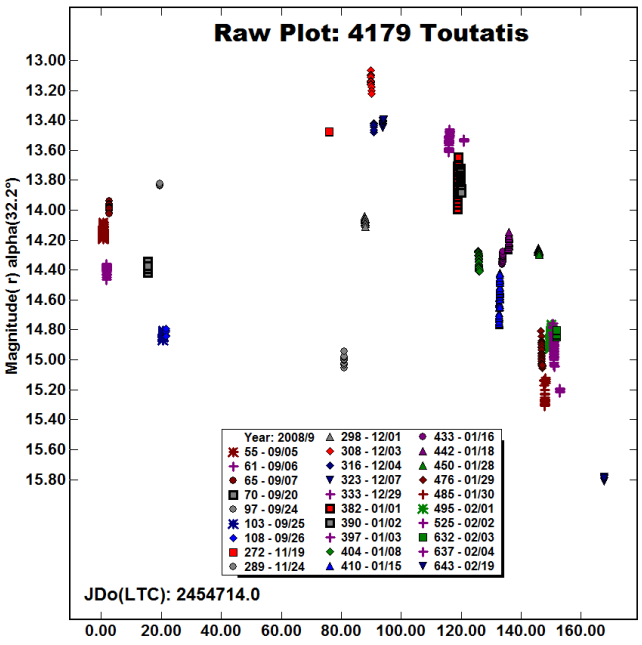

4205 David Hughes. This Mars-crosser is a Lowell 'Pluto Camera' discovery. Three widely separated nights of photometry gave only a hint that the lightcurve has large amplitude and the period is very long. A raw plot (including H,G correction) is shown below. The first night is 0.7-m data, while the two 2011 Jan nights are from the LONEOS Schmidt.

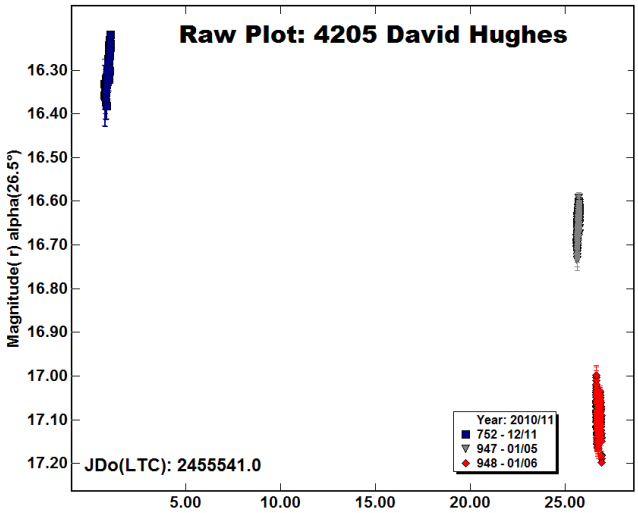

4894 Ask. Raoul Behrend (2015web) used data obtained by René Roy to determine a provisional period of 3.78 h for this main-belt Flora. Our two-night run in 2011 Apr using the 0.7-m telescope yields a somewhat shorter period. Although the data are a bit noisy, multiple cycles were covered each night. The RMS scatter on the lightcurve fit is 0.030 mag.

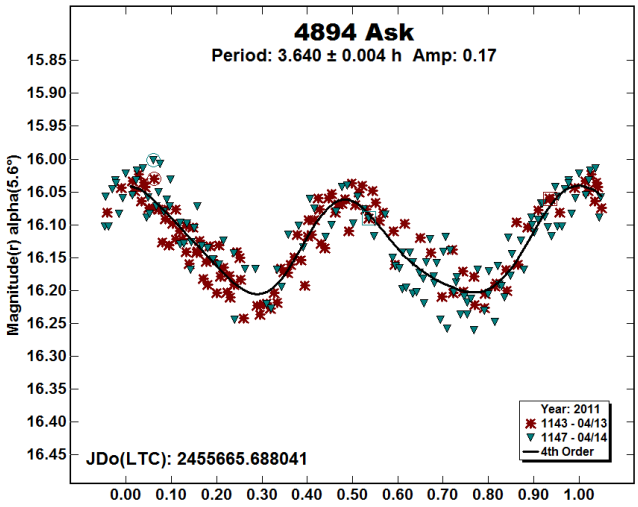

5011 Ptah. In Paper 2 we described our 2009 Apr LONEOS Schmidt observations of this Apollo. Revision of the comparison star photometry permits a notional fit to the period, as shown below. No, we don't believe it either. Even ignoring the unconstrained minimum, the amplitude is nearly two magnitudes at this fairly high phase-angle.

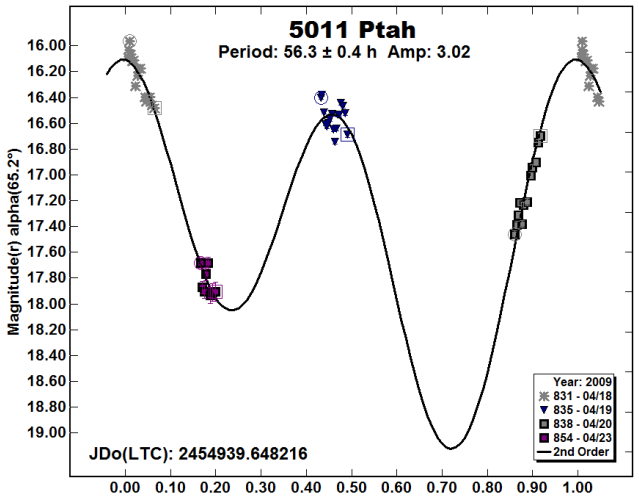

5253 Fredclifford. Brian Warner (2014) correctly chastised us for posting a rotation period for this Mars-crosser based on a single night of rather poor data. Those were taken under an 88%-illuminated waxing Moon with the unfiltered *f*/1.9 LONEOS Schmidt, so the sky background was very bright. A few weeks later (2010 Dec) we used the same instrument to get two nights with no Moonlight when the asteroid was almost twice as bright, yielding much smaller internal errors.

We show the two phased lightcurves at the same scale. In an effort to reduce the noise, the first has the 30-second exposures averaged into three-image 3-minute bins and the period force-fit; the second is a normal fit to all the data. The RMS scatter on the first is 0.029 mag, while for the second it is 0.014 mag. The morphology of the lightcurves is broadly similar, though the amplitude in the second plot is less than half that of the first.

5261 Eureka. Not long after its discovery by Hank Holt and David Levy, this asteroid was recognized as the first Mars Trojan by Ted Bowell (Marsden, 1990). Rivkin et al. (2003) obtained the first spectra and portions of a lightcurve, but found the nightly segments did not match up, possibly due to the then-unrecognized binary. Our more extensive photometric series began in late 2011, capturing several mutual events that allowed the system to be solved. Observations were taken over twelve nights with the LONEOS Schmidt, and the 0.7-m and 1.1-m telescopes. All the data have now been adjusted more closely to the Sloan r′ system.

Petr Pravec provided the binary orbital solution for Paper 2. We do not repeat his phased lightcurves, but show raw plots from successive nights on the 0.7-m telescope of the two sorts of mutual events manifest during that apparition: one sharp, the other flat-bottomed and a little shallower. The RMS scatter on the complete solution was 0.020 mag for data from the two larger telescopes; the Schmidt data were much less good. The LCDB indicates there is no additional lightcurve photometry, surely overdue in this case.

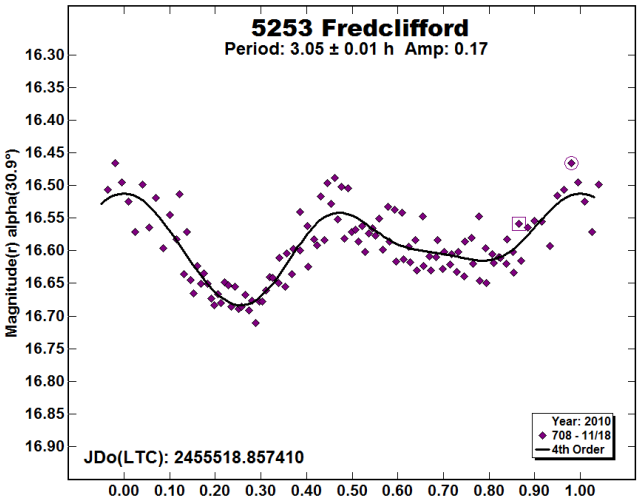

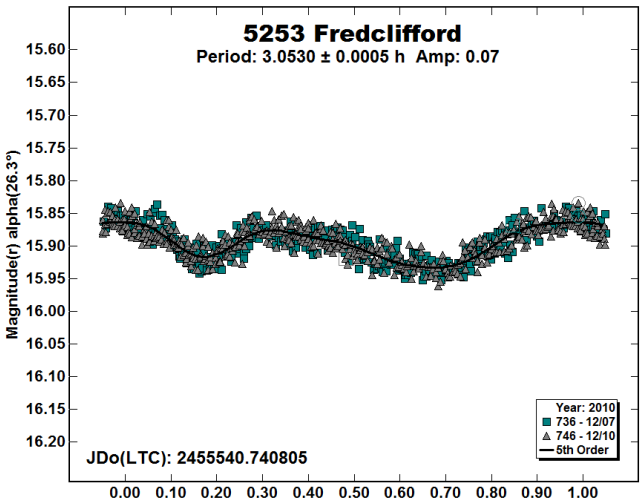

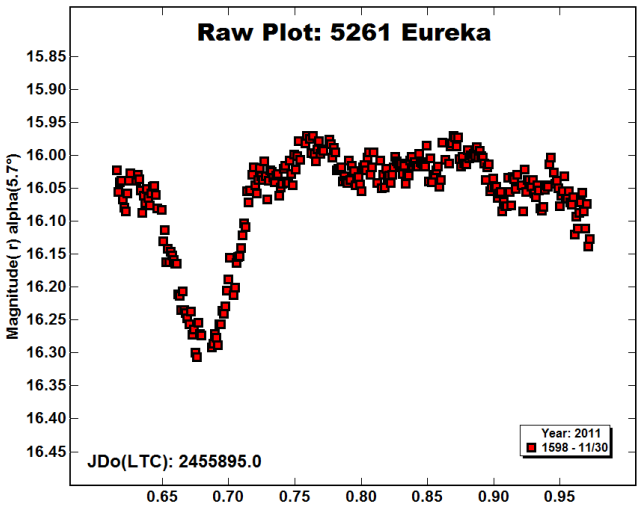

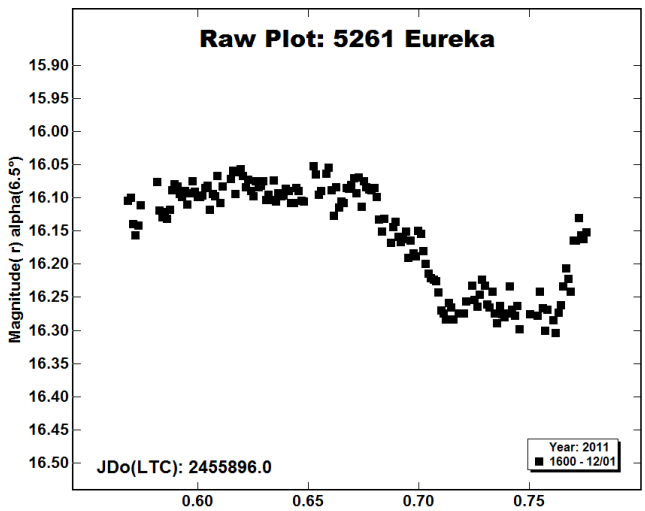

5404 Uemura. This inner main-belt object is one of two exemplar asteroids in the much-cited paper by Harris et al. (2014) dealing with the maximum allowable amplitudes of harmonics in asteroid lightcurves. In private discussions leading up to this, Adrián Galád suspected the asteroid might be rotating faster than the spin-barrier limit. However, comprehensive analysis of his, ours, and other data assembled by Harris et al. showed that the complex lightcurve was best represented by a period near 3.45 h, which is *not* unusual. Our contribution was series at two different apparitions using the 0.7-m and 1.1-m telescopes as well as the LONEOS Schmidt. It is inappropriate to repeat those results, but we record here that our dataset is now adjusted closely to Sloan r′ and included in the ALCDEF files for the asteroid. The second asteroid discussed in Harris *et al*. is the small Apollo 2010 RC130, which is described below.

(5604) 1992 FE. This Aten was picked up on four nights in 2009 Mar-Apr using the Schmidt, but we obtained only sparse sampling. An approximate solution was offered in Paper 2. After adjustment of the comparison stars to Sloan r′, the data can be fit reasonably well to the period previously determined by Higgins and Warner (2009) from data taken during the same lunation we observed. We round-off the period-determination to 0.01 h due to the sparse coverage; the RMS scatter on the fit is 0.015 mag.

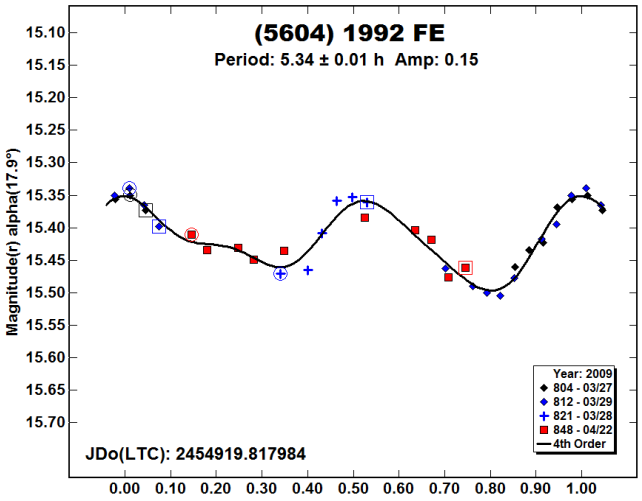

5620 Jasonwheeler. Some of these are easy! The large-amplitude lightcurve with comparison stars adjusted to Sloan r′ is essentially identical to what we showed in Paper 2. The derived period is close to that first published by Durkee (2010) from data taken one month after ours.

The RMS scatter on the fit, from Schmidt data on five of six consecutive nights using 48-second exposures, is 0.027 mag. The deeper, sharp minimum is not fully traced by the order-13 curve: a more accurate full amplitude is 1.22 ± 0.02 mag. The Amor asteroid has not been bright since the 2009 apparition, so there are no recent lightcurves.

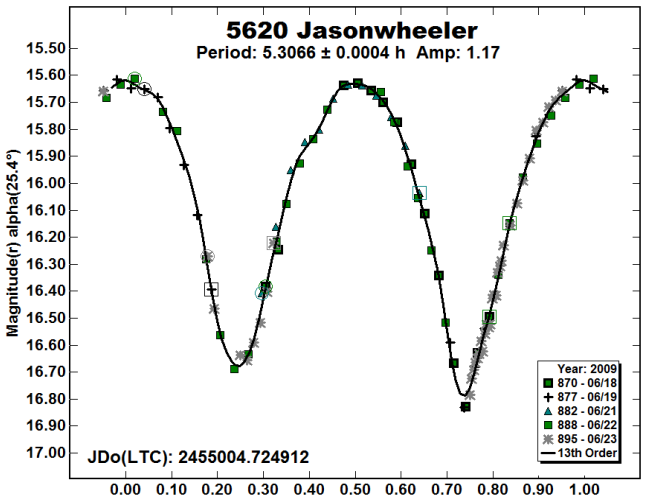

5869 Tanith. Four nights in 2010 Nov using the Schmidt on this Amor produced a complex quadrumodal lightcurve. Double- and triple-mode fits at shorter periods are unsatisfactory. Compare the similar lightcurves for asteroid (20446) 1999 JB80 in our Paper 3. Some low-level tumbling seems likely, but clearly more data will be required to resolve this. The phased lightcurve shows the original 1666 data-points (mostly 45-second exposures) averaged into three-image 5-minute bins. The RMS scatter on the fit is 0.018 mag.

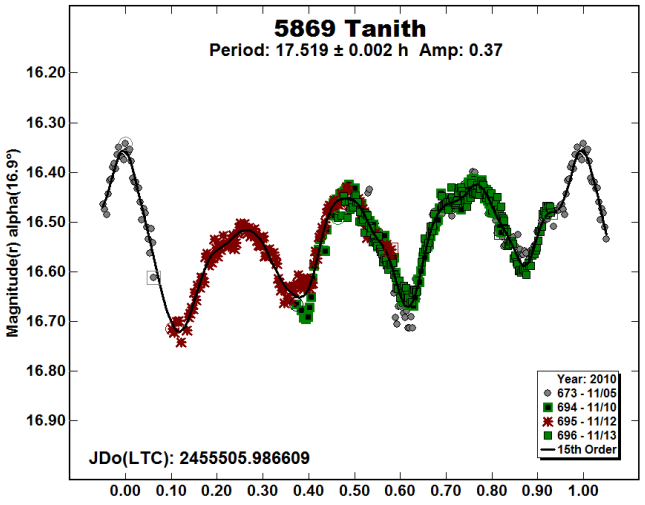

5945 Roachapproach. This main-belt Flora was discovered on Lowell 'Pluto Camera' plates, and is named for electronic 'ambient' musician Steve Roach. We acquired three useful series of photometry at well-separated phase-angle bisectors, as shown in the table of observing circumstances, so the lightcurve morphologies are also distinct. The first two apparitions were done with the 0.7-m telescope, all 3-minute exposures with an R_c filter. The 2019 Mar nights were 5-minute exposures with the 1.1-m telescope and 'VR' filter. The phased plots are shown at the same vertical scale. The RMS scatter for the 2014 run is 0.015 mag, while for the larger-amplitude 2017 lightcurve it is only 0.008 mag. The 2019 data, when the asteroid was two magnitudes fainter, have 0.014 mag scatter.

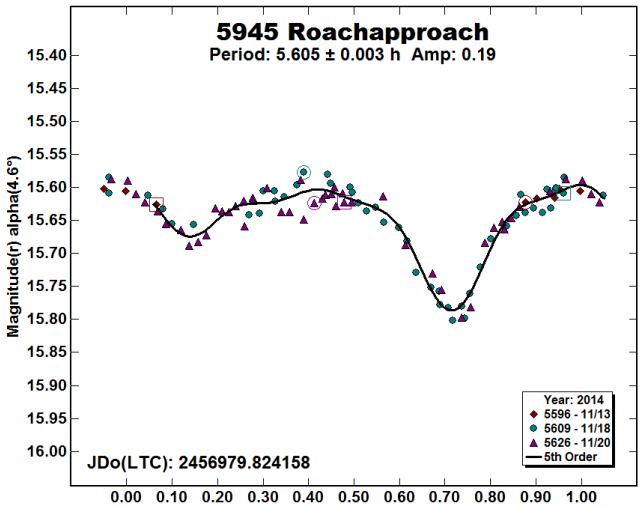

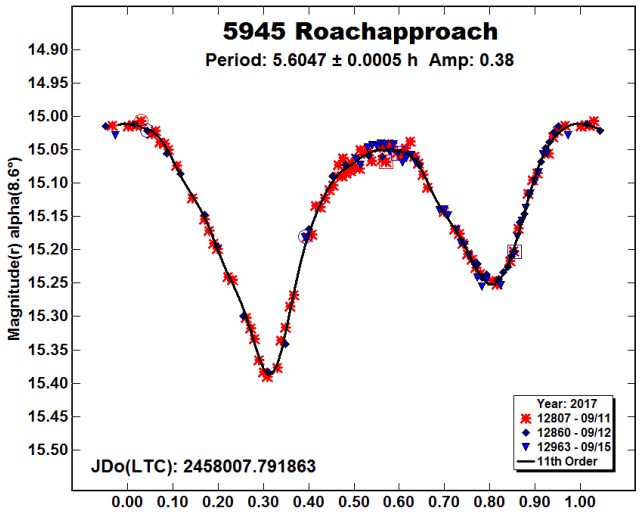

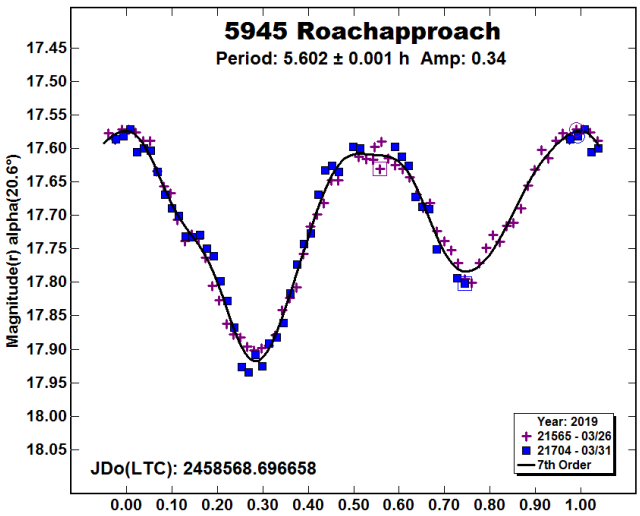

5999 Plescia. The lightcurve amplitude of this Mars-crosser varies strongly with phase angle. The period has been previously determined by Pravec (2011web) and by Warner (2018b). We obtained data in two successive lunations using the 0.7-m telescope. The two nights in 2011 Jan gave complete rotational phase coverage, and that period is used to force-fit the single night from the month before. The RMS scatter on the fits are 0.040 mag (2010 Dec, amplitude 0.98 mag) and 0.016 mag (2011 Jan).

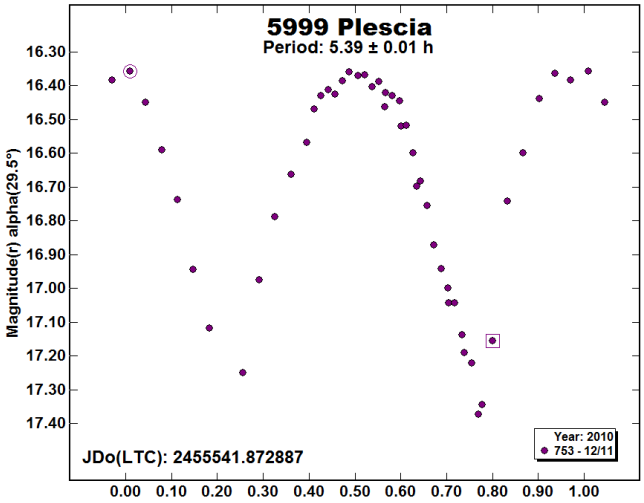

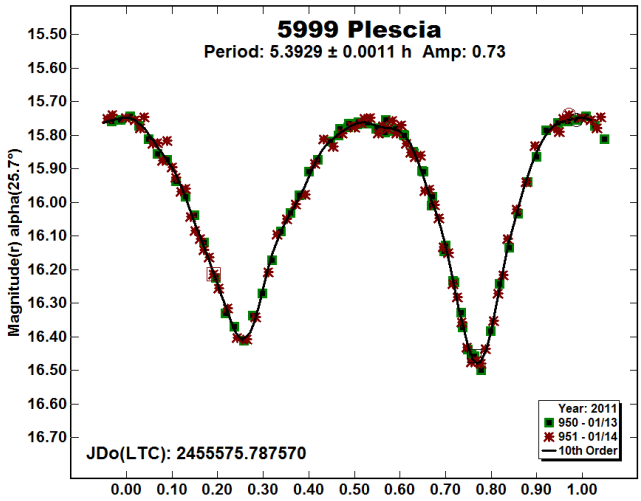

6012 Williammurdoch. This main-belt object was discovered in 1990 by Rob McNaught at Siding Spring. We observed it for several hours on two consecutive nights in 2011 using the 0.7-m telescope. The short-period, moderate-amplitude lightcurve is well-defined despite internal errors somewhat larger than we would prefer. The RMS scatter on the fit is 0.032 mag. These are the only lightcurve data published hitherto.

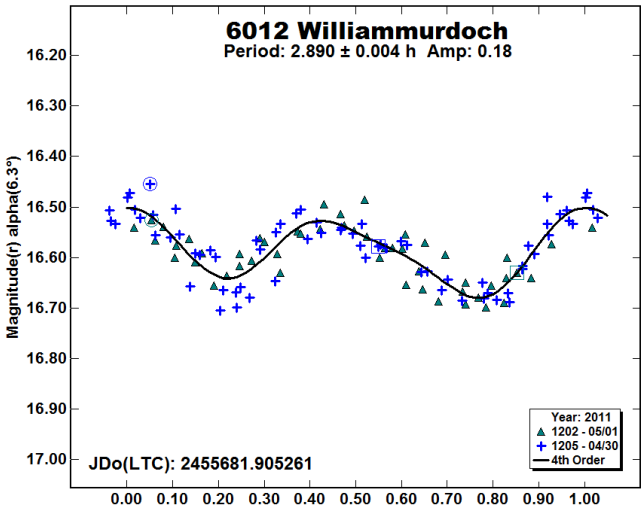

6239 Minos. This Apollo has been studied previously by Pravec (2004web) and by Warner (2016a), who observed small amplitude lightcurves with periods between 3.55 and 3.60 hours. We obtained only a single run just short of 8 hours on 2010 Sep 5 using 30-second exposures with the Schmidt. This yielded a quadrumodal lightcurve with a somewhat longer period of 3.67 hours. The PAB longitude is modestly offset from the previous data. The RMS scatter on the fit is 0.020 mag.

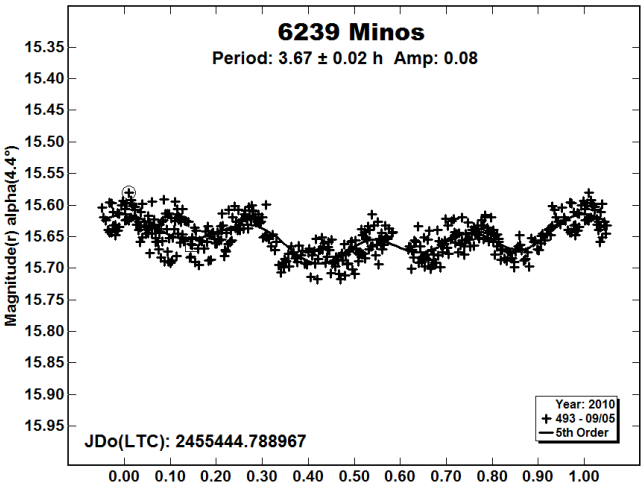

(6455) 1992 HE. Several observers have obtained photometry of this Apollo, the earliest probably being Pravec (2002web). The period is given alternately as 2.74 hours or twice this value. Our two nights in 2012 Apr using the 0.7-m telescope indicate only the shorter double-mode period, confirmed by a split-halves plot of the fairly small-amplitude lightcurve. The RMS scatter on the fit is 0.015 mag.

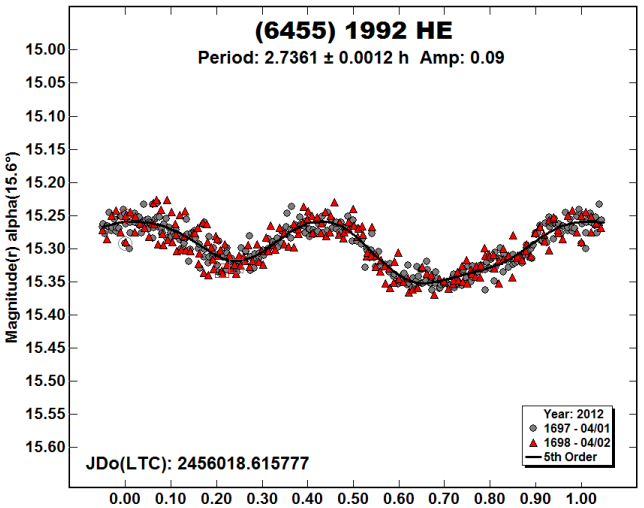

7267 Victormeen. The purpose of revisiting this Mars-crossing asteroid was to obtain data at previously unobserved phase angle bisectors. In 2019 May it was located well south of –30° Dec, where the SkyMapper photometric catalogue (Wolf et al. 2018) was essential. Three nights of observation using the 0.7-m telescope were a little rough due to poor weather and bright Moonlight. We confirm, however, the period by Pravec (2008web). The RMS scatter on the fitted lightcurve is 0.035 mag. The PAB values are offset by about 40° in longitude and 30° in latitude from previous work.

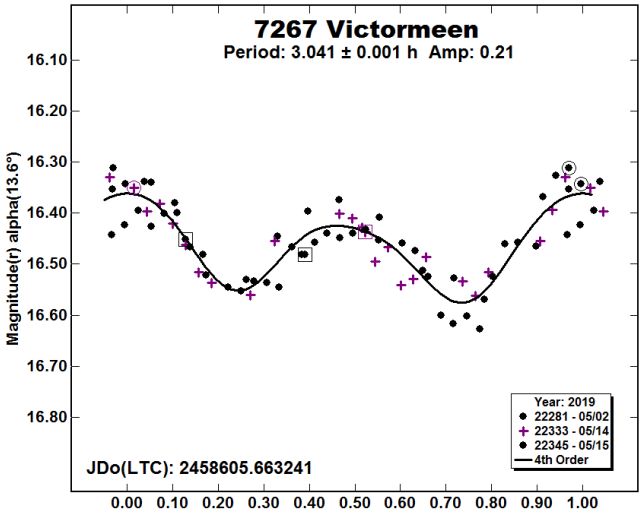

7965 Katsuhiko. This Phocaea was observed in 2019 Apr with the 0.7-m telescope to provide a lightcurve at new viewing geometry compared to previous results. During this apparition, the PAB longitude was offset by more than 100 degrees relative to data by both Oey et al. (2009) and Behrend (2012web, observer Pierre Antonini); the lightcurve morphology is considerably different as a consequence. The RMS scatter on the fit is 0.014 mag.

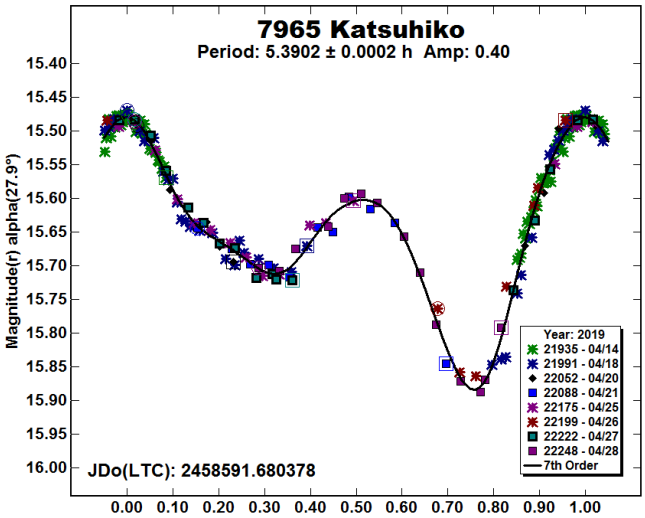

8444 Popovich. We followed this Mars-crosser for nearly four weeks through 2010 Nov using the 0.7-m telescope, extending from phase angle 2° to 16°. The increase in the lightcurve amplitude away from opposition necessitated changing the phase-function coefficient G to 0.3 to get things to fit reasonably well. The adjustment may not be perfect, partly due to incomplete

rotational phase coverage, but the default value 0.15 is certainly incorrect. The RMS scatter on the fit is 0.024 mag.

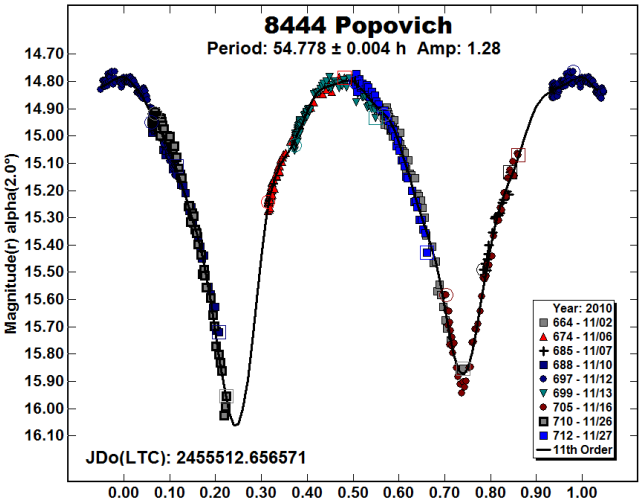

9564 Jeffwynn. Two nights of 1.1-m data near the 2019 Jun Full Moon produced a clean lightcurve for this Mars-crossing Phocaea. The period matches that of Warner (2013), but with rather better internal precision (0.011 mag versus ~0.03 mag). The PAB values are offset by about 80° in longitude from the earlier work. Our lightcurve amplitude is smaller despite higher phase angle, and the morphology is somewhat different.

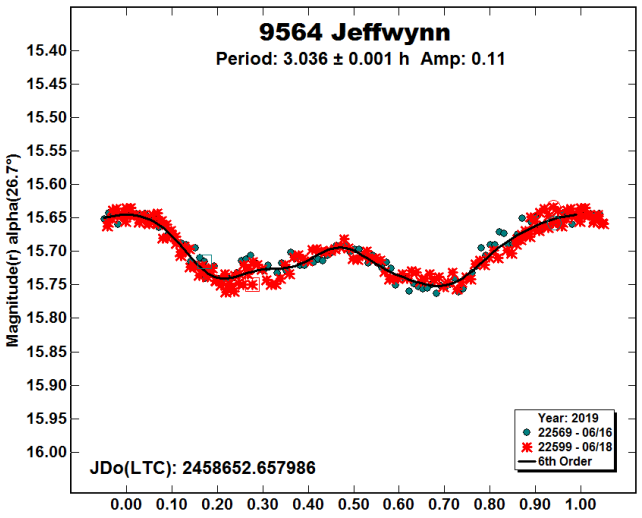

(12538) 1998 OH. Brian Warner has agonized over several datasets for this Apollo, the most recent being the "continuing non-resolution" of Warner (2019) from data in 2018 Oct. We obtained two nights of data in 2019 May-Jun using the 1.1-m telescope under Moon-free photometric conditions. The phase angle was much higher and PABs different than previously; nearly two rotational cycles were obtained each night. The data seem to point unambiguously to a single period near 2.58 hours. The high phase angle changed enough in the six-day gap that the amplitude is significantly different, so phased plots are shown for each night. The RMS scatter for both nights is 0.007 mag, quite a bit better than the Warner data (~0.027 mag). The double-mode period near 5.2 hours is excluded by split-halves plots.

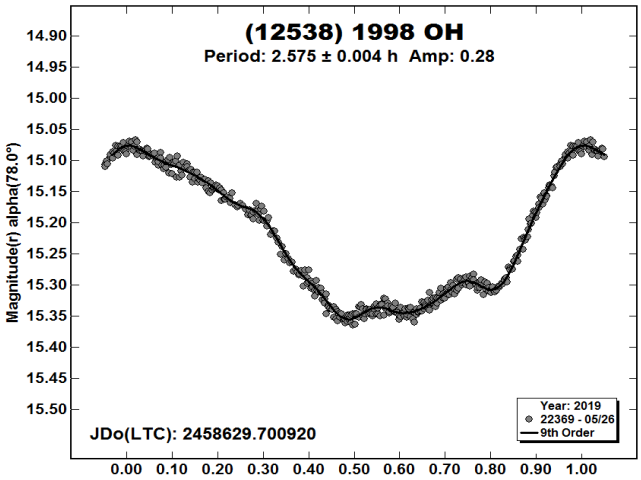

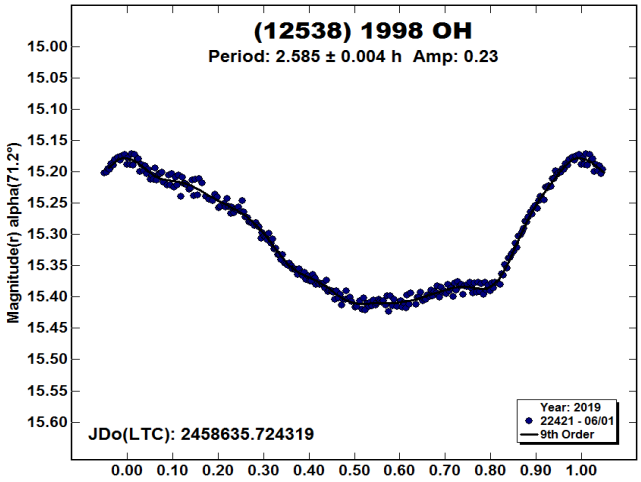

(14402) 1991 DB. In Paper 2 we showed unconvincing results for this Amor. By contrast Pravec (2000web), displays a complete, well-defined lightcurve from data taken in 2000 Mar. However, making magnitude corrections to the comparison stars allowed us to recognize that the rapidly increasing phase angle caused the amplitude to increase significantly. We now show two lightcurves from the beginning and end of our 2009 Mar Schmidt series; three additional intervening nights are included in the ALCDEF file. The RMS scatter on the two phased plots is 0.040 and 0.049 mag, roughly 3-sigma detections from only 28 and 41 data-points, respectively.

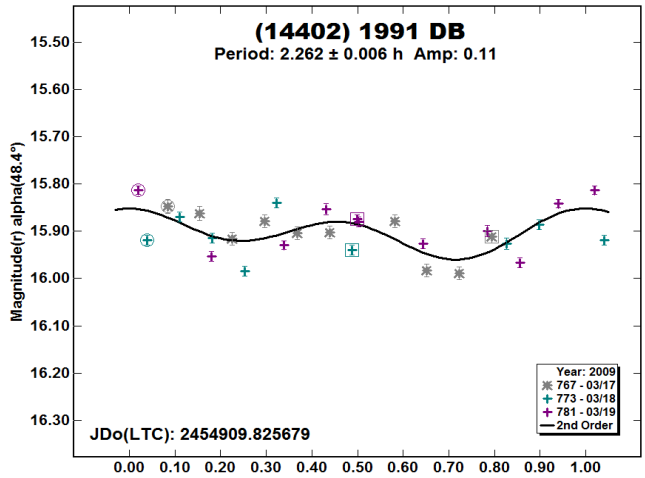

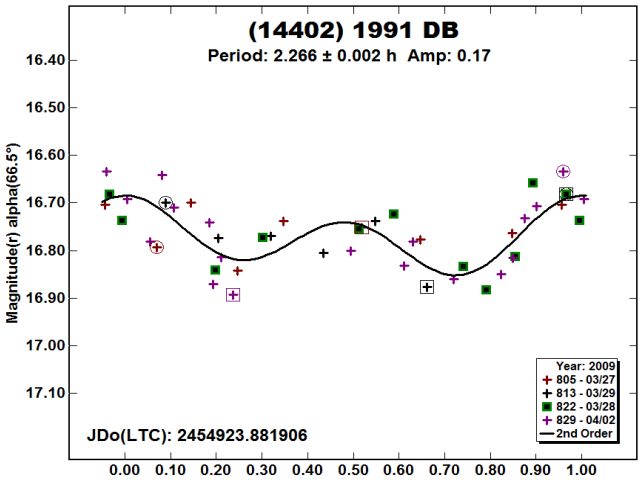

(15700) 1987 QD. Durkee et al. (2010) announced that this Mars-crosser was a candidate binary from observations taken in 2010 Sep-Oct. We observed the asteroid on four nights 2010 Jul-Sep. The first plot below shows one night at fairly high phase-angle from the 0.7-m telescope with the data force-fit to the known short rotation period. The RMS scatter is 0.027 mag. Two successive nights closer to opposition using the Schmidt are also shown; the amplitude is much smaller and the morphology has changed. The RMS scatter here is 0.016 mag. A short run on an isolated night is included in the ALCDEF dataset.

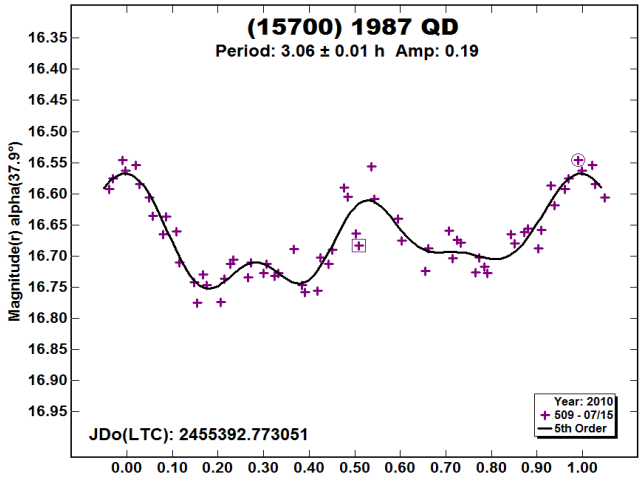

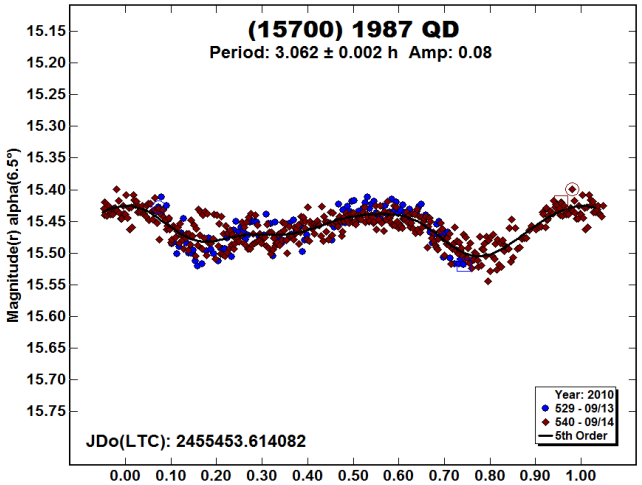

(19402) 1998 EG14. Our observations of this Mars-crosser appear to be the only such photometry available. We obtained fairly sparse data on three nights in 2010 Nov using the 0.7-m telescope. These yielded a short-period, moderate-amplitude lightcurve. On the first and last nights the runs extended beyond 8 hours, nearly three rotational cycles. The RMS scatter on the fit is 0.020 mag.

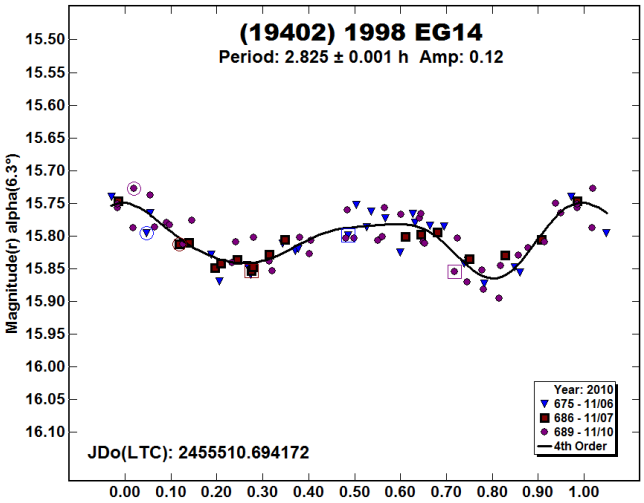

(20691) 1999 VY2. Several observers caught this Mars-crosser during the apparition of 2010/11 Dec/Jan, all with similar results. We used the 0.7-m telescope on two nights during this time to get runs of nearly 8 hours, just shy of three rotational cycles each night. The lightcurve is smooth and uncomplicated; the RMS scatter on the fit is 0.016 mag.

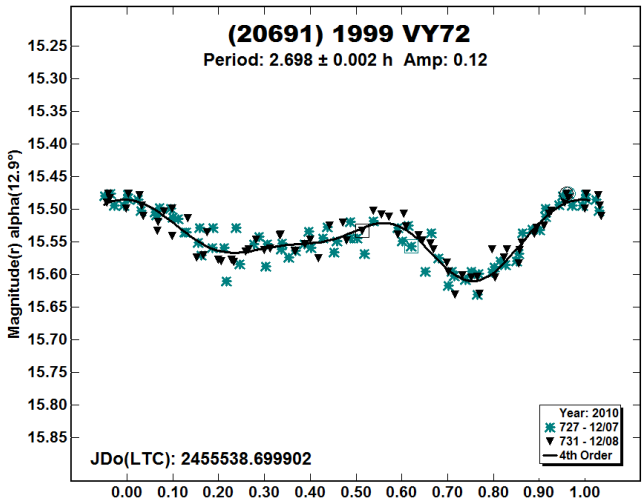

20936 Nemrut Dagi. In a 2011 CALL post we preferred a double-mode 6.5-hour rotation period for this Hungaria. In several later papers, starting with data taken during the same apparition, Brian Warner (2011b) found that the half-period was more likely. Our revised data are shown below from pairs of nights at two successive lunations in 2011 Jan-Feb, and again in 2019 Apr. All three were done with the 0.7-m telescope and R_c filter. The amplitudes for the first two series are small compared to the noise in the data (RMS scatter 0.020 and 0.028 mag, respectively), between 3- and 4-sigma. In 2019 Apr we obtained rather better data (RMS scatter 0.011 mag) at fresh phase-angle bisectors. The object is evidently nearly spherical, so the amplitude remains

small, and the lightcurve morphology similar. The three plots below are at the same vertical scale.

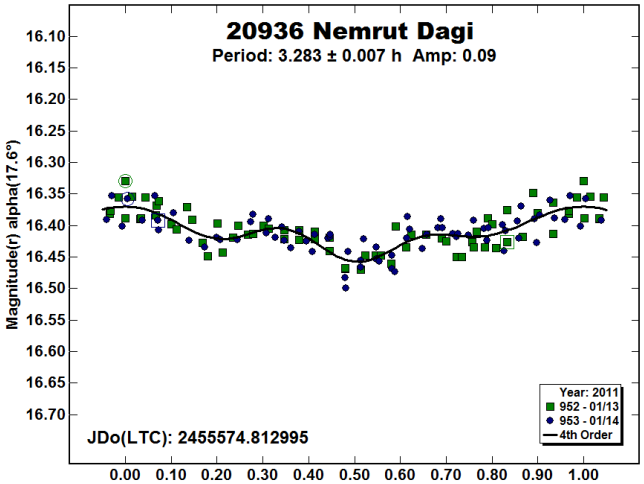

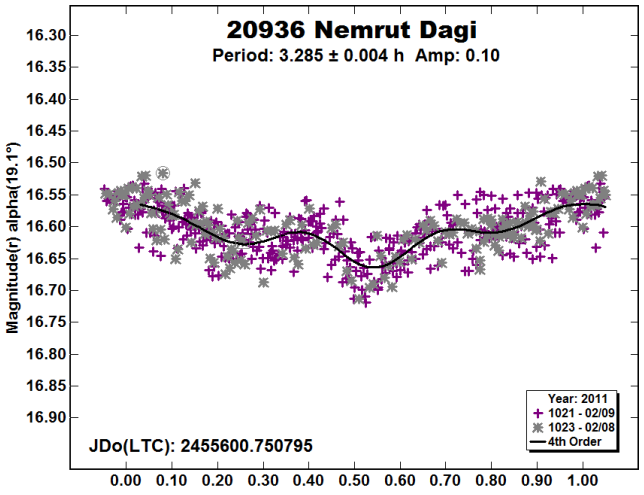

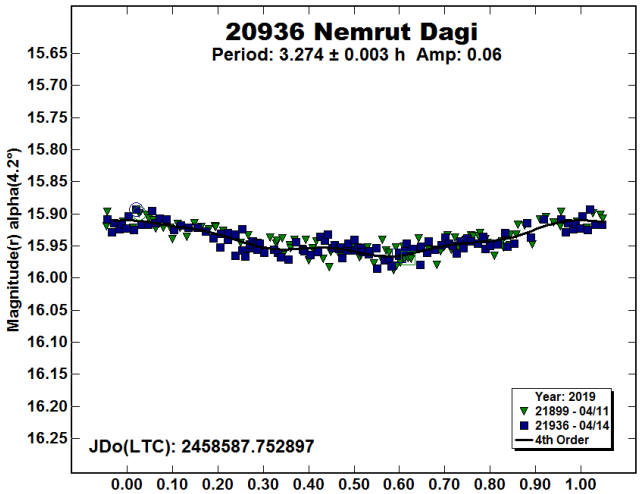

21104 Sveshnikov. Five of six consecutive, mostly clear nights in 2010 Oct with the 0.7-m telescope yielded a clean lightcurve for this Mars-crosser. The R_c-filter exposures were 45- or 60-seconds, usually taken in pairs and mixed with other targets during the night. The RMS scatter on the fit is 0.018 mag. This confirms to similar accuracy the period in sparse data from the Palomar Transient Factory (Waszczak et al., 2015).

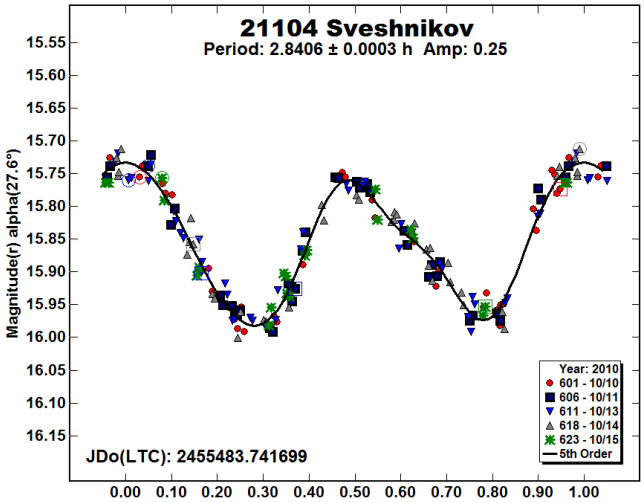

(22262) 1980 PZ2. This Phocaea has no previous lightcurve. We observed it using the 0.7-m telescope in the weeks following opposition in 2019 Apr, when it was well south of the ecliptic. The period turned out to be moderately long, which made getting complete rotational phase coverage difficult since the nightly viewing window was short. The results appear to be satisfactory, although the order-6 fit does not quite capture the sharp primary maximum accurately. The RMS scatter on the fit is 0.015 mag.

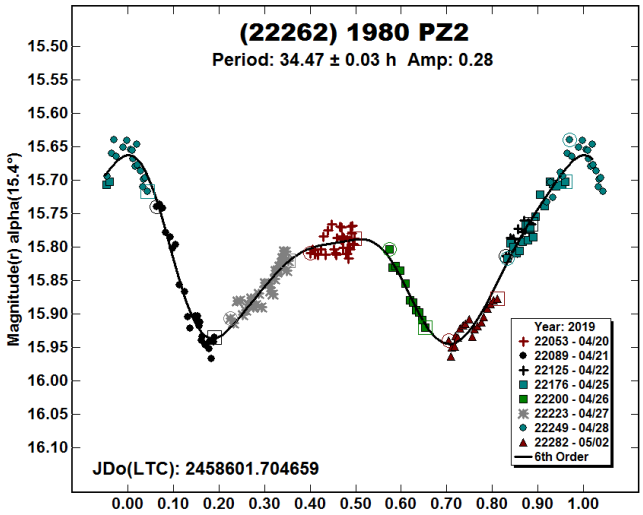

(23183) 2000 OY21. Warner (2016b) published the first lightcurve for this Amor from data taken in 2016 Jan. Three long consecutive nights from five years earlier with the LONEOS Schmidt (20- and 30-second exposures) produced a very nice clean lightcurve. The runs were about 7, 7, and 8½ hours each. An order-13 Fourier fit was required to pick up the sharp minimum accurately. The RMS scatter on the fit to the 1300+ data-points is 0.023 mag.

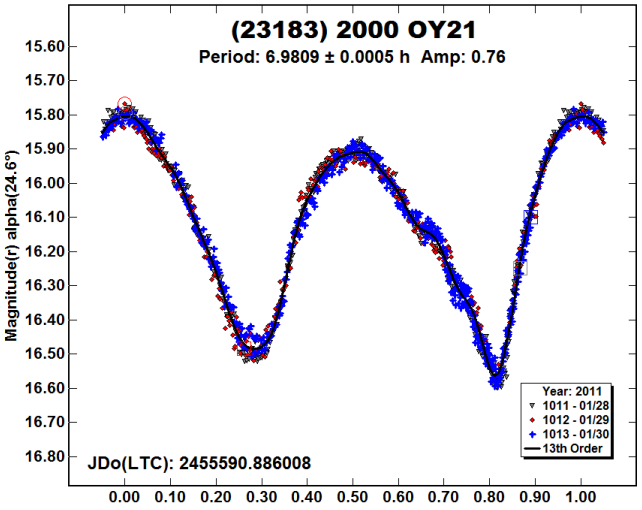

(24029) 1999 RT198. We obtained data at two apparitions at similar PABs for this Mars-crosser using the 0.7-m telescope. Both lightcurves exhibit fairly large amplitudes and sharp minima, requiring order-10 fits to capture them accurately (the sparsely-sampled maxima are over-fit, so the fitted curves are omitted here). The RMS scatter on the 2010 Nov lightcurve is 0.022 mag, while for the 2017 Oct data it is 0.015 mag. The full amplitudes are 0.70 and 0.82 mag, respectively.

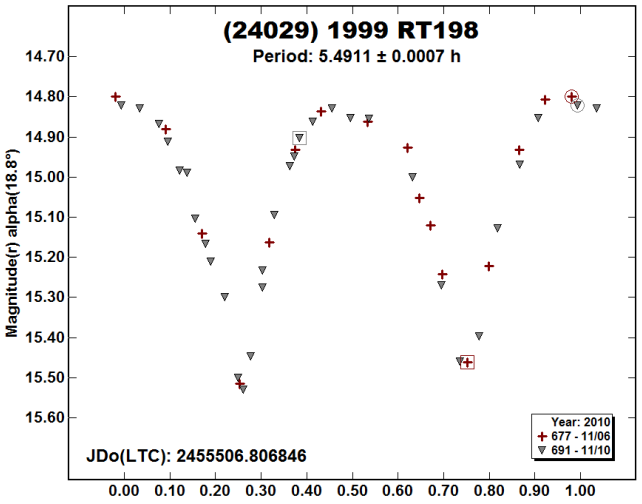

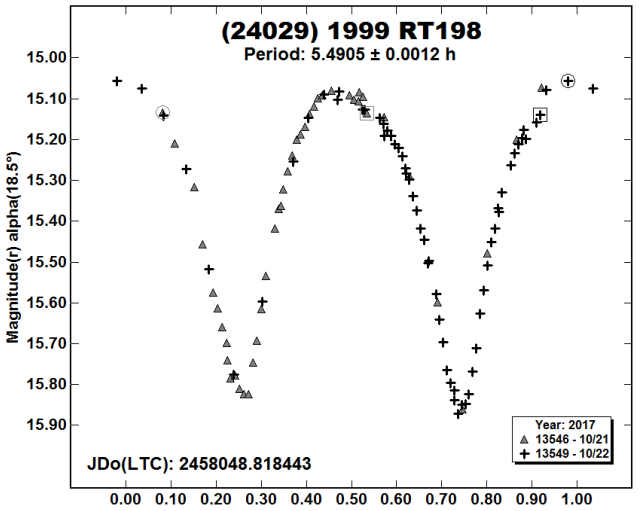

24643 MacCready. Two nights of 1.1-m telescope data on this Mars-crossing Phocaea showed that previously announced uncertain periods (Pravec 2005web, 4.507 h; Erasmus et al. 2017, 2.06 h) are both incorrect. The 5-hour runs in 2019 Jun spanned more than 1½ cycles each night, so the correct period was evident from visual inspection of the nightly raw plots. The RMS scatter is 0.012 mag.

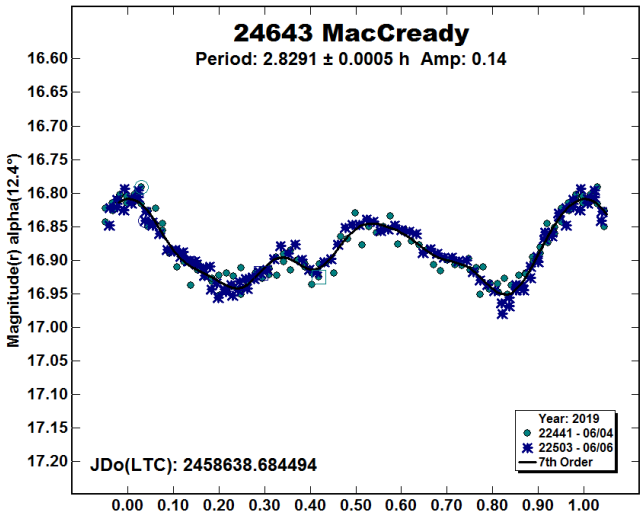

26471 Tracybecker. This Mars-crossing binary Hungaria has been observed many times for lightcurves starting with Behrend (2001web), who gave the period derived from data by Bernasconi, Charbonnel, and himself. The binary nature was reported by Warner et al. (2009a). Our four nights using the 0.7-m telescope in 2019 Mar were taken when the asteroid was at about –30° Dec and at PAB values not observed hitherto. Again the purpose was to provide leverage for future shape-modelling. Mutual events were not evident. The RMS scatter on the fit is 0.019 mag.

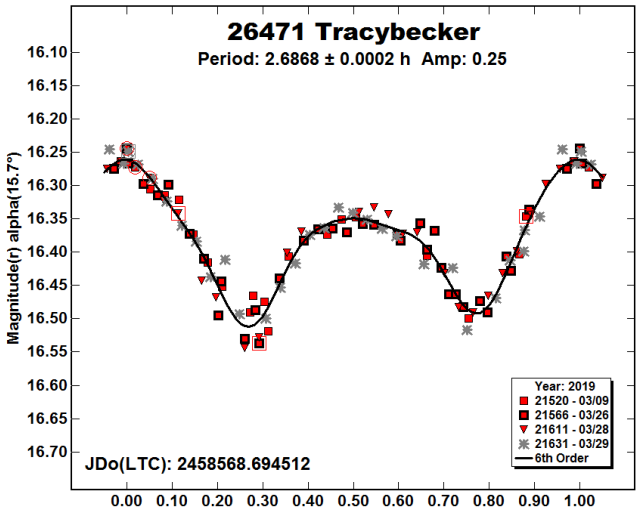

(35107) 1991 VH. As described in Paper 2, we did not obtain enough independent data to disentangle the periods of this well-known Apollo binary, identified originally from its lightcurve but now resolved via direct imaging. The 570 observations were obtained on five nights in 2008 May and six nights in 2009 Jan using the LONEOS Schmidt, and 0.7-m and 1.1-m telescopes. The revised data are included in the ALCDEF files.

(37384) 2001 WU1. This Mars-crosser had a northern apparition in spring 2019, which we caught on two nights as it emerged from the evening twilight using the 1.1-m telescope. The secondary maximum has a curious dimple (at fairly high phase-angle and phase-angle bisector latitude +30°), but otherwise the lightcurve is uncomplicated. The RMS scatter on the fit is 0.014 mag.

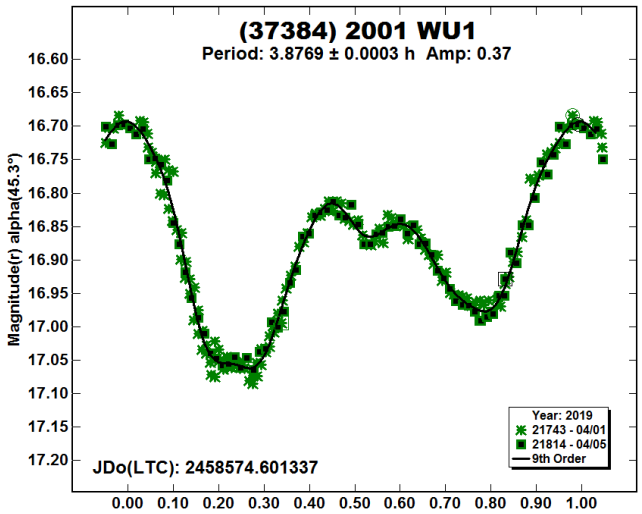

(38074) 1999 GX19. Two short nights with the 1.1-m telescope at the 2019 Jun summer solstice gave nearly complete rotational coverage for this low-inclination Mars-crosser. The RMS scatter on the fitted lightcurve is 0.009 mag.

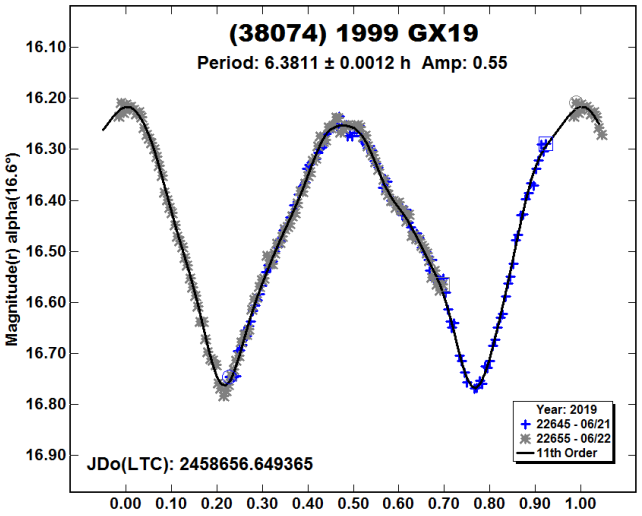

(42811) 1999 JN81. This is another trial to get data at previously unobserved viewing geometry in hopes of providing leverage for future shape modelling. Data were acquired on two nights in 2019 Apr using the 0.7-m telescope and R_c filter. Three previous lightcurves at nearly identical PABs were obtained by Warner (2008, 2012) and by Benishek (2018). For the new lightcurve, the angles are offset from those by about 100° in longitude and more than 50° in latitude. The RMS scatter on the lightcurve is 0.018 mag.

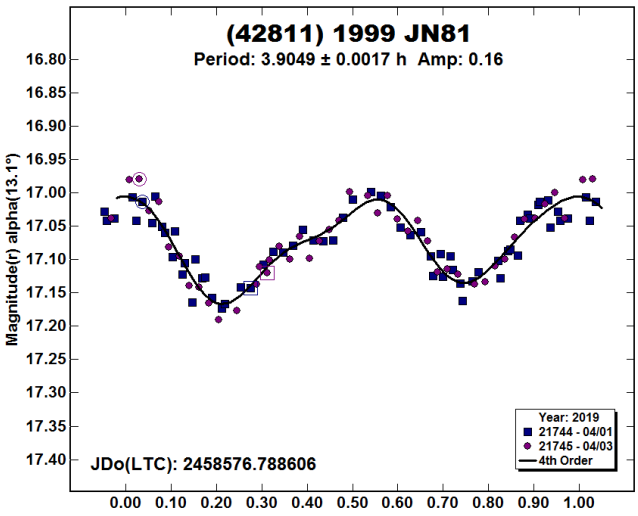

(42930) 1999 TM11. This Phocaea-type asteroid had its rotation period previously determined from sparse Palomar Transient Factory data (Waszczak et al. 2015). We confirm their results from two nights of 5-minute R_c-filter exposures using the 0.7-m telescope in 2019 Apr. The viewing geometry was nearly the same. The RMS scatter on the fitted curve is 0.012 mag.

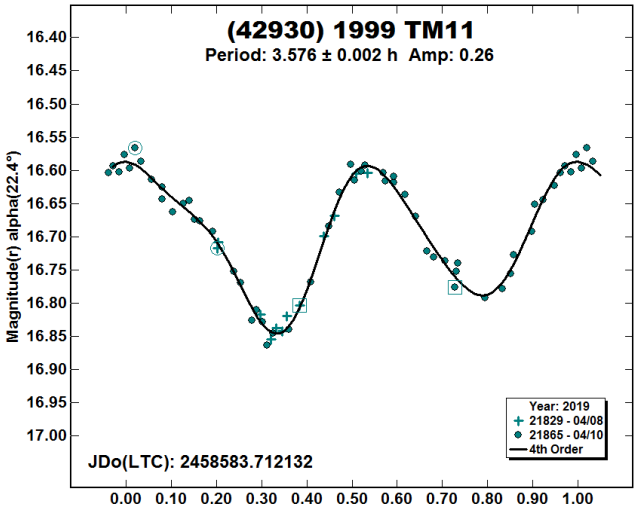

(52768) 1998 OR2. We used the LONEOS Schmidt to observe this Amor on eight nights in 2009 Jan-Feb, as presented in Paper 2. Some of the nightly runs span six hours. The data are ample, of good quality, and the period-determination is unambiguous.

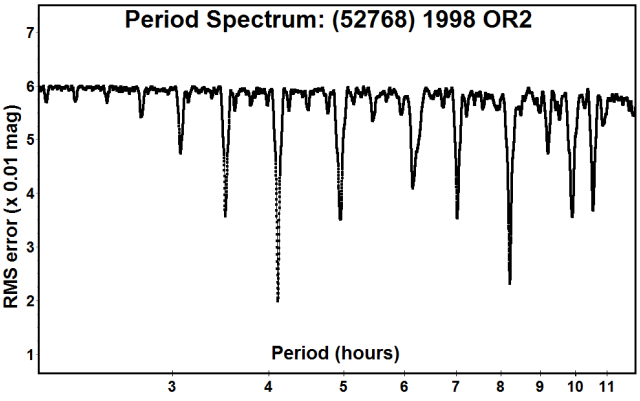

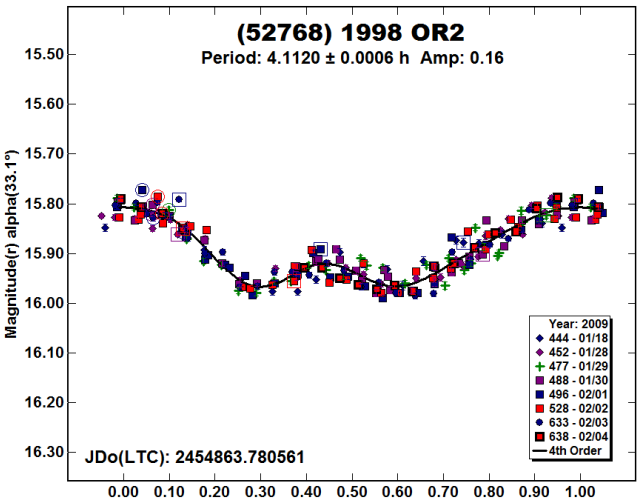

The results presented by Betzler and Novaes (2009) have large internal errors, up to 0.2 mag, and the period they find is incorrect. The RMS scatter on our phased lightcurve is 0.020 mag.

This is exhibited along with the period spectrum between 2 and 12 hours, which indicates that the Betzler and Novaes 3.2-h period is not present in our data (the nearby weak minimum is at 3.07 h). It might be useful to fit their original data to the new period and determine post-facto which points are the deviant ones.

(53319) 1999 JM8. We obtained two series of observations for this tumbling Apollo (Pravec et al. 2005). The first was four nights in 2008 Mar-Apr using the 1.1-m telescope; in 2008 Oct we got seven more nights using the LONEOS Schmidt. Neither run was sufficient to deal with the long-period tumbling aspect. All data are now adjusted to Sloan r′ and included in the ALCDEF file.

(65679) 1989 UQ. Petr Pravec et al. (1998a) obtained the first lightcurve for this 1-km PHA Aten in 1996, which is the only published result. Our two-night series in 2010 Oct with the Schmidt yielded over seven hundred 45-second exposures. Our period matches the previous one and has similar internal scatter (RMS error 0.031 mag).

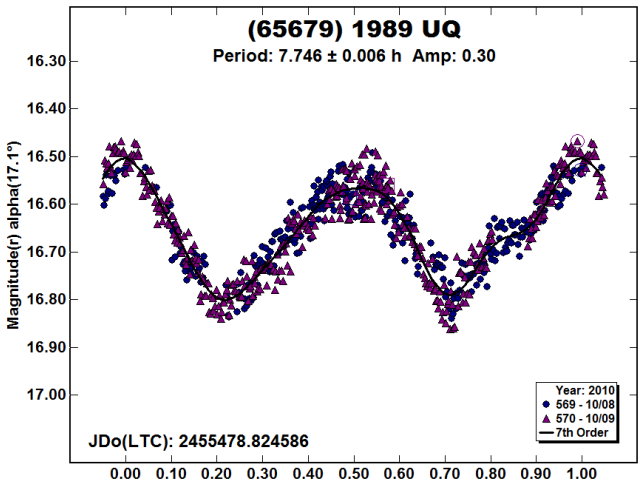

(68134) 2001 AT18. This Mars-crosser is a LONEOS discovery. We targeted it for two nights in 2010 Dec using the 0.7-m telescope, and obtained about two hundred 90-second exposures. The large-amplitude lightcurve has sharp minima, fit here with an order-13 Fourier curve. The RMS scatter on the fit is 0.032 mag. There is no other published photometry. A favorable northern apparition occurs in autumn 2020, which will have phase-angle bisectors completely different from those of the 2010 apparition.

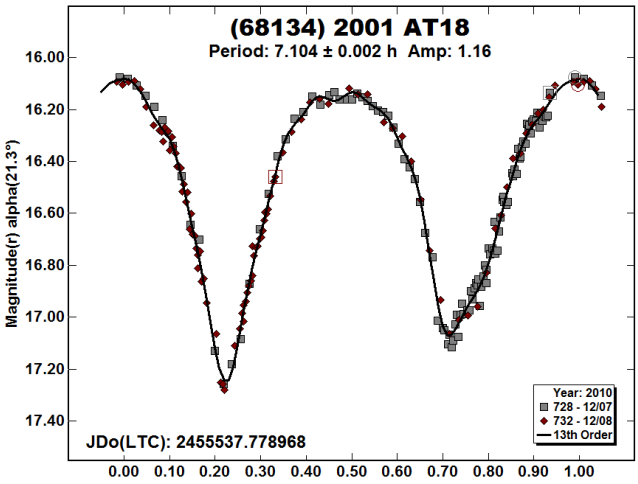

(68216) 2001 CV26. Several observers have obtained rotational lightcurves for this 1-km Apollo as early as the 2010 apparition in which we followed it. Our best night was a 6½-hour run with the 1.1-m telescope and R_c filter. This produced the clean result shown below (RMS scatter 0.009 mag).

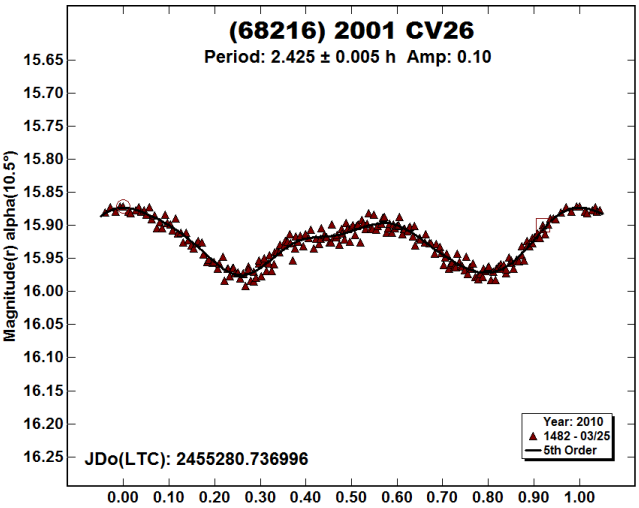

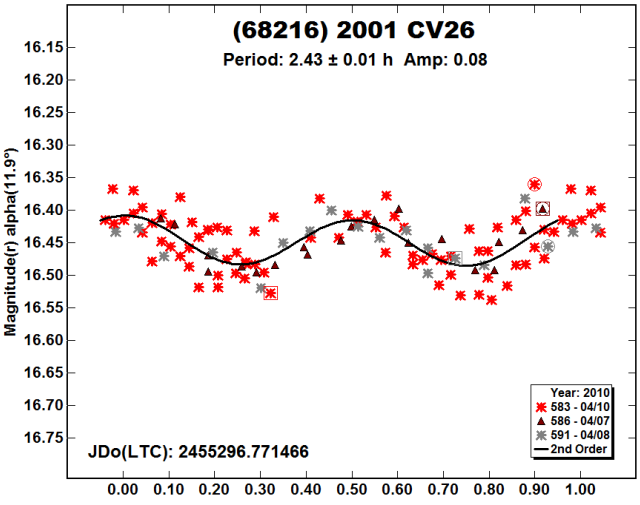

On three later nights we used the LONEOS Schmidt, where the results were poorer, as shown in the second phased plot (RMS scatter 0.031 mag). An earlier isolated night, 2009 Dec 19, is included in the ALDEF dataset.

(68350) 2001 MK3. Albino Carbognani (2011) published a complete lightcurve for this Amor from data taken during the same interval we observed it in early 2009. His period (3.273 h) is somewhat longer than ours; the morphology is identical but the lightcurve is under-fit, and some stray data-points may have skewed the period. Our LONEOS Schmidt lightcurve in Paper 2 is confirmed here to higher precision after revision of the photometry. Many of the nightly runs exceed six hours. An 8½-hour dataset isolated from these is plotted separately with the period force-fit. The phase-angle was smaller, so the lightcurve amplitude had shrunk and was of somewhat different form. The RMS scatter on the two fits is 0.019 and 0.033 mag.

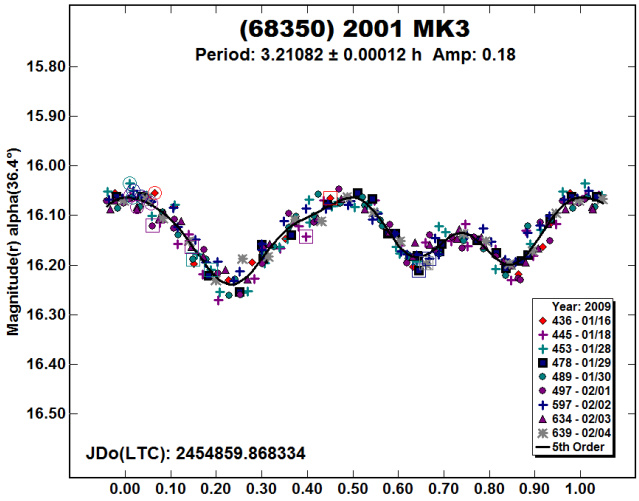

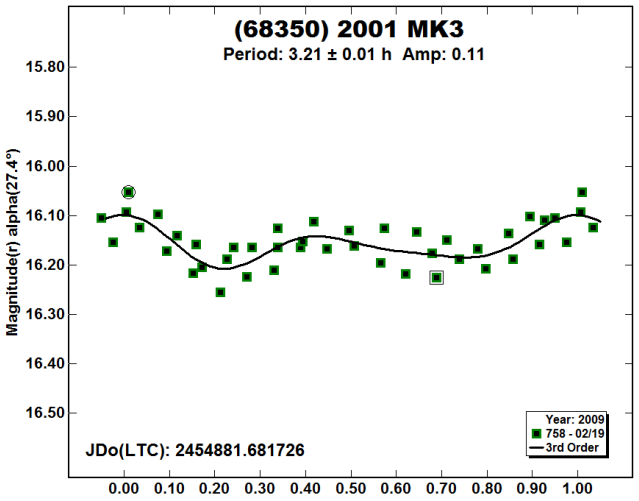

(74779) 1999 RF241. We appear to have obtained the only lightcurve photometry so far for this Mars-crossing Phocaea. Significant portions of three nights using the 0.7-m telescope in 2010 Dec defined the large-amplitude variation very clearly. The RMS scatter on the fit is 0.023 mag.

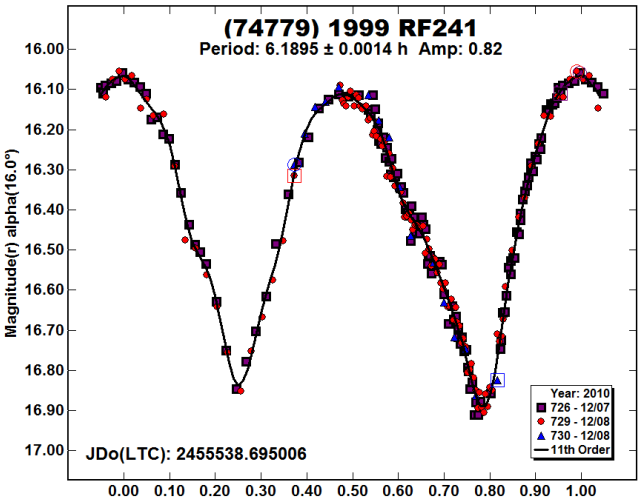

(74823) 1999 TD15. Our data through 2010 Nov from the 0.7-m telescope for this Mars-crosser ranged from 2° to 20° phase angle, so the lightcurve amplitude increased significantly. We could adjust for this fairly well by changing the phase-function coefficient *G* to 0.4. The rotational phase coverage is incomplete, but the period is uncertain by only perhaps 0.1 hour at most. The RMS scatter on the fit is 0.024 mag.

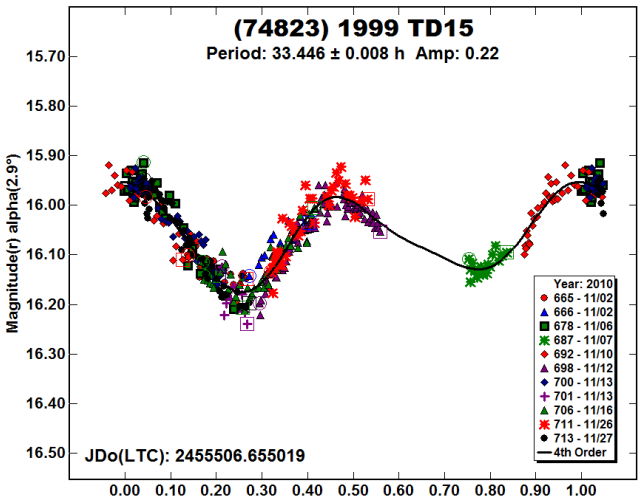

(85839) 1998 YO4. Previously, Warner (2010) concluded there was no sensible variation in this Amor from three nights of data taken one month prior to ours. We obtained only a single 4-hour run using the Schmidt in 2010 Apr 14, so can certainly agree that the variation is small. A notional fit is given even so, which has RMS scatter of 0.014 mag. See the discussion for asteroid (208023) for a cautionary tale about inferring too much from short observing runs.

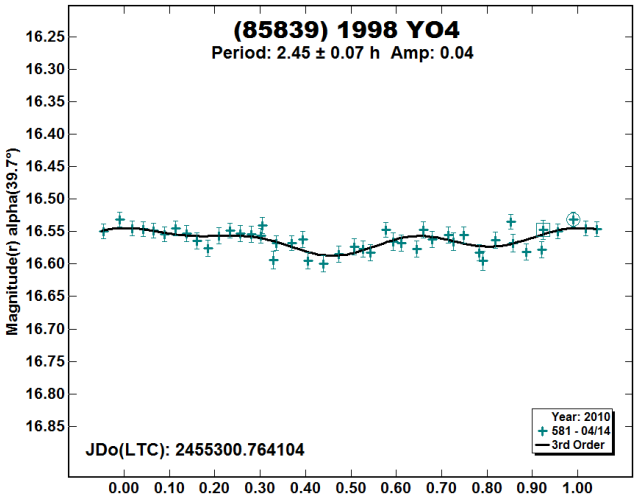

(85867) 1999 BY9. A notional plot of LONEOS Schmidt data from 2009 Mar-Apr was shown in Paper 2, mainly to indicate that this Amor was a likely tumbler. Adopting Sloan r´ magnitudes for the comparison stars from Pan-STARRS showed there were significant shifts in the nightly zero-points from the earlier work, but no change in the conclusions. There is likely to be a pseudo-periodicity of some tens of hours involved, evident from the slopes of the nightly runs in the upper-left portion of the plot below. However, we do not have enough data to make a proper solution since not even one extremum was captured. Data collected by Hasegawa et al. (2018) on five nights in 2009 Jan are likewise indeterminate. The raw plot shows our ten nights without H,G correction.

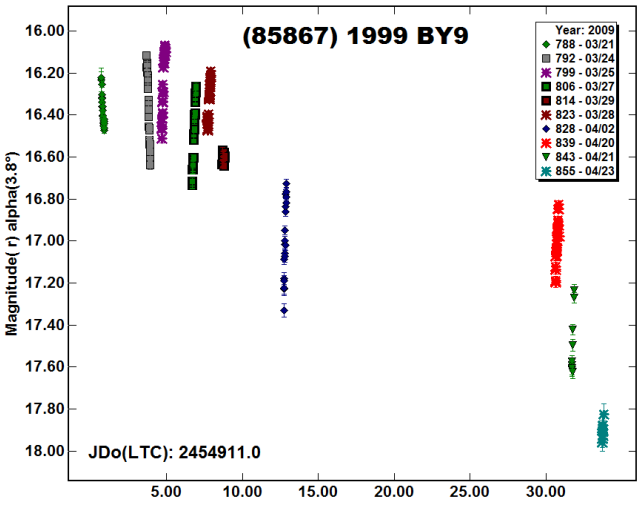

(87684) 2000 SY2. In Paper 1 we gave a plot of the photometry from a single night (2008 Sep 7) for this Aten. These were obtained mainly with the 1.1-m telescope plus a few additional points from the LONEOS Schmidt, both used unfiltered. The combined series spanned only about 3½ hours. We have re-measured the original images using the same comparison stars in both sets, and adopt better Sloan r´ values for those stars. Despite the short run, a small-amplitude lightcurve emerged whose period, within our larger uncertainty, matches that of Warner (2017b; N.B. a typo for the period in the *text and table* there: the period of 2.57 hours given in the *figure* is correct). The weak triple-mode morphology is also very similar to Warner's. The RMS scatter on the fitted curve is 0.011 mag.

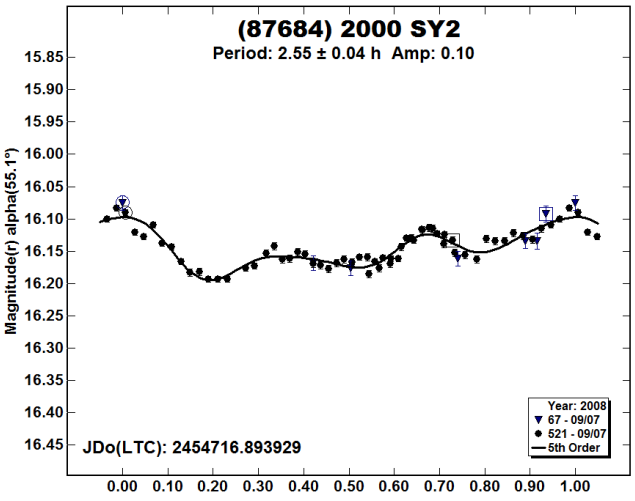

(99913) 1997 CZ5. Based on data from 2011 Jan, Higgins et al. (2011) announced that this Mars-crosser was binary. No lightcurve has been published from those data. Earlier in that apparition, (2010 Oct) we obtained two 4-hour runs on consecutive nights using 20-second exposures on the Schmidt, which clearly revealed the short period of the system but no evidence of a binary. The PAB values are offset from Higgins et al. by about 50° in longitude and 40° in latitude and also at much higher phase-angle. The RMS scatter on the fit is 0.019 mag.

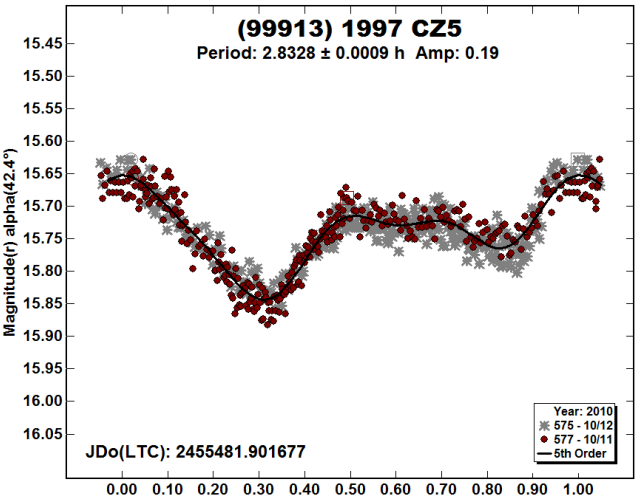

(100926) 1998 MQ. This 1-km Amor was the first NEO found by the LONEOS survey in 1998 Jun, identified by then-undergraduate summer student Chris Onken, more recently project manager of the valuable SkyMapper survey. Warner (2011a) obtained a lightcurve in 2011 Oct, producing a triple-mode rotation period of 2.33 hours. Three weeks later we got a few data-points at somewhat lower phase angle on one night using the 0.7-m telescope. We show a force-fit the Warner period, which indicates an amplitude only half that of his. The RMS scatter on the fit is 0.015 mag.

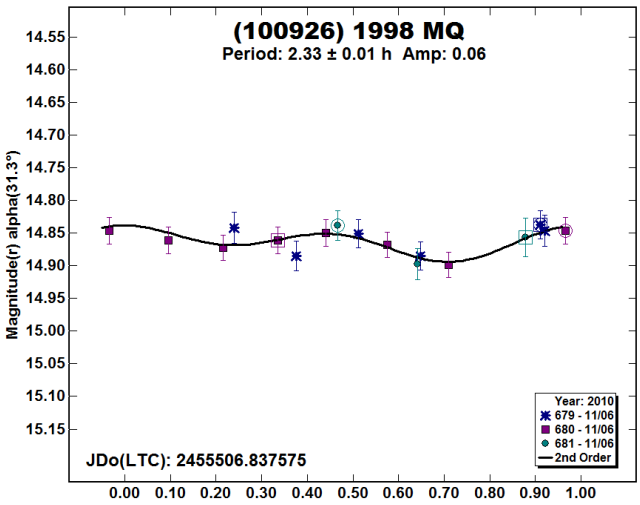

(102873) 1999 WK11. This Amor was observed on three nights in 2008 May-Jun using the 0.7-m and 1.1-m telescopes without filters. The 0.7-m results were quite noisy due to fringing from night-sky emission, so many of those data-points had to be omitted. The rotation period is short for a 1-km object; the RMS scatter on the fit is 0.017 mag. The asteroid has not been brighter than mag 20 since 2008, so there is no further photometry.

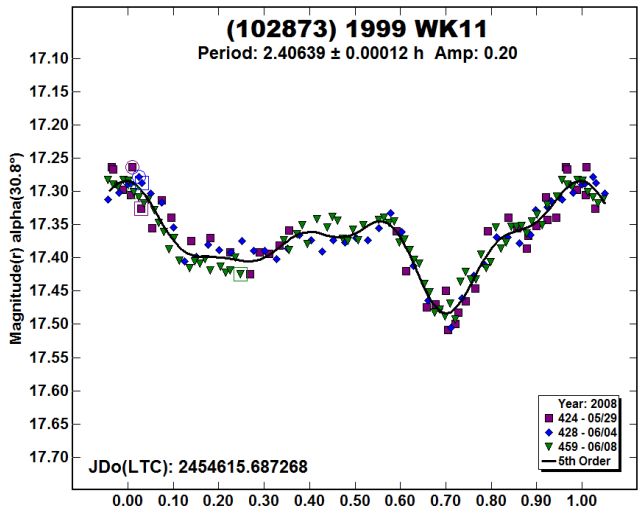

(136568) 1980 XB. Benishek (2019b) observed this Mars-crosser in early Dec 2018; about six weeks later, before those results were published, we got with another run. We used the 1.1-m telescope on two nights in bright moonlight. The two lightcurves are very similar. The RMS scatter on the fit to our data is 0.008 mag.

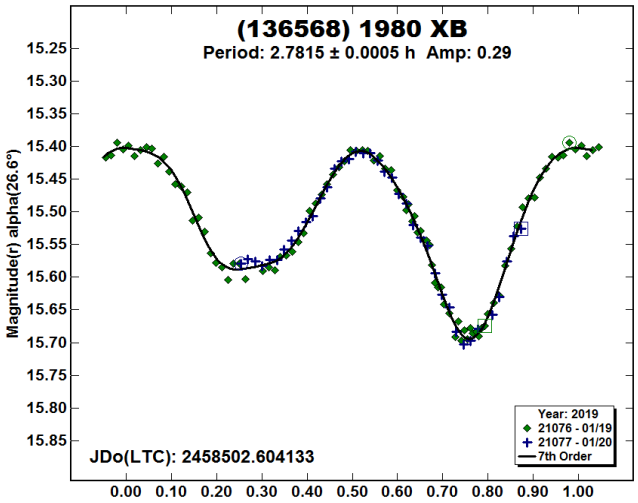

(138883) 2000 YL29. Revision of our complete LONEOS Schmidt dataset of this Apollo produced a puzzle. At the insightful suggestion of Brian Warner (*priv. comm.*), we have changed the phase-function coefficient *G* to 0.3 from the default value of 0.15. This allowed the 2009 Sep-Oct nights to be phased with the same period as shown in Paper 2, but with a peculiar morphology (the Paper 2 lightcurve itself is completely erroneous). The RMS scatter on the somewhat over-fit order-9 curve is 0.037 mag. A raw plot from 2009 Sep 23 highlights the sharp minimum appearing that night. Two additional isolated nights of data are included in the ALCDEF file, but not shown here.

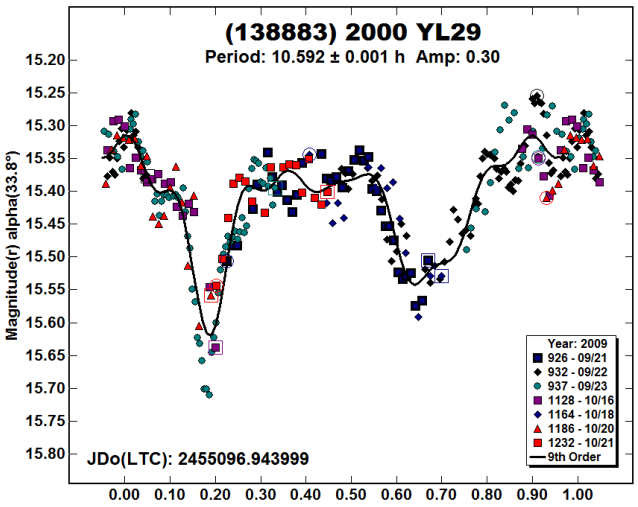

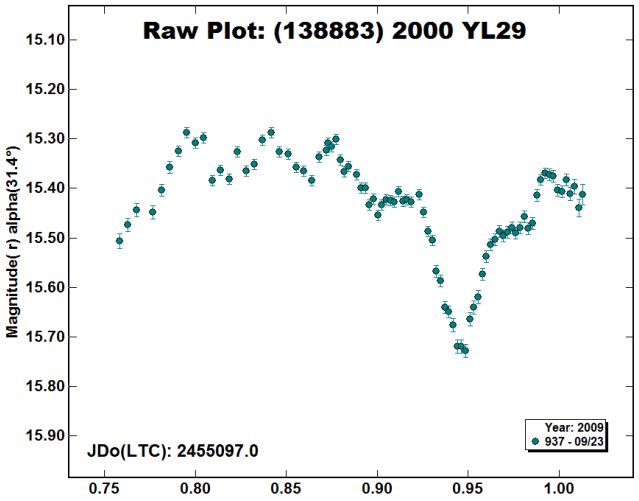

(141432) 2002 CQ11. David Polishook (2012) obtained a rough lightcurve for this 250-meter Aten from Wise Observatory in 2007 Feb. Our two nights came in 2011 May using the Schmidt, when the PAB longitude was offset about 50° from his. From more than 550 30-second exposures, our data phase to a period similar to that of Polishook and the morphology may be somewhat different (only one well-defined minimum in the fitted lightcurve). The amplitude is fairly small relative to the internal scatter (0.036 mag), so the result is not as nice as we would like to see.

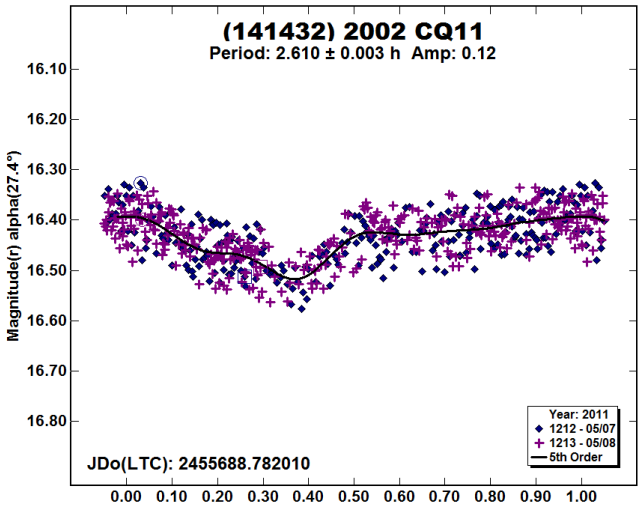

(141498) 2002 EZ16. Warner and Stephens (2019b) have observed this Aten recently, obtaining a provisional period of 8.35 h. Our three nights from 2010 Nov using the Schmidt do not confirm this, but neither are we happy with the results due to the noisy data. The separate sessions each night point to a 5-hour period, but periods near 10 and 12.5 hours seem admissible. The phased lightcurve with the shorter period is shown below along with a period spectrum between 2 and 35 hours. The RMS scatter on the fit is 0.040 mag.

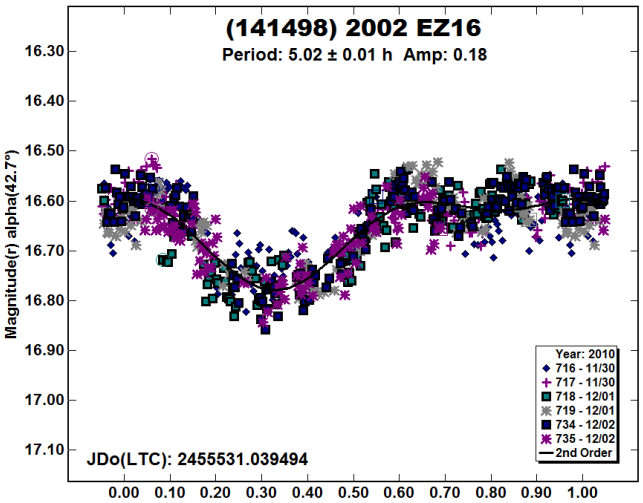

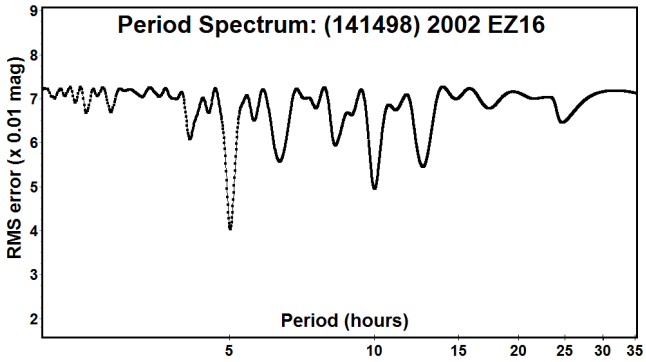

(143381) 2003 BC21. We got several runs on this Amor during northern autumn 2010 using the Schmidt and the 0.7-m telescope. The large amplitude and fairly short period made it easy to follow specifically to pick up maxima. Surprisingly, there is no entry for the asteroid in the LCDB; it has not been brighter than mag 19 since 2010. Six phased plots are given at the same vertical scale for each group among the thirteen observing nights. The last two are force-fit to the approximate period since they result from single-night runs. The series covers a substantial range in phase-angle before and after opposition, but only a modest range in phase-angle bisectors, so the morphology is little changed. The RMS scatter is about 0.04 mag for each plot.

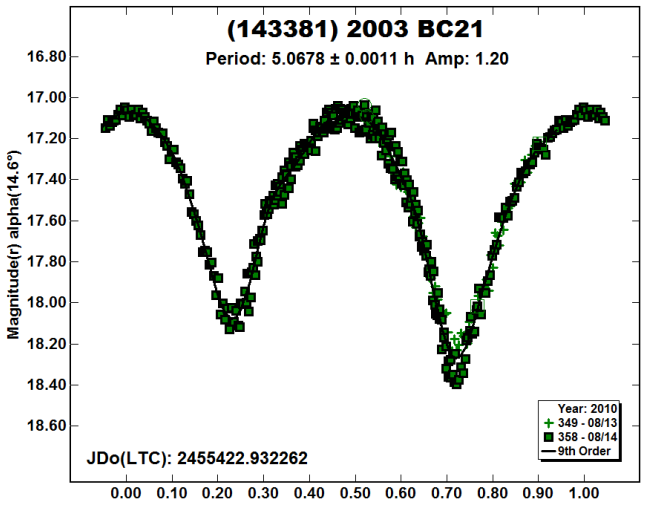

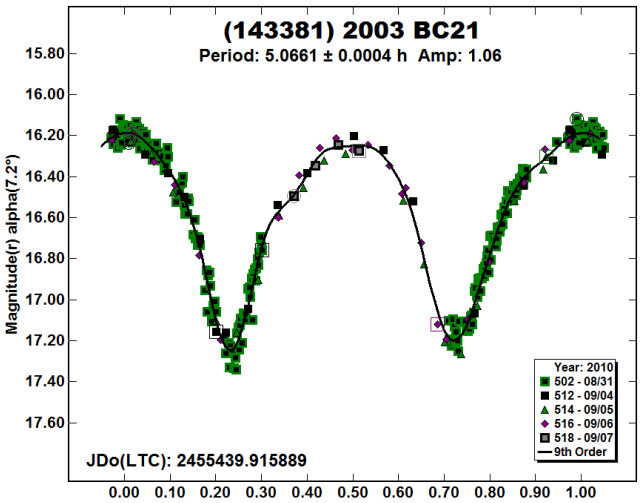

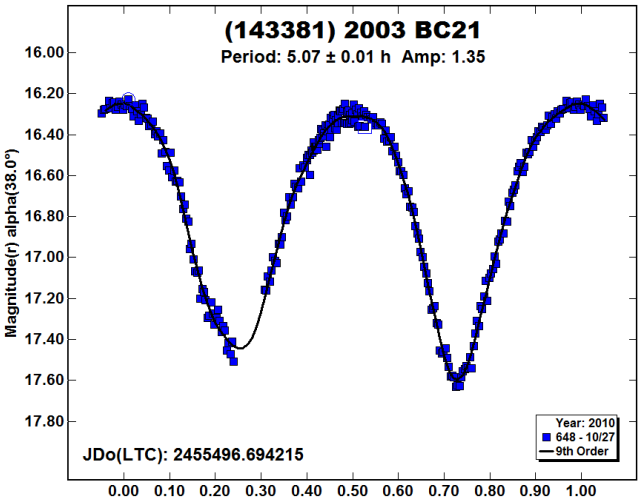

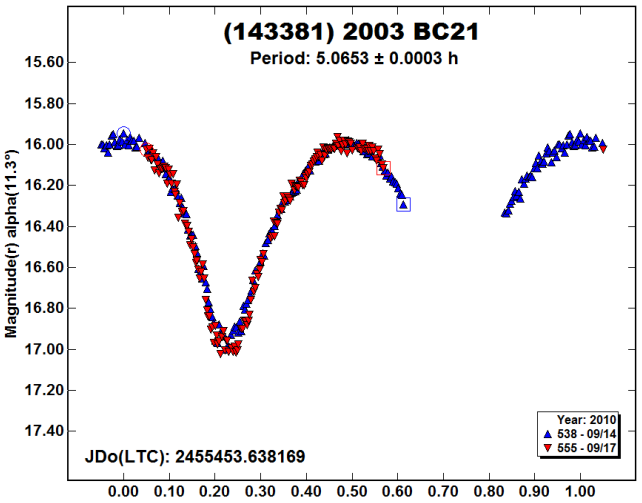

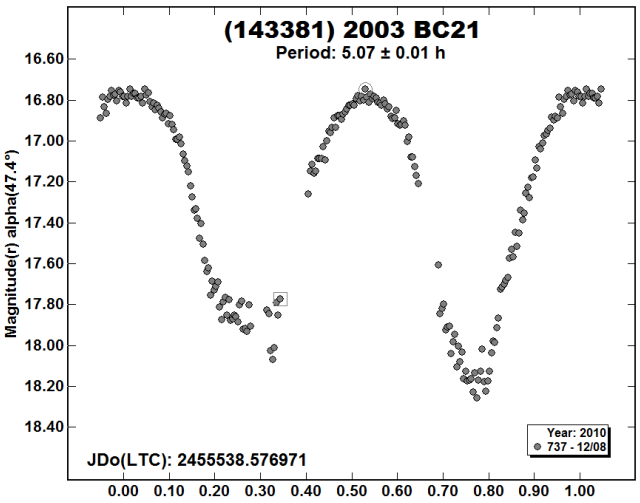

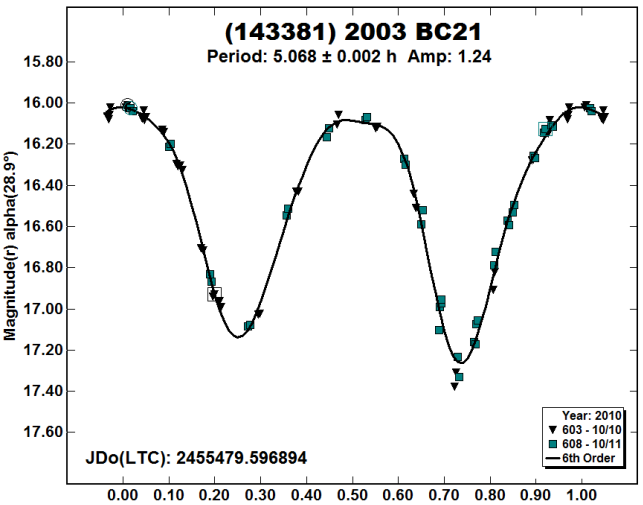

(143651) 2003 QO104. We were one of three groups to observe this Apollo asteroid during its close approach in spring 2009 (cf. Warner et al. 2009c and Birtwhistle 2009). The lightcurves from all three are similar (we must have looked at the same object!), featuring a long period near 114 hours, large amplitude, and mildly non-repeating tumbling aspect. Our LONEOS Schmidt data, first given in Paper 2, were taken on 15 nights with exposures ranging from 3 minutes down to 75 seconds.

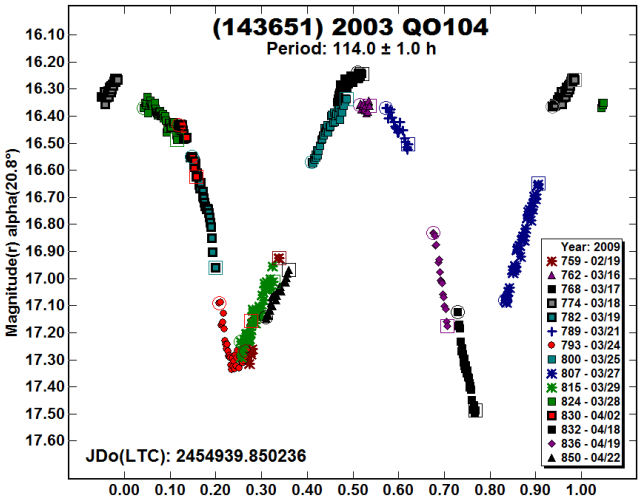

The new fit has the period rounded to 1 h, merely to indicate the likely approximate dominant period. The RMS scatter on the data is 0.040 mag because of the poor single-period fit; nightly internal errors are better.

(152558) 1990 SA. We used 30-second exposures with the Schmidt on successive nights to get fairly long runs on this Amor, totaling about 12 hours on the target. The lightcurve is smooth within the errors in the data, which have RMS scatter of 0.021 mag around the fit.

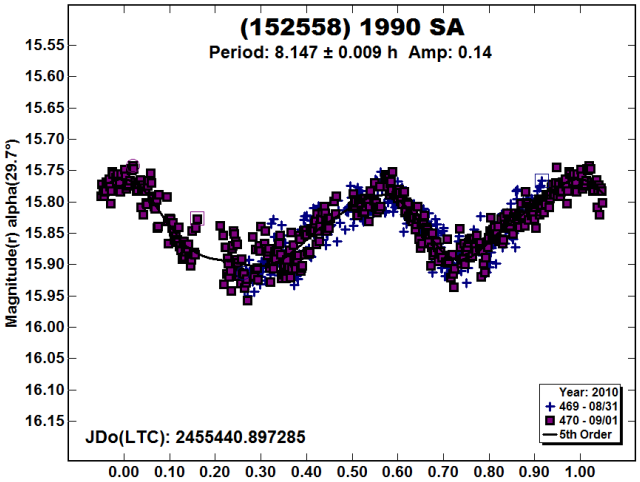

(152952) 2000 GC2. We caught this faint, fast-moving Amor on three nights in 2010 Sep using the Schmidt and 0.7-m telescope. The amplitude turned out to be small, giving only 3-sigma significance in the period determination. The noisy segments of each 'session' (~0.06 mag RMS) could be linked reliably only by being confident that the magnitudes for the comparison stars were consistent to ~0.01 mag across the series (mainly from Pan-STARRS). We show here a phased plot with the data averaged in three-image 6-minute intervals. The RMS scatter is 0.040 mag. The double period near 8.4 hours is not excluded, and gives a simpler-looking double wave.

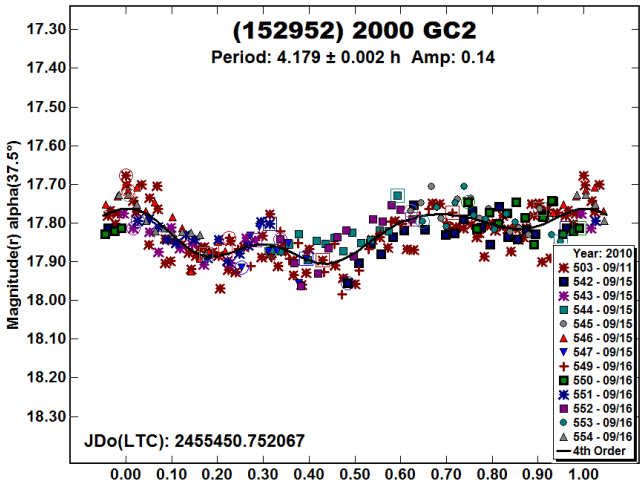

(153814) 2001 WN5. Two photometry runs about two weeks apart were obtained for this 1-km PHA Apollo, which is a LONEOS discovery. We used the LONEOS Schmidt itself in 2010 Oct for the data: two nights of 15-second exposures at fairly high phase-angle, then a single 6-hour run of 30-second exposures at lower phase-angle. The form of the triple-mode lightcurve is not dramatically different between the two, but the amplitude is greatly reduced in the second plot. The RMS scatter on the fits is 0.038 and 0.027 mag, respectively.

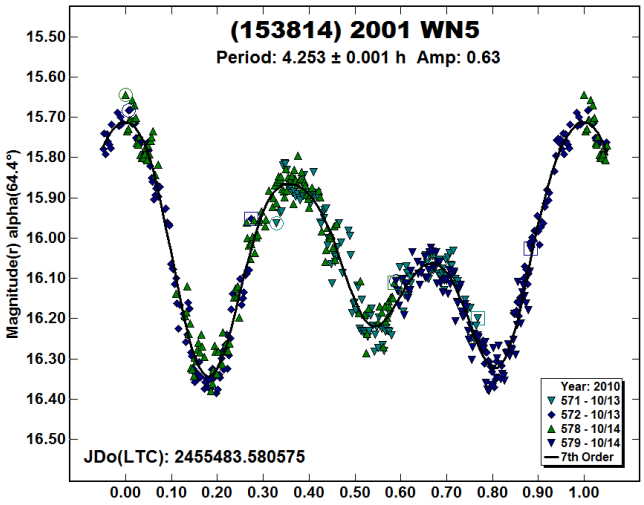

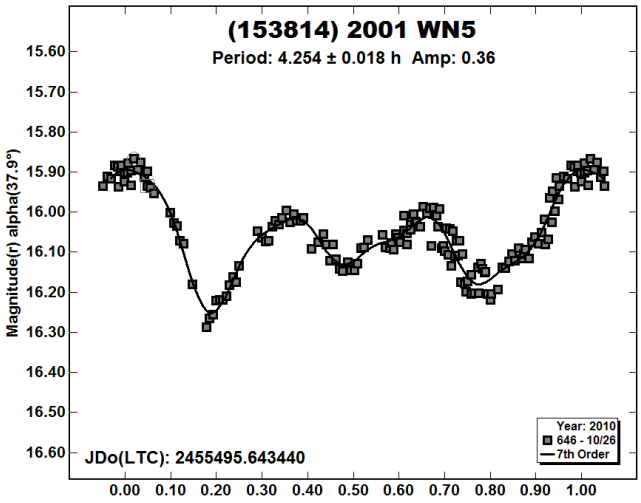

(154029) 2002 CY46. Warner et al. (2011) used data from Palmer Divide and Lowell taken in early Sep 2010 to provide a very clean, small-amplitude lightcurve for this Apollo, which had been observed via radar. There is no reason to repeat those results other than to note we have now adjusted the LONEOS data more closely to Sloan r´. The period derived from our data alone (856 observations) is identical to the combined one presented by Warner et al.; the RMS scatter is 0.014 mag.

(154244) 2002 KL6. Satisfactory datasets were obtained using the LONEOS Schmidt across four lunations between 2009 Jun and Oct, as originally described in Paper 2. Exposures ranged from 30 to 90 seconds. The first lightcurve for this Amor was published by Galád et al. (2010) from data taken at the same time as our first run. The four new phased lightcurves are shown at the same vertical scale, showing the reduction in amplitude and more symmetrical morphology later in the apparition when the phase-

angle was lower. The RMS scatter on each of the fits is about 0.04 mag.

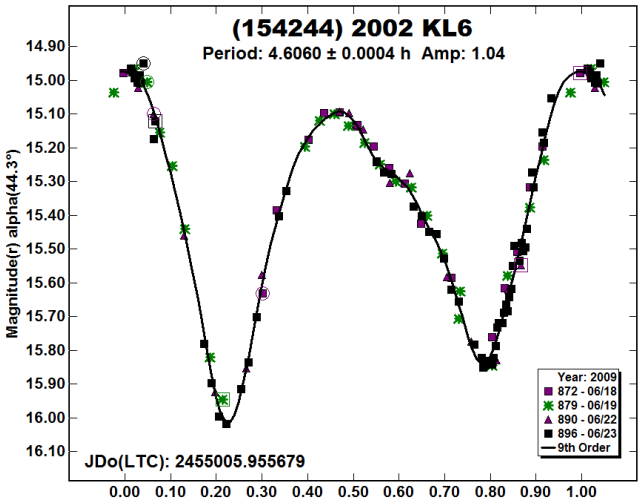

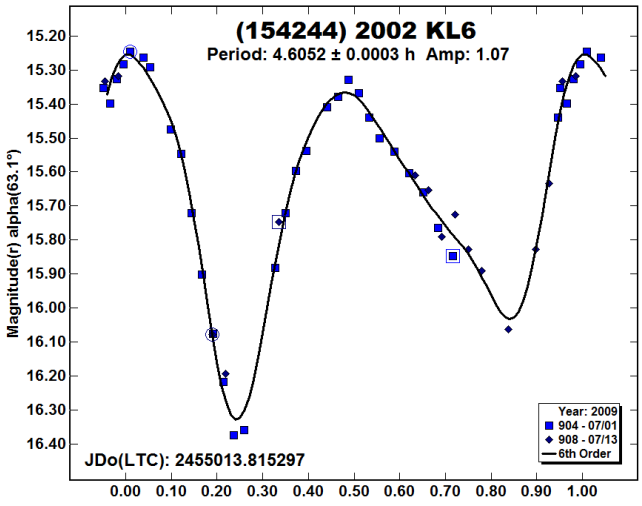

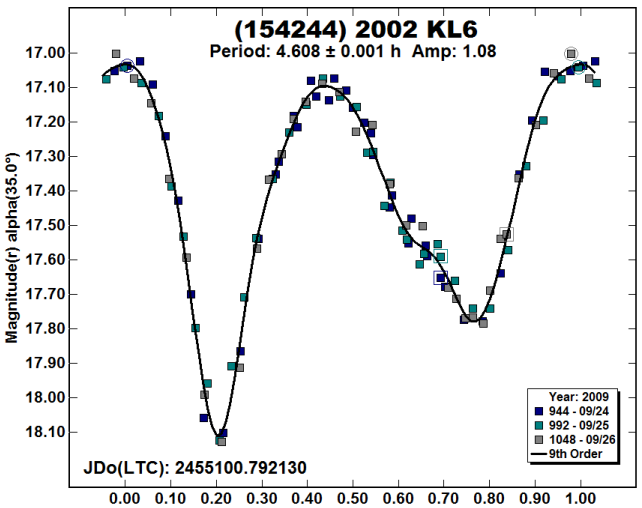

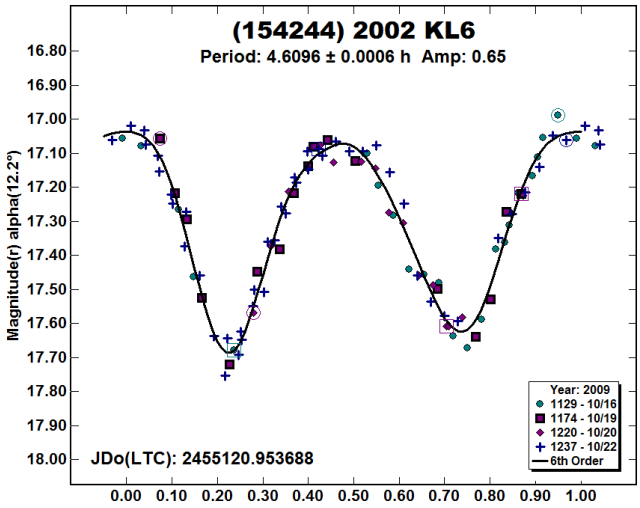

(154278) 2002 TB9. We did not acquire enough data to get complete rotational phase coverage for this Apollo, missing one of the sharp minima. Data on three short nights in 2008 Jun were obtained using the 1.1-m telescope unfiltered. A naïve Fourier fit showed a single-mode lightcurve with half the period indicated, so we adopt the double-mode period, rounded here to 0.01-h precision. The RMS scatter on the order-11 fit is 0.020 mag.

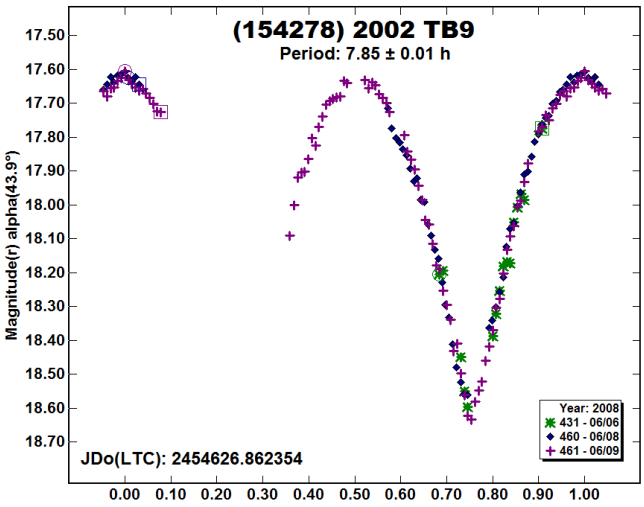

161989 Cacus. We obtained only fourteen observations with the Schmidt over less than 3½ hours on 2009 Feb 19 for this Apollo (cf. Paper 2). UBV colors and period of 3.75 h, considered very rapid at the time, have been known since shortly after its discovery (Surdej and Surdej, 1978; Degewij, 1978). We show a simple order-2 force-fit to this period. Ignoring the unconstrained maximum, the asteroid varied by about 1.1 mag in this interval.

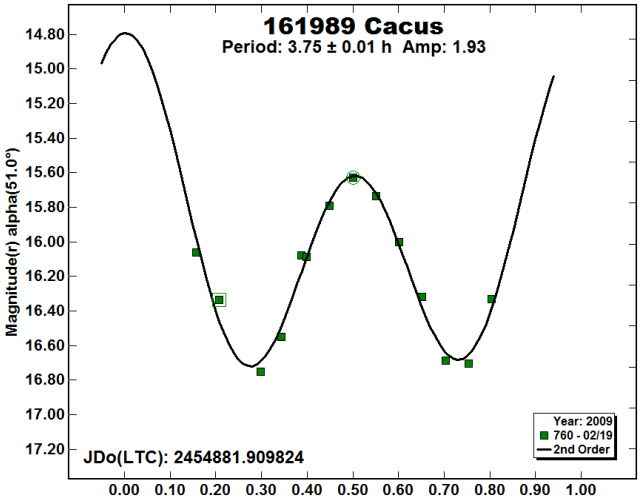

(162385) 2000 BM19. Our observations of this Aten were made using the Schmidt in the few hours before dawn on several nights in 2009 Jan-Feb. Thus we have little overlapping phase coverage. The period is nevertheless unambiguous, as noted in Paper 2; the nightly zero-point offsets mentioned there are removed by revising the comparison star magnitudes using the Pan-STARRS catalogue. The RMS scatter on the fit is 0.046 mag.

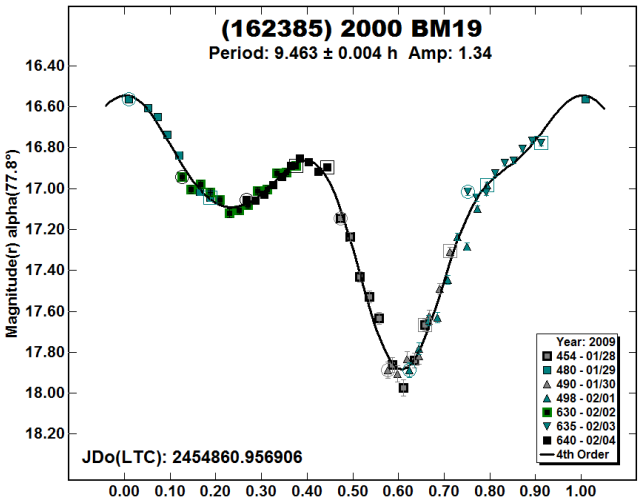

(162900) 2001 HG31. There is no significant change in what we presented for this tumbling Amor in Paper 1: about 660 Schmidt observations through 2008 Oct-Dec plus two nights in 2009 Mar. No simple periodic lightcurve is found from our data. Only the comparison stars have been adjusted more closely to Sloan r´ throughout the apparition, and the revised data deposited in the ALCDEF database. The temporal coverage is shown in a plot of the raw data with no H,G correction.

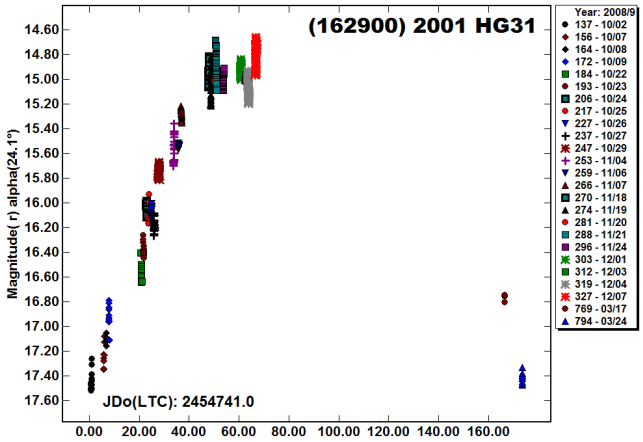

(163000) 2001 SW169. This Amor is another object for which our observations are inadequate. In Paper 1 we gave a poor, notional fit from Schmidt data taken in 2008 Sep-Oct. After adjustment of the comp stars, we now show another unsatisfying fit, and almost certainly wrong. Stephens (2016) showed a lightcurve fit to one of several similarly valid periods from his more extensive data. It could be that the situation is complicated, involving tumbling or very long periods, so there is no firm conclusion yet.

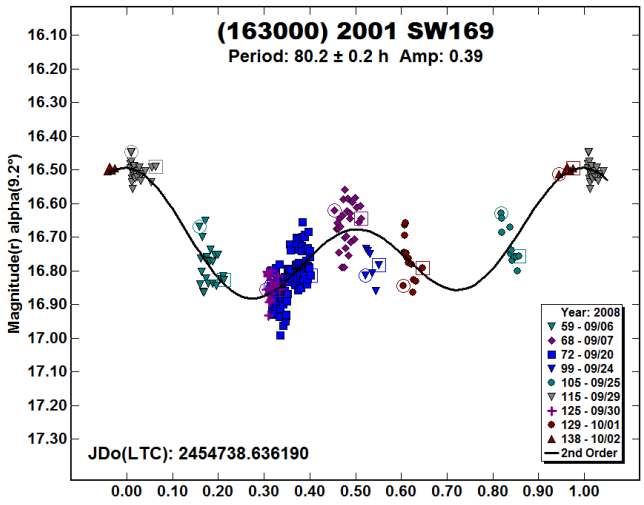

(164716) 1998 GH. We obtained only a single night on this Hungaria using the 0.7-m telescope in 2010 Nov, but the 9.7-hour run covered about 3½ rotational cycles of the small-amplitude lightcurve. Our period is not far from the 2.645-h period given by Waszczak et al. (2015) from sparse data in the Palomar Transient Factory survey. This is rated quality U = 1 in the LCDB, but we essentially confirm it as correct within our mutual errors. The RMS scatter on the simple order-2 fit is 0.026 mag.

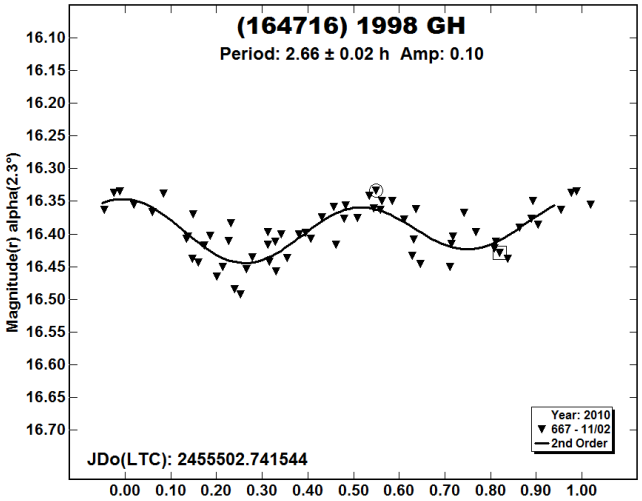

(174599) 2003 QM70. The rotation period of this Mars-crosser must be several tens of hours, but we obtained only two nights on the target using the 0.7-m telescope. We show a notional fit to the data, which is possibly half the true period. The RMS scatter on the fit is 0.030 mag.

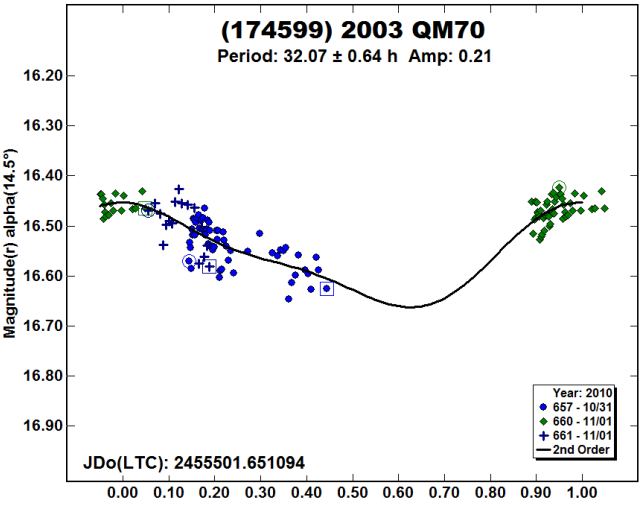

(175706) 1996 FG3. This is a well-known binary Apollo having a very dark surface and low orbital velocity relative to Earth (Walsh et al., 2012). We observed it on five nights in 2009 Mar-Apr using the Schmidt with exposures of about two minutes. The phase-function coefficient *G* was found to be –0.07 by Pravec et al. (2012), which we adopted for the reductions here. In Paper 2 we were not able to fit the photometry properly due to assuming the incorrect default value for G (0.15); the lightcurve there is wrong. The new period determination is similar to the short period of the binary first identified by Mottola and Lahulla (1998) and Pravec et al. (1998b), though our data are fairly noisy (RMS scatter 0.045 mag), probably from not also accounting for the longer 16-h orbital period.

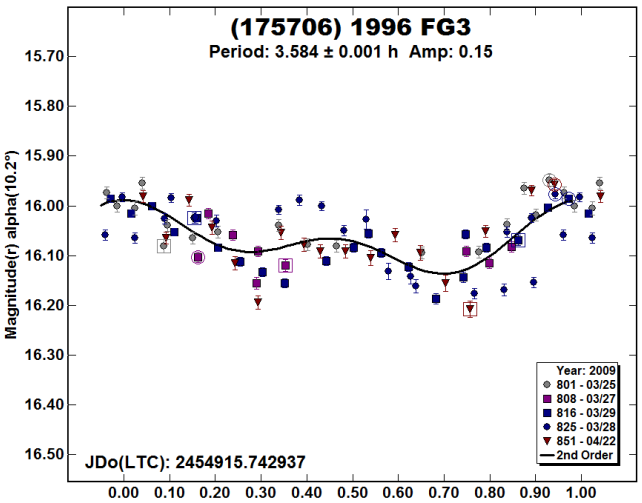

(184990) 2006 KE69. This 2-km Apollo is a LONEOS discovery. In 2008 May we obtained two nights of unfiltered photometry using the 1.1-m telescope. The asteroid was faint, so the data are noisy, but produce a weak lightcurve with a period similar to the provisional one determined by Behrend (2006web) from other observers' data. The RMS scatter on our lightcurve is 0.045 mag. Clearly the object needs further attention.

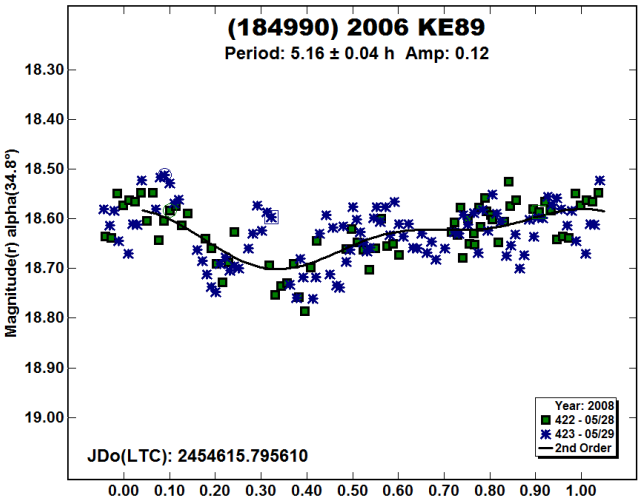

(185851) 2000 DP107. We observed this well-established binary Apollo asteroid (Pravec et al. 2006) throughout 2008 with the LONEOS Schmidt, and 1.1-m and 1.8-m telescopes on 29 nights. Only 17 of these were described in Paper 1; all are now adjusted to Sloan r´ magnitudes. While some isolated groups of nights can reproduce the short-period component of the lightcurve, there is not enough coverage to resolve the complex longer period independently. Below is an example of the short-period variation in Schmidt data from sparsely sampled 30-second exposures on successive nights when it was bright (RMS scatter 0.017 mag). For reference we also show a raw plot without H,G correction of our complete temporal coverage appearing in the ALCDEF database.

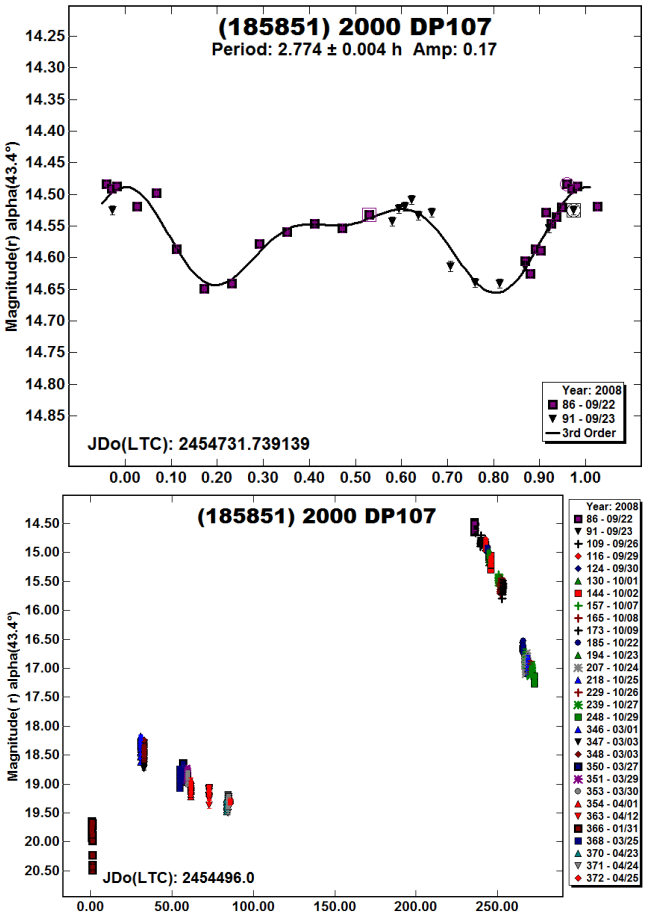

(185854) 2000 EU106. Revision of the comparison stars has not significantly changed the incomplete two-night Schmidt lightcurve for this Mars-crosser from Paper 1. We reproduce this with the period force-fit to 3.5 h, consistent with the later, more complete coverage by Warner (2015). The formal RMS scatter on the fit here is 0.046 mag.

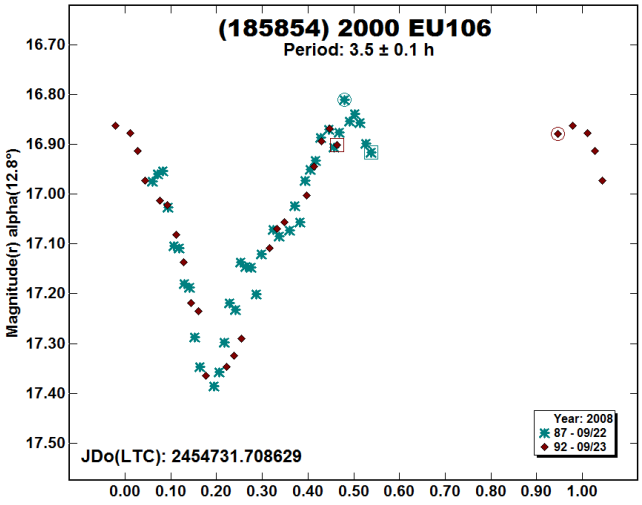

(188452) 2004 HE62. A single 4½-hour run using the 1.1-m telescope on 2008 Sep 7 yielded only ~3/4 of a complete lightcurve for this Amor, capturing two minima but only the secondary maximum properly. The raw data show that the period must be about 5.4 hours, and we adopt a minimum in the period spectrum near that period. The RMS scatter on the fit is about 0.015 mag, but it is somewhat uncertain. The high phase-angle produced the large 1.15 mag amplitude.

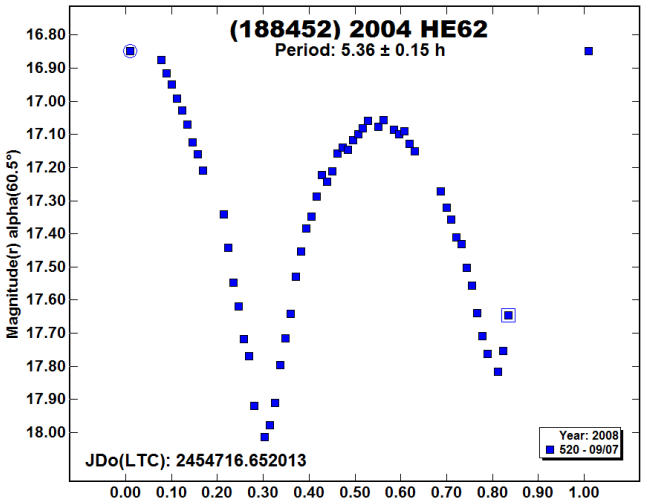

(194386) 2001 VG5. The lightcurve we showed for this Apollo in Paper 2 was basically correct, but did not include all the LONEOS Schmidt data from 2009 Jun. Adopting Pan-STARRS photometry for the comparison stars led to a substantial shift in the apparent magnitudes (brighter), allowed an entire night that was previously omitted to be added (doubling the number of data-points!), and eliminated the large nightly zero-point offsets that were applied. The revised lightcurve is far more secure and is only slightly different than the one published by Warner (2016b). The RMS scatter on the fit is 0.05 mag. An isolated night, 2009 Jan 15, is included in the ALCDEF file for this asteroid.

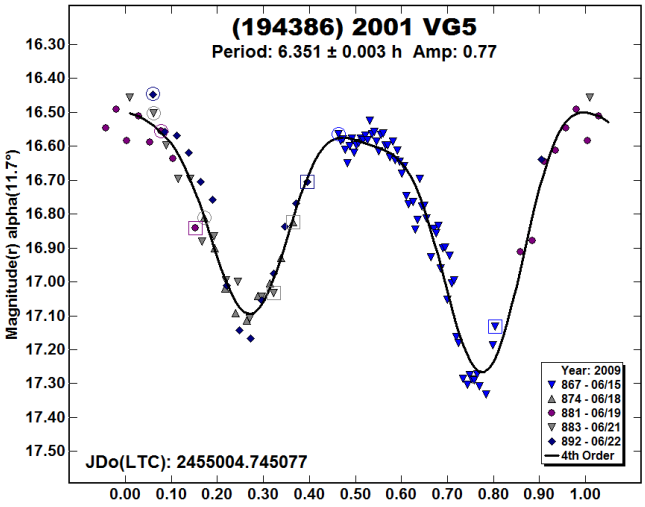

(207945) 1991 JW. A rather scattered lightcurve for this Apollo was shown in Paper 2 from Schmidt data taken in 2009 Apr-May. After adjusting the comparison stars more closely to Sloan r′ we give a cleaner result with better precision on the period. The RMS scatter on the fit is 0.028 mag. These remain the only lightcurve photometry for this asteroid.

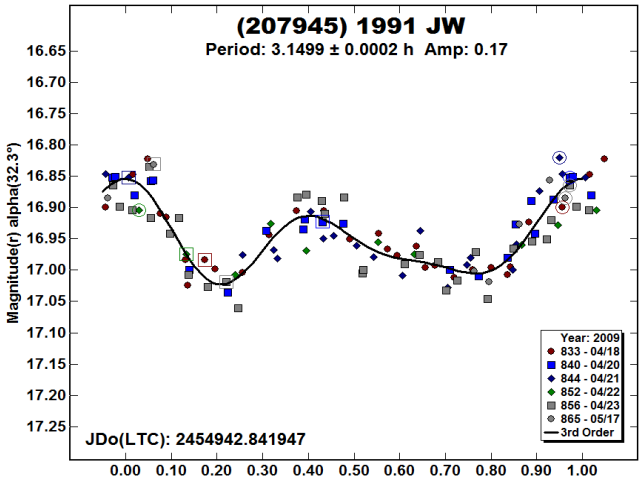

(208023) 1999 AQ10. We gave a data-description but no lightcurve for this Aten in Paper 2, claiming no variation within the uncertainties. Betzler and Novaes (2009), observing for only 4 hours on 2009 Feb 14, gave a period of 2.79 h. Using another short run from the following night by Silvano Casulli, Behrend (2009web) found a provisional period of 2.67 hours.

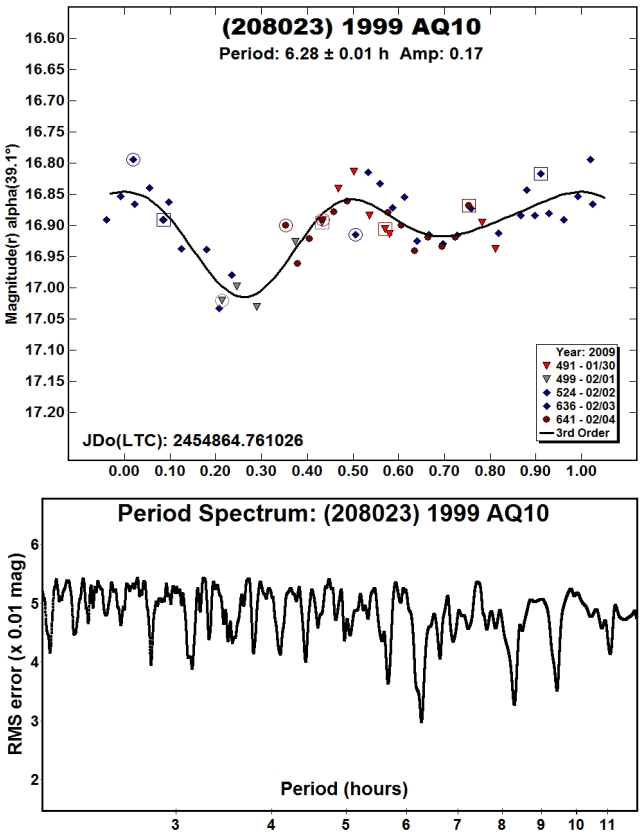

We obtained sparse Schmidt data starting two weeks prior to these on five of the six nights 2009 Jan 30 to Feb 4 with exposures between two and three minutes. After adjusting the comparison star magnitudes, the data now yield a somewhat uncertain period of 6.28 h, which we round to 0.01 h precision. The RMS scatter on the fit is 0.030 mag. We find only a weak minimum near 2.78 h in the period spectrum. The Betzler and Novaes and Casulli-Behrend data could possibly be linked to provide an independent test of both the shorter and longer periods.

(219071) 1997 US9. Observations of this Apollo extended for more than 8 hours on two consecutive nights in 2010 Nov using 45-second exposures with the Schmidt. Thus about 2½ rotational cycles were witnessed each night. The period is somewhat different than that given by Pravec (1998web, 3.52 h). The RMS scatter on the fit to our data is 0.036 mag.

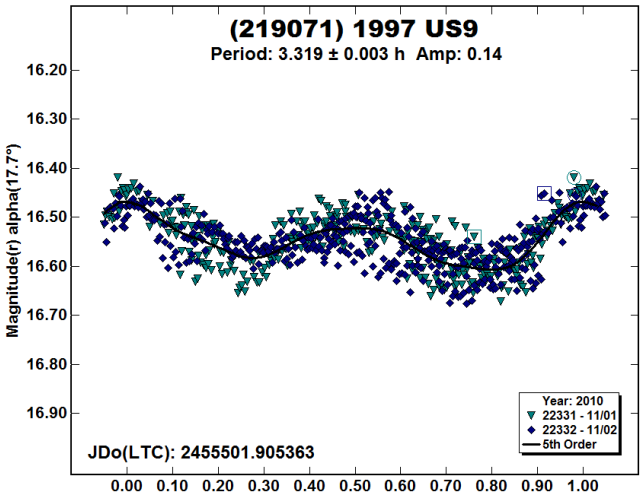

(220124) 2002 TE66. We obtained three consecutive photometric nights of sparse data in 2010 Apr for this 600-meter Apollo using 3-minute exposures with the Schmidt. The data are fairly noisy, but seem to show a moderately short-period lightcurve of small amplitude at 3-sigma significance (RMS scatter 0.05 mag). This is contrary to the 45.4-hour period reported by Warner (2017a).

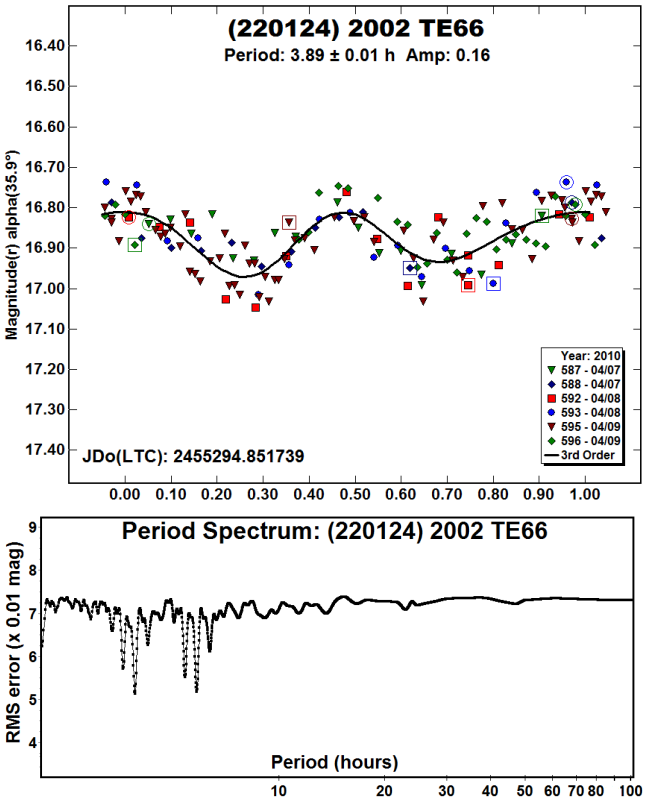

The phased lightcurve along with the period spectrum of the data are shown. The minimum near 5.8 hours is a triple-mode solution (not utterly excluded since the amplitude is small), but no longer

periodicity is present out to the 54-hour baseline of our data. It is possible that the disparate periods reflect some aspect of a very wide binary.

(242211) 2003 QB90. Despite a fair effort to get several nights of data on this Amor, we were unsuccessful in finding the rotation period in 2010 Sep. The series includes one night with the 1.1-m telescope, three more nights using the Schmidt, and finally a night with the 0.7-m telescope. A raw plot with H,G correction is shown below, indicating either a long period and/or small amplitude well below the noise level in our data.

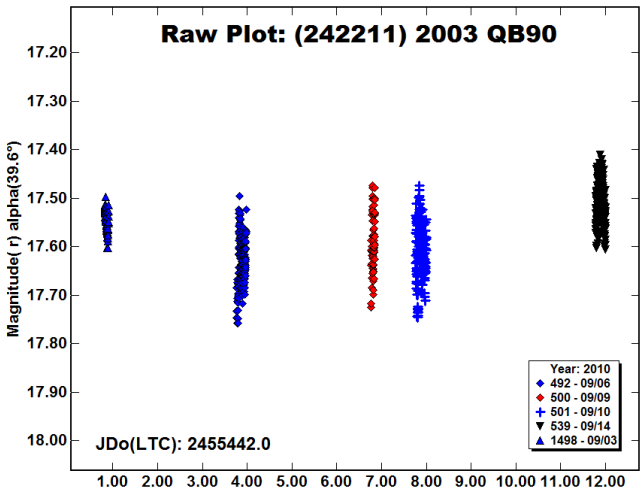

(242643) 2005 NZ6. Our two-hour run from 2008 May on this high-eccentricity Apollo using the 1.1-m telescope unfiltered shows perhaps one-third of a complete lightcurve. A notional fit suggests a period roughly in the range of 6 or 7 hours, but the correct period could be somewhat longer.

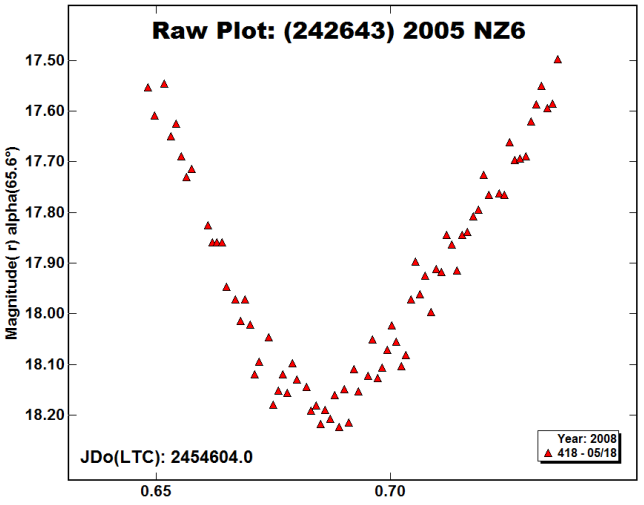

(248818) 2006 SZ217. In Paper 1 we gave only a summary of sparse photometry from LONEOS Schmidt data for this Amor. Revision of the comparison stars now allows us to find a likely period similar to, but different from, an uncertain one by Ye et al. (2009), who observed the asteroid the same week as we did in 2008 Dec. Our period determination is nevertheless also somewhat uncertain, which we round to 0.01-h precision. The RMS scatter on the fit is 0.020 mag, much smaller than the Ye et al. data, where it is approximately 0.07 mag.

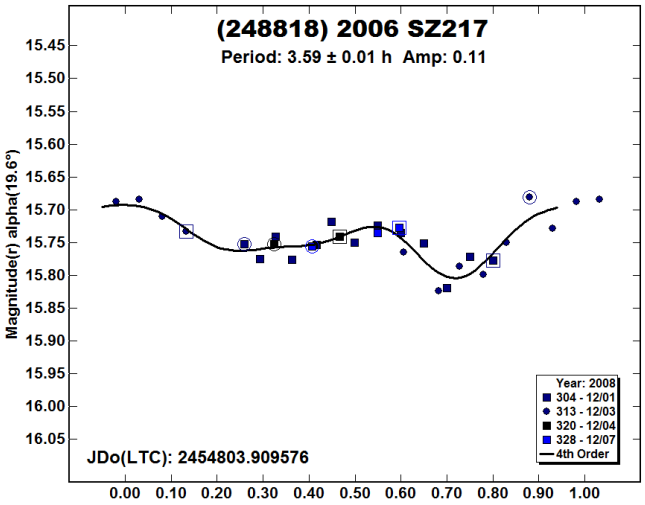

(256412) 2007 BT2. Our observations of this Amor in spring 2009 were insufficient to produce a complete lightcurve, as explained in Paper 2. After revision of the comparison star magnitudes, one could suspect a period of several tens of hours and amplitude of at least 0.6 mag. The asteroid has not been particularly bright since 2009, so there are no further photometric data.

(260141) 2004 QT24. We observed this PHA Apollo on two nights in 2011 Apr using the Schmidt. These high phase-angle data were sufficient to define the large-amplitude lightcurve. The phased plot shows the 671 useful 30-second exposures averaged by threes into 226 data-points. The RMS scatter on the fit is 0.038 mag. The asteroid has not been brighter than V = 18 since 2011, so there is no further photometry.

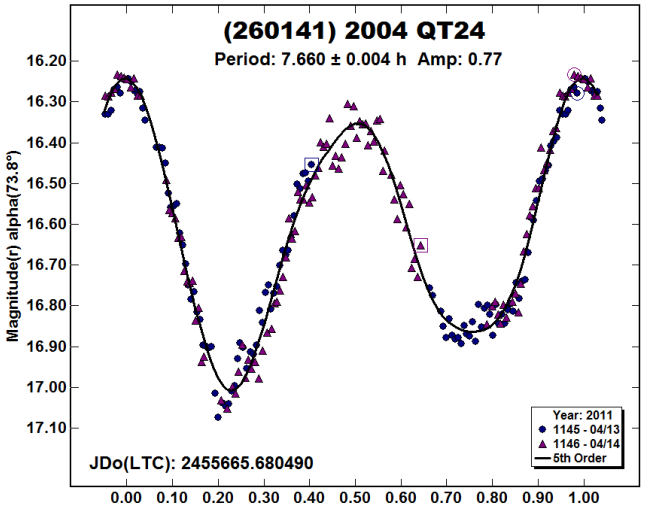

(277039) 2005 CF41. Two nights of data in 2008 May using the 1.1-m telescope were insufficient to give complete rotational phase coverage for this Apollo. The segments do suggest a period near 16 hours, which we round to 0.1-h precision. The RMS scatter on the fit is 0.02 mag.

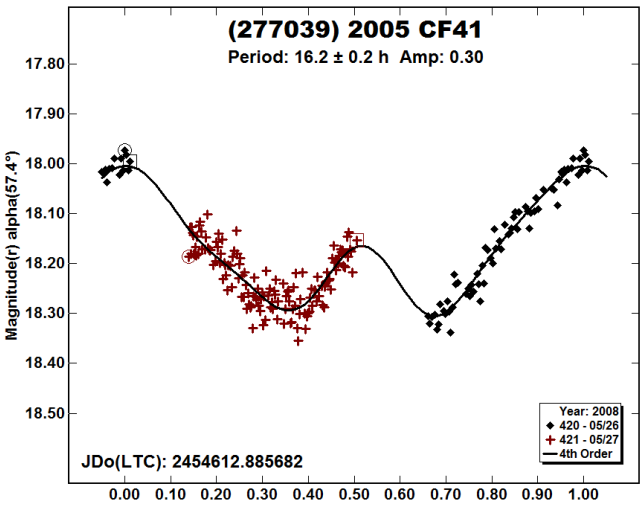

(305090) 2007 VQ4. In Paper 1 we showed a combined lightcurve for this Amor from two isolated nights of 1.1-m data in 2008 May-Jun. After revision of the comp stars it appears preferable to show them separately. The first night covers more than six hours, nearly 2½ rotation cycles, and seems to be reliable, if noisy. The asteroid was much fainter on the second night and so the results are more uncertain. The RMS scatter on the fitted curves is the same for both, 0.024 mag; the second curve is somewhat over-fit.

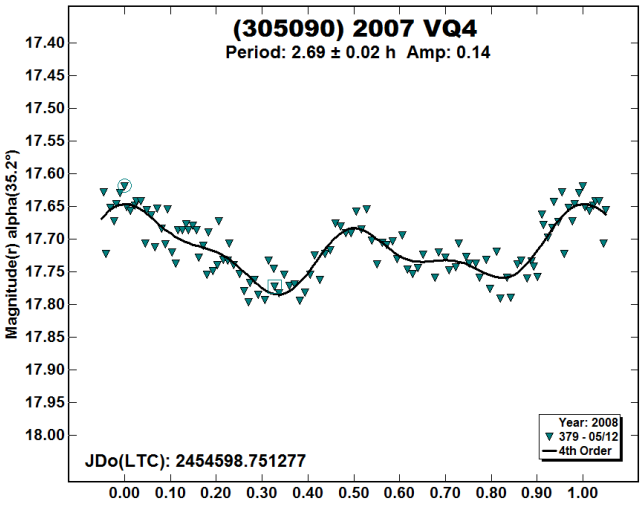

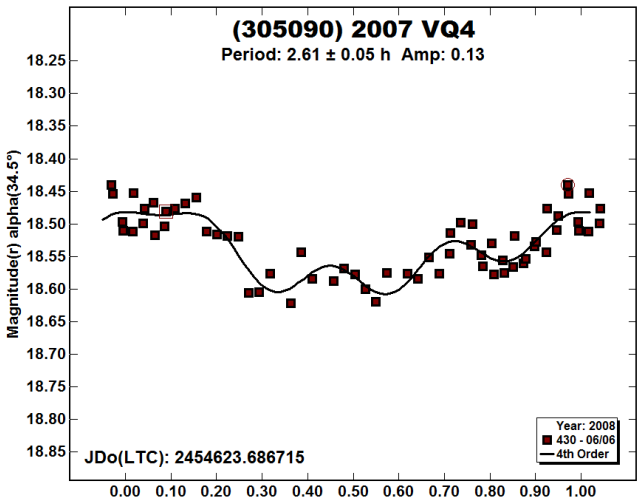

(325769) 2010 LY63. We observed this Amor on four nights using the Schmidt and 0.7-m telescopes in 2010 Sep-Oct. These were insufficient to get a handle on the rotation period beyond saying that it must be long and has a large amplitude, possibly involving tumbling. Periods of many tens of hours are likely, but cannot constrain limits to any useful extent. Only a raw plot of the data (with H,G correction) is offered here.

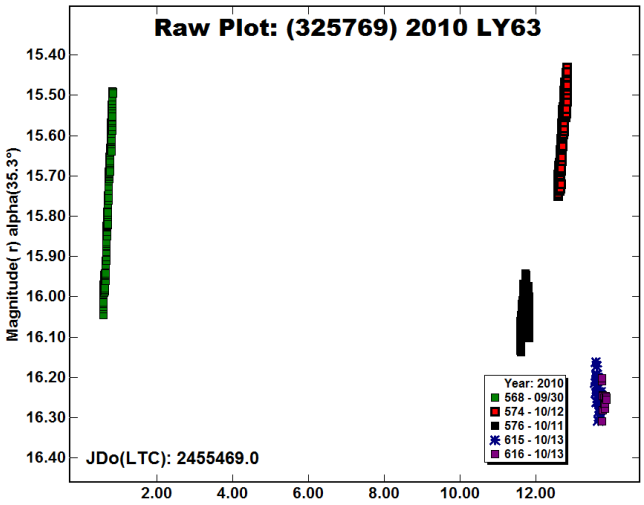

(341843) 2008 EV5. This is a 400-m Aten. Because of a subtle change in amplitude between our two nights of Schmidt data, which were combined in Paper 1, we show them separately here. Note the drop in brightness of half a magnitude in three days. The tiny variation and single-night runs preclude a precise period determination despite having more than two cycles covered each night (8 and 9 hours, respectively). The morphology is the same in the two lightcurves, but the maxima are shifted in phase in the plots. Within our significant errors the periods are the same as those found by others, notably Galád et al. (2009), who also observed it during the final week of 2008. Their lightcurves show much rapid, small-scale variation that is unresolved here; they also note possible intra-night changes in morphology. The RMS scatter on our two phased lightcurves is 0.007 and 0.010 mag.

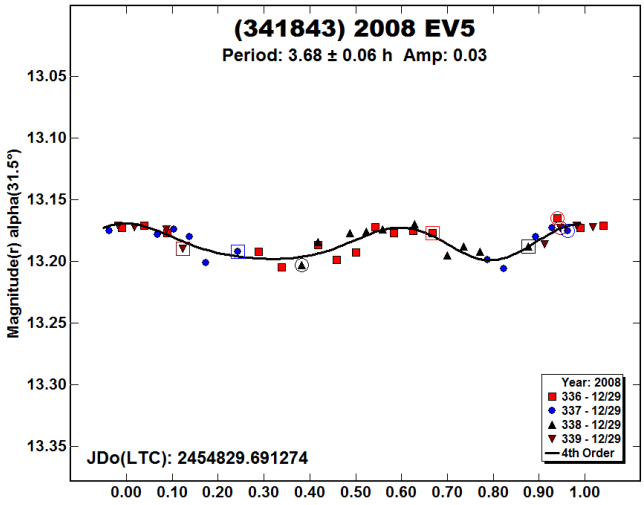

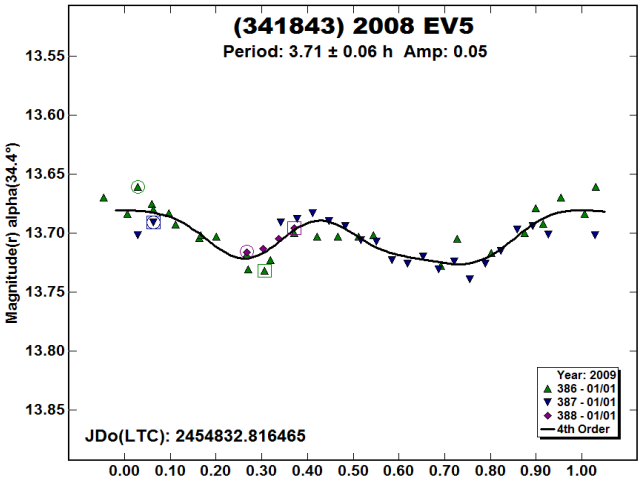

(345705) 2006 VB14. We previously showed Schmidt data in Paper 1 for this 400-m Aten. After revision of the comparison stars, the sparse data from 2008 Dec yield a noisy lightcurve with a period matching two series by Warner (2016c, 2017a). The RMS scatter here is 0.06 mag. The seven-hour run from 2010 Nov 27 covers two rotation cycles, but seems to fit only a somewhat longer period; the RMS scatter is 0.05 mag. The two phased lightcurves are shown below at the same vertical scale. The periods are both rounded to 0.01-h precision due to the sparse sample in 2008 Dec and having only the single night in 2010 Nov.

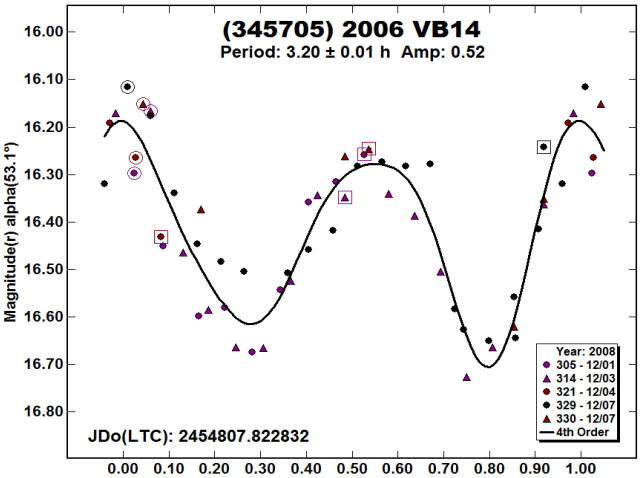

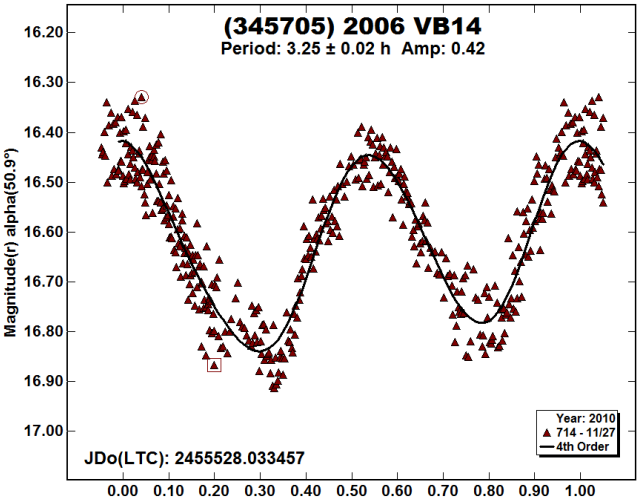

(367248) 2007 MK13. This 400-meter PHA Apollo was observed by Hicks and Somers (2010) at the end of Dec 2009. At the same time, we obtained two nights of sparse data using the LONEOS Schmidt with exposures between 85 and 105 seconds, followed a week later by a single full night with the 1.1-m telescope and 60- or 90-second exposures. Periods derived from these data are similar to Hicks and Somers. The two phased lightcurves are shown to document the spectacular amplitude on 2009 Dec 26. It would be surprising if this was not a contact binary. The RMS scatter on the fits are 0.038 mag (LONEOS) and 0.027 mag (1.1-m).

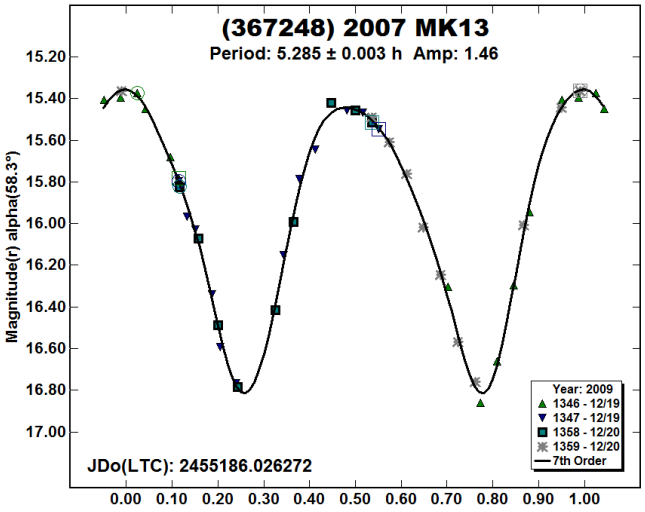

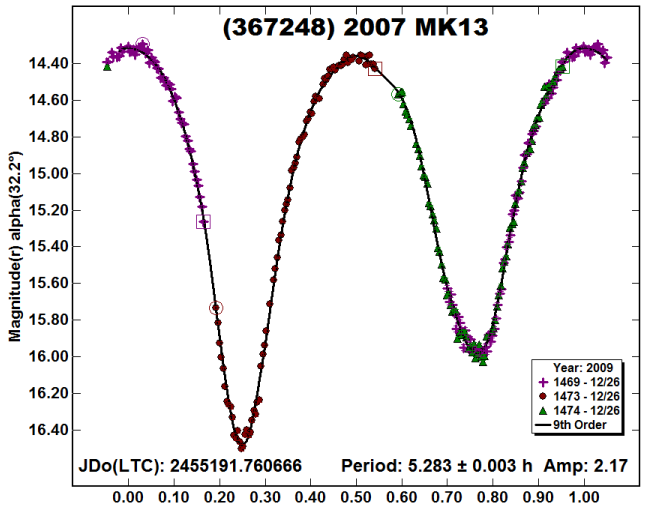

(410650) 2008 SQ1. No lightcurve was shown in Paper 1 for this Amor since the period appeared to be "long" but indeterminate. After correcting the comparison star magnitudes in the Schmidt data taken 2008 Oct-Nov, we found that a single-mode solution of about 23½ hours is possibly valid. We thus show here the double-mode fit at twice this period, which is merely tentative. The phased plot shows the original 414 data-points averaged into 220 three-image 10-minute bins. The RMS scatter is 0.048 mag. As we noted in Paper 1, periods of several hundred hours are not formally excluded, but the data are simply inadequate to infer anything with certainty.

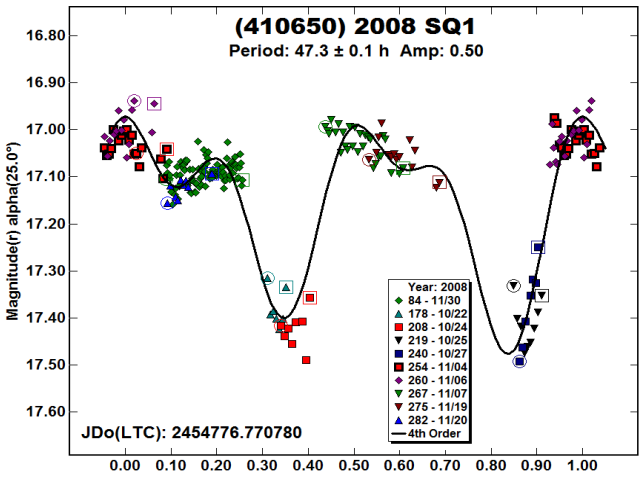

(410777) 2009 FD. We got only a single six-hour run of Schmidt data for this Apollo on 2009 Mar 24. A notional phased lightcurve is shown, which resembles the one published by Carbognani (2011). The morphology is peculiar, and we are skeptical of our results since the derived period is the same as the length of the dataset. Notice the large uncertainty on the period determination. The RMS scatter on the fit is 0.06 mag.

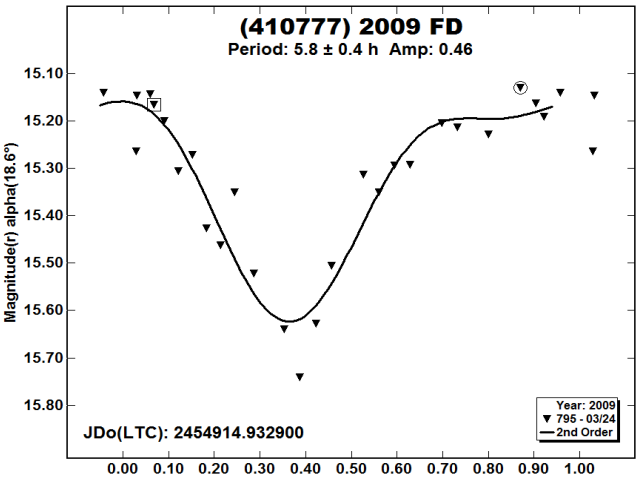

(416801) 2005 GC120. After getting three nights of data in 2010 Dec it became clear that this 1-km Apollo is a tumbler with a non-repeating lightcurve. Analysis was hampered by the rapid change in phase-angle.

By way of example we show a raw plot of the first night below. The complete dataset comprises 800 exposures of 12 and 20 seconds using the Schmidt, covering in total about 12½ hours on target.

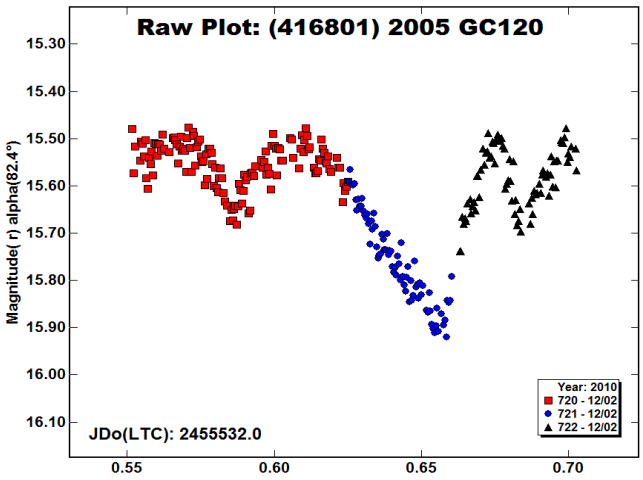

(446791) 1998 SJ70. This is a 1-km Apollo. By correcting the comparison stars in the 2008 Sep-Oct Schmidt data more closely to Sloan r´, we no longer need to make large zero-point adjustments to the separate nightly fragments to make them fit, as was done in Paper 1. Even so, due to insufficient phase coverage and likely weakly tumbling state (Pravec et al. 2014), the periodicity is poorly expressed, and we give a solution similar to the previous one. The RMS scatter on the fit is large, 0.09 mag, caused by the incomplete phase coverage and necessarily low-order fit.

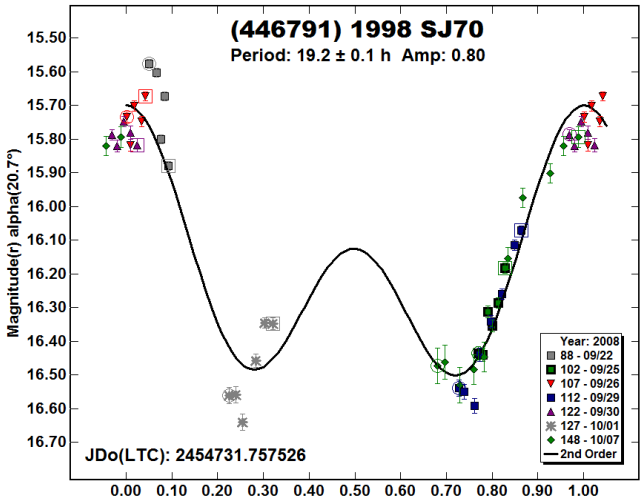

(453778) 2011 JK. By tracking the 1.1-m telescope at half the ephemeris motion of this Amor, we got good results on two nights in 2019 June using 90-second exposures. The short-period, modest-amplitude lightcurve shows relatively subtle asymmetry. The RMS scatter on the fit is 0.011 mag.

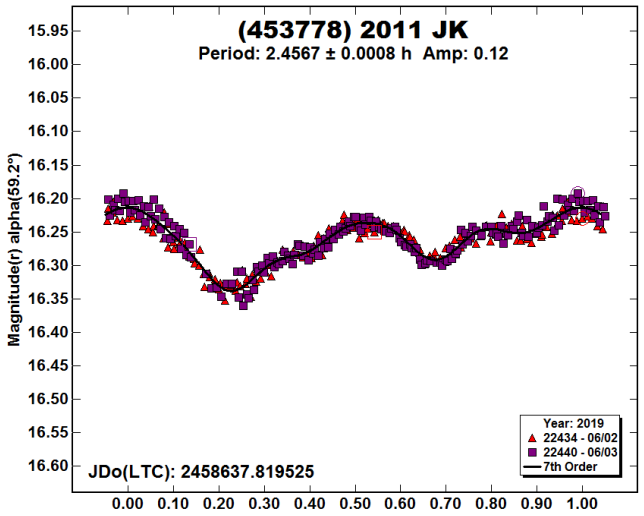

(488515) 2001 FE90. This 200-meter Apollo is a LONEOS discovery; it was observed by three groups during its close passage in 2009 Jun: Hicks et al. (2009), Oey (2011), and ourselves in Paper 2. We obtained Schmidt data on five nights, but only on the last was coverage dense enough and the cadence sufficiently fast (4-second exposures) to capture the rapid, large-amplitude variation. The value for the phase-function coefficient *G* (0.43) was adopted from Hicks et al., as reported in the LCDB. The resulting lightcurve is very smooth, which was calibrated mainly against SkyMapper (Wolf et al., 2018) reference stars. The RMS scatter on the order-6 fit is 0.025 mag. On the earlier nights the phase angle was as high as 103° (2009 Jun 21), and the amplitude implied by the fragmentary lightcurve was well over two magnitudes. Data from all the nights is included in the ALCDEF file.

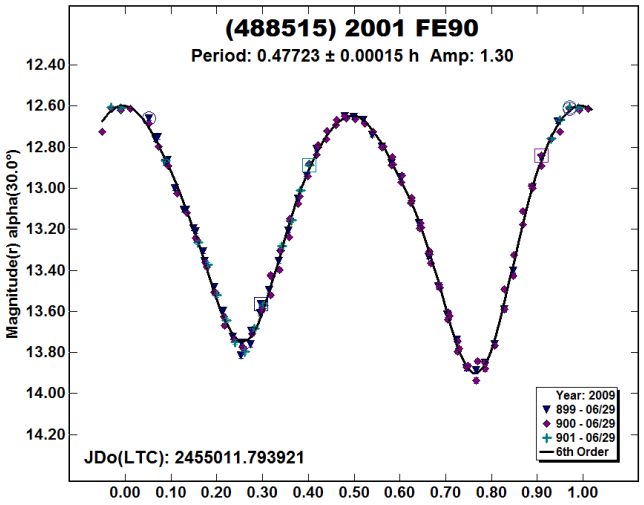

(503941) 2003 UV11. Warner (2018a) obtained a period of 18.25 hours for this 250-meter Apollo. Our two half-nights from 2010 Oct were thus insufficient to get more than a hint of the period. We show a raw plot of the series below, which was done using 60-second exposures on the Schmidt.

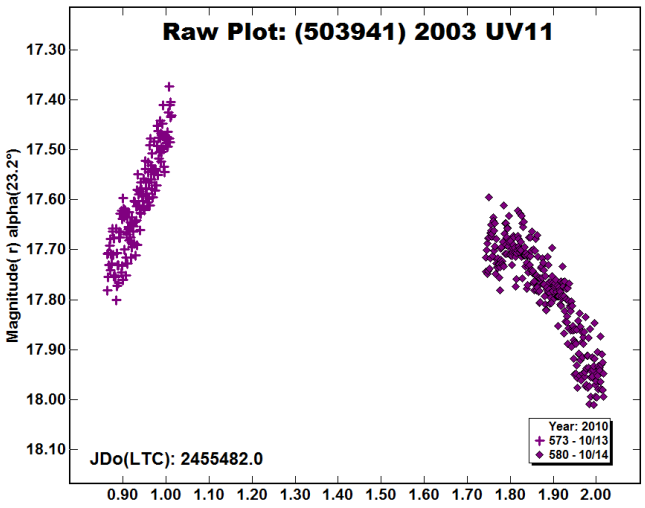

(504025) 2005 RQ6. We obtained two groups of data for this Amor in 2009 Oct using the Schmidt and the 0.7-m telescope. The Schmidt data cover seven of eight consecutive nights and provide an accurate period determination. This period was imposed on the two overlapping nights of 0.7-m data, which has incomplete rotational phase coverage, shown in the second plot. The RMS scatter on the fitted curves is 0.025 and 0.023 mag, respectively.

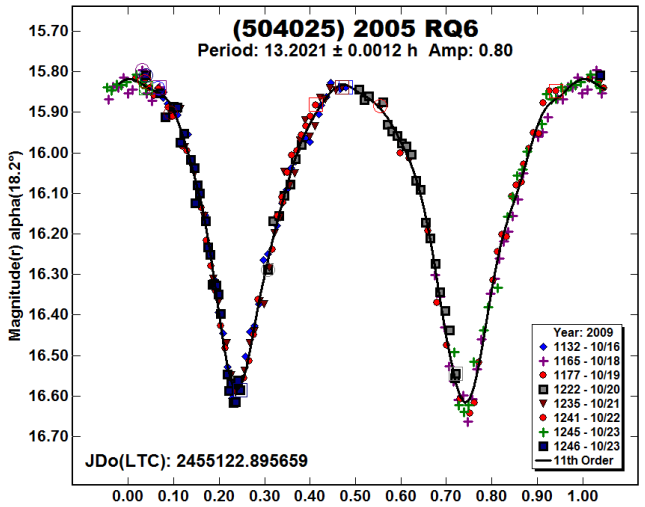

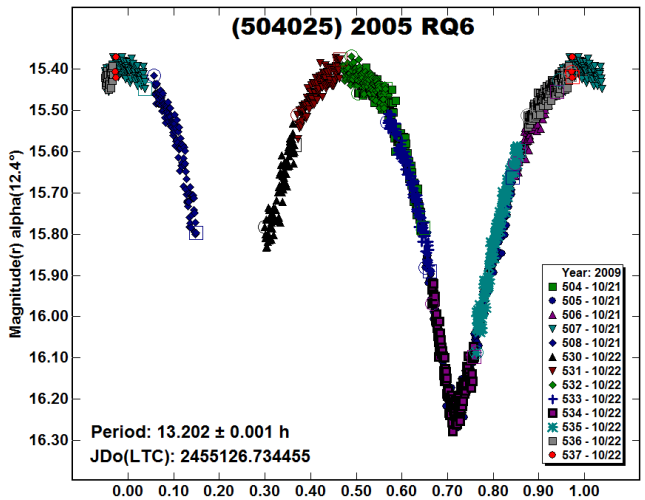

(518638) 2008 JP14. We observed this half-kilometer Apollo shortly after its discovery by the Catalina survey in 2008 May. The two nights of 1.1-m telescope data have an unfortunate eight-day gap, so there is some half- or whole-rotation ambiguity in the period determination, with the aliases separated by ~0.03-hour increments from the period shown in the phased plot. The original 294 data-points are binned here into 150 two-image 5-minute averages. The RMS scatter on the fit is 0.023 mag.

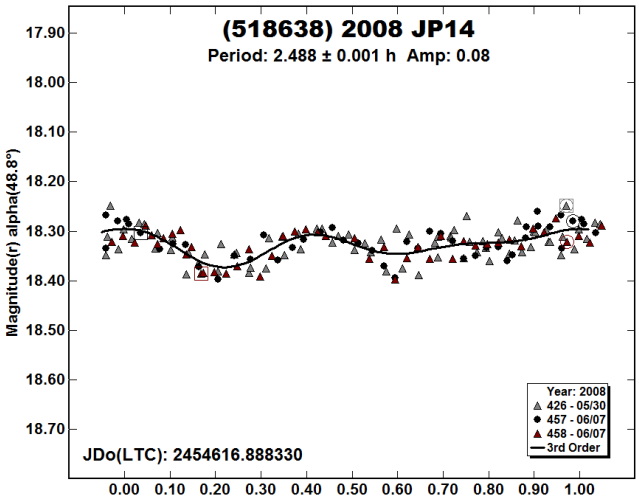

(524522) 2002 VE68. This PHA Aten is a known tumbler with characteristic cycle-length of about 13.5 hours (Pravec 2002web). Although the tumbling aspect of the lightcurve is certain, the two periods involved are not. Our four nights in 2010 Oct with the LONEOS Schmidt are far from adequate to derive this. Thus we show only the rough solution simply to exhibit what we have.

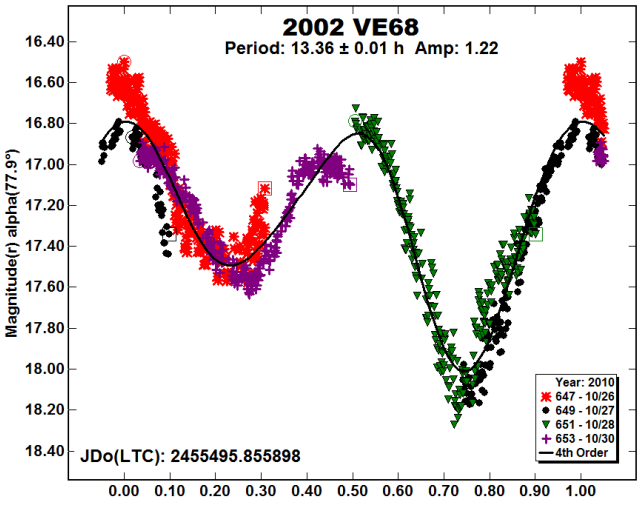

(528159) 2008 HS3. Our three nights using the 1.1-m telescope in 2008 May-Jun gave us only part of the fairly long, large-amplitude lightcurve. A rough double-mode solution is shown, suggesting a period in the 10.7-hour range. The RMS scatter is 0.05 mag.

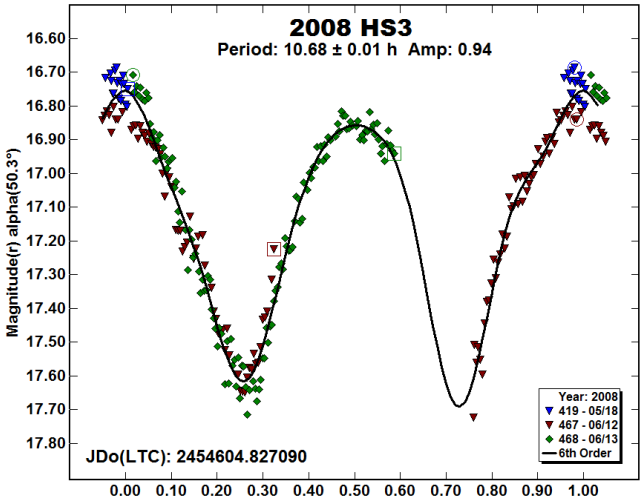

(529668) 2010 JL33. Radar observations of this 2-km Apollo were acquired on the same nights we took photometry in 2010 Dec (cf. Agle 2011). Blaauw et al. (2011) obtained a lightcurve about two weeks afterward. We used the LONEOS Schmidt with 4-second exposures to get about 750 data-points over three nights. Our period is slightly longer than that derived by Blaauw et al.; the data were taken at much higher phase-angle, so the amplitude is larger as well. The RMS scatter on the fitted curve is 0.015 mag. We omit data for Dec 10 (phase angle 76°) since the slope in the data in much steeper than the later nights (larger amplitude implied).

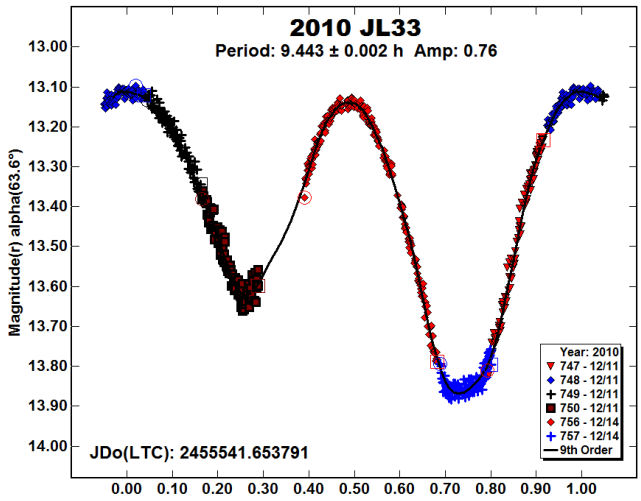

2004 XK3. Observations of this small (~40-meter) Apollo were described in Paper 1, apparently a unique dataset, but no period was determined. Adjustment of the comparison stars on the 7-hour run of 1-minute Schmidt exposures allows a tentative rapid rotation to be found. The data were taken on a cirrus-y night, so the period is suggestive only, though two of the three 'sessions' also show the 0.48-h period. The RMS scatter is 0.07 mag, making the lightcurve of barely 3-sigma significance.

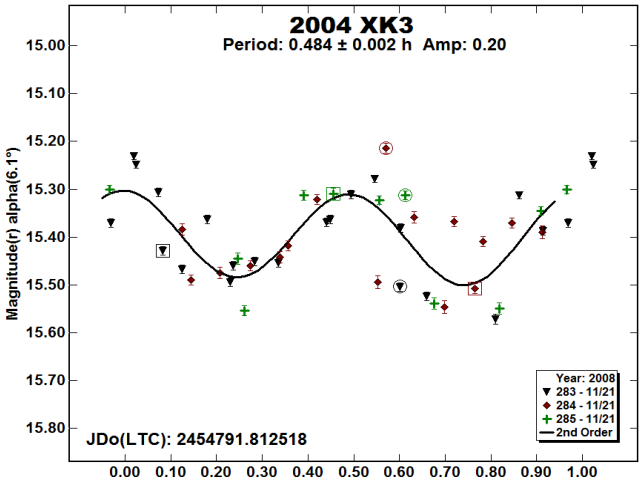

2007 RU17. Three nights of relative sparse data using the 0.7-m telescope yielded only limits on the variation of this Apollo. The raw plot indicates either long period and/or small amplitude with RMS scatter of roughly 0.03 mag.

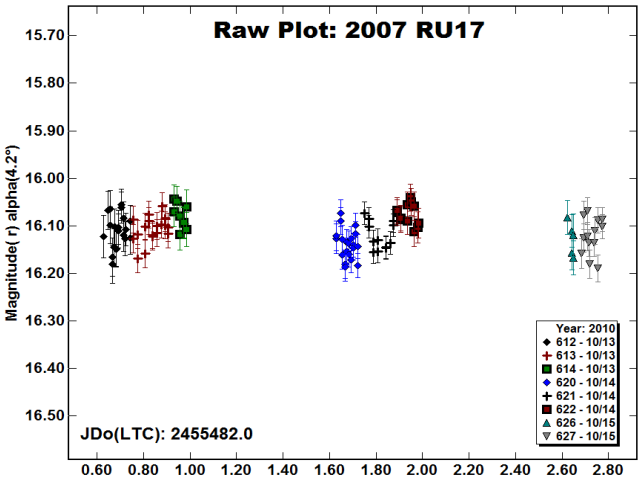

2008 JT35. This 200-meter Amor has not been observed since the discovery apparition. We obtained two nights of photometry in 2008 Jun using the 1.1-m telescope, totaling about 9 hours on the target with 260 unfiltered 75-second exposures.

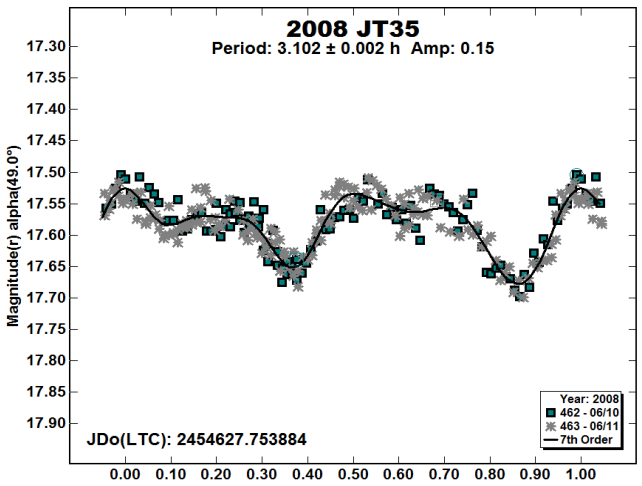

The lightcurve is somewhat complex, featuring broad, double-peaked maxima. The RMS scatter on the fit is 0.020 mag.

2008 QS11. Our presentation of data for this Apollo in Paper 1 was erroneous due to inconsistent comparison star photometry. The ~47-hour period we showed there is invalid. A previously unreduced night of LONEOS Schmidt data was recovered and is now included. The SkyMapper catalogue (Wolf et al., 2018) was used to establish a stable photometric zero-point for this series while the asteroid was well south of –30° Dec, and for the many bright (mag 10-12) comp stars adopted. Although the period must be fairly long, we remain uncertain of the revised results because of gaps in observing. The phased plot shows our best guess, but it is only a notional fit. Many of the exposures were only 10 or 12 seconds in order to reduce trailing. For clarity, the phased plot shows the original 1443 data-points binned into 295 five-image 10-minute averages. The resulting RMS scatter is 0.019 mag.

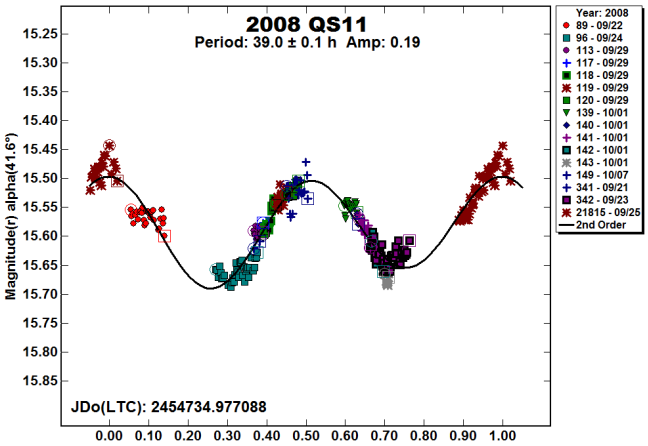

2008 SA. This quite small Apollo (H = 25, roughly 25 meters diameter) was followed astrometrically for only four days in 2008 and has not been seen since. We got a 5-hour run of 45-second exposures with the LONEOS Schmidt on the night after discovery, evidently the only such data.

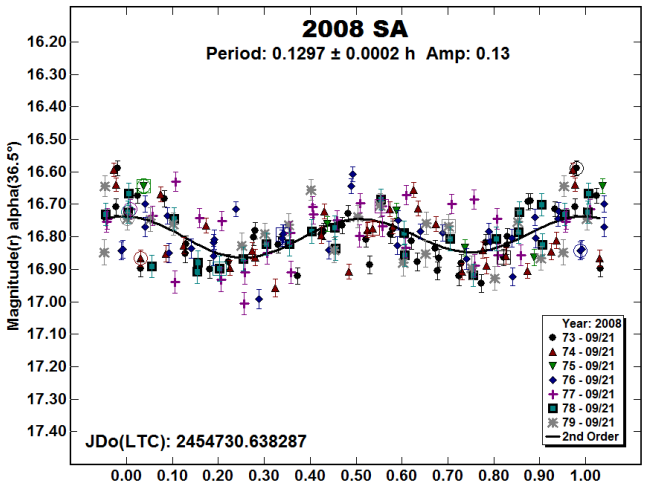

In Paper 1 we showed a raw plot of most of the data, but found no rotation period. The small size allows rather fast periods, and indeed we now find a weakly defined cycle of about 0.13 hours (about 8 minutes). The phased plot now shows all the data. The RMS scatter is 0.07 mag compared to the full amplitude of just 0.13 mag, thus under 2-sigma significance. However, most of the

separate 'sessions' also show periods near 0.13 hours. This is in the middle range of known periods for asteroids of this size. The exposures were roughly 10% of the cycle length, so lightcurve features are smoothed over and the apparent amplitude is reduced.

2008 SE. We observed this Amor on two nights in 2008 Oct using the LONEOS Schmidt and 3-minute exposures. Adjusting the comparison stars did not improve the results compared to Paper 1. We thus show essentially the same lightcurve as before; the approximate period is only roughly similar (and inferior) to those by Warner (2009, 4.57 h) and Statler et al. (2013, 4.44 h), who both observed one month later. The RMS scatter on the fit is very wide, 0.11 mag.

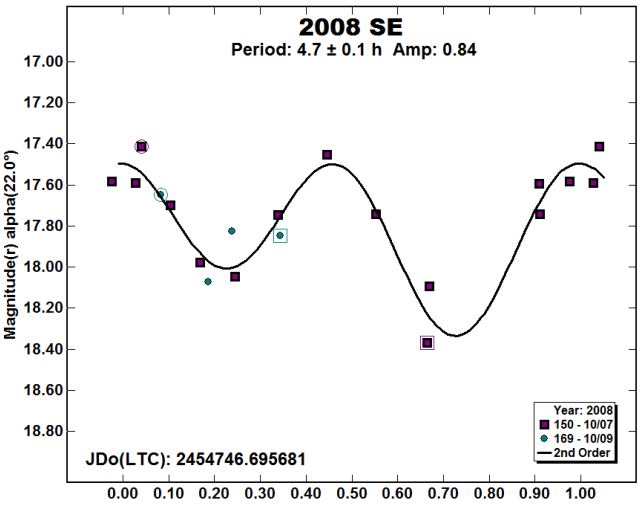

2008 SR1. As outlined in Paper 1, we obtained only a handful of measurements on two nights with the LONEOS Schmidt for this Apollo asteroid, which has not been recovered. Revision of the photometry allows the suggestion (and no more) that there could be periodicity near 11 or 22 hours. We show a notional fit below.

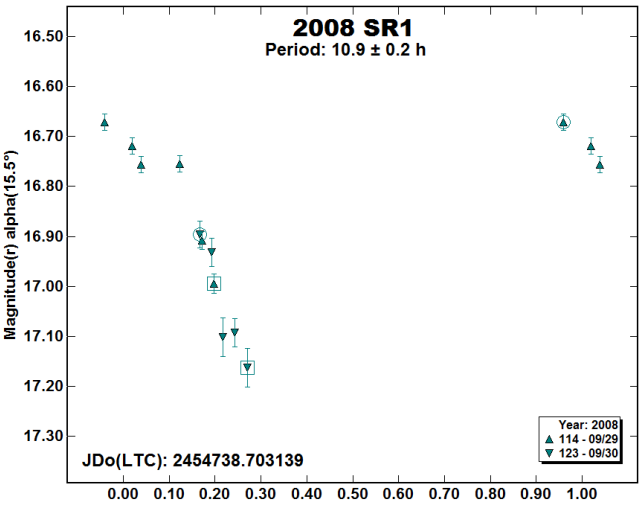

2008 WL 60. Our data from Paper 2 are the only ones available hitherto for this Amor. Revision of the comparison stars improved the results significantly. The new lightcurve has RMS scatter of 0.038 mag from 129 unfiltered 3-minute exposures using the Schmidt.

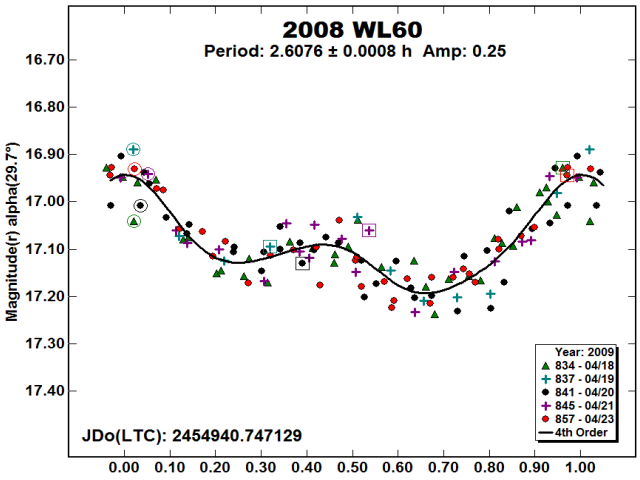

2009 DO111. We reported a rough but correct lightcurve for this rapidly-rotating 80-m Apollo in Paper 2. The first two nights of observation with the LONEOS Schmidt were done with 50- and 30-second exposures, and so the lightcurve is smeared out and has reduced amplitude over the 3-minute rotation period. On the final night we took 15- and 16-second exposures, which captured the morphology more clearly, but we simply did not get enough data-points. The fits on the two phased lightcurves have RMS scatter of 0.032 and 0.024 mag. The excellent lightcurve by Adrián Galád at Modra (Vaduvescu et al., 2017) from 2009 Mar 16 is greatly preferred.

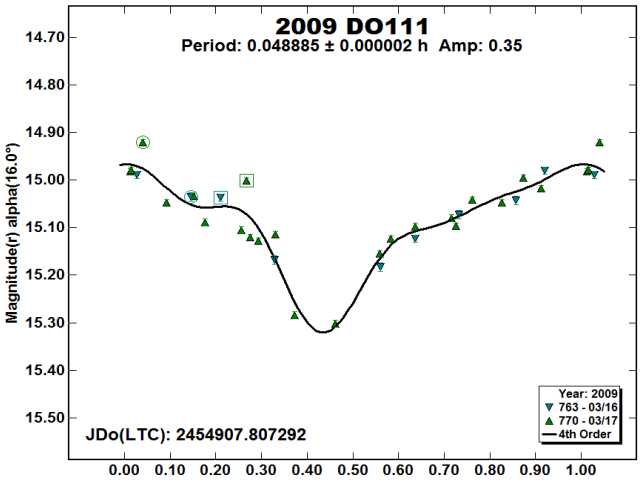

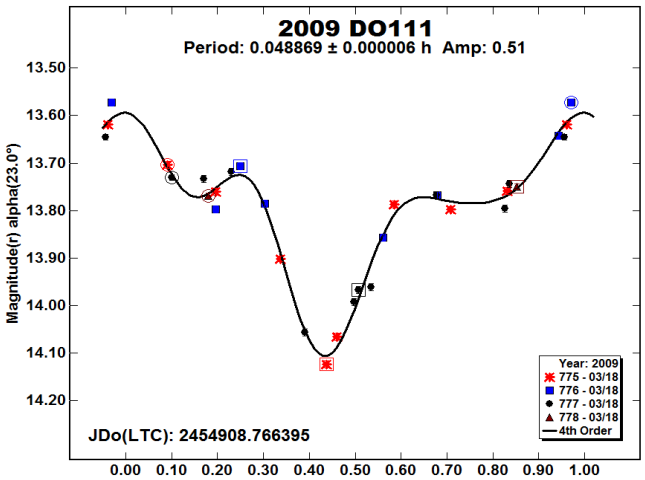

2009 JM2. The 2009 May lightcurve we showed in Paper 2 from Schmidt data exhibited little variation for this Apollo. After adjusting the comparison stars carefully, it seems clear the period is at least many tens of hours, but our data are insufficient to get a convincing solution. We show a fit to a local minimum in the period spectrum, but this is probably wrong. The only other minimum is near 80 h, which is the total length of the time series, and thus also suspect.

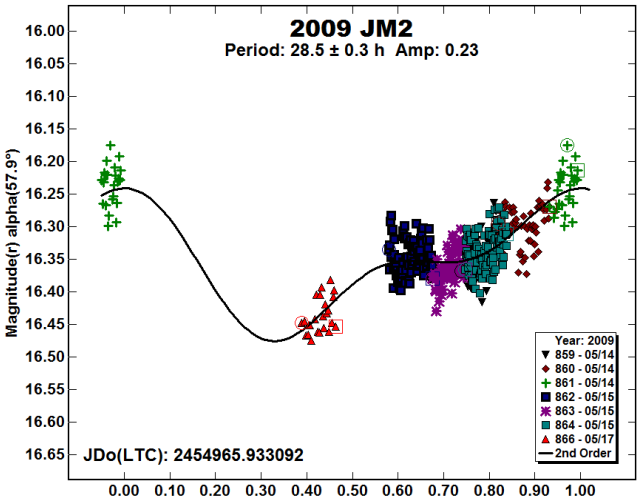

2009 UU1. We got only a short run of images on 2009 Oct 24 using the Schmidt for this very small (H = 24.7), fast-moving Apollo asteroid. Ryan (2009web) previously found a period of 0.12367 h (7.4 minutes) from high-quality data taken with the 2.4-m Magdalena Ridge telescope. Forcing our much lower quality data to this period produces a jumbled lightcurve. We show here a double-mode fit to our revised photometry, which is both sparse and compromised by relatively long exposures (22 seconds). This is not the half-period, but something slightly longer, and could be significantly in error. The RMS scatter is 0.19 mag because the object was essentially disappearing in the deep minima. Ryan's results are surely to be preferred. We very much appreciate Bill Ryan (*priv. comm.*) re-examining his unpublished trove of archive photometry for this object, which aided the interpretation of our results.

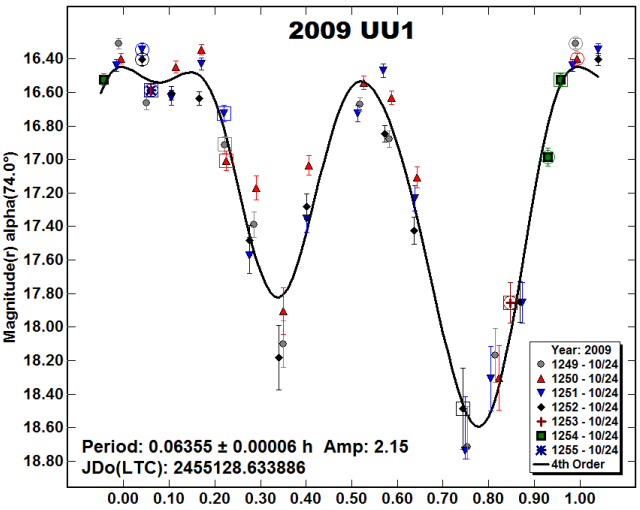

2010 LF86. Linder et al. (2013) observed this Amor during the lunation after we did late in 2010 and got the identical rotation period and lightcurve of very similar morphology. Our data were taken in 2010 Nov under bright ,oonlight with the Schmidt using 45-second exposures, covering about 7 hours each night. The RMS scatter on the fitted lightcurve is slightly over 0.05 mag, with the brightness near the comfortable limit of the Schmidt.

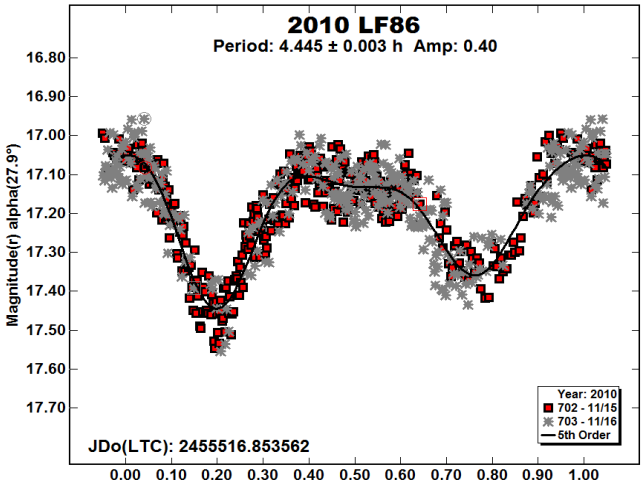

2010 RC130. This Apollo, perhaps 100 to 150 meters diameter, is the second of the exemplar asteroids dealt with in the paper by Harris et al. (2014) on the maximum amplitudes of lightcurve harmonics (cf. 5404 Uemura above). In this case the asteroid is tumbling rapidly, producing, on the face of them, wild-looking variations, which are physically untenable because of the large amplitudes. A pseudo-period of about 8.7 hours results from resonances of the two shorter periods of the tumbling state. All this, including the resolved lightcurves, is outlined in Harris et al. The four nights of LONEOS Schmidt data that we contributed to this work, about 1150 30- and 45-second exposures from 2010 Sep 26-29, are now adjusted closely to Sloan r´. The asteroid has not been bright since the discovery apparition and remains unrecovered.

2010 RF181. We got only a 5-hour run using the Schmidt for this Apollo on the night prior to data by Vaduvescu et al. (2017). They claimed a possible period of 4.6 hours, but our raw plot below shows only a fraction of a normal double-mode lightcurve, so the period must in fact be much longer, several tens of hours. The asteroid was followed only in late 2010, and has not been recovered since then.

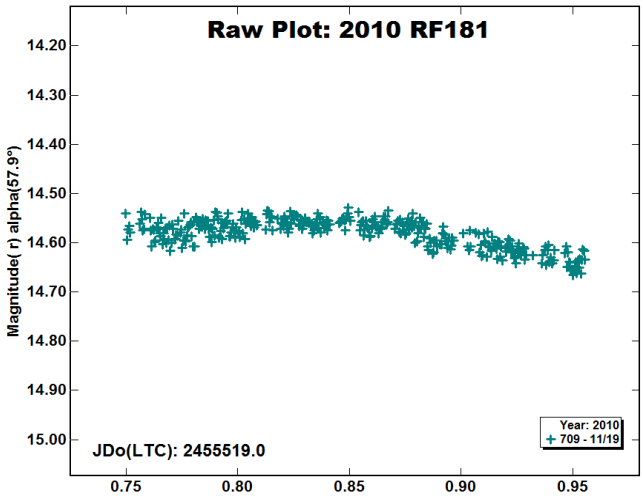

2010 SC41. This Apollo appears not to have been observed photometrically except by us. We obtained three nights in 2010 Nov using the 1.1-m telescope and R_c filter. These phase together very nicely into a nearly symmetrical lightcurve. The RMS scatter on the fit is 0.022 mag. Another night using the LONEOS Schmidt was taken under cirrus and bright moonlight. These results are poor, but they are included in the ALCDEF dataset.

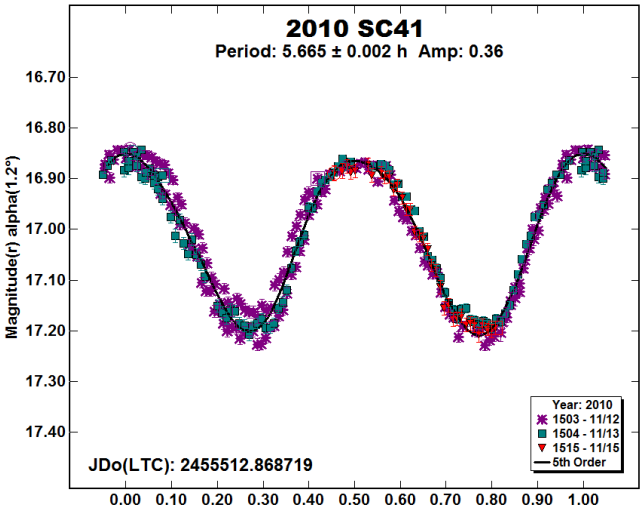

2010 TC55. Statler et al. (2013) observed this 300-meter Amor for about 4 hours on one night in 2010 Oct. Their rotation period is similar to ours from two nights of Schmidt data taken ten days later, and agrees within our mutual uncertainties. We show the phased lightcurve with the original 566 data-points binned into three-image 4-minute averages. The RMS scatter on the fit (0.042 mag) is fairly noisy compared to the modest lightcurve amplitude. The asteroid has not been brighter than V = 23 since 2010, so has not been recovered.

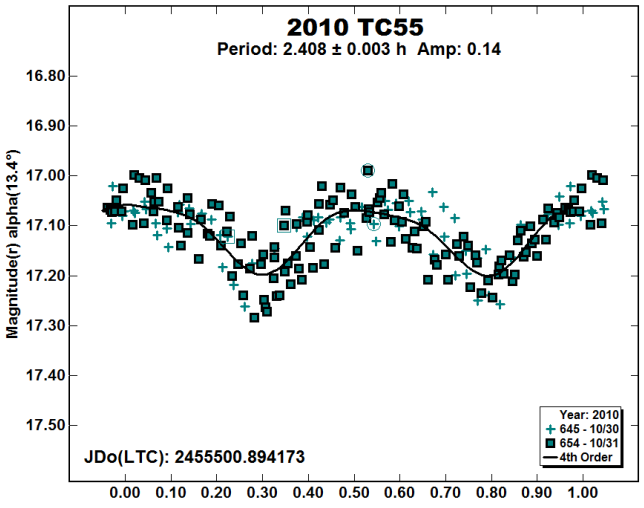

2010 TU5. This is another unrecovered Apollo, which has not been seen since 2011 Jul. We followed it over three nights using the Schmidt in 2011 May. The phase-angle was quite high, which explains the large lightcurve amplitude. The 829 original 45-second exposures are shown below binned into 282 three-image 5-minute averages. The RMS scatter on the fit is 0.037 mag.

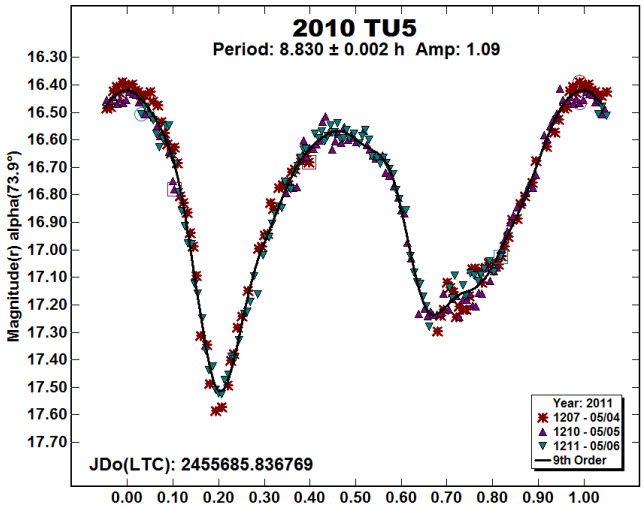

2010 TX168. This Apollo lacks previous study in the LCDB. We obtained two nights of data, extending over 9 hours each, using the Schmidt in 2010 Nov. The results are noisy compared to the small amplitude. Averaging images by threes within a 5-minute interval we get the lightcurve shown below, which we regard with some uncertainty (shy of 3-sigma significance). The RMS scatter on the fit is 0.034 mag.

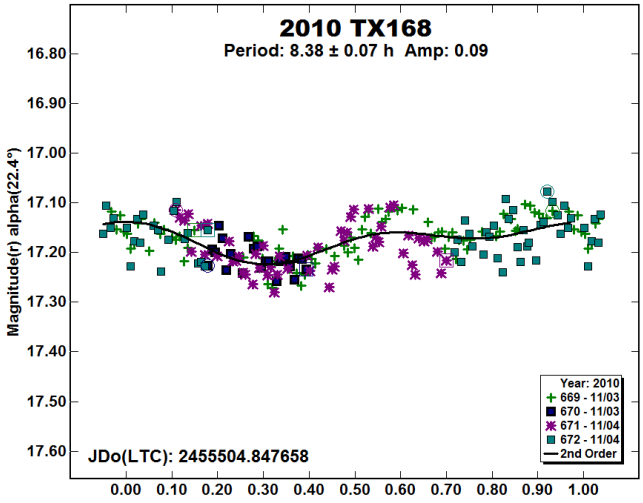

2010 UX6. This small (~80-meter) Apollo has only a 100-day orbital arc from the discovery apparition. We used the Schmidt on two nights in 2010 Nov, a week following discovery at La Sagra, to give what appears to be a partial lightcurve. We show a notional fit to the data. A simple order-2 fit gives a rough double-mode lightcurve with half this period, so the period shown below is *possibly* more nearly correct, but it could be completely wrong. Since it is fairly small, some tumbling is not out of the question. The asteroid was near the faint limit of the instrument, so the data are quite noisy, with RMS scatter of 0.06 mag.

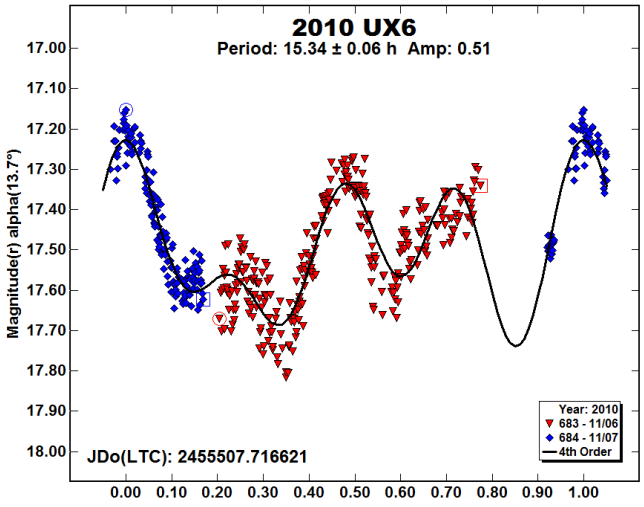

2011 AL37. On 2011 Jan 26 we used the LONEOS Schmidt to get a 3½-hour series of 4-second exposures on this very small (H = 24.3), fast-moving Apollo. The object was approaching Earth, moving at ~45°/day, and gradually brightened during the run. The photometry from fourteen separate pointings (and groups of comparison stars) link together very well and produce a clean lightcurve that shows no indication of tumbling or change in amplitude. The RMS scatter on the fitted lightcurve is 0.022 mag. These are the only lightcurve data for this asteroid, which has not been recovered since 2011.

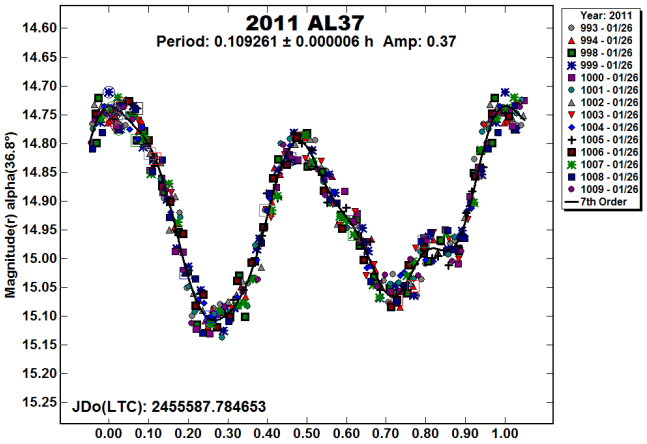

2011 HP. This ~150-meter Apollo passed close to Earth in 2011 May-Jun. It was observed by Hicks et al. (2011) and ourselves within a few days of each other. We obtained two 7-hour runs using 20- and 30-second exposures with the Schmidt. The lightcurve is fairly smooth and undistinguished in morphology. The RMS scatter on the fit is 0.039 mag.

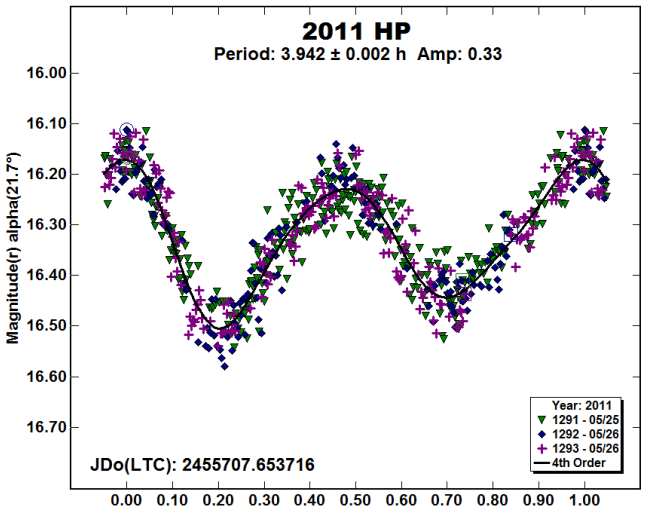

Incidental photometry

The following table summarizes single- or few-night photometry where the data were insufficient to derive any useful results. The date shown is either the sole or the first date of observation. This is followed by an approximate mean Sloan r′ magnitude and the number of useful observations we took. The individual observations are submitted to the ALCDEF database.

Num	Name	UT date	r'	obs
5693	1993 EA	2009-05-13	17.36	35
8566	1996 EN	2009-04-02	17.09	21
14223	1999 XM169	2010-12-11	16.8	82
16834	1997 WU22	2009-06-18	17.	22
22753	1998 WT	2009-01-30	17.2	20
66146	1998 TU3	2008-10-22	15.0	4
85774	1998 UT18	2008-11-20	16.9	10
137805	1999 YK5	2008-11-24	17.1	5
146134	2000 SE1	2010-07-15	18.1	52
162173	Ryugu	2008-04-13	18.7	31
163758	2003 OS13	2009-06-18	17.5	14
171576	1999 VP11	2008-10-26	17.0	6
190135	2005 QE30	2008-09-24	17.9	7
190491	2000 FJ10	2008-10-01	16.8	44
203217	2001 FX9	2009-01-28	17.42	13
212546	2006 SV19	2009-06-21	17.8	24
250697	2005 QY151	2010-11-16	17.02	132
259585	2003 UG220	2008-02-01	19.65	29
284114	2005 TZ51	2008-09-24	17.76	8
306769	2001 BX2	2010-10-14	16.5	50
309214	2007 LL	2008-07-10	19.3	49
348314	2005 BC	2009-01-16	16.40	12
354713	2005 SG19	2009-03-29	16.68	11
366366	2009 PR9	2010-12-08	17.33	287
414586	2009 UV18	2009-11-22	16.2	152
435548	2008 QT3	2009-01-16	16.6	32
450293	2004 LV3	2009-01-01	15.85	17
484795	2009 DE47	2009-04-20	17.0	17
	2008 JJ	2008-05-17	18.6	47
	2009 EP2	2009-03-16	15.9	10

Acknowledgements

Funding for the Near-Earth Asteroid Photometric Survey (NEAPS) from 2008 to 2010 was provided by NASA grant NNX08AR28G awarded to Ted Bowell. Since then, Skiff has been supported in this activity by the Lowell Observatory research fund. We also gratefully acknowledge Sasha Brownsberger (now at Harvard Univ), who transformed the old image-preparation code to IDL based on Marc Buie's algorithms. Student observers

included Emily K. Bevins, Jared Nelson, and Graham Vickowski. The Lowell technical staff were *sine qua non* for maintenance of telescopes, domes, camera electronics, computer systems, and software – especially Larry Wasserman, Ralph Nye, Ted Dunham, Peter Collins, Len Bright, and Mike Collins. The first author is also grateful to the Lowell library and its archivist Lauren Amundson for providing access to printed journals so that references could be browsed in-person. As with many *MPB* papers, the fingerprints of Brian Warner are all over this; his help with *MPO Canopus* and with lightcurve interpretation is appreciated.

This research has made extensive use of the VizieR catalogue access tool provided by the CDS, Strasbourg, France. Indeed, we would not have attempted it if this indispensable utility did not exist. Cécile Loup and Patricia Vannier have been especially helpful in this regard.

References

Agle, D.C. (2011). "NASA radar reveals features on asteroid." *https://www.jpl.nasa.gov/news/news.php?feature=2873*

Apostolovska, G.; Ivanova, V.; Borisov, G. (2004). "Lightcurves and rotational periods for 1474 Beira, 1309 Hyperborea, and 2525 O'Steen." *Minor Planet Bull*. **31**, 44-45.

Aznar Macías, A. (2014web). Posting on CALL web site. *http://www.MinorPlanet.info/call.html*

Behrend, R. (2001web, 2002web, 2006web, 2009web, 2012web, 2015web). "Courbe de rotation et luminosité d'asteroïdes…" *https://obswww.unige.ch/~behrend/page_cou.html*

Benishek, V. (2018). "Lightcurves and rotation periods for 29 asteroids." *Minor Planet Bull*. **45**, 82-91.

Benishek, V. (2019a). "Lightcurves and rotation periods for ten asteroids." *Minor Planet Bull*. **46**, 87-90.

Benishek, V. (2019b). "Lightcurves and rotation periods for ten Asteroids." *Minor Planet Bull*. **46**, 208-210.

Betzler, A.S.; Novaes, A.B. (2009). "Photometric observations of 1998 OR2, 1999 AQ10, and 2008 TC3." *Minor Planet Bull*. **36**, 145-147.

Birtwhistle, P. (2009). "Lightcurves for five close approach asteroids." *Minor Planet Bull*. **36**, 186-187.

Blaauw, R.C.; Cooke, W.J.; Suggs, R.M. (2011). "Lightcurve analysis of asteroids 890 Waltraut and 2010 JL33." *Minor Planet Bull*. **38**, 131-132.

Carbognani, A. (2011). "Lightcurves and periods of eighteen NEAs and MBAs." *Minor Planet Bull*. **38**, 57-63.

Clark, M. (2006). "Lightcurve results for 383 Janina, 899 Jokaste, 1825 Klare, 2525 O'Steen, 5064 Tanchozuru, and (17939) 1999 HH8." *Minor Planet Bull*. **33**, 53-56.

Degewij, J.; Lebofsky, L.; Lebofsky, M. (1978). "1978 CA and 1978 DA." IAU *Circ*. 3193. *http://www.cbat.eps.harvard.edu/iauc/03100/03193.html*

Durkee, R.I. (2010). "Asteroids observed from the Shed of Science Observatory: 2009 July-September." *Minor Planet Bull*. **37**, 18-19.

Durkee, R.; Pravec, P.; Hornoch, K.; and twelve additional co-authors (2010). "(15700) 1987 QD." *CBET* 2540.

Erasmus, N.; Mommert, M.; Trilling D.E.; and three additional co-authors (2017). "Characterization of near-Earth asteroids using KMTNET-SAAO." *Astron. J*. **154**, 162.

Galád, A.; Világi, J.; Kornoš, L.; Gajdoš, Š. (2009). "Relative photometry of nine asteroids from Modra." *Minor Planet Bull*. **36**, 116-118.

Galád, A.; Kornoš, L.; Világi, J. (2010). "An ensemble of lightcurves from Modra." *Minor Planet Bull*. **37**, 9-15.

Harris, A.W.; Young, J.W.; Scaltritti,F.; Zappala, V. (1984). "Lightcurves and phase relations of the asteroids 82 Alkmene and 444 Gyptis." *Icarus* **57**, 251-258.

Harris, A.W.; Young, J.W. (1989). "Asteroid lightcurve observations from 1979-1981." *Icarus* **81**, 314-364.

Harris, A.W.; Pravec, P.; Galád,A.; Skiff, B.A.; Warner, B.D.; and eleven additional co-authors (2014). "On the maximum amplitude of harmonics of an asteroid lightcurve." *Icarus* **235**, 55-59.

Hasegawa, S.; Kuroda, D.; Kitazato, K.; and 40 additional co-authors (2018). "Physical properties of near-Earth asteroids with a low delta-*v*: survey of target candidates for the Hayabusa2 mission." *Publ. Astron. Soc. Japan* **70**, 114-144.

Hicks, M.D.; Lawrence, K.; Rhoades, H.; Somers, J.; McAuley, A.; Barajas, T. (2009). *The Astronomer's Telegram*, **2116**.

Hicks, M.; Somers, J. (2010). "2007 MK13: a high elongated C-type potentially hazardous asteroid." *The Astronomer's Telegram,* **2372**.

Hicks, M.; Somers, J.; Truong, T.; McCormack, M.; Teague, S.; Rhoades, H. (2011). "Broadband photometry of 2011 HP: a possibly water-rich, low delta-V near-Earth asteroid." *The Astronomer's Telegram*, **3419**.

Higgins, D.; Gonsalves, R.M.D. (2007). "Asteroid lightcurve analysis at Hunters Hill Observatory and collaborating stations – June-September 2006." *Minor Planet Bull*. **34**, 16-18.

Higgins, D.; Warner, B.D. (2009). "Lightcurve analysis at Hunters Hill Observatory and collaborating stations -- autumn 2009." *Minor Planet Bull*. **36**, 159-160.

Higgins, D.; Pravec, P. and thirteen additional co-authors (2011). "(99913) 1997 CZ5." *CBET* **2648**.

Koehn, B.W.; Bowell, E.L.G.; Skiff, B.A.; Sanborn, J.J.; McLelland, K.P.; Pravec, P.; Warner B.D. (2014). "Lowell Observatory Near-Earth Asteroid Photometric Survey (NEAPS) -- 2009 January through 2009 June." *Minor Planet Bull*. **41**, 286-300. [Paper 2]

Kušnirák, P.; Pravec, P.; and ten additional co-authors (2007). "(3073) Kursk." *CBET* **792**.

Lagerkvist C.-L. (1976). "Photographic photometry of the asteroid 1975 RB." *Icarus*, **29**, 143-145.

Linder, T.R.; Sampson, R.; Holmes, R. (2013). "Astronomical Research Institute photometric results." *Minor Planet Bull*. **40**, 4-6.

Magnier, E.A., Schlafly, E.F., Finkbeiner, D.P., and eighteen additional co-authors (2019). "Pan-STARRS photometric and astrometric calibration." arXiv:1612.05242, version 3 of 2019 Jan 27. *https://arxiv.org/abs/1612.05242*

Marsden, B.G. (1990). "1990 MB." IAU *Circular* **5067**. *http://www.cbat.eps.harvard.edu/iauc/05000/05067.html*

Menzies, K. (2011web). Posting on CALL web site. *http://www.MinorPlanet.info/call.html*

Mommert, M.; Hora, J.L.; Harris, A.W.; and eight additional co-authors (2014). "The discovery of cometary activity in near-Earth asteroid (3552) Don Quixote." *Astrophys. J.*; **781**, 25.

Mommert, M.; Polishook, D.; Moskovitz, N. (2018). "(3552) Don Quixote." *CBET* **4502**.

Mottola, S.; Lahulla, F. (1998). "1996 FG3." IAU *Circ*. **7069**. *http://www.cbat.eps.harvard.edu/iauc/07000/07069.html*

Oey, J.; Cooney, W.; Gross, J.; and eight additional co-authors (2009). "Photometry of asteroids 7516 Kanjc, 7965 Katsuhiko, and (15515) 1999 VN80 from Leura, and other collaborating observatories." *Minor Planet Bull*. **36**, 50-51.

Oey, J. (2011web). *http://minorplanet.haoeydental.com.au*

Polakis, T.A. (2019). "Lightcurves of twelve main-belt minor plaents." *Minor Planet Bull*. **46**, 287-292.

Polishook, D. (2012). "Lightcurves and spin periods of near-Earth asteroids, the Wise Observatory, 2005 - 2010." *Minor Planet Bull*. **39**, 187-192.

Pravec, P. (1998web, 1999web, 2000web, 2002web, 2004web, 2005web, 2008web, 2011web, 2013web, 2019web). "Ondřejov asteroid photometry project." *http://www.asu.cas.cz/~asteroid/1991db_a.png*

Pravec, P.; Wolf, M.; Šarounová, L. (1998a). "Lightcurves of 26 near-Earth asteroids." *Icarus* **136**, 124-153.

Pravec, P.; Šarounová, L.; Wolf, M. (1998b). "1996 FG3". IAU *Circ*. **7074**, item 2.

Pravec, P.; Harris, A.W.; Scheirich, P.; and 17 additional co-authors (2005). "Tumbling asteroids." *Icarus* **173**, 108-131.

Pravec, P.; Scheirich, P.; Kušnirák, P.; Šarounová, L.; and 53 additional co-authors (2006). "Photometric survey of binary near-Earth asteroids." *Icarus* **181**, 63-93.

Pravec, P.; Harris, A.W.; Kušnirák, P.; Galád, A.; Hornoch, K. (2012). "Absolute magnitudes of asteroids and a revision of asteroid albedo estimates from WISE thermal observations." *Icarus* **221**, 365-387.

Pravec, P.; Scheirich, P., Ďurech, J., Pollock, J.; and sixteen additional co-authors (2014). "The tumbling spin state of (99942) Apophis." *Icarus* **233**, 48-60.

Rivkin, A.S.; Binzel, R.P.; Howell, E.S.; Bus, S.J.; Grier, J.A. (2003). "Spectroscopy and photometry of Mars Trojans." *Icarus* **165**, 349-354.

Ryan, W. (2009web), and e-mail correspondence in 2019 March. *http://www.nmt.edu/~bryan/research/work/mro_images/k09u01u*

Skiff, B.A.; Bowell, E.; Koehn, B.W.; Sanborn, J.J.; McLelland, K.P.; Warner, B.D. (2012). "Lowell Observatory Near-Earth Asteroid Photometric Survey (NEAPS) - 2008 May through 2008 December." *Minor Planet Bull*. **39**, 111-130. [Paper 1]

Skiff, B.A.; Bowell, E.; Koehn, B.W.; Sanborn, J.J.; McLelland, K.P.; Warner, B.D. (2019). "Lowell Observatory Near-Earth Asteroid Photometric Survey (NEAPS): Paper 3." *Minor Planet Bull*. **46,** 238-264. [Paper 3]

Spencer, J.R.; and 39 additional co-authors (1995). "The lightcurve of 4179 Toutatis: evidence for complex rotation." *Icarus* **117**, 71-89.

Statler, T.S., Cotto-Figueroa, D.; Riethmiller, D.A., Sweeney, K.M. (2013). "Size matters: the rotation rates of small near-Earth asteroids." *Icarus* **225**, 141-155.

Stephens, R.D. (2016). "Asteroids observed from CS3: 2015 October-December." *Minor Planet Bull*. **43**, 158-159.

Stephens, R.D.; Warner, B.D. (2019). "Main-belt asteroids observed from CS3: 2019 January-March." *Minor Planet Bull*.; **46**, 298-301.

Surdej, J.; Surdej. A. (1978). "1978 CA and 1978 DA." IAU *Circ*. **3185**. *http://www.cbat.eps.harvard.edu/iauc/03100/03185.html*

Tonry, J.L., Denneau, L., Flewelling, H., and six additional co-authors. (2019). "The ATLAS all-sky stellar reference catalog." Astrophys. J., **867**. 105.

Vaduvescu, O.; Aznar Macías, A.; Tudor, V.; Predatu, M.; and 23 additional co-authors (2017). "The EURONEAR lightcurve survey of near Earth asteroids." *Earth, Moon, & Planets* **120**, 41-100.

Walsh, K.; Delbò, M.; Mueller, M.; Binzel, R.P.; DeMeo, F.E. (2012). "Physical characterization and origin of binary near-Earth asteroid (175706) 1996 FG3." *Astrophys. J.* **748**, 104.

Warner, B.D. (2005). "Asteroid lightcurve analysis at the Palmer Divide Observatory – Winter 2004-2005." *Minor Planet Bull*. **32**, 54-58.

Warner, B.D. (2008). "Asteroid lightcurve analysis at the Palmer Divide Observatory – June-October 2007." *Minor Planet Bull*. **35**, 56-60.

Warner, B.D. (2009). "Asteroid lightcurve analysis at the Palmer Divide Observatory: 2008 September-December." *Minor Planet Bull*. **36**, 70-73.

Warner, B.D.; Harris, A.W.; Pray, D. (2009a). "(26471) 2000 AS152." *CBET* **1881**.

Warner, B.D.; Harris, A.W.; Pravec, P. (2009b). "The asteroid lightcurve database." *Icarus* **202**, 134-146. queried 2019 Mar. *http://www.minorplanet.info/lightcurvedatabase.html*

Warner, B.D.; Stephens, R.D.; Carbognani, A. (2009c). "Analysis of the slow rotator (143651) 2003 QO104." *Minor Planet Bull*. **36**, 179-180.

Warner, B.D. (2010). "Asteroid lightcurve analysis at the Palmer Divide Observatory: 2009 December-2010 March." *Minor Planet Bull*. **37**, 112-118.

Warner, B.D. (2011a). "Asteroid lightcurve analysis at the Palmer Divide Observatory: 2010 September-December." *Minor Planet Bull*. **38**, 82-86.

Warner, B.D. (2011b). "Asteroid lightcurve analysis at the Palmer Divide Observatory: 2010 December-2011 March." *Minor Planet Bull*. **38**, 142-149.

Warner, B.D.; Skiff, B.A.; McLelland, K. (2011). "Lightcurve analysis of the near-Earth asteroid (154029) 2002 CY46." *Minor Planet Bull*. **38**, 32-33.

Warner, B.D. (2012). "Asteroid lightcurve analysis at the Palmer Divide Observatory: 2012 March-June." *Minor Planet Bull*. **39**, 245-252.

Warner, B.D.; Megna, R. (2012). "Lightcurve for 1090 Sumida." *Minor Planet Bull*. **39**, 231.

Warner, B.D. (2013). "Asteroid lightcurve analysis at the Palmer Divide Observatory: 2012 June-September." *Minor Planet Bull*. **40**, 26-29.

Warner, B.D. (2014). "Asteroid lightcurve analysis at CS3-Palmer Divide Station: 2014 January-March." *Minor Planet Bull*. **41**, 144-155.

Warner, B.D. (2015). "Near-Earth asteroid lightcurve analysis at CS3-Palmer Divide Station: 2015 March-June." *Minor Planet Bull*. **42**, 267-276.

Warner, B.D. (2016a). "Near-Earth asteroid lightcurve analysis at CS3-Palmer Divide Station: 2015 June-September." *Minor Planet Bull*. **43**, 66-79.

Warner, B.D. (2016b). "Near-Earth asteroid lightcurve analysis at CS3-Palmer Divide Station: 2015 October-December." *Minor Planet Bull*. **43**, 143-154.

Warner, B.D. (2016c). "Near-Earth asteroid lightcurve analysis at CS3-Palmer Divide Station: 2016 January-April." *Minor Planet Bull*. **43**, 240-250.

Warner, B.D. (2017a). "Near-Earth asteroid lightcurve analysis at CS3-Palmer Divide Station: 2016 July-September." *Minor Planet Bull*. **44**, 22-36.

Warner, B.D. (2017b). "Near-Earth asteroid lightcurve analysis at CS3-Palmer Divide Station: 2016 October-December." *Minor Planet Bull*. **44**, 98-107.

Warner, B.D.; Benishek, V.; Harris, A.W. (2017). "1943 Anteros: A possible near-Earth binary asteroid." *Minor Planet Bull*. **44**, 186-188.

Warner, B.D. (2018a). "Near-Earth asteroid lightcurve analysis at CS3-Palmer Divide Station: 2017 October-December." *Minor Planet Bull*. **45**, 138-147.

Warner, B.D. (2018b). "Near-Earth asteroid lightcurve analysis at CS3-Palmer Divide Station: 2018 April-June." *Minor Planet Bull*. **45**, 380-386.

Warner, B.D. (2019). "(12538) 1998 OH: a continuing non-resolution." *Minor Planet Bull*. **46**, 157-160.

Warner, B.D.; Stephens, R.D. (2019a) "Near-Earth asteroid lightcurve analysis at the Center for Solar System Studies: 2018 July-September." *Minor Planet Bull*. **46**, 27-40.

Warner, B.D.; Stephens, R.D. (2019b) "Near-Earth asteroid lightcurve analysis at the Center for Solar System Studies: 2018 September-December." *Minor Planet Bull*. **46**, 144-152.

Waszczak, A.; Chang, C.-K.; Ofek, E.O.; Laher, R.; Masci, F.; Levitan, D.; Surace, J.; Cheng, Y.-C.; Ip, W.-H.; Kinoshita, D.; Helou, G.; Prince, T.A.; Kulkarni, S. (2015). "Asteroid Light Curves from the Palomar Transient Factory Survey: Rotation Periods and Phase Functions from Sparse Photometry." *Astron. J.* **150**, A75.

Wisniewski, W.Z. (1991). "Physical studies of small asteroids. I – Lightcurves and taxonomy of 10 asteroids." *Icarus*, **90**, 117-122.

Wisniewski W.Z.; Michałowski, T.M.; Harris, A.W.; McMillan, R.S. (1997). "Photometric observations of 125 asteroids." *Icarus*, **126**, 395-449.

Wolf, C.; Onken C.; Luvaul, L.C.; Schmidt, B.P.; and thirteen additional co-authors (2018). "SkyMapper southern survey: first data release (DR1)." *https://arxiv.org/abs/1801.07834 Publ. Astron. Soc. Austral*. **35**, e10; *https://arxiv.org/abs/1801.07834* and *https://skymapper.anu.edu*

Ye, Q.; Shi, L.; Xu, W.; Lin, H-C.; Zhang, J. (2009). "Photometric observations and lightcurve analysis of near-Earth asteroids (136849) 1998 CS1, 2006 SZ217, and 2008 UE7." *Minor Planet Bull*. **36**, 180-181.

Number	Name	20yy mm/dd	Phase	L_{PAB}	B_{PAB}	Period(h)	P.E.	Amp	A.E.	Grp
985	Rosina	19 05/30-05/31	22.3,22.3	17	-2	3.015	0.002	0.18	0.01	MC
1090	Sumida	19 06/19-06/20	19.6,19.7	230	17	2.7186	0.0007	0.14	0.01	PHO
1293	Sonja	10 04/24-04/26	11,4,11.9	354	-4	2.8761	0.0014	0.18	0.01	MC
1387	Kama	10 12/09-12/11	17.6,17.8	353	3	50.1	0.1	0.37	0.01	MB-O
1468	Zomba	19 04/15-04/18	10.7,9.7	219	-13	2.7727	0.0004	0.36	0.01	MC
1865	Cerberus	08 09/30-10/09	18.6,10.6	24	8	6.8044	0.0005	1.65	0.03	NEA
1865	Cerberus	08 10/22-10/29	9.5,17.4		4	6.8037	0.0007	1.67	0.05	NEA
1865	Cerberus	08 11/04-11/07	24.6,28.0	18	1	6.8013	0.0018	1.99	0.05	NEA
1943	Anteros	09 06/18-07/01	55.4,50.7	324	12	2.87	0.01	0.14	0.03	NEA
2212	Hephaistos	10 09/15-09/15	18.2	84	9					NEA
2281	Biela	10 12/09-12/10	4.4,4.9	69	-1	54.	10.	0.10	0.05	MB-O
2525	O'Steen	19 05/14-05/15	17.1,16.9	288	-1	3.569	0.003	0.16	0.01	MB-O
2585	Irpedina	10 12/09-12/10	.8,.5	121	-3					MB-O
2629	Rudra	10 10/13-10/15	17.5,17.2	29	24			0.	0.05	MC
2744	Birgitta	10 10/10-10/11	15.2,14.8	29	11	8.990	0.005	0.17	0.01	MC
3040	Kozai	19 03/09-03/23	.5,25.6	155	28	4.5129	0.0003	0.31	0.01	MC
3073	Kursk	08 04/12-04/15	12.9,11.7	229	2	3.446	0.002	0.21	0.01	MB-O
3086	Kalbaugh	19 03/30-03/31	17.8,18.0	182	-26	5.177	0.002	0.84	0.01	H
3552	Don Quixote	09 11/17-01/16	41.1,27.0	0	17	6.6605	0.0002	1.24	0.03	CEN
3552	Don Quixote	18 08/30-09/11	32.2,28.9	39	22	6.6625	0.0005	0.45	0.03	CEN
3554	Amun	09 03/17-03/29	48.2,50.1	139	13	2.5298	0.0003	0.19	0.01	NEA
3554	Amun	11 03/13-03/15	46.5,45.0	179		2.5308	0.0004	0.16	0.01	NEA
3671	Dionysus	10 04/07-04/08	19.8,.1	191	22	2.705	0.001	0.09	0.03	NEA
3672	Stevedberg	14 08/25-09/13	12.3,2.7	350	-4	2.7784	0.0002	0.17	0.02	FLO
3838	Epona	10 11/30-11/30	15.9	32	5	2.40	0.03	0.06	0.01	NEA
3875	Staehle	11 04/27-05/12	10.4,16.7	198	8	78.72	0.02	1.69	0.03	FLO
4179	Toutatis	08 09/05-02/19	*31.8,17.3							NEA
4205	David Hughes	10 12/11—01/06	26.7,10.6	115	-4					MC
4894	Ask	11 04/13-04/14	5.5,6.0	193	-3	3.640	0.004	0.17	0.02	FLO
5011	Ptah	09 04/18-04/23	65.5,59.8	162	-1	56.3	0.4	2.0	0.2	NEA
5253	Fredclifford	10 11/18-11/18	30.9	99	10	3.05	0.01	0.17	0.02	MC
5253	Fredclifford	10 12/07-12/10	26.4,25.7	104	18	3.0530	0.0005	0.07	0.01	MC
5261	Eureka	11 11/30-12/01	5.4,6.3	62	1					MC
5404	Uemura									MB-O
5604	1992 FE	09 03/27-04/22	18.1,33.2	186	-12	5.34	0.01	0.15	0.01	NEA
5620	Jasonwheeler	09 06/18-06/23	25.3,26.4	256	16	5.3066	0.0004	1.22	0.02	NEA
5869	Tanith	10 11/05-11/13	17.1,12.4	58	-3	17.519	0.002	0.37	0.01	NEA
5945	Roachapproach	14 11/13-11/20	4.5,8.2	43	3	5.605	0.003	0.19	0.01	FLO
5945	Roachapproach	17 09/11-09/15	8.5,10.6	337	-5	5.6047	0.0005	0.38	0.01	FLO
5945	Roachapproach	19 03/26-03/31	.6,21.4	132	5	5.602	0.001	0.34	0.01	FLO
5999	Plescia	10 12/11-12/11	29.5	117	19	5.39	0.01	0.98	0.03	MC
5999	Plescia	11 01/13-01/14	25.7	126	30	5.3929	0.0011	0.73	0.01	MC
6012	Williammurdoch	11 04/30-05/01	6.1,6.2	215	11	2.890	0.004	0.18	0.02	MB-O
6239	Minos	10 09/05-09/05	4.9	345	-0	3.67	0.02	0.08	0.01	NEA
6455	1992 HE	12 04/01-04/02	15.7,15.6	190		2.7361	0.0012	0.09	0.01	NEA
7267	Victormeen	19 05/02-05/15	13.5,17.3	211	-	3.041	0.001	0.21	0.03	MC
7965	Katsuhiko	19 04/14-04/28	27.8,30.9	160	-23	5.3902	0.0002	0.40	0.01	PHO
8444	Popovich	10 11/02-11/27	1.9,15.7	39	2	54.778	0.004	1.28	0.02	MC
9564	Jeffwynn	19 06/16-06/18	26.7,26.9	268	35	3.036	0.001	0.11	0.01	MC
12538	1998 OH	19 05/26-05/26	78.4	198	23	2.575	0.004	0.28	0.01	NEA
12538	1998 OH	19 06/01-06/01	71.5	8	29	2.585	0.004	0.23	0.23	NEA
14402	1991 DB	09 03/17-03/19	47.7,52.0	194	25	2.262	0.006	0.11	0.03	NEA
14402	1991 DB	09 03/27-04/02	65.9,72.4	212	36	2.266	0.002	0.17	0.03	NEA
15700	1987 QD	10 07/15-07/15	38.0	335	27	3.06	0.01	0.19	0.02	MC
15700	1987 QD	10 09/13-09/14	15.4,15.4	346	6	3.062	0.002	0.08	0.01	MC
19402	1998 EG14	10 11/06-11/10	6.5,4.9	49	-5	2.825	0.001	0.12	0.02	MC
20691	1999 VY72	10 12/07-12/08	13.0,12.8	78	-19	2.698	0.002	0.12	0.01	MC
20936	Nemrut Dagi	11 01/13-01/14	17.6,17.5	1	27	3.283	0.007	0.09	0.01	H
20936	Nemrut Dagi	11 02/08-02/09	18.8,19.1	121	26	3.285	0.004	0.10	0.02	H
20936	Nemrut Dagi	19 04/11-04/14	4.1,5.4	196	4	3.274	0.003	0.06	0.01	H
21104	Sveshnikov	10 10/10-10/15	27.5,29.1	344	23	2.8406	0.0003	0.25	0.01	MC
22262	1980 PZ2	19 04/20-05/02	15.3,.7	0	-19	34.47	0.03	0.28	0.01	PHO
23183	2000 OY21	11 01/28-01/30	24.6,24.8	137	22	6.9809	0.0005	0.76	0.02	NEA
24029	1999 RT198	10 11/06-11/10	18.9,18.4	58	-19	5.4911	0.0007	0.70	0.02	MC
24029	1999 RT198	17 10/21-10/22	18.6,18.3	49	-12	5.4905	0.0012	0.82	0.01	MC
24643	MacCready	19 06/04-06/06	12.2,13,2	238	14	2.8291	0.0005	0.14	0.01	MC
26471	Tracybecker	19 03/09-03/29	15.7,16.3	177	-27	2.6868	0.0002	0.25	0.02	H

Table I. Observing circumstances and results. The phase angle is given for the first and last date. If preceded by an asterisk, the phase angle reached an extrema during the period. L_{PAB} and B_{PAB} are the approximate phase angle bisector longitude/latitude at mid-date range (see Harris et al., 1984). Grp is the asteroid family/group (Warner et al., 2009b). CEN: Centaur, FLO: Flora, H: Hungaria, MB-O: outer main-belt, MC: Mars-crosser, NEA: near-Earth asteroid, PHO: Phocaea,

Number	Name	20yy mm/dd	Phase	L_{PAB}	B_{PAB}	Period(h)	P.E.	Amp	A.E.	Grp
38074	1999 GX19	19 06/21-06/22	16.4,17.0	251	8	6.3811	0.0012	0.54	0.01	MC
42811	1999 JN81	19 04/01-04/03	13.0,13.6	177	-17	3.9049	0.0017	0.16	0.01	MC
42930	1999 TM11	19 04/08-04/10	22.4,22.7	190	35	3.576	0.002	0.26	0.01	PHO
52768	1998 OR2	09 01/18–02/04	33.1,35.7	153	12	4.11	0.0006	0.16	0.01	NEA
53319	1999 JM8	2008								NEA
65679	1989 UQ	10 10/08-10/10	17.8,16.0	26	-2	7.746	0.006	0.30	0.02	NEA
68134	2001 AT18	10 12/07-12/08	21.5,20.9	106	3	7.104	0.002	1.16	0.02	MC
68216	2001 CV26	10 03/26-03/26	9.9	189	8	2.425	0.005	0.10	0.01	NEA
68216	2001 CV26	10 04/08-04/10	16.3,16.5	189	3	2.43	0.01	0.08	0.02	NEA
68350	2001 MK3	09 01/16-02/04	36.6,26.8	151	10	3.21082	0.00012	0.18	0.01	NEA
68350	2001 MK3	09 02/19-02/19	27.3	154	26	3.21	0.01	0.11	0.02	NEA
74779	1999 RF241	10 12/07-12/08	15.9,16.4	53	-7	6.1895	0.0014	0.82	0.01	PHO
74823	1999 TD15	10 11/02-11/27	2.8,19.5	39	-7	33.446	0.008	0.22	0.02	MC
85839	1998 YO4	10 04/14-04/14	39.6	168	7	2.45	0.07	0.04	0.01	NEA
85867	1999 BY9	09 03/21-04/23	3.9,20.5	189	-2					NEA
87684	2000 SY2	08 09/07-09/07	55.4	28	-15	2.55	0.04	0.10	0.01	NEA
99913	1997 CZ5	10 10/11-10/12	42.2,42.3	82	25	2.8328	0.0009	0.19	0.01	MC
100926	1998 MQ	10 11/08-11/08	31.5	63	-12	2.33	0.01	0.06	0.01	NEA
102873	1999 WK11	08 05/29-06/08	30.6,38.6	223	4	2.40639	0.00012	0.20	0.01	NEA
136568	1980 XB	19 01/19-01/20	26.5,26.9	105	28	2.7815	0.0005	0.29	0.01	MC
138883	2000 YL29	09 09/21-10/21	34.2,23.5	23	-15	10.592	0.001	0.30	0.03	NEA
141432	2002 CQ11	11 05/07-05/08	26.5,29.7	212	8	2.610	0.003	0.12	0.03	NEA
141498	2002 EZ16	10 11/30-12/02	44.0,37.7	80	25	5.02	0.01	0.18	0.03	NEA
143381	2003 BC21	10 08/13-08/14	14.7,14.2	337	6	5.0678	0.0011	1.20	0.03	NEA
143381	2003 BC21	10 08/31-09/07	7.2,7.7	341	8	5.0661	0.0004	1.06	0.03	NEA
143381	2003 BC21	10 09/14-09/17	11.1,13.1	343	9	5.0653	0.0003	1.05	0.03	NEA
143381	2003 BC21	10 10/10-10/11	28.7,29.4	350	10	5.068	0.002	1.24	0.03	NEA
143381	2003 BC21	10 10/27-10/27	37.9	358	11	5.07	0.01	1.35	0.03	NEA
143381	2008 BC21	10 12/08-12/08	47.3	27	8	5.07	0.01	1.43	0.03	NEA
143651	2003 QO104	09 02/19-04/22	20.7,59.8	163	24	114.	1.	1.25	0.05	NEA
152558	1990 SA	10 08/31-09/01	30.2,28.3	350		8.147	0.009	0.14	0.01	NEA
152952	2000 GC2	10 09/11-09/16	37.8,34.6		15	4.179	0.002	0.14	0.03	NEA
153814	2001 WN5	10 10/13-10/14	64.9,62.0	344	12	4.253	0.001	0.63	0.03	NEA
153814	2001 WN5	10 10/26-10/26	38.1	9	8	4.254	0.018	0.36	0.02	NEA
154029	2002 CY46	10 09								NEA
154244	2002 KL6	09 06/18-06/23	43.8,50.8	296	12	4.6060	0.0004	1.04	0.03	NEA
154244	2002 KL6	09 07/01-07/13	62.5,74.5	324	15	4.6052	0.0003	1.07	0.03	NEA
154244	2002 KL6	09 09/24-09/26	35.4,33.4	31	3	4.608	0.001	1.08	0.03	NEA
154244	2002 KL6	09 10/16-10/22	12.6,6.6	35	1	4.6096	0.0006	0.65	0.03	NEA
154278	2002 TB9	08 06/06-06/09	44.0,42.6	268	49	7.85	0.01	1.02	0.02	NEA
161989	Cacus	09 02/19-02/19	50.9	187	0	3.75	0.01	1.1	0.1	NEA
162385	2000 BM19	09 01/28-02/04	7.9,76.9	160	37	9.463	0.004	1.34	0.03	NEA
162900	2001 HG31	2008-2009								NEA
163000	2001 SW169	08 09/06-10/02	*9.4,20.4	350	-3	80.2	0.2	0.39	0.05	NEA
164716	1998 GH	10 11/02-11/02	2.1	38	2	2.66	0.02	0.10	0.02	H
174599	2003 QM70	10 10/31-11/01	14.4,14.8	32	17	32.1	0.6	0.21	0.02	MC
175706	1996 FG3	09 03/25-04/22	*10.5,46.7	188	-7	3.584	0.001	0.15	0.03	NEA
184990	2006 KE89	08 05/28-05/29	34.7,35.0	223	45	5.16	0.04	0.12	0.03	NEA
185851	2000 DP107	08 09/22-09/23	44.2,41.3	24	4	2.774	0.004	0.17	0.01	NEA
185854	2000 EU106	08 09/22-09/23	12.9,12,2	15	6	3.5	0.1	0.53	0.04	MC
188452	2004 HE62	08 09/07-09/07	60.5	326	43	5.36	0.15	1.15	0.01	NEA
194386	2001 VG5	09 06/15-06/22	11.5,15.9	255	6	6.351	0.003	0.77	0.03	NEA
207945	1991 JW	09 04/18-05/17	*32.6,19.0	226	11	3.1499	0.0002	0.17	0.02	NEA
208023	1999 AQ10	09 01/30-02/04	39.3,37.6	152	10	6.28	0.01	0.17	0.02	NEA
219071	1997 US9	10 11/01-11/02	17.9,17.3	50	-10	3.319	0.003	0.14	0.02	NEA
220124	2002 TE66	10 04/07-04/09	35.3,38.3	194	25	3.89	0.01	0.16	0.03	NEA
242211	2003 QB90	10 09/03-09/14	40.8,36.1	15	-9					NEA
242643	2005 NZ6	08 05/18-05/18	66.1	187	-0					NEA
248818	2006 SZ217	08 12/01-12/07	19.2,25.4	72	-17	3.59	0.01	0.11	0.01	NEA
256412	2007 BT2	09 03/27-04/22	35.7,27.6	188	21					NEA
260141	2004 QT24	11 04/13-04/14	74.2,72.5	169	31	7.660	0.004	0.77	0.03	NEA
277039	2005 CF41	08 05/26-05/27	57.0,58.5	250	43	16.2	0.2	0.30	0.01	NEA
305090	2007 VQ4	08 05/12-05/12	35.2	198	21	2.69	0.02	0.14	0.02	NEA
305090	2007 VQ4	08 06/06-06/06	34.5	210	9	2.61	0.05	0.13	0.02	NEA
325769	2010 LY63	10 09/30-10/13	35.3,36.0	351	14					NEA
341843	2008 EV5	08 12/29-12/29	31.5	109	12	3.68	0.06	0.03	0.01	NEA
341843	2008 EV5	09 01/01-01/01	33.9	106	17	3.71	0.06	0.05	0.01	NEA

Table I (continued). Observing circumstances and results. The phase angle is given for the first and last date. If preceded by an asterisk, the phase angle reached an extrema during the period. L_{PAB} and B_{PAB} are the approximate phase angle bisector longitude/latitude at mid-date range (see Harris et al., 1984). Grp is the asteroid family/group (Warner et al., 2009b).

Number	Name	20yy mm/dd	Phase	L_{PAB}	B_{PAB}	Period(h)	P.E.	Amp	A.E.	Grp
345705	2006 VB14	2008 12/01-12/07	53.6,47.5	104	2	3.20	0.01	0.52	0.04	NEA
345705	2006 VB14	2010 11/27-11/27	51.4	93	18	3.25	0.02	0.42	0.03	NEA
367248	2007 MK13	2009 12/19-12/20	60.0,56.1	115	-17	5.285	0.003	1.46	0.03	NEA
367248	2007 MK13	2009 12/26	32.9	112	3	5.283	0.003	2.17	0.02	NEA
410650	2008 SQ1	2008 10/22-11/30	17.7,24.9	37	13	47.3	0.1	0.50	0.03	NEA
410777	2009 FD	2009 03/24-03/24	18.1	192	5	5.8	0.4	0.46	0.04	NEA
416801	2005 GC120	2010 12/02-12/02	83.8	25	-5					NEA
446791	1998 SJ70	2008 09/22-10/07	*21.5,8.3	8	-6	19.2	0.1	0.80	0.06	NEA
453778	2011 JK	2019 06/02-06/03	59.5,58.3	223	24	2.4567	0.0008	0.12	0.01	NEA
488515	2001 FE90	2009 06/29-06/29	34.1	262	9	0.47723	0.00015	1.30	0.02	NEA
503941	2003 UV11	2010 10/13-10/14	23.4,22.8	37	-2					NEA
504025	2005 RQ6	2009 10/16-10/23	18.5,10.1	27	-9	13.2021	0.0012	0.80	0.02	NEA
504025	2005 RQ6	2009 10/21-10/22	12.8,11.5	29	-8	13.202	0.001	0.87	0.02	NEA
518638	2008 JP14	2008 05/30-06/07	48.3,65.2	232	34	2.488	0.001	0.08	0.01	NEA
524522	2002 VE68	2010 10/26-10/30	78.8,68.1	66	26	13.36	0.01	1.22	0.05	NEA
528159	2008 HS3	2008 05/15-06/13	50.1,54.8	234	26	10.68	0.01	0.94	0.03	NEA
529668	2010 JL33	2010 12/11-12/14	65.6,40.9	65	24	9.443	0.002	0.76	0.01	NEA
	2004 XK3	2008 11/21-11/21	7.3	55	1	0.484	0.002	0.20	0.05	NEA
	2007 RU17	2010 10/13-10/15	5.1,3.0	23	2					NEA
	2008 JT35	2008 06/10-06/11	49.0,48.9	236	16	3.102	0.002	0.15	0.01	NEA
	2008 QS11	2008 09/21-10/07	41.3,92.8	25	-17	39.0	0.1	0.19	0.02	NEA
	2008 SA	2008 09/21-09/21	34.5	342	6	0.1297	0.0002	0.13	0.05	NEA
	2008 SE	2008 10/07-10/09	22.2,20.9	29	8	4.7	0.1	0.84	0.07	NEA
	2008 SR1	2008 09/29-09/30	15.2,16.1	2	-9	10.9	0.2	0.5	0.1	NEA
	2008 WL60	2009 04/18-04/23	4.9,5.8	16	-11	2.6076	0.0008	0.25	0.02	NEA
	2009 DO111	2009 03/16-03/17	15.6,14.9	177	8	0.048885	0.000002	0.35	0.03	NEA
	2009 DO111	2009 03/18-03/18	21.5	176	11	0.048869	0.000006	0.51	0.02	NEA
	2009 JM2	2009 05/14-05/17	59.0,47.5	220	28	28.5	0.3	0.23	0.05	NEA
	2009 UU1	2009 10/24-10/24	68.6	357	8	0.06355	0.00006	2.15	0.20	NEA
	2010 LF86	2010 11/15-11/16	29.8,30.1	31	17	4.445	0.003	0.40	0.03	NEA
	2010 RC130	2010 09/26-09/29	30.1,24.1	351	8					NEA
	2010 RF181	2010 11/19-11/19	56.6	81	17					NEA
	2010 SC41	2010 11/12-11/15	1.5,2.3	51	0	5.665	0.002	0.36	0.01	NEA
	2010 TC55	2010 10/30-10/31	13.7,12.2	33	7	2.408	0.003	0.14	0.03	NEA
	2010 TU5	2011 05/04-05/06	75.4,67.3	234	41	8.830	0.002	1.09	0.03	NEA
	2010 TX168	2010 11/03-11/04	21.3,25.2	31	12	8.38	0.07	0.09	0.02	NEA
	2010 UX6	2010 11/06-11/07	14.2,12.3	36	-1	15.34	0.06	0.51	0.04	NEA
	2011 AL37	2011 01/26-01/26	28.9	140	4	0.109261	0.000006	0.37	0.01	NEA
	2011 HP	2011 05/25-05/26	20.7,24.3	244	12	3.942	0.002	0.33	0.02	NEA

Table I (continued). Observing circumstances and results. The first line gives the results for the primary of a binary system. The second line gives the orbital period of the satellite and the maximum attenuation. The phase angle i given for the first and last date. If preceded by an asterisk, the phase angle reached an extrema during the period. L_{PAB} and B_{PAB} are the approximate phase angle bisector longitude/latitude at mid-date range (see Harris et al., 1984). Grp is the asteroid family/group (Warner et al., 2009b).

COLLABORATIVE ASTEROID PHOTOMETRY FOR 3653 KLIMISHIN, 4748 TOKIWAGOZEN AND 9951 TYRANNOSAURUS

Alessandro Marchini
Astronomical Observatory, DSFTA - University of Siena (K54)
Via Roma 56, 53100 - Siena, ITALY
alessandro.marchini@unisi.it

Lorenzo Franco
Balzaretto Observatory (A81), Rome, ITALY

Riccardo Papini, Massimo Banfi, Fabio Salvaggio
Wild Boar Remote Observatory (K49)
San Casciano in Val di Pesa (FI), ITALY

Charles Galdies
Znith Observatory
Armonie, E. Bradford Street, Naxxar NXR 2217, MALTA

Stephen M. Brincat
Flarestar Observatory (171)
San Gwann SGN 3160, MALTA

(Received: 2019 July 15)

Photometric observations of three main-belt asteroids were made in order to acquire lightcurves. The synodic period and light curve amplitude were found for: 3653 Klimishin 6.783 ± 0.001 h, 0.21 mag; 4748 Tokiwagozen 39.78 ± 0.01 h, 0.42 mag.; 9951 Tyrannosaurus 3.767 ± 0.004 h, 0.21 mag. Asteroid 4748's lightcurve shows a few interesting features which suggest the opportunity of further observations in order to verify a possible "tumbling" nature.

Collaborative asteroid photometry was made in the second quarter of 2019. The targets were selected in order to acquire lightcurves for determining their rotational period. The CCD observations were performed in April-June 2019 using the instrumentation described in the Table I. Lightcurve analysis was done with MPO Canopus (BDW Publishing, 2018). All the images were calibrated with dark and flat frames and converted to R magnitudes using solar colored field stars from CMC15 catalogue, distributed with MPO Canopus. Table II shows the observing circumstances and results.

3653 Klimishin is a main belt asteroid discovered on April 25 1979, by N. Chernykh, at Nauchnyj. Collaborative observations were made over six nights. We found a synodic period of P = 6.783 ± 0.001 h with an amplitude A = 0.21 ± 0.02 mag.

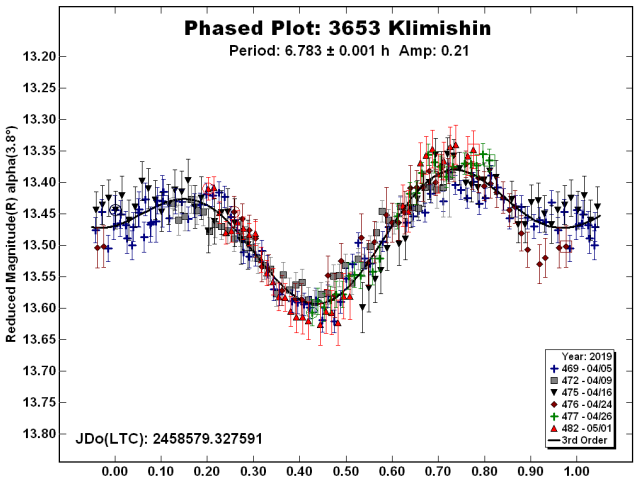

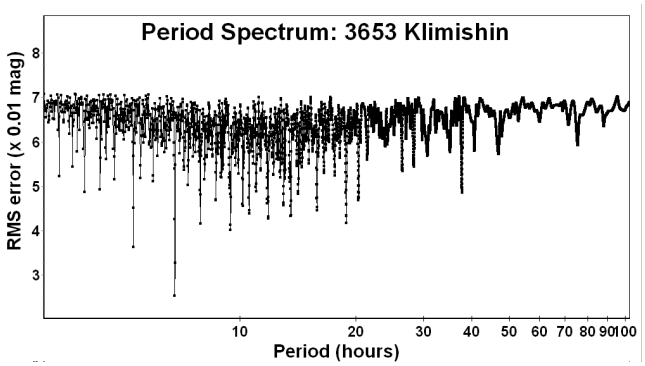

4478 Tokiwagozen is a main-belt asteroid discovered on November 20 1989, by Suzuki and Urata at Toyota. Collaborative observations were made over fifteen nights. The folded lightcurve was very tough to fold using the MPO's tools. We found a synodic rotation period of P = 39.78 ± 0.01 h with an amplitude A = 0.42 ± 0.06 mag. The lightcurve shows some phase and amplitude variations that could indicate a tumbling nature of the asteroid. A dual period search shows a possible secondary period close to 46 h.

Observatory (MPC code)	Telescope	CCD	Filter	Observed Asteroids
DSFTA Observatory (K54)	0.30-m MCT f/5.6	SBIG STL-6303e	Rc,C	3653, 4748, 9951
WBRO (K49)	0.23-m SCT f/10	SBIG ST8-XME	Rc,C	3653, 4748, 9951
Znith	0.20-m SCT f/10	Moravian G2-1600	C	4748
Flarestar (171)	0.25-m SCT f/10	Moravian G2-1600	C	4748

Table I. Observing Instrumentations. MCT: Maksutov-Cassegrain, SCT: Schmidt-Cassegrain.

Number	Name	2019 mm/dd	Phase	L_{PAB}	B_{PAB}	Period(h)	P.E.	Amp	A.E.	Grp
3653	Klimishin	04/05-05/01	*4.3,11.0	202	3	6.783	0.001	0.21	0.025	FLOR
4748	Tokiwagozen	05/06-06/08	6.6,11.9	232	11	39.78	0.01	0.42	0.06	MB-O
9951	Tyrannosaurus	06/01-06/04	11.3,12.6	233	10	3.767	0.004	0.21	0.06	V

Table II. Observing circumstances and results. The first line gives the results for the primary of a binary system. The second line gives the orbital period of the satellite and the maximum attenuation. The phase angle is given for the first and last date. If preceded by an asterisk, the phase angle reached an extrema during the period. L_{PAB} and B_{PAB} are the approximate phase angle bisector longitude/latitude at mid-date range (see Harris *et al.*, 1984). Grp is the asteroid family/group (Warner *et al.*, 2009).

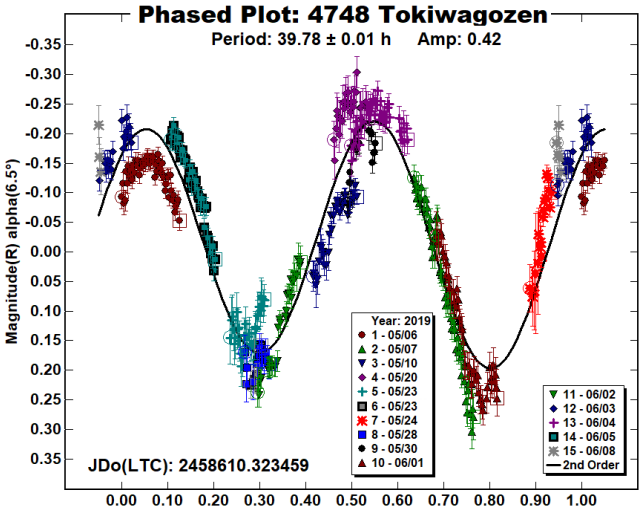

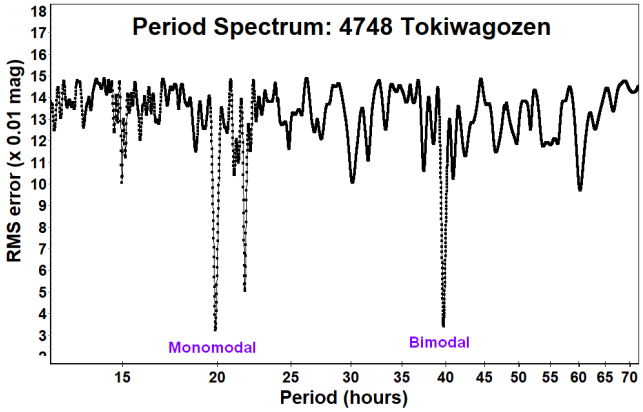

9951 Tyrannosaurus was discovered on November 15 1990 by E. W. Elst at the European Southern Observatory. Collaborative observations were performed over three nights. We found a synodic rotation period of P = 3.767 ± 0.004 h with an amplitude A = 0.21 ± 0.06 mag.

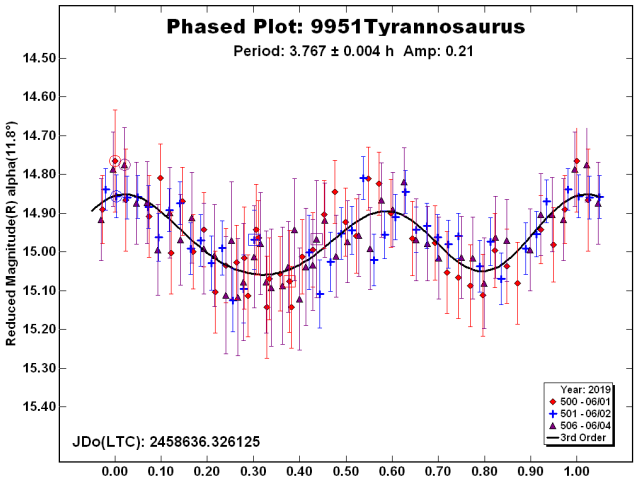

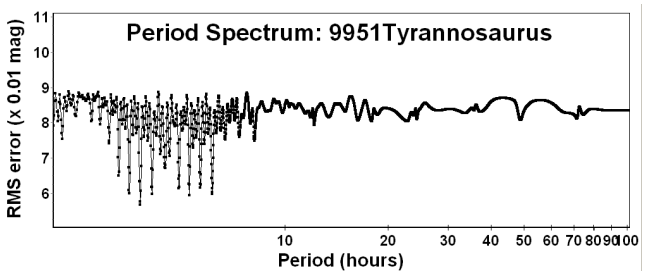

Acknowledgements

This research was made possible in part based on data from the AAVSO Photometric All-Sky Survey (APASS), funded by the Robert Martin Ayers Sciences Fund.

References

Harris, A.W.; Young, J.W.; Scaltriti, F.; Zappala, V. (1984). "Lightcurves and phase relations of the asteroids 82 Alkmene and 444 Gyptis." *Icarus* **57**, 251-258.

Warner, B.D. (2018). MPO Software, MPO Canopus v10.7.7.0. Bdw Publishing. *http://minorplanetobserver.com*

Warner, B.D.; Harris, A.W.; Pravec, P. (2009). "The Asteroid Lightcurve Database." *Icarus* **202**, 134-146. Updated 2019 Jan. *http://www.minorplanet.info/lightcurvedatabase.html*

LIGHTCURVES AND SYNODIC ROTATION PERIODS FOR SEVEN ASTEROIDS: 2019 APRIL–JULY

Vladimir Benishek
Belgrade Astronomical Observatory
Volgina 7, 11060 Belgrade 38, SERBIA
vlaben@yahoo.com

(Received: 2019 July 15)

Results are given on lightcurve and synodic rotation period determinations for seven asteroids from data collected at Sopot Astronomical Observatory between 2019 April to July.

Photometric observations of seven asteroids were conducted at Sopot Astronomical Observatory (SAO) from 2019 April to July in order to determine their synodic rotation periods. For this purpose, two 0.35-m *f*/6.3 Meade LX200GPS Schmidt-Cassegrain telescopes were used. The telescopes are equipped with an SBIG ST-8 XME and an SBIG ST-10 XME CCD cameras. The exposures were unfiltered and unguided for all targets. Both cameras were operated in 2x2 binning mode, which produces image scales of 1.66 arcsec/pixel and 1.25 arcsec/pixel for ST-8 XME and ST-10 XME cameras, respectively. Prior to measurements, images were corrected using dark and flat field frames.

Photometric reduction, lightcurve construction, and period analysis were done using *MPO Canopus* (Warner, 2018). Differential photometry with up to five comparison stars of near solar color ($0.5 \leq B\text{-}V \leq 0.9$) was performed using the Comparison Star Selector (CSS) utility. This helped ensure a satisfactory quality level of night-to-night zero point calibrations and correlation of the measurements within the standard magnitude framework. Field comparison stars were calibrated using standard Cousins R magnitudes derived from the Carlsberg Meridian Catalog 15 (VizieR, 2019) Sloan r´ magnitudes using the formula: R = r´ – 0.22. In some instances, small zero point adjustments were necessary to achieve the best match between individual data sets in terms of minimum RMS residual of a Fourier fit.

Table I gives the observing circumstances and results.

Some of the targets presented in this paper were observed within the Photometric Survey for Asynchronous Binary Asteroids (BinAstPhot Survey) under the leadership of Petr Pravec from Ondřejov Observatory, Czech Republic.

2460 Mitlincoln. Analysis of the photometric data collected at SAO from 2019 April 16-21 indicates a bimodal period of P = 3.0068 ± 0.0007 h as the most plausible solution. Previous period results (Warner, 2011; 2.667 h) and Kryszczynska et al. (2012; 2.8277 h) produced significantly worse fits using the latest combined data set. The period result shown here is in a very good agreement with that obtained by Behrend (2004), 3.009 h.

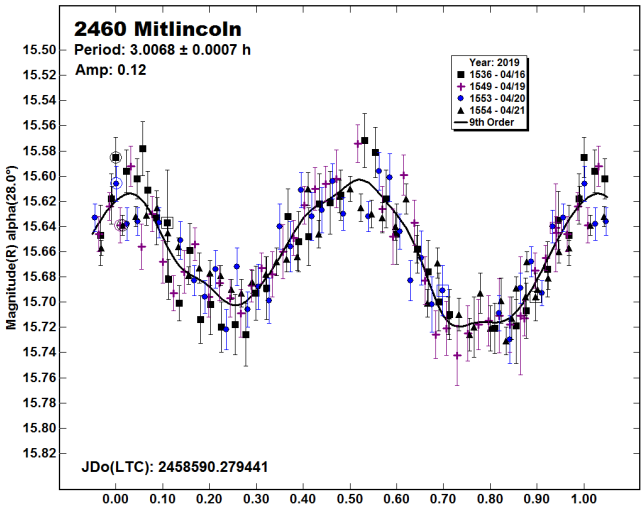

2937 Gibbs. Behrend (2005) and Stephens (2017) found synodic rotation periods for this Mars-crossing asteroid of 3.06153 h and 3.189 h, respectively. Period analysis conducted upon the SAO photometric data obtained over four nights from 2019 June 30-July 4 shows P = 2.9820 ± 0.0004 h as a more likely solution.

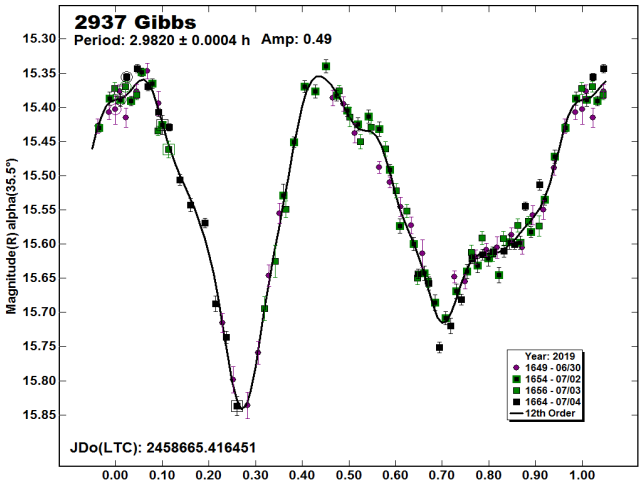

Number	Name	2019/mm/dd	Phase	L_{PAB}	B_{PAB}	Period (h)	P.E.	Amp	A.E.	Grp
2460	Mitlincoln	04/16-04/21	28.0,28.5	147	-1	3.0068	0.0007	0.12	0.02	FLOR
2937	Gibbs	06/30-07/04	35.5,35.3	329	22	2.9820	0.0004	0.49	0.01	MC
3315	Chant	06/06-07/01	6.6,13.1	254	12	13.463	0.002	0.38	0.01	MB-M
9564	Jeffwynn	06/13-07/06	26.5,29.0	270	36	3.0346	0.0002	0.14	0.03	MC
10422	1999 AN22	04/25-06/10	*7.9,16.0	227	8	35.2	0.1	≥0.47		MB-O
10524	Maniewski	04/04-04/08	*3.1,2.3	198	4	5.201	0.003	0.19	0.02	FLOR
12538	1998 OH	06/06-06/15	66.1,63.6	220	33	2.5814	0.0005	0.21	0.02	NEA

Table I. Observing circumstances and results. Phase is the solar phase angle at the start and end of date range. If preceded by an asterisk, the phase angle reached an extrema during the period. L_{PAB} and B_{PAB} are the average phase angle bisector longitude and latitude. Grp is the asteroid family/group (Warner *et al.;* 2009): FLOR: Flora, MB-M/O: main-belt middle/outer, MC: Mars-crosser, NEA: near-Earth asteroid.

3315 Chant was a BinAstPhot Survey program target observed exclusively at SAO on eight nights from 2019 June 6-July 1.

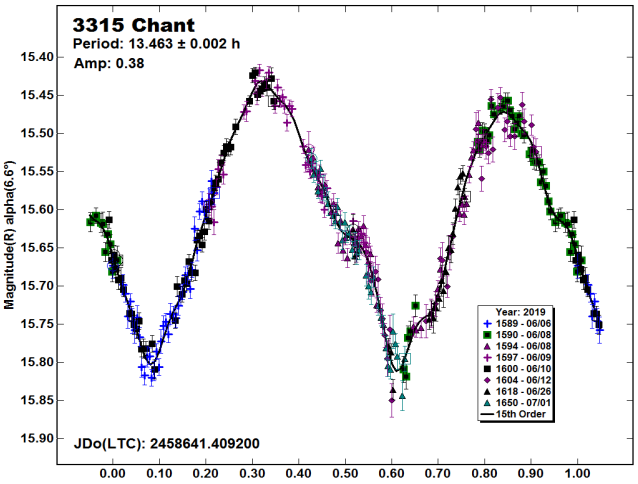

Period analysis found an unequivocal bimodal solution for a rotation period of 13.463 ± 0.002 h that is associated with a large amplitude (0.38 mag) lightcurve. This result is somewhat different from the previous results but with significant errors: Chang et al. (2015; 13.71 ± 0.200 h) and Waszczak et al. (2015, 13.749 ± 0.2458 h). An uncertainty flag of U = 2 has been assigned in the asteroid lightcurve database (LCDB; Warner et al., 2009) to both the earlier results.

9564 Jeffwynn. Warner (2013) determined a value of 3.035 h for the rotation period of this Mars-crosser. A newly found rotation period, P = 3.0346 ± 0.0002 h, derived from the six data sets obtained at SAO in 2019 June and July fully confirms the result found by Warner.

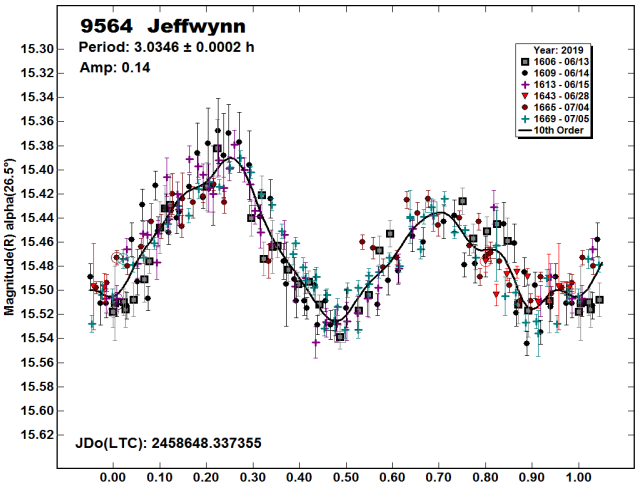

(10422) 1999 AN22 was another BinAstPhot target with no previously known rotation period. After the first few data sets were obtained, it became clear that this asteroid is a slow rotator. Observations were made over a six week period starting in late 2019 April. A total of seven independent data sets was obtained.

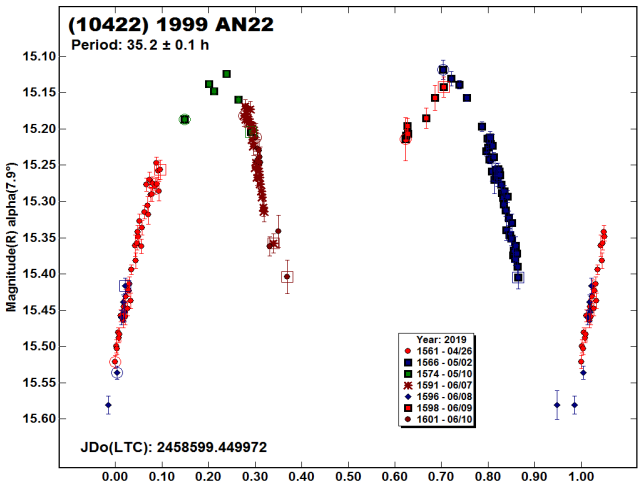

After a slow rotation has been determined, the strategy of taking several groups of multiple exposures with longer time intervals between them was applied in some cases in order to save valuable observing time for other priority targets. Although the full rotation cycle is not fully covered, given the large amplitude (≥ 0.47 mag) at a low phase angle, it is almost certain that the correct solution is a bimodal lightcurve with a period of 35.2 h (Harris et al., 2014).

10524 Maniewski. A search of records shows no previous lightcurves for this Flora family asteroid. Period analysis of the dense photometric data taken on four nights in 2019 April led to a highly reliable solution of P = 5.201 ± 0.003 h.

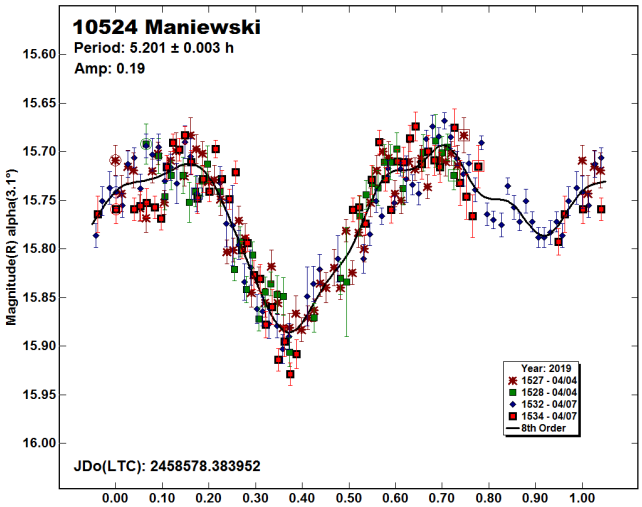

(12538) 1998 OH. Several previously reported synodic rotation periods were found in the LCDB for this near-Earth asteroid. Almost all the results were either a period of 2.6 h or the double period of about 5.2 h (e.g. Warner 2017, 5.154 h; Lozano et al. 2017, 5.088 h; and Vaduvescu et al. 2017, 2.582 h). The only notable exception is the value originally determined by Warner (2015) of 5.833 h.

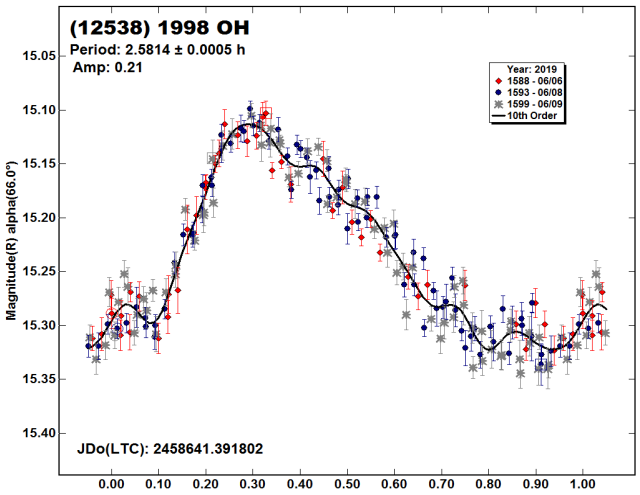

An analysis using the photometric observations carried out at SAO over three nights in 2019 June favors of the shorter periods, finding P = 2.5814 ± 0.0005 h with a monomodal lightcurve. The double period is associated with the bimodal lightcurve that produced identical halves when using the "split-halves" method in *MPO Canopus*; it was ruled out as a spurious solution. The shoter period solution shown here is in very good agreement with that recently found by Warner (2019) of 2.5804 h.

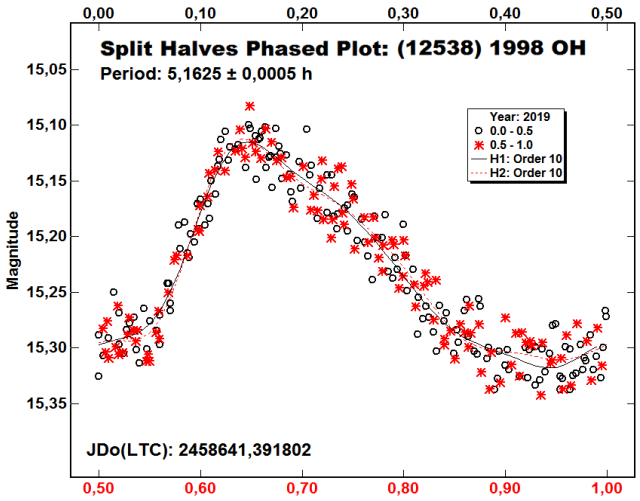

Acknowledgements

Observational work at Sopot Astronomical Observatory is supported by a 2018 Gene Shoemaker NEO Grant from The Planetary Society.

References

Behrend, R. (2004, 2005). CdL Observatoire de Geneve web site: *http://obswww.unige.ch/~behrend/page_cou.html*

Chang, C.-K.; Ip, W.-H.; Lin, H.-W.; Cheng, Y.-C.; Ngeow, C.-C.; Yang, T.-C.; Waszczak, A.; Kulkarni, S.R.; Levitan, D.; Sesar, B.; Laher, R.; Surace, J.; Prince, T.A. (2015). "Asteroid Spin-rate Study Using the Intermediate Palomar Transient Factory." *Ap. J. Suppl. Ser.* **219**, A27.

Harris, A.W.; Pravec, P.; Galad, A.; Skiff, B.A.; Warner, B.D.; Vilagi, J.; Gajdos, S.; Carbognani, A.; Hornoch, K.; Kusnirak, P.; Cooney, W.R.; Gross, J.; Terrell, D.; Higgins, D.; Bowell, E.; Koehn, B.W. (2014). "On the maximum amplitude of harmonics on an asteroid lightcurve." *Icarus* **235**, 55-59.

Kryszczynska, A.; Colas, F.; Polinska, M.; Hirsch, R.; Ivanova, V.; Apostolovska, G.; Bilkina, B.; Velichko, F.P.; Kwiatkowski, T.; Kankiewicz, P. and 20 colleagues. (2012). "Do Slivan states exist in the Flora family? I. Photometric survey of the Flora region." *Astron. Astrophys*. **546**, A72.

Lozano, J.; Flores, A.; Mas, V.; Fornas, G.; Rodrigo, O.; Brines, P.; Forna, A.; Herrero, D.; Carreno, A.; Arce, E. (2017). "Seven Near-Earth Asteroids at Asteroids Observers (OBAS) - MPPD: 2016 June-November." *Minor Planet Bull.* **44**, 108-111.

Stephens, R.D. (2017). "Asteroids Observed from CS3: 2016 October – December." *Minor Planet Bull.* **44**, 120-122.

Vaduvescu, O.; Macias, A.A.; Tudor, V.; Predatu, M.; Galad, A.; Gajdoš, Š.; Vilagi, J.; Stevance, H.F.; Errmann, R.; Unda-Sanzana, E.; Char, F.; Peixinho, N.; Popescu, M.; Sonka, A.; Cornea, R. and 12 colleagues (2017). "The EURONEAR Lightcurve Survey of Near Earth Asteroids." *Earth, Moon & Planets* **120**, 41-100.

VizieR (2019). *http://vizier.u-strasbg.fr/viz-bin/VizieR.*

Warner, B.D.; Harris, A.W.; Pravec, P. (2009). "The Asteroid Lightcurve Database." *Icarus* **202**, 134-146. Updated 2019 Jan. *http://www.minorplanet.info/lightcurvedatabase.html*

Warner, B.D. (2011). "Upon Further Review: VI. An Examination of Previous Lightcurve Analysis from the Palmer Divide Observatory." *Minor Planet Bull.* **38**, 96-101.

Warner, B.D. (2013). "Asteroid Lightcurve Analysis at the Palmer Divide Observatory: 2012 June – September." *Minor Planet Bull.* **40**, 26-29.

Warner, B. D. (2015). "Near-Earth Asteroid Lightcurve Analysis at CS3-Palmer Divide Station: 2014 October-December." *Minor Planet Bull.* **42**, 115-127.

Warner, B.D. (2017). "Near-Earth Asteroid Lightcurve Analysis at CS3-Palmer Divide Station: 2016 October-December." *Minor Planet Bull.* **44**, 98-107.

Warner, B.D. (2018). *MPO Canopus* software, version 10.7.11.3. *http://www.bdwpublishing.com*

Warner, B.D. (2019). Center for Solar System Studies Web Site. *http://www.planetarysciences.org/PHP/CS3_Lightcurves.php*

Waszczak, A.; Chang, C.-K.; Ofek, E.O.; Laher, R.; Masci, F.; Levitan, D.; Surace, J.; Cheng, Y.-C.; Ip, W.-H.; Kinoshita, D.; Helou, G.; Prince, T.A.; Kulkarni, S. (2015). "Asteroid Light Curves from the Palomar Transient Factory Survey: Rotation Periods and Phase Functions from Sparse Photometry." *Astron. J.* **150**, A75.

LIGHTCURVE PHOTOMETRY OPPORTUNITIES: 2019 OCTOBER-DECEMBER

Brian D. Warner
Center for Solar System Studies / MoreData!
446 Sycamore Ave.
Eaton, CO 80615 USA
brian@MinorPlanetObserver.com

Alan W. Harris
MoreData!
La Cañada, CA 91011-3364 USA

Josef Ďurech
Astronomical Institute
Charles University
18000 Prague, CZECH REPUBLIC
durech@sirrah.troja.mff.cuni.cz

Lance A.M. Benner
Jet Propulsion Laboratory
Pasadena, CA 91109-8099 USA
lance.benner@jpl.nasa.gov

We present lists of asteroid photometry opportunities for objects reaching a favorable apparition and have no or poorly-defined lightcurve parameters. Additional data on these objects will help with shape and spin axis modeling using lightcurve inversion. We also include lists of objects that will or might be radar targets. Lightcurves for these objects can help constrain pole solutions and/or remove rotation period ambiguities that might not come from using radar data alone.

We present several lists of asteroids that are prime targets for photometry during the period 2019 October through December.

In the first three sets of tables, "Dec" is the declination and "U" is the quality code of the lightcurve. See the latest asteroid lightcurve data base (LCDB; Warner et al., 2009) documentation for an explanation of the U code:

http://www.minorplanet.info/lightcurvedatabase.html

The ephemeris generator on the CALL web site allows you to create custom lists for objects reaching V ≤ 18.0 during any month in the current year, e.g., limiting the results by magnitude and declination.

http://www.minorplanet.info/PHP/call_OppLCDBQuery.php

We refer you to past articles, e.g., *Minor Planet Bulletin* **36**, 188, for more detailed discussions about the individual lists and points of advice regarding observations for objects in each list.

Once you've obtained and analyzed your data, it's important to publish your results. Papers appearing in the *Minor Planet Bulletin* are indexed in the Astrophysical Data System (ADS) and so can be referenced by others in subsequent papers. It's also important to make the data available at least on a personal website or upon request. We urge you to consider submitting your raw data to the ALCDEF database. This can be accessed for uploading and downloading data at

http://www.alcdef.org

Containing almost 3.5 million observations for more than 14760 objects, we believe this to be the largest publicly available database of raw asteroid time-series lightcurve data.

Now that many backyard astronomers and small colleges have access to larger telescopes, we have expanded the photometry opportunities and spin axis lists to include asteroids reaching V = 15.5 and brighter (sometimes 15.0 when the list has more than 100 objects.

Lightcurve/Photometry Opportunities

Objects with U = 3– or 3 are excluded from this list since they will likely appear in the list for shape and spin axis modeling. Those asteroids rated U = 1 should be given higher priority over those rated U = 2 or 2+, but not necessarily over those with no period. On the other hand, d*o not overlook asteroids with* U = 2/2+ *on the assumption that the period is sufficiently established.* Regardless, do not let the existing period influence your analysis since even highly-rated result have been proven wrong at times. Note that the lightcurve amplitude in the tables could be more or less than what's given. Use the listing only as a guide.

An entry in bold italics is a near-Earth asteroid (NEA).

		Brightest			LCDB Data		
Number	Name	Date	Mag	Dec	Period	Amp	U
4686	Maisica	10 01.3	15.3	+9			
10516	Sakurajima	10 01.5	15.2	-1			
5534	1941 UN	10 01.8	14.2	+3	4.1	0.97	2
1885	Herero	10 01.9	14.8	+12	7.609	0.21-0.23	2
19719	Glasser	10 01.9	15.5	-11			
4422	Jarre	10 02.2	13.9	-2	5.428	0.12	2
7081	Ludibunda	10 03.5	15.0	+12			
5047	Zanda	10 03.8	15.5	+5			
5102	Benfranklin	10 03.9	15.4	+15			
26853	1992 UQ2	10 03.9	15.3	-27	8.27	0.14	2+
7408	Yoshihide	10 04.9	15.2	+7			
2517	Orma	10 05.4	15.2	+1			
4940	Polenov	10 05.8	15.3	+1			
8028	Joeengle	10 05.9	15.5	-2	9.1	0.35	2
6979	Shigefumi	10 06.2	14.6	+12			
3055	Annapavlova	10 07.1	15.3	+10	44.626	0.41	2
6964	Kunihiko	10 09.1	15.1	+6			
5565	Ukyounodaibu	10 09.4	15.0	-8			
15161	2000 FQ48	10 10.1	15.3	+22	6.663	0.10	2
48540	1993 TW8	10 11.0	15.3	+6			
1882	Rauma	10 12.2	15.0	+8	25.	0.1	2
2051	Chang	10 13.7	14.7	+8			
12230	1986 QN	10 16.3	15.2	+2			
6485	Wendeesther	10 17.3	15.2	+32	74.82	1.00	2
8020	Erzgebirge	10 17.5	15.4	+8			
6527	Takashiito	10 18.5	15.2	+18			
6982	1993 UA3	10 18.8	15.3	+10	16.08	0.10	2
3295	Murakami	10 19.7	14.8	+0			
16506	1990 UH1	10 19.9	15.5	-9			
11230	1999 JV57	10 20.3	14.6	+9			
2789	Foshan	10 20.7	14.9	+15			
6061	1981 SQ2	10 21.3	15.3	+11			
29180	1990 SW1	10 21.3	15.3	-4			
10936	1998 FN11	10 21.4	13.8	+21	25.7	0.28-0.40	2
6341	1993 UN3	10 21.8	15.5	+13			
3629	Lebedinskij	10 22.3	15.1	+15	9.338	0.2	2
8141	Nikolaev	10 22.5	14.7	+15			
9474	Cassadrury	10 22.9	15.3	+11			
3606	Pohjola	10 25.4	14.6	+26	2.92	0.11	2
10730	White	10 25.8	15.4	+17			
1673	van Houten	10 26.7	15.2	+12			
10615	1997 UK3	10 26.9	15.2	+15			
39197	2000 XA	10 27.1	15.4	+8	5.221	0.72	2
162082	***1998 HL1***	***10 27.3***	***12.5***	***+17***			
11420	1999 KR14	10 27.4	15.2	+4			
9333	Hiraimasa	10 27.5	14.8	+13			
53025	1998 WD	10 27.8	15.4	+5			
1944	Gunter	10 28.9	15.0	+13			
47908	2000 GH72	10 29.4	15.3	+10			
5827	Letunov	10 31.6	15.2	+7		0.97	
3347	Konstantin	11 01.5	15.5	+11			
14923	1994 TU3	11 01.6	15.3	+8	7.3	0.34	2+
3171	Wangshouguan	11 02.1	14.5	+17			
10987	1967 US	11 02.8	15.2	+7			
9348	1991 RH25	11 02.9	15.5	+9			
768	Struveana	11 03.3	13.1	+16	8.76	0.26-0.54	2+

(cont'd)		Brightest			LCDB Data		
Number	Name	Date	Mag	Dec	Period	Amp	U
12520	1998 HV78	11 03.3	15.3	+21			
12738	Satoshimiki	11 03.3	15.4	-12	8.708	0.20-0.25	2+
2099	Opik	11 04.1	15.1	+11	6.443	0.21- 0.7	2
3024	Hainan	11 05.3	15.0	+21	11.746	0.10-0.14	2+
2516	Roman	11 07.3	15.0	+14			
48433	1989 US1	11 07.5	15.5	+23			
16244	Broz	11 09.9	15.5	+12			
5795	Roshchina	11 10.0	15.2	+11			
2569	Madeline	11 11.7	13.5	+8		0.1	
13388	1999 AE6	11 11.8	15.3	+24			
1057	Wanda	11 15.4	13.5	+21	28.8	0.14-0.41	2
79789	1998 VL1	11 16.0	15.5	+12			
3460	Ashkova	11 16.1	15.5	+17	4.562	0.31	2
3085	Donna	11 16.8	15.3	+23			
3643	Tienchanglin	11 17.9	14.7	+18			
99248	***2001 KY66***	***11 18.5***	***15.5***	***+54***	***19.7***	***0.30***	***2-***
24417	2000 BK5	11 19.8	15.2	+25		0.49	
9628	Sendaiotsuna	11 20.7	14.9	+31			
3489	Lottie	11 20.9	15.5	+27			
4735	Gary	11 20.9	15.1	+13			
18130	2000 OK5	11 23.2	15.2	+19			
5792	Unstrut	11 23.3	15.1	+12			
9717	Lyudvasilia	11 23.3	15.4	+27			
13007	1984 AU	11 23.4	15.4	+26			
2758	Cordelia	11 25.1	15.2	+27			
6945	Dahlgren	11 25.6	15.5	+35			
5164	Mullo	11 25.8	15.4	+26			
10426	Charlierouse	11 27.1	14.8	+1			
16272	2000 JS55	11 29.7	15.4	+20			
2394	Nadeev	11 30.0	14.8	+19			
39525	1989 TR2	11 30.8	15.5	+28			
7992	Yozan	12 01.3	15.2	+23			
1359	Prieska	12 01.7	14.2	+23		0.04-0.05	
14031	Rozyo	12 01.8	15.2	+14	2.901		2
53916	2000 GW7	12 02.0	15.3	+17			
10707	1981 UV23	12 03.5	14.9	+25			
3644	Kojitaku	12 05.4	15.0	+29			
51149	2000 HF52	12 05.8	15.4	+34			
13696	1998 HU43	12 07.0	15.4	+32			
30963	Mount Banzan	12 08.1	15.5	+19		0.63	
8323	Krimigis	12 11.0	15.1	+6			
5822	Masakichi	12 11.8	15.2	+22			
862	Franzia	12 17.1	13.3	+37	7.52	0.10-0.13	2
3609	Liloketai	12 17.4	14.9	+26	15.636	0.17	2
4700	Carusi	12 20.8	14.5	+26			
7300	Yoshisada	12 23.1	15.3	+21			
14931	1994 WR3	12 23.1	15.5	+29			
18837	1999 NY62	12 23.3	15.5	+18			
7097	Yatsuka	12 25.0	15.2	+24			
4916	Brumberg	12 25.1	15.4	+10	6.683	0.19	2+
4421	Kayor	12 29.8	14.4	+24			

Low Phase Angle Opportunities

The Low Phase Angle list includes asteroids that reach very low phase angles. The "α" column is the minimum solar phase angle for the asteroid. Getting accurate, calibrated measurements (usually V band) at or very near the day of opposition can provide important information for those studying the "opposition effect." Use the on-line query form for the LCDB to get more details about a specific asteroid.

http://www.minorplanet.info/PHP/call_OppLCDBQuery.php

You will have the best chance of success working objects with low amplitude and periods that allow covering at least half a cycle every night. Objects with large amplitudes and/or long periods are much more difficult for phase angle studies since, for proper analysis, the data must be reduced to the average magnitude of the asteroid for each night. This reduction requires that you determine the period and the amplitude of the lightcurve; for long period objects that can be difficult. Refer to Harris *et al.* (1989; *Icarus* **81**, 365-374) for the details of the analysis procedure.

As an aside, some use the maximum light to find the phase slope parameter (*G*). However, this can produce a significantly different values for both *H* and *G* versus when using average light, which is the method used for values listed by the Minor Planet Center.

The International Astronomical Union (IAU) has adopted a new system, H-G_{12}, introduced by Muinonen *et al.* (2010; *Icarus* **209**, 542-555). It will be some years before H-G_{12} becomes widely used. Furthermore, it still needs refinement. That can be done mostly by having data for more asteroids, but only if at very low and moderate phase angles. We strongly encourage obtaining data every degree between 0° to 7°, the non-linear part of the curve that is due to the opposition effect. At angles $\alpha > 7°$, well-calibrated data every 2° or so out to about 25-30°, if possible, should be sufficient. Coverage beyond about 50° is not generally helpful since the H-G system is best defined with data from 0-30°.

Num	Name	Date	α	V	Dec	Period	Amp	U
5534	1941 UN	10 01.7	0.25	14.2	+03	4.10	0.97	2
533	Sara	10 04.4	0.56	13.8	+03	11.654	0.19-0.30	3
77	Frigga	10 05.6	0.34	11.3	+05	9.012	0.07-0.20	3
299	Thora	10 06.0	0.94	13.8	+07	272.9	0.37-0.50	3-
3014	Huangsushu	10 06.6	0.82	14.5	+04	15.697	0.32-0.35	3-
168	Sibylla	10 10.0	0.38	12.1	+07	47.009	0.16	3
720	Bohlinia	10 11.5	0.39	13.4	+06	8.919	0.16-0.46	3
72	Feronia	10 12.7	0.77	11.0	+09	8.097	0.11-0.15	3
33	Polyhymnia	10 14.7	0.41	10.2	+09	18.608	0.13-0.20	3
3533	Toyota	10 17.7	0.55	14.5	+08	2.981	0.16-0.20	3
26	Proserpina	10 25.5	0.48	11.1	+11	13.110	0.08-0.21	3
76	Freia	10 27.5	0.21	12.0	+12	9.973	0.05-0.33	3
1130	Skuld	10 29.0	0.05	13.5	+13	4.810	0.26-0.61	3
1102	Pepita	10 29.9	0.14	13.1	+14	5.105	0.31-0.36	3
429	Lotis	10 30.4	0.48	12.3	+15	13.577	0.21-0.24	3
3171	Wangshouguan	11 02.0	0.85	14.5	+17			
768	Struveana	11 03.3	0.31	13.1	+16	8.76	0.26-0.54	2+
1961	Dufour	11 03.7	0.68	14.5	+17	15.79	0.31-0.35	3-
1343	Nicole	11 06.7	0.20	14.4	+16	14.76	0.38-0.42	3-
233	Asterope	11 09.9	0.44	11.2	+16	19.70	0.25-0.35	3
116	Sirona	11 10.0	0.54	11.6	+15	12.028	0.42	3
4288	Tokyotech	11 10.8	0.66	13.9	+19	3.181	0.19	3
1223	Neckar	11 16.4	0.34	14.0	+20	7.81	0.16-0.45	3
332	Siri	11 25.8	0.82	13.3	+23	8.007	0.10-0.35	3
10	Hygiea	11 26.5	0.96	10.3	+24	27.630	0.09-0.33	3
409	Aspasia	11 27.1	0.25	11.1	+20	9.022	0.09-0.16	3
960	Birgit	11 28.5	0.26	14.5	+22	8.85	0.28-0.28	2+
416	Vaticana	11 28.8	0.75	12.6	+24	5.372	0.06-0.38	3
596	Scheila	11 30.2	0.35	13.6	+20	15.848	0.06-0.10	3
1359	Prieska	12 01.8	0.50	14.2	+23		0.04-0.05	
140	Siwa	12 05.0	0.89	12.4	+20	34.445	0.05-0.15	3
2512	Tavastia	12 08.1	0.66	14.1	+24	7.296	0.26-0.31	3
583	Klotilde	12 08.3	0.20	12.9	+23	9.214	0.17-0.30	3
1602	Indiana	12 09.8	0.18	14.5	+23	2.601	0.12-0.19	3
996	Hilaritas	12 11.8	0.37	14.5	+24	10.05	0.54-0.70	3
431	Nephele	12 13.9	0.47	13.1	+22	13.530	0.03-0.23	3
237	Coelestina	12 17.0	0.02	13.1	+23	29.215	0.16-0.25	3
1691	Oort	12 17.3	0.63	14.4	+22	10.271	0.38	3
86	Semele	12 19.5	0.18	11.8	+24	16.634	0.09-0.18	3
1074	Beljawskya	12 21.0	0.37	13.5	+24	6.284	0.32-0.37	3
786	Bredichina	12 21.1	0.12	13.4	+23	29.434	0.05-0.60	3-
1681	Steinmetz	12 22.6	0.48	13.6	+22	8.999	0.42	3
347	Pariana	12 23.5	0.78	11.9	+25	4.053	0.09-0.50	3
1423	Jose	12 23.6	0.87	14.5	+26	12.307	0.68-0.96	3
6555	1989 UU1	12 27.6	0.58	14.5	+24	12.678	0.27	3-
263	Dresda	12 28.3	0.61	13.9	+22	16.809	0.37-0.55	3
4421	Kayor	12 29.8	0.38	14.4	+24			
656	Beagle	12 30.8	0.28	13.8	+22	7.035	0.57-1.20	3
1003	Lilofee	12 31.4	0.71	14.0	+21	8.255	0.52-0.57	3

Shape/Spin Modeling Opportunities

Those doing work for modeling should contact Josef Ďurech at the email address above. If looking to add lightcurves for objects with existing models, visit the Database of Asteroid Models from Inversion Techniques (DAMIT) web site

http://astro.troja.mff.cuni.cz/projects/asteroids3D

Additional lightcurves could lead to the asteroid being added to or improving one in DAMIT, thus increasing the total number of asteroids with spin axis and shape models.

Included in the list below are objects that:

1. Are rated U = 3– or 3 in the LCDB
2. Do not have reported pole in the LCDB Summary table
3. Have at least three entries in the Details table of the LCDB where the lightcurve is rated U ≥ 2.

The caveat for condition #3 is that no check was made to see if the lightcurves are from the same apparition or if the phase angle bisector longitudes differ significantly from the upcoming apparition. The last check is often not possible because the LCDB does not list the approximate date of observations for all details records. Including that information is an on-going project.

Favorable apparitions are in bold text. NEAs are in italics.

		Brightest			LCDB Data		
Num	Name	Date	Mag	Dec	Period	Amp	U
522	Helga	10 03.3	13.5	-2	8.129	0.13-0.31	3
273	Atropos	10 03.5	13.5	-13	23.924	0.52-0.65	3
533	Sara	10 04.3	13.8	+3	11.654	0.19-0.30	3
1029	La Plata	10 05.7	14.8	+4	15.31	0.26-0.58	3
5240	Kwasan	10 09.8	15.0	+13	5.673	0.42-0.53	3
854	Frostia	10 13.2	14.7	+6	37.56	0.33-0.38	3
33	**Polyhymnia**	**10 14.6**	**10.2**	**+9**	**18.608**	**0.13-0.20**	**3**
1069	Planckia	10 15.0	14.3	-7	8.665	0.14-0.42	3
1425	Tuorla	10 15.1	15.1	+3	7.75	0.17-0.40	3
1186	Turnera	10 17.1	12.9	+4	12.085	0.20-0.34	3
3533	**Toyota**	**10 17.7**	**14.5**	**+8**	**2.9807**	**0.16-0.20**	**3**
1152	Pawona	10 21.5	14.2	+17	3.4154	0.16-0.26	3
1563	Noel	10 21.8	15.1	+6	3.5495	0.14-0.18	3
156	Xanthippe	10 21.9	13.4	+18	22.37	0.10-0.12	3
811	Nauheima	10 22.3	14.5	+7	4.0011	0.11-0.20	3
1799	Koussevitzky	10 22.9	15.2	-2	6.318	0.25-0.40	3
1060	Magnolia	10 24.6	14.7	+14	2.911	0.05-0.32	3
785	Zwetana	10 26.0	13.9	+0	8.8882	0.13-0.20	3
5369	Virgiugum	10 27.6	15.3	+6	5.8422	0.13-0.26	3-
6823	1988 ED1	11 01.2	15.2	-8	2.546	0.10-0.30	3
1355	Magoeba	11 02.8	14.6	+19	2.9712	0.06-0.22	3
1129	Neujmina	11 04.8	14.0	+25	5.0844	0.06-0.20	3
1806	Derice	11 05.1	14.1	+21	3.224	0.07-0.19	3
3986	Rozhkovskij	11 06.4	14.8	+24	3.548	0.25-0.35	3
3915	Fukushima	11 06.5	15.5	-2	9.418	0.50-0.79	3
773	Irmintraud	11 08.4	13.5	+40	6.7514	0.09-0.15	3
2083	Smither	11 08.7	15.2	+37	2.6717	0.08-0.11	3
2294	Andronikov	11 14.1	14.8	+27	3.1529	0.35-0.42	3
204	Kallisto	11 15.4	13.1	+13	19.489	0.09-0.26	3
294	Felicia	11 16.1	14.3	+10	10.4227	0.19-0.24	3
855	Newcombia	11 17.8	15.5	+29	3.003	0.33-0.41	3
463	Lola	11 20.2	13.9	+30	6.206	0.20-0.22	3
3754	Kathleen	11 22.3	14.9	+11	11.18	0.13-0.20	3-
3115	**Baily**	**11 24.0**	**13.5**	**+26**	**16.012**	**0.08- 0.2**	**3-**
332	Siri	11 25.8	13.2	+23	8.0074	0.10-0.35	3
956	Elisa	11 26.6	14.9	+13	16.492	0.35-0.37	3
6500	**Kodaira**	**11 26.7**	**14.8**	**-34**	**5.4**	**0.52-0.80**	**3**
309	Fraternitas	11 26.8	14.3	+26	22.398	0.10-0.35	3
1131	Porzia	11 27.6	14.4	+17	4.6584	0.15-0.23	3
459	**Signe**	**11 30.1**	**12.7**	**+34**	**5.5362**	**0.25-0.54**	**3**
633	Zelima	12 01.5	14.1	+6	11.73	0.14-0.49	3
4874	Burke	12 06.3	15.3	+1	3.657	0.22-0.23	3-
583	Klotilde	12 08.4	12.9	+23	9.2135	0.17-0.30	3
1602	Indiana	12 09.9	14.5	+23	2.601	0.12-0.19	3
2650	Elinor	12 10.1	14.6	+45	2.762	0.02-0.18	3
374	Burgundia	12 10.4	12.9	+15	6.972	0.05-0.18	3
465	Alekto	12 12.7	14.8	+27	10.936	0.12-0.18	3
721	Tabora	12 13.0	13.9	+31	7.982	0.19-0.30	3
70	Panopaea	12 13.5	12.2	+33	15.8052	0.07-0.18	3
1117	Reginita	12 14.5	15.0	+17	2.946	0.10-0.33	3
1829	**Dawson**	**12 16.7**	**14.4**	**+29**	**4.254**	**0.05-0.32**	**3**
3483	**Svetlov**	**12 20.4**	**15.1**	**+25**	**6.79**	**0.21-0.28**	**3**
715	Transvaalia	12 23.5	14.0	+39	11.83	0.19-0.32	3
1220	**Crocus**	**12 23.7**	**15.5**	**+17**	**491.4**	**0.15-1.00**	**3**
563	**Suleika**	**12 23.9**	**10.6**	**+26**	**5.69**	**0.13-0.28**	**3**
256	Walpurga	12 24.7	14.5	+4	16.664	0.25-0.58	3
929	Algunde	12 25.1	14.7	+19	3.3102	0.13-0.17	3
834	Burnhamia	12 26.8	14.8	+18	13.875	0.15-0.22	3
2478	**Tokai**	**12 28.2**	**14.3**	**+18**	**25.885**	**0.41-0.90**	**3**
5448	Siebold	12 29.1	14.9	+30	2.9546	0.24-0.53	3

Radar-Optical Opportunities

Past radar targets:
http://echo.jpl.nasa.gov/~lance/radar.nea.periods.html

Arecibo targets:
http://www.naic.edu/~pradar
http://www.naic.edu/~pradar/ephemfuture.txt

Goldstone targets:
http://echo.jpl.nasa.gov/asteroids/goldstone_asteroid_schedule.html

These are based on *known* targets at the time the list was prepared. It is very common for newly discovered objects to move up the list and become radar targets on short notice. We recommend that you keep up with the latest discoveries the Minor Planet Center observing tools

In particular, monitor NEAs and be flexible with your observing program. In some cases, you may have only 1-3 days when the asteroid is within reach of your equipment. Be sure to keep in touch with the radar team (through Dr. Benner's email or their Facebook or Twitter accounts) if you get data. The team may not always be observing the target but your initial results may change their plans. In all cases, your efforts are greatly appreciated.

Use the ephemerides below as a guide to your best chances for observing, but remember that photometry may be possible before and/or after the ephemerides given below. Note that *geocentric* positions are given. Use these web sites to generate updated and *topocentric* positions:

MPC: *http://www.minorplanetcenter.net/iau/MPEph/MPEph.html*
JPL: *http://ssd.jpl.nasa.gov/?horizons*

In the ephemerides below, ED and SD are, respectively, the Earth and Sun distances (AU), V is the estimated Johnson V magnitude, and α is the phase angle. SE and ME are the great circle distances (in degrees) of the Sun and Moon from the asteroid. MP is the lunar phase and GB is the galactic latitude. "PHA" indicates that the object is a "potentially hazardous asteroid", meaning that at some (long distant) time, its orbit might take it very close to Earth.

About YORP Acceleration

Many, if not all, of the targets in this section are near-Earth asteroids. These objects are particularly sensitive to YORP acceleration. YORP (Yarkovsky–O'Keefe–Radzievskii–Paddack) is the asymmetric thermal re-radiation of sunlight that can cause an asteroid's rotation period to increase or decrease. High precision lightcurves at multiple apparitions can be used to model the asteroid's *sidereal* rotation period and see if it's changing.

It usually takes four apparitions to have sufficient data to determine if the asteroid rotation rate is changing under the influence of YORP. This is why observing asteroids that already have well-known periods is still a valuable use of telescope time. It is even more so when considering the BYORP (binary-YORP) effect among binary asteroids that has stabilized the spin so that acceleration of the primary body is not the same as if it would be if there were no satellite.

To help focus efforts in YORP detection, Table I gives a quick summary of this quarter's radar-optical targets. The family or group for the asteroid is given under the number name. Also under the name will be additional flags such as "PHA" for Potentially Hazardous Asteroid, NPAR for a tumbler, and/or "BIN" to

indicate the asteroid is a binary (or multiple) system. "BIN?" means that the asteroid is a suspected but not confirmed binary. The period is in hours and, in the case of binary, for the primary. The Amp column gives the known range of lightcurve amplitudes. The App columns gives the number of different apparitions at which a lightcurve period was reported while the Last column gives the year for the last reported period. The R SNR column indicates the estimated radar SNR using the tool at

http://www.naic.edu/~eriverav/scripts/index.php

The "A" is for Arecibo; "G" is for Goldstone.

Asteroid	Period	Amp	App	Last	R	SNR
(141593) 2002 HK12	**12.690**	**1.5**	**1**	**2002**	**A**	**470**
NEA					**G**	**160**
(1620) Geographos	5.222	0.95	4	2019	G	25
NEA		2.03				
(467317) 2000 QW7	71.3	1.0	1	2000	A	2950
NEA					G	990
(2100) Ra-Shalom	19.797	0.30	4	2016	A	35
NEA		0.55			G	10
(354030) 2001 RB18	-	-	-	-	A	40
NEA					G	15
(297418) 2000 SP43	-	-	-	-	G	50
NEA						
(153814) 2001 WN5	-	-	-	-	A	40
NEA					G	13
(395289) 2011 BJ2	7.03	0.48	1	2014		
NEA						
(162082) 1998 HL1	**-**	**-**	**-**	**-**	**A**	**700**
NEA					**G**	**230**
2015 JD1	**-**	**-**	**-**	**-**	**A**	**530**
NEA					**G**	**180**
(481394) 2006 SF6	**11.517**	**0.97**	**1**	**2019**	**A**	**1470**
NEA					**G**	**490**
2010 JG	**-**	**-**	**-**	**-**	**A**	**90**
NEA					**G**	**30**
(99248) 2001 KY66	**19.7**	**0.30**	**1**	**2015**		
NEA						
(85236) 1993 KH	5.057	0.32	1	2019		
NEA						
(162723) 2000 VM2	-	-	-	-		
NEA						
(216258) 2006 WH1	**7.30**	**0.20**	**1**	**2006**	**A**	**510**
NEA					**G**	**170**

Table I. Summary of radar-optical opportunities for the current quarter. Period and amplitude data are from the asteroid lightcurve database (Warner *et al.,* 2009; *Icarus* **202**, 134-146). SNR values are *estimates* that are affected by power output of the radar along with rotation period, size, and distance. They are given for relative comparisons among the objects in the list.

The SNRs were calculated using the current MPCORB absolute magnitude (H), a period of 4 hours (2 hours if $D \leq 200$ m) if it's not known, and the approximate minimum Earth distance during the current quarter. These are estimates only and assume that the radars are fully functional.

If the SNR value is in bold text, the object was found on the radar planning pages listed above. Otherwise, the planning tool at

http://www.minorplanet.info/PHP/call_OppLCDBQuery.php

was used to find known NEAs that were V < 18.0 during the quarter. An object is usually placed on the list only if the estimated Arecibo SNR > 10 when using the SNR calculator mentioned above.

There are a number of hold-overs from the previous quarter (with shortened ephemerides to cover the current quarter). While the best radar opportunities may have gone by, these objects are still within reach and should be observed, if possible. It's rarely the case, especially when shape/spin axis modeling, that there are too many data. Remember that the best set for modeling includes not just data from multiple apparitions but from as wide a range of phase angles during each apparition as well.

(141593) 2002 HK12 (H = 18.1)

The rotation period for 2002 HK12 is about 12.7 hours. A single station can eventually cover the entire lightcurve but two observers at well-separated longitudes could make much quicker work of completing the lightcurve. The estimated diameter is 710 meters.

DATE	RA	Dec	ED	SD	V	α	SE	ME	MP	GB
09/26	02 54.3	+29 26	0.20	1.14	16.5	41.2	131	93	-0.11	-26
10/03	02 36.0	+27 23	0.23	1.19	16.6	30.9	142	154	+0.23	-30
10/10	02 20.0	+25 19	0.26	1.24	16.7	21.5	153	68	+0.87	-33
10/17	02 06.6	+23 18	0.30	1.29	16.8	13.4	163	25	-0.91	-36
10/24	01 55.8	+21 26	0.35	1.34	17.0	7.4	170	117	-0.23	-39
10/31	01 47.9	+19 48	0.41	1.39	17.4	6.7	171	136	+0.11	-41
11/07	01 42.7	+18 26	0.47	1.45	17.9	10.4	165	49	+0.74	-43

(1620) Geographos (H = 15.6)

The period is well known (P ~ 5.22204 h) but data from each new apparition help refine the amount that YORP is increasing the asteroid's rotation rate (decreasing the period), which has been given as $(1.15\pm0.15)\times10^{-8}$ rad d^{-2} (Durech et al., 2008, *A&A* **489**, L25-28).

DATE	RA	Dec	ED	SD	V	α	SE	ME	MP	GB
10/01	20 32.3	-01 23	0.30	1.19	15.1	46.2	121	90	+0.08	-23
10/06	20 48.2	+00 48	0.34	1.21	15.4	45.1	121	34	+0.53	-25
10/11	21 02.1	+02 31	0.39	1.24	15.7	44.3	120	35	+0.93	-27
10/16	21 14.7	+03 55	0.44	1.27	16.0	43.8	119	86	-0.96	-29
10/21	21 26.4	+05 05	0.49	1.29	16.3	43.4	117	140	-0.56	-31
10/26	21 37.5	+06 05	0.54	1.31	16.5	43.2	115	139	-0.07	-33
10/31	21 48.2	+06 57	0.59	1.34	16.7	42.9	113	77	+0.11	-34
11/05	21 58.7	+07 46	0.64	1.36	17.0	42.7	111	27	+0.56	-36
11/10	22 09.0	+08 31	0.69	1.38	17.2	42.5	109	47	+0.94	-37
11/15	22 19.1	+09 13	0.75	1.41	17.4	42.3	107	101	-0.94	-38

(467317) 2000 QW7 (H = 19.8)

The period for this NEA is known to be long (~71 h) and, to make things more difficult, is nearly commensurate with an Earth day (close to the same section of the curve is observed every three days). This calls for another well-coordinated observing campaign.

On the plus side, the estimated size of 330 meters and minimum distance of about 0.036 AU mean that the SNR for Arecibo could be near 3000 and 1000 for Goldstone.

DATE	RA	Dec	ED	SD	V	α	SE	ME	MP	GB
10/01	02 57.6	-18 00	0.07	1.05	15.7	40.0	137	151	+0.08	-60
10/06	03 15.8	-14 12	0.09	1.07	16.2	38.8	138	112	+0.53	-54
10/11	03 25.9	-11 26	0.11	1.08	16.6	36.3	140	62	+0.93	-51
10/16	03 31.2	-09 17	0.12	1.10	16.9	33.0	143	23	-0.96	-48
10/21	03 33.4	-07 30	0.14	1.12	17.1	29.3	147	65	-0.56	-47
10/26	03 33.6	-05 56	0.17	1.14	17.3	25.5	150	131	-0.07	-46
10/31	03 32.5	-04 31	0.19	1.17	17.6	21.9	154	148	+0.11	-45
11/05	03 30.8	-03 09	0.21	1.19	17.8	18.7	157	90	+0.56	-45
11/10	03 28.7	-01 51	0.24	1.22	18.0	16.3	160	34	+0.94	-45

(2100) Ra-Shalom (*H* = 16.1)

Because of orbital geometries, Ra-Shalom (1.8 km) has reported rotation periods from only four apparitions between 1978 and 2016. The period is about 19.8 h, which makes it a difficult target. For those with larger telescopes, it's accessible for the first six weeks of the quarter.

DATE	RA	Dec	ED	SD	V	α	SE	ME	MP	GB
10/01	23 00.8	-28 16	0.19	1.16	14.2	31.6	143	116	+0.08	-66
10/06	22 36.1	-33 53	0.21	1.15	14.6	41.3	131	46	+0.53	-60
10/11	22 14.4	-38 05	0.23	1.13	15.0	49.6	120	31	+0.93	-55
10/16	21 56.1	-41 07	0.25	1.11	15.4	56.6	112	88	-0.96	-52
10/21	21 41.3	-43 18	0.27	1.09	15.7	62.5	104	146	-0.56	-49
10/26	21 29.5	-44 55	0.29	1.07	16.0	67.7	97	125	-0.07	-46
10/31	21 20.2	-46 09	0.31	1.04	16.2	72.4	90	59	+0.11	-45
11/05	21 12.6	-47 08	0.33	1.01	16.4	76.8	84	29	+0.56	-43
11/10	21 06.0	-47 59	0.34	0.98	16.6	81.2	79	74	+0.94	-42
11/15	20 59.6	-48 44	0.36	0.95	16.8	85.6	73	129	-0.94	-41

(354030) 2001 RB18 (*H* = 18.5)

There's no reported period in the LCDB for this 600 meter NEA. It's accessible the entire quarter. The prolonged period and range of phase angles makes for an opportunity to do a detailed study of lightcurve changes as the phase angle decreases to a minimum of about 10° and then rises.

DATE	RA	Dec	ED	SD	V	α	SE	ME	MP	GB
10/01	01 57.4	+19 59	0.09	1.08	14.7	25.7	152	167	+0.08	-40
10/11	03 19.8	+16 48	0.10	1.09	15.1	31.7	145	66	+0.93	-33
10/21	04 10.1	+13 01	0.13	1.10	15.6	32.7	143	48	-0.56	-27
10/31	04 35.2	+10 15	0.16	1.13	16.0	29.1	146	169	+0.11	-24
11/10	04 45.4	+08 39	0.20	1.17	16.4	23.0	153	53	+0.94	-23
11/20	04 47.3	+08 02	0.24	1.22	16.7	16.2	160	79	-0.49	-23
11/30	04 45.5	+08 10	0.29	1.27	17.0	11.2	165	139	+0.13	-23
12/10	04 43.4	+08 53	0.36	1.33	17.6	11.0	165	21	+0.95	-23
12/20	04 42.8	+09 56	0.43	1.40	18.2	14.5	159	118	-0.41	-23
12/30	04 44.7	+11 10	0.52	1.46	18.9	18.7	151	108	+0.14	-22

(297418) 2000 SP43 (*H* = 18.5)

2000 SP43 is a 600-meter NEA with no reported rotation period. The large phase angles could produce unusual lightcurve shapes.

DATE	RA	Dec	ED	SD	V	α	SE	ME	MP	GB
10/01	19 32.1	-03 42	0.12	1.04	16.3	67.7	106	75	+0.08	-11
10/03	19 50.4	-02 37	0.13	1.05	16.5	64.3	109	53	+0.23	-14
10/05	20 05.3	-01 45	0.15	1.06	16.7	61.8	111	34	+0.43	-17
10/07	20 17.5	-01 01	0.16	1.07	16.8	59.9	112	21	+0.63	-20
10/09	20 27.8	-00 25	0.18	1.08	17.0	58.4	113	25	+0.80	-22
10/11	20 36.7	+00 05	0.19	1.09	17.2	57.3	113	40	+0.93	-23
10/13	20 44.4	+00 32	0.21	1.10	17.4	56.5	113	60	+0.99	-25
10/15	20 51.3	+00 55	0.23	1.11	17.5	55.9	113	80	-0.99	-26
10/17	20 57.5	+01 15	0.24	1.12	17.7	55.4	113	102	-0.91	-27
10/19	21 03.2	+01 33	0.26	1.12	17.8	55.0	113	124	-0.76	-28

(153814) 2001 WN5 (*H* = 18.2)

There's no reported period for 2001 WN5. Mainzer et al. (2016) give a diameter of about 930 meters when using *H* = 18.3. This one goes through a very wide range of phase angles in the first two months of the quarter. This makes it a good target for finding *H* and *G*.

DATE	RA	Dec	ED	SD	V	α	SE	ME	MP	GB
10/01	05 36.1	+34 29	0.18	1.05	17.0	68.3	102	131	+0.08	+1
10/08	05 13.4	+33 10	0.20	1.10	17.0	56.7	114	130	+0.72	-3
10/15	04 51.8	+31 45	0.22	1.14	16.9	45.7	125	44	-0.99	-8
10/22	04 30.5	+30 10	0.24	1.19	17.0	35.1	137	54	-0.45	-12
10/29	04 09.9	+28 26	0.27	1.23	17.0	25.0	148	158	+0.01	-17
11/05	03 51.0	+26 36	0.30	1.28	17.0	15.6	160	103	+0.56	-21
11/12	03 34.9	+24 49	0.34	1.33	17.0	7.4	170	17	+1.00	-25
11/19	03 22.1	+23 12	0.39	1.38	17.2	3.5	175	81	-0.60	-28
11/26	03 12.7	+21 49	0.45	1.43	17.8	8.3	168	172	-0.01	-30
12/03	03 06.6	+20 44	0.51	1.47	18.4	13.5	160	84	+0.38	-32

(395289) 2011 BJ2 (*H* = 18.3)

There is only one period given in the LCDB: Warner (2014), who determined *P* = 7.03 h but new observations are encouraged. Because of the moon, the best conditions are early or late in October.

DATE	RA	Dec	ED	SD	V	α	SE	ME	MP	GB
10/10	05 17.3	-05 11	0.30	1.16	17.9	51.6	115	100	+0.87	-23
10/15	05 20.0	+03 00	0.23	1.13	17.3	50.1	120	47	-0.99	-19
10/20	05 22.3	+17 43	0.17	1.10	16.5	47.8	125	17	-0.66	-11
10/25	05 24.0	+44 36	0.13	1.07	15.9	49.4	125	83	-0.14	+5
10/30	05 23.3	+79 40	0.13	1.05	16.3	62.7	110	117	+0.05	+23
11/04	17 28.8	+75 20	0.18	1.02	17.2	75.7	94	101	+0.46	+31
11/09	17 28.4	+61 40	0.24	0.99	18.0	82.2	84	99	+0.88	+33

(162082) 1998 HL1 (*H* = 18.9)

This NEA is accessible from the first of October through mid-December. The ephemeris concentrates on the time when it is brightest. The diameter is about 500 meters.

DATE	RA	Dec	ED	SD	V	α	SE	ME	MP	GB
10/20	23 48.5	+64 35	0.06	1.03	14.7	55.0	122	74	-0.66	+2
10/22	00 42.9	+55 22	0.05	1.03	14.1	44.2	134	87	-0.45	-8
10/24	01 23.6	+41 57	0.04	1.03	13.4	29.8	149	110	-0.23	-21
10/26	01 53.2	+25 34	0.04	1.03	12.8	12.9	167	143	-0.07	-35
10/28	02 15.0	+09 17	0.04	1.04	12.6	3.9	176	177	+0.00	-48
10/30	02 31.3	-04 12	0.05	1.04	13.4	17.3	162	150	+0.05	-57
11/01	02 43.8	-14 16	0.06	1.04	14.1	27.4	151	121	+0.18	-61
11/03	02 53.5	-21 31	0.07	1.05	14.6	34.5	143	96	+0.37	-62
11/05	03 01.2	-26 45	0.08	1.05	15.1	39.6	137	76	+0.56	-61
11/07	03 07.5	-30 35	0.09	1.06	15.5	43.3	133	60	+0.74	-60

2015 JD1 (*H* = 20.6)

The diameter is about 200 meters, so the period is likely *P* > 2 h. Make no assumptions. The asteroid moves quickly from the northern into the southern celestial hemisphere. The ephemeris has two-day intervals and is centered on the time the asteroid is brightest.

DATE	RA	Dec	ED	SD	V	α	SE	ME	MP	GB
10/30	20 09.0	+41 36	0.05	1.00	16.7	79.5	98	82	+0.05	+5
11/01	21 17.7	+34 02	0.04	1.01	15.9	68.7	109	74	+0.18	-11
11/03	22 33.1	+20 34	0.03	1.01	15.2	54.9	124	59	+0.37	-32
11/05	23 40.9	+04 05	0.03	1.02	15.0	43.6	135	40	+0.56	-54
11/07	00 33.5	-09 30	0.04	1.02	15.3	40.0	138	23	+0.74	-72
11/09	01 11.7	-18 28	0.05	1.03	15.8	41.3	137	19	+0.88	-80
11/11	01 39.4	-24 04	0.06	1.03	16.3	43.5	134	32	+0.98	-79
11/13	01 59.8	-27 38	0.07	1.04	16.7	45.4	132	49	-1.00	-75
11/15	02 15.2	-29 59	0.09	1.05	17.1	46.9	129	68	-0.94	-71
11/17	02 27.2	-31 34	0.10	1.05	17.5	48.0	128	88	-0.80	-69

(481394) 2006 SF6 (*H* = 19.9)

Warner (2019) found a period of 11.517 h for this 300-m NEA. The period is nearly commensurate with an Earth day, so two observers at widely separated longitudes could make easier work of confirming the result. The galactic latitude is low into November; that makes for more of a challenge.

DATE	RA	Dec	ED	SD	V	α	SE	ME	MP	GB
10/10	03 56.0	+33 24	0.22	1.15	18.5	40.7	131	91	+0.87	-15
10/15	03 58.4	+33 14	0.19	1.14	18.1	37.9	135	35	-0.99	-15
10/20	03 58.9	+32 46	0.16	1.13	17.6	34.5	140	35	-0.66	-15
10/25	03 57.0	+31 49	0.14	1.11	17.1	30.4	146	102	-0.14	-16
10/30	03 51.7	+30 07	0.11	1.09	16.5	25.1	152	167	+0.05	-18
11/04	03 41.5	+27 04	0.09	1.07	15.7	18.1	160	113	+0.46	-22
11/09	03 23.3	+21 23	0.06	1.05	14.6	7.9	172	48	+0.88	-29
11/14	02 49.9	+09 37	0.04	1.03	13.8	9.9	170	25	-0.98	-43
11/19	01 42.1	-16 05	0.03	1.01	14.0	43.7	135	116	-0.60	-74
11/24	23 20.9	-48 11	0.03	0.99	15.6	90.0	88	118	-0.09	-63

2010 JG (*H* = 20.9)

The rotation period is unknown for this 200-m NEA (Mainzer et al., 2016). The size is close to where the possibility of $P < 2$ h increases significantly. The window of opportunity is short and for those with larger telescopes.

DATE	RA	Dec	ED	SD	V	α	SE	ME	MP	GB
11/15	12 03.0	+42 59	0.05	0.98	18.2	100.9	76	83	-0.94	+71
11/16	12 03.5	+50 51	0.06	0.98	18.1	94.7	82	70	-0.88	+65
11/17	12 04.1	+57 39	0.06	0.99	18.0	89.2	87	61	-0.80	+58
11/18	12 04.9	+63 26	0.07	0.99	18.0	84.4	92	56	-0.70	+53
11/19	12 05.8	+68 19	0.07	1.00	18.1	80.4	95	56	-0.60	+48
11/20	12 06.9	+72 28	0.08	1.00	18.1	76.9	99	59	-0.49	+44
11/21	12 08.3	+75 59	0.09	1.01	18.2	74.0	101	66	-0.37	+41
11/22	12 09.9	+79 00	0.09	1.01	18.3	71.4	103	73	-0.26	+38
11/23	12 12.0	+81 36	0.10	1.02	18.4	69.3	105	82	-0.17	+35
11/24	12 14.8	+83 52	0.11	1.02	18.5	67.3	107	90	-0.09	+33

(99248) 2001 KY66 (*H* = 16.4)

The NEA is accessible throughout the quarter, but the galactic longitude is low starting in mid-November. Warner (2015) found a period of 19.7 h but it's a weak solution (U = 2–). Well-calibrated data will be particularly helpful. The diameter is 1.6 km.

DATE	RA	Dec	ED	SD	V	α	SE	ME	MP	GB
10/01	12 33.5	+67 20	0.20	0.95	16.4	98.3	70	80	+0.08	+50
10/11	10 31.7	+71 21	0.22	0.99	16.1	85.4	82	118	+0.93	+42
10/21	08 37.0	+69 53	0.24	1.04	15.9	71.9	95	48	-0.56	+34
10/31	07 14.1	+65 37	0.26	1.10	15.7	58.1	109	130	+0.11	+27
11/10	06 13.6	+59 48	0.28	1.17	15.7	44.1	125	80	+0.94	+19
11/20	05 29.0	+52 56	0.31	1.24	15.6	30.5	140	66	-0.49	+10
11/30	04 57.8	+45 45	0.35	1.31	15.7	18.7	155	143	+0.13	+2
12/10	04 38.1	+39 12	0.42	1.39	15.9	12.2	163	30	+0.95	-5
12/20	04 27.7	+33 51	0.50	1.46	16.5	13.7	159	116	-0.41	-10
12/30	04 24.1	+29 49	0.60	1.54	17.2	18.4	150	107	+0.14	-14

(85236) 1993 KH (*H* = 18.7)

Warner (2019) reported a period of 5.057 h. That could use confirmation and/or refinement. The diameter of the NEA is about 500 meters. It's accessible for the last two months of the quarter, which should provide plenty of time to get observations.

DATE	RA	Dec	ED	SD	V	α	SE	ME	MP	GB
11/01	10 13.0	-13 46	0.11	0.94	18.1	114.0	60	107	+0.18	+34
11/08	09 47.4	+05 00	0.10	0.97	17.1	96.4	78	150	+0.82	+41
11/15	09 21.9	+23 41	0.11	1.01	16.6	77.4	97	55	-0.94	+43
11/22	08 52.8	+39 02	0.12	1.04	16.4	61.0	113	53	-0.26	+40
11/29	08 17.0	+50 01	0.14	1.08	16.5	48.4	125	146	+0.07	+34
12/06	07 34.0	+56 55	0.17	1.11	16.7	39.5	134	104	+0.66	+28
12/13	06 48.2	+60 27	0.20	1.15	16.9	33.9	139	39	-0.99	+23
12/20	06 07.1	+61 30	0.24	1.18	17.3	31.0	142	92	-0.41	+19
12/27	05 36.1	+60 56	0.28	1.22	17.7	30.1	142	139	+0.01	+15
01/03	05 16.4	+59 32	0.33	1.25	18.1	30.5	140	80	+0.48	+12

(162723) 2000 VM2 (*H* = 17.4)

This NEA is about 1 km in diameter. There is no period given in the LCDB. The galactic longitude is highest, though not particularly favorable, when the asteroid is faintest and lowest when the asteroid is brightest. Neither is a winning combination.

DATE	RA	Dec	ED	SD	V	α	SE	ME	MP	GB
10/20	03 12.5	+34 50	0.53	1.47	17.9	21.7	147	45	-0.66	-20
10/25	03 05.9	+36 34	0.47	1.42	17.5	20.1	151	110	-0.14	-19
10/30	02 55.7	+38 32	0.40	1.37	17.1	19.0	153	155	+0.05	-18
11/04	02 40.3	+40 46	0.35	1.31	16.7	19.1	154	104	+0.46	-18
11/09	02 17.5	+43 16	0.29	1.26	16.3	21.5	152	51	+0.88	-17
11/14	01 42.9	+45 54	0.24	1.20	16.0	27.2	146	43	-0.98	-16
11/19	00 50.1	+48 06	0.20	1.14	15.7	36.9	136	97	-0.60	-15
11/24	23 32.6	+48 16	0.17	1.08	15.6	51.3	121	129	-0.09	-13
11/29	21 56.6	+43 31	0.15	1.02	15.8	71.0	101	82	+0.07	-9

(216258) 2006 WH1 (*H* = 20.2)

The LCDB lists one previous period, 7.30 h (Warner, 2007). It's rated U = 2, so it's possible that the true period is significantly different. The diameter is about 270 meters. The Fates are again unkind in that the asteroid remains at low galactic latitudes from mid-November to late December.

DATE	RA	Dec	ED	SD	V	α	SE	ME	MP	GB
11/20	05 14.0	+22 53	0.23	1.20	18.4	18.2	158	69	-0.49	-9
11/24	05 21.0	+22 07	0.20	1.18	17.9	16.6	160	125	-0.09	-8
11/28	05 29.5	+21 02	0.17	1.15	17.4	15.3	162	179	+0.02	-7
12/02	05 40.6	+19 26	0.14	1.12	16.9	14.6	163	131	+0.29	-6
12/06	05 56.2	+16 58	0.11	1.09	16.4	15.4	163	86	+0.66	-4
12/10	06 20.3	+12 50	0.08	1.06	15.9	18.9	160	44	+0.95	-1
12/14	07 01.5	+05 08	0.06	1.04	15.4	28.2	150	18	-0.96	+5
12/18	08 20.1	-10 04	0.04	1.01	15.2	49.5	129	44	-0.64	+15
12/22	10 39.2	-30 11	0.04	0.99	16.1	83.8	94	56	-0.20	+25
12/26	12 58.8	-37 54	0.05	0.96	17.9	109.3	68	66	+0.00	+25

INDEX TO VOLUME 46

Franco, L.; Marchini, A.; Casalnuovo, G.B.; Chinaglia, B.; Baj, G.; Scarfi, G.; Galli, G.; Bacci, P.; Maestripieri, M.; Valvasori, L.; Caselli, C.; Punzo, P.; Montigiani, N.; Mannucci, M.; Bachini, M.; Succi, R.; Bacci, R. "Lightcurves for 227 Oceana, 359 Georgia, 1453 Fennia and 1717 Arlon" 350–352.

Franco, L.; Marchini, A.; Galdies, C.; Brincat, S.M.; Grech, W. "Spin Axis and Shape Model for 1117 Reginita" 269–271.

Franco, L.; Marchini, A.; Papini, R.; Banfi, M.; Salvaggio, F.; Noschese, A.; Vecchione, A.; Catapano, A. "H-G Parameters for (37652) 1994 JS1" 373.

Franco, L.; Montigiani, N.; Mannucci, M.; Benedetti, W. "Lightcurve and a Spin-shape Model for 16847 Sanpoloamosciano" 196–198.

Franco, L.; Pilcher, F. "A New Lightcurve and Spin-shape Model for 46 Hestia" 140–142.

Franco, L.; Pilcher, F.; Marchini, A.; Baj, G.; Bacci, P.; Maestripieri, M.; Bacci, R. "Spin-shape Model for 131 Vala" 392–394.

Fuller, K.; Sanchez, C.; Montgomery, K. "Rotational Periods and Lightcurves of Four Asteroids" 1–2.

Galdies, C.; Brincat, S.M.; Grech, W. "Photometric Observations of Main-belt Asteroids 232 Russia, 1117 Reginita, and (11200) 1999 CV121" 61–62.

Gao, X.; Tan, H. "The Rotation Period of (32209) 2000 OW9" 215.

Gonçalves, R.M.D. "Lightcurve and Revised Rotation Period for 1277 Dolores" 95.

Gonzalez, L.; Bentz, M.C.; Paredes, L. "V-Band Photometric Monitoring of 852 Wlandilena" 8–9.

Hayes-Gehrke, M.; Anil, A.; Baffes, P.; Ferrel, B.; Gandham, S.; Gregory, M.; Menon, R.; Moore, C.; Pongchit, A.; Proulx, A.; Sackalosky, C.; Sefik, Y.; Weddle, T.; Yates, E. "Lightcurve for 3816 Chugainov" 387.

Hayes-Gehrke, M.N.; Berk, M.; Fatodu, A.; Kanani, B.; Kropschot, Q.; Marks, J.; Misangyi, E.; Nguyen, M.; Stone, J.; Suniga, J.; Thompson, M.; Vorsteg, M.; Wagman, T.; Marchini, A.; Banfi, M.; Papini, R.; Salvaggio, F.; Brincat, S.M.; Galdies, C.; Grech, W. "Lightcurve Analysis and Rotation Period of 6372 Walker" 388.

Hayes-Gehrke, M.N.; Singh, A.; Malwitz, A.; Wilson, C.; Huang, D.; Nava, D.; Yu, I.; Chappell, N.; Lin, J.; Du, L.; Vijaykumar, A.; Dries, R.; Lou, Y.; Brincat, S.M.; Galdies, C.; Grech, W. "Lightcurve Analysis of Five Main-belt Asteroids: 3446 Combes, (9410) 1995 BJ1, (17780) 1998 FY13, (24491) 2000 YT 123, and 28341 Bingaman" 385–386.

Hayes-Gehrke, M.N.; Yates, E.; Sewell, C.; Tapscott, E.; Margolis, A.; Goren, E.; Merlo-Coyne, J.; Zahid, S.; Reinhardt, A.; Malone, S.; Gardner, C.; Seidell, T.; Koehn, J.; Pattanayak, S. "2638 Gadolin Lightcurve Analysis" 384.

Izzo, L.; Cerdan, H.F.B.; Diaz, M.A.D.; Suarez, J.L.; Rodriguez, E.M.; Megias, B.M.; Romero. J.N.; De La Llave, A.R.; Vergara, I..Y.; Nosches, A.; Mollica, M, Vecchione, A. "On the Rotation Period of 1599 Giomus" 71–72.

Izzo, L.; Franciscis, S.; Rodrigáñez, F.J.R.S.; Romero, A.C.; García, A.M.; Martínez, M.S.; Roa, A.G.; Rodríguez, J.A.G; Lopez, P.F.F.; Muñoz, J.G.; Noschese, A.; Mollica, M.; Vecchione, A. "The Rotation Period of 5351 Diderot" 377.

Klinglesmith, D.A. III "Photometric Lightcurve for 4807 Noboru" 199.

Klinglesmith, D.A. III; Lovato, E.A. "Etscorn Asteroids: 2018 July–September" 81–82.

Klinglesmith, D.A. III; Goodwrench, Z. "Etscorn Lightcurves: January 2019–April 2019" 329–330.

Loera-González, P.; Olguín, L.; Contreras, M.E.; Morales, J.S.; Schuster, W.; Sada, P.V. "Results of the First Semester of the 2018 Mexican Asteroid Photometry Campaign" 283–285.

Loera-González, P.; Olguín, L.; Saucedo, J.C.; Núñez-López, R.; Yahia-Keith, N.A. "Lightcurve Based Rotational Period Determination for Asteroids at Unison Observatory: First Half of 2018" 97–98.

López-Oquendo, A.J.; Cotto-Figueroa, D. "Lightcurve Analysis for 2018 UQ1 and 2018 UR2" 190–191.

López-Oquendo, A.J.; Cotto-Figueroa, D. "Lightcurve Analysis of Three Potentially Hazardous Asteroids" 204–205.

Macías, A.A.; Licandro, J.; Serra-Ricart, M. "Mainbelt Asteroids Lightcurve Analysis from *TAR* Telescope Network: 2018 October – 2019 May" 395–399.

Mannucci, M.; Montigiani, N. "Rotational Period Determination for Asteroids 1802 Zhang Heng and (110767) 2001 UB25" 277–278.

Marchini, A.; Franco, L.; Papini, R.; Banfi, M.; Salvaggio, F.; Galdies, C.; Brincat, S.M. "Collaborative Asteroid Photometry for 3653 Klimishin, 4748 Tokiwagozen, and 9951 Tyrannosaurus" 504–505.

Marchini, A.; Papini, R.; Banfi, M.; Salvaggio, F. "Rotation Period Determination for 5351 Diderot and 7230 Lutz" 90–91.

Marchini, A.; Papini, R.; Banfi, M.; Salvaggio, F. "Rotation Period Determination of Three Main Belt Asteroids: 3769 Arthurmiller, 3995 Sakaino and (7520) 1990 BV" 213–214.

Marchini, A.; Papini, R.; Banfi, M.; Salvaggio, F.; Bachini, M.; Galdies, C.; Brincat, S.M. "Rotation Period Determination for 3157 Novikov and 7485 Changchun" 211–212.

Marchini, A.; Papini, R.; Banfi, M.; Salvaggio, F.; Bachini, M.; Galdies, C.; Brincat, S.M. "Rotation Period Determination for 3157 Novikov – Addendum" 357.

Marchini, A.; Papini, R.; Banfi, M.; Salvaggio, F.; Franco, L. "Rotation Period Determination for the Asteroids 3329 Golay and (37652) 1994 JS1" 338–339.

Mollica, M.; Noschese, A.; Vecchione, A. “Lightcurve Analysis and Rotation Period for 5321 Jagras” 206–207.

Mollica, M.; Vecchione, A. “Lightcurve Analysis and Rotation Period for (11650) 1997 CN” 76.

Noschese, A.; Catapano, A.; Vecchione, A. “Lightcurve Analysis and Rotation Period for 19911 Rigaux” 24.

Noschese, A.; Mollica, M.; Catapano, A.; Vecchione, A. “Lightcurve Analysis, Rotation Period and H-G Parameters Determination for 2727 Paton” 439–440.

Noschese, A.; Vecchione, A. “Lightcurve Analysis and Rotation Period for 4262 Devorkin” 25.

Noschese, A.; Vecchione, A. “Lightcurve Analysis and Rotation Period for (28281) 1999 CT29” 26.

Noschese, A.; Vecchione, A. “Rotation Period Determination for 1229 Tilia” 77.

Noschese, A.; Vecchione, A. “Rotational Periods and Lightcurves of 1475 Yalta and 7230 Lutz” 194–195.

Noschese, A.; Vecchione, A.; Catapano, A. “Lightcurve Analysis and Rotation Period for (37652) 1994 JS1” 331.

Odden, C.; Abruzzese, Z.; Beckwith, R.; Chandran, R.; El Alam, Z.; Glover, E.; Kacergis, J.; Carrasco, I.L.; Solomon, H.; Wang, J.; Klinglesmith, D.; Goodwrench, Z.; Pilcher, F. “Lightcurve and Period Determination for Asteroid 4148 McCartney” 293–294.

Odden, C.E.; Abruzzese, Z.N.; Beckwith, R.M.; Chandran, R.J.; El Alam, Z.; Glover, E.W.; Kacergis, J.P.; Julia, I.L.C, Nyiha, I.N.; Solomon, H.V.; Wang, J.S.; Yu, Z.; Zhu, J. “Lightcurve Analysis of Asteroid 2305 King” 363–364.

Oey, J.; Groom, R. “Lightcurve Analysis of Asteroids from BMO and DRO in 2016. II” 119–125.

Owings, L.E. “Lightcurve Analysis of Ten Asteroids” 272–274.

Papini, R.; Banfi, M.; Salvaggio, F.; Marchini, A. “Rotation Period Determination of Asteroids 7736 Nizhnij Novgorod and (42701) 1998 MD13” 99–100.

Papini, R.; Banfi, M.; Salvaggio, F.; Marchini, A.; Franco, L. “Rotation Period Determination of the Asteroid 5321 Jagras (1985 VN)” 218–219.

Percy, S.C. “Rotation Period for 1711 Sandrine” 374–376.

Percy, S.C. “Rotation Period for 2053 Nuki” 265–266.

Percy, S.C. “Rotation Period for 2326 Tololo” 13–14.

Percy, S.C. “Rotation Period for 3670 Chuvashia” 227–228.

Pilcher, F. “Call for Observations” 187.

Pilcher, F. “General Report of Position Observations by the ALPO Minor Planets Section for the Year 2018” 322–329.

Pilcher, F. “Minor Planets at Unusually Favorable Elongations in 2019” 40–42.

Pilcher, F. “New Lightcurves of 50 Virginia, 57 Mnemosyne, 59 Elpis, 194 Prokne, 444 Gyptis, and 997 Priska” 445–448.

Pilcher, F. “New Lightcurves of 153 Hilda, 293 Brasilia, and 318 Magdalena” 130–131.

Pilcher, F. “New Lightcurves of 156 Xanthippe, 445 Edna, and 676 Melitta” 58–60.

Pilcher, F. “Rotation Period Determinations for 58 Concordia, 384 Burdigala, 464 Megaira, 488 Kreusa, and 491 Carina” 360–363.

Pilcher, F.; Benishek, V. “Lightcurves of 153 Hilda at Large Phase Angles” 318–319.

Pilcher, F.; Franco, L.; Marchini, A. “Rotation Period Determination for 449 Hamburga” 267.

Pilcher, F.; Klinglesmith, D., III; Oey, J. “1744 Harriet: Another Very Slowly Rotating Asteroid” 456–457.

Polakis, T. “Lightcurve Analysis for Seven Main-belt Minor Planets” 78–80.

Polakis, T. “Lightcurves of Twelve Main-belt Minor Planets” 287–292.

Polakis, T. “Photometric Observations of Seventeen Minor Planets” 400–406.

Polakis, T.; Skiff, B. “Lightcurves of Eleven Main-belt Minor Planets” 132–137.

Reshetnyk, V.; Godunova, V.; Izvekova, I.; Simon, A.; Sergeev, O.; Polyakov, V. “Photometry of NEA (144332) 2004 DV24 at the Terskol Observatory” 96.

Rowe, B. “Lightcurve Analysis of 6 Asteroids from RMS Observatory” 92–94.

Rowe, B. “Lightcurve Analysis of 9 Asteroids from RMS Observatory” 353–356.

Rowe, B. “A Re-evaluation of Asteroid 4181 Kivi” 292.

Ruthroff, J. “Low Phase Angle Observations of Asteroid 291 Alice” 319–320.

Salthouse, A. “Distribution of Minor Planet Numbers vs Cumulative Number Observed” 235.

Salthouse, A. “A Model of Minor Planet Number Distributions: Visual Observations” 378–380.

Salthouse, A. “Pattern of Minor Planet Numbers Versus Cumulative Number Observed” 118.

Salthouse, A. “Visual Observation of Minor Planets” 5–7.

Salvaggio, F.; Marchini, A.; Papini, R.; Banfi, M. “Lightcurve and Rotation Period Determination for 2496 Fernandus, 2727 Paton, and 69971 Tanzi” 340–341.

Skiff, B.A.; McLelland, K.P.; Sanborn, J.J.; Pravec, P.; Koehn, B.W.; Bowell, E. “Lowell Observatory Near-Earth Asteroid Photometric Survey (NEAPS)”
Paper 3 238–265.
Paper 4 458–503.

IN THIS ISSUE

This list gives those asteroids in this issue for which physical observations (excluding astrometric only) were made. This includes lightcurves, color index, and H-G determinations, etc. In some cases, no specific results are reported due to a lack of or poor quality data. The page number is for the first page of the paper mentioning the asteroid. EP is the "go to page" value in the electronic version.

Number	Name	EP	Page
50	Virginia	73	445
57	Mnemosyne	73	445
59	Elpis	73	445
131	Vala	20	392
194	Prokne	73	445
234	Barbara	69	441
261	Prymno	23	395
338	Budrosa	23	395
349	Dembowska	50	422
444	Gyptis	73	445
714	Ulula	23	395
722	Frieda	28	400
767	Bondia	9	381
805	Hormuthia	28	400
856	Backlunda	28	400
904	Rockefellia	28	400
985	Rosina	86	458
997	Priska	73	445
1036	Ganymed	51	423
1090	Sumida	86	458
1166	Sakuntala	69	441
1178	Irmela	28	400
1199	Geldonia	28	400
1229	Tilia	9	381
1269	Rollandia	34	406
1293	Sonja	86	458
1387	Kama	86	458
1397	Umtata	28	400
1468	Zomba	86	458
1475	Yalta	9	381
1483	Hakoila	28	400
1516	Henry	28	400
1517	Beograd	28	400
1551	Argelander	46	418
1558	Jarnefelt	28	400
1677	Tycho Brahe	46	418
1711	Sandrine	2	374
1744	Harriet	84	456
1774	Kulikov	46	418
1865	Cerberus	86	458
1902	Shaposhnikov	34	406
1914	Hartbeespoortdam	28	400
1914	Hartbeespoortdam	69	441
1943	Anteros	86	458
2025	Nortia	77	449
2212	Hephaistos	86	458
2281	Biela	86	458
2357	Phereclos	17	389
2363	Cebriones	17	389
2378	Pannekoek	77	449
2396	Kochi	28	400
2433	Sootiyo	28	400
2433	Sootiyo	69	441
2460	Mitlincoln	134	506
2510	Shandong	77	449
2525	O'Steen	86	458
2564	Kayala	46	418
2585	Irpidina	86	458
2602	Moore	40	412
2629	Rudra	86	458
2638	Gadolin	12	384
2727	Paton	67	439
2744	Birgitta	86	458
2778	Tangshan	77	449
2784	Domeyko	28	400
2937	Gibbs	40	412
2937	Gibbs	134	506
2956	Yeomans	23	395
3040	Kozai	86	458
3073	Kursk	86	458
3086	Kalbaugh	86	458
3103	Eger	51	423
3147	Samantha	23	395
3315	Chant	134	506
3446	Combes	13	385
3451	Mentor	17	389
3552	Don Quixote	86	458
3554	Amun	86	458
3570	Wuyeesun	28	400
3577	Putilin	34	406
3653	Klimishin	132	504
3671	Dionysus	86	458
3672	Stevedberg	86	458
3816	Chugainov	15	387
3838	Epona	86	458
3843	OISCA	34	406
3875	Staehle	86	458
3880	Kaiserman	40	412
4160	Sabrina-John	77	449
4179	Toutatis	86	458
4205	David Hughes	86	458
4581	Asclepius	51	423
4748	Tokiwagozen	132	504
4807	Noboru	9	381
4892	Chrispollas	77	449
4894	Ask	86	458
5011	Ptah	86	458
5253	Fredclifford	86	458
5261	Eureka	86	458
5262	Brucegoldberg	28	400
5332	Davidaguilar	51	423
5351	Diderot	5	377
5404	Uemura	86	458
5604	1992 FE	86	458
5620	Jasonwheeler	86	458
5627	1991 MA	77	449
5693	1993 EA	51	423
5869	Tanith	86	458
5945	Roachapproach	86	458
5999	Plescia	86	458
6012	Williammurdoch	86	458
6239	Minos	86	458
6310	Jankonke	77	449
6329	Hikonejyo	23	395
6372	Walker	16	388
6455	1992 HE	86	458
6582	Flagsymphony	9	381
6859	Datemasamune	77	449
7267	Victormeen	86	458
7305	Ossakajusto	9	381
7673	Inohara	23	395
7965	Katsuhiko	86	458
8444	Popovich	86	458
9410	1995 BJ1	13	385
9564	Jeffwynn	77	449
9564	Jeffwynn	86	458
9564	Jeffwynn	134	506
9951	Tyrannosaurus	132	504
10422	1999 AN22	134	506
10480	Jennyblue	77	449
10524	Maniewski	134	506
10997	Gahm	23	395
11155	Kinpu	46	418
12538	1998 OH	51	423
12538	1998 OH	86	458
12538	1998 OH	134	506
12929	1999 TZ1	17	389
14105	Nakadai	23	395
14402	1991 DB	86	458
15700	1987 QD	86	458
15925	Rokycany	23	395
17492	Hippasos	17	389
17780	1998 FY13	13	385
19402	1998 EG14	86	458
20691	1999 VY72	86	458
20936	Nemrut Dagi	77	449
20936	Nemrut Dagi	86	458
21104	Sveshnikov	86	458
22262	1980 PZ2	86	458
23183	2000 OY21	86	458
24029	1999 RT198	86	458
24491	2000 YT123	13	385
24643	MacCready	86	458
26355	Grueber	46	418
26471	Tracybecker	86	458
27568	2000 PT6	40	412
28341	Bingaman	13	385
32772	1986 JL	77	449
33324	1998 QE56	77	449
33729	1999 NJ21	23	395
36274	2000 AV107	34	406
37652	1994 JS1	1	373
38074	1999 GX19	86	458
39266	2001 AT2	34	406
42811	1999 JN81	86	458
42930	1999 TM11	86	458
47369	1999 XA88	46	418
52768	1998 OR2	86	458
53319	1999 JM8	86	458
53440	1999 XQ33	77	449
55854	Stoppani	77	449
62836	2000 UC59	23	395
65679	1989 UQ	86	458
66346	1999 JU71	77	449
66391	1999 KW4	69	441
66391	1999 KW4	72	444
68134	2001 AT18	86	458
68216	2001 CV26	51	423
68216	2001 CV26	86	458
68350	2001 MK3	86	458
68950	2002 QF15	51	423
74779	1999 RF241	86	458
74823	1999 TD15	86	458
85236	1993 KH	51	423
85839	1998 YO4	86	458
85867	1999 BY9	86	458
85989	1999 JD6	51	423
87684	2000 SY2	86	458
99913	1997 CZ5	86	458
100926	1998 MQ	86	458
102873	1999 WK11	86	458
112221	2002 KH4	51	423
136568	1980 XB	86	458
138883	2000 YL29	86	458
141432	2002 CQ11	86	458
141498	2002 EZ16	86	458
141525	2002 FV5	51	423
142040	2002 QE15	40	412
143381	2003 BC21	86	458
143651	2003 QO104	86	458
144898	2004 VD17	51	423
152558	1990 SA	86	458
152952	2000 GC2	86	458
153814	2001 WN5	86	458
154029	2002 CY46	86	458
154244	2002 KL6	86	458
154278	2002 TB9	86	458
161989	Cacus	86	458
162181	1999 LF6	51	423
162385	2000 BM9	86	458
162820	2001 BK36	77	449
162900	2001 HG31	86	458
163000	2001 SW169	86	458
163696	2003 EB50	51	423
164716	1998 GH	86	458
174599	2003 QM70	86	458
175706	1996 FG3	86	458
184990	2006 KE89	86	458
185851	2000 DP107	86	458
185854	2000 EU106	86	458
188542	2004 HE62	86	458
194386	2001 VG5	86	458
207945	1991 JW	86	458
208023	1999 AQ10	86	458
219071	1997 US9	86	458
220124	2002 TE66	86	458
224211	2003 QB90	86	458
242643	2005 NZ6	86	458
244670	2003 KN18	51	423
248818	2006 SZ217	86	458
256412	2007 BT2	86	458
257744	2000 AD205	51	423
260141	2004 QT24	86	458
277039	2005 CF41	86	458
302111	2001 MM3	77	449

Number	Name	EP	Page	Number	Name	EP	Page	Number	Name	EP	Page
305090	2007 VQ4	86	458	524522	2002 VE68	86	458		2010 RC130	86	458
305090	2007 VQ4	86	458	528159	2008 HS3	86	458		2010 RF181	86	458
325769	2010 LY63	86	458	529668	2010 JL33	86	458		2010 SC41	86	458
326777	2003 SV222	51	423		2002 JW15	51	423		2010 TC55	86	458
341843	2008 EV5	86	458		2004 XK3	86	458		2010 TU5	86	458
341843	2008 EV5	86	458		2006 KE	51	423		2010 TX168	86	458
345705	2006 VB14	86	458		2007 RU17	86	458		2010 UX6	86	458
355256	2007 KN4	51	423		2008 HS3	51	423		2011 AL37	86	458
410650	2008 SQ1	86	458		2008 JT35	86	458		2011 HP	51	423
410777	2009 FD	86	458		2008 QS11	86	458		2011 HP	86	458
416801	2005 GC120	86	458		2008 SA	86	458		2014 LJ21	51	423
446791	1998 SJ70	86	458		2008 SE	86	458		2014 SZ303	51	423
453778	2011 JK	51	423		2008 SR1	86	458		2018 EB	51	423
453778	2011 JK	86	458		2008 WL60	86	458		2018 XG5	51	423
455736	2005 HC3	51	423		2008 WX32	51	423		2019 FP2	51	423
488515	2001 FE90	86	458		2009 DL1	51	423		2019 HC	51	423
494999	2010 JU39	51	423		2009 DO111	86	458		2019 JB1	51	423
503941	2003 UV11	86	458		2009 JM2	86	458		2019 JX7	51	423
504025	2005 RQ6	86	458		2009 UU1	86	458		2019 KZ3	51	423
518638	2008 JP14	86	458		2010 LF86	86	458		2019 MB4	51	423

THE MINOR PLANET BULLETIN (ISSN 1052-8091) is the quarterly journal of the Minor Planets Section of the Association of Lunar and Planetary Observers (ALPO). Current and most recent issues of the *MPB* are available on line, free of charge from:

http://www.minorplanet.info/MPB/mpb.php

Nonmembers are invited to join ALPO by communicating with: Matthew L. Will, A.L.P.O. Membership Secretary, P.O. Box 13456, Springfield, IL 62791-3456 (will008@attglobal.net). The Minor Planets Section is directed by its Coordinator, Prof. Frederick Pilcher, 4438 Organ Mesa Loop, Las Cruces, NM 88011 USA (fpilcher35@gmail.com, assisted by Lawrence Garrett, 206 River Rd., Fairfax, VT 05454 USA (LSGasteroid@msn.com). Dr. Alan W. Harris (Space Science Institute; awharris@spacescience.org), and Dr. Petr Pravec (Ondrejov Observatory; ppravec@asu.cas.cz) serve as Scientific Advisors. The Asteroid Photometry Coordinator is Brian D. Warner, Palmer Divide Observatory, 446 Sycamore Ave., Eaton, CO 80615 USA (brian@MinorPlanetObserver.com).

The Minor Planet Bulletin is edited by Professor Richard P. Binzel, MIT 54-410, 77 Massachusetts Ave, Cambridge, MA 02139 USA (rpb@mit.edu). Brian D. Warner (address above) is Associate Editor, and Dr. David Polishook, Department of Earth and Planetary Sciences, Weizmann Institute of Science (david.polishook@weizmann.ac.il) is Assistant Editor. The *MPB* is produced by Dr. Robert A. Werner, 3937 Blanche St., Pasadena, CA 91107 USA (rawerner@polygrav.org) and distributed by Derald D. Nye. Direct all subscriptions, contributions, address changes, etc. to:

Mr. Derald D. Nye - Minor Planet Bulletin
10385 East Observatory Drive
Corona de Tucson, AZ 85641-2309 USA
(nye@kw-obsv.org) (Telephone: 520-762-5504)

Effective with Volume 38, the *Minor Planet Bulletin* is a limited print journal, where print subscriptions are available only to libraries and major institutions for long-term archival purposes. In addition to the free electronic download of the *MPB* noted above, electronic retrieval of all *Minor Planet Bulletin* articles (back to Volume 1, Issue Number 1) is available through the Astrophysical Data System

http://www.adsabs.harvard.edu/.

Authors should submit their manuscripts by electronic mail (rpb@mit.edu). Author instructions and a Microsoft Word template document are available at the web page given above. All materials must arrive by the deadline for each issue. Visual photometry observations, positional observations, any type of observation not covered above, and general information requests should be sent to the Coordinator.

* * * * *

The deadline for the next issue (47-1) is October 15, 2019. The deadline for issue 47-2 is January 15, 2020.